DOE/LC/11060--2846

DE90 009656

Oil Shale Retorting Using Electromagnetic Methods

Final Report

R. Inguva
J. Baker-Jarvis

September 1988

Work Performed Under Contract No.: DE-AC21-85LC11060

For
U.S. Department of Energy
Office of Fossil Energy
Morgantown Energy Technology Center
Morgantown, West Virginia

By
University of Wyoming
Department of Physics and Astronomy
Laramie, Wyoming

DISCLAIMER

Available to DOE and DOE contractors from the Office of Scientific and Technical Information, P.O. Box 62, Oak Ridge, TN 37831; prices available from (615)576-8401, FTS 626-8401.

Available to the public from the National Technical Information Service, U.S. Department of Commerce, 5285 Port Royal Rd., Springfield, VA 22161.

Price: Printed copy A15
Microfiche AO1

Codes are used for pricing all publications. The code is determined by the number of pages in the publication. Information pertaining to the pricing codes can be found in the current issues of the following publications, which are generally available in most libraries: *Energy Research Abstracts (ERA), Government Reports Announcements* and *Index (GRA* and *I); Scientific and Technical Abstracts Reports (STAR);* and publication NTIS-PR-360 available from NTIS at the above address.

DOE/LC/11060-2846
(DE90009656)

Oil Shale Retorting Using Electromagnetic Methods

Final Report

R. Inguva
J. Baker-Jarvis

Work Performed Under Contract No.: DE-AC21-85LC11060

For
U.S. Department of Energy
Office of Fossil Energy
Morgantown Energy Technology Center
P.O. Box 880
Morgantown, West Virginia 26507-0880

By
University of Wyoming
Department of Physics and Astronomy
Laramie, Wyoming 82071

September 1988

ACKNOWLEDGMENTS

The work presented in this report could not have been accomplished without the help of several individuals and the facilities at several laboratories over the past several years. In particular we are pleased to acknowledge the contributions of the following:

1. *Students:* Mr. Atish Sen (Dielectric Measurements); Mr. V. Nagaraj (Phased Arrays); Mr. Prashant Sansgiri (Modeling); Mr. Larry Bryant (Permeability Measurements); Mr. Adwait Chawathe (Permeability Measurements).

2. Mr. V.K. Saxena, microwave engineer, helped design and fabricate the bench scale retort and maintained all the microwave equipment.

3. We are grateful to Professor M.P. Sharma for help with the permeability measurements. Chapter 4 has been written in collaboration with Dr. Sharma and Mr. Chawathe.

4. Chapter 3 on the dielectric measurements setup has been written in collaboration with Mr. Atish Sen.

5. Mr. Ramon Jesch and Dr. Howard Bussey assisted in the design and fabrication of the dielectric measurement setup.

6. We are grateful to Professor Richard Ewing for his partial support in the acquisition of the permeability measurement setup.

7. We are deeply indebted to Mr. William Little who provided assistance and encouragement at every stage of the project. Without his vision and support this project could not have been accomplished.

8. A debt of graditude is due to Dr. Ted Bartke and Mr. Carl Roosmagi for their interest and encouragement throughout the project duration.

9. The various personnel in the Arts and Sciences workshop helped in the construction of bench scale reactor. The many hours spent are gratefully appreciated.

10. Various staff members of Western Research Institute offered assistance whenever needed. In particular, we are grateful to Dr. Chang-Yul-Cha and Mr. David Sheesley for their help.

11. Its is a pleasure to acknowledge the invaluable assistance of Ms. Marce Mitchum for all the nontrivial paperwork related to contractual matters and accounting. Thanks are due to Ms. Evelyn Haskell, Ms. Kristy Anderson, Ms. Cora Streyle, and Mr. Michael Mann for help with the expert typing of the many reports and several versions of the final report.

TABLE OF CONTENTS

LIST OF TABLES

LIST OF FIGURES

EXECUTIVE SUMMARY

The enclosed report presents the results of a three year study on the retorting of oil shales by electromagnetic methods. The main aim of this study was twofold: (1) to obtain reliable data on the various retorting parameters such as dielectric constants, temperature profiles, permeabilities, oil yields, etc., for the case of bench scale retorting of a shale block by electromagnetic methods using a monopole antenna; and (2) to develop and validate a mathematical model using this data.

Reliable data have been obtained using a bench scale retort to heat shale blocks using monopole antennas under various conditions. Data have been obtained for dielectric constants and permeabilities. A mathematical model has been developed to interpret the present data. Combined with all the earlier experimental work in the literature, economics of the heating process has been studied following the earlier work by Bridges and his group, and Mellon. Feasibility studies of other configurations such as phased arrays have been conducted. The data base and modeling effort should be of great value for all future large scale efforts.

The simple monopole configuration was investigated mainly to obtain a basic understanding of the electromagnetic retorting process. With a proper design we feel (in agreement with the earlier conclusions of Bridges and his coworkers) that the electromagnetic retorting method will ultimately provide a viable process for erxtracting oil from oil shales. Bench scale retorting experiments using more realistic configurations such as phased arrays would be very worthwhile before undertaking large scale efforts.

CHAPTER 1

DIELECTRIC HEATING OF OIL SHALES BY MONOPOLES AND COAXIAL APPLICATORS

CHAPTER SUMMARY

The concept of dielectric heating of oil shales by high power, high frequency electromagnetic fields using monopole, dipole and modified coaxial applicators is studied and tested. The various physical and modeling parameters are introduced and discussed in the context of *in situ* heating of fossil fuels. Based on numerical model results a radio frequency power delivery system and echoic test chamber were designed and fabricated for high temperature heating experiments. A series of experiments were performed using both monopoles and modified coaxial applicators. It was found that dielectric breakdown near pyrolysis temperatures limited the power level for the heating process. It was also found that a modified coaxial applicator with the TM_{01} mode and an open circuited line at the bottom confined the fields and has potential as a useful applicator in large scale field tests.

1.1 BACKGROUND: Radiation Heating of Oil Shales

It has been shown that it is possible to heat large volumes of oil shales and tar sands *in situ* using radio frequency (r.f.) heating technology. [1–9] The radiation heating process converts electrical power from an a.c. generator into heat by rotating polar molecules; energy is dissipated as heat when work is performed by the electric fields in rotating the molecules. Past strategies that have been used for electromagnetic heating of oil shales fall under two categories: 1) radiation or high frequency methods and 2) low frequency methods. High frequency methods include both microwave heating and radio frequency heating processes. On oil shales, microwave heating has been performed by duBow and Rajeshwar [3], and by Wall *et al.* [4]. These experiments were carried out on small samples of shale in the laboratory. Radio frequencies have been used to heat oil shale by guided wave applicators by Bridges et al [1,2]. Bridges reported encouraging heating results at 13.56 Mhz using an applicator that was a modified triplate transmission line in which plates were replaced by rows of electrodes. This pioneering work demonstrated that it is possible to heat shale *in situ* to pyrolysis temperatures and recover reasonable amounts of oil. However, the IITRI design does require extensive mining and drilling to insert the system. Raytheon [10] has proposed the use of dipoles to heat fossil fuels *in situ*, but little experimental work has been performed to prove the concept.

Simple applicators have the advantage of minimizing the work of mining when inserting the system into the resource. Monopole or dipole applicators (see Fig. 1.1) are quite attractive because of the ease of emplacement. If phasing of arrays of applicators could be accomplished in such a fashion as to confine the fields to a localized area, then large regions could be heated *in situ*. In order to describe the heating profile of a phased array of monopoles it is first necessary to understand, in detail, the characteristics of a single monopole (see e.g. [11]). To this end a series of experiments were carried out at the Department of Physics and Astronomy, University of Wyoming. The goal of our project was to study the total dielectric heating process when monopole and coaxial applicators are utilized as applicators. The structure of the project is indicated in Fig. 1.2. The goal of the present chapter is to report on the results found from simple applicator experiments.

1.2 FUNDAMENTALS OF ENERGY DISSIPATION IN A LOSSY MEDIUM

In a low conducting, lossy medium such as oil shale, the heating due to high frequency electric fields is primarily the result of rotation of polar molecules. In a rapidly fluctuating electromagnetic field, polar molecules are rotated by the external torque on the dipole moments. This rotation, of course, is resisted by the damping forces in the medium so that heat is generated in the process. In the electromagnetic heating process the ability of the electromagnetic fields to heat the shale depends on both the magnitude and the frequency of the applied field. The attenuation of the electromagnetic fields in the medium depends on the frequency of the fields and the dielectric constant of the material. The attenuation lengths of the electromagnetic fields in lossy media are inversely proportional to the frequency and the imaginary component of the dielectric constant. The dielectric constant of oil shales has a strong temperature dependence (see [1,2,3] and Chapter 3).

By considering conservation of energy for fields in a lossy medium it is possible to obtain formulae for the dissipated heat energy as a function of the medium and field parameter.

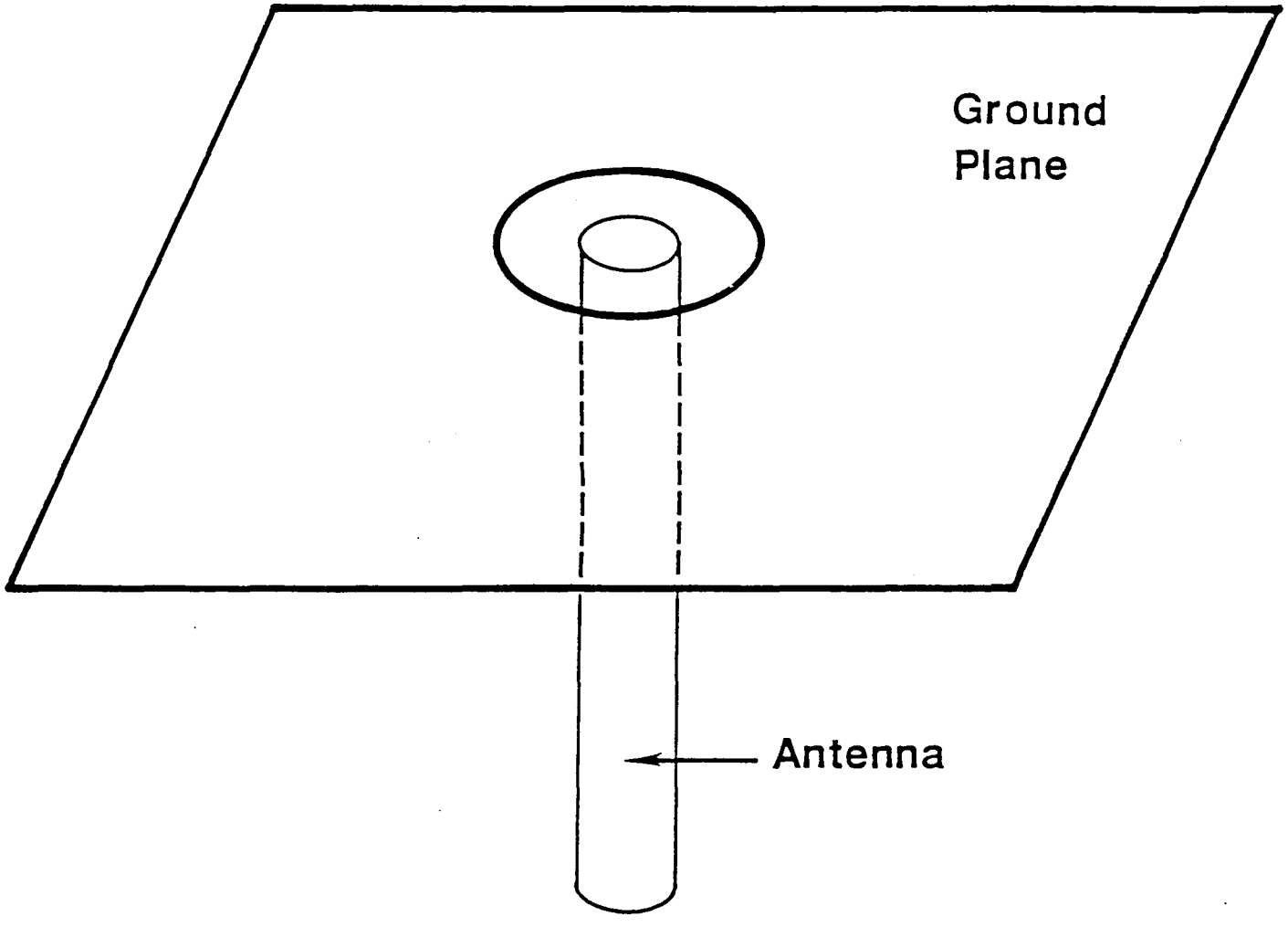

Figure 1.1. Monopole with ground plane.

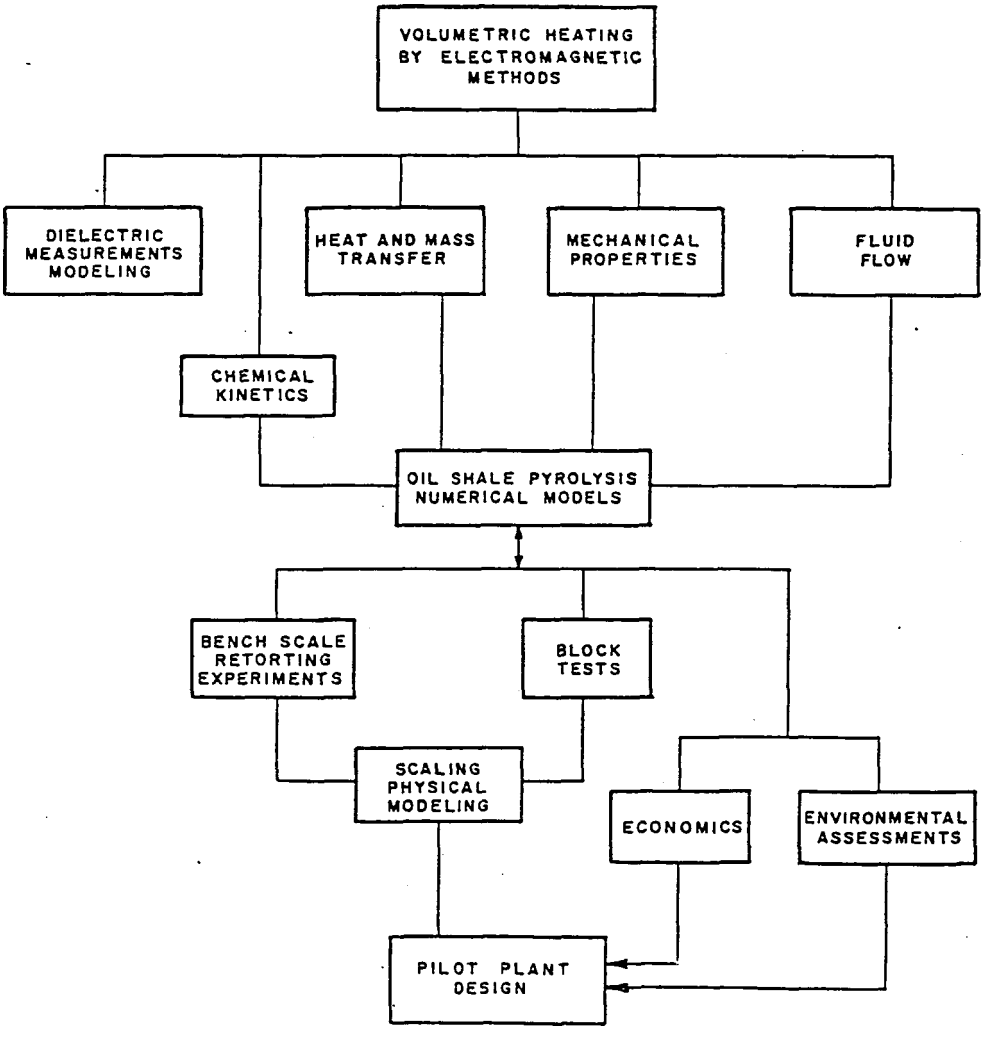

Figure 1.2. Electromagnetic heating project organization.

For a given volume, Poynting's theorem states that:

$$\int_S \vec{E}X\vec{H}^* \cdot \vec{n}\, dA = -\frac{1}{2}\int_V \sigma|\vec{E}|^2 dV + \frac{1}{2}j\omega\int_V \left[\mu|\vec{H}|^2 - \epsilon|\vec{E}|^2\right] dV. \tag{1.1}$$

Here, S is the bounding surface, V is the volume, $\epsilon = \epsilon' - j\epsilon''$ is the dielectric constant, j is the square root of -1, σ = the conductivity, ω = the angular frequency and E and H are Fourier transforms of the electric and magnetic fields, and μ = magnetic permeability. If we assume that the magnetic loss is small then taking the real part of Equation (1.1) yields the power dissipated into the media:

$$Re\int_S \vec{E}X\vec{H}^* \cdot \vec{n}\, dA = -\frac{1}{2}\int \sigma|\vec{E}|^2 dV \tag{1.2}$$

The conductivity σ consists of d.c., low frequency losses and high frequency, polarization losses:

$$\sigma = \sigma_{dc} + \omega\epsilon'' \tag{1.3}$$

At high frequencies, generally the d.c. losses are small compared to polarization losses. We can write the power density dissipated in a non-magnetic lossy medium due to high frequency fields as

$$P_{\text{diss}} = \frac{1}{2}\omega\epsilon''|\vec{E}|^2 \times (\text{watts/m}^3). \tag{1.4}$$

It has been found experimentally that the power density that can be applied to oil shale at pyrolysis temperature is limited by dielectric breakdown of the pyrolysis products. This limitation is a severe constraint on applicator design. The power density at breakdown is a strong function of frequency. The breakdown power densities, at P_1, P_2, at frequencies f_1 and f_2 can be related as a ratio using Equation (1.4):

$$\frac{P_1}{P_2} = \frac{\epsilon_1''\omega_1}{\epsilon_2''\omega_2}. \tag{1.5}$$

Here we have assumed that breakdown E-fields are independent of frequency. We see, therefore, at higher frequencies greater power densities can be used before breakdown occurs.

In oil shales the dielectric polarization losses are mainly due to the interaction with bound water and to a lesser extent on the polar molecules contained in kerogen and Maxwell-Wagner relaxation [12]. A typical absorption curve vs. frequency is shown in Fig. 1.3. Here, we see the characteristic absorption peak due to water at 2.45 GHz. The strong temperature dependence of the dielectric constant is due to the various chemical reactions that occur in the shale as it is heated and the release and migration of steam throughout the shale. In the far field where the waves approximate a plane wave, the power attenuates in an exponential manner and we can define an attenuation constant α:

$$P = P_0 \exp\left(-\frac{z}{\alpha}\right). \tag{1.6}$$

It can be shown that α is a function of the imaginary part of the dielectric constant and also is a function of the frequency

$$\alpha = \frac{1}{\omega}\left[\frac{2}{\mu\epsilon'}\right]^{\frac{1}{2}}\left(\left(\left(1+\left(\frac{\epsilon''}{\epsilon'}\right)^2\right)^{\frac{1}{2}} - 1\right)^{-\frac{1}{2}}\right). \tag{1.7}$$

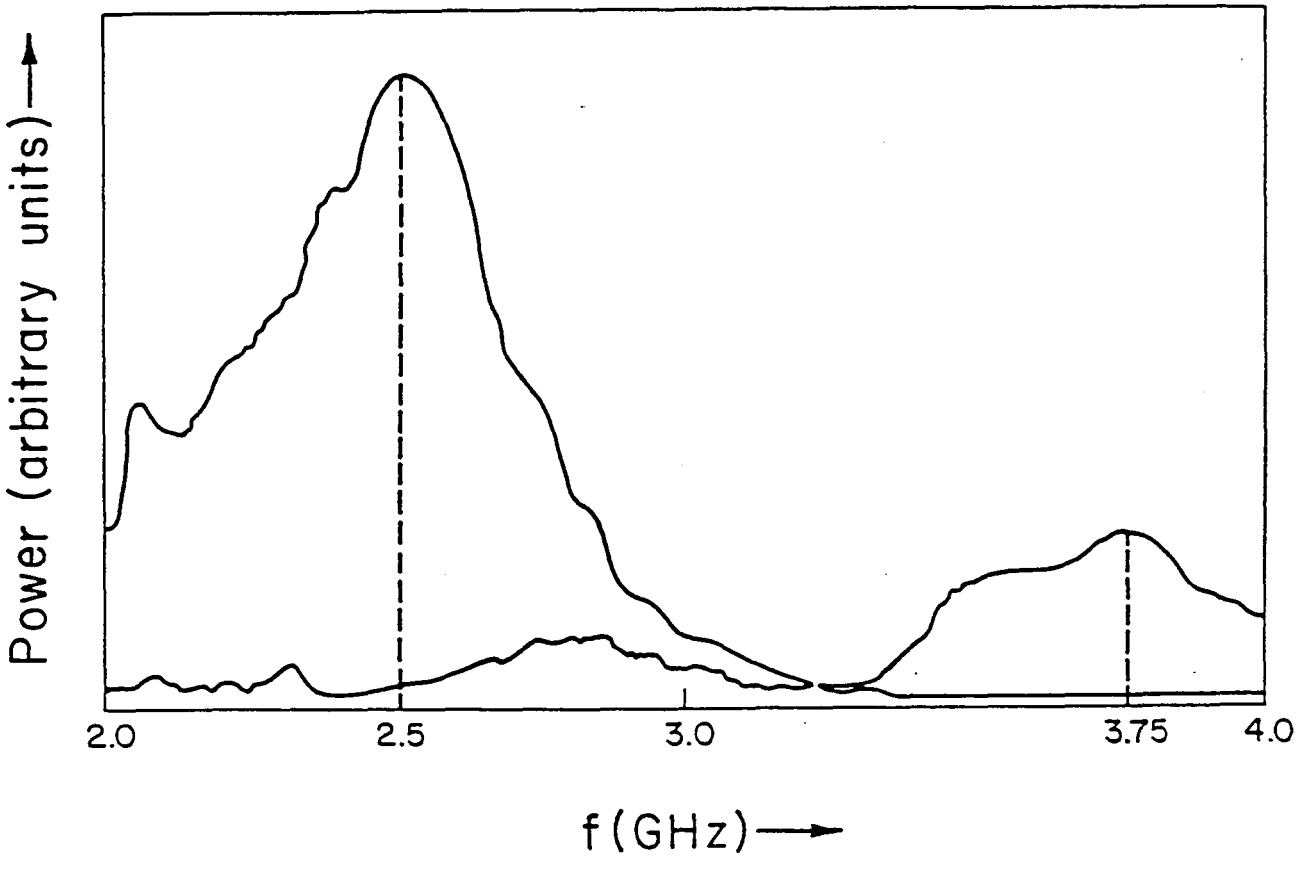

Figure 1.3. Power absorption as a function of frequency in Anvil Points shale (23 GPT).

For an applicator such as a monopole, the near field dissipates energy very rapidly. Also, because of the near field resistance, the total power pumped from the monopole is not easily expressed as in the lossless case as $\frac{1}{2}|I(0)|^2 R_{\text{rad}}$, where R_{rad} = the radiation resistance of the monopole and I(0) is the input current. In general, the simplest way to calculate the total power dissipated by the monopole is to numerically integrate Equation (1.4) over a large volume. Calculation of the attenuation lengths are, of course, of interest when considering any heating problem, but the problem of heating with monopoles is much more complex than a simple application of Equation (1.7). It turns out that the fields due to a monopole are attenuated both radially away from the monopole and vertically down from the feed point due to the damping of the excitation fields (see Fig. 1.4). Therefore, we found it necessary to develop a complicated numerical model from first principles to describe adequately the heating process.

1.3 EXPERIMENTAL CONFIGURATION FOR MONOPOLE TESTS

Power delivery system:

In order to determine the optimum heating frequency and power, a numerical model of the heating process was developed. This model included equations for heat-mass transfer, electromagnetic source terms [9,11], chemical reactions and flow equations. Also a model was developed to simulate the electromagnetic fields around a monopole. A sample calculation is shown in Fig. 1.4. Extensive modeling was carried out to determine the parameters for the design of the experiment.

The modeling produced results for attenuation lengths as a function of frequency and dielectric constant in the shale, the microwave absorption as a function of frequency and the expected heating profiles for various power levels and frequencies. Fig. 1.5 displays the calculated attenuation as a function of frequency and Fig. 1.6 shows measured power density vs. theory for a sample of western shale. The experimental values were obtained by probes inserted into holes drilled into the shale block. Modeling was used to predict heating parameters for a block size of $(0.3 \times 0.3 \times 0.15)\text{m}^3$ for a heating time of 8 hours. It was found that a generator in the frequency range of 900–2500 MHz with a power in the range of 1000–3000 watts was required. A generator was purchased from Cobar Electronics at 2.45 GHz and 0–3000 watts. This generator has a small bandwidth and produces very stable output power. Also two other generators were also used, one at frequency of 450 MHz and 2000 watts and one at 915 MHz and 1000 watts. To protect the magnetron a circulator and a hybrid tuner were also acquired. With the tuner it was possible to tune out almost any impedance mismatch encountered. Dual directional couplers were employed to sample the forward and reflected power. Sampling power was at 60 dB and 50 dB down, respectively. The power transfer was accomplished by waveguides up to the spool piece and thereafter 0.041 m. coax was used. A flow chart of the system is given in Fig. 1.7. to allow a small flexibility in the system a flex coax line was utilized for a section of the coax. Due to the high temperatures encountered in the heating process it was necessary to replace the teflon support beads in the flex line near the shale block with specially machined quartz beads. The monopole consisted of an extension of the inner conductor of a 0.041 m. coax mounted on a ground plane. A hole was drilled into the shale block and the antenna inserted and mounted to the ground plane. Cooling coils were placed on the elbow miter near the ground

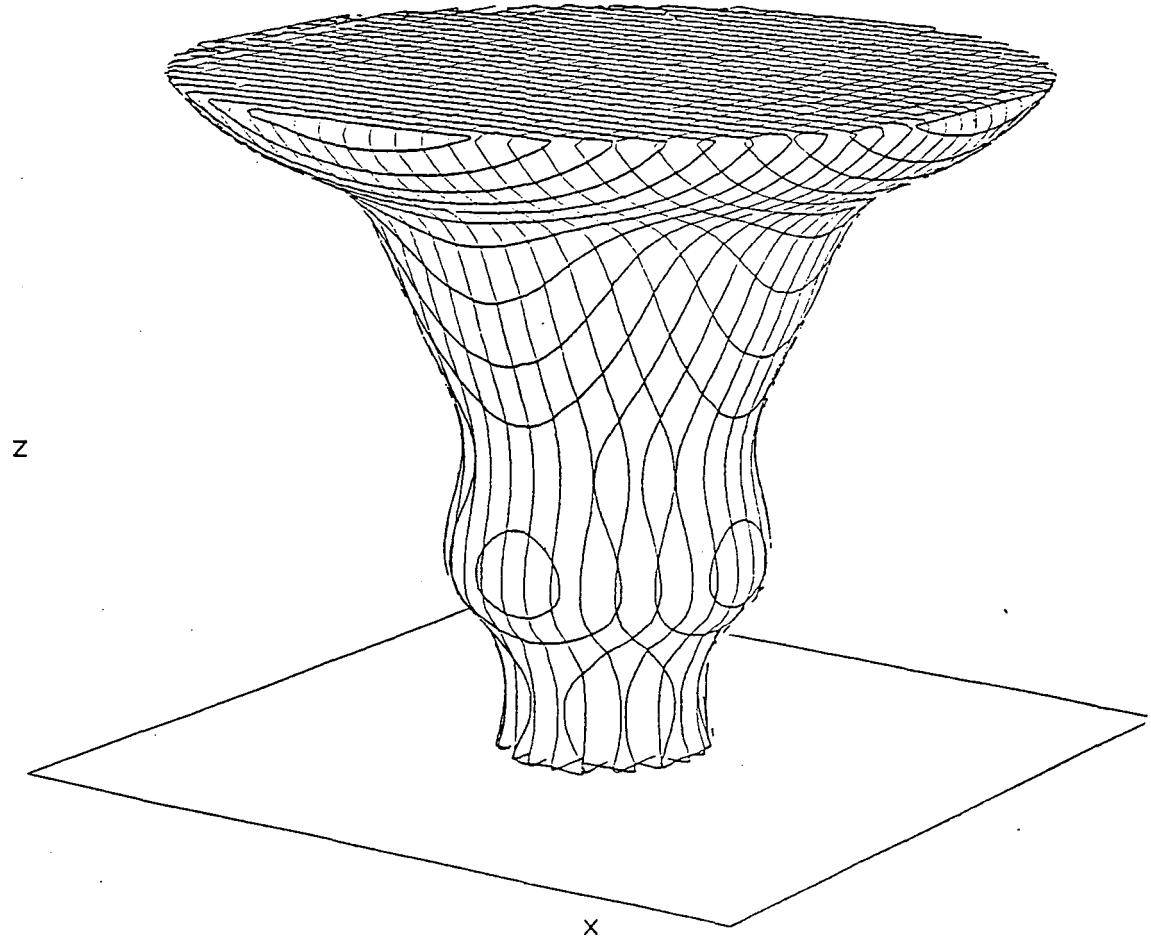

Figure 1.4. Power density from a monopole in lossy medium.

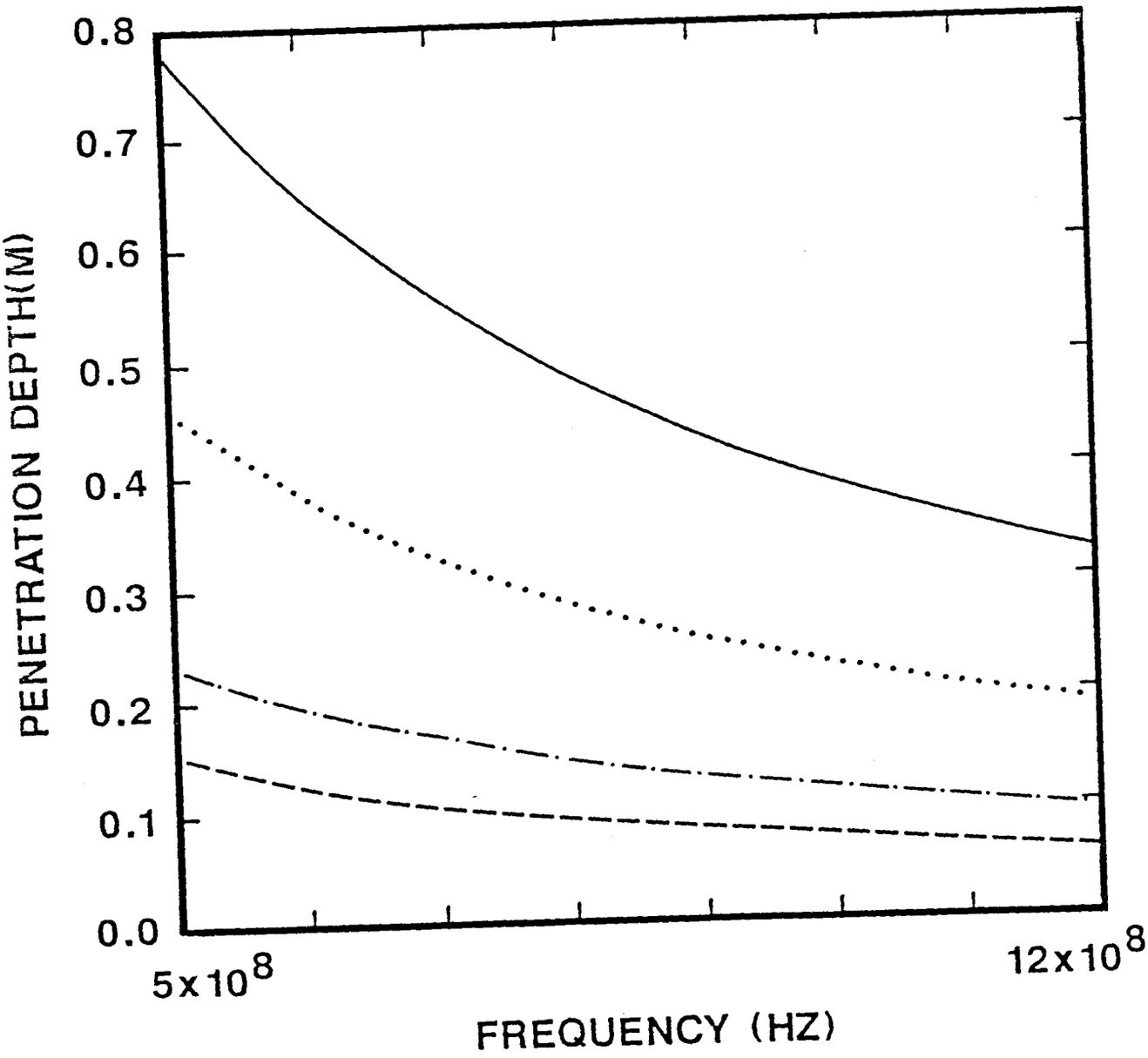

Figure 1.5. Penetration depth as a function of frequency $(- - -)$ $\epsilon = 3$, $(- \cdot -)$ $\epsilon = 1$, $(\cdots)$ $\epsilon = 0.5$, $(—)$ $\epsilon = 0.1$.

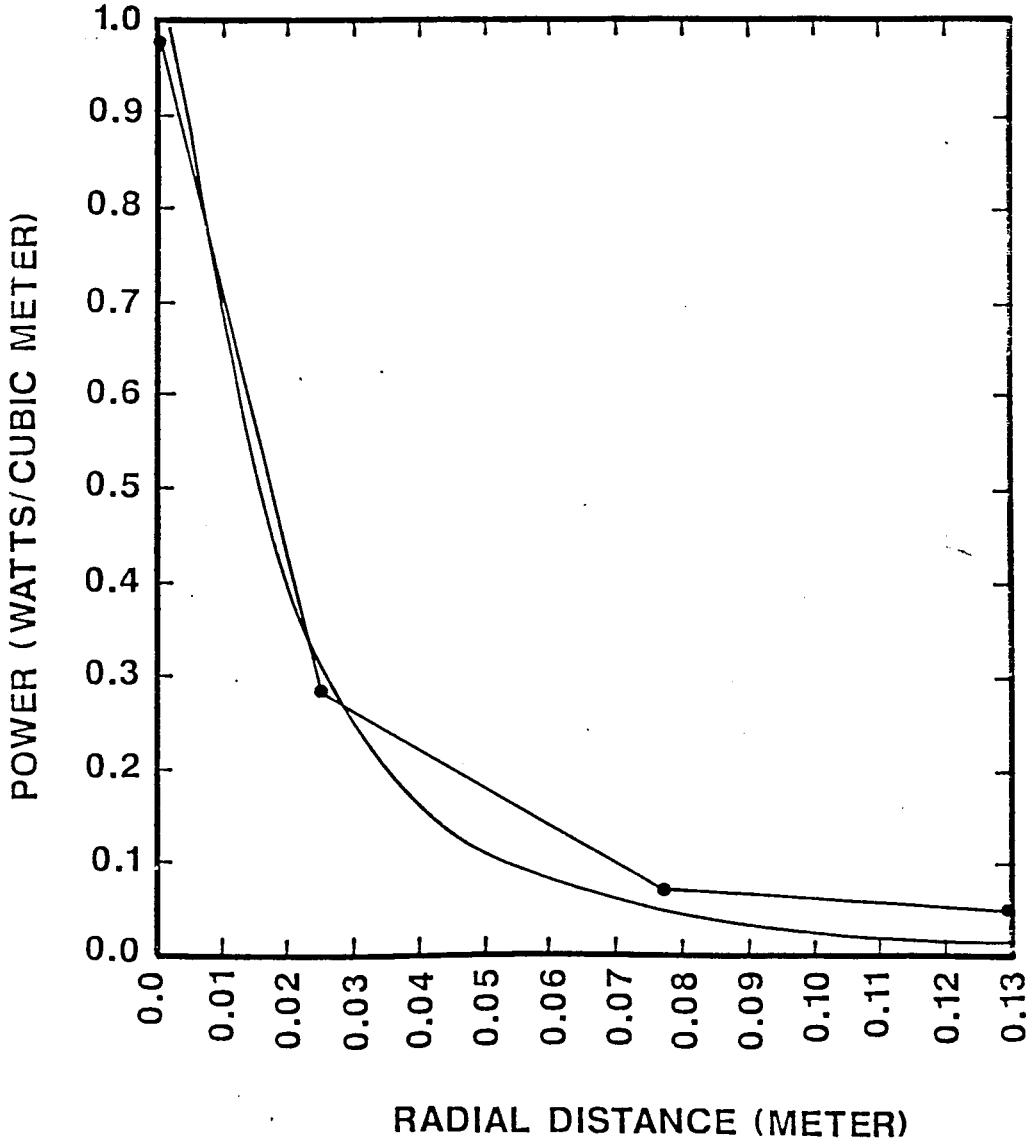

Figure 1.6. Experimental vs. theoretical power as a function of distance from monopole in Anvil Points western shale sample.

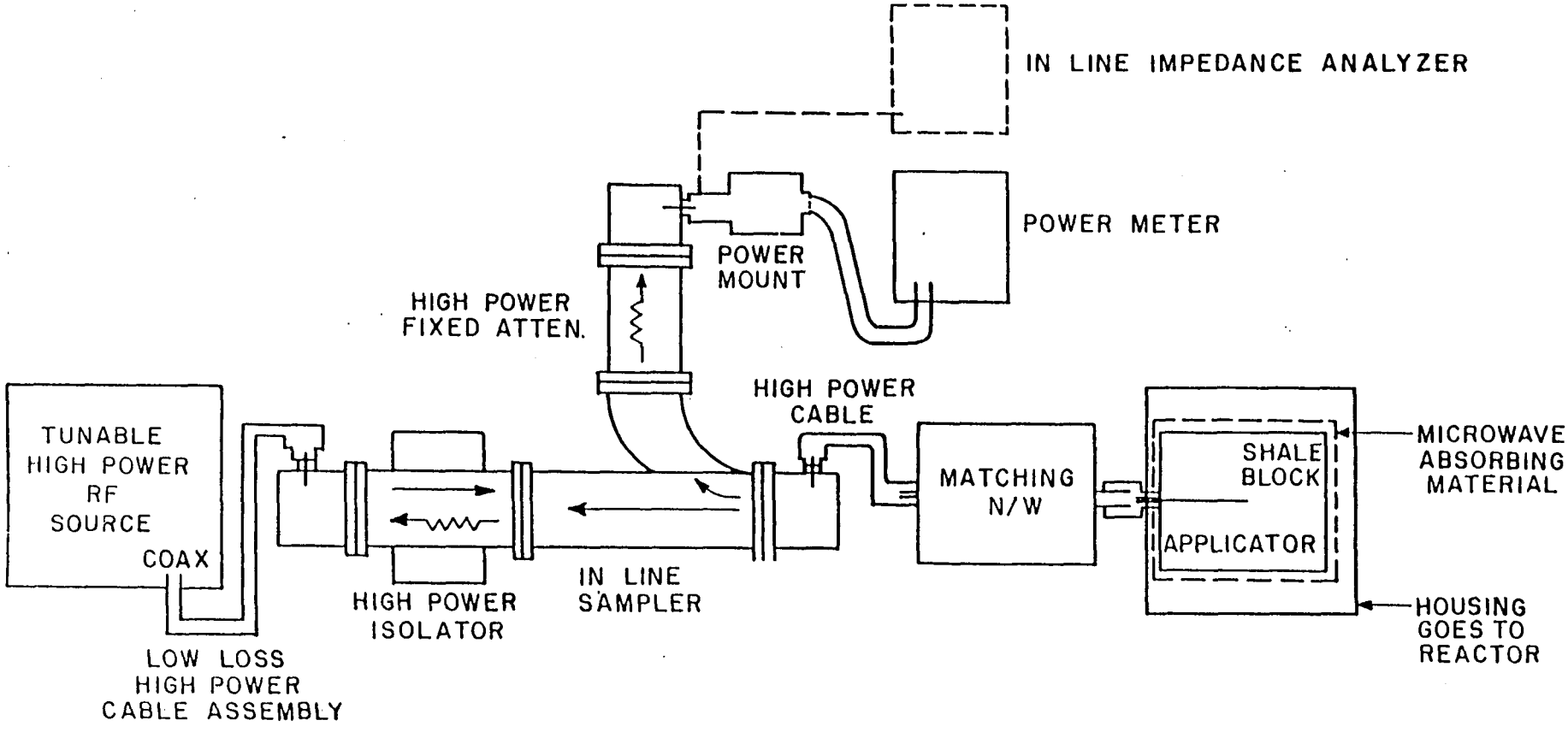

Figure 1.7. System design.

plane. In the first series of experiments no air gap was left between shale and antenna, but dielectric breakdown was encountered. To remedy this, a quartz tube was fabricated to fit over the antenna. The tube contains small ventilation holes in it and the tube was subjected to a constant purge of dry nitrogen gas. This arrangement, show in Fig. 1.8, minimized the dielectric breakdown phenomena.

Design of Spool Piece:

A high temperature spool piece was designed to contain the sample shale block during test runs; a schematic is given in Fig. 1.9. It was required to design the spool piece to withstand high temperatures and pressures of up to 2 atmospheres and at the same time be a good container of electromagnetic waves. The finished spool piece was of dimensions $\{0.8 \times 0.8 \times 0.7\}$ m^3. The vessel was constructed of 0.63 cm steel plate and was designed to be airtight in order to confine product gases. In order to suppress internal reflection of electromagnetic waves, ferrite absorbing tiles were purchased from Emerson and Cumming Inc. and were installed on all inside spool piece surfaces. A hydraulic press was fastened to the top plate so that up to 100 psi simulated overburden could be applied to the block. Inside of the spool piece the sample was contained in another ceramic spool piece in order to confine the products. This simple arrangement made it possible to obtain a reasonable product recovery estimate. In order to monitor temperatures throughout the heating process, thermocouples were inserted into the shale block at various distances. Modeling results indicated that in order to minimize coupling between monopole fields and metallic thermocouples, the thermocouples should be cross polarized with respect to the field polarization. Also, so that temperature measurements could be made at full power, special thermocouples were constructed by Gordon Inc. in which an additional layer of copper foil was wound around the wires, thus decreasing the skin depth appreciable. It was found that temperature measurements could be taken even when high power was applied. The product was collected through a grate at the bottom of the spool piece which funneled into a series of collection condensers.

1.4 TEST RESULTS FOR MONOPOLE APPLICATORS

In Table 1.1 the parameters for tests are given. Thermocouples were inserted into the sides of block at the positions indicated in Fig. 1.10 and cemented in place with ceramic cement. In the first series of experiments the antenna was uninsulated, but it was found that dielectric breakdown was encountered. So in subsequent tests, the hole in the shale was increased to a diameter of 0.041 m. so that there was an air gap around the antenna. This tactic decreased the dielectric breakdown phenomena to some extent, but after pyrolysis temperatures (350°C) were obtained the breakdown reoccurred. In the next series of tests a number of changes were made. First of all a dry nitrogen purge was utilized, also additional cooling of the flex line was installed, and finally a quartz tube was installed to insulate the antenna by preventing the pyrolysis products from coming in contact with the antenna. In these tests much better results were encountered, and it was possible to deliver much higher power levels to the block. In these experiments we were able to deliver 1000 watts continuously during pyrolysis without impedance anomalies occurring. The product (oil) yield was on the order of 25% of Fischer assay. Gas samples were taken at various times during the test and later analyzed, results are given in Table 1.2 for a typical sample during

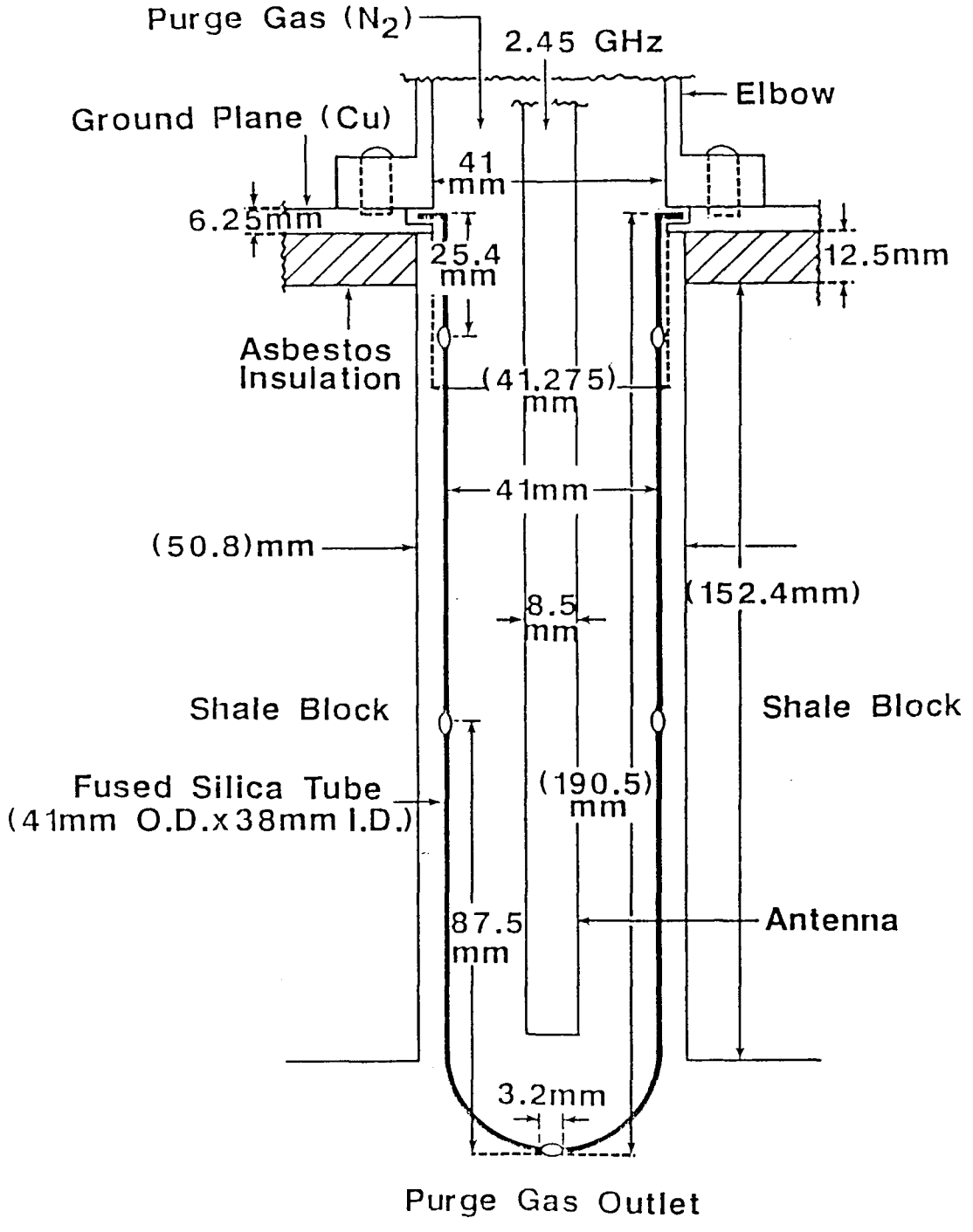

Figure 1.8. Insulated antenna design.

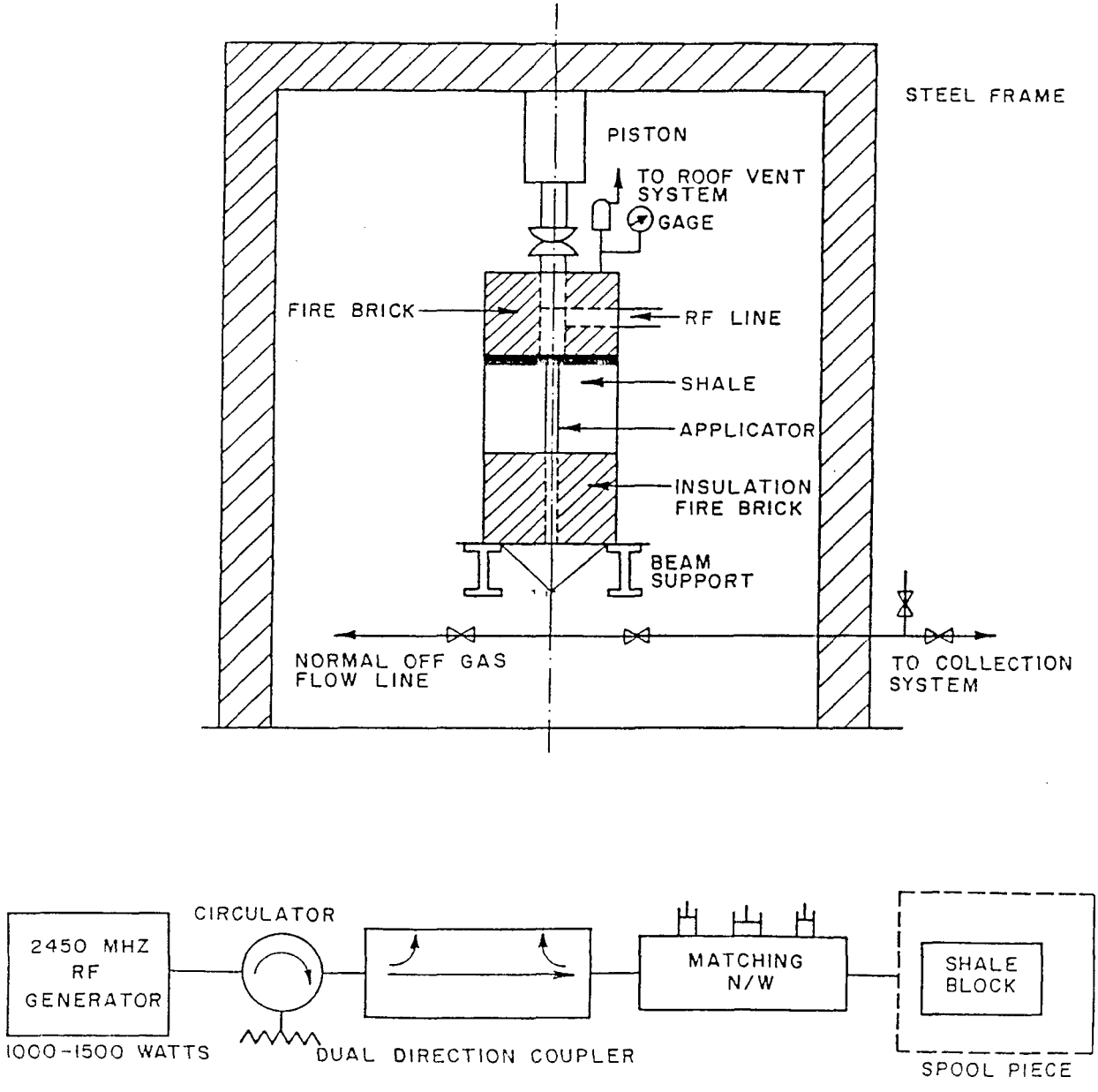

Figure 1.9. Spool piece design.

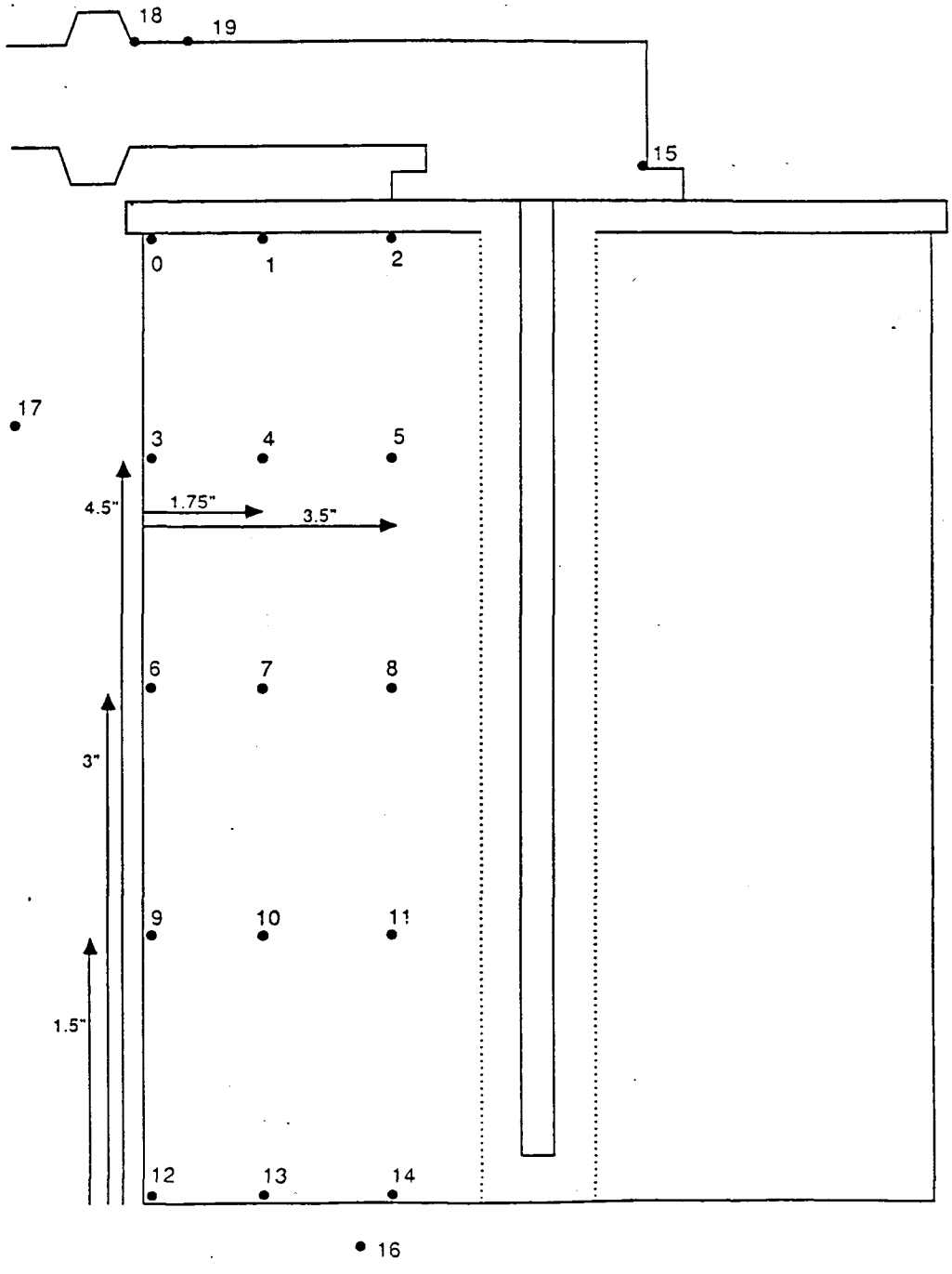

Figure 1.10. Thermocouple positions.

r.f. retorting of Anvil Points western shale. In Table 1.3 the analysis of the oil is given for a 23 GPT Anvil Points western shale after r.f. retorting.

TABLE 1.1

Parameters for Monopole Heating Experiments

Antenna length	0.14 m
Antenna Diameter	0.008 m
Block Dimension	$\{0.3 \cdot 0.3 \cdot 0.15\}$ m^3
Frequency	2.45 GHz, 450 MHz, 915 MHz
Power	500–2000 watts
Shale Grade	23–30 GPT

TABLE 1.2

Typical Gas Analysis for Monopole Heating (23 GPT Anvil Points Western Shale)

Compound	Percent
Hydrogen	21.5
Carbon monoxide	35.3
Carbon dioxide	24.3
Methane	13
Ethane	1.9
Ethylene	1.1
Propane	0.7
Propylene	0.7
C4's	0.6
C5's	0.1
C6–10's	0.5

TABLE 1.3

Oil Analysis for Monopole Test
(Anvil Points Western Shale 23 GPT

Compound	Percent
Carbon	84.8
Hydrogen	12.1
Nitrogen	2.0
Sulfur	1.1
Pour Point	21°C

Temperature profiles at thermocouple positions indicated in Fig. 1.10 are shown in Figs. 1.11 and 1.12.

1.5 MODIFIED COAXIAL APPLICATOR

In an attempt to overcome the dielectric breakdown limitations of the monopole antenna, a test was carried out to study another applicator design concept. This applicator consisted of a coaxial line terminated in an open circuit as depicted in Fig. 1.13. Somlo [13] has studied the coax line terminated in an open circuit with the outer sheath extending a small distance beyond the end of the inner conductor and found that the TM_{01} mode will not propagate more than a Somlo length beyond the end of the inner conductor. This mode cut-off condition is valid for frequencies give by:

$$\frac{f}{(\epsilon)^{\frac{1}{2}}} < \frac{7.8}{b}, \tag{1.8}$$

where f is the frequency in GHz, and b is the radius of the outer conductor in centimeters. If the frequency meets this criterion then modes will not propagate past the open circuit. Experiments were performed to test the validity of Equation (1.8) by measuring transmitted power past the end of an open circuited coax as a function of frequency and it was found that Equation (1.8) holds quite well. In these experiments frequencies from 1 to 500 MHz were studied and the transmitted power was always less than 30 dB down from input power. The electric field distribution in a coax can be approximated by

$$E = \frac{V}{\ln\left(\frac{b}{a}\right) r}. \tag{1.9}$$

Therefore, the power densities will vary as $\frac{1}{r^2}$ in the coax, so a reasonable heating distribution can be obtained.

The advantage of this applicator over a monopole is that power is confined to a given region on all sides and the power distribution is more uniform. Also, this type of applicator can easily be inserted into a resource using only surface drilling.

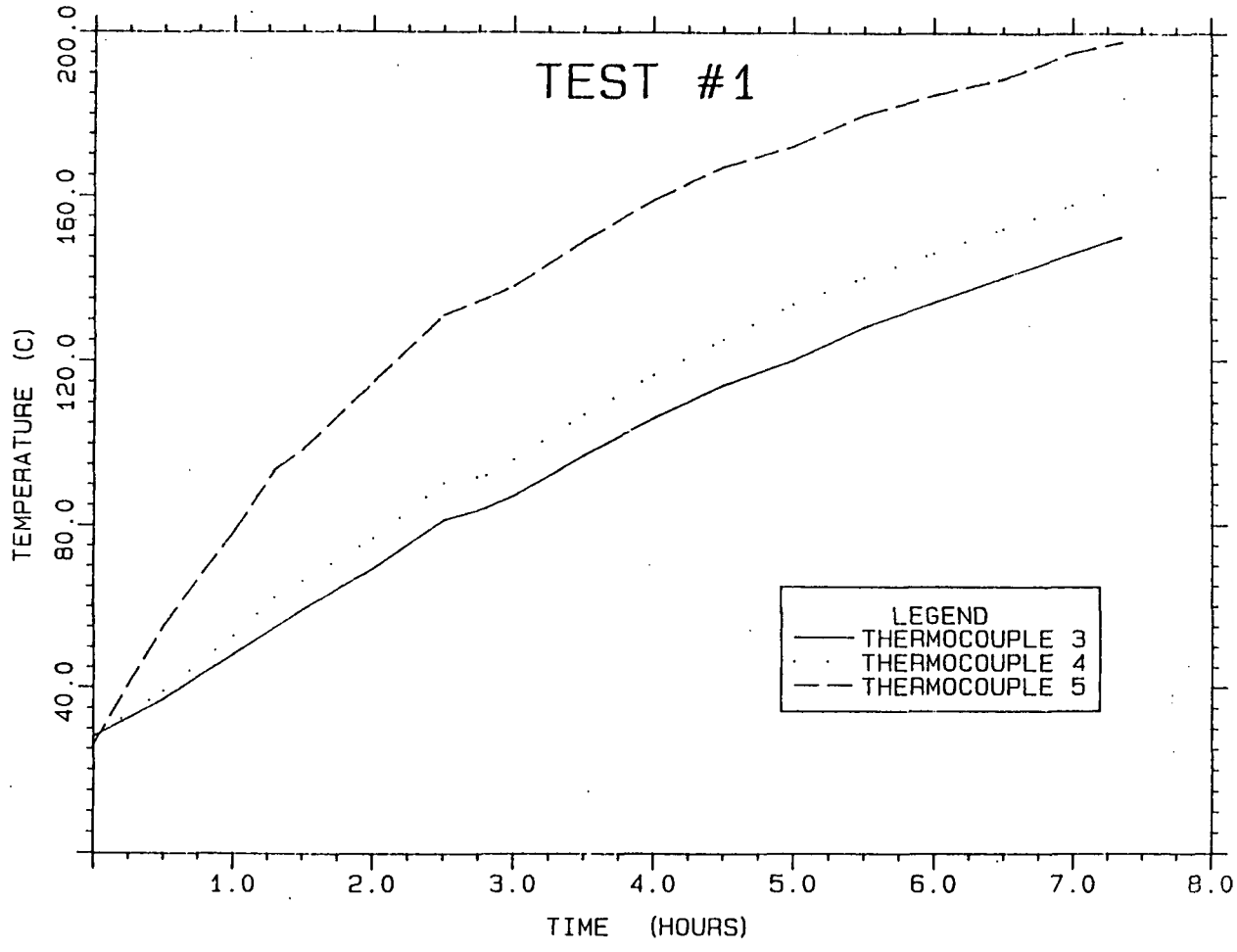

Figure 1.11. Temperature as a function of time for a monopole in shale with 1000 watts at thermocouple positions 3, 4, 5.

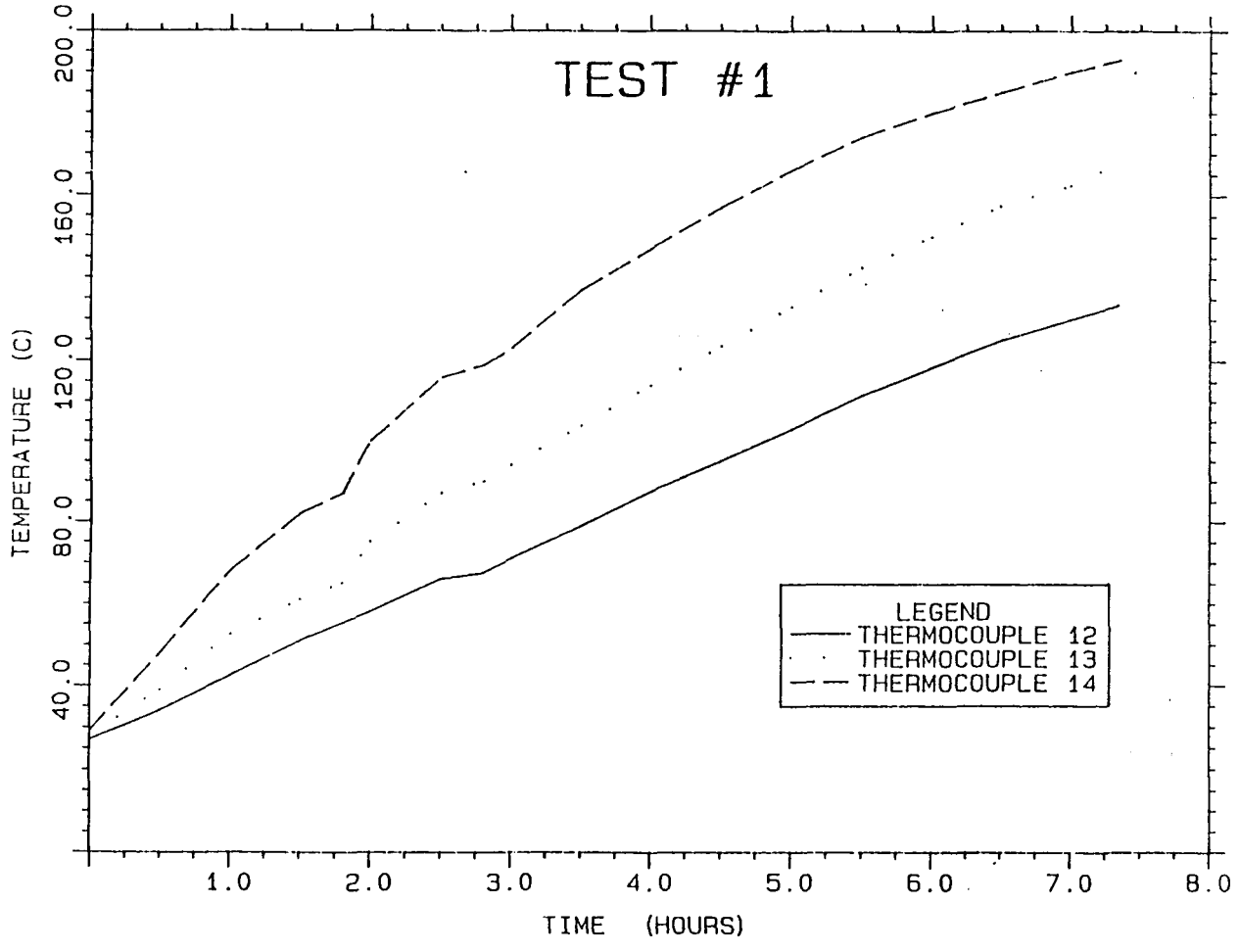

Figure 1.12. Temperature as a function of time for a monopole in shale with 1000 watts applied at thermocouples 12, 13, 14.

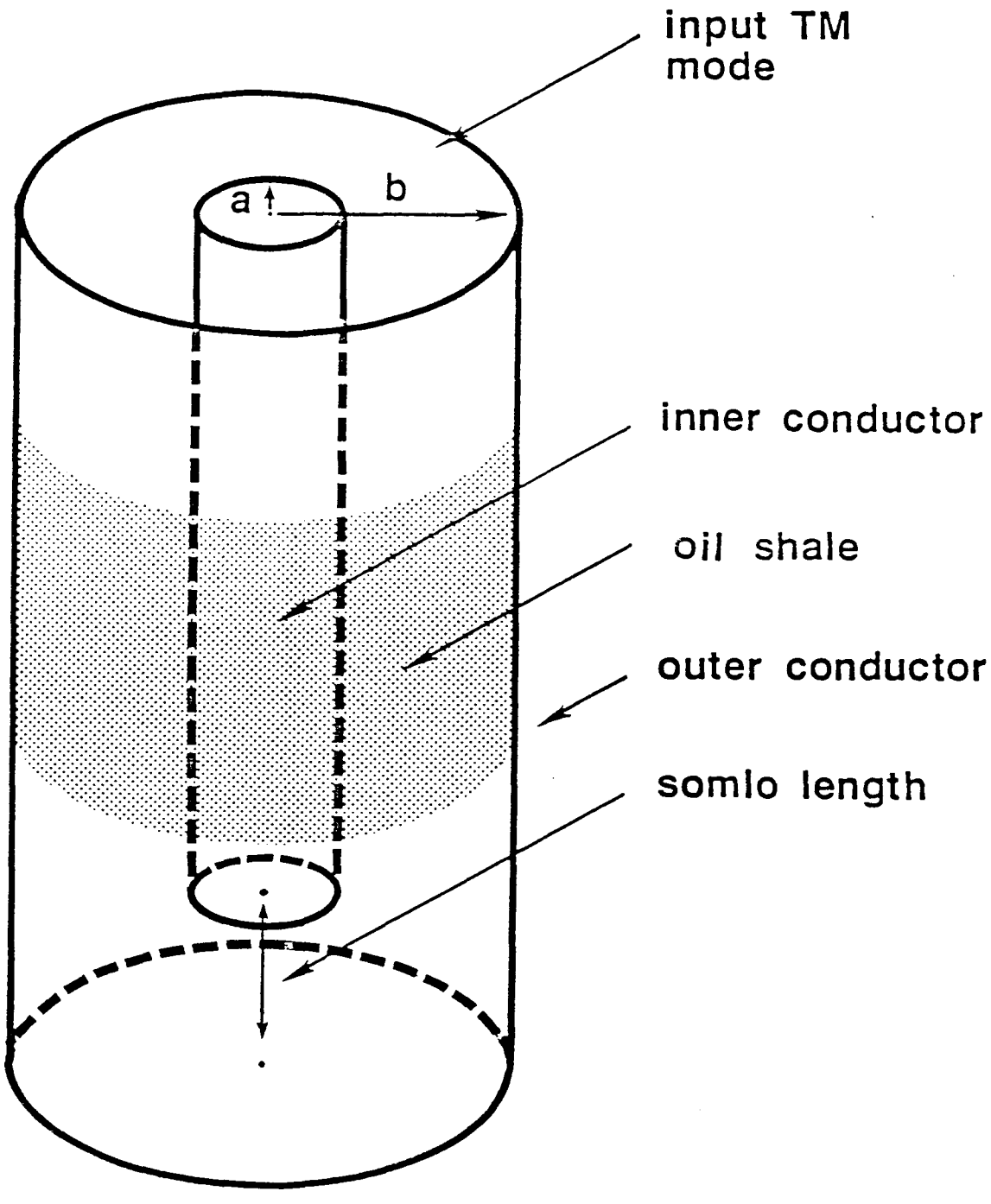

Figure 1.13. Modified coax applicator with short circuite TM_{01} mode.

Experimental work:

In order to test this applicator a series of tests were performed. A section of coax was filled with oil shale. The coax was wrapped with layers of insulation and thermocouples were attached to the outside skin of the coax. The coax was then energized at various power levels (500 or 1000 watts) at 2.45 GHz and the temperatures of the shale were measured as a function of time. In Fig. 1.14 the temperatures are plotted as a function of time for a typical test. We see a very rapid increase in temperature as a function of time. Power was terminated once pyrolysis began. Impedance anomalies were observed for power levels above 1000 watts at pyrolysis temperature.

In large scale experiments the outer conductor would be replaced by a series of tubular electrodes spaced at approximated $\frac{\lambda}{30}$, and the inner conductor would be a tubular electrode. A schematic of the design is shown in Fig. 1.15. At the top, the TM_{01} mode would be excited and at the bottom the energy would be trapped according to the cut-off condition. This simple energy confining system would be easy to insert and yield a relatively uniform heating profile. Using Equation (1.8) we find that frequencies in the range 0.1–200 MHz would be useful for field applications. Taking the breakdown measurement of Bridges [2] as 30 w/kg., we see from Equation (1.5) that for a frequency f (in MHz), a power of $4867 \times f$ w/m^3 can be applied at breakdown. Therefore the allowed application powers for frequencies in the range 0.1–200 MHz are 486–97200 w/m^3. These power levels have been found to be adequate in model calculations to heat monolithic slabs of shale in time periods of less than one month [9].

1.6 DISCUSSION

The experimental results indicate that a single monopole produces a relatively uneven heating rate in the medium. Much of the heat is dissipated in the near field and near the ground plane (see Fig. 1.4). Dielectric breakdown is a real problem with the process, but the effects of dielectric breakdown can be minimized by insulating the antenna in quartz or ceramic. Bridges [2] found that dielectric breakdown occurred at power levels of 10–60 watts/kg at 13.56 MHz; this should scale to much higher levels at 2.45 GHz as indicated in Equation (1.5). This was verified experimentally in that at 2.45 GHz the power densities at breakdown near the monopole were >5000 watts/m^3. The temperature profiles in Figs. 1.11 and 1.12 indicate the uneven power distribution due to monopole applicators. The temperatures are hotter near top and decrease toward the bottom. This effect is due to the damping of the excitation fields vertically along the antenna. Also the fields attenuate radially away from the antenna. Very hot temperatures are encountered near the antenna due to the dissipation of heat in the antenna's near field region. The near field problem can be controlled to some extent by using the quartz tube around the antenna. Product (oil) recovery using the monopole was near 25% of Fischer Assay. This recovery is mainly due to the uneven heating of the block, thus producing warm and cold spots. The coaxial applicator shows promise as an easily insertable system in the field. This applicator confines the fields to a given region, thus optimizing use of electrical energy and reasonable levels of power can be pumped to the load before dielectric breakdown occurs.

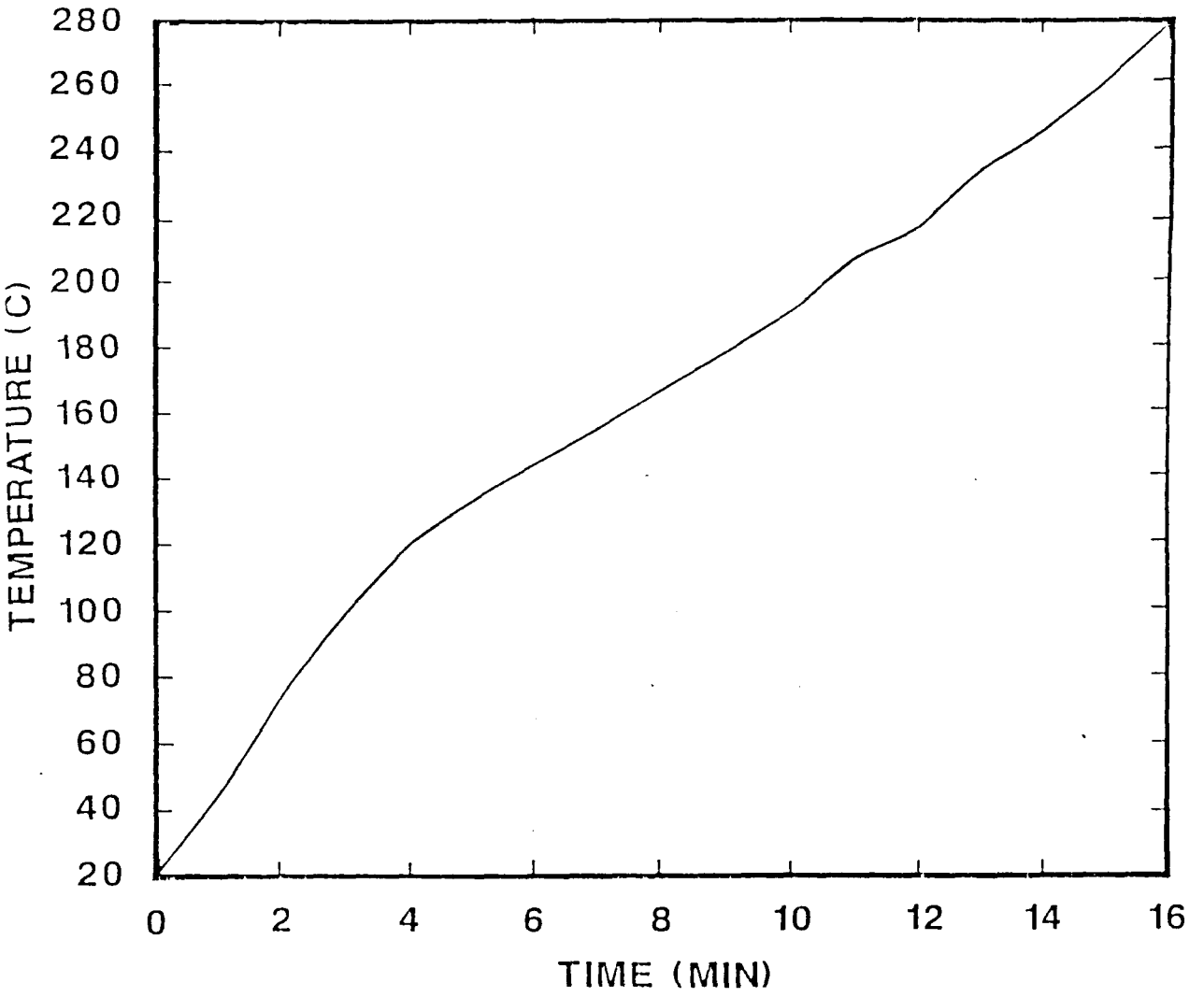

Figure 1.14. Temperature as a function of time for modified coax applicator.

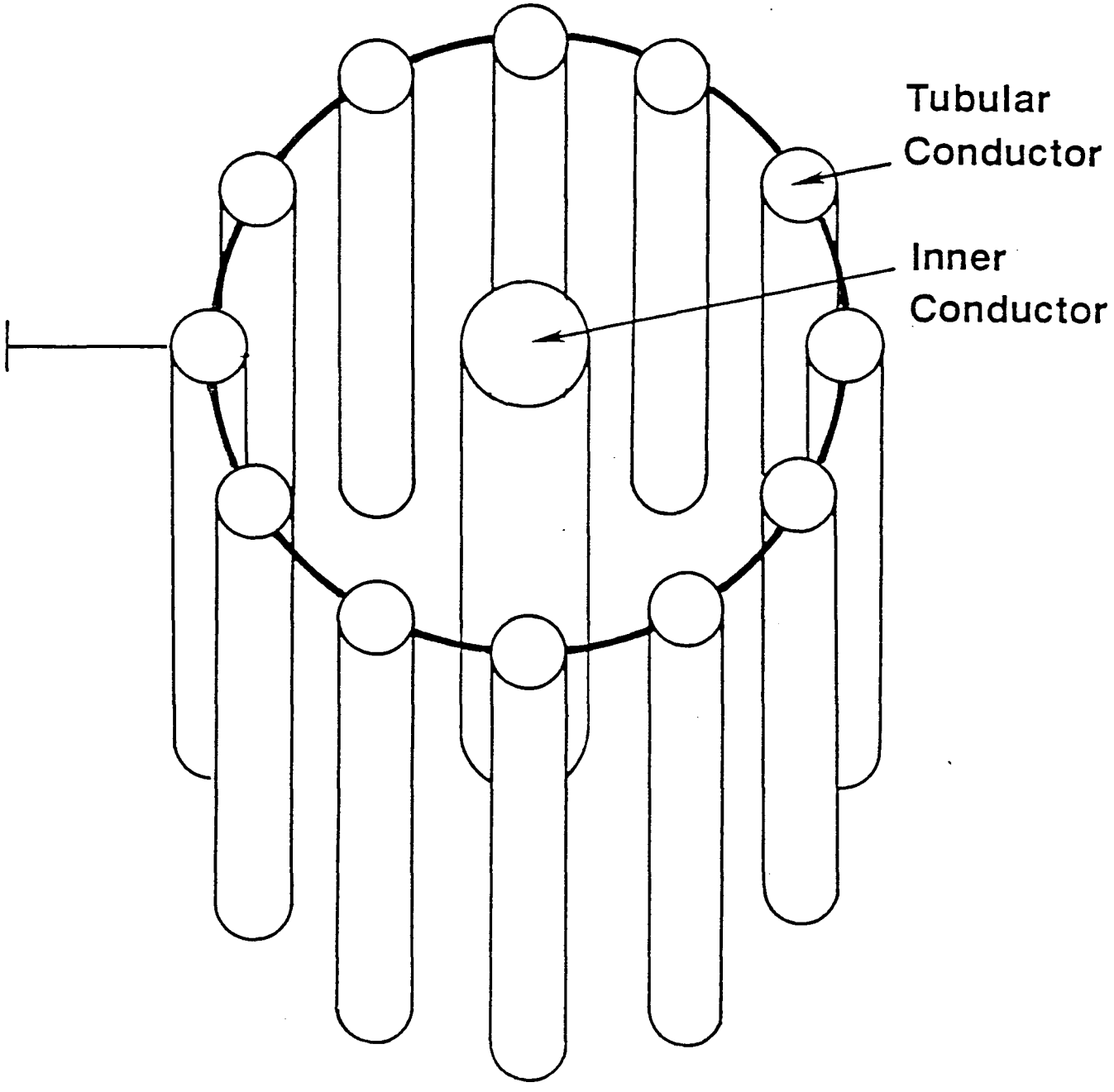

Figure 1.15. Configuration of modified coax for field applications.

CHAPTER 2

MATHEMATICAL MODEL FOR IN SITU OIL SHALE RETORING BY ELECTROMAGNETIC RADIATION

CHAPTER SUMMARY

A mathematical model for electromagnetic heating of oil shales is developed. The model simulates the process of oil and gas evolution and transfer through consolidated blocks of oil shale. The model includes equations for temperature, pressure, saturations, chemical reactions, mass conservation, and source terms. The inert gases are all assumed to form one bulk species and the oil is assumed to be either in gaseous or liquid phases. The chemical reactions include pyrolysis of kerogen and char, release of bound water, coking, and decomposition of carbonates. Porosity and permeability are dynamic functions of the shale constituents. Nonlinear relationships for viscosity, thermal properties, and source terms are used as inputs to the model. A detailed solution to the monopole applicator fields is presented. A finite difference approximation to the differential equations is derived and solved using Newton's iteration technique. For the cases studied the solutions are quite stable.

Numerical results are included and a preliminary study of the optimization of the heating process is presented. Reasonable agreement is obtained between the model and experimental results when a monopole antenna is used as a heat source.

2.1 INTRODUCTION

An abundance of models for *in situ* oil shale retorting have been developed in recent years (see for example Braun [14], Travis *et al.* [15], and Coats [16]). These models of combustion retorts all require some sort of rubblizing to take place to increase permeability of the shale in order to maintain a combustion front. The results of Bridges *et al.* [1,2] and Sresty [17] have shown that it should be possible to perform true *in situ* recovery using the energy from radio frequency waves to heat the shale. They have demonstrated that permeabilities increase upon heating to values of up to one darcy, which is a significant permeability. They have also shown that the oil is recoverable from the shale by the autogeneous gas drive developed by the steam and gases evolved in pyrolysis. That is, as the shale heats the permeability increases which permits the evolved gases of the pyrolysis to drive the oil to recovery wells. A numerical model for electromagnetic heating of oil shale would be useful in that analytical solutions to the complicated non-linear system are not possible. The development of a code yields insight into the basic physical processes of mass transfer in oil shale blocks or particles. A realistic model for *in situ* recovery via electromagnetic heating requires a mathematical formulation of the problem, a reliable numerical procedure, and empirical relations for such quantities as thermal conductivity, specific heats, permeabilities, dielectric constant and viscosities. In this paper the mathematical foundations describing the underlying physical processes for *in situ* retorting by electromagnetic heating are presented. In the special case of monopole applicators the complete field distribution is calculated in Appendix B. In Section 2.2 the electromagnetic heating process is reviewed. Sections 2.3 and 2.4 develop a mathematical model to describe the heating process and Section 2.5 develops a numerical model to solve the system of partial differential equations and an example is presented in Section 2.6.

2.2 RADIATION HEATING PROCESS

The radiation heating process converts electrical power supplied by an a.c. oscillator into thermal energy to heat oil shale. Energy is dissipated from the electrical field as work is performed in rotating the polar molecules in the shale. The dissipated energy produces the heat necessary for pyrolysis. There are many advantages in using dielectric heating as a means for recovering oil from shale. Dielectric heating techniques make it possible to heat large volumes of shale *in situ*, in a uniform manner and under controlled conditions. The dielectric heating process is not limited by the poor thermal diffusion of oil shales, rather the shale heats from within.

Various strategies have been developed in the past for electromagnetic heating of shales and oil sands. Among the most notable are filament heating [18], ohmic heating [10,20], microwave heating [21], and radio frequency (R.F.) heating [1,2]. Also Fisher [20] proposed the concept of induction heating of carbonaceous deposits.

The use of oscillating electric fields in the microwave or radio frequency band to heat shale internally has been studied by Abernathy [21], duBow and Rajeshwar [3], Bridges [1,2], and Wall *et al.* [4]. The advantage of the volumetric heating process over ohmic heating processes is that it does not rely on the electrical conduction of the shale to transport energy and is not limited by the arcing problem of ohmic heating. Raytheon [10] has also carried out a series of studies on radiating systems in oil shales.

In the volumetric heating process, the ability of electromagnetic fields to heat shale depends both on the magnitude and frequency of the applied fields. The attenuation of the electric fields in the shale depends on the frequency of the fields and dielectric constant of the shale. It has been found experimentally that the magnitude of the fields that can be used to heat the shale are limited by electrical breakdown characteristics of the shale. (Electrical breakdown occurs when field strengths reach a point where arcing across a narrow path in the shale effectively shorts out the system). At microwave frequencies the attenuation lengths are quite short (0.1–2.0 meters) and could be useful for heating small beds of shale. Short attenuation lengths cause uneven heating rates in the shale bed, which in turn cause some regions to be over or under heated. Radio frequency waves, on the other hand, have large attenuation lengths (on the order of 2–200 meters) and if they can be confined to a given region they have great potential for realistic *in situ* oil recovery.

In the dielectric heating process there are basically two approaches to heating a given resource. Either a waveguide type of system or a radiating antenna system can be used to heat. Bridges' [1,2] approach was an example of the waveguide approach. Bridges *et al.* used a modified triplate transmission line. Raytheon's work [10] on the other hand was an example of the radiated field approach where antennas are inserted into the resource. Our work presently is in the area of radiating systems, in particular we have studied in depth the monopole and dipole antenna in a lossy medium.

Monopole applicators (which by symmetry are the bottom half of a dipole) consist of a tubular antenna and a ground plane. Dipole applicators of electromagnetic energy are easy to insert into the shale bed (whereas monopoles are easier to test in the lab) and when a number of these applicators are in phase it is possible to confine the fields and obtain a relatively uniform heating profile in the shale bed. In Appendix B the monopole applicator is studied in detail. The analysis of the dipole is a straight forward extension of this.

2.3 MODEL DESCRIPTION

The present model is a transient, two dimensional description of oil shale as it is heated by electromagnetic sources. The model geometry is cylindrical with the radial and axial coordinates describing the position in space. It is possible to use a non- uniform grid in the numerical model for spatial discretization. The model can be used to simulate laboratory studies or simulate actual field tests. The role of the model is to calculate as a function of time and spatial position, the temperatures, pressures, saturations, densities of substances, as well as net energy recoveries. The solid species are described by six independent variables. These are: organics, inert inorganics, dolomite, calcite, char, and coke. The liquid phase is described by variables oil. The inert gases are combined into a single system which consists of a mixture of steam, H_2, CO, CO_2, CH_4, and CH_x. The oil is separated into light and heavy ends; each can be either gas or liquid. Various sets of boundary conditions for the temperature and flow can be used in the model. For example, when simulating laboratory experiments it is possible to use adiabatic boundary conditions.

The mathematical formulation consists of equations for conservation of species, saturations, capillary pressure, momentum, energy, and electromagnetic source term. These equations constitute a system of coupled non-linear partial differential equations which must be solved numerically. The empirical relations used for a description of the chemical reactions

are primarily those of Campbell *et al.* [22], Burnham [23], Braun [14] and Sresty [17]. The permeability relations are derived from the data of Sresty [17] and the formulas of Kozeny (see reference [24]). Thermal conductivity and heat capacities are extracted from the data of duBow and Rajeshwar [3] and Braun [16]. Viscosity data is taken from the work of Jenkins *et al.* [25] and Christenson [26].

The model describes the time evolution of the organic and inorganic materials as the shale is heated. The porosity and permeability are dynamic functions of the shale constituents. The model classifies all organics under the bulk name of kerogen (there is no attempt to distinguish between bitumen and kerogen).

The inorganic materials consist of a bulk mineral component (primarily quartz), calcite and dolomite, and bound water. As the shale is heated the kerogen reacts chemically, yielding gases, char, and oil. The carbonates decompose to form gases. It is assumed that the water is released in form of steam. The r.f. heating technique requires relatively low operating temperatures for pyrolysis (340–400°C) for efficiency. Because of these low temperatures and slow heating rates for *in situ* heating, coking is the dominant degradation mode for the oil. Cracking reactions are not treated in the present model. Because oxygen will be limited, combustion reactions are neglected in the low temperature modeling. Additionally, reactions of evolved carbon with evolved gases at these temperatures is assumed minimal (see Travis *et al.* [15]).

2.4 MATHEMATICAL MODEL DESCRIBING KINETICS, HEAT-MASS TRANSFER, AND ELECTROMAGNETIC HEATING

Following Braun [14], we assume for the kerogen decomposition the following scheme:

$$\begin{aligned}[1\text{kg kerogen}] \rightarrow\ & [f_1\text{kg char}] + [f_2\text{kg oil}] + [f_3\text{kg CO}] + [f_4\text{kg } CO_2] \\ & + [f_5\text{kg } H_2] + [f_6\text{kg } CH_4] + [f_7\text{kg } CH_x] + [f_g\text{kg } H_2O]\end{aligned}$$

where CH_x are other gases and f_i are stoichiometric coefficients ($\sum_{i=1} f_i = 1$).

$$\begin{aligned} f_1 &= .1709\ [\text{kg char/kg kerogen}] \\ f_2 &= .6585\ [\text{kg oil/kg kerogen}] \\ f_3 &= .0106\ [\text{kg CO/kg kerogen}] \\ f_4 &= .0390\ [\text{kg } CO_2\text{/kg kerogen}] \\ f_5 &= .0042\ [\text{kg } H_2\text{/kg kerogen}] \\ f_6 &= .0189\ [\text{kg } CH_4\text{/kg kerogen}] \\ f_7 &= .0601\ [\text{kg } CH_x\text{/kg kerogen}] \\ f_8 &= .0378\ [\text{kg } H_2O\text{/kg kerogen}] \end{aligned}$$

Additionally, char is formed by coking. The equations which describe the mass balance of the organics can be written as

$$\frac{dU_k}{dt} = -K_k U_k, \qquad U_k(t=0) = U_k^0 \tag{2.1}$$

$$\frac{dU_{cl}}{dt} = f_1 U_k + g_1 U_c, \qquad U_{c1}(t=0) = 0 \tag{2.2}$$

Here K denotes kerogen, cl denotes char and $U_{(i)}$ denotes densities of substances in kg/m^3 of shale, $K_{(i)}$ denote rate constants for the various reactions. The rate constants are given by:

$$K_k = 2.81 \times 10^{13} \ \exp(-26390/T) \ \ (1/\text{sec}) \tag{2.3}$$

The coking reactions are taken from the work of Burnham and Braun [23], as was the release of bound water

$$\frac{dU_w}{dt} = -k_w U_w \left[1 - \frac{P_{H_2O}}{P_{eq}}\right]\left[\frac{P_0}{P_t}\right] \tag{2.4}$$

where $P_{eq} = 4.2\times10^{10} \ \exp(-5033/T)$, $k_w = 3\times10^{48} \ \exp(-62000/T)$ and P_t is total pressure. All pressures are in Pa. The reactions of dolomite can be expressed as

$$\mathrm{MgC(CO_3)_2} \rightarrow \mathrm{MgO\bar{}} + \mathrm{CaCO_3} + \mathrm{CO_2}$$

The heat of reaction of the carbonates is:

$$H_{\text{carbonates}} = 2.9 \times 10^6 J/\text{kg } \mathrm{CO_2}.$$

The inorganic carbonates are assumed to decompose according to:

$$\frac{dU_{mg}}{dt} = -KU_{mg}, \quad U_{mg}(t=0) = U^0_{mg} \tag{2.5}$$

where mg denotes dolomite.

$$K_{mg} = 2.5 \times 10^{10} \ \exp(-29090/T)(1/\text{sec}). \tag{2.6}$$

Equation (2.5) can be integrated to yield:

$$U_{mg} = U^0_{mg} \ \exp\left(-\int_0^t X_{mg}(r,\tau)d\tau\right). \tag{2.7}$$

The rest of the inorganic materials are assumed to be unaffected by heating.

The porosity of the shale depends on the temperature history at a given point in the bed. Initially, the porosity is assumed to be on the order of one percent. As the shale is heated the decomposition of the organics and swelling increases the porosity. The porosity is assumed to be given as a linear function of the shale components:

$$\begin{aligned}\phi = \ & \frac{U^0_k}{\rho_K} + \frac{U^0_{cl}}{\rho_{cl}} + \frac{U^0_w}{\rho_w} + \frac{U^0_{ca}}{\rho_{ca}} + \frac{U^0_{mg}}{\rho_{mg}} + \frac{U^0_{\text{inorg}}}{\rho_{\text{inorg}}} \\ & - \left(\frac{U_k}{\rho_K} + \frac{U_{cl}}{\rho_{cl}} + \frac{U_w}{\rho_w} + \frac{U_{ca}}{\rho_{ca}} + \frac{U_{mg}}{\rho_{mg}} + \frac{U_{\text{inorg}}}{\rho_{\text{inorg}}}\right) + \epsilon\end{aligned} \tag{2.8}$$

where $\rho_{(i)}$ denotes densities of substances and ϵ is the initial porosity and can include the effects of swelling.

The absolute permeability of the shale is also a function of the temperature history. In this model the permeability is defined in each region in the shale as a function of the porosity. Initially, the shale permeability is of the order of 10^{-4} darcy. As it is heated the permeability increases to around 0.1–0.5 darcies. Sresty [17] has determined experimentally the global

evolution of the permeability with temperature for varying grades of shale. The usefulness of Sresty's data is limited since the measurements are for bulk permeabilities of the total shale sample, whereas this model needs as an input a local permeability. In order to express the temperature evolution of the permeability as a function of the organic content, various functional relationships were tried and the formula of Kozeny given below produced good results [24].

$$K_a = C\frac{\phi^3}{(1-\phi)^2} + \delta. \tag{2.9}$$

The total permeability can be written as a product of the absolute and relative permeabilities. The permeability of the oil shale is in general a very complicated function of many variables and may vary drastically from shale to shale depending on the shale micro-structure. Equation (2.9) is an attempt to model the permeability in a simplified form.

In addition, density relations are needed for gases and liquids

$$\begin{aligned} &\text{(a)} \quad \rho_g = \frac{MP}{ZRT} \\ &\text{(b)} \quad \rho_0 = (A + BT)\ \exp(C(P - D)) \end{aligned} \tag{2.10}$$

where P is the pressure, M the molecular weight, R is the gas constant, T the temperature, and Z the compressibility factor. The density of the liquid oil in Equation (2.10b) is assumed temperature dependent and A, B, C and D are constants which are fit empirically.

A capillary pressure is also assumed between gas and liquid. The sum of the saturations of oil and gas must equal unity. The fluid species equations characterize the time evolution of the gases and oil. In the present model gases are separated into inert and gaseous oil. The inert gas satisfies the following equation:

$$\frac{\partial}{\partial t}(y_i \phi S_g \rho_g) + \vec{\nabla} \cdot (Y_i \rho_g \vec{v}) = \sum_{i=3}^{8} f_i U_k K_k + \frac{dU_w}{dt} + I_{gi} \tag{2.11}$$

where $S_g, \vec{\nabla}_g, I_{gi}$, and ρ_g are the saturations, velocities, sources, and densities of the gas phase.

The liquid oil is separated into light and heavy oil. The light oil can be present in either liquid or gas phases and the heavy oil is assumed to remain in liquid form. The species equation for the light oil can be written as

$$\frac{\partial}{\partial t}(\phi X_{lo} S_o \rho_o + \phi Y_{l0} s_g \rho_g) + \nabla \cdot (X_{lo} \rho_o \vec{v}_o + Y_{lo} \rho_g \vec{v}_g) = (1-\delta) f_2 K_k U_k + I_{lo}$$

where S_g, S_0 are the saturations, $\vec{v}_i$ are the velocities, Y_i are the mole fractions of the gases, X_i are the liquid mole fractions of the light and heavy oil, δ is the fraction of oil that is heavy, and ρ_0, ρ_g are the densities of the oil and gas phases. The heavy oil satisfies

$$\frac{\partial}{\partial t}(\phi X_{ho} S_o \rho_o + \phi Y_{ho} S_g \rho_g) + \nabla \cdot (X_{ho} \rho_o \vec{v}_o + Y ho \rho_g \vec{v}_g) = \delta f_2 K_k U_k + I_{ho}. \tag{2.12}$$

The total mass of the system is conserved in that the sum of all the rate and species equations yields an equation of bulk continuity.

We also need relations between the various species of gases and oils

$$Y_i + Y_{lo} + Y_{ho} = 1 \tag{2.13}$$

$$X_{lo} + X_{ho} = 1. \tag{2.14}$$

Here the sum over X and Y are the constraints that the sum of all the mole fractions of the oils gases are unity; *lo* and *ho* stand for light oil and heavy oil. The mole fractions of light and heavy oils in vapor and liquid phase are given:

$$Y_{lo} = KX_{lo} \tag{2.15}$$

$$Y_{ho} = KX_{ho} \tag{2.16}$$

where K is the equilibrium constant. For disappearance or appearance of the oil phases the pseudoequilibrium ratios [27] are used. This technique allows a small amount of all phases to always remain and eliminates the need for variable substitution.

The momentum equation for flow in porous media is approximated by Darcy's Law.

$$\vec{v}_i = -\frac{\overline{\overline{K}}_i}{\mu} \cdot [\nabla P + \rho_i \vec{g}] \tag{2.17}$$

where i denotes gas or oil phase, $\overline{\overline{K}}$ is the total permeability tensor, $\vec{g}$ is the gravity vector. Consider now the energy balance for the gas-liquid-solid system. The energy balance includes effects of convection, conduction, and sources. Some simplifying assumptions are necessary for the modeling. Since the electromagnetic heating is relatively constant over the region of interest and since velocities and pore size are small, to a good approximation the temperatures of the gas, liquid, and solid are equal at any point in space. We can write a bulk energy balance equation

$$\begin{aligned} &\frac{\partial}{\partial t}\{(c_{po}\phi S_0 \rho_0 T) + (c_{pg}\phi S_g \rho_g T) + (c_{mg}U_{mg}T) + (c_k U_k T) + (c_{\text{inorg}}U_{\text{inorg}}T) \\ &+(C_w U_w T) + (c_{\text{coke}}U_{\text{coke}}T)\} + \nabla \cdot (\rho_0 c_{po} T \vec{v}_o + \rho_g C_{pg} T \vec{v}_g) \\ = \;& \nabla \cdot (\overline{\overline{\lambda}} \cdot \nabla T) + g_e(r,t) + H_k + H_{mg} + H_{ca} + H_w \end{aligned} \tag{2.18}$$

where T is the temperature above the initial resource temperature, $\overline{\overline{\lambda}}$ is the thermal conductivity tensor, $c_{p(i)}$ are specific heats, $g_e(r,t)$ is the electromagnetic source term. For a monopole applicator the field distribution is worked out in Section 2.7, and $H_{(i)}$ are the heats due to reactions.

A constitutive relation is also needed to express the electromagnetic source in terms of the frequency of the applied fields and properties of the medium:

$$g_e(r,t) = \frac{1}{2}\vec{E} \cdot \vec{J} = \frac{1}{2}\omega\epsilon''|\vec{E}|^2 \frac{\text{watts}}{\text{M}^3}, \tag{2.19}$$

Here, ω is the radial frequency, ϵ'' is the imaginary part of the dielectric constant, and $\vec{E}$ is the electric field. In general the source term is a function of radial distance in the

shale (attenuation length) and also temperature dependent, since as the shale is heated the electrical properties of the shale change (see Fig. 2.1). The electrical dissipative source term $g_e(r,t)$ has units of watts/m^3 of shale. The present source being used is that of a monopole applicator.

The viscosities are temperature dependent. For the liquid oil phase the viscosity is

$$V_0 = A \ \exp(B/T) \tag{2.20}$$

and the gas viscosity is given by:

$$V_g = [A + BT + CT^2]. \tag{2.21}$$

The thermal conductivity is assumed to be a function of the amount of organics in the shale (see duBow and Rajeshwar [3]). Also, since the shale is layered the anisotropic nature of the thermal conductivity must be input [28,29]. Effective values for thermal conductivity are used for heat flow parallel and perpendicular to the bedding planes (assumed to be layered in a periodic fashion):

$$\begin{aligned} \lambda_{\text{parallel}} &= \lambda_1 n_1 + \lambda_2(1 - n_1) \\ \lambda_{\text{perpendicular}} &= \frac{\lambda_1 \lambda_2}{n_1 \lambda_1 + (1 - n_1)\lambda_2} \end{aligned} \tag{2.22}$$

where n_1 denotes the volume fraction of layers of type one. The thermal conductivities of those layers is given by:

$$\lambda_i = \left[\lambda_{\text{raw}(i)} \left(\frac{U_{\text{organic}}}{U^0_{\text{organic}}}\right) + \lambda_{\text{spent}(i)} \left(1 - \frac{U_{\text{organic}}}{U^0_{\text{organic}}}\right)\right] (AT + B) \tag{2.23}$$

The specific heats depend both on shale grade (gal/ton) and temperature

$$c_p = (AT + B)(C + DX) \tag{2.24}$$

where X is the grade of the shale in gal/ton and T is the temperature in °K, the units of c_p is (J/°K).

The total model then consists of a system of coupled equations for the unknowns X_{ho}, X_{lo}, Y_{ho}, Y_{lo}, Y_i, S_g, S_p, P_g, P_o, T, $U_{(k)}$, $U_{(cl)}$, $U_{(mg)}$, $U_{(ca)}$, $U_{w,vg,vo}$, $g_e(r,t)$. The equations can be solved by a finite difference scheme to yield predictions for the time and space evolution of the temperature, pressure, saturation, and oil yields. In order to complete the mathematical model we need appropriate boundary conditions for the fluids and temperatures on the bounding surfaces. In the present model the normal components of the gases and oil are specified as zero on the outer boundaries. At the well bore it is possible to specify the pressure, or flow, or a convective flow condition given by

$$v_{\text{well}(i)} = \frac{hKK_r}{\mu}[P_{\text{atmos}} - P_i] \tag{2.25}$$

where h is an empirical constant and i denotes the velocity of the component (gas or oil). For the temperature flux on the boundaries we may write a convective boundary condition

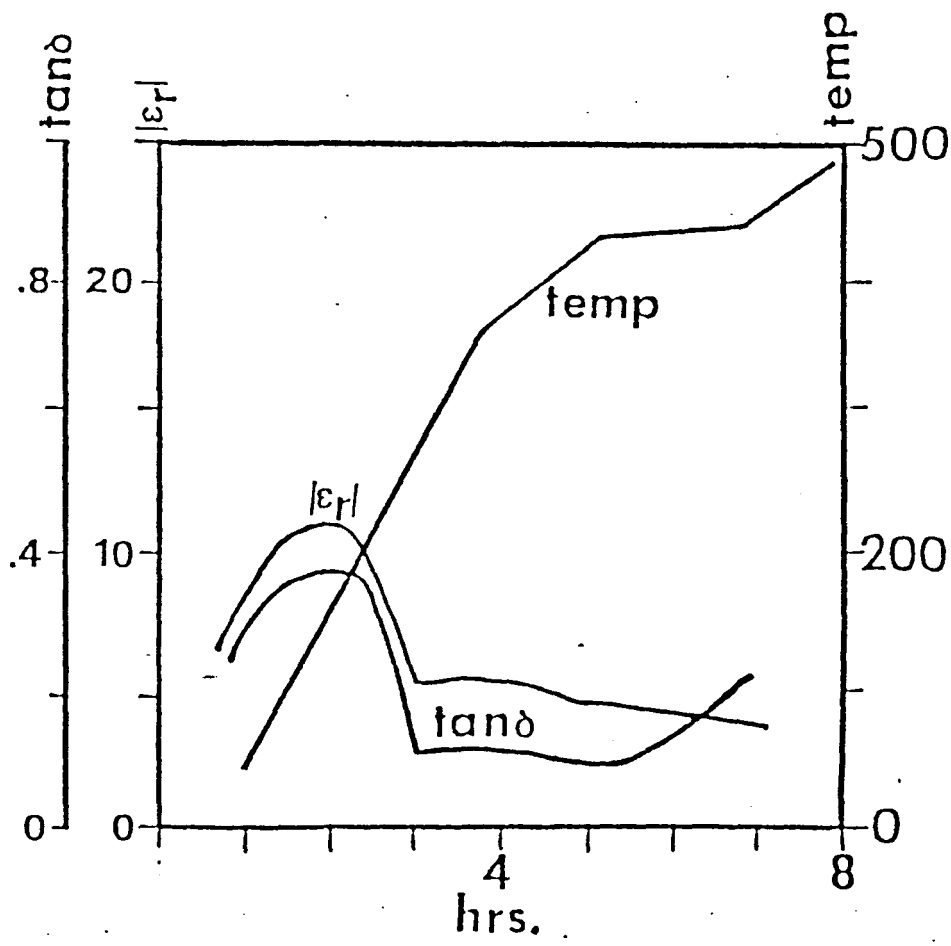

Figure 2.1. Typical example of how the dielectric properties vary as a sample is heated [2].

$$-(\bar{\bar{\lambda}} \cdot \nabla T) \cdot \vec{n} = H[T_c - T] \tag{2.26}$$

H and T_c are constants.

2.5 NUMERICAL SCHEME

We discretized Equations (2.12), (2.13) and (2.19) in the spatial coordinate only, so that the problem then was reduced to solving a set of coupled, first order, ordinary differential equations in time.

After running the model, various interesting quantities were plotted. Oil yields were plotted by a knowledge of saturations, porosites, coke, and kerogen concentrations at each point in the shale. The yields were normalized to the calculated potential oil in the shale.

2.6 LARGE SCALE SIMULATION

As an application of the model, an idealized commercial run has been simulated. The geometry consists of a well bored in the shale (Fig. 2.2). In this idealized simulation it is assumed that the heating source is uniform within the retort region. The simulation is idealized in that there has not been sufficient experimental research to yield accurate estimates of some of the input physical parameters such as the relative permeabilities, and absolute permeabilities. As first approximation the following relations for the permeabilities were used: $P_{rg} = (1-S_0)^2$, $P_{ro} = S_0^2$. Figs. 2.3–2.6 portray the evolution of various quantities with time for an average heating rate of 0.54°C/hr and an initial porosity of 1%. In this case the shale grade varies in the bed in a periodic fashion for a maximum of 33 gal/ton to 5 gal/ton. It can be seen that the effects of layering on the temperature profile is minimal. The layering can be seen quite clearly in the plots for organics, coke, and char. Fig. 2.7 shows the evolution of the oil as the shale is heated. Note that the oil yield is normalized to the calculated potential oil in the shale.

In order to study the effects of grid size on the model, results a series of tests were run. In these tests the region heated was held fixed whereas the number of spatial grid blocks were varied.

The average heating rates were 21°C/hr until 390°C, and thereafter the source was turned off. In Figs. 2.8 and 2.9 gas saturations and temperatures are plotted for 63 grid blocks (dashed lines), 48 grid blocks (+ lines), and 35 grid blocks (solid lines). The saturation and temperature profiles are functions of radial distance in the shale for a fixed z coordinate. The z coordinate used was the center of the heated region. It can be seen that for 63 and 48 grid blocks the saturations are almost identical, whereas at 35 grid blocks the solutions diverge. The origin of the numerical dispersion is spatial truncation error and the effects of upstream weighting in the relative permeability terms. For the temperatures all the solutions are fairly close when considering the scale on which they are plotted. It seems that numerical dispersion has affected the temperature profiles to a lesser degree than the saturations. This is probably due to the fact that the relatively constant heating rate produces temperature profiles which have small thermal gradients.

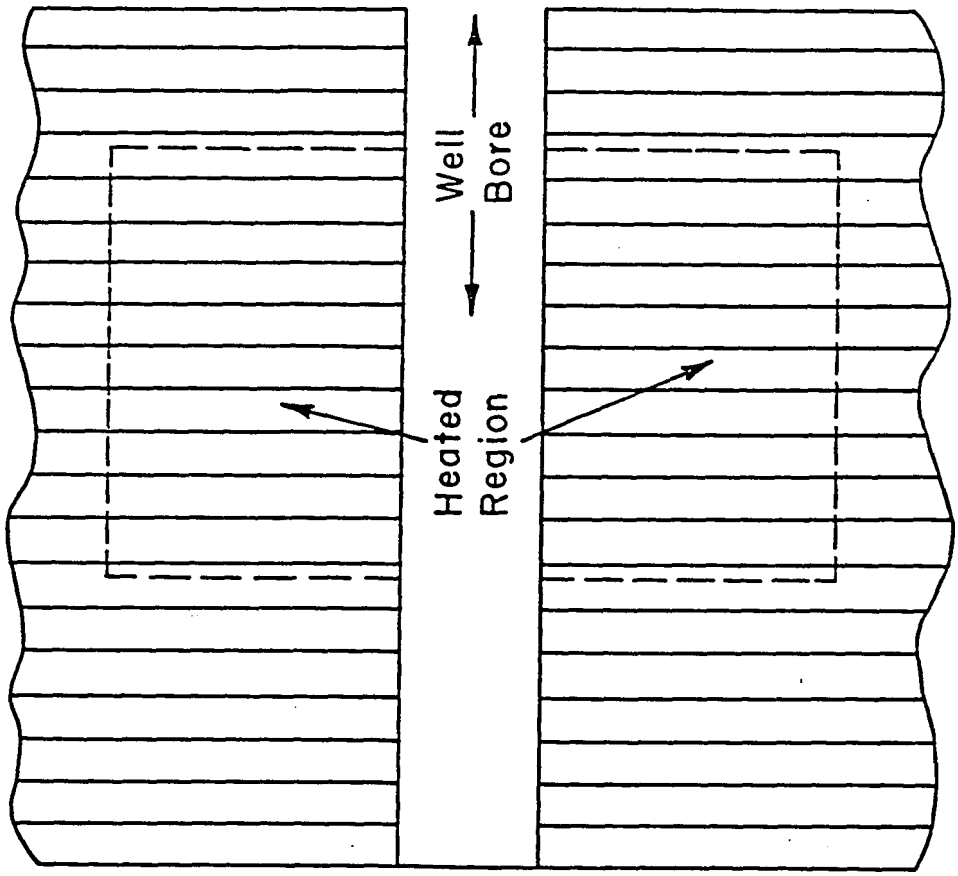

Figure 2.2. A large scale retort. The system consists of a well bored into the shale bed and an antenna inserted in the wellbore. The region enclosed by the dashed lines is the region heated by the antenna. The first set of plots assume the shale to be layered in a periodic fashion, alternating from high (33 gal/ton) to low (5 gal/ton) concentrations of shale. It is assumed that the fields are confined by use of some waveguide-like technique to the enclosed region.

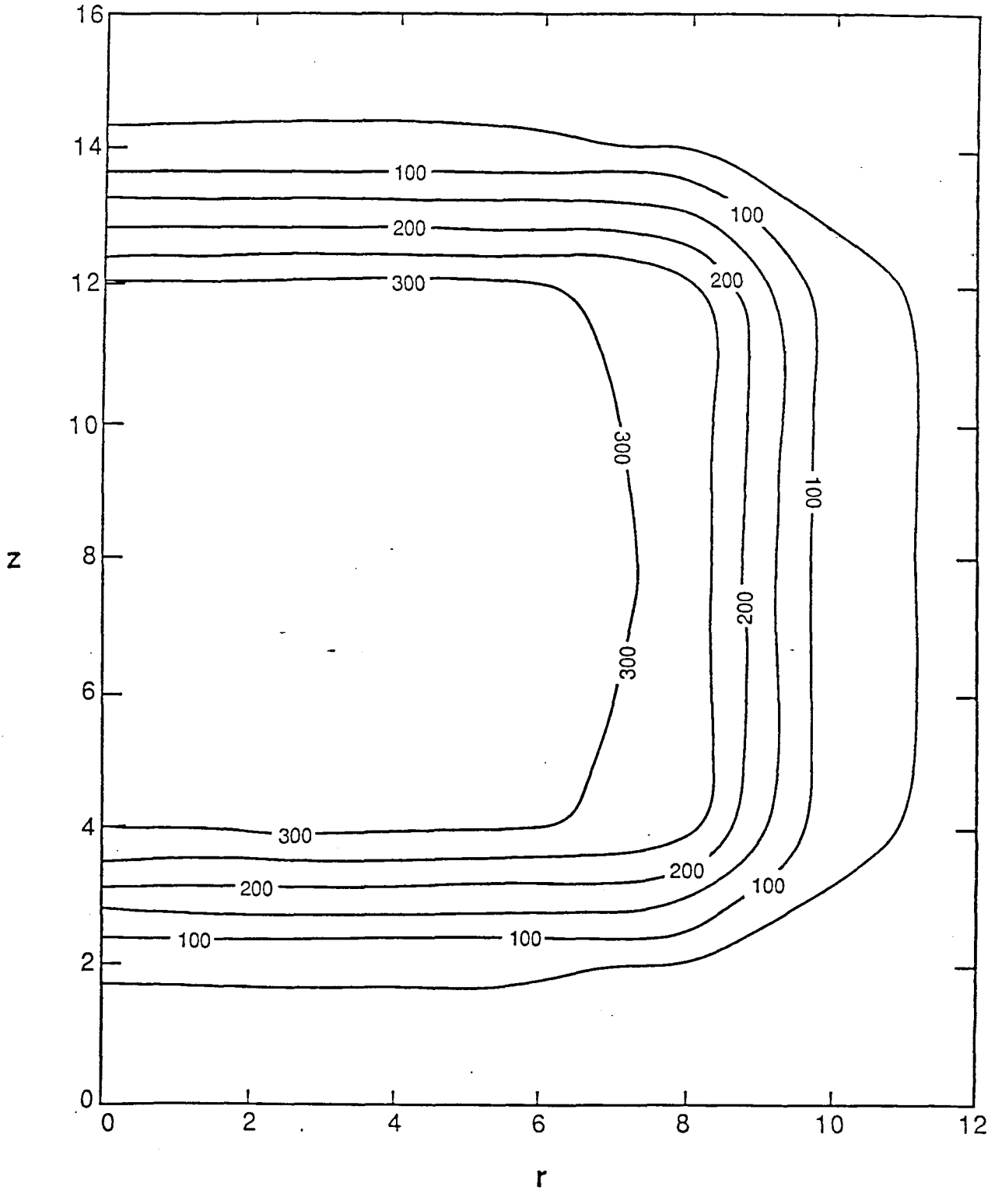

Figure 2.3. Simulation of temperature profiles (°C) for a full scale commercial retort after 10 days heating. The dimensions of the retorted shale is 10 meters in radial direction and 10 meters in vertical direction (cylindrical symmetry). The heating rate of 0.54°C/hr and the frequency of the input is 2×10^6 Hz with attenuation length of 100 meters.

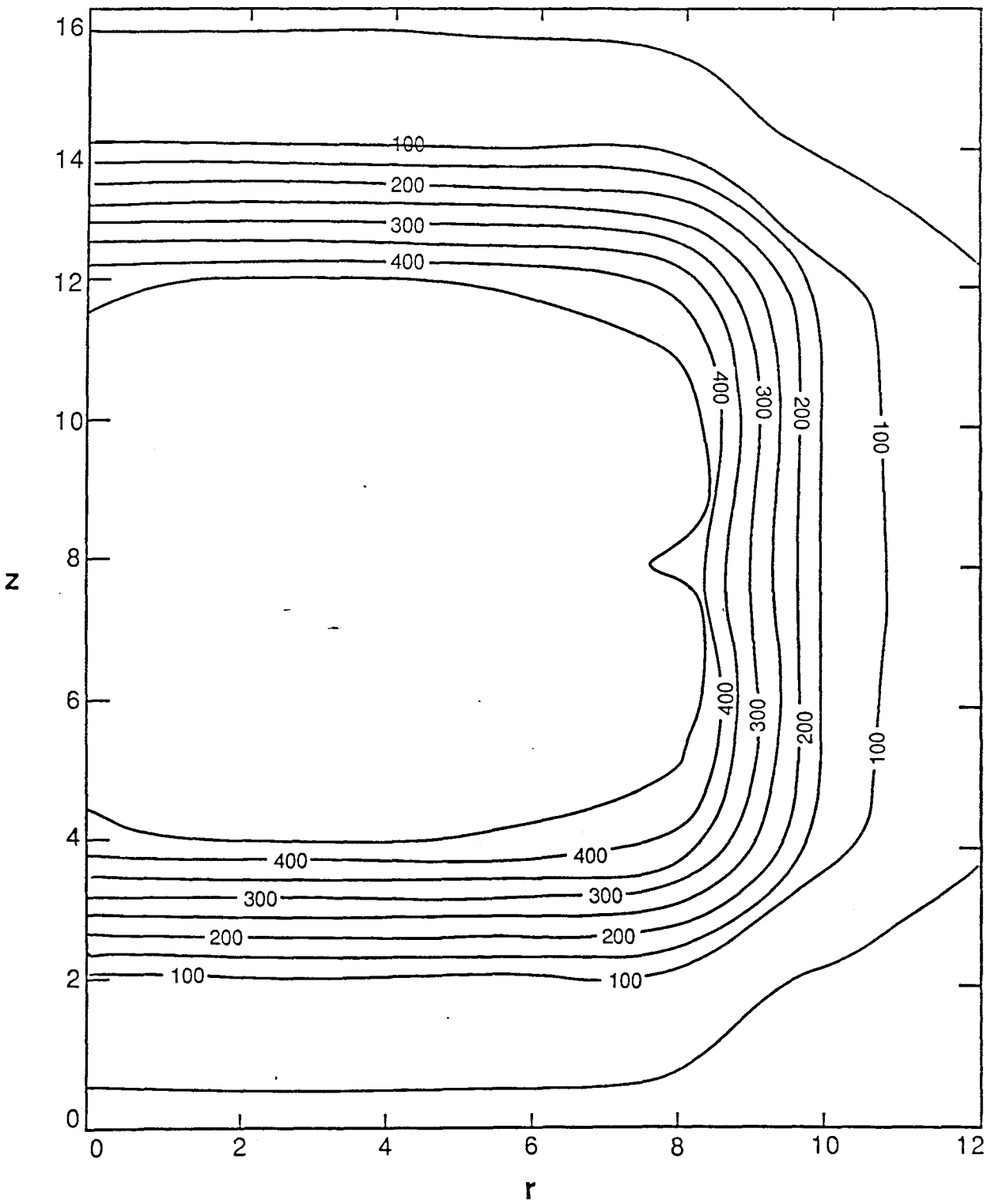

Figure 2.4. Same as Figure 2.3, but after 40 days.

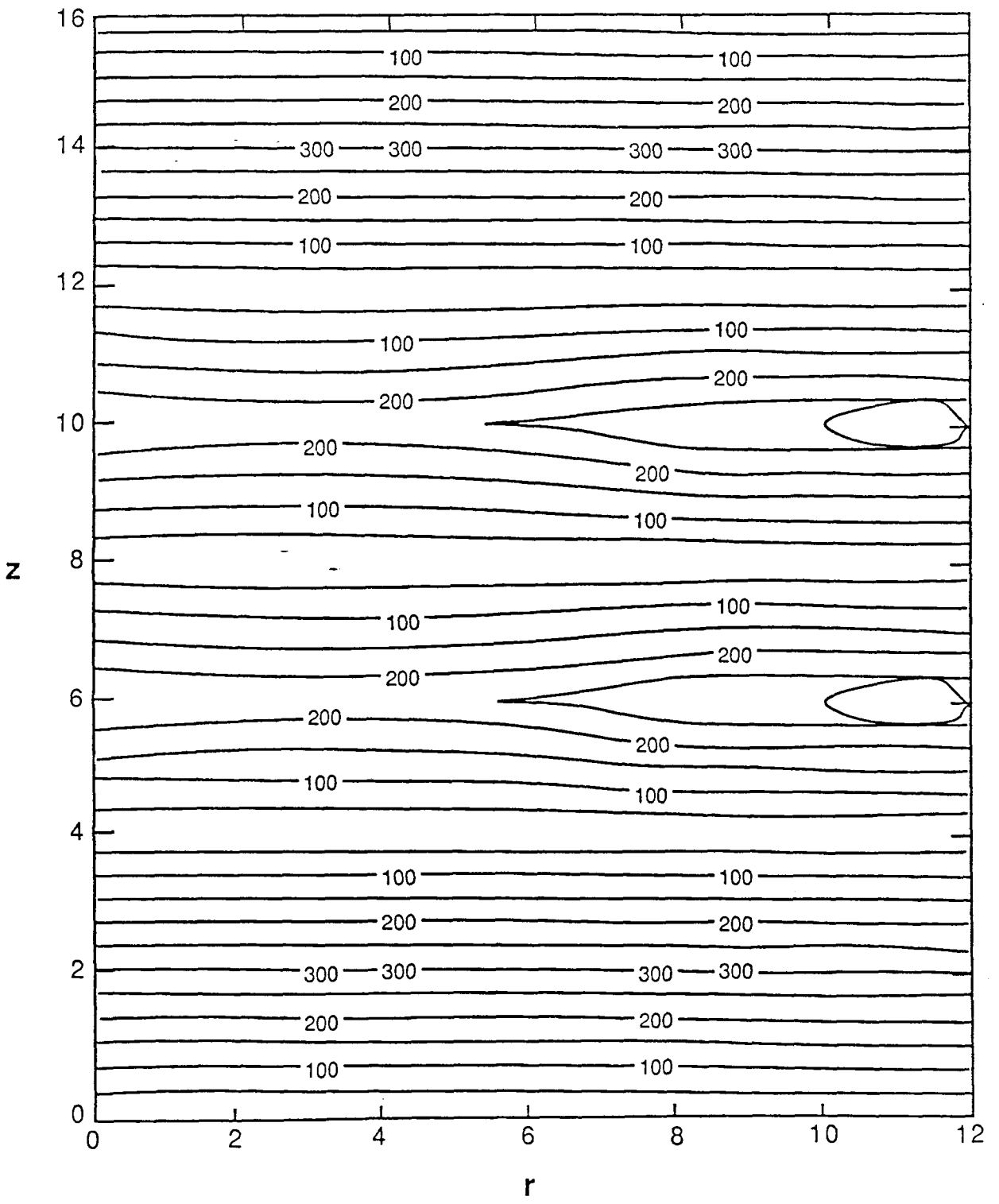

Figure 2.5. Organic content remaining in the shale at 10 days (kg/m^3). The shale was layered periodically with layers of high and low organic content as stated in Figure Caption 2.3.

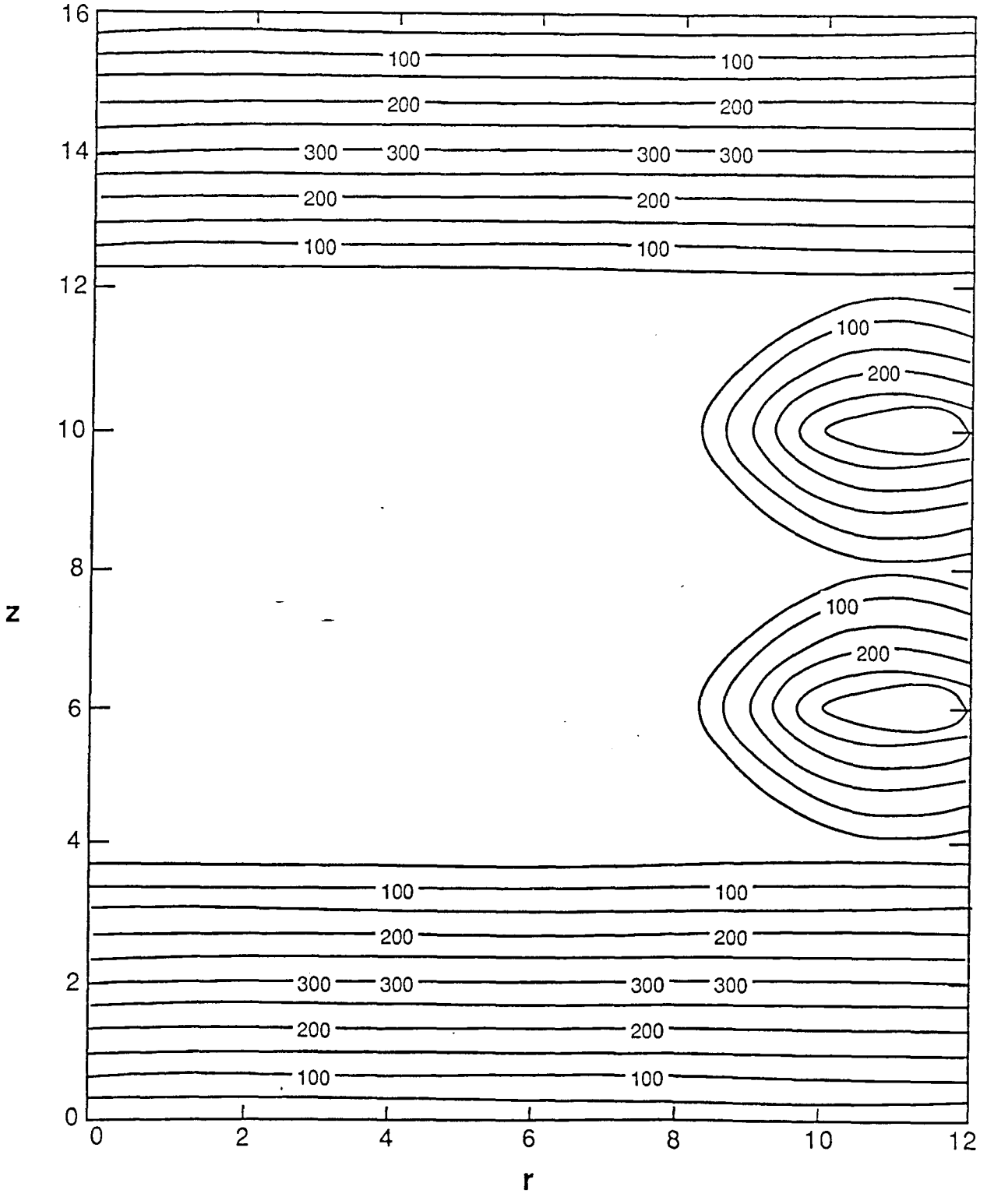

Figure 2.6. Same as Figure 2.5, but for 40 days.

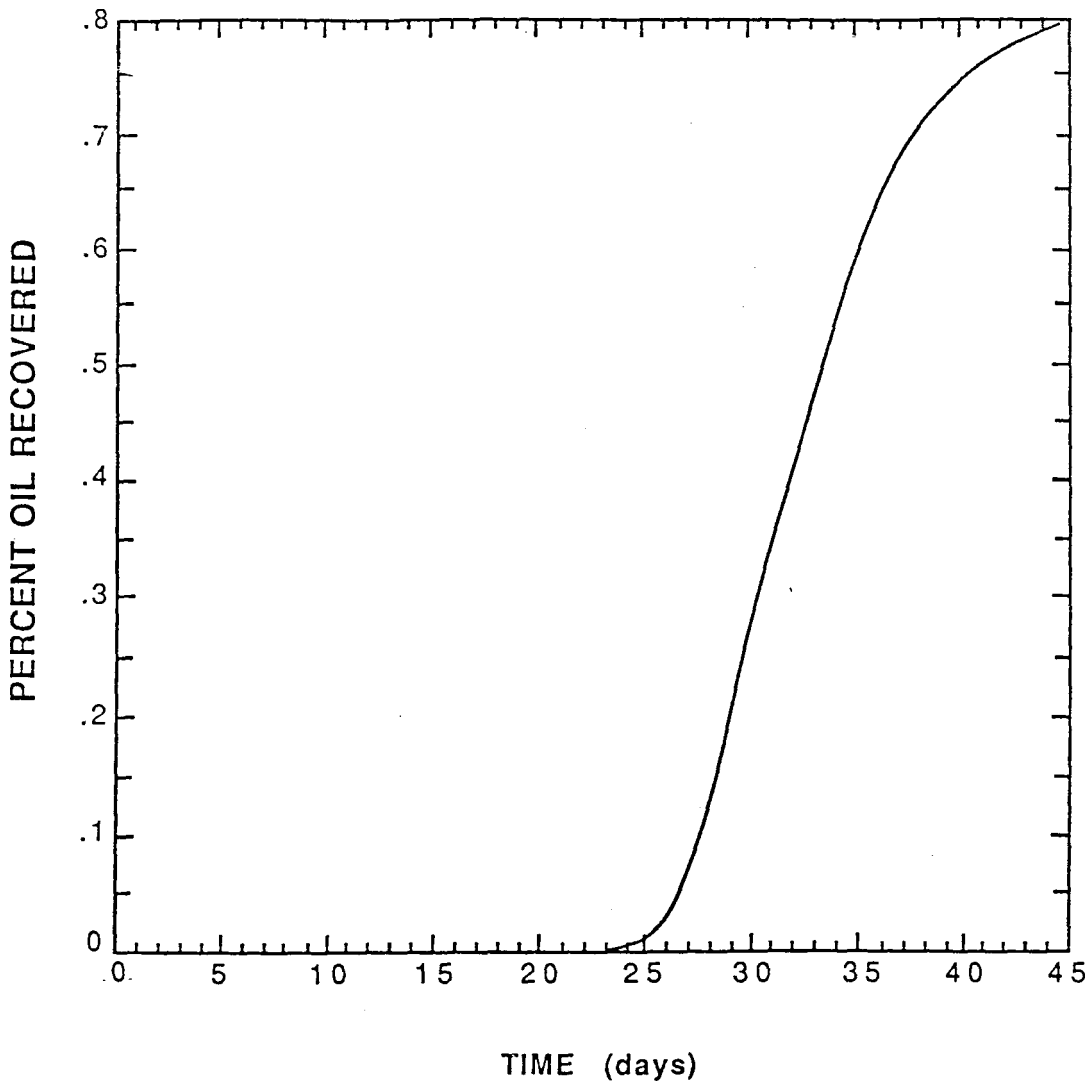

Figure 2.7. Oil yield as a function of time for the above large scale simulation.

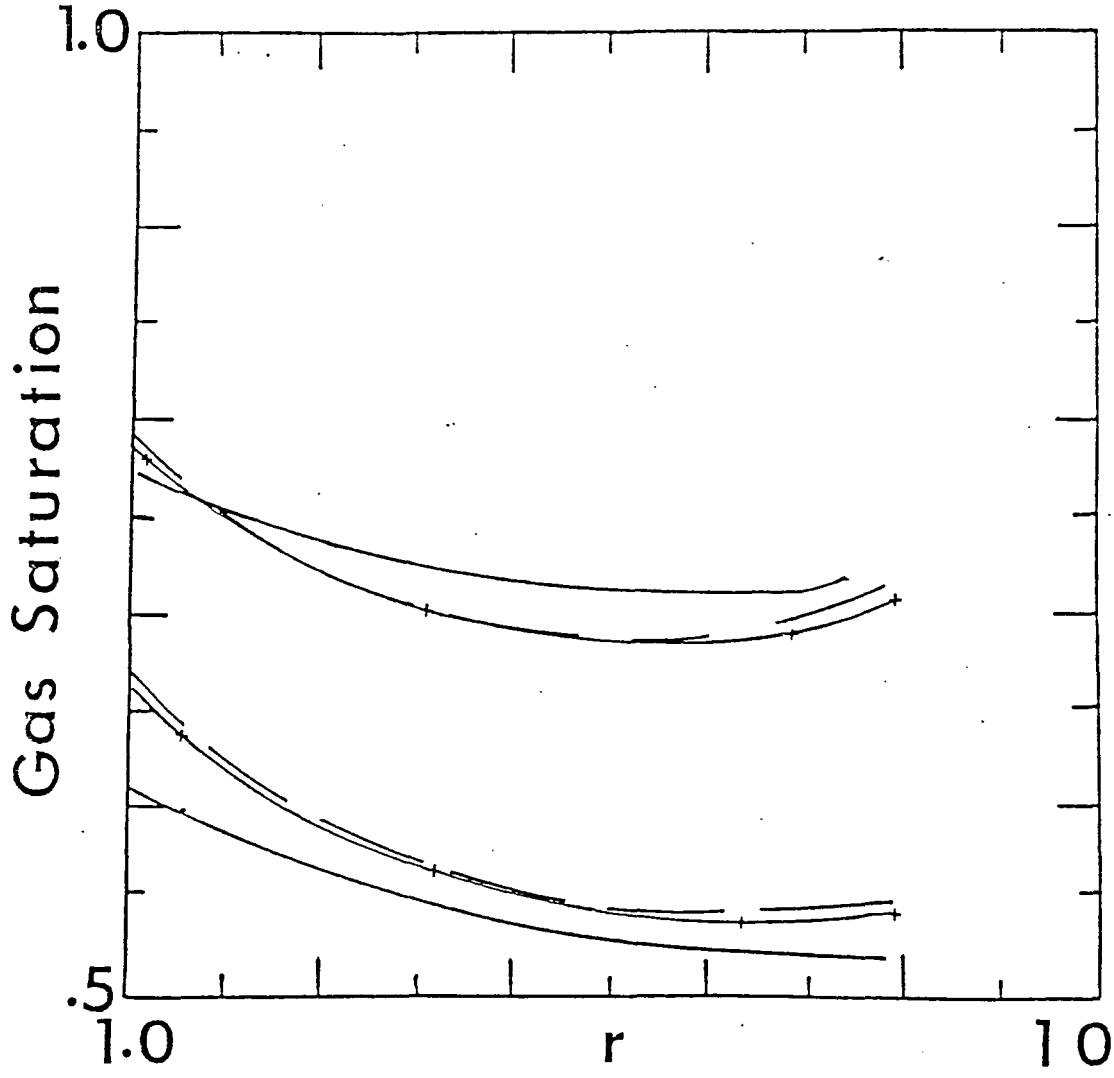

Figure 2.8. Radial saturation profiles as the number of grid points is varied are in a large scale simulation. The dashed lines are for 63 grid blocks, the +−+−+ lines are for 48 grid blocks, and the solid lines are for 35 grid blocks. The axial coordinate is located in the middle of the retort.

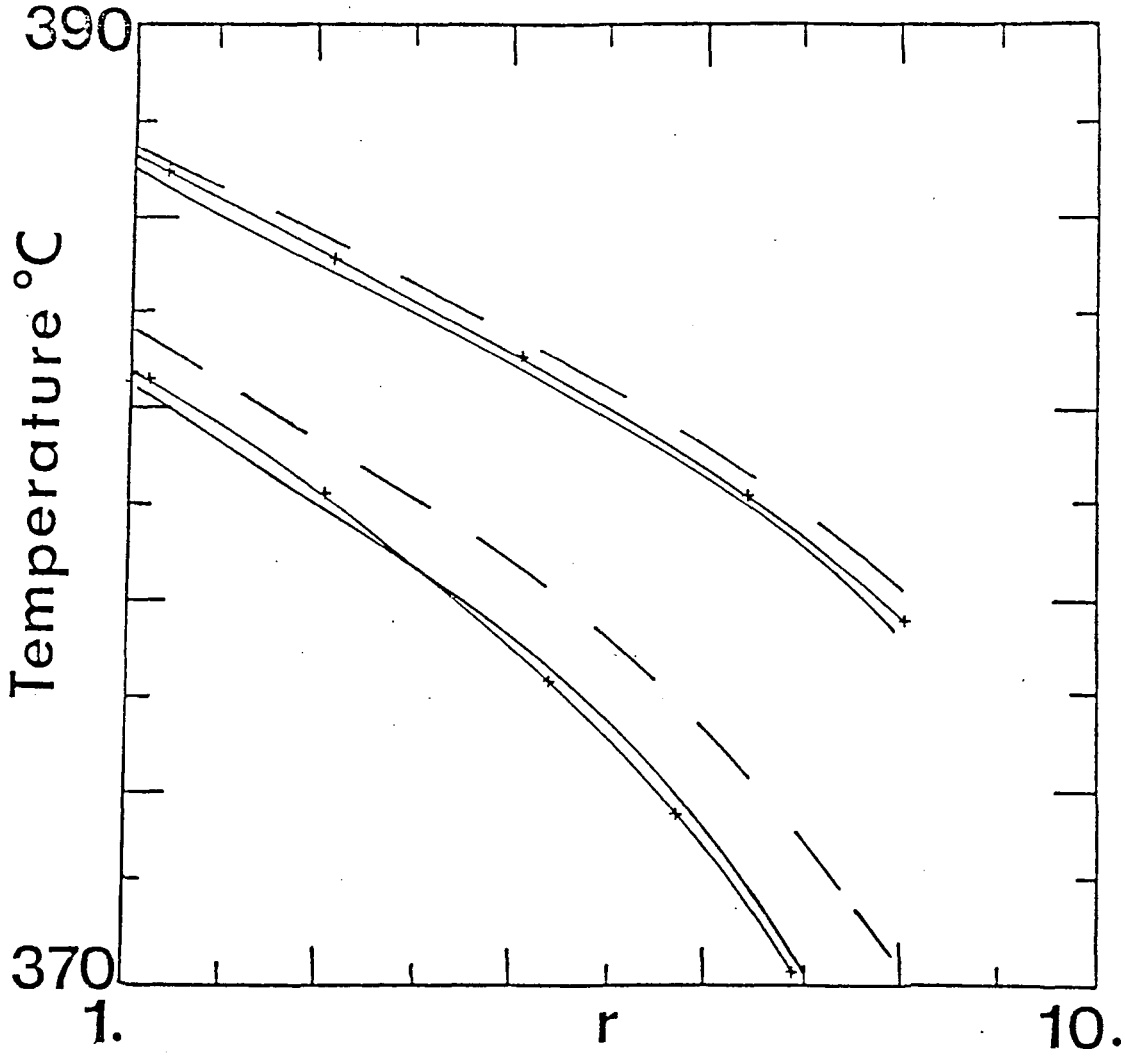

Figure 2.9. Radial temperature profiles (°C) *as the number of grid points is varied in a large scale simulation. The dashed lines are for 63 grid blocks, the* $+-+-+$ *lines are for 48 grid blocks, and the solid lines are for 35 grid blocks. The axial coordinate is located in the middle of the retort.*

2.7 HEATING USING A MONOPOLE ANTENNA

A simple heating applicator is the monopole (or dipole) antenna (see Fig. 2.10). This consists of a ground plane and a tubular conductor inserted into the shale bed. The advantage of a dipole for heating applications is the simplicity of insertion and that when phased with a number of other dipoles inserted nearby it is possible to obtain a relatively uniform heating pattern.

For a monopole of length L oriented along the z axis (see Fig. 2.10) the current has only a z component. From Maxwell's equations the vector potential can be obtained from (see Appendix B for details)

$$A_z = \frac{\mu}{4\pi} \int_{-L}^{L} dz' I(z') K(r, r'), \tag{2.27}$$

where the kernal K is given by

$$K(r, r') = \frac{1}{2}\pi \int_{-\pi}^{\pi} \exp(-ikR(\theta))/R(\theta) d\theta \tag{2.28}$$

with

$$R = ((z - z')^2 + \rho^2 + a^2 - 2a\rho\cos\theta)^{\frac{1}{2}}. \tag{2.29}$$

Here z is the observation point, a is the antenna radius, and θ is the angle between ρ and ρ'.

However, for the field calculations the reduced or average kernal was used to reduce computation time:

$$K = \exp(-ikR)/R, \tag{2.30}$$

$$R = ((z - z')^2 + \rho^2)^{\frac{1}{2}}. \tag{2.31}$$

This approximation is valid for thin antennas and introduces error in the field calculations only for points extremely close to the antenna. The vector potential is then given by

$$A_z = \frac{\mu}{4\pi} \int_{-L}^{L} dz' L(z') \exp(-ikR)/R. \tag{2.32}$$

The electric field can then be obtained from

$$E_\rho = -\frac{i}{4\pi\omega\epsilon} \int_{-L}^{L} dz' I(z') \left[\frac{\partial^2}{\partial\rho\partial z}\right] K(R) \tag{2.33}$$

$$E_z = -\frac{i}{4\pi\omega\epsilon} \int_{-L}^{L} dz' I(z') \left[\frac{\partial^2}{\partial z^2} + k^2\right] K(R) \tag{2.34}$$

The derivatives of K can be calculated analytically to yield:

$$\frac{\partial^2 K}{\partial\rho\partial z} = \frac{(z - z')(\rho - \rho')}{4\pi} \exp(-ikR)/R \left[ik\left(\frac{ik}{R^2} + \frac{1}{R^3}\right) + \left(\frac{2ik}{R^3} + \frac{3}{R^4}\right)\right] \tag{2.35}$$

$$\frac{\partial^2 K}{\partial z^2} = \frac{1}{4\pi} \exp(-ikR)/R) \left[-i\frac{k}{R} - \frac{(1 + k^2(z - z')^2)}{R^2} + i\frac{3k(z - z')^2}{R^3} + \frac{3(z - z')^2}{R^4}\right] \tag{2.36}$$

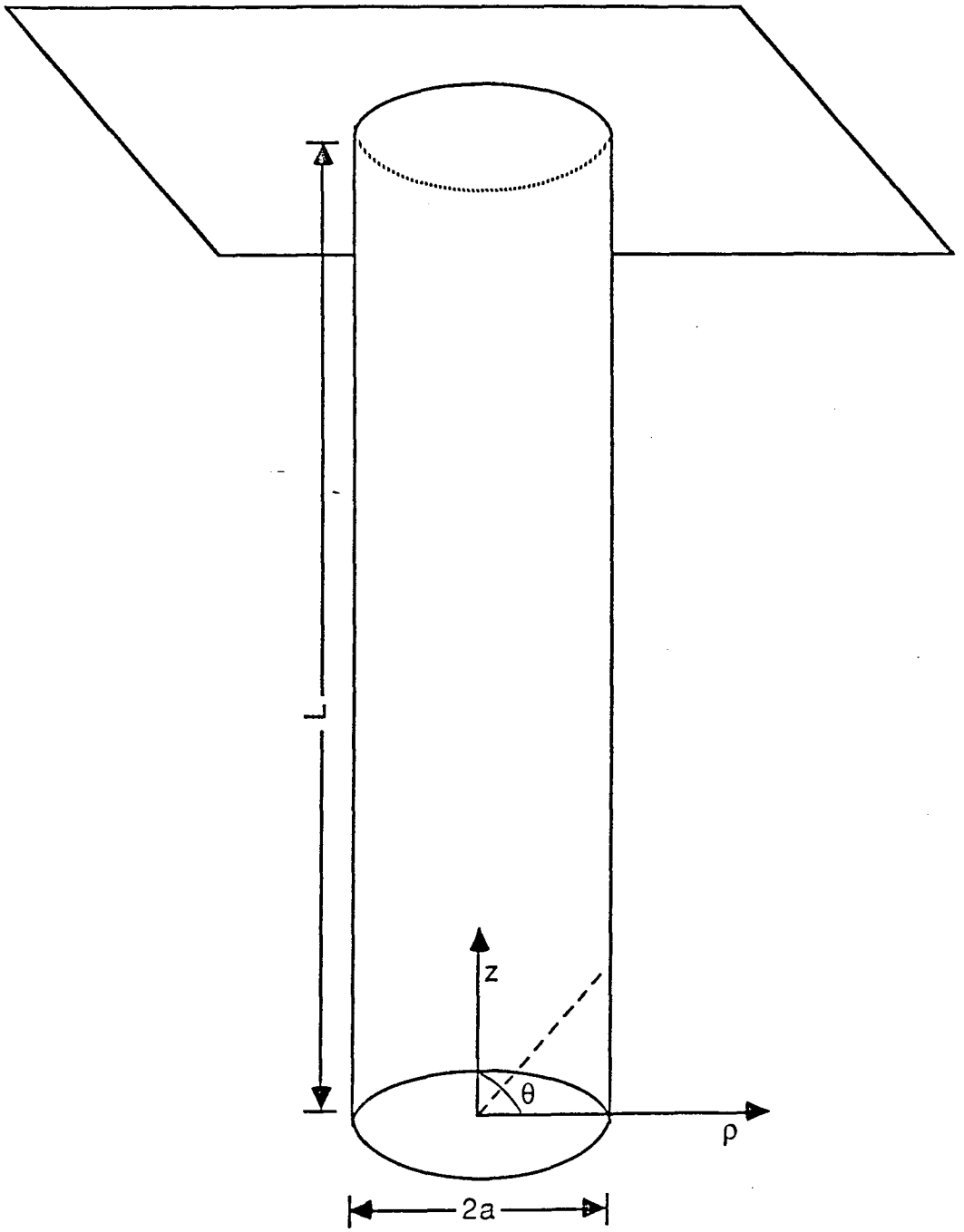

Figure 2.10. A monopole antenna with ground plane.

In the calculations it was assumed that the input excitation is that of a TEM mode given by

$$E_\rho = \frac{V}{2\ln(b/a)\rho} \tag{2.37}$$

where a is the monopole radius, b is the outer coax radius. The following assumptions were made:

1. The averaged kernal was utilized.
2. The antenna is assumed to have no conductive losses.
3. The antenna is assumed electrically thin ($L/a > 60$).

Pocklington's integral equation for an antenna of length 2L is given by

$$E_z = \frac{1}{i\omega\epsilon} \int_{-L}^{L} \left[\frac{\partial^2 K(z,z')}{\partial z^2} + k^2 K(z,z') \right] I(z') dz' d\theta \tag{2.38}$$

where E_z is the excitation field from Equation (2.38).

Pocklington's equation was solved numerically using the method of moments to obtain the current on the antenna and then Equations (2.34) and (2.35) were integrated numerically to find the field distribution in the shale, which was then put into Equation (2.20) to give the power distribution pattern (an example of the power distribution is given in Figs. 2.11 and 2.12). Further details are given in Appendix B.

2.8 EXPERIMENTS WITH A MONOPOLE

We performed a number of experiments using a monopole to heat small blocks of shale at 2.45 GHz to calibrate both our field models and the heat-mass transfer model. In these tests, blocks of western Anvil Points oil shale were heated by a monopole antenna inserted into the middle of the block. The monopole heating system is shown in Fig. 2.13. In Table 2.1 the input parameters used are summarized.

TABLE 2.1

Block Size	0.5 × 0.5 × 0.5 m
Frequency	450 MHz
Power Level	2200 w
Shale Grade	23 GPM
Thermal Data	Reference [11]
Viscosity	Reference [18]
Density Data	Reference [24]
Equilibrium Coefficients	Reference [24]
Reaction Kinetic Parameters	Reference [15]

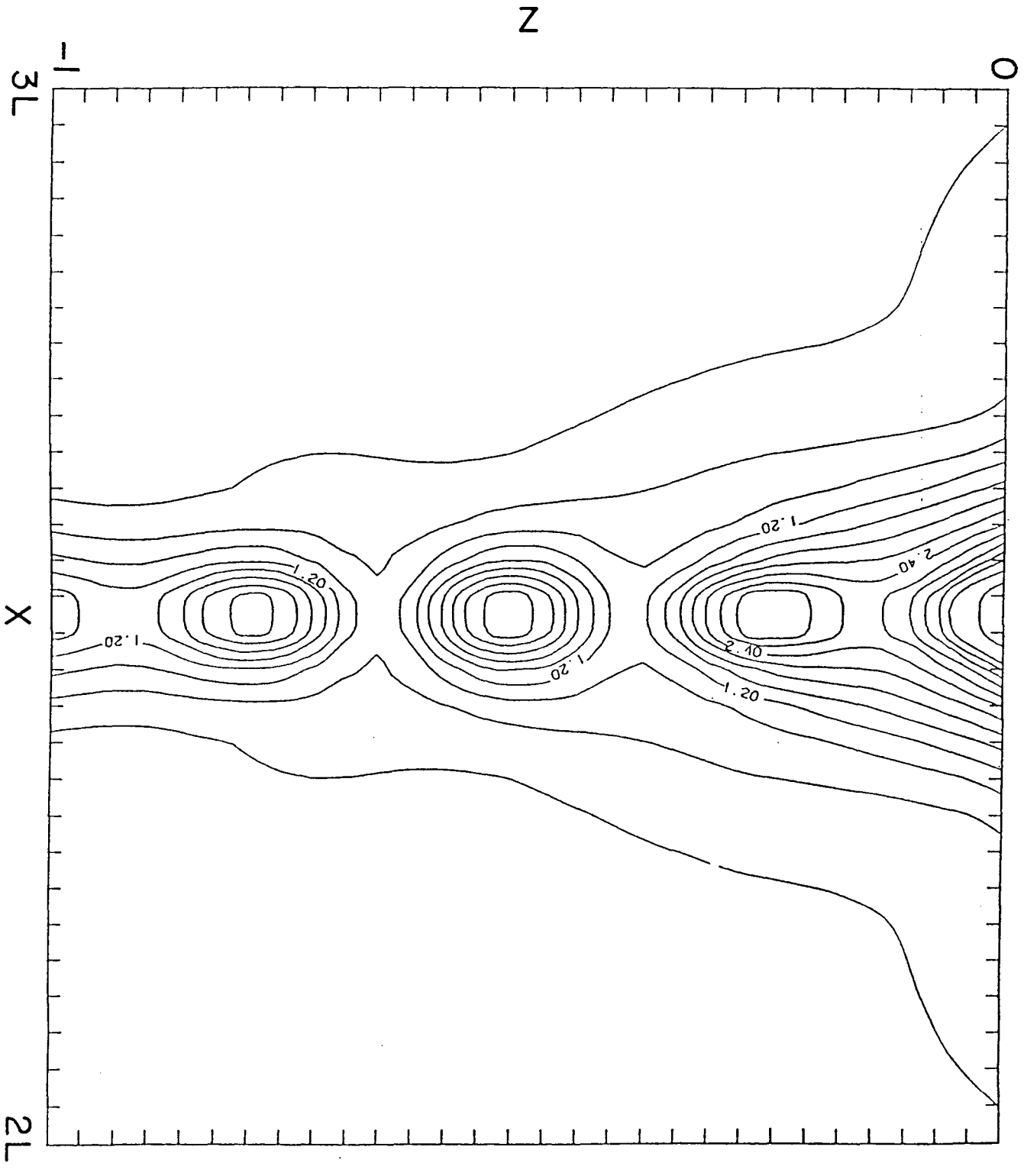

Figure 2.11. Typical power contour for a monopole antenna.

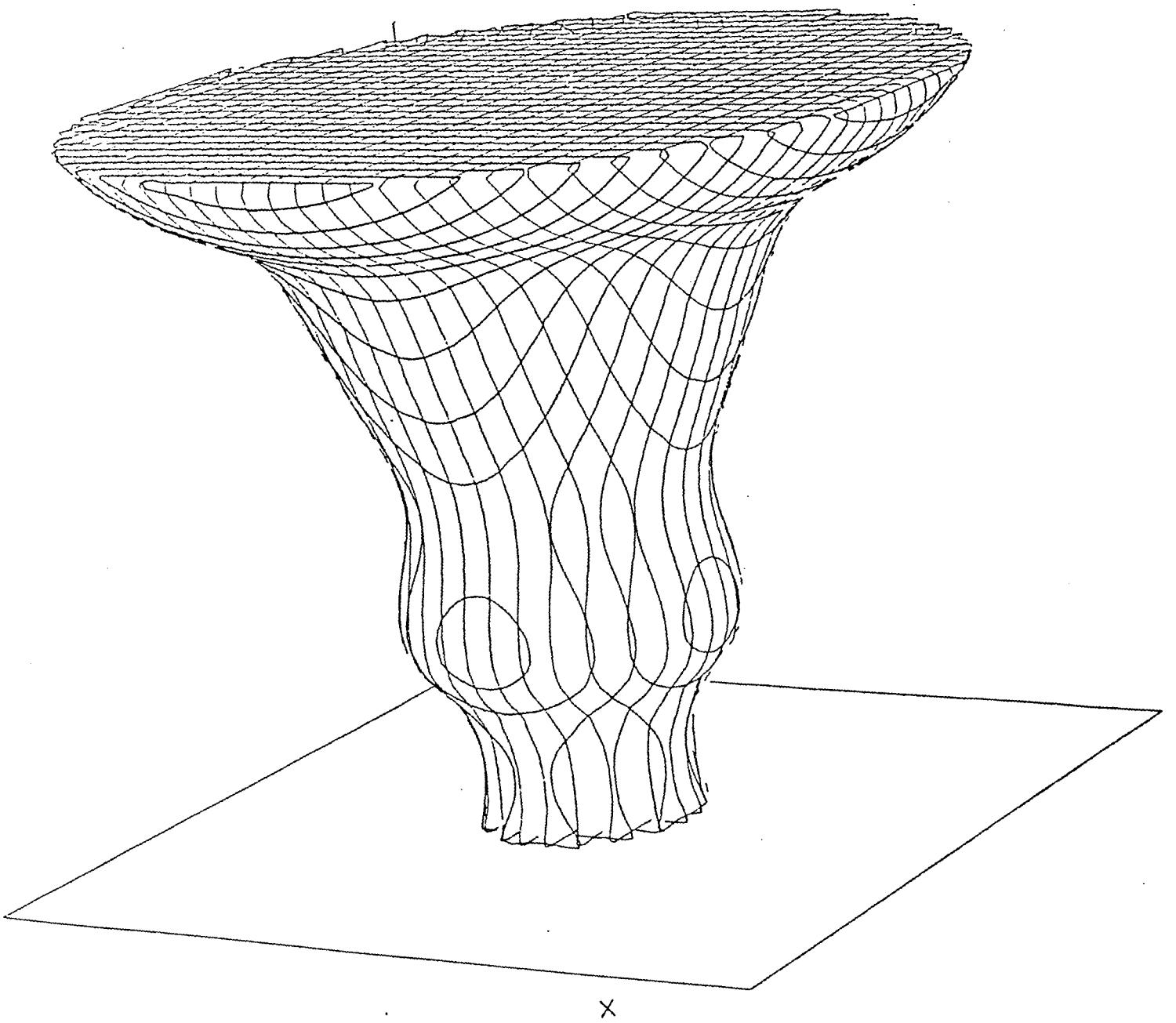

Figure 2.12. Power distribution around a monopole in lossy media in normalized units.

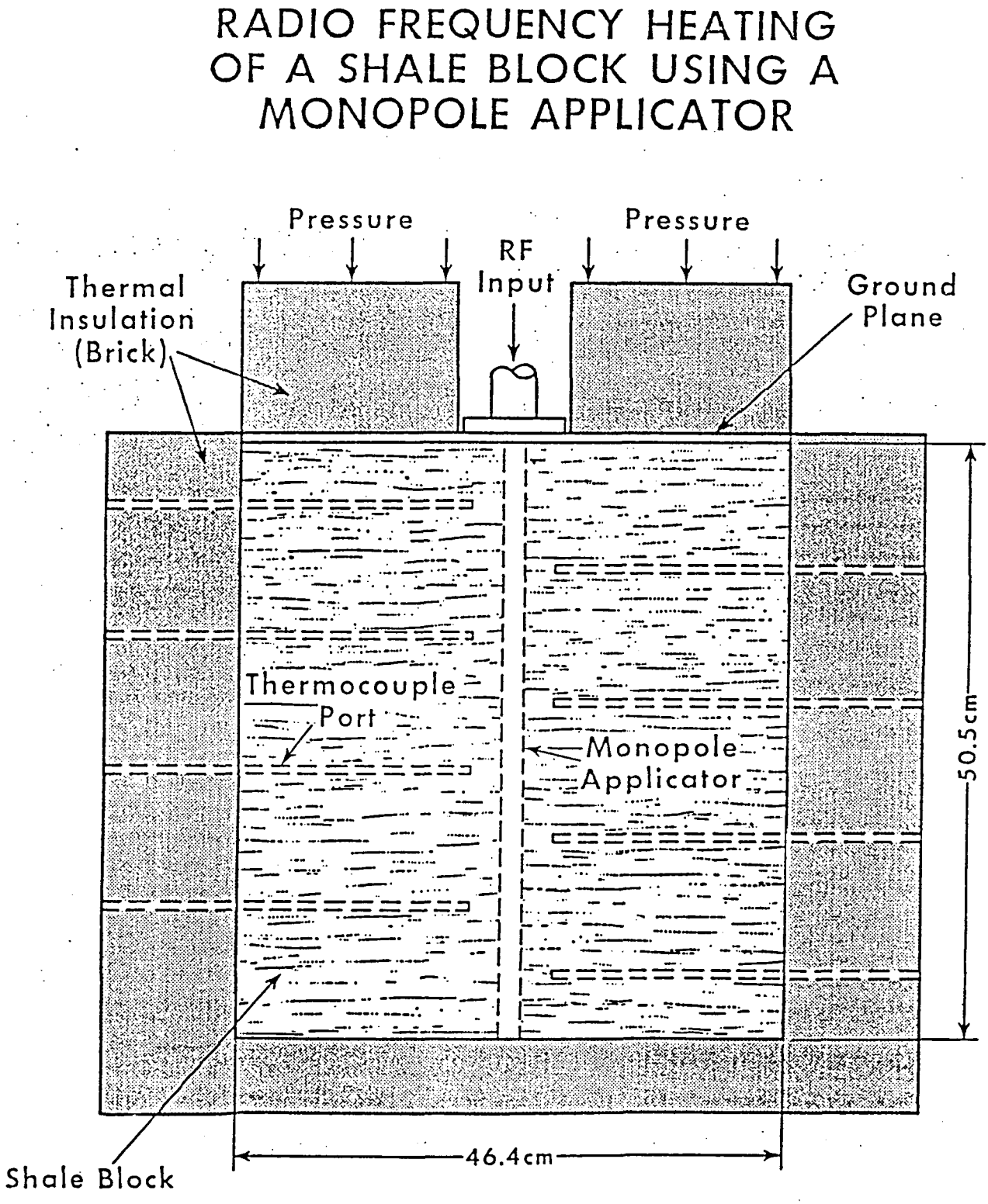

Figure 2.13. A monopole antenna inserted into the block.

In Figs. 2.15–21 the experimental results at various thermocouple positions (see Fig. 2.14) are compared to the model results. The temperature distributions predicted by the model compare reasonably well with experimental results. It was noticed that overheating occurred at the input point and near the antenna. This overheating problem was due to the near fields around the antenna. Little oil was recovered in this test because of the relatively low temperatures obtained.

In Appendix D we present additional results on model simulations and comparison with the various heating tests summarized in Appendix A.

2.9 CONCLUSIONS AND RECOMMENDATIONS

The model appears to be numerically stable for the cases tested. For the geometries studied it appears that oil may be recovered at about 200 kw/hr of electricity per barrel of recovered oil. To enhance recovery, sweep gases could be injected at various points in the heated region. Another advantage of the r.f. heating process is that it produces cracks in the bed (at least when the block is not constrained radially), thus eliminating the need for blasting and enhancing the recovery.

Future modeling should include more information on the flow of the oil in the shale. That is, one would expect that some of the oil would be trapped in the shale in regions of low permeability. The experimental studies performed by Sresty [17] were too small to see the effects of oil trapping, and were probably performed on selected samples of shale.

In the comparison of the model with experiment we see in Figs. 2.15–2.20 that the model performed reasonably. In Figs. 2.15, 2.18 and 2.20) the model deviated from experiment. The reason for this is that all of these thermocouples were very near the antenna and the present field model is not good very near the monopole.

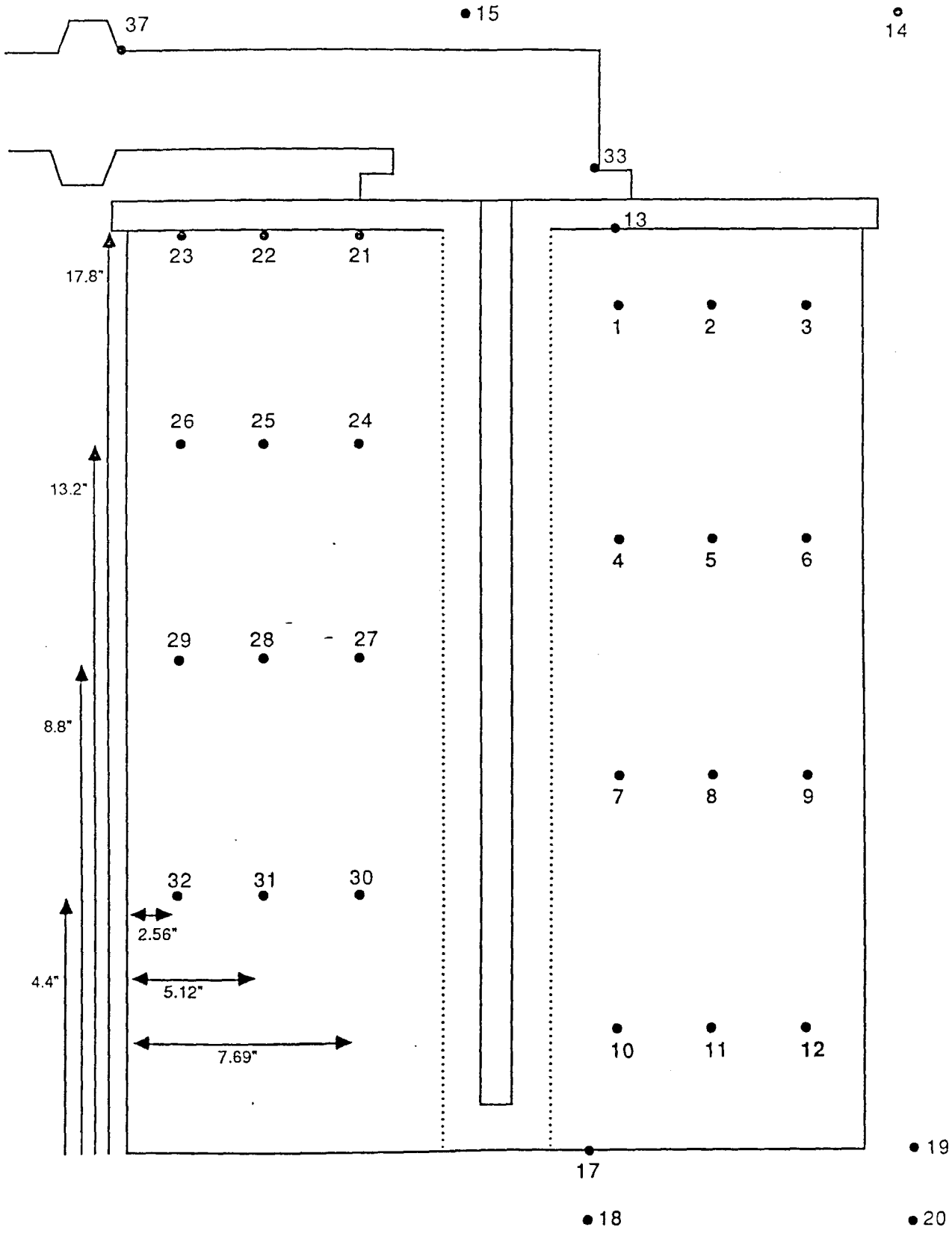

Figure 2.14. Thermocouple positions in shale block.

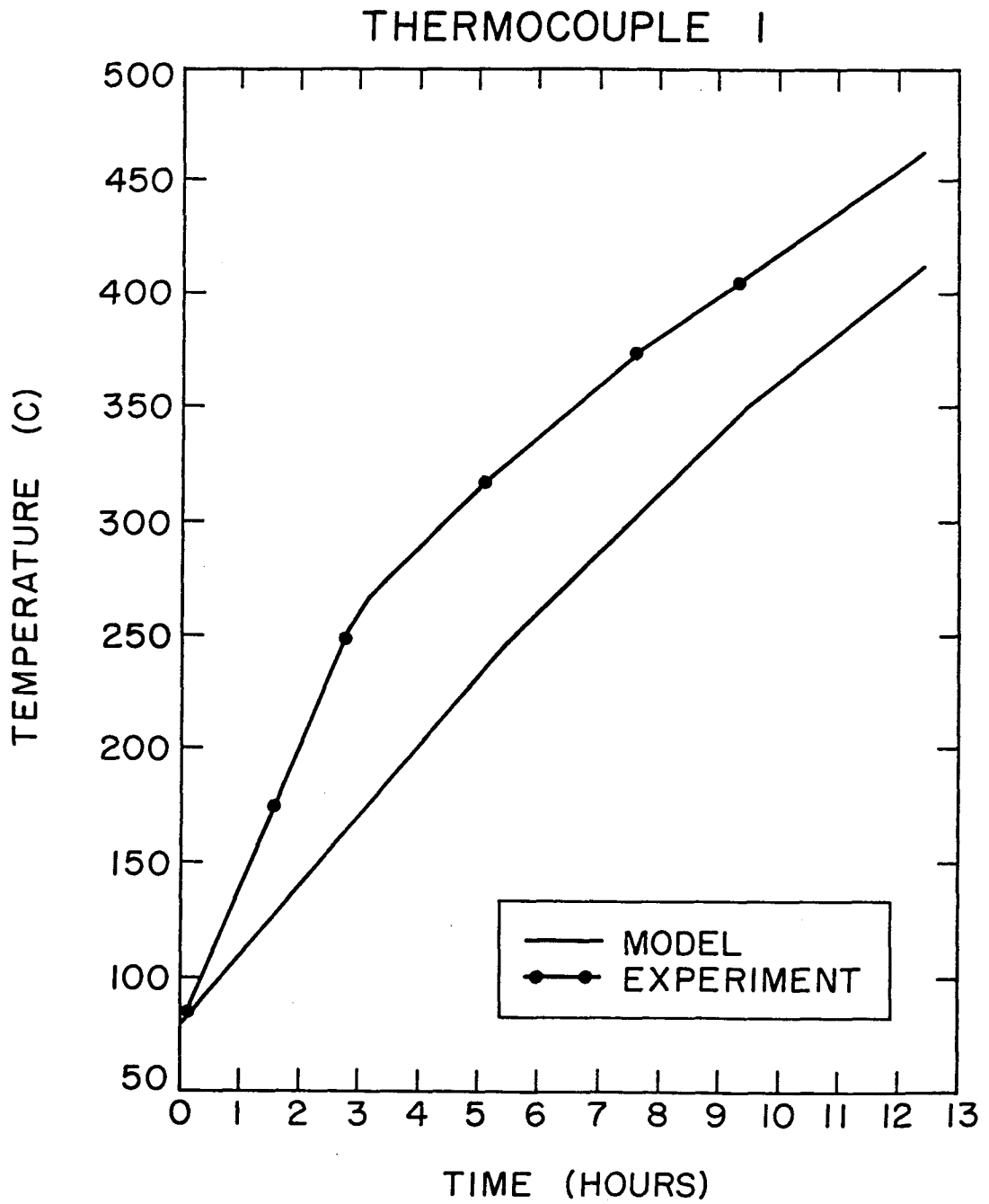

Figure 2.15. Model predications (—) vs experimental measurements in a shale block (– – –) for #1 thermocouple position.

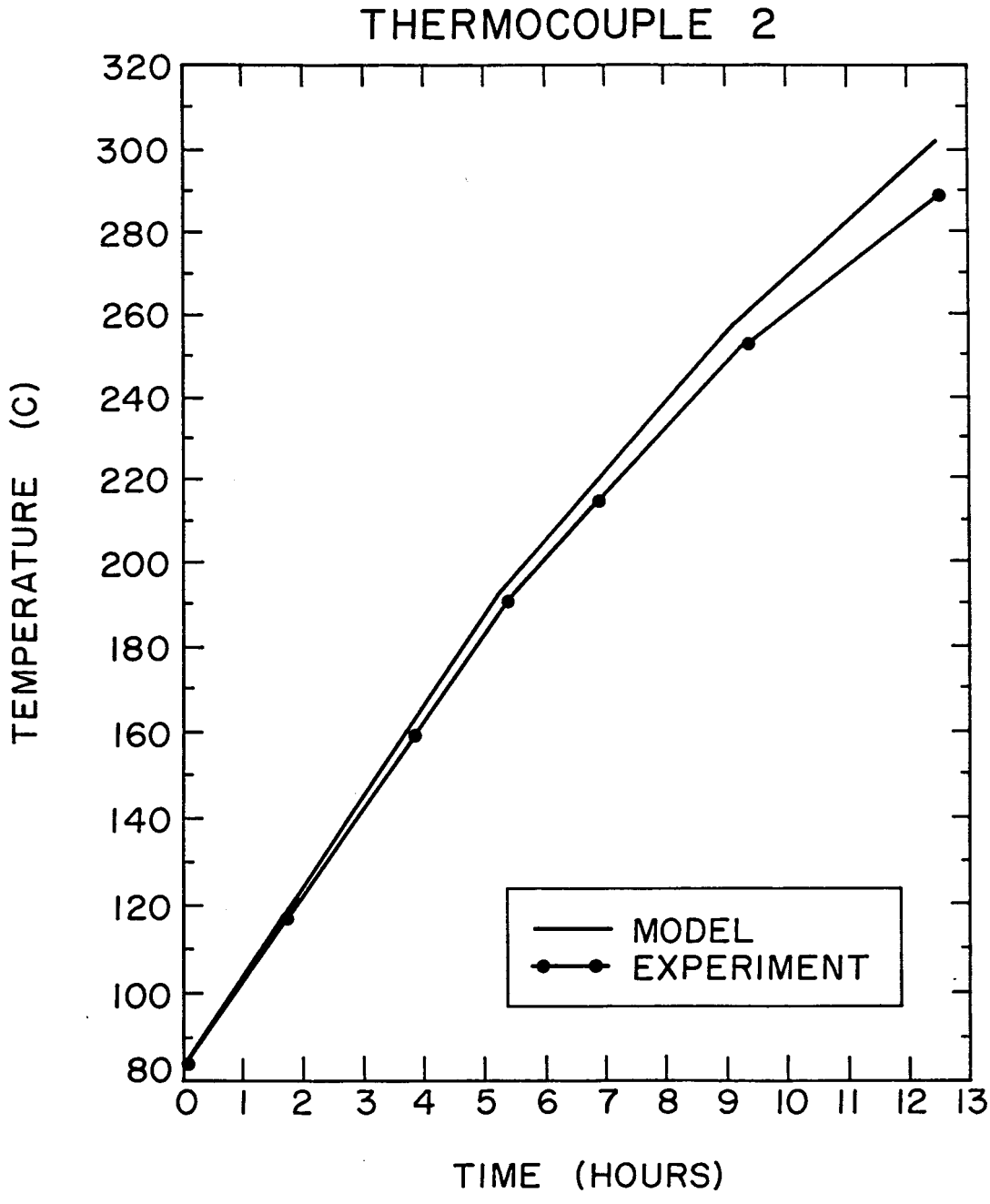

Figure 2.16. Model predications (—) vs experimental measurements in a shale block (– – –) for #2 thermocouple position.

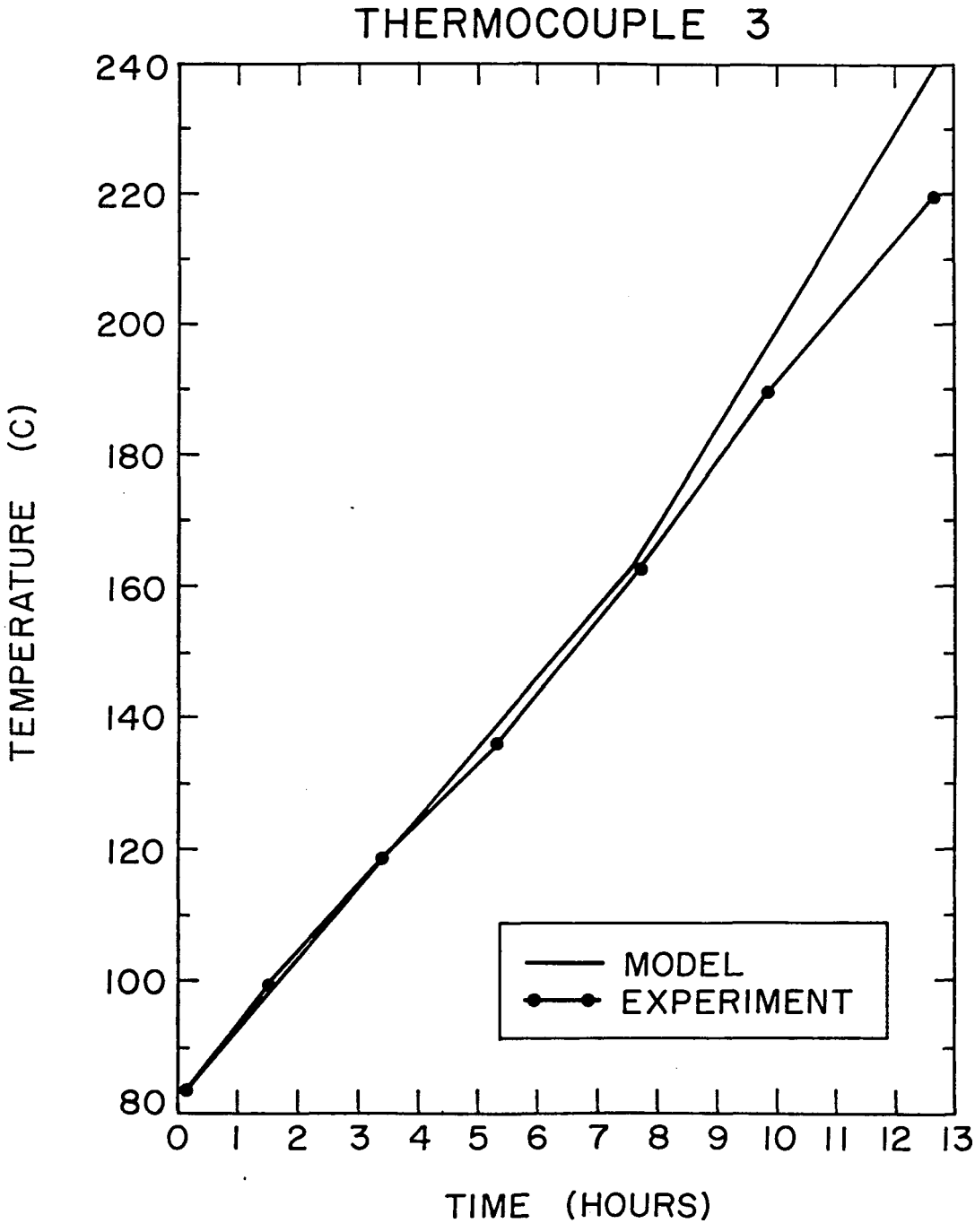

Figure 2.17. Model predications (—) vs experimental measurements in a shale block (– – –) for #3 thermocouple position.

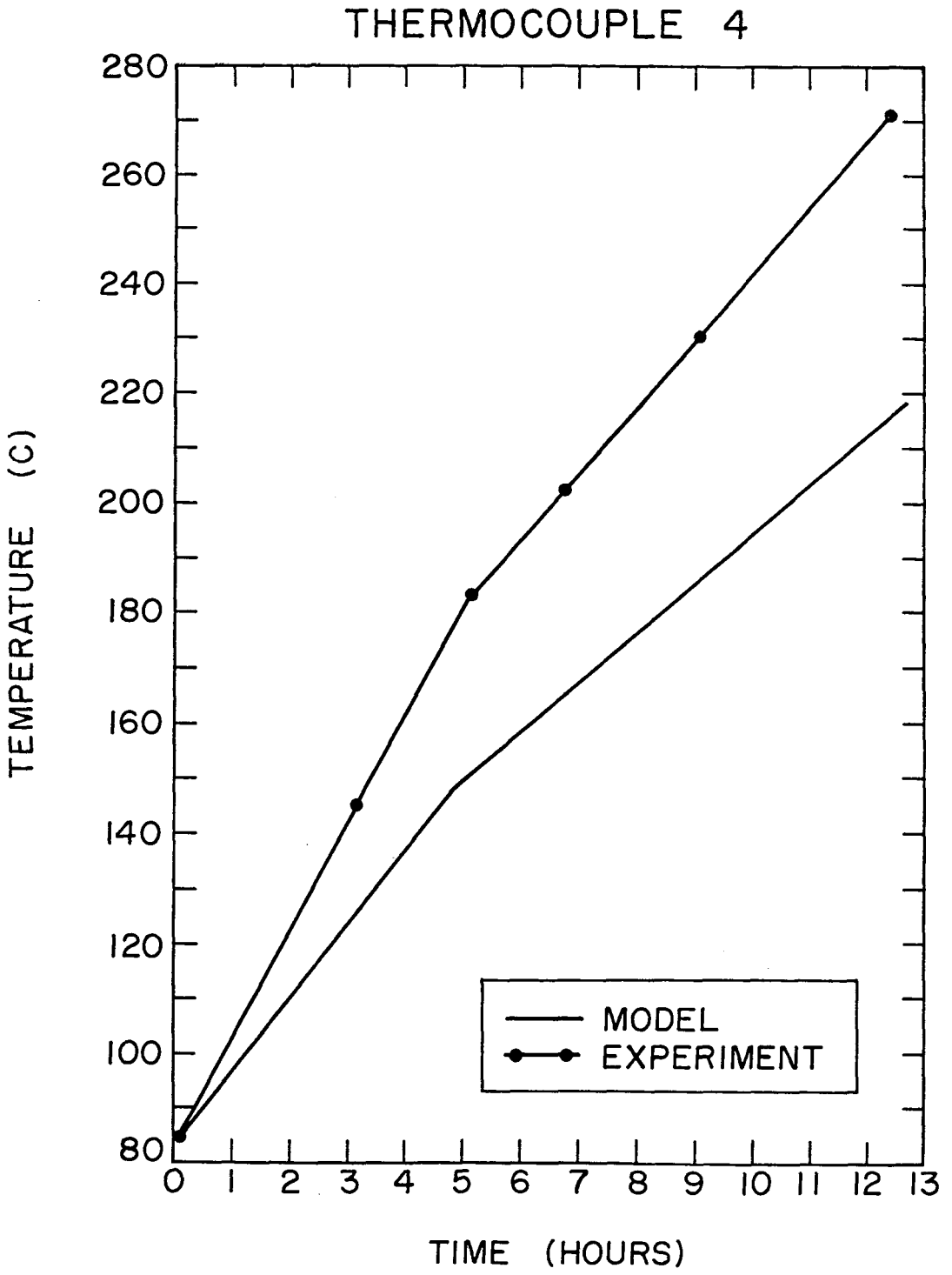

Figure 2.18. Model predications (—) vs experimental measurements in a shale block (– – –) for #4 thermocouple position.

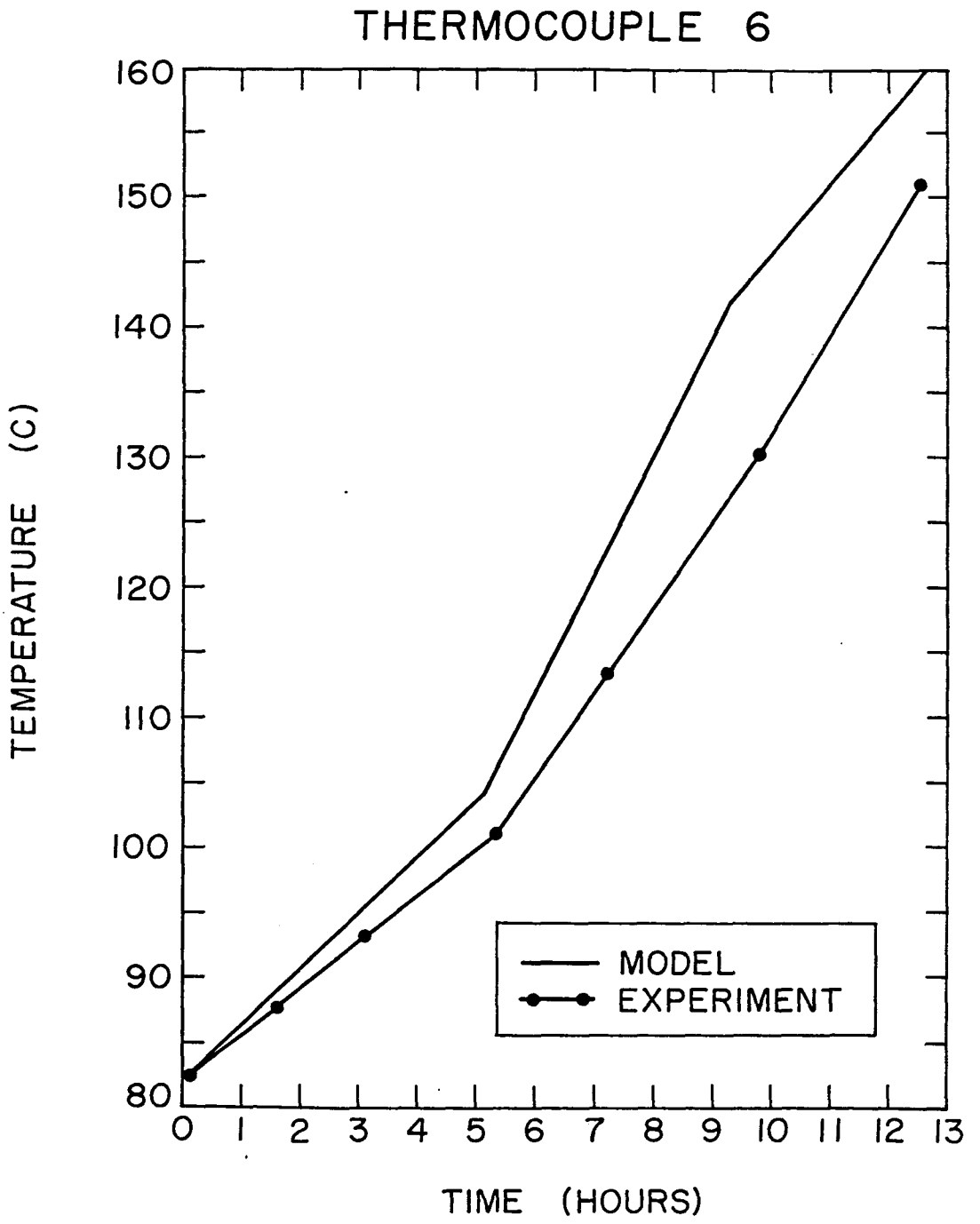

Figure 2.19. Model predications (—) vs experimental measurements in a shale block (– – –) for #6 thermocouple position.

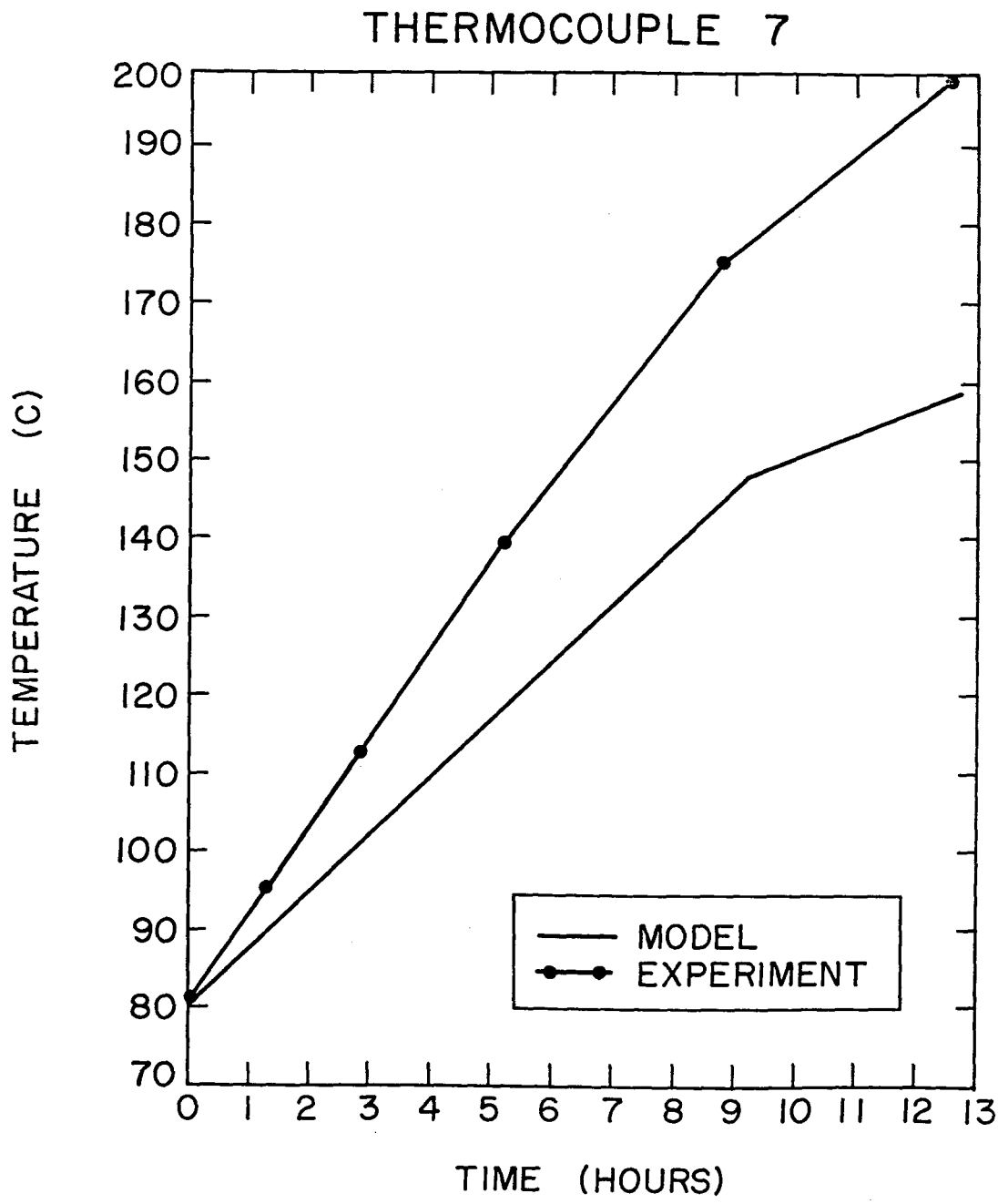

Figure 2.20. Model predications (—) vs experimental measurements in a shale block (– – –) for #7 thermocouple position.

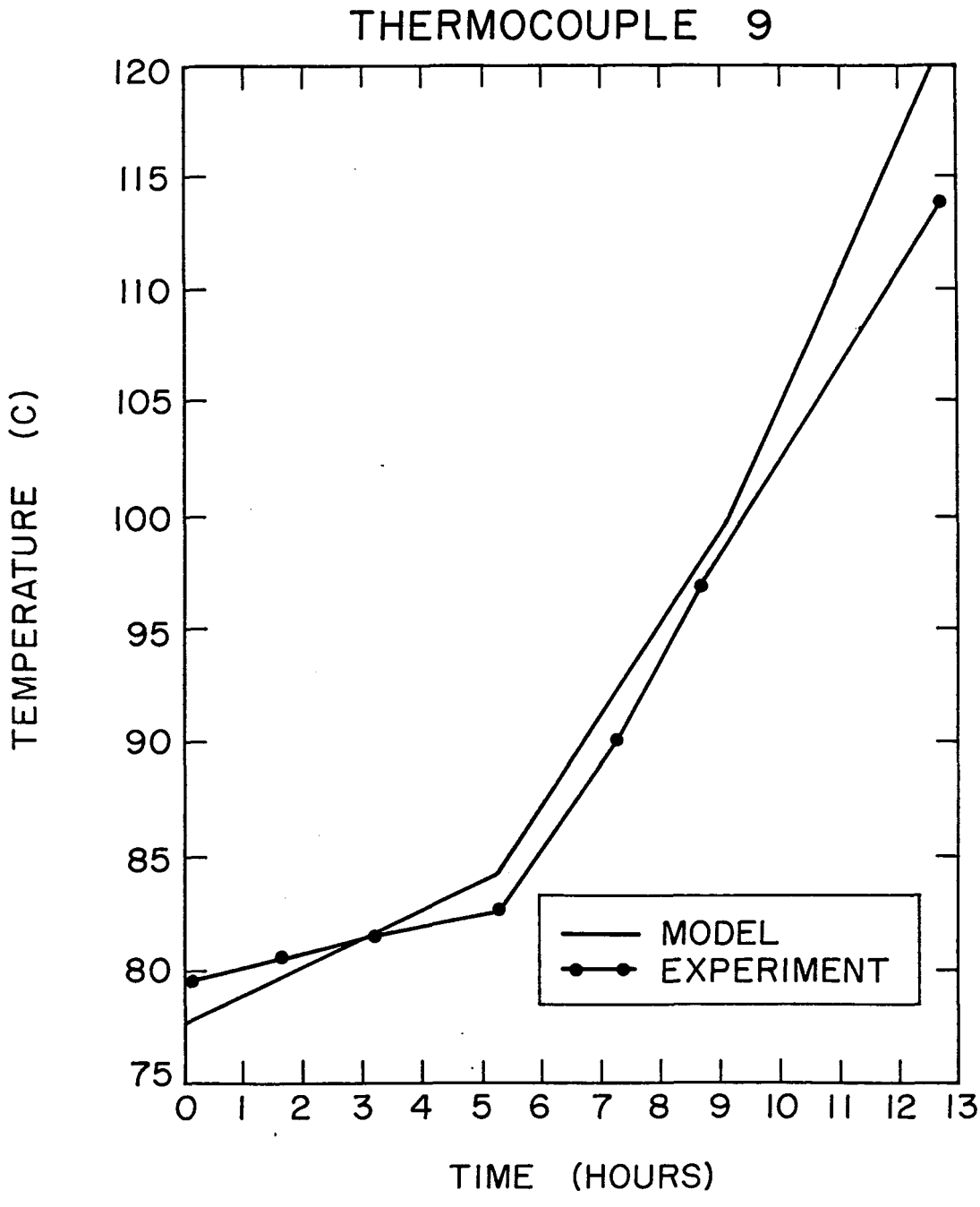

Figure 2.21. Model predications (—) vs experimental measurements in a shale block (– – –) for #9 thermocouple position.

CHAPTER 3

DIELECTRIC CONSTANT MEASUREMENTS

CHAPTER SUMMARY

Using a new technique developed in collaboration with Ramon Jesch and Howard Bussey a new sample holder has been designed and fabricated for dielectric constant measurements. Using this sample holder we present detailed measurements on the real and imaginary parts of the dielectric constant for the oil shales.

3.1 INTRODUCTION

The use of electromagnetic (em) techniques to heat oil shale requires a knowledge of its dielectric properties. The power dissipated in a medium with a complex dielectric constant $\epsilon^* = \epsilon' - j\epsilon''$ is

$$P_{\text{diss}} = \frac{\omega}{2}\epsilon_0\epsilon''|\vec{E}|^2 \tag{3.1}$$

where $\vec{E}$ is the electric field of the incident em wave, at frequency $f(f = \omega/2\pi)$. Another factor affecting em heating is the dielectric attentuation

$$\alpha = \frac{\pi}{\lambda}\frac{\epsilon''}{\epsilon'} \tag{3.2}$$

where λ is the wavelength of the em wave in the dielectric. Thus the dielectric constant of a material is used to estimate the necessary incident em power, frequency and the size of the sample optimum for an effective em heating process.

Oil shale is a lossy dielectric and therefore its dielectric constant is a function of frequency and temperature [33]. Oil shales have a certain free and bound water content [3] which are released at elevated temperatures. The loss of moisture from the oil shale is indicated by an abrupt change in the dielectric constant [33].

Previous experiments measuring the dielectric constant of oil shale [2,34,35] as a function of frequency and temperature have yielded conflicting results. The present experiment was designed as a further effort to unravel the problem. The following sections describe the operating principle, design and characterization of the sample holder. The measurement technique is discussed in detail. Sample holder characteristics are discussed carefully. Finally the results of measurements of the dielectric constant of oil shale are presented.

Theory

Transmission line measurements of a dielectric sample terminated by either a short circuit or an open circuit are well known [36]. Coaxial transmission line techniques have been previously used to measure the dielectric constant of oil shales [34,35], various grains [37], soils [38], and lunar soil [39].

At radio frequencies the measurable quantity at any transverse plane is the admittance, defined as the ratio of longitudinal current to transverse voltage. The sample holder is treated as a coaxial transmission line terminating in an open circuit. A TEM mode propagates down the coaxial line whose output admittance is zero. The open circuit line has the advantage that the sample is easily inserted through the open end.

In any uniform section of a coaxial line the input admittance is given by [40]

$$Y_{\text{in}} = Y_0\left(\frac{Y_0 + Y_e \coth\gamma d}{Y_0 \coth\gamma d + Y_e}\right) \tag{3.3}$$

where the TEM characteristic admittance Y_0 is

$$Y_0 = \frac{2\pi}{\ln(b/a)}\left(\frac{\epsilon_0\epsilon^*}{\mu_0\mu^*}\right)^{\frac{1}{2}}. \tag{3.4}$$

Y_e is the output admittance of the section.

$$\gamma = \alpha + j\beta = \left(-\omega^2 \mu_0 \mu^* \epsilon_0 \epsilon^*\right)^{\frac{1}{2}} \tag{3.5}$$

is the complex propagation constant in the section. $\epsilon^* = \epsilon' - j\epsilon''$ and μ^* are the complex dielectric constant and permeability of the dielectric in the section. For nonmagnetic materials, like oil shales, $\mu^* = 1$. a and b are the inner and outer radii of the coaxial line. d is the length of the section. $\omega(= 2\pi f)$ is the radial frequency of the TEM wave. $\epsilon_0(= 8.854 \times 10^{-12} F \cdot m^{-1})$ and $\mu_0(= 4\pi \times 10^{-7} H \cdot m^{-1})$ are the permittivity and permeability of free space. Note that both Y_0 and γ depend on ϵ^*.

The admittance at a dielectric interface is continuous except when changes in radii a and b occur [41,42]. Any change in the radii introduces a step capacitance C_s. Then the corresponding shunt admittance is given by [42]

$$Y_s = j\omega \epsilon^* C_s \tag{3.6}$$

where ϵ^* is the dielectric constant of the dielectric that is against the radially stepped surface(s). Therefore, in a coaxial transmission line terminating in an open circuit, the truncated center conductor introduces a shunt admittance. Then at the terminating point the output admittance is Y_s instead of zero.

The step capacitance can also be represented by moving the location of the open circuit to a plane beyond the end of the terminated center conductor [13]. This effectively increases the length of the center conductor to

$$d = d_0 + d_s \tag{3.7a}$$

where d_0 is the physical length of the center conductor and d_s is the length representing the step capacitance. Therefore, at the transverse plane at a distance d_s beyond the end of the center conductor, the output admittance of the coaxial line is zero.

In a line with 50Ω characteristic impedance, the extended length of the center conductor is [13,43]

$$d_s = (b-a)(0.6034 + 0.9464x^2 + 18.19x^{5.127}), \quad \text{for } x < 0.3 \tag{3.7b}$$

where $x = b/\lambda$.

3.3 SAMPLE HOLDER

The sample holder is an open circuit coaxial transmission line with a terminated center conductor. It can be broadly divided into three sections.

A. Sample Section: This section is a 38.8 mm (1.527″) diameter stainless steel coaxial line, as shown in Figs. 3.1 and 3.2. The center conductor is a 16.9 mm (0.664″) diameter stainless steel rod. The center conductor is terminated and the outer conductor extends beyond the end of the center conductor. Thus for air dielectric ($\epsilon^* = 1$), the characteristic impedance of a TEM mode is 50Ω.

The em field extends beyond the end of the center conductor. Therefore the outer conductor must extend a distance sufficiently large beyond the end of the center conductor

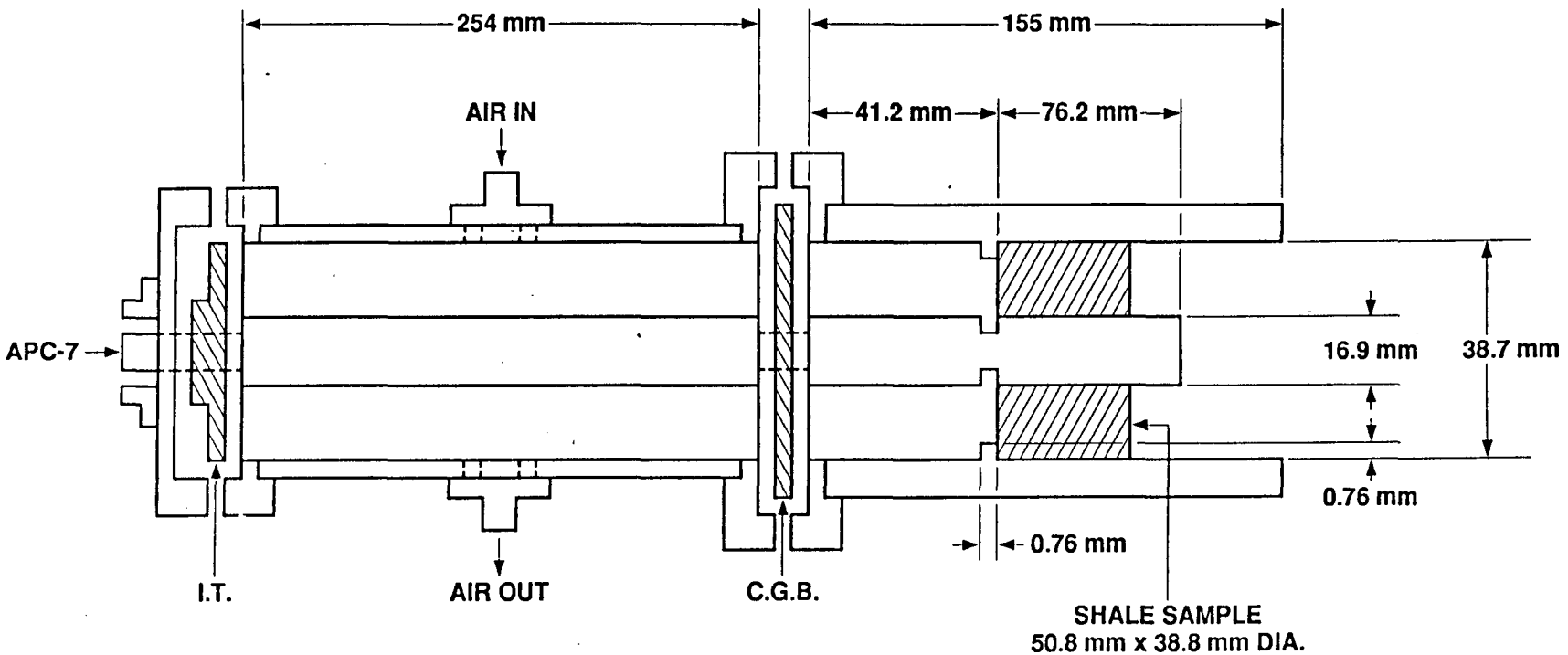

Figure 3.1. Sample holder showing the sample, adaptor and transformer section. IT: Impedance Transformer, CGB: Ceramic Gas Barrier.

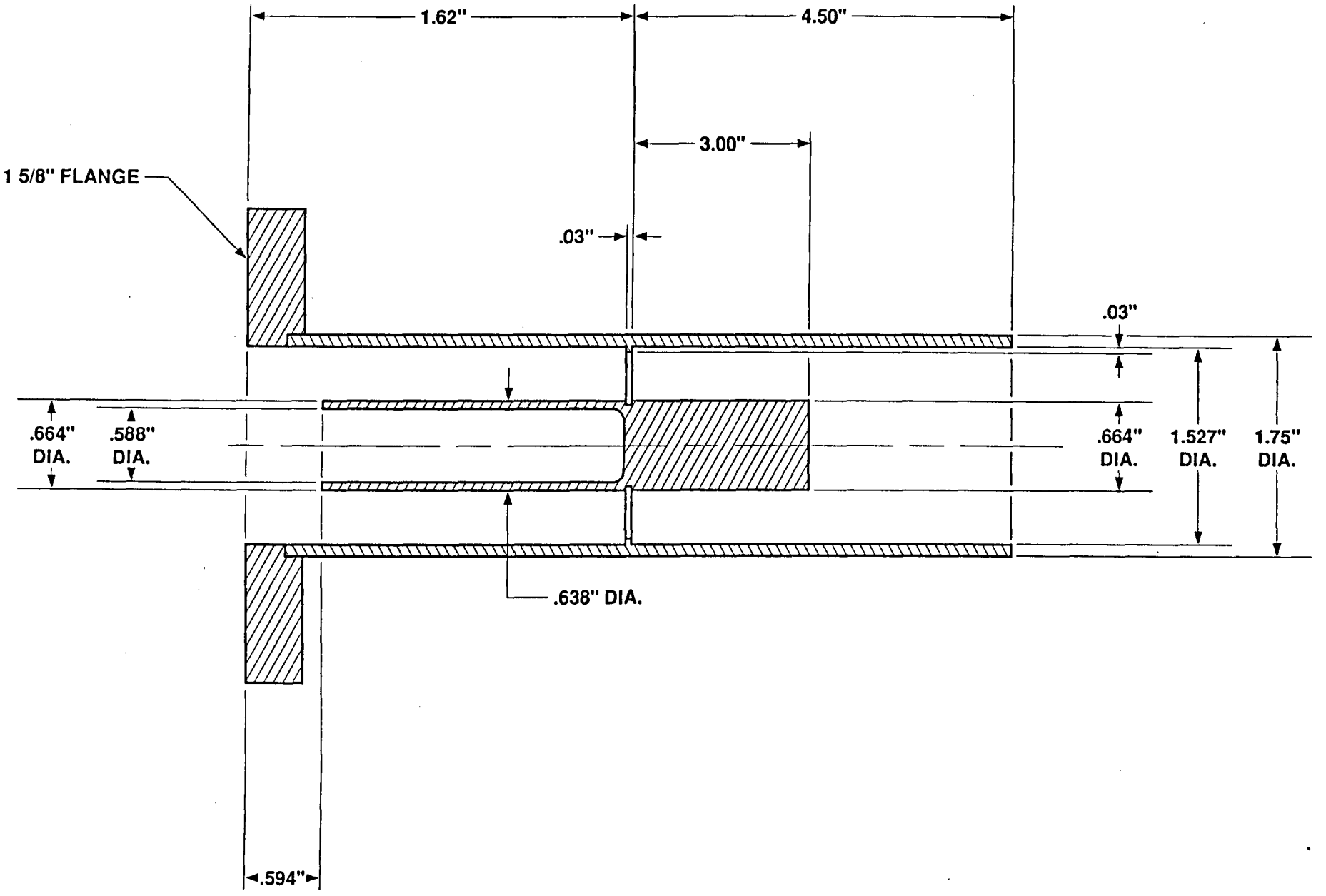

Figure 3.2. Sample section of sample holder.

so that the em fields do not emerge from the section. Theoretically this distance should be infinity. Practically, if the frequency is well below cutoff

$$f \ll \frac{0.387c}{b\sqrt{\epsilon'}} \tag{3.8}$$

then the outer conductor needs to extend at least a distance of $3b/2$ beyond the terminated center conductor. For the sample holder ($b = 19.9$ mm) and oil shale sample ($\epsilon' \approx 6$), the cutoff frequency is 2.38 GHz. So, the operating range of frequency (10–1000 MHz) is well below cutoff.

There is a positioning ring on the outer conductor with a compensating groove cut into the center conductor. The sample rests against this ring and so the sample plane is fixed for all experiments. The center conductor extends beyond the sample length (4 cm), a distance greater than $3b/2$. This ensures that the propagating mode is TEM throughout this section.

B. Adaptor Section: The adaptor setion is a 38.8 mm (1.527″) diameter brass coaxial line, as shown in Figs. 3.1 and 3.3. The inner conductor is a 16.9 mm (0.664″) diameter brass rod. these dimensions give a TEM mode characteristic impedance of 50Ω, for air dielectric. The adaptor section surfaces are rhodium flashed to prevent corrosion and consequent alteration of the electrical characteristics. There is an air inlet-outlet manifold on the outer conductor. Cold dry air is passed through this section when the sample is heated.

There is a gas barrier between the sample and the adaptor sections. It stops the flow of gases, effusing out of the sample at high temperatures, up the sample holder. These gases can alter the electrical characteristics of the adaptor section. The gas barrier also allows for cooling of the adaptor section without affecting the sample temperature. The barrier is a ceramic disk with a high dielectric constant ($\epsilon' \approx 9$). The 50Ω characteristic impedance of the line is maintained by increasing the ratio b/a.

C. Transformer-Connector Section: This section contains an APC–7 connector and an impedance transfer. The impedance transfer compensates for the change in the diemeter from 7 mm to 38.8 mm. This introduces some extra capacitance. The transformer corrects for the extra capacitance while maintaining the 50Ω characteristic impedance between the APC–7 connector and the adaptor section.

3.4 ELECTRICAL MEASUREMENTS

The common measurement technique with an open circuit coaxial line is to treat the sample holder as a number of separate electrical sections [43]. The input admittance Y_{in} is measured, and using Equations (3.3)–(3.5) the output admittance Y_e is calculated for the first section. Y_e is then the input admittance of the second section. Progressing through each section Y_{in} is transformed to Y'_{in}, the input admittance of the section containing the sample. The output admittance of the sample section is zero if the sample extends beyond the open circuit plane ($d = d_0 + d_s$). Then for the sample section Equation (3.3) reduces to

$$Y'_{\text{in}} = Y_0 \tanh \gamma d. \tag{3.9}$$

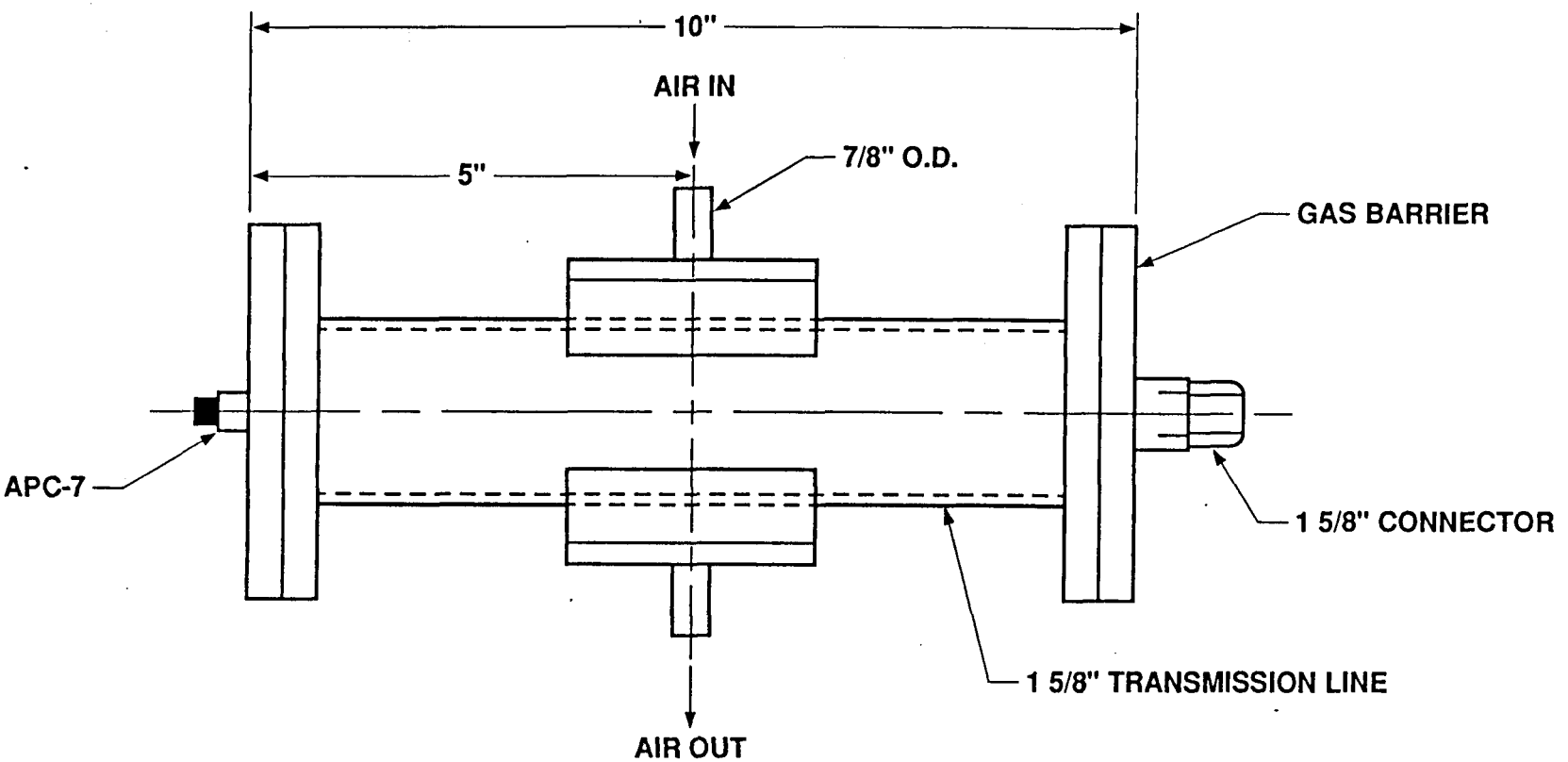

Figure 3.3. Adaptor and transformer. Connector section of the sample holder.

This is a transcendental equation for the unknown ϵ^* in the sample section.

For our sample holder the number of electrical sections were too many ($\sim$ 10). This would increase the errors involved in transforming Y_{in} to Y'_{in}. An alternate method was used taking advantage of the reflection mode operation of an impedance analyzer. The impedance analyzer measures the reflection coefficient the load

$$\Gamma = \Gamma_x + j\Gamma_y = |\Gamma|\exp(j\theta) = |\Gamma|(\cos\theta + j\sin\theta) \tag{3.10}$$

where $\theta = \tan^{-1}(\Gamma_y/\Gamma_x) = |\Gamma_0| = \left(\Gamma_x^2 + \Gamma_y^2\right)^{\frac{1}{2}}$. Then the resistance R and the reactance X of the load are calculated.

$$R = Z_0\frac{1-\Gamma_x^2-\Gamma_y^2}{(1-\Gamma_x)^2+\Gamma_y^2} = Z_0\frac{1-|\Gamma|^2}{(1-|\Gamma|\cos\theta)^2+(|\Gamma|\sin\theta)^2} \tag{3.11}$$

$$X = Z_0\frac{2\Gamma_y}{(1-\Gamma_x)^2+\Gamma_y^2} = Z_0\frac{2|\Gamma|\sin\theta}{(1-|\Gamma|\cos\theta)^2+(|\Gamma|\sin\theta)^2}. \tag{3.12}$$

R and X provide the value of $Y = |Y|\exp(j\theta)$ as

$$\begin{aligned} &\text{(a)} \quad |Y| = (R^2+X^2)^{-\frac{1}{2}} \\ &\text{(b)} \quad \phi = \tan^{-1}(X/R) \end{aligned} \tag{3.13}$$

In our measurement technique, the sample holder is characterized by an electrical length ℓ up to the sample plane. The electrical length is then used to transform the reflection coefficient from the measurement plane at APC-7, $\ell = 0$, to the sample plane as

$$\begin{aligned} \Gamma_\ell &= \Gamma\exp(-2j\beta\ell) \\ &= |\Gamma_0|\exp\{j(\theta-2\beta\ell)\} \\ &= |\Gamma_0|\exp(j\theta_\ell) \end{aligned} \tag{3.14}$$

where

$$\theta_\ell = \theta - 2\beta\ell. \tag{3.15}$$

$\beta = \omega/c$ is the phase constant and Γ_0 is the reflection coefficient at $\ell = 0$.

This technique bypasses the errors involved in repeated admittance transformation. The electrical length is obtained by shorting the sample holder at the sample plane. Then, at the short plane $\Gamma = -1 = |1|\exp(-j\pi)$. The value of ℓ giving $\Gamma = -1$ is the electrical length. When measuring Y_{in}, the appropriate value of ℓ is entered into the impedance analyzer. The instrument has the capability to transform Y_{in} to Y'_{in} and Y'_{in} is measured directly.

Once Y'_{in} is obtained, the sample holder is treated as two electrical sections. The first is the sample section with an unknown dielectric. The second is an air section whose output admittance is zero at $d = d_0 + d_s$. In this section $\epsilon^* = 1$. Therefore, in the sample section, from Equation (3.3),

$$Y_{es} = Y_{os}\left(\frac{Y_{os} - Y'_{\text{in}}\coth\gamma_s d_1}{Y'_{\text{in}} - Y_{os}\coth\gamma_s d_1}\right). \tag{3.16}$$

In the air section $Y_{ea} = 0$, and so

$$Y_{\text{in}}^{\text{air}} = Y_{es} = Y_{oa} \tanh \gamma_a d_a. \tag{3.17}$$

Y_{os} and Y_{oa} are given by Equation (3.4) with appropriate dielectric constants. Similarly γ_s and γ_a are given by Equation (3.5). d_1 is the length of the sample and

$$d_a = d_0 + d_s - d_1 \tag{3.18}$$

is the length of the air section. Equations (3.16) and (3.17) define a transcendental equation whose root is the value of the dielectric constant of the sample.

The equation has multiple roots. However, at a low frequency, $d_a/\lambda < 0.03$, the lowest root is appropriate. The root finder routine was Newton-Raphson iteration. The unknown ϵ^* is explicitly in the expression for Y_{os} and γ_s.

Fig. 3.4 shows the block diagram of the experiment. A computer (HP 9153/300) controls the entire experiment. It is connected to the impedance analyzer (HP 4191A), an oven (L&L TB512) and a data logger (Fluke 2240B). The sample holder with the sample is inserted into the oven. A type K thermocouple senses the sample temperature. The data logger measures the temperature and also conveys the information to the computer. Based on the sample temperature, the computer controls the oven. At the appropriate temperatures, it allows the impedance analyzer to measure the input admittance from 1 MHz to 1000 MHz.

Staring at room temperature admittance measurements are made every 25°C up to 300°C. Above room temperature the sample length d_1 must be corrected for thermal expansion, since most dielectrics have large thermal expansion coefficients. The thermal expansion of a conductor at the operating temperatures is negligible. Therefore, d_0 and the electrical length are unchanged throughout the experiment. The sample temperature is increased very slowly, so that there are no significant temperature gradients in the sample.

The samples are 5.08 cm long and machined very carefully so as to fit the sample holder just right.

3.5 SAMPLE HOLDER CONSTANTS AND STANDARD SAMPLES

One of the important design considerations is to maintain a 50Ω characteristic impedance of the sample holder. Fig. 3.5 shows a plot of frequency vs VSWR of the empty sample holder. It has a maximum of 1.10 at about 765 MHz. This is due to the ceramic gas barrier is the adaptor section. The real part of the dielectric constant of the ceramic is high (≈ 9). This increases the reflections at barrier interface. Without the ceramic barrier, the VSWR < 1.05 over the entire frequency range.

Another important consideration is the stability of the electrical length. Any fluctuations in the value of the electrical length during the experiment would render all measurements useless. On repeated determinations of the electrical length of the sample holder, it was found that the length changed by less than ± 0.01 cm over the duration of the experiment. Since the HP 4191A can resolve electrical length up to 0.01 cm, the electrical length of the sample holder is stable over the operating range of frequencies.

The simplest standard sample to measure is air, i.e., an empty sample holder. Strictly, the dielectric constant of air is $\epsilon^*_{\text{air}} = 1 - j0$. For measurement purposes it can be considered

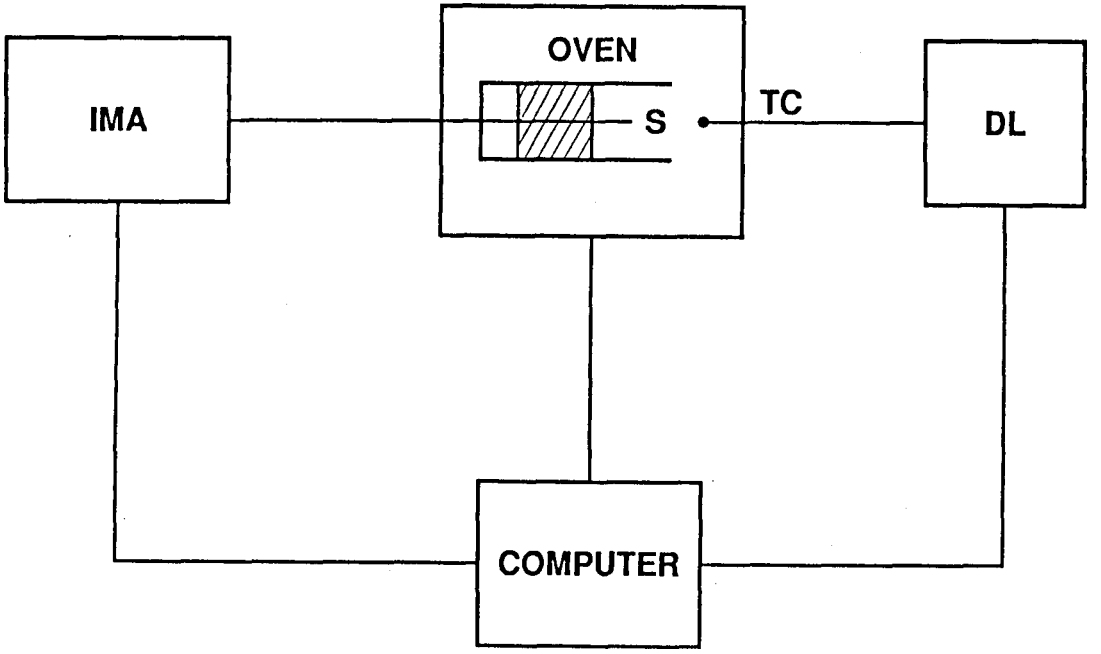

Figure 3.4. Block diagram of the experiment. IMA: Impedance Analyzer, TC: thermocouple, S: Sample Holder, and DL: Datalogger.

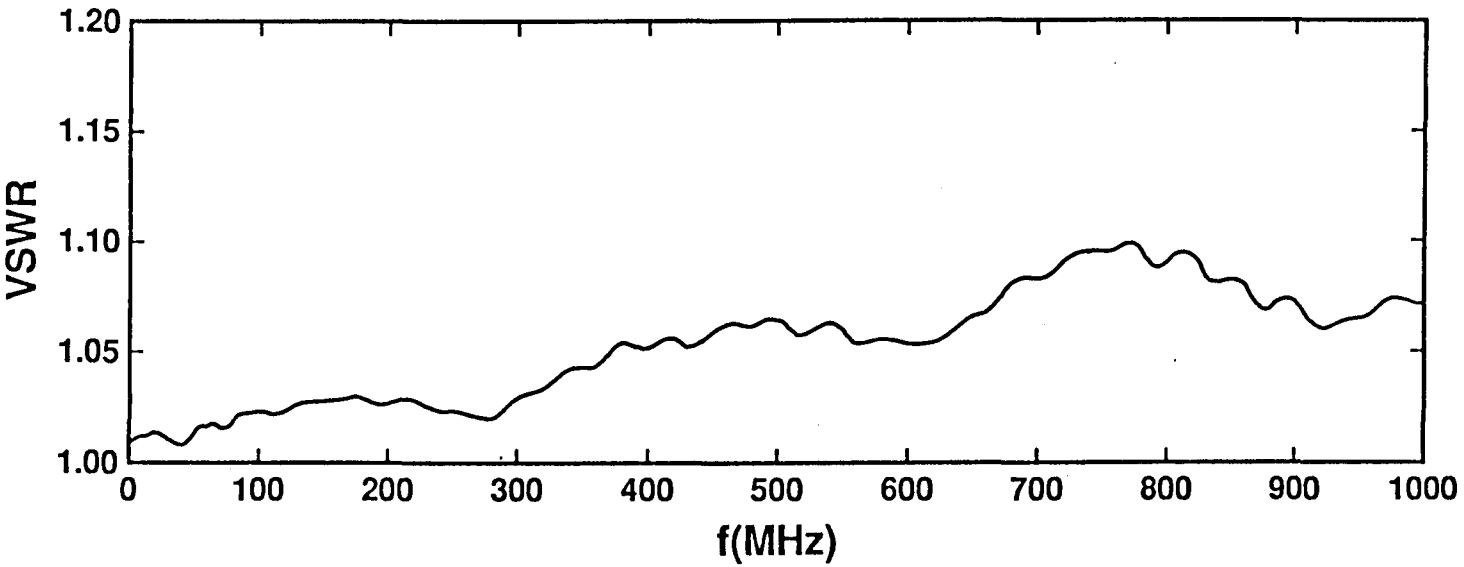

Figure 3.5. Plot of VSWR vs f (MHz) for the empty sample holder.

as $\epsilon^*_{air} = 1 - j0.01$. Fig. 3.6a shows the real part of the dielectric constant of air measured from 1 MHz to 1000 MHz. Fig. 3.6b shows the measured values of imaginary part of the dielectric constant of air. The broken line in both the figures indicate the standard value. Measured values of ϵ'_{air} and ϵ''_{air} are very close to the standard values. ϵ'_{air} deviates by a maximum of 0.19% at 700 MHz. ϵ''_{air} has a maximum value of 0.025 at 900 MHz. These results show excellent agreement with the expected values of ϵ'_{air} and ϵ''_{air}. ϵ''_{air} is so low that it is difficult to measure and consequently there is more scatter in the measured values.

Samples of Teflon and Nylon were fabricated and the real part of their dielectric constant were measured. The dielectric values of these materials are known for a wide range of frequencies [44]. Fig. 3.7 shows a plot of ϵ' and frequency for Teflon at room temperature. The standard value is indicated by the dashed line at 2.1. Fig. 3.8 shows a similar plot for Nylon. The standard value of ϵ' for Nylon is 3.08. For both materials the measured values of ϵ' are within 5% of the standard values. For both samples, $\epsilon' \leq 0.05$ and was hard to measure since they are quite small.

3.6 RESULTS AND DISCUSSION

Two samples were cored from each shale block. One sample was cored such that the shale stratification was perpendicular to the direction of propagation of the incident em wave. The second sample was cored such that the shale stratification was parallel to the direction of propagation. The sample cuts are shown in Fig. 3.9. With two samples the effect of shale anisotropy on the dielectric constant could be measured. In a previous study [45] it was observed that when the incident em wave propagated through the shale layers, there was only a single propagated mode. This mode corresponded to a single medium of propagation whose real part of the dielectric constant was 5.4. When the em wave was incident along the shale layers, various modes were propagated. The medium behaved as if it were composed of a few discrete dielectric layers.

The heating rate utilized in all the experiments was about 1.6°C/min. This time-temperature profile heated the sample from room temperature (25°C) to 300°C in about 3 hours. High quality thermocouples were used to monitor the temperature of the sample throughout the experiment. The blocks from which the samples were cored were analyzed by Fischer assay technique at the Western Research Institute, Laramie, Wyoming for oil and water yields. Table 3.1 shows the results of the analysis.

TABLE 3.1

Oil and Water Yields of Oil Shale & Samples

Sample Designation	Oil Yield		Water Yield	
	L/Kg	gal/ton	L/Kg	gal/ton
W1	0.08	20.0	0.006	1.4
W2	0.14	33.7	0.02	4.5

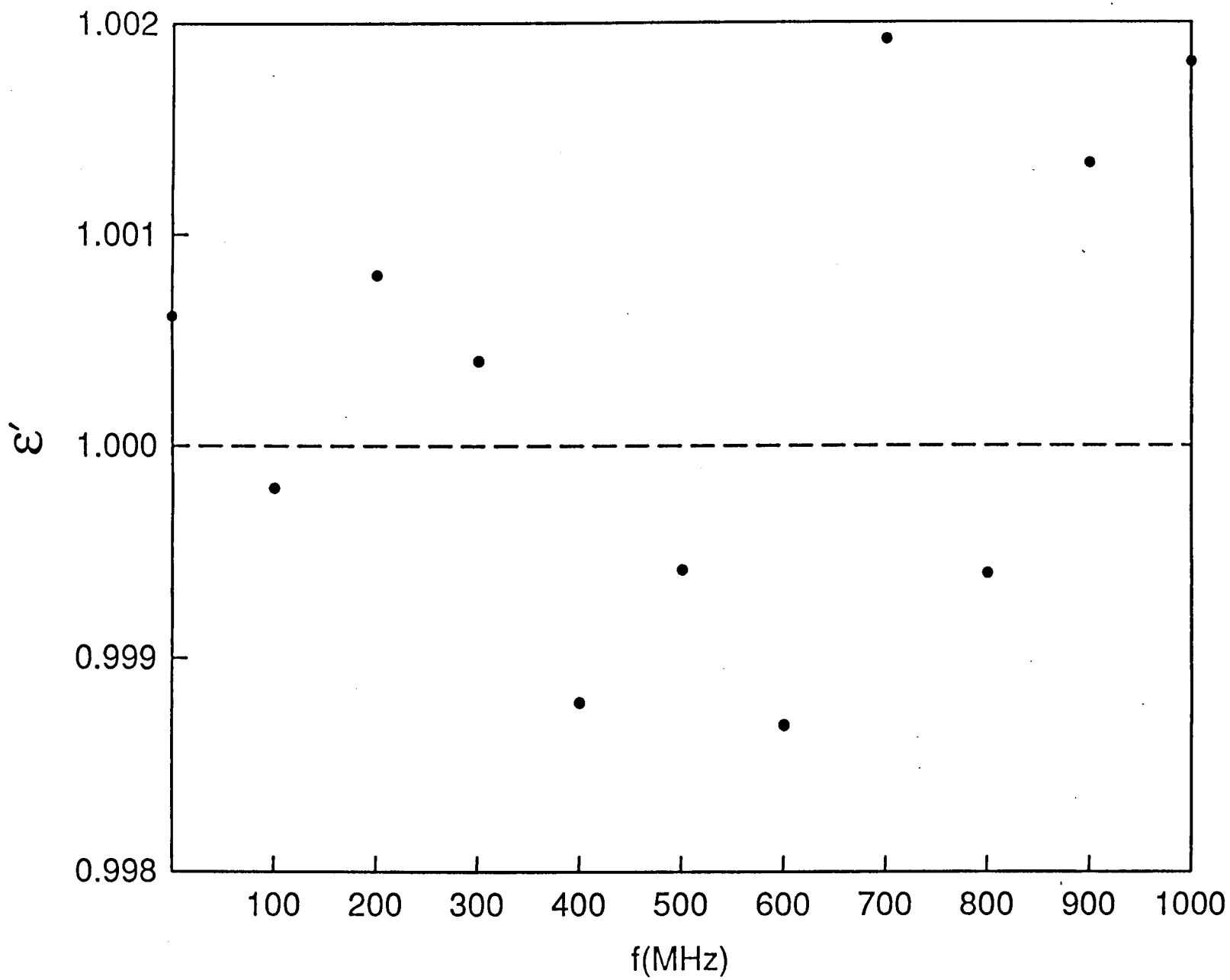

Figure 3.6a. Plot of ϵ' vs f (MHz) for air at room temperature.

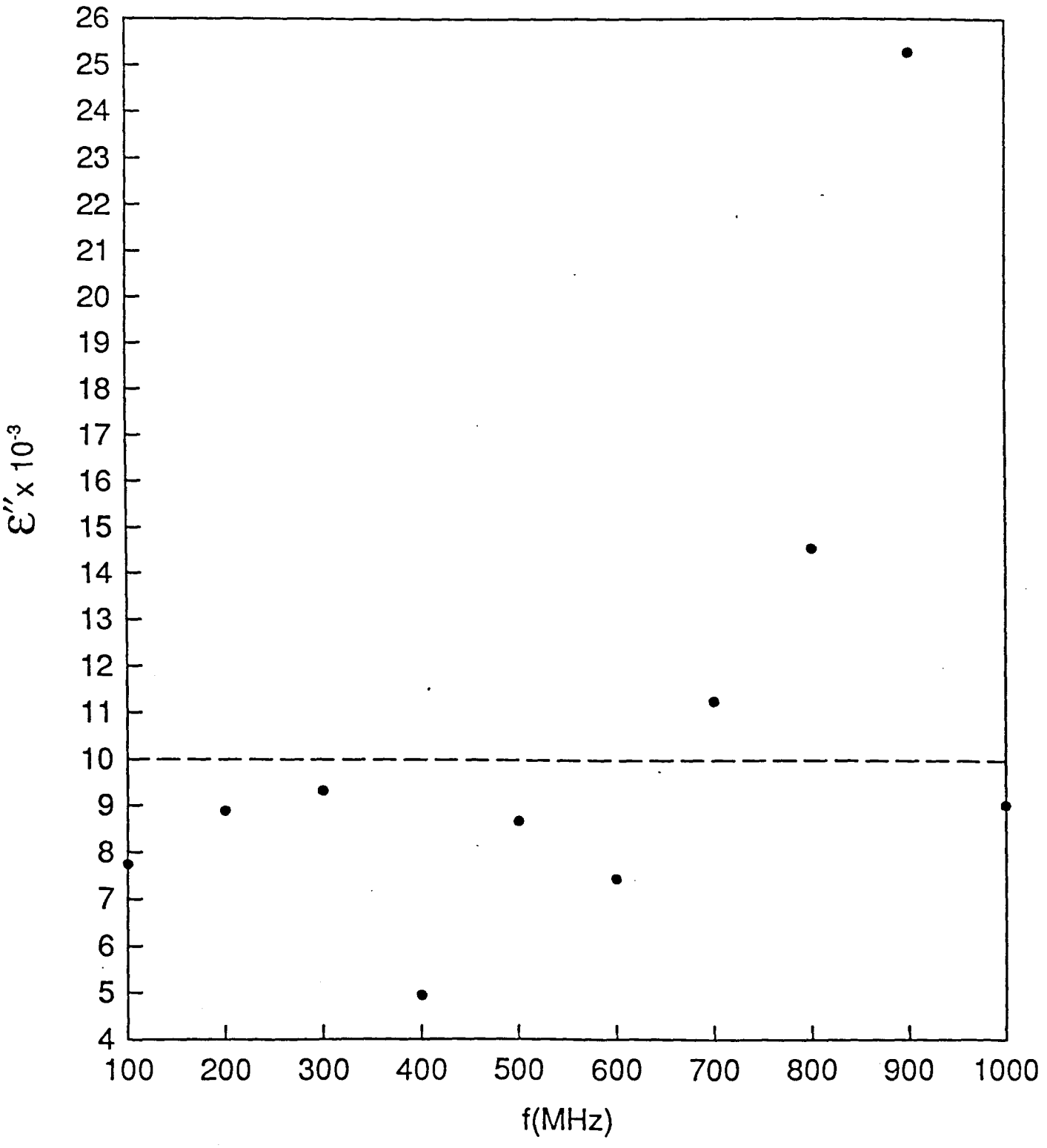

Figure 3.6b. Plot of ϵ'' vs f (MHz) for air at room temperature.

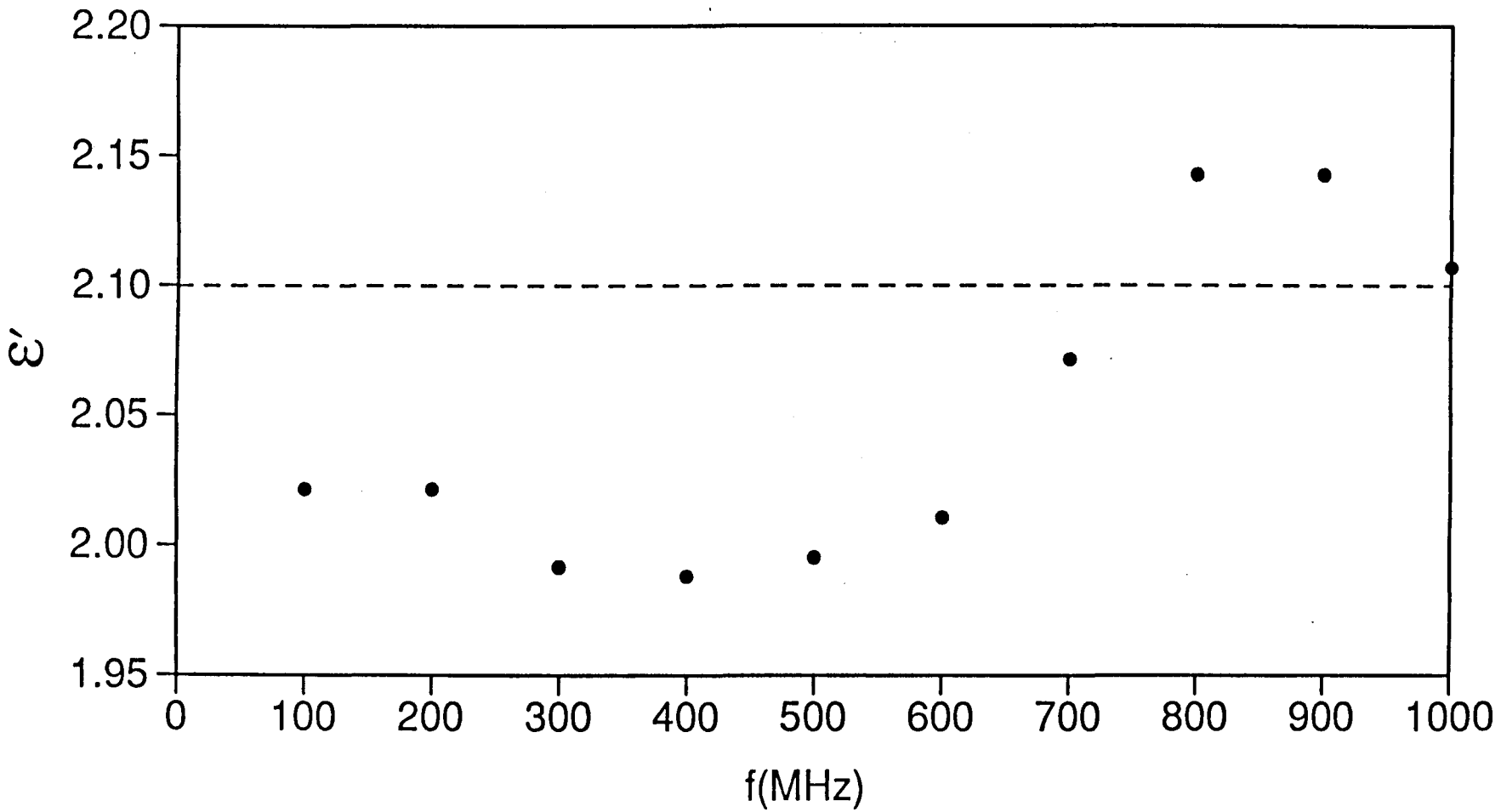

Figure 3.7. Plot of ϵ' vs f (MHz) for teflon at room temperature.

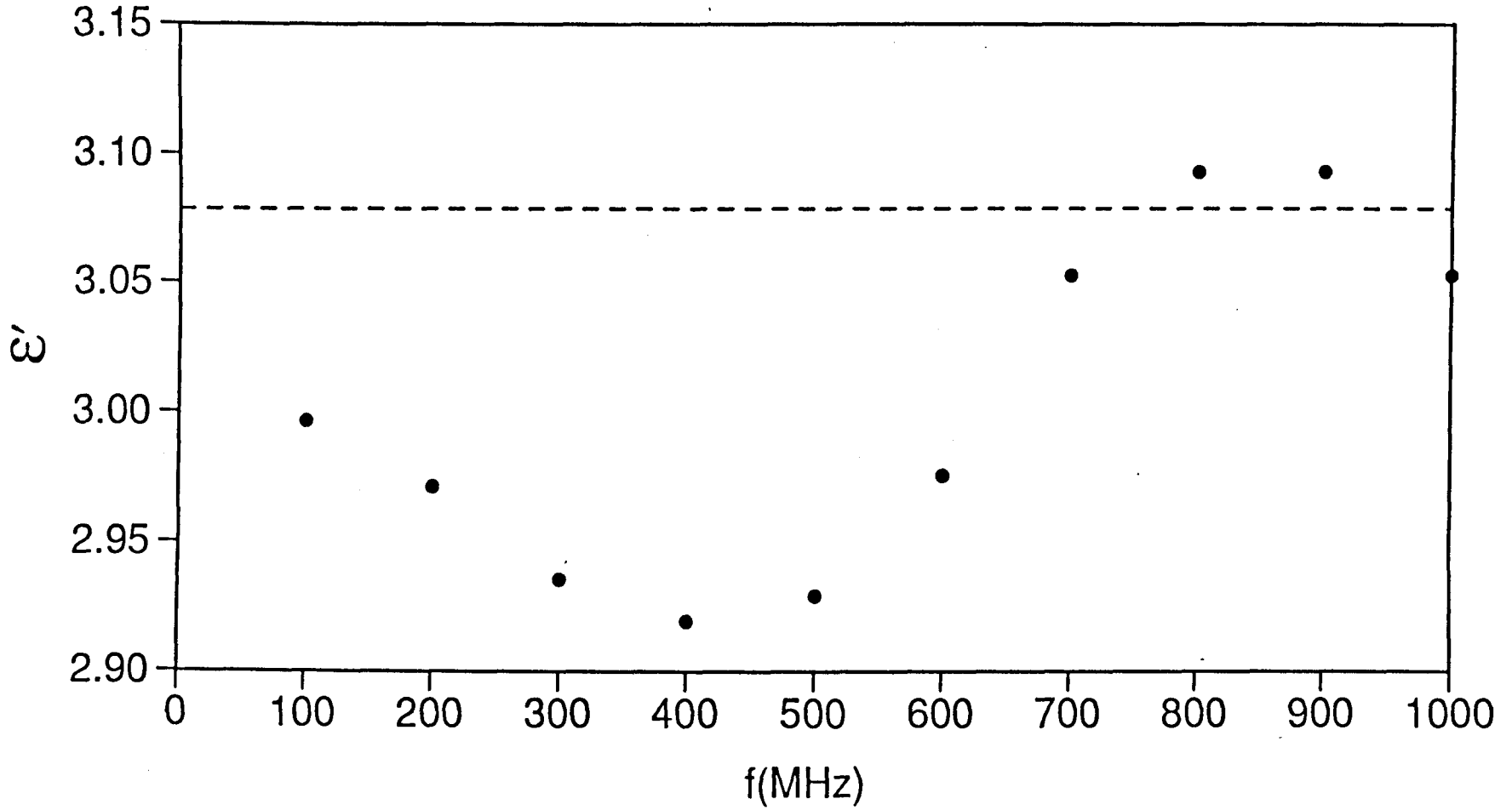

Figure 3.8. Plot of ϵ' vs f (MHz) for nylon at room temperature.

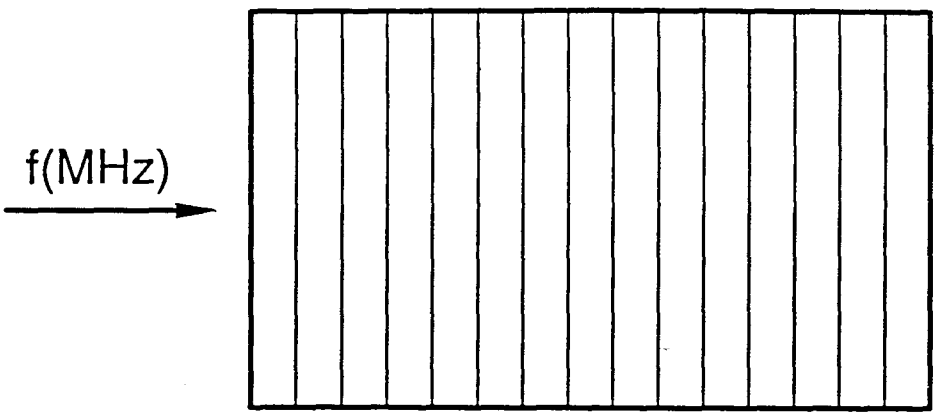

(a) Perpendicular ($\perp$).

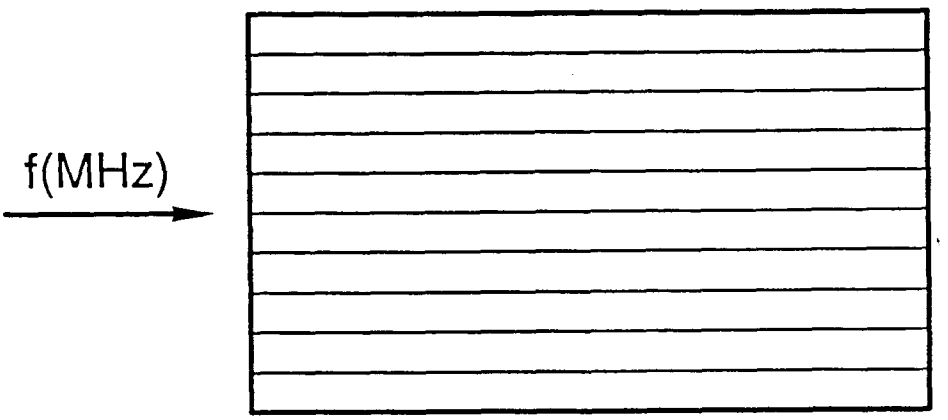

(b) Parallel ($||$).

Figure 3.9. Sample cuts showing shale configuration.

Fig. 3.10a is a plot of ϵ' and temperature for three typical frequencies. ϵ' does not vary much with temperature or frequency. The sample (W1) has very little water and is moderately lean in oil. There is a very slight decrease in the value of ϵ' at $\approx$200°C. The variation of ϵ'' with temperature (Fig. 3.10b) is much more drastic. The value of ϵ'' decreases sharply after $\approx$200°C. The abrupt fall in the value of ϵ'' above 200°C can be associated with the expulsion of water from the shale [33]. Since the water content is low (only 0.6% by weight) the effect is marginal on ϵ'.

Figs. 3.11a and 3.11b show the dielectric behavior of the sample W2 with increasing temperature. This sample is richer in oil and water. The major result of note is that the dielectric values of this sample are higher than sample W1. This result is in contradiction to the observations by Jesch and McLaughlin [33,34]. In their study the dielectric values decreased with increasing oil yield. The expulsion of water from the sample at 200°C is quite apparent. The effect is quite clear even in ϵ' since the percentage loss is larger (1.9% by weight).

The samples described above were the normal perpendicular cut (Fig. 3.9). Fig. 3.12a and 3.12b show the temperature effect on the dielectric constant for sample W1 in the parallel configuration. The anisotropy does not seem to affect much. The dielectric behavior is the same as in Figs. 3.10a and 3.10b. In sample W2 the configuration change seems to alter the dielectric values (Figs. 3.13a and 3.13b). The values are higher by $\approx$5–10% in the parallel cut than those in the perpendicular case (Figs. 3.11a and 3.11b).

Room temperature measurement were conducted on spent oil shale samples. The samples were cored from a block whch had been pyrolyzed by heating with a monopole antenna (see Chapters 1 and 2). The shale block had an oil yield of 0.1 L/Kg. The values of ϵ' and ϵ'' are considerably higher than those of fresh shale of similar oil yield (sample W1) over the entire frequency range (Figs. 3.14a and 3.14b). This result is in accordance with the findings of Jesch and McLaughlin [33,34]. They observed that ϵ' and ϵ'' increased sharply after the onset of pyrolysis ($\approx$400°C). It is quite conceivable that during pyrolysis many chemical reactions occur. Oxidation of materials is probably the major chemical change. This process would form high dielectric constant products in the shale, increasing the dielectric values of the sample.

3.7 CONCLUSIONS

A description of a high temperature sample holder is described along with the measurement technique. Characterization with standard samples show that the sample holder measures the dielectric constant of solids quite well over the frequency range of 1–1000 MHz. The measurement uncertainty is about 5% for ϵ' and about 10% for ϵ'' at all frequencies. Larger sample lengths would provide better results. The best results would be for samples extending beyond the equivalent length describing the admittance of a terminated coaxial transmission line [13].

From the measurement of dielectric constant it is clear that the water content of oil shales has a marked effect on ϵ'', while the kerogen content affects ϵ'. The effect of shale stratification is not very clear. While there is a hint of an anisotropy effect for the 0.14 L/Kg sample, there is inadequate information to draw concrete conclusions. The significant

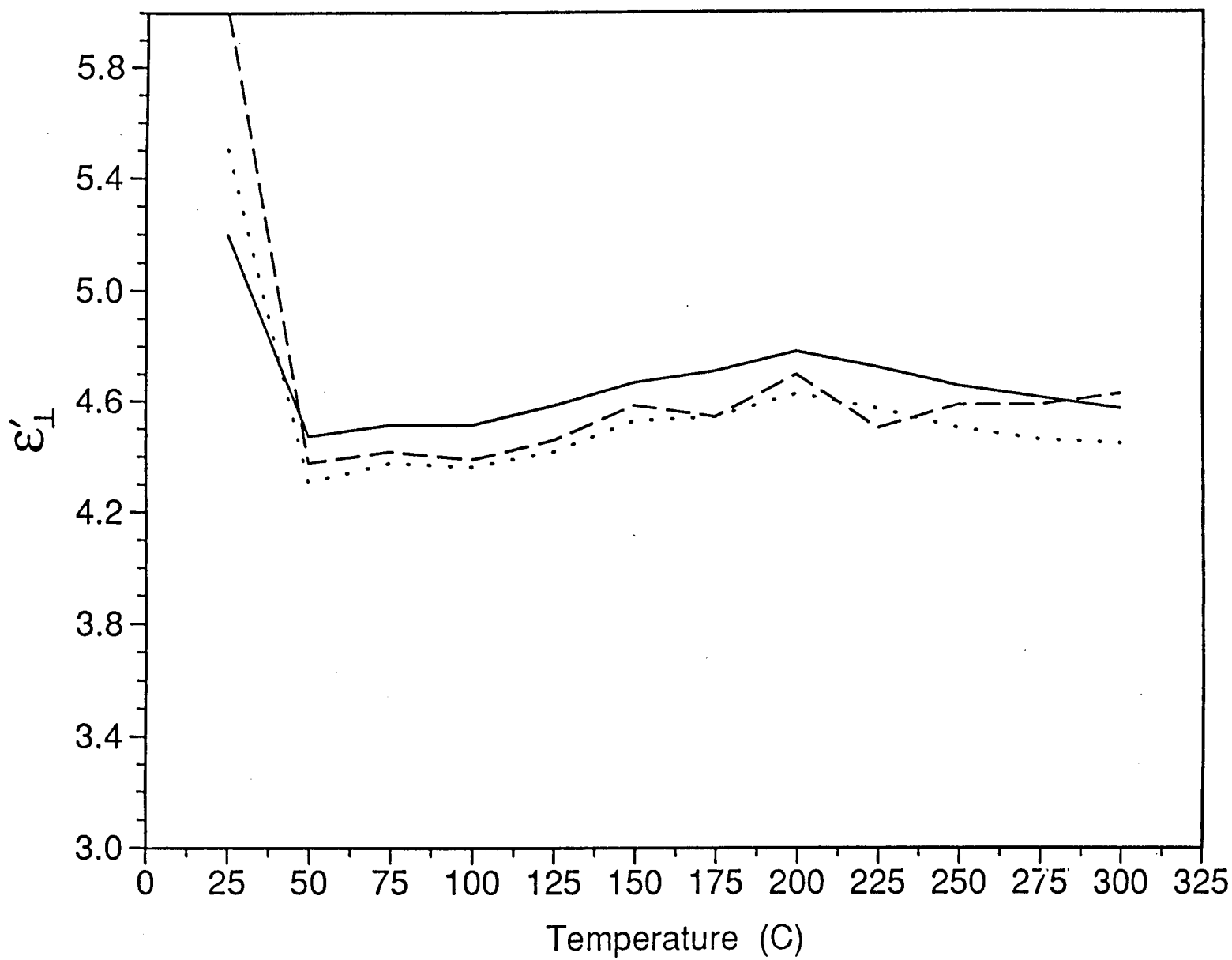

Figure 3.10a. Plot of $\epsilon'_{\perp}$ vs temperature for sample W1 at different frequencies, 300 MHz, 500 MHz and 900 MHz.

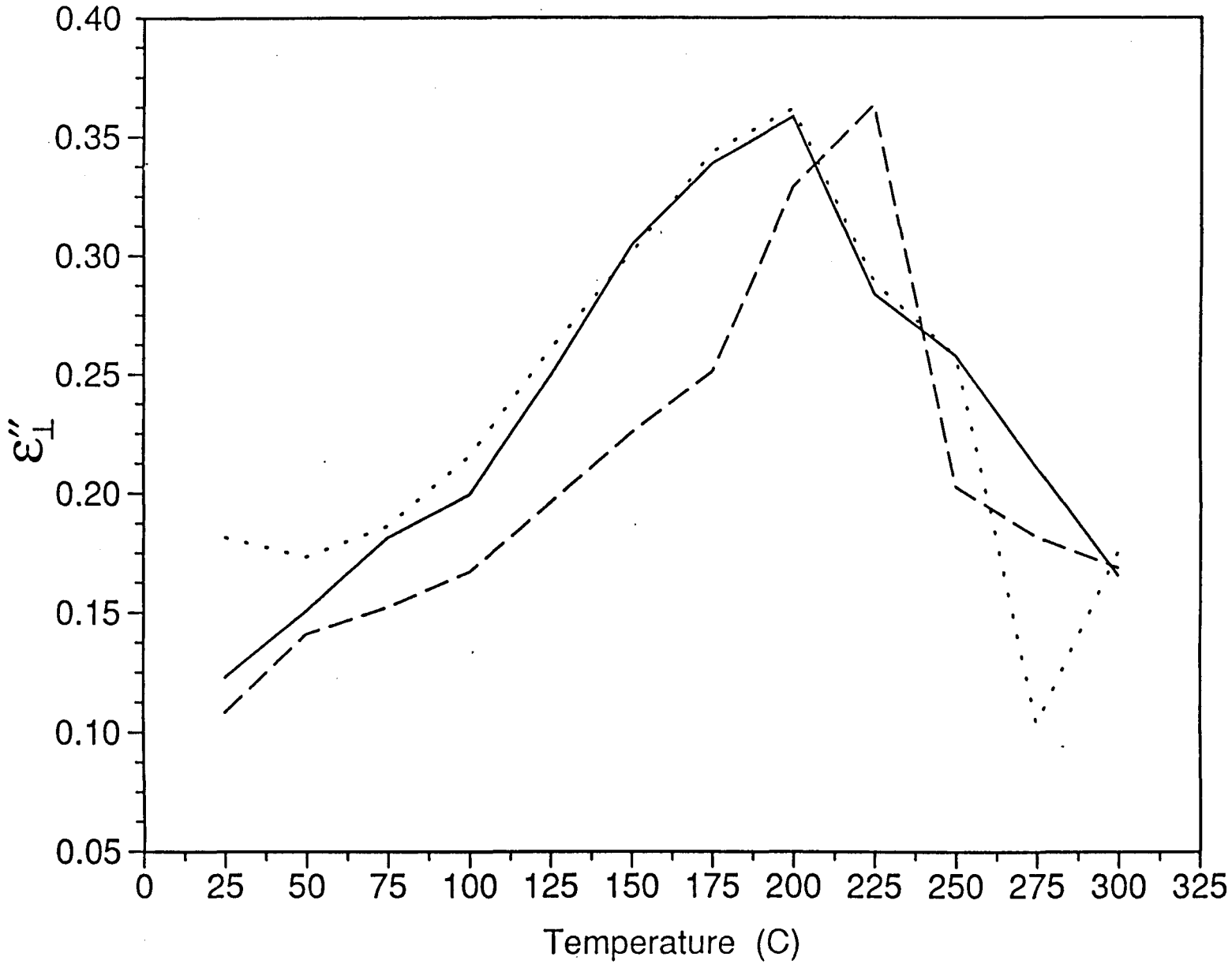

Figure 3.10b. Plot of $\epsilon''_\perp$ vs temperature for sample W1 at different frequencies, 300 MHz, 500 MHz, and 900 MHz.

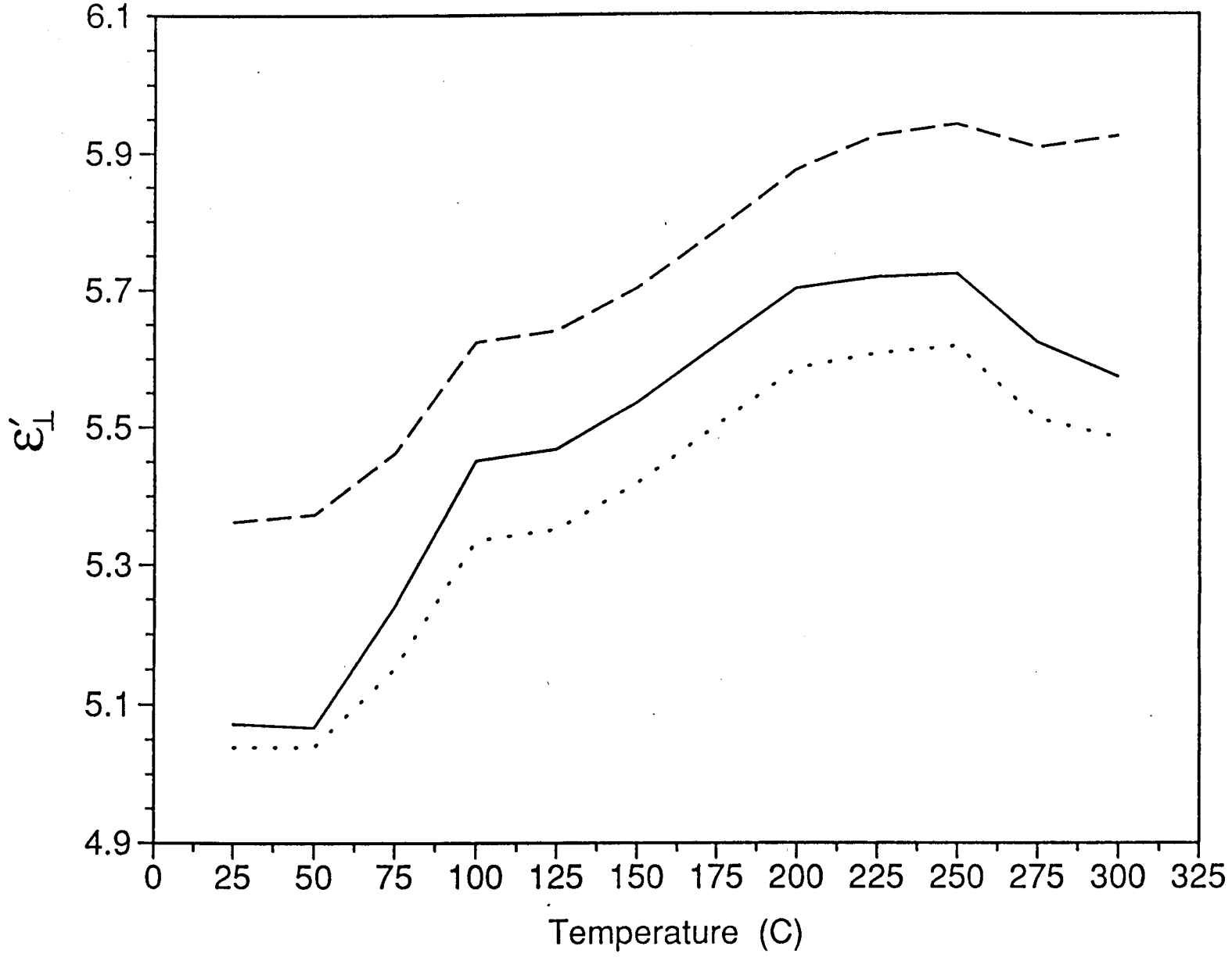

Figure 3.11a. Plot of $\epsilon'_{\perp}$ vs temperature for sample W2 at different frequencies (300 MHz, 500 MHz, and 900 MHz).

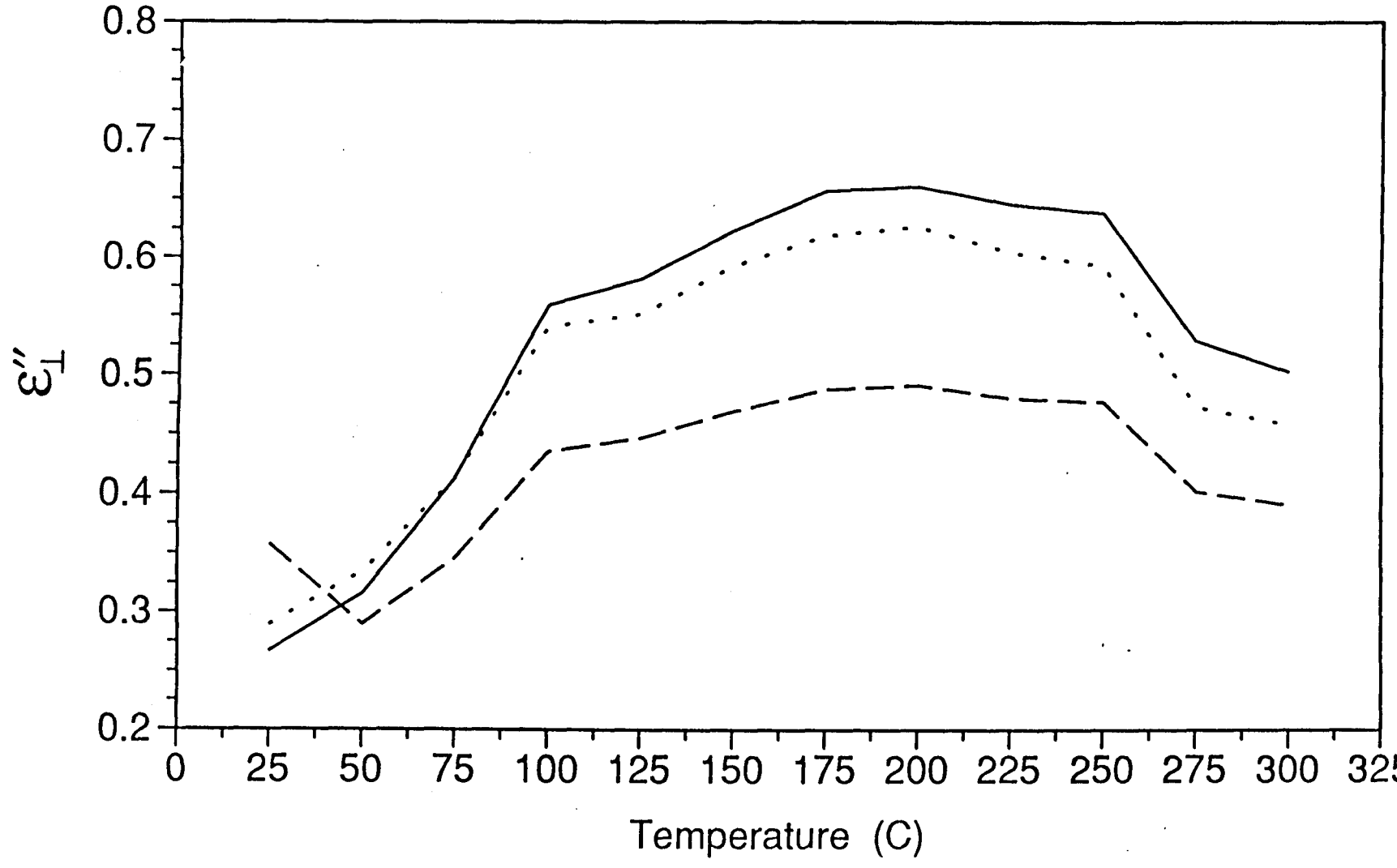

Figure 3.11b. Plot of $\epsilon''_\perp$ vs temperature for sample W2 at different frequencies (300 MHz, 500 MHz, and 900 MHz).

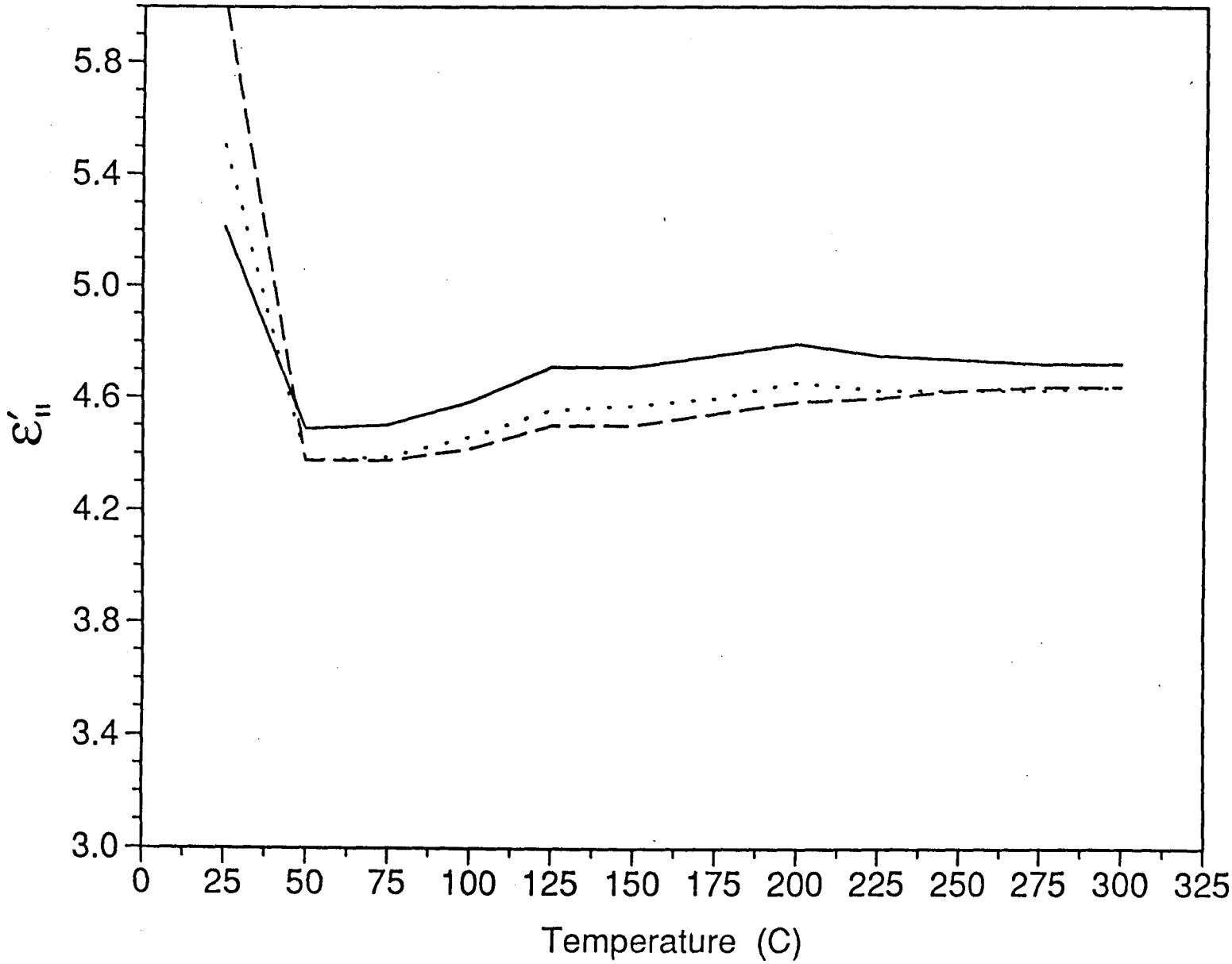

Figure 3.12a. Plot of $\epsilon''_{||}$ vs temperature for sample W1 at different frequencies (300 MHz, 500 MHz, and 900 MHz).

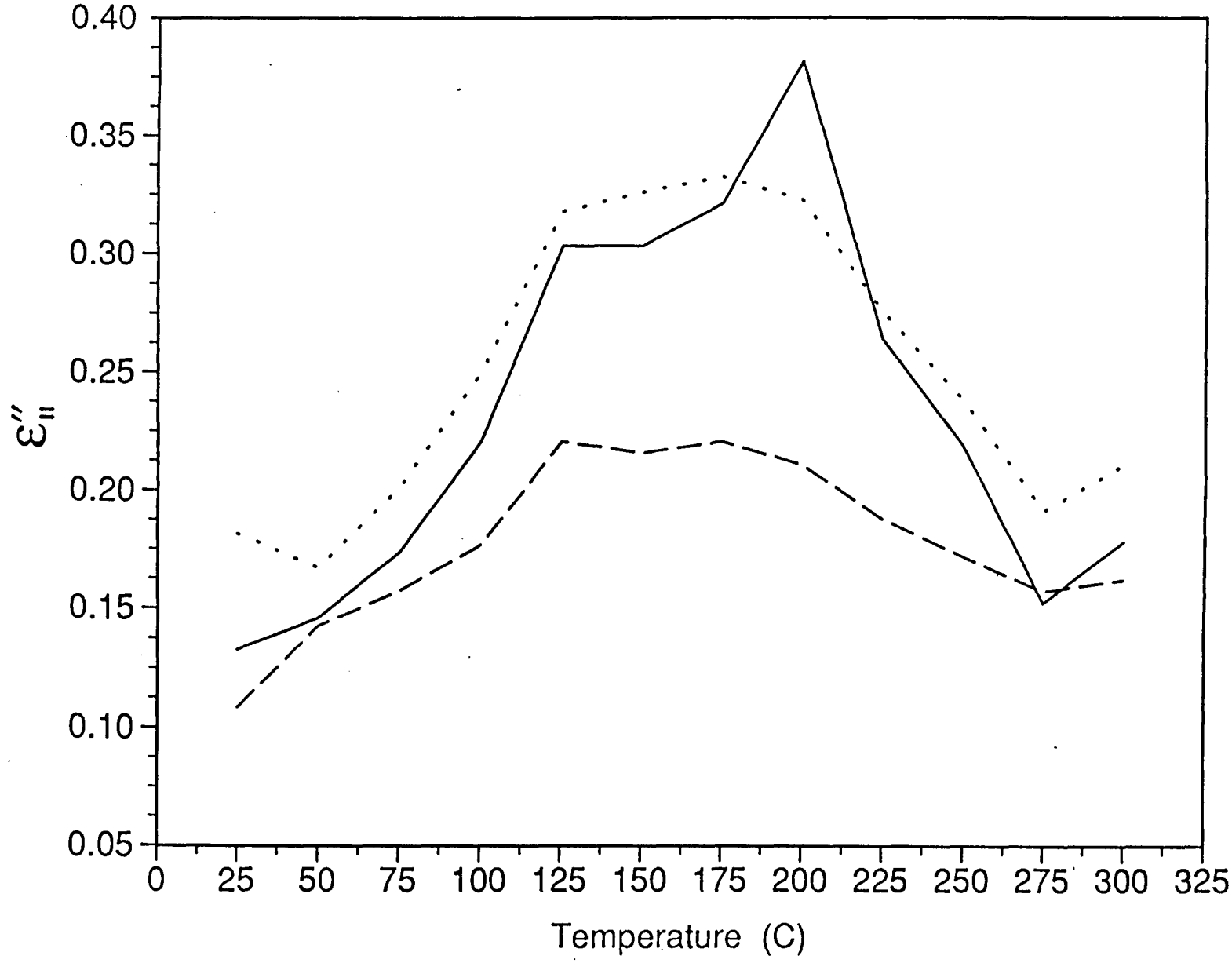

Figure 3.12b. Plot of $\epsilon''_{||}$ for sample W1 at frequencies, 300 MHz, 500 MHz, and 900 MHz.

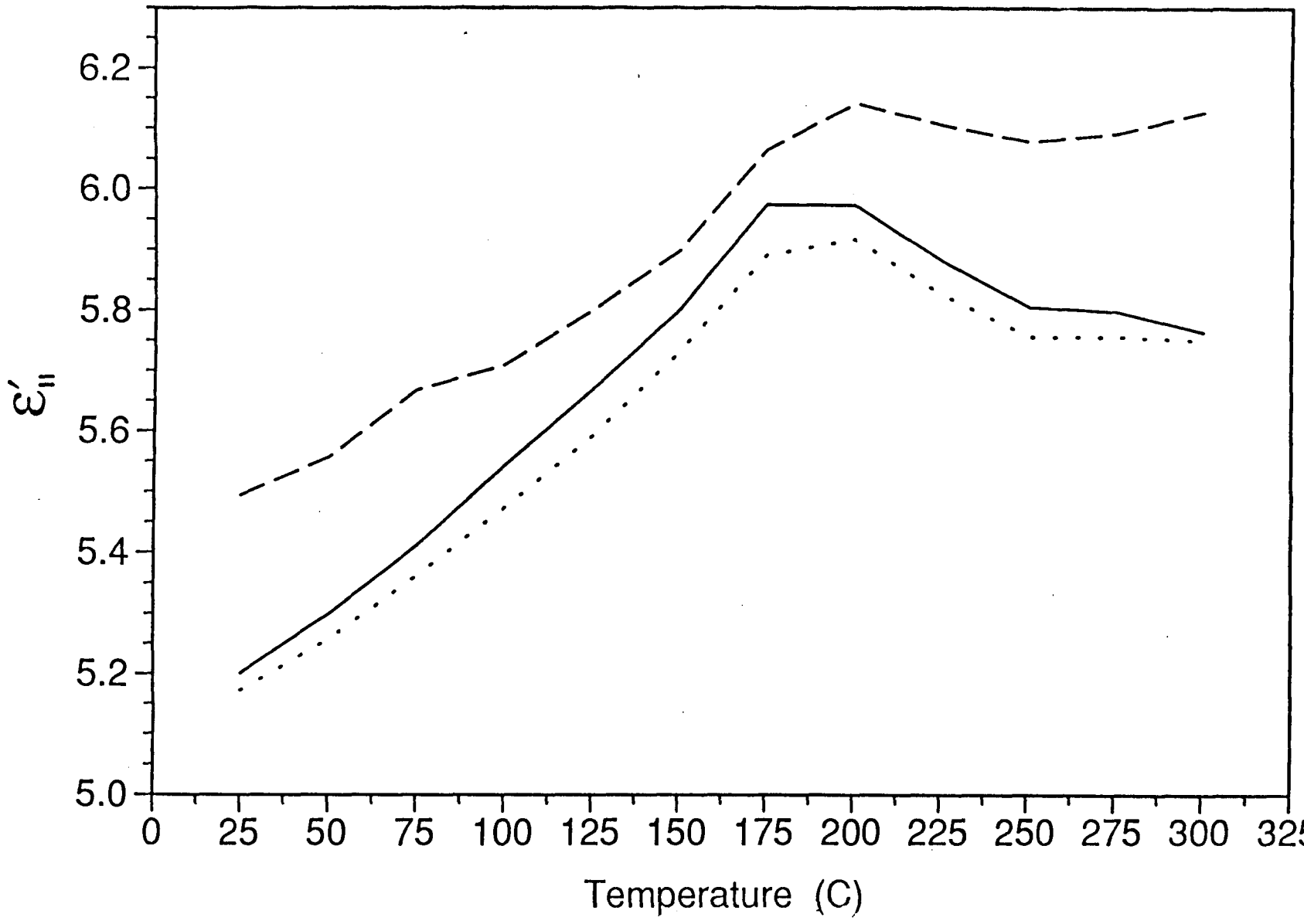

Figure 3.13a. Plot of $\epsilon'_{||}$ vs temperature for sample W2 at frequencies 300 MHz, 500 MHz, and 900 MHz.

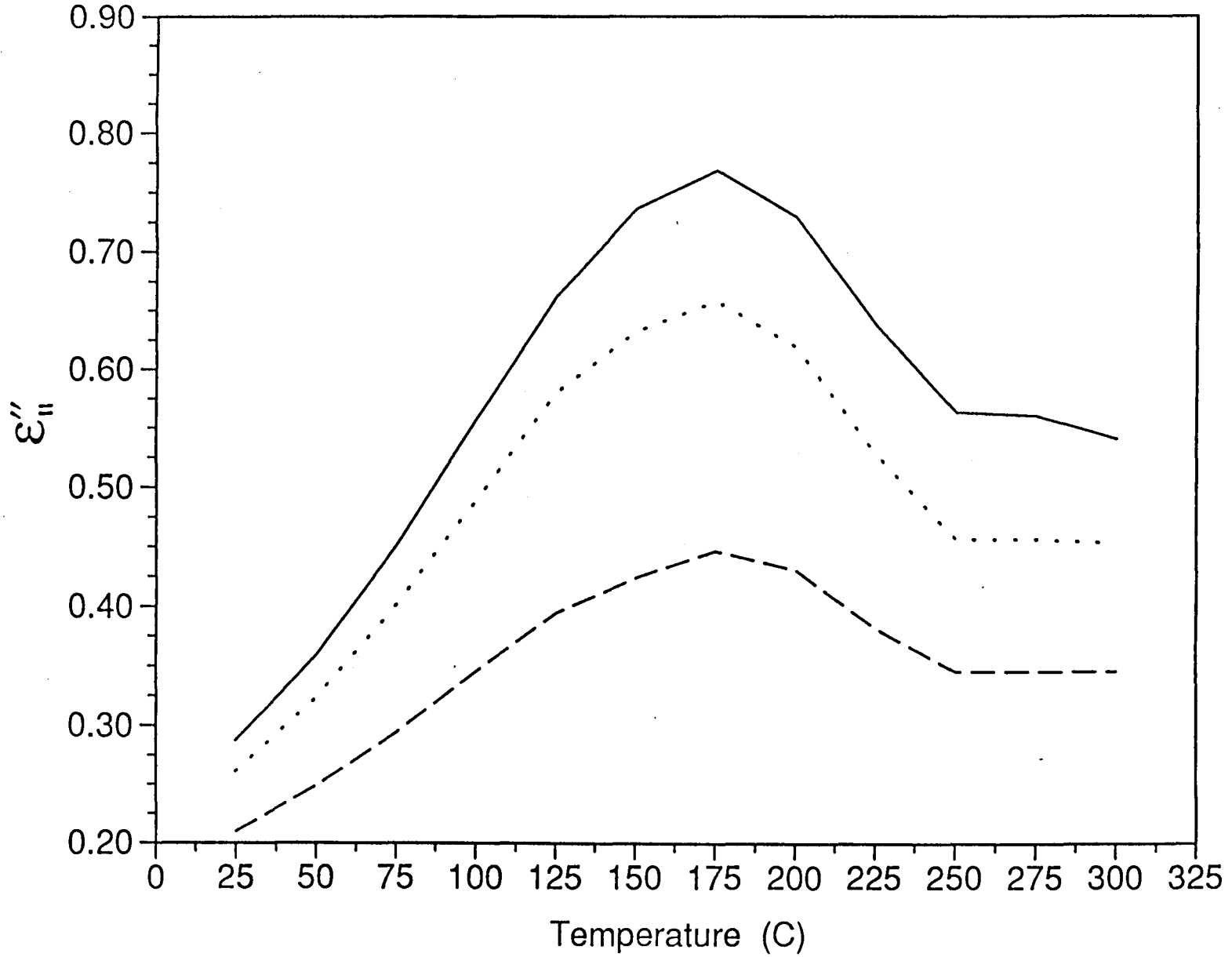

Figure 3.13b. Plot of $\epsilon''_{\parallel}$ vs temperature for sample W2 at frequencies 300 MHz, 500 MHz, and 900 MHz.

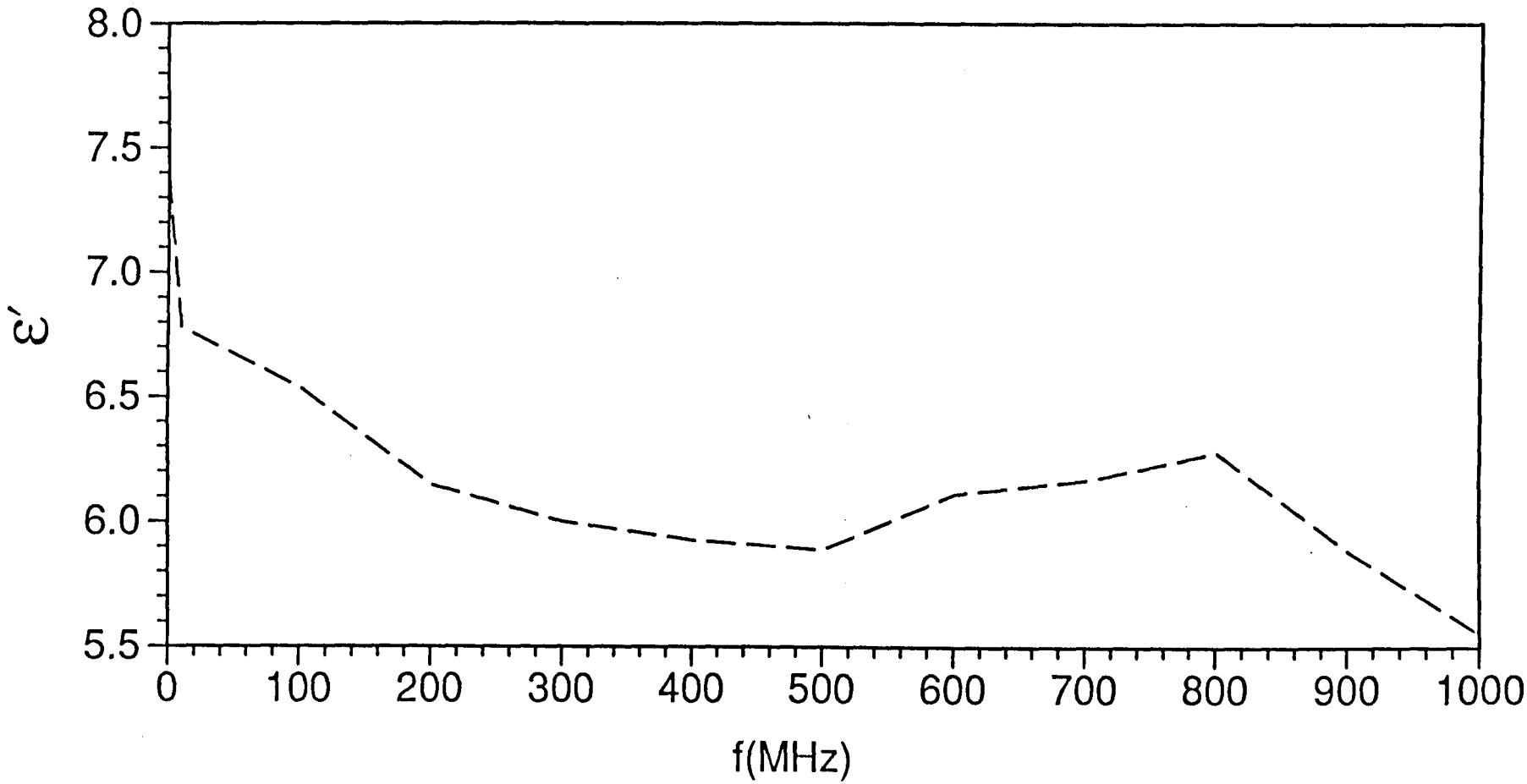

Figure 3.14a. Plot of ϵ' vs f (MHz) for spent shale at room temperature.

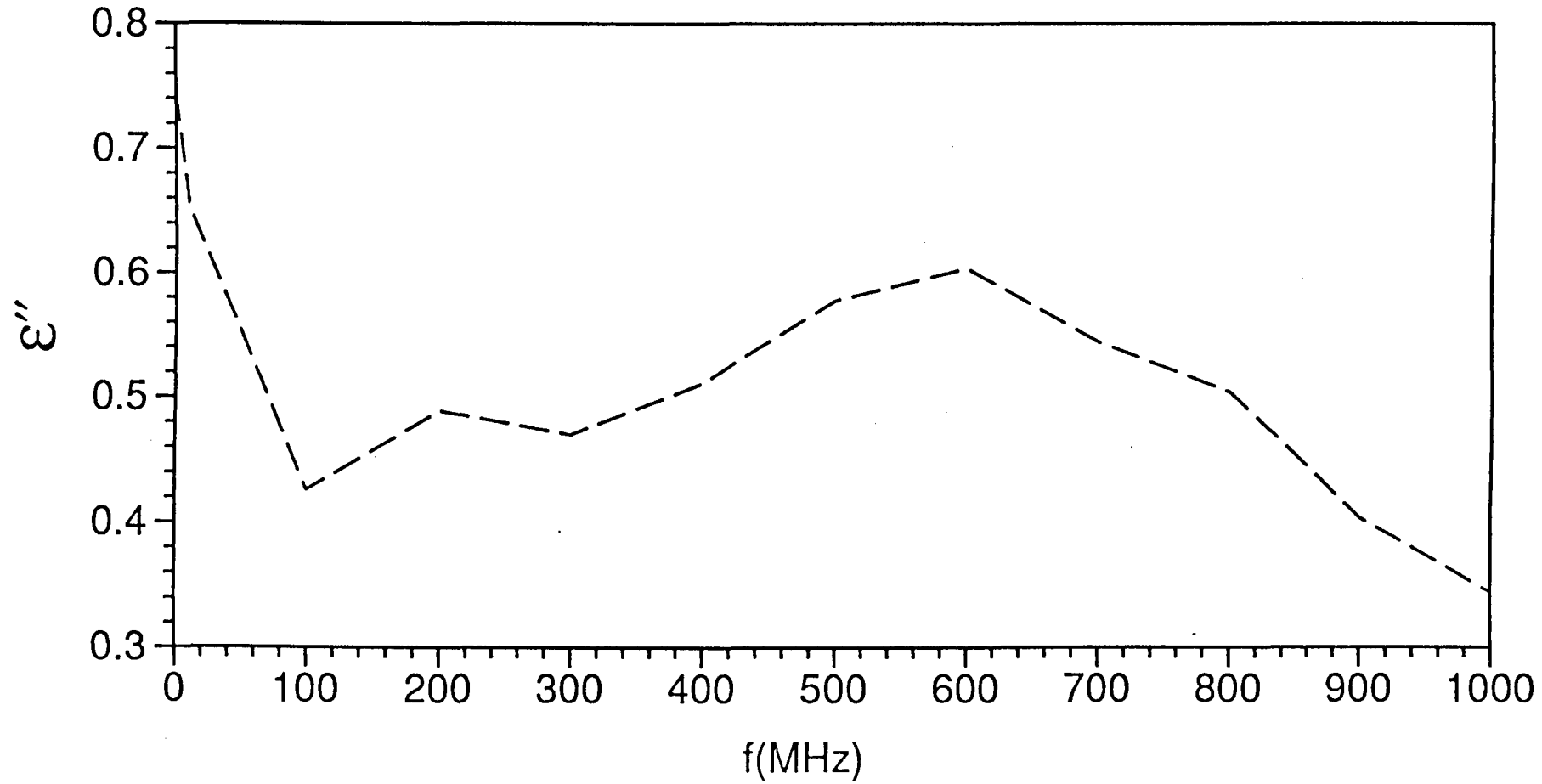

Figure 3.14b. Plot of ϵ'' vs f (MHz) for spent shale at room temperature.

result of the study is that the dielectric constant of oil shales increases with increasing oil yield. This result is not unexpected, since the addition of kerogen and water to the shale rock matrix would increase the dielectric constant of the material.

CHAPTER 4

MEASUREMENTS OF OIL SHALE PERMEABILITY AT HIGH TEMPERATURES AND PRESSURES

CHAPTER SUMMARY

An improved method is presented for measuring the Klinkenberg permeability of oil shales at high temperatures and pressures. The method incorporates unsteady-state technique for speed and accuracy, and the data acquired from various cores has been presented and analyzed.

4.1 INTRODUCTION

It has been determined that calculations of Klinkenberg permeability using the steady-state technique is slow and can also lead to serious errors. Klinkenberg permeability of tight cores like oil shales can have an error of 40 to 80 percent or more using the conventional technique and hence the unsteady state method has been used. The theory of operation has been adapted and developed from the theory presented by S.C. Jones [46] and various cores were tested for permeability. The equipment calibration was done using sandstone cores and the following three methods were adopted:

A. Frank Jones Method.

B. Conventional Steady-State Technique

C. Unsteady-State Technique

4.2 THEORETICAL ANALYSIS

The gas used in the system is Nitrogen which is chemically inert with respect to the core. Nitrogen at pressures such as 300–400 psi is passed through the core and the pressure decline characteristics with respect to time are plotted.

The volumetric flow rate of Nitrogen is proportional to the number of moles of Nitrogen flowing through the cross-section under consideration per unit time.

$$q_0(t) = \frac{M}{\rho(t)}\left[-\frac{dn}{dt}\right] \tag{4.1}$$

where $q_0(t)$ = flow rate at the inlet face of the core expressed as a function of time only in ml/sec, n = no. of moles, and $\rho(t)$ = gas density at the inlet face of the core in gm/ml. The negative sign indicate the decrease in number of moles as time increases. Since

$$pV = nRT \qquad \ldots \text{general gas law}$$

$$\frac{dn}{dt} = V\frac{dp}{dt}.$$

For a certain inlet pressure p_0

$$\frac{dn}{dt} = \frac{V_t}{RT}\left[\frac{dp_0}{dt}\right], \qquad V_t \rightarrow \text{ volume of a storage reservoir}$$

$$p_0 \rightarrow \text{ is in psig.}$$

Substituting this in Equation (4.1) we have

$$q_0(t) = \frac{-MV_t}{\rho(t)RT}\left[\frac{dp_0}{dt}\right]. \tag{4.2}$$

Also from

$$p_0V = nRT$$

we have

$$\begin{aligned} p_0 V &= \frac{m}{M} RT \\ m &= \text{mass of gas in gm} \\ M &= \text{molecular weight of Nitrogen (gm/gm mol)} \\ \frac{m}{V} &= \rho(t) = \frac{M}{RT} p_0(t) \quad \ldots \text{expressed as a function of time.} \end{aligned}$$

Hence Equation (4.2) can be written as

$$q_0(t) = -\frac{V_t}{p_0(t)} \frac{dp_0}{dt}. \tag{4.3}$$

The assumption that gas flow rate is not a function of its position throughout the length of the core is not entirely correct, hence, we express q_0 as

$$q_0(x,t) = -\frac{V_t}{p(x,t)} \frac{dp_0}{dt}.$$

Assuming Darcy flow in one dimension only, we express q_0 in terms of Darcy's law

$$q_0(x,t) = -\frac{V_t p_0'(t)}{p(x,t)} = -\frac{K_\ell A \left(1 + \frac{b}{p(x,t)}\right)}{\mu} \times \frac{\partial p(x,t)}{\partial x}$$

where

$$\begin{aligned} p_0'(t) &= \frac{dp_0}{dt} \\ b &= \text{slip factor} \\ \mu &= \text{viscosity of Nitrogen} \\ (1 + b/p(x,t)) &= \text{correction factor} \\ K_\ell &= \text{Klinkenberg Permeability} \end{aligned}$$

The above equation can also be written as

$$-\frac{V_t \mu p_0'(t) \partial x}{K_\ell A} = (p(x,t) + b)\partial p(x,t).$$

Integrating

$$-\frac{V_t \mu p_0'(t) L}{K_\ell A} = \frac{(p_\ell(t)^2 - p_0(t)^2)}{2} + b(p_\ell(t) - p_0(t))$$

where $p_\ell(t)$ = outlet pressure as a function of time.

Multiplying both sides by $2/(p_\ell(t) - p_0(t))$ we get

$$-\frac{2V_t \mu p_0'(t) L}{K_\ell A(p_0(t) - p_\ell(t))} = p_\ell + p_0 + 2b. \tag{4.4}$$

Expressing pressures in terms of psig and permeabilities in terms of mD instead of Darcies, we have $p_\ell = 0$ psig. Therefore

$$-\frac{V_t p_0'(t)}{p_0(t)} = \frac{K_\ell A}{(2000)14.69\mu L}\ [p_0(t) + 2(p_a + b)] \tag{4.5}$$

where

$$14.69 = \text{std. atmospheric pressure}, \quad p_a = \text{atmospheric pressure}.$$

We can write Equation (4.5) as

$$y = -\frac{V_t p_0'(t)}{p_0(t)} = i + m p_0(t). \tag{4.6}$$

Now y can be evaluated from two discrete values of p_1 and p_2 taken at times t_1 and t_2. Subsequent integration and multiplication by $(p_g + i/m)$

$$-\left(\frac{V_t i}{m}\right) \ln \frac{p_1\left(p_2 + \frac{i}{m}\right)}{p_2\left(p_1 + \frac{i}{m}\right)} = m(t_2 - t_1). \tag{4.7}$$

Since $\frac{i}{m}$ is unknown, above two equations are combined to give

$$-\frac{V_t p_0'(t)}{p_0(t)} = m\left(p_0(t) + \frac{i}{m}\right) = \frac{V_t\left(p_0(t) + \frac{i}{m}\right)}{(t_2 - t_1)\left(\frac{i}{m}\right)} \times \ln \frac{p_1\left(p_2 + \frac{i}{m}\right)}{p_2\left(p_1 + \frac{i}{m}\right)}. \tag{4.8}$$

The RHS of the equation for any value p_0 between p_1 and p_2 is insensitive to the value of $\frac{i}{m}$ used. Jones [46] determined this value of $\frac{i}{m}$ to be between 24 to 70 psi. Within this range p_0 is equal to the geometric mean of p_1 and p_2

$$p_0 = p_g = (p_1 p_2)^{\frac{1}{2}}. \tag{4.9}$$

Jones [46] points out that for an arbitrary value of 30 psi for $\frac{i}{m}$, the error is 0.1%. Simplifying, the equation becomes

$$y(p_g) = i + m p_g(t) \tag{4.10}$$

where

$$y(p_g) = \frac{V_t p_g'(t)}{p_g(t)} \tag{4.11}$$

$$m = \frac{K_\ell \times A}{29390\mu L} \tag{4.12}$$

where

A = cross-sectional area of core in cm^2

L = length of core in cm

μ = viscosity of Nitrogen in cp

K_ℓ = Klinkenberg permeability in mD.

4.3 EXPERIMENTAL SET-UP AND PROCEDURE (FIG. 4.1)

1. Nitrogen is passed under high pressure from the main cylinder to reservoir (capacity 1000 cc). The pressure is controlled by the pressure regulator safety valve.
2. The furnace is programmed to fire according to the previously determined temperature-time profile. The furnace increases the temperature to a certain set point similar to the one shown in Fig. 4.2 and holds it at that particular temperature for a predetermined amount of time. The process of increasing the temperature between two set points is termed as ramping while holding temperature at a particular set point is called soaking. Hence the profile is called RAMP and SOAK profile.
3. This gas now stored in the reservoir is then released to the core and the pressure decline data is recorded on the calibrated data logger as well as on a back-up pressure gauge. The data is transferred to the data logger via a pressure transducer.
4. For the steady measurement, a flow meter was also incorporated to measure the flow rate of the exiting gas.
5. The by-pass system has been incorporated to ensure the safety for the cores in case of accidental pressure overloads.
6. The modifications done to account for the high temperature and pressure runs include:
   (a) Special core holders were designed for extreme temperature operation.
   (b) The gas reservoir is in the furnace so that the gas is at a uniform temperature when it enters the core. This eliminates errors due to cooling.
   (c) High temperature rubber sleeves were used to ensure proper sealing of the core.
   (d) All threads need to be coated with anti-seize and silicone compounds.
7. Two computer programs convert all the data into values from which the Klinkenberg permeability may be calculated.

Parameters Measured

1. Inlet Pressure
2. Outlet Pressure
3. Furnace Temperature
4. Ambient Temperature
5. Gas Flow Rate
6. Time

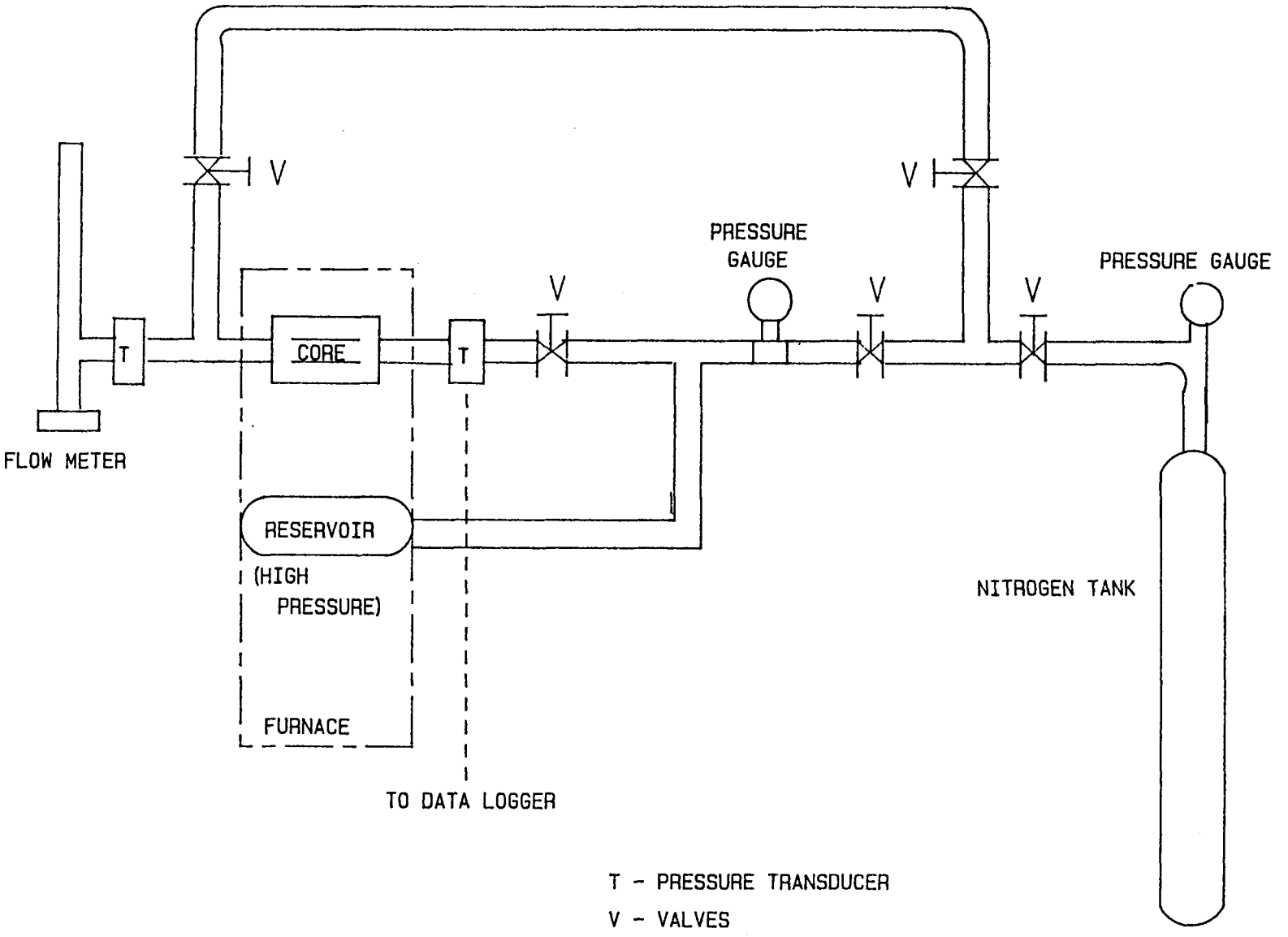

Figure 4.1. Schematic pulse decay technique.

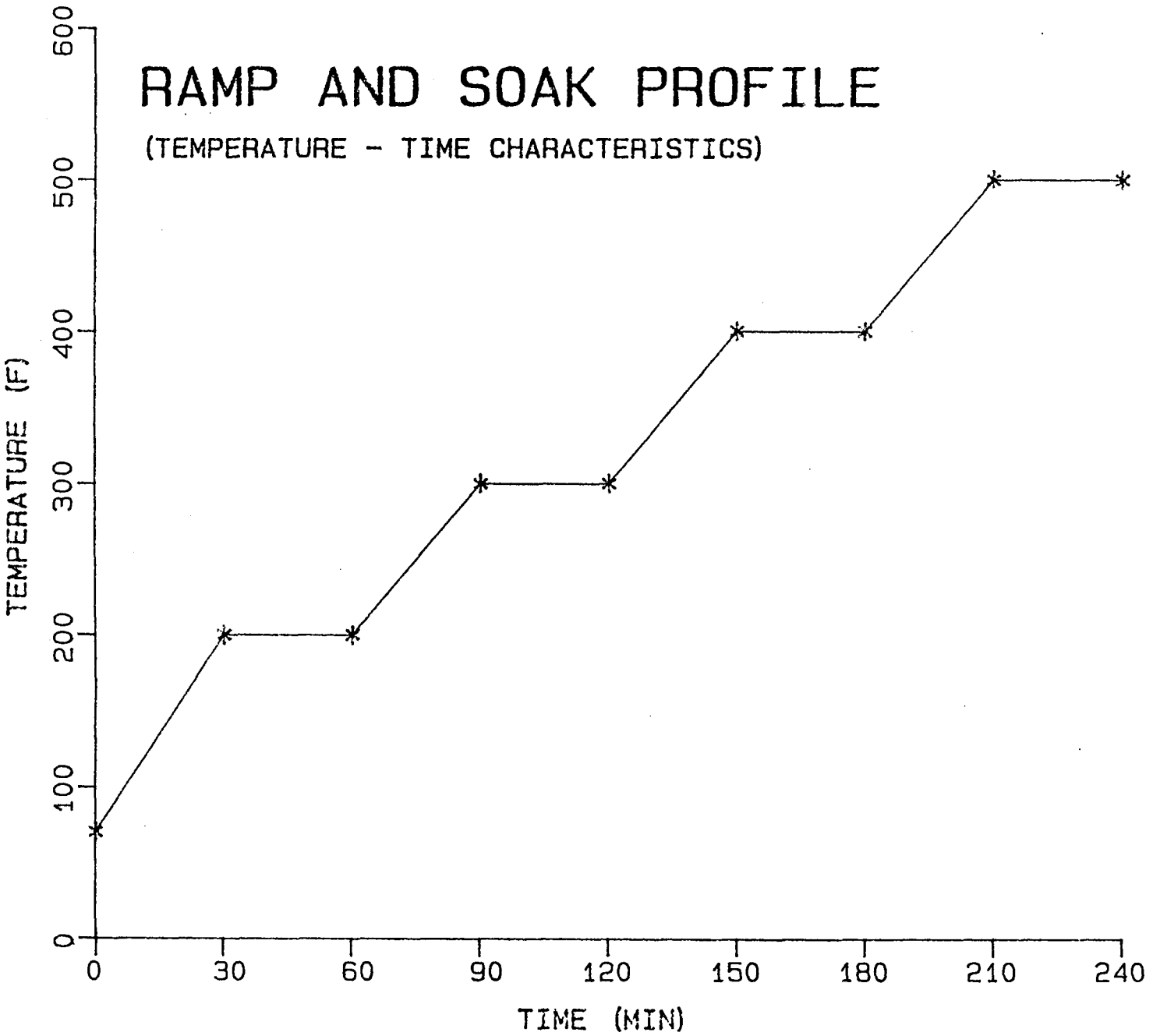

Figure 4.2. Ramp and soak profile: Temperature-time characteristic.

Data from the logger is converted into a pressure-time plot (Fig. 4.3).

Two discrete points in the P–t plot are used to calculate the value of Y of Equation (4.11) and another Y versus pressure plot obtained which is a straight line after linear regression (Fig. 4.4). Y refers to the calculated value $Y(p_g)$ in Equation (4.11).

Klinkenberg permeability is calculated from the slope of this line as:

$$K_\ell = \frac{29,390 \times \mu \times \ell \times m}{A}$$

where

μ = viscosity of Nitrogen corrected for temperature (cp)

ℓ = length of the core (cm)

K_ℓ = Klinkenberg permeability in mD

m = slope of the line

A = cross sectional area of the core (cm^2)

4.4 RESULTS

A. Calibration Results (Using Sandstone):

Temperature = 70°F, Pressure = 350 psi

Permeability	Core 1	Core 2	Core 3	Core 4
Unsteady State	153.1	108	82.4	312.5
Frank Jones	132.0	94.2	72.8	584.0
Length	4.54	4.5	3.52	5.2
Diameter	2.53	2.5	2.51	2.51

All permeabilities in mD and all dimensions in cm.

B. Oil Shale Permeability Results (Example):

Oil shale experimental runs were carried out in two ways:

1. *Intermittent.* The intermittent run was performed as follows: The core was heated using the temperature-time profile similar to the one shown in Fig. 4.2. The core is sealed in the holder (Fig. 4.5) and the furnace is programmed to increase the temperature in steps and hold it at that temperature for a certain predetermined amount of time.

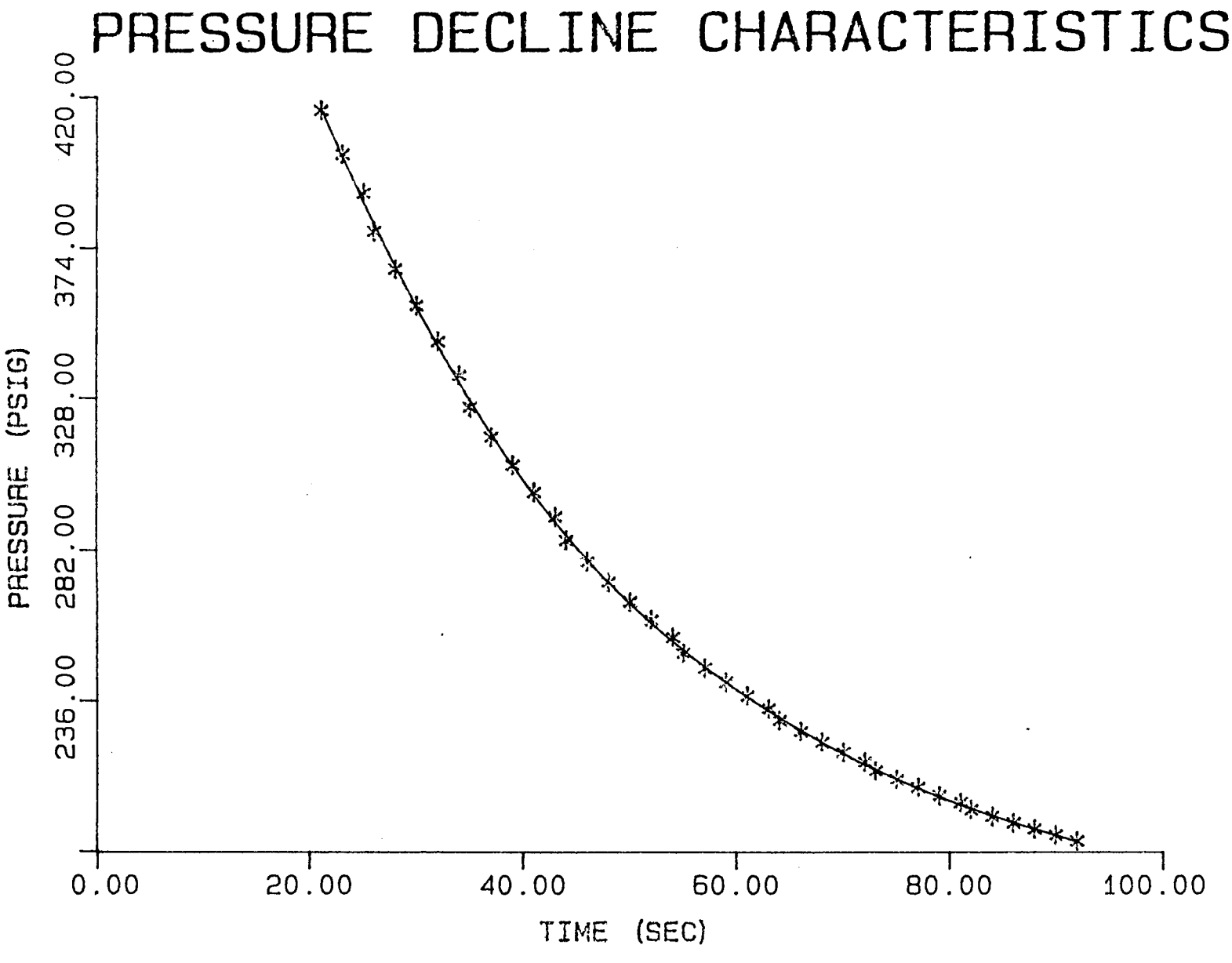

Figure 4.3. Pressure decline characteristic (pressure vs time).

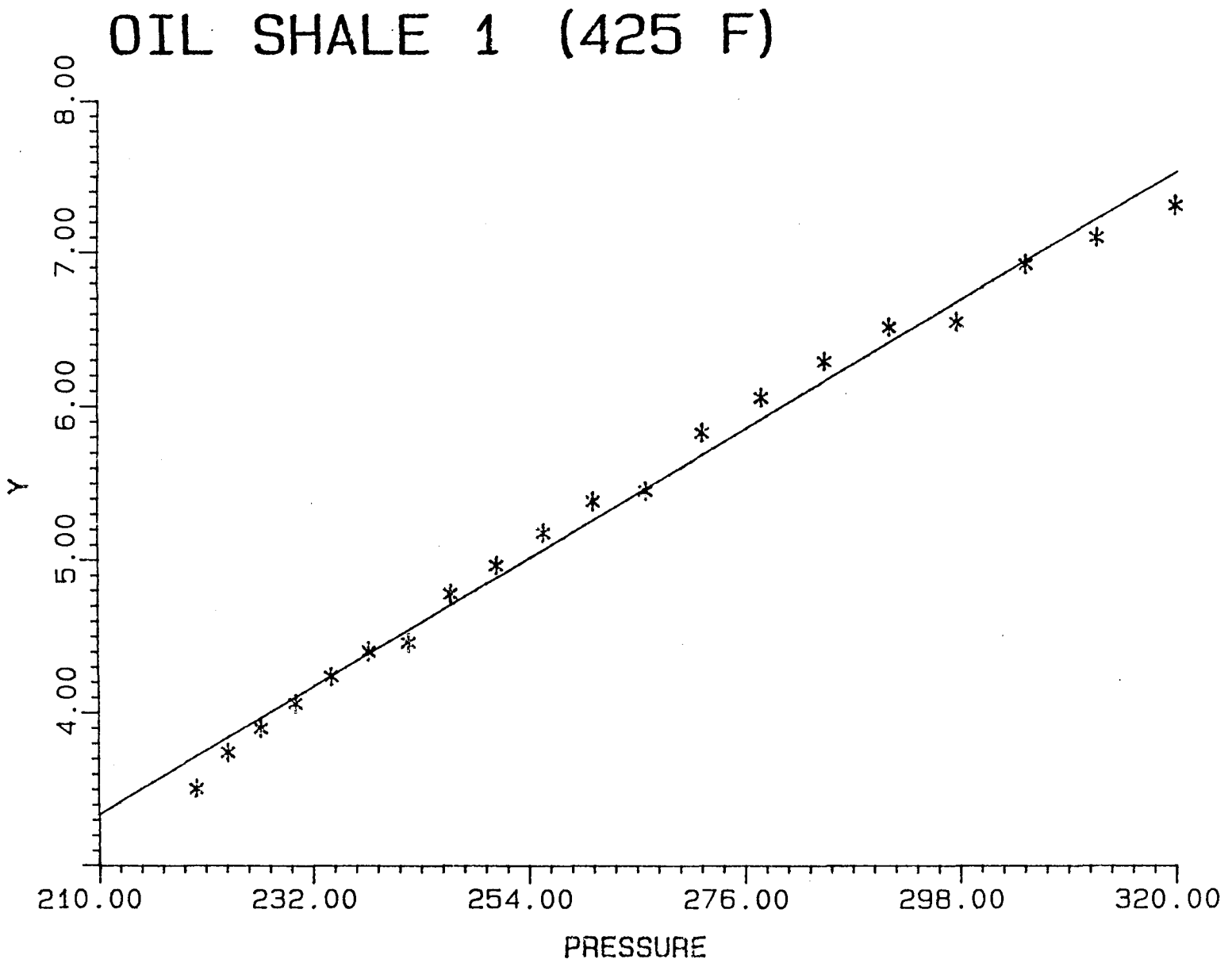

Figure 4.4. The quantity Y of Equation (4.11) vs pressure.

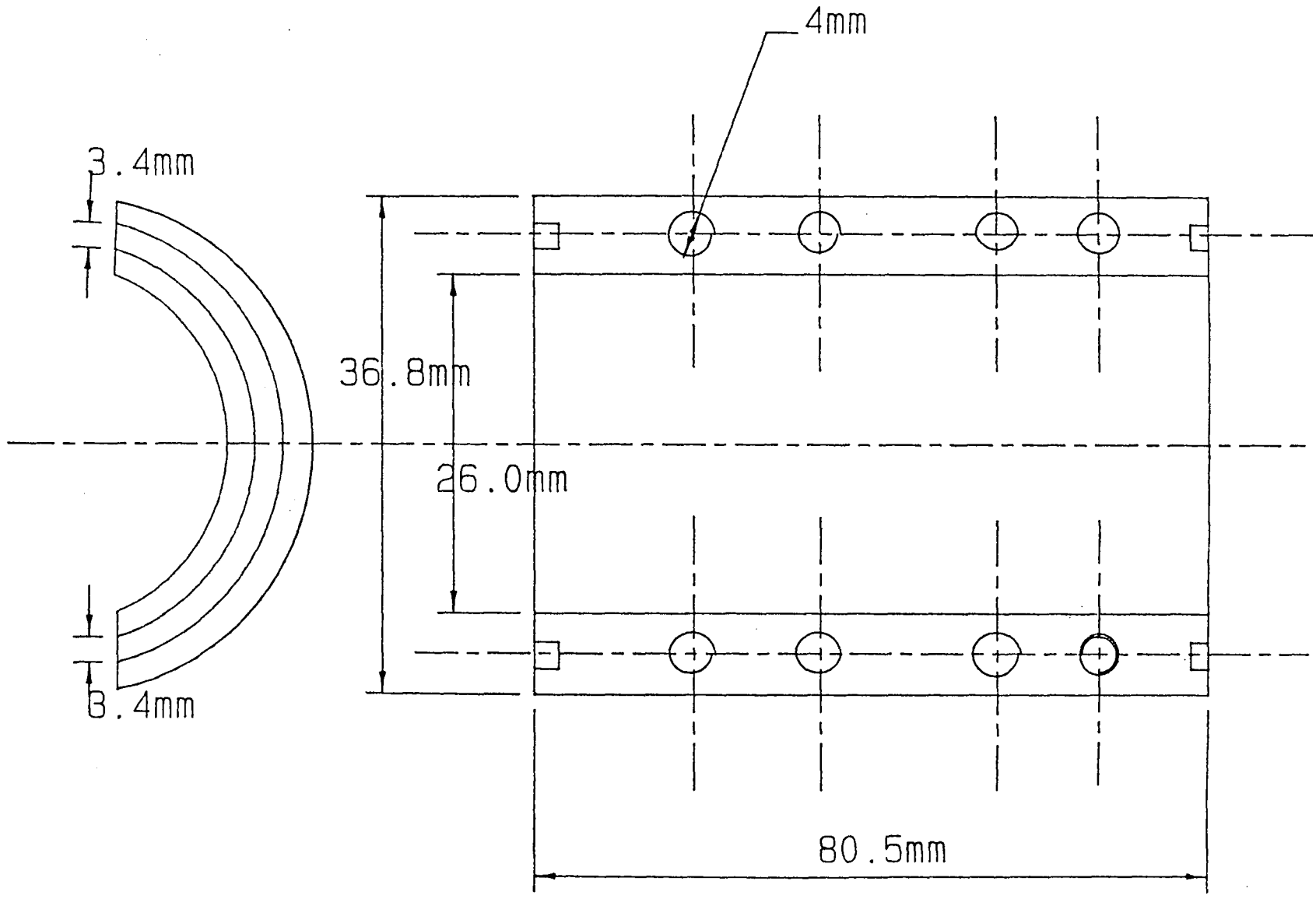

Figure 4.5. Design of core holder.

(a) @ 550 F for 1 hour — permeability was 1.5 mD

(b) @ 575 F for 1 hour — permeability was 2.4 mD

(c) @ 580 F for 1 hour — permeability was 3.4 mD

2. *Continuous.* The continuous run was performed at 580 F for 6 hours and the readings were taken every two hours. The average permeability during this time period was 1.3 mD. At the end of the sixth hour, after opening the core holder it was found that the core had undergone total disintegration.

4.5 CONCLUSIONS

Oil shale is impermeable till 540 F. After 540 F a permeability is seen which increases slowly with increase in temperature and time. The range is about 1.5 to 3.5 mD. It was also seen that any further increase in the temperature causes total disintegration of the core.

CHAPTER 5

ECONOMIC STUDY OF RF HEATING BY PHASED ARRAYS OF DIPOLE ANTENNAE

CHAPTER SUMMARY

We present a study of the economic feasibility of recovering oil from oil shale by heating with dipole applicators.

5.1 INTRODUCTION

The object of this study is to estimate the economic viability of recovering oil from oil shale by heating with dipole applicators. In the process we assume that various wells are drilled into the resource and in each well a dipole or monopole applicator is installed. The spacing of the wells is a function of the applied frequency. Frequencies in the range of 1–50 MHz have been found to be optimum. The attenuation lengths at these frequencies are from 2 to 200 meters. The process is invisioned as consisting of arrays of dipoles or monopoles inserted into the resource (Figs. 5.1–5.3). The well spacing is assumed to be $\lambda/2$ and phase shifters exist between the various applicators. The wells are operated in unison, however when overheating is noted at a particular well the power affecting this spot may be decreased. The phasing takes place according to model results to optimize the uniformity of heating. The oil flows through the induced permeability to recovery wells by the autogeneously produced pressure as shown in Fig. 5.4. We assume in the analysis that the retort temperature occurs at 400°C which is low enough so that the carbonates are not reacted (which is an endothermic reaction). This is an important assumption since this reaction requires a lot of energy. Also we assume that only a small fraction of the oil is vaporized. The present study does not include the price of drilling and r.f. equipment. An estimate of these is given in Bridges [1].

5.2 ECONOMIC PARAMETERS

Temperature of Pyrolysis

Slow pyrolysis can occur at temperatures of 350–400°C. We assume that pyrolysis takes place at 400°C, a temperature that can be achieved in 1–3 days of heating.

Potential Energy in Recovered Product

If the recovered product were burned we estimate that approximately 40 MJ/kg oil would be released in the liquid and gaseous products [50].

Kerogen Decomposition

As the kerogen in the shale reaches retort temperatures, oil, coke and gas is evolved [14].

Energy Required for Pyrolysis and Vaporization

A conservative estimate for the amount of energy to pyrolyze the shale and vaporize a portion of the oil and water is 0.43 MJ/kg kerogen [14,51].

Percent Fischer Assay Recovery

Due to overheating and underheating by monopoles, a conservative estimate of recovery is 60–80% of Fischer Assay.

Enthalpy of Shale

The amount of energy required to heat the shale of specific heat of $c_p = 1000$ J/kg/°C to retort temperatures is $c_p m \Delta T$, where T is temperature and m is mass.

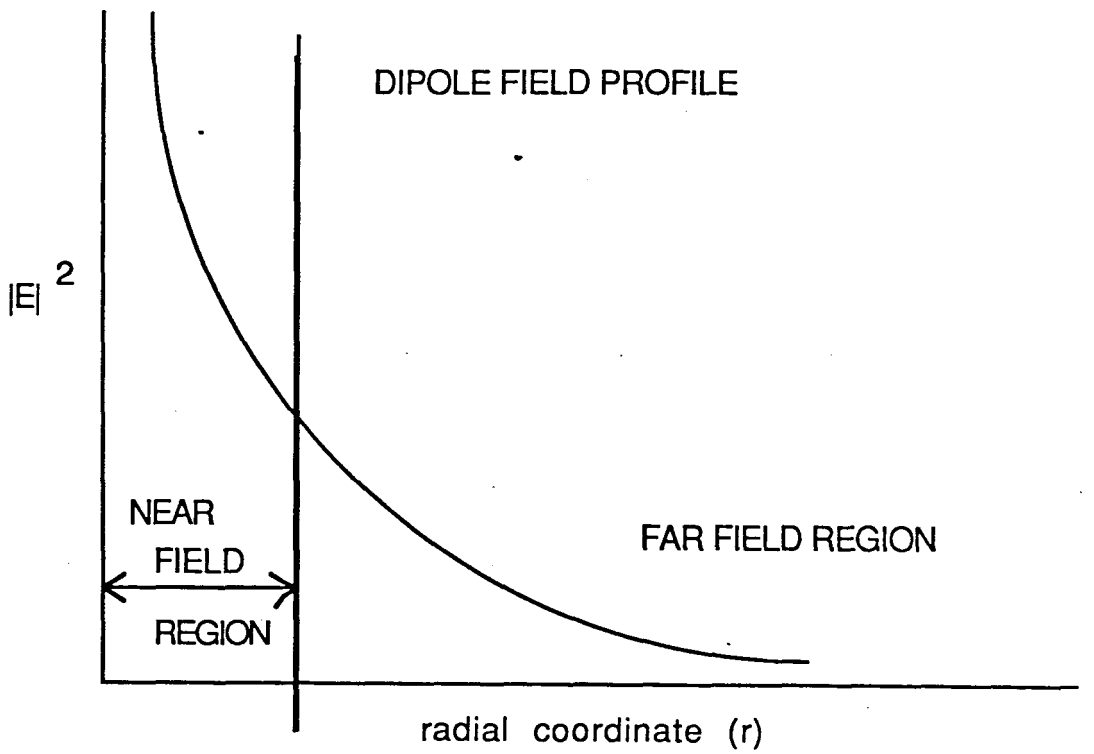

Figure 5.1. Dipole electric field profile.

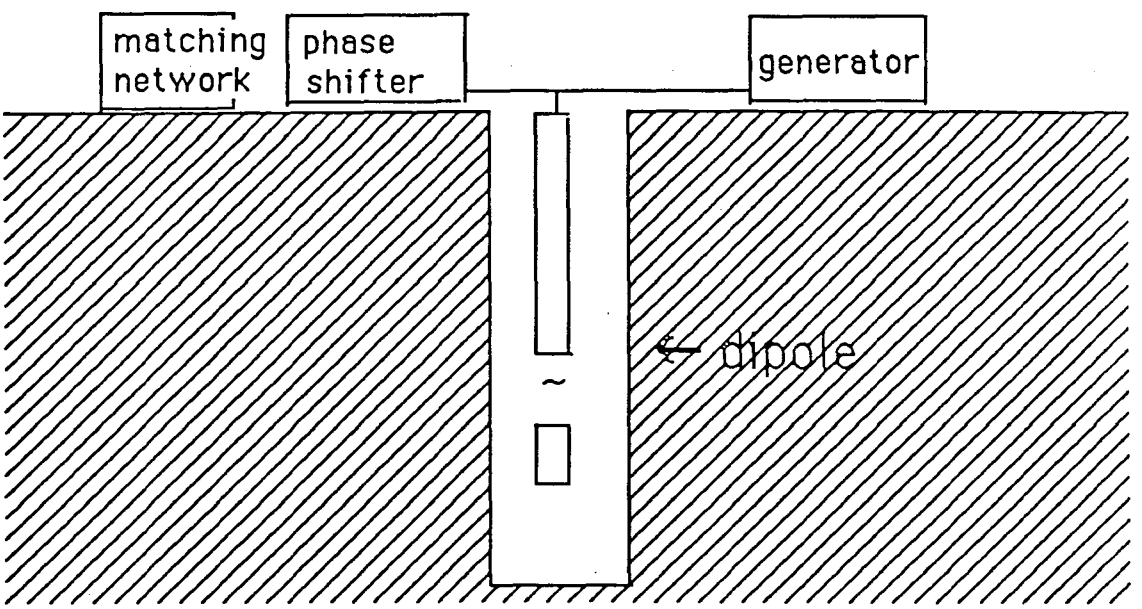

Figure 5.2. Dipole applicator.

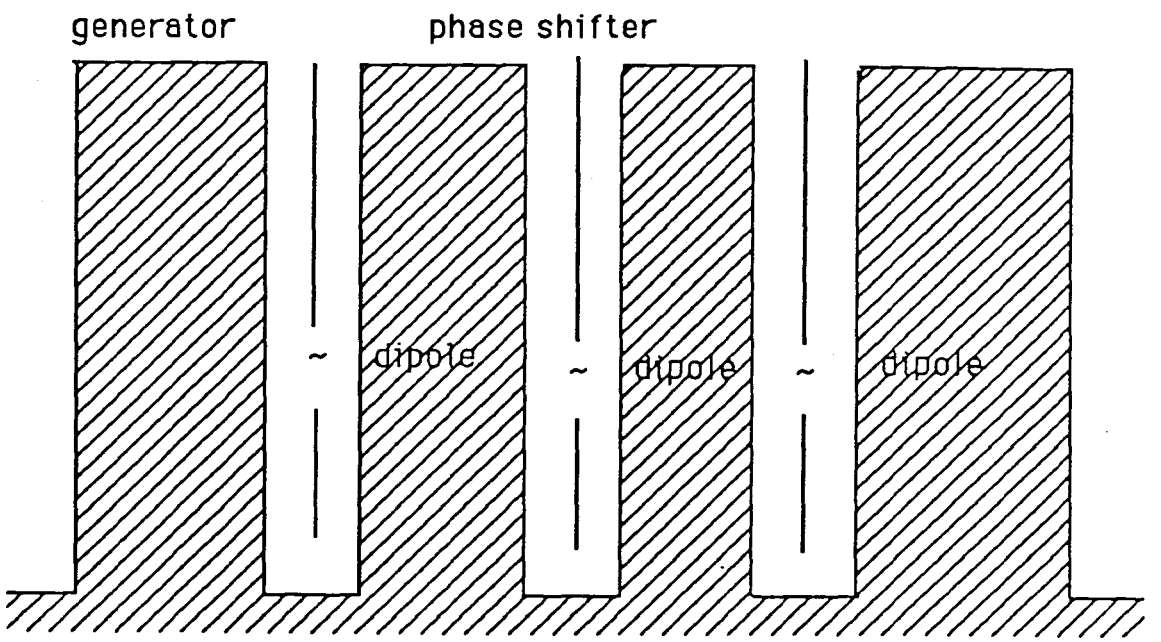

Figure 5.3. Array of dipoles in resource.

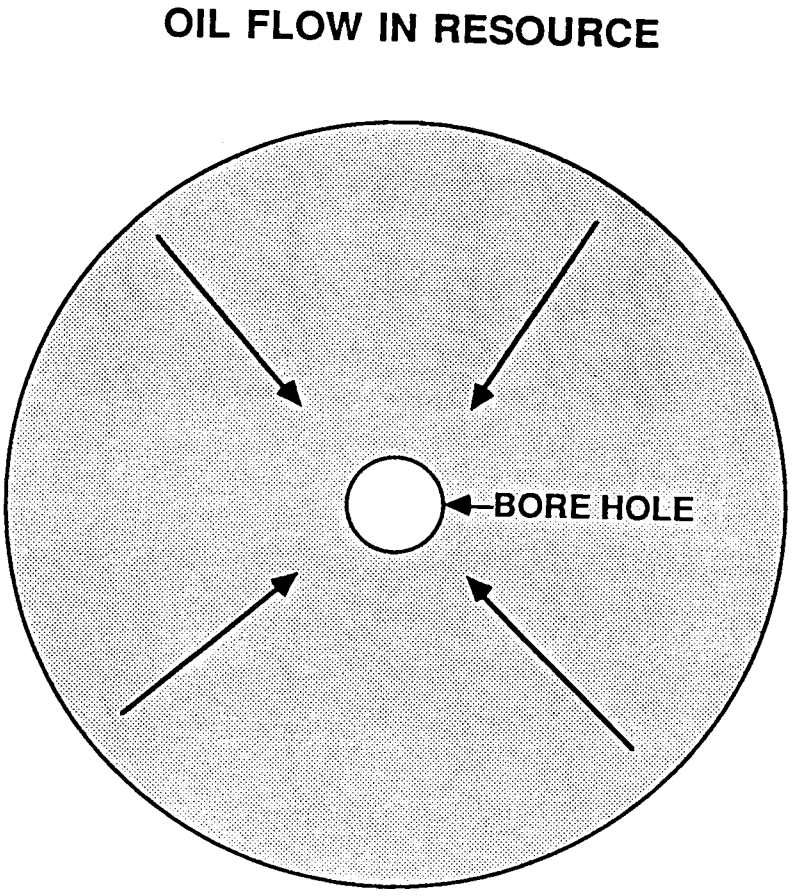

Figure 5.4. Flow of oil in resource.

Efficiences

(a) Efficiency of power plant from converting coal to electricity: 45%

(b) Efficient of r.f. generator for converting a.c. to r.f.: 95%

(c) In the dipole process some of the applied r.f. energy is dissipated in regions that will not be retorted. Some of the heat is wasted in over and underheating. We estimate from model results that the percent of applied heat that actually goes to heat shale is 60–80%.

Recycling of Heat

After retorting is complete it should be possible to utilize some of this energy to preheat unretorted areas generally by waiting for diffusion to transport heat to adjacent regions. We assume a value of 40% of the heat can be recycled [52,53].

Coking

Oil is lost in terms of coke. The coking rate depends on the heating rate. In this report we will assume a heating rate of 0.001°C/sec. The rate of coking is given by [14]

$$R_c = .00363 R_k/(R_t)^{\frac{1}{2}}$$

where R_c is rate of coking in kg coke/m^3 shale per second, R_k is rate of kerogen decomposition in kg kerogen/m^3 shale per second.

5.3 SUMMARY OF PARAMETERS

The following parameters are assumed in the analysis:

Heat derived from products	40 MJ/kg oil
Heat to pyrolyze	0.43 MJ/kg kerogen
Enthalpy of unretorted shale	0.38 MJ/kg shale
% Fischer Assay	80%
Efficiency of r.f. generator	95%
Efficiency of power plant	45%
% Useful heat (heat actually used to pyrolyze shale)	60%
% of Recycled Heat	0.0–40%
Temperature of pyrolysis	400°C

In the following example we present the results for a cubic meter of western shale which is 15% kerogen by weight. In Case #1 we assume no recycling of heat, an 80% Fischer assay recovery of shale oil and gas, and a 60% utilization of applied r.f. power. We consider this as a worst case scenario.

CASE #1: No Recycling of Resource Heat

Mass	2375 kg
Shale grade	15% kerogen (wt)
Fischer Assay minus coke loss	80%
Kilograms kerogen	352
Total oil recovered	164 kg
Combustion energy of oil and gas	6560 MJ
Enthalpy at retort temperature	909 MJ
Pyrolysis energy	150 MJ
Total retorting energy	1059 MJ
Total r.f. energy necessary to heat shale (60%)	1765 MJ
Total input energy out of generator (95%)	1857 MJ
Total energy in coal to generator plant (45%)	4129 MJ
Net recovery ratio	1.59

In the next example we assume a 40% recycling of heat, an 80% recovery and a 60% utilization of r.f. energy. We consider this case as very realistic.

Case #2: 40% Recycling of Resource Heat

Mass	2375 kg
Recycling heat	40%
Shale grade	15% kerogen (wt)
Fischer Assay minus coke loss	80%
Kilograms kerogen	352
Total oil recovered	165 kg
Combustion energy of oil and gas	6560 MJ
Enthalpy at retort temperature	546 MJ
Pyrolysis energy	150 MJ
Total retorting energy	696 MJ
Total r.f. energy necessary to heat shale (60%)	1160 MJ
Total input energy out of generator (95%)	1221 MJ
Total energy in coal to generator plant (45%)	2713 MJ
Net recovery ratio	2.41

In the final example we display the results for a recovery scheme which is optimistic, but we feel could be achieved. In this case we assume 80% recovery of products and 80% useful utilization of r.f. energy and a 40% recycling of reservoir heat energy.

Case #3: 80% Recovery and R.F. Heating Efficiency

Mass	2375 kg
Recycling heat	40%
Shale grade	15% kerogen (wt)
Fischer Assay minus coke loss	80%
Kilograms kerogen	352
Total oil recovered	165 kg
Combustion energy of oil and gas	6560 MJ
Enthalpy at retort temperature	546 MJ
Pyrolysis energy	150 MJ
Total retorting energy	696 MJ
Total r.f. energy necessary to heat shale (80%)	870 MJ
Total input energy out of generator (95%)	916 MJ
Total energy in coal to generator plant (45%)	2035 MJ
Net recovery ratio	3.22

The relative magnitudes of the various energy requirements is shown in Figs. 5.5 and 5.6.

5.4 COMPARISON WITH PREVIOUS STUDIES

Bridges [1] with his modified triplate array has found NER of 3–5. In their analysis they assumed 90% recovery, which we consider to be very optimistic. They also assume almost all input heat is utilized to pyrolyze, whereas in the present technique we lose some heat in the leakage of the fields out of the retort zone. Also they assume a recycling of heat and gasification of carbon.

Mallon [8] has determined NER's roughly similar to Bridges results, however they assume a recovery of 83%. Butt [53] has determined NER's from 2–6. In their analysis they assume a 90% recovery.

We see that our estimates are on the low side of what others have estimated. The reason for this is the energy lost outside of the retort zone in the monopole process. However, the monopole process does require much less mining than the previously proposed processes.

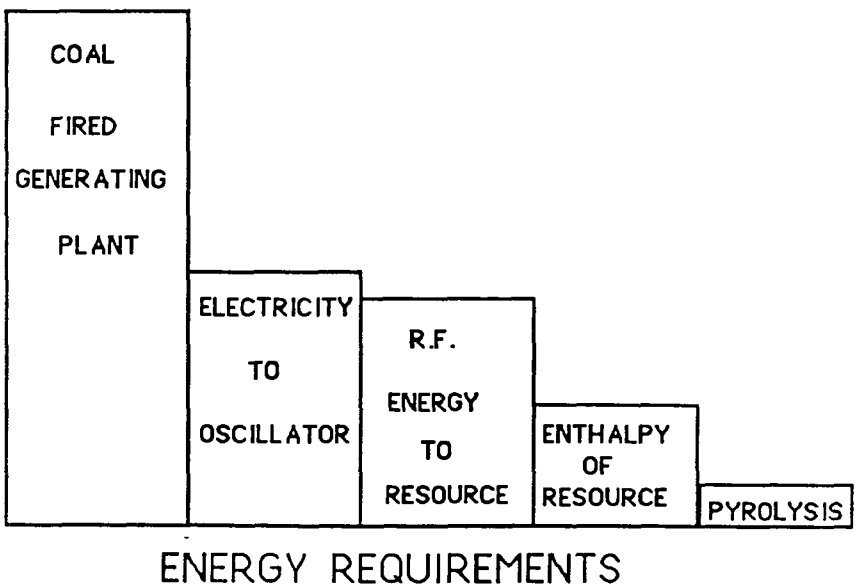

Figure 5.5. Energy requirements.

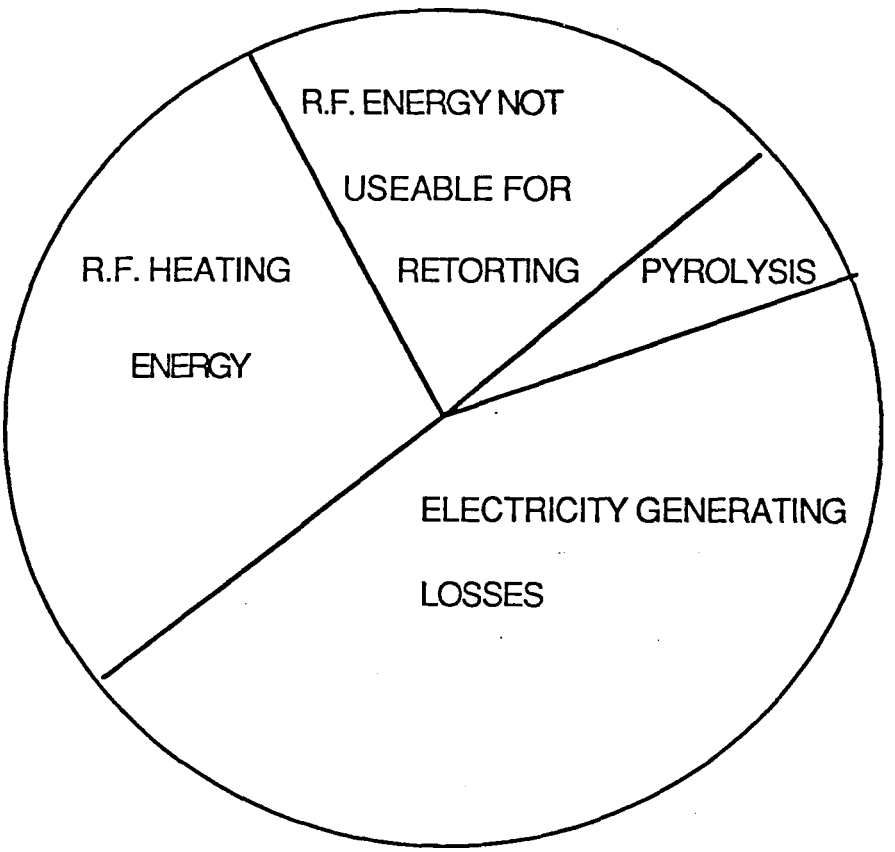

Figure 5.6. Pie chart of heating losses.

APPENDIX A:

RESULTS OF BENCH SCALE HEATING EXPERIMENTS

THEORETICAL MODELING FOR THE DESIGN OF THE R.F. SYSTEM

In order to determine the appropriate frequencies and power for the r.f. heating experiments extensive modeling was performed. first attenuation lengths as functions of frequency were found and plotted as shown in Figs. A1–A7. From these plots it was possible to estimate appropriate heating frequencies.

In order to estimate power requirements it was necessary to run the numerical heat-mass transfer model using the monopole field model as input. In the following, the model predictions for an experiment run jointly between Western Research Institute and U. of Wyoming are shown. In these tests the block to be heated was of dimensions $(0.5 \times 0.5 \times 0.5)$ m^3. Model results are indicated in Figs. A8–A17. For these model runs the following parameters were used:

Frequency:	450 MHz
Input Power:	2015 watts
Antenna Length:	0.5 m
Shale Grade:	27 gal/ton
Dielectric Constant:	(6.0, 0.2)

SUMMARY OF R.F. BENCH SCALE EXPERIMENTS

Test #0,00 (shakedown tests):

These were shakedown tests with the goal to test r.f. system and the reactor assembly. In these test the following parameters were used:

Block Size:	$12'' \times 12'' \times 6''$
Shale Grade:	22 gal/ton
Original Block Weight:	29.65 kg
Ending Block Weight:	28.65 kg
Weight of Oil Collected:	20 gm
Antenna Length:	$5.88''$
Frequency:	2.45 GHz

The goal of these tests were to test the heating and collection system. The tests proceeded very well, although dielectric breakdown was found to occur at relatively low power levels.

Test #1 (First heating test):

In these tests the following parameters were used:

Block Size:	$12'' \times 12'' \times 6''$
Shale Grade:	22 gal/ton
Original Block Weight:	29.95 kg
Ending Block Weight:	27.65 kg
Weight of Oil Collected:	260 gm
Antenna Length:	$5.88''$
Antenna Radius:	$0.66''$
Frequency:	2.45 GHz

In this test the hole in the shale block was 1 5/8″ in diameter. A dry nitrogen gas was used for purging this time in order to minimize breakdown due to water moisture. The antenna diameter for this test was reduced from 0.66″ to 0.33″ in order to change the input impedance and thus minimize the heating near the ground plane. The hole was purged with a nitrogen gas flow. It was found that the maximum power that could be delivered in this test was 350 watts before dielectric breakdown occurred. Retorting began after 13 hours of heating. It was found that near the ground plane the temperatures were very hot and decreased as you went down the bore hole. The temperature profiles at the various thermocouple position are given in Figs. A18–A33.

Test #2

In this test the following parameters were used:

Block Size:	$12'' \times 12'' \times 6''$
Shale Grade:	23 gal/ton
Original Block Weight:	29.95 kg
Ending Block Weight:	27.25 kg
Weight of Oil collected:	678.8 gm
Antenna Length:	$5.88''$
Antenna Radius:	$.33''$
Frequency:	2.45 GHz

In this test the hole in the shale block was 1 7/8″ in diameter, but there was a insulating dielectric sleeve as shown in Fig. A34. In this test we also provided extra cooling coils around the meter elbow that is attached to the ground plane. The antenna diameter for this test was again 0.33″. We found that with the quartz insulating sleeve we could deliver power of 800 watts throughout pyrolysis. We considered this test very successful. The temperature distributions around the thermocouples are given in Figs. A35–A39.

Test #3

In this test the following parameters were used:

Block Size:	$12'' \times 12'' \times 6''$
Shale Grade:	23 gal/ton
Original Block Weight:	28.35 kg
Ending Block Weight:	26.25 kg
Antenna Length:	$5.88''$
Antenna Radius:	$0.33''$
Frequency:	2.45 GHz

The object of this test was to see the effect of decreasing the hole diameter. In this test the hole in the shale block was 1 1/4″ in diameter, and a insulating dielectric sleeve was used. We found that in this test a maximum of only 600 watts could be delivered before breakdown.

Test #4

Block Size:	12″ × 12″ × 6″
Shale Grade:	23 gal/ton
Antenna Length:	5.88″
Antenna Radius:	0.33″
Frequency:	2.45 GHz

The object of this test was to see the effect of increasing the antenna diameter. In this test the hole in the shale block was 1 1/4″ in diameter, and there was a insulating dielectric sleeve. We found that in this test a maximum of only 500 watts could be delivered before breakdown. We observed dielectric breakdown at bottom of antenna.

Test #5:

In this test the following parameters were used:

Block Size:	12″ × 12″ × 6″
Shale Grade:	23 gal/ton
Antenna Length:	5.88″
Antenna Radius:	0.33″
Frequency:	2.45 GHz

The object of this test was to see the effect of decreasing the antenna diameter. In this test the hole in the shale block was 1 1/4″ in diameter and there was a insulating dielectric sleeve around the antenna. We found that in this test a maximum of only 500 watts could be delivered before breakdown. We observed dielectric breakdown at bottom of antenna. We conclude that the variables comprising test #2 appear to be optimum.

Test #6

In this test the following parameters were used:

Block Size:	12″ × 12″ × 6″
Shale Grade:	23 gal/ton
Original Block Weight:	28.9 kg
Ending Block Weight:	26.965 kg
Antenna Length:	5.88″
Antenna Radius:	0.33″
Frequency:	2.45 GHz

The object of this experiment was to reproduce the results of experiment #2. In this test the hole in the shale block was 1 7/8″ in diameter, and there was a insulating dielectric sleeve of dimensions 1 3/8″ around the antenna. We found that in this test at maximum of 900 watts could be delivered before breakdown. The temperature obtained in this experiment are shown in Figs. A40–A72.

Test #7

This was a test performed in conjunction with Western Research Institute. In this test the following parameters were used:

Block size:	51.5cm × 50.5cm × 46.4cm
Shale Grade:	25 gal/ton
Antenna Length:	50 cm
Antenna Radius:	0.66″
Frequency:	450 MHz
Power:	500 watts for 30 min, 1000 watts for 30 min and thereafter 1500 watts

The experimental temperature distributions are shown in Figs. A73–A77. The model predictions of this run are shown in Figs. A78–A82.

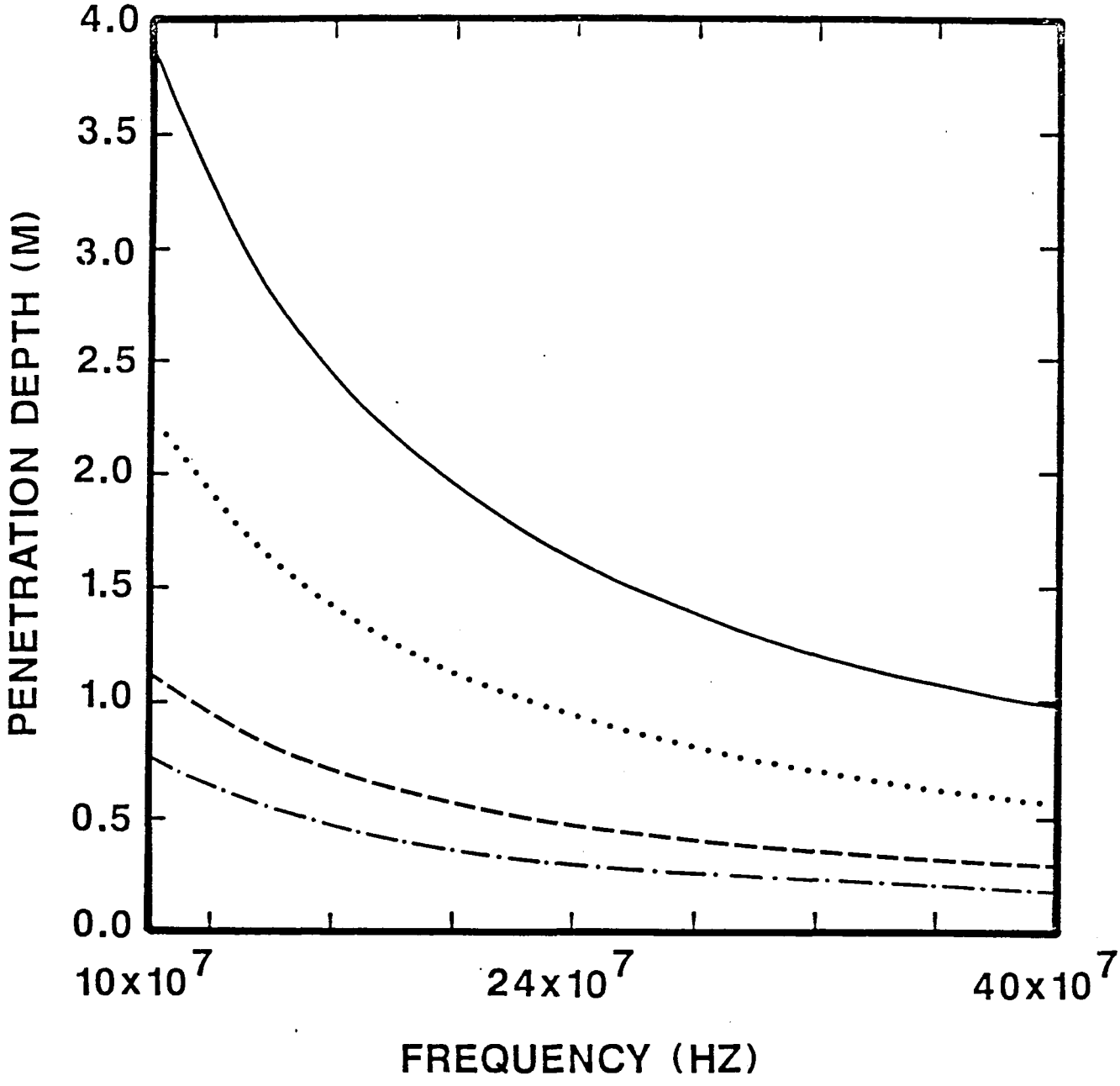

Figure A1. Penetration depth vs frequency for various values of ϵ''; (—) $\epsilon'' = 0.1$; $(\cdots)$ $\epsilon'' = 0.5$; $(- - -)$ $\epsilon'' = 1.0$; $(- \cdot - \cdot -)$ $\epsilon'' = 3.0$.

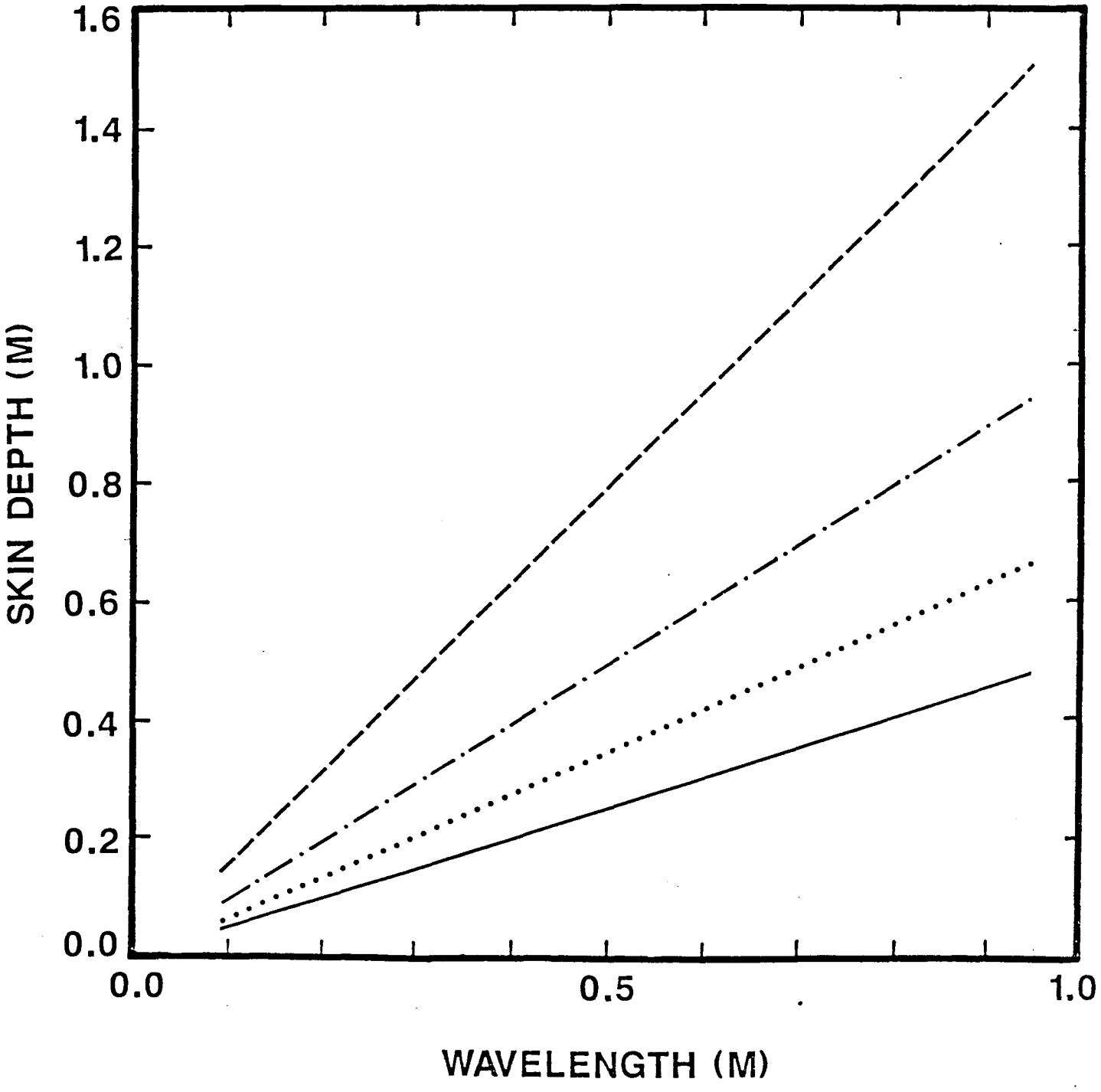

Figure A2. Skin depth vs wavelength (in meters) for various ϵ''; (—) $\epsilon'' = 0.1$; (···) $\epsilon'' = 0.5$; (– – –) $\epsilon'' = 3.0$; (– · – · –) $\epsilon'' = 1.0$.

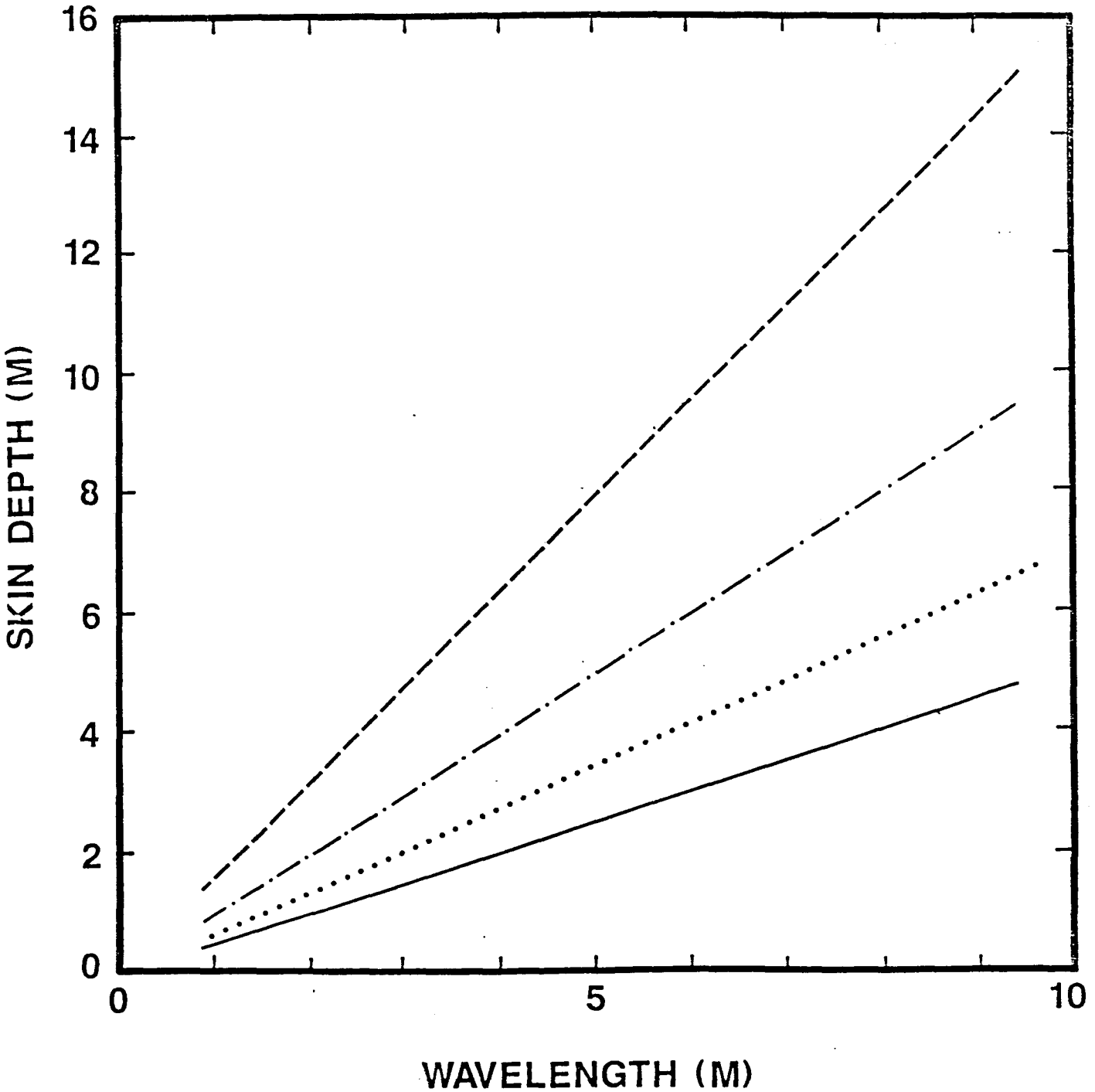

Figure A3. Skin depth vs wavelength for various ϵ''; (—) $\epsilon'' = 0.1$; $(\cdots)$ $\epsilon'' = 0.5$; $(- - -)$ $\epsilon'' = 3.0$; $(- \cdot - \cdot -)$ $\epsilon'' = 1.0$.

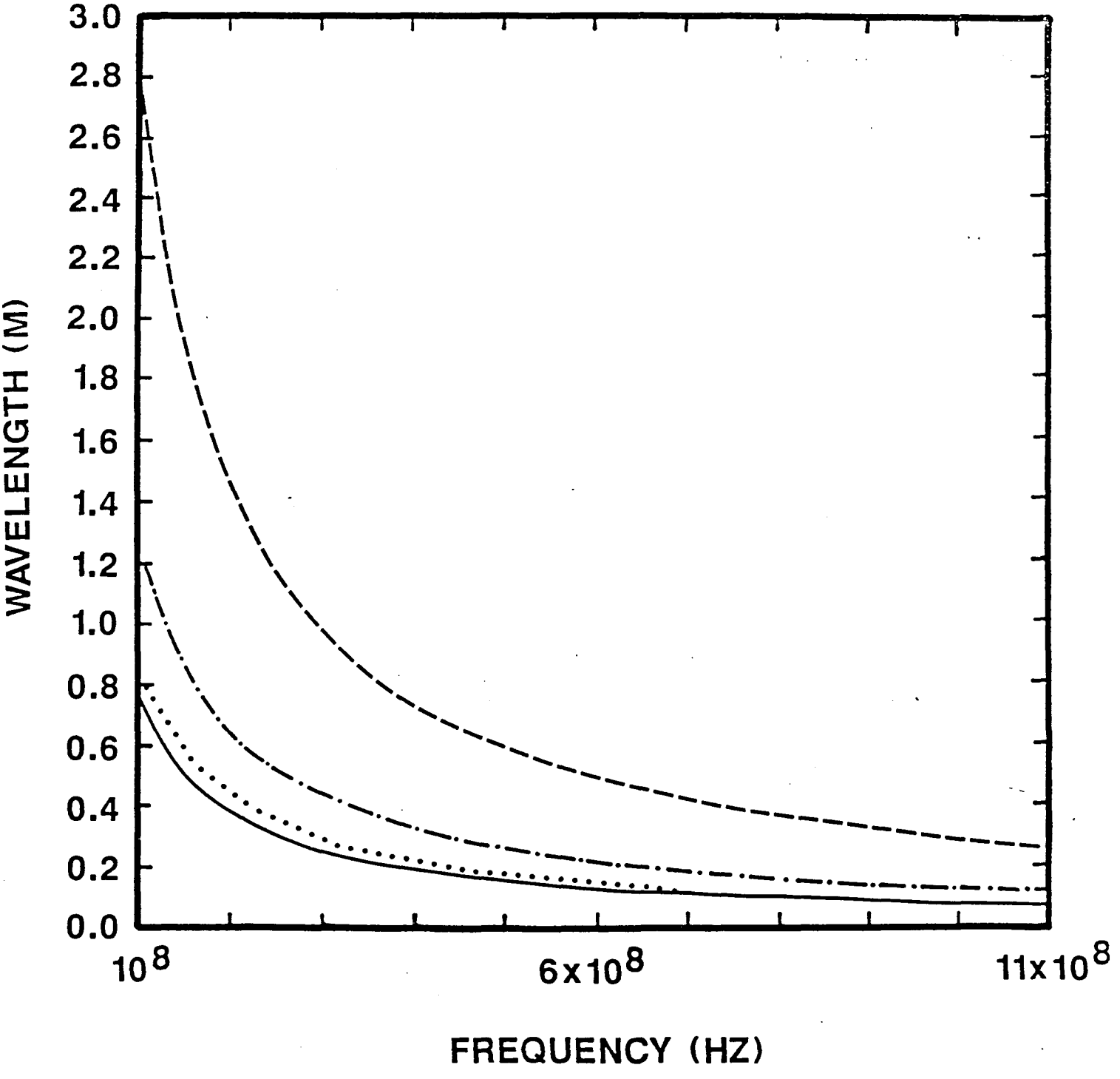

Figure A4. Wavelength vs frequency: (—) $\epsilon'' = 0.1$; $(\cdots)$ $\epsilon'' = 0.5$; $(- - -)$ $\epsilon'' = 3.0$; $(- \cdot - \cdot -)$ $\epsilon'' = 1.0$.

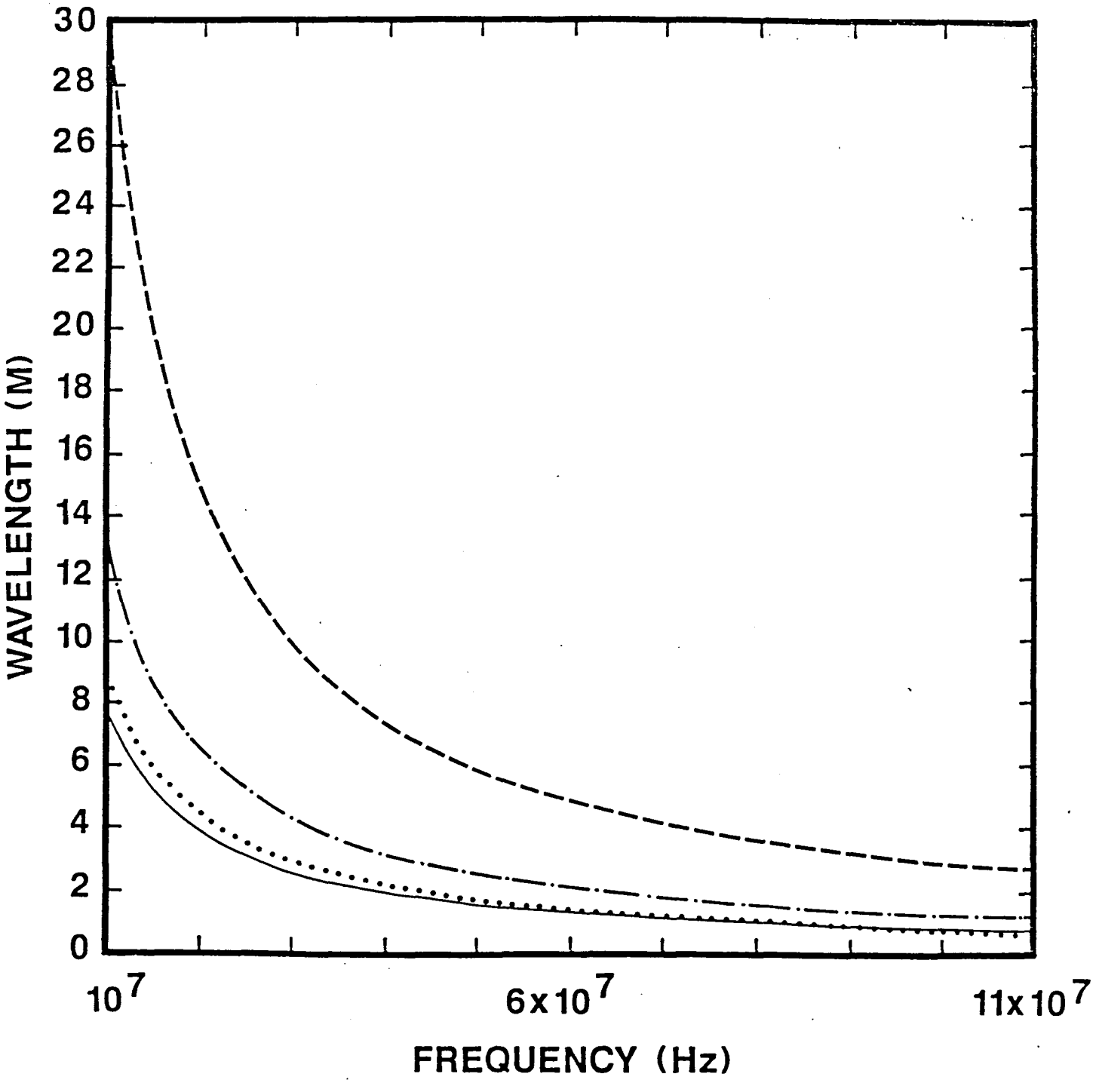

Figure A5. Same as Fig. A4 for a different frequency regime.

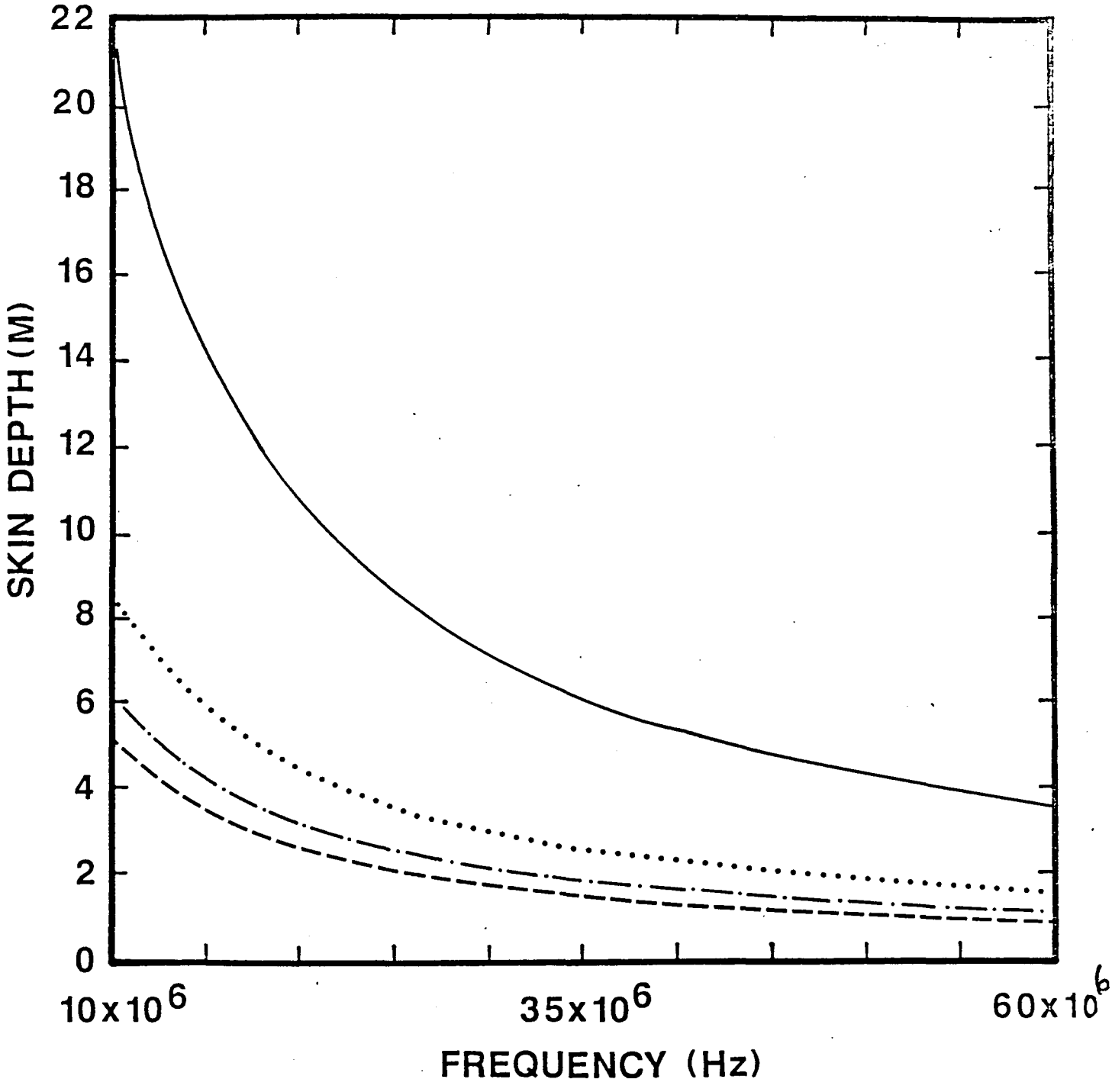

Figure A6. Skin depth vs frequency: (—) $\epsilon'' = 0.1$; (···) $\epsilon'' = 0.5$; (– – –) $\epsilon'' = 3.0$; (–·–·–) $\epsilon'' = 1.0$.

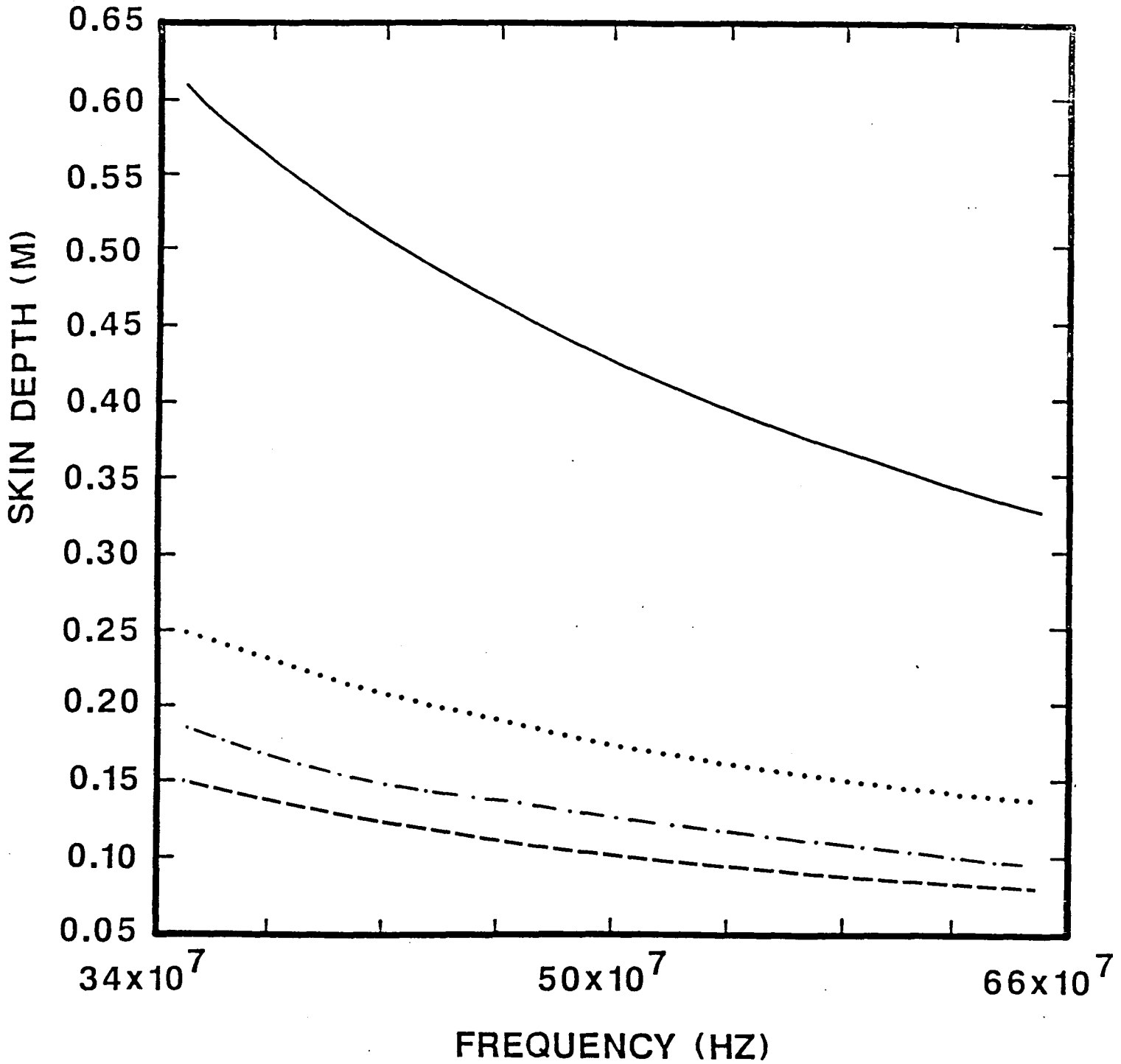

Figure A7. Same as in Fig. A6 for different frequency regime.

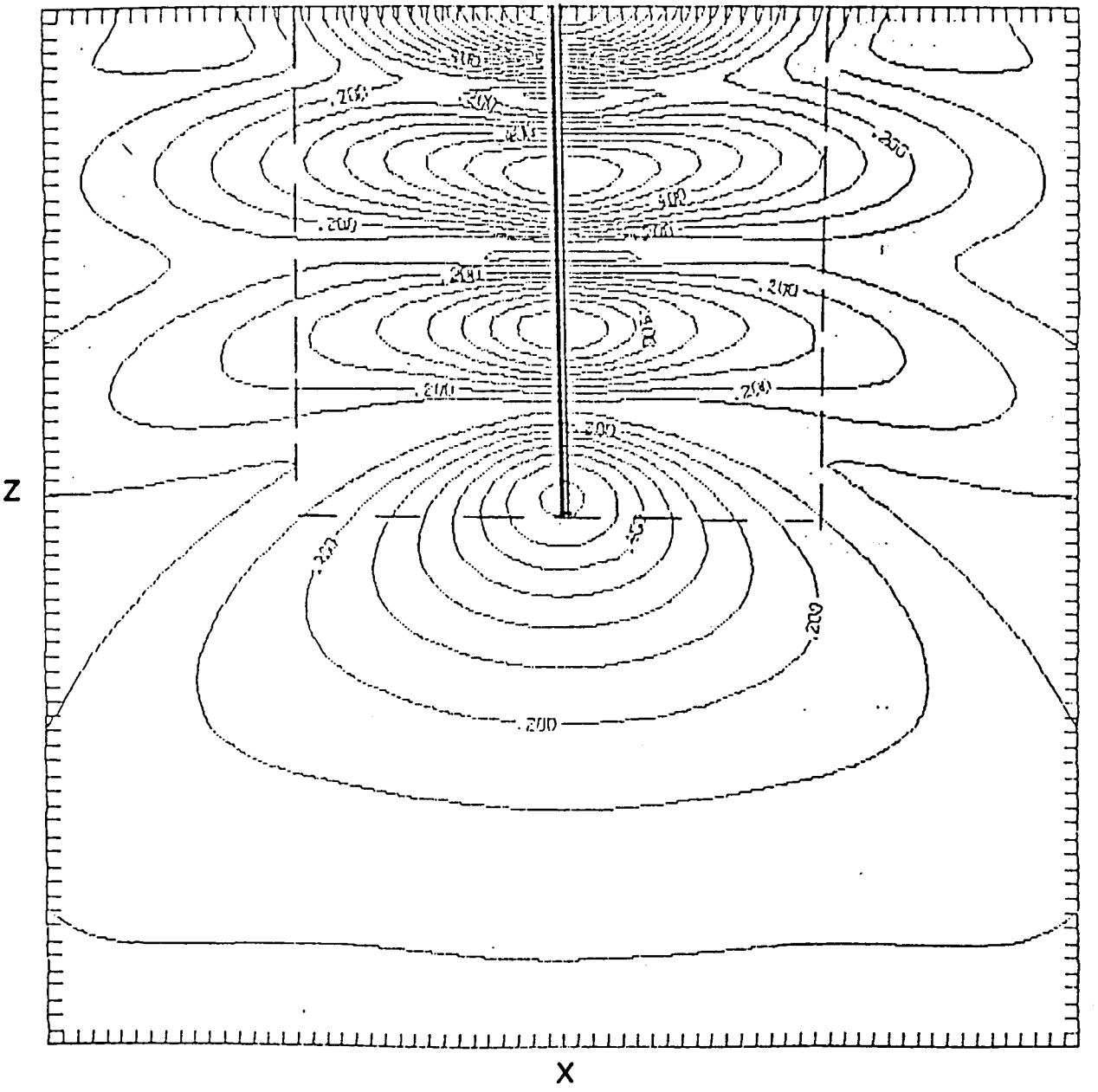

Figure A8. Electric field distribution around a monopole.

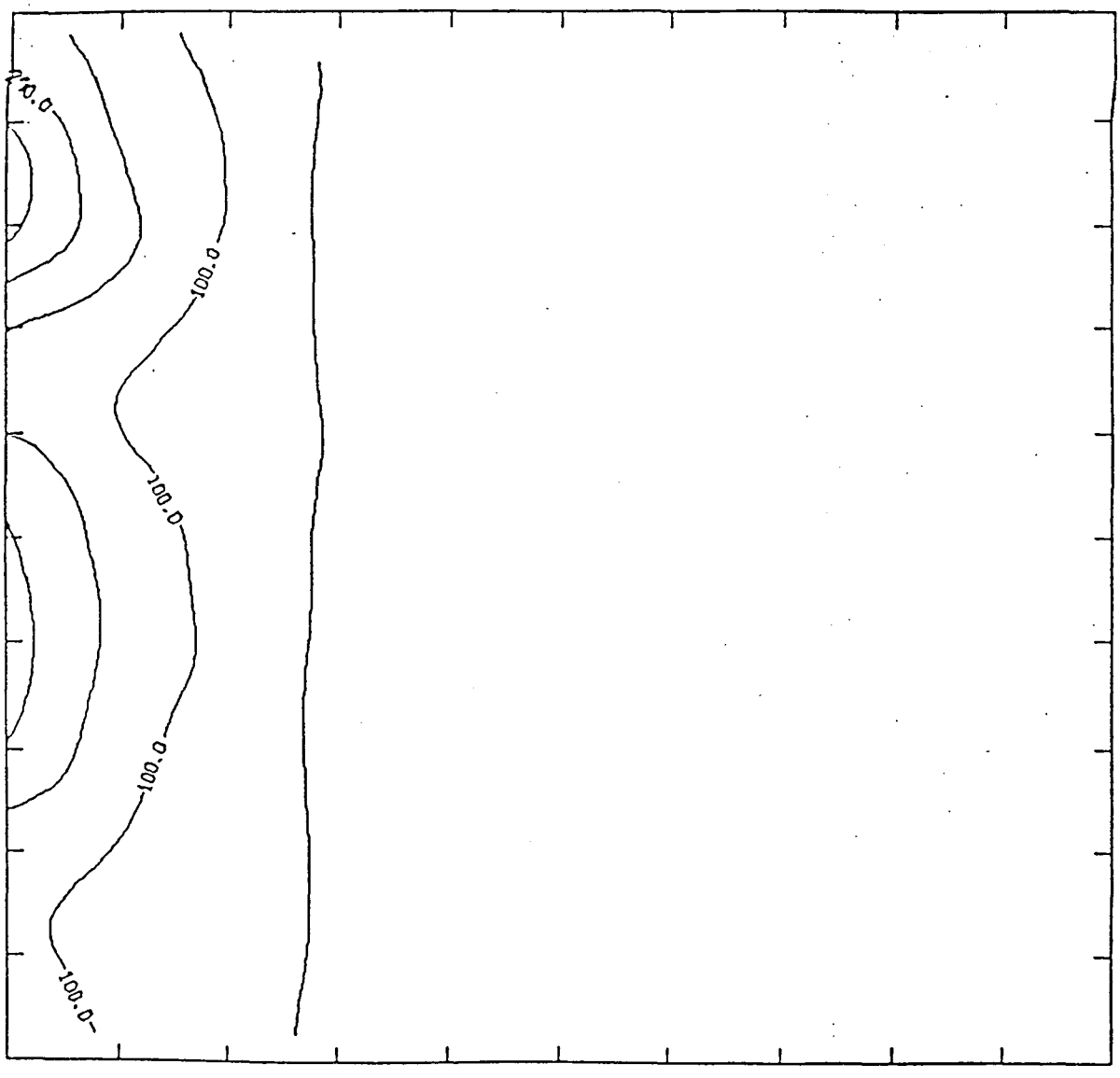

Figure A9. Temperature distribution at 5 hours.

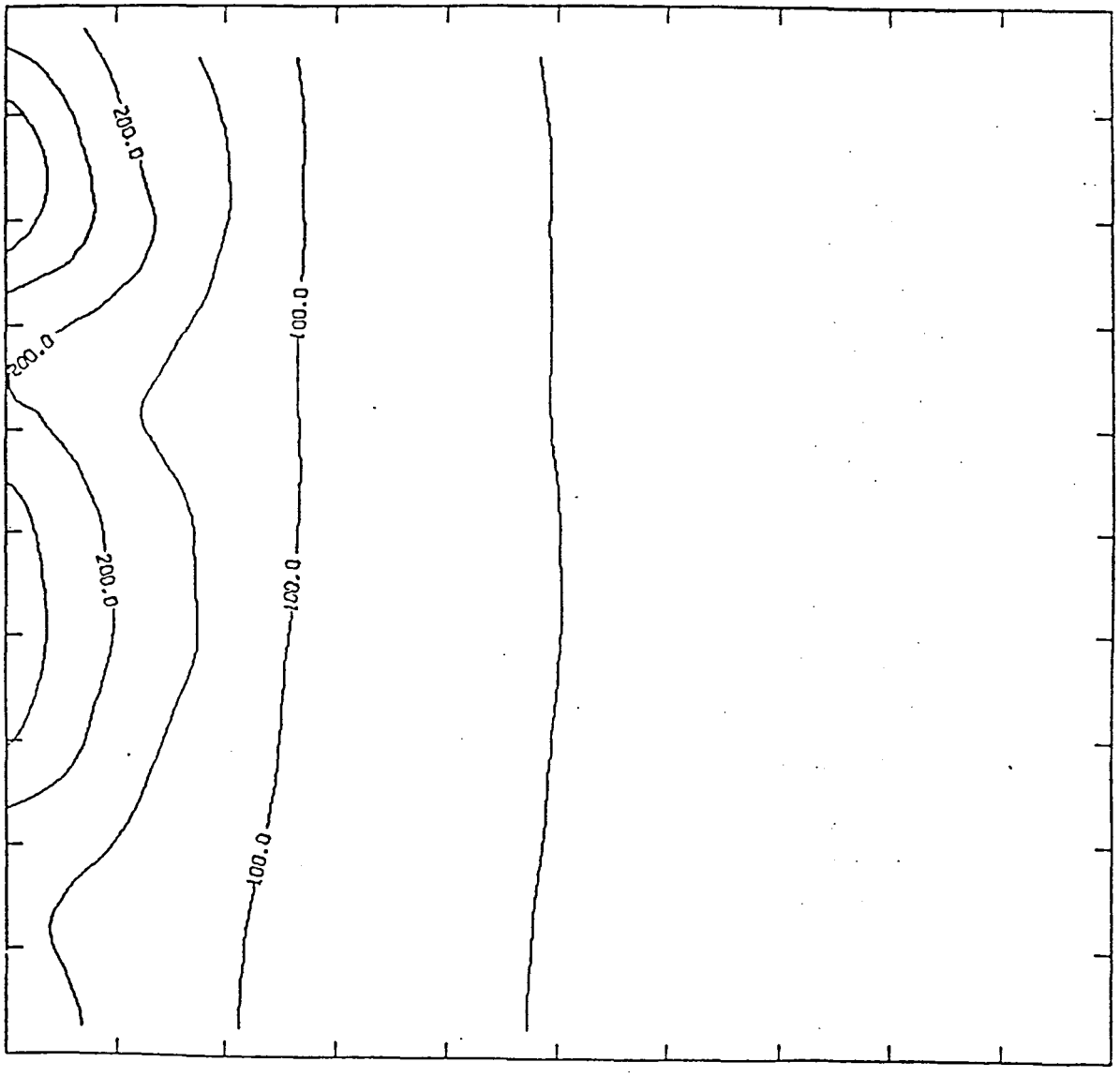

Figure A10. Temperature distribution at 10.9 hours.

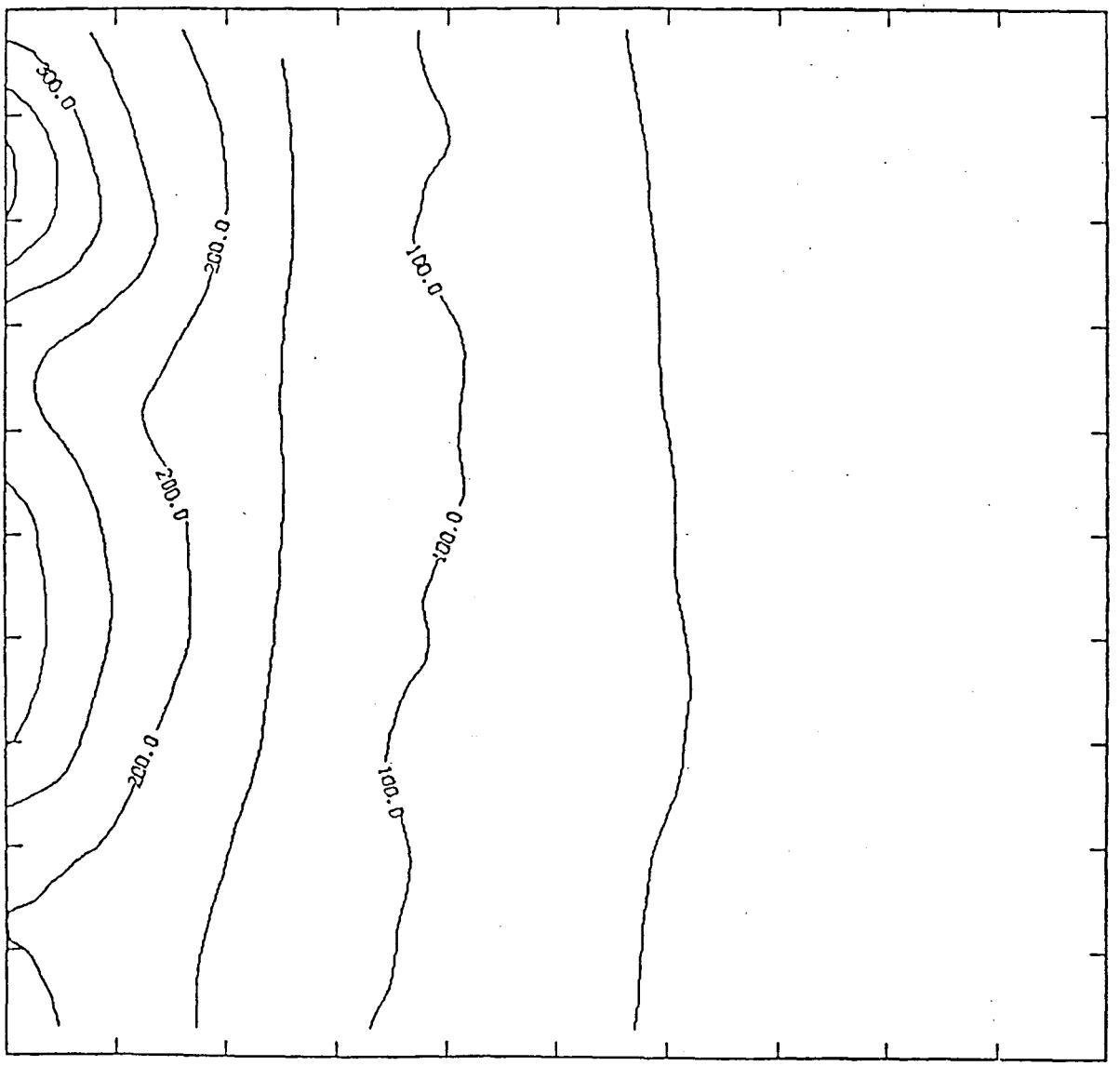

Figure A11. Temperature distribution at 19.8 hours.

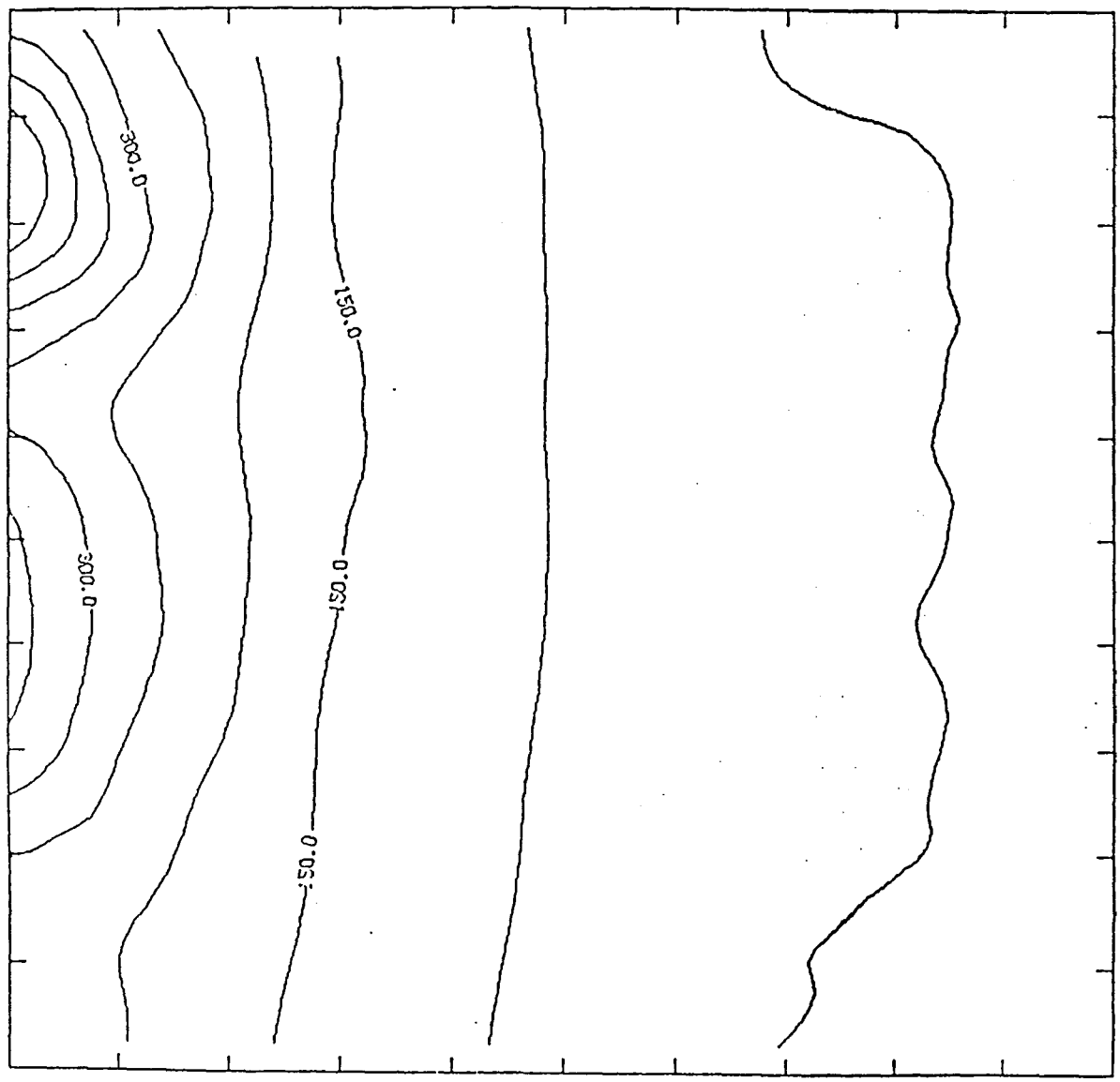

Figure A12. Temperature distribution (in °C) at 28.0 hours.

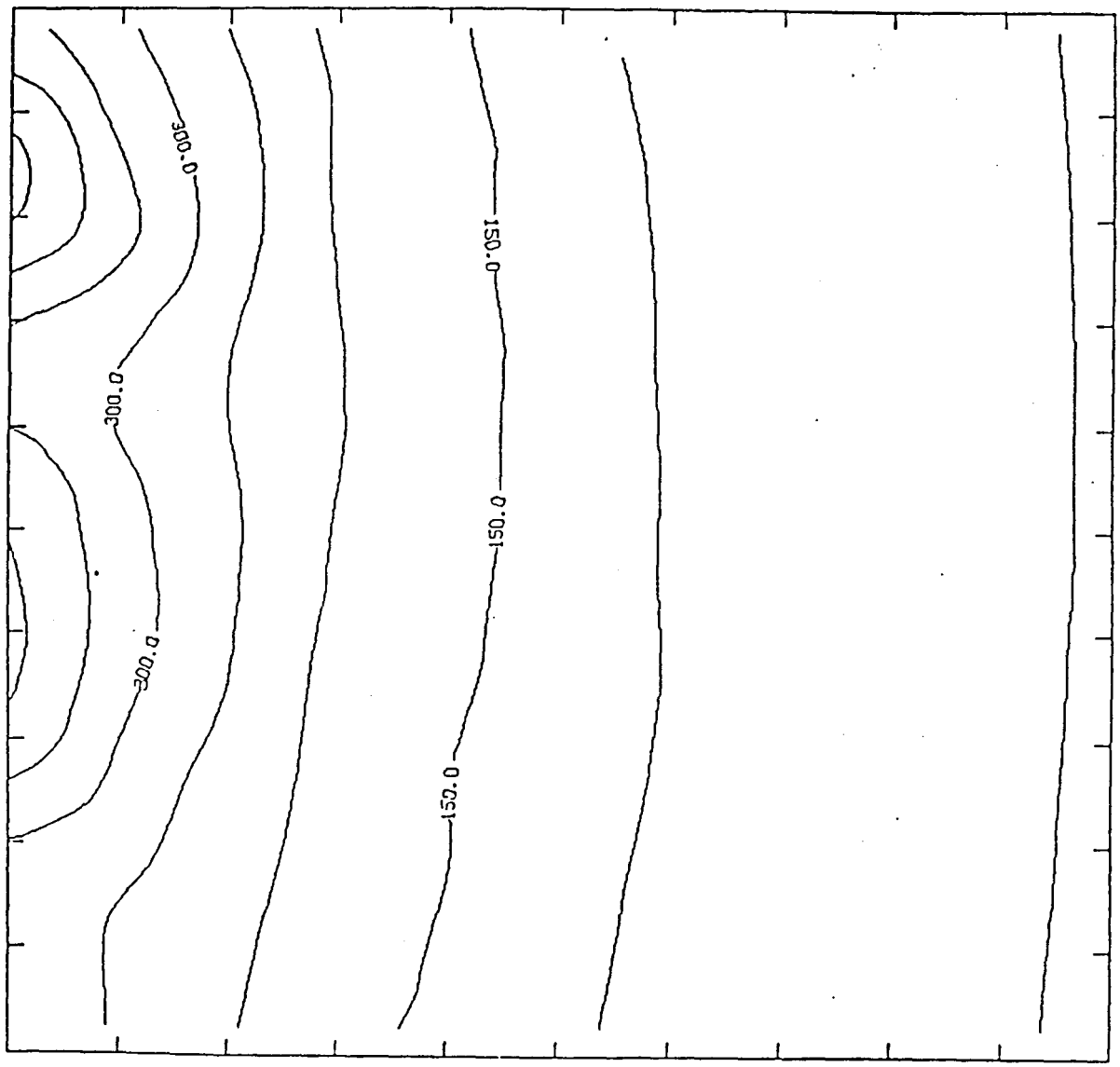

Figure A13. Temperature distribution (°C) at 47.9 hours.

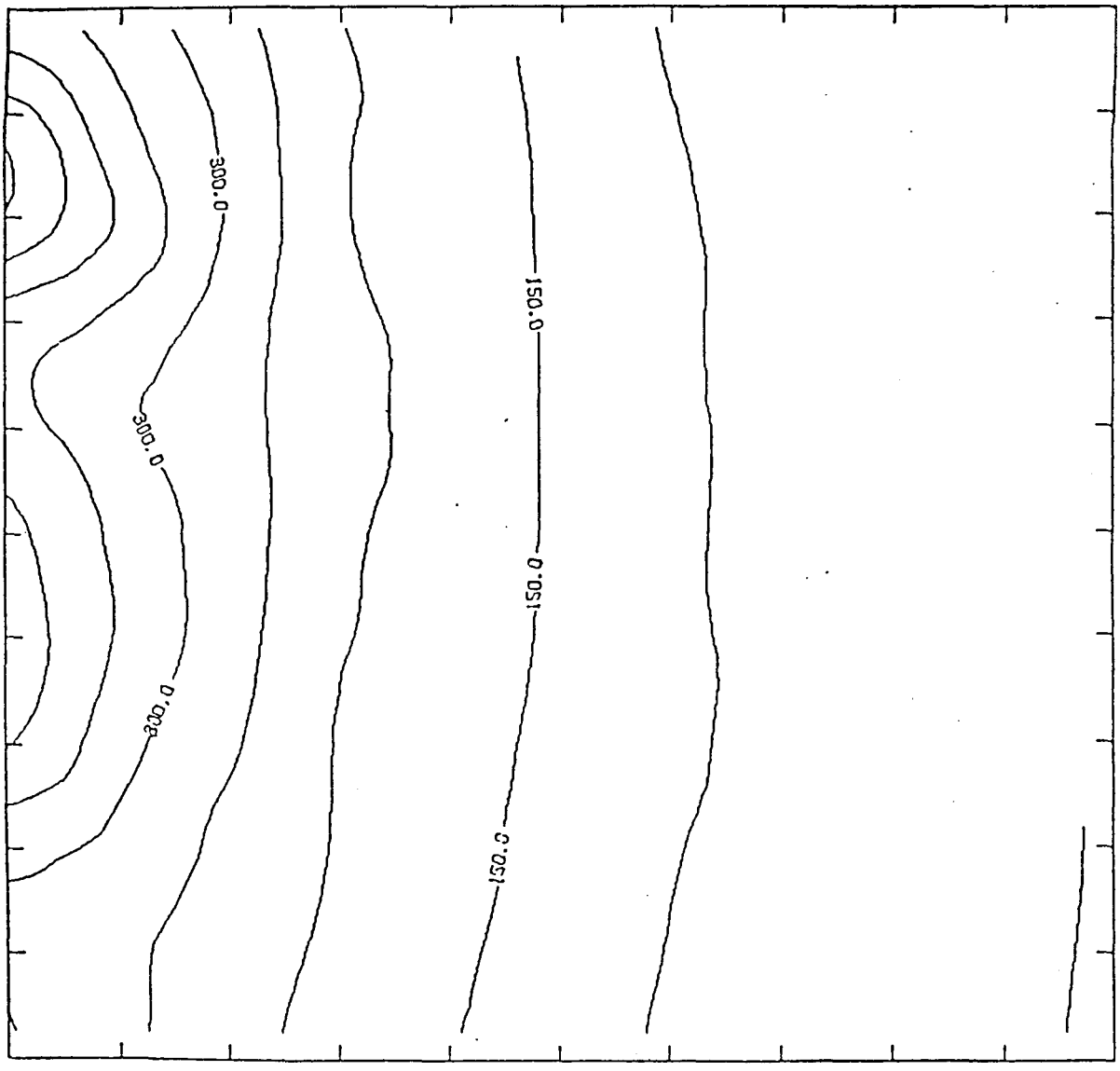

Figure A14. Temperature distribution (°C) at 60.8 hours.

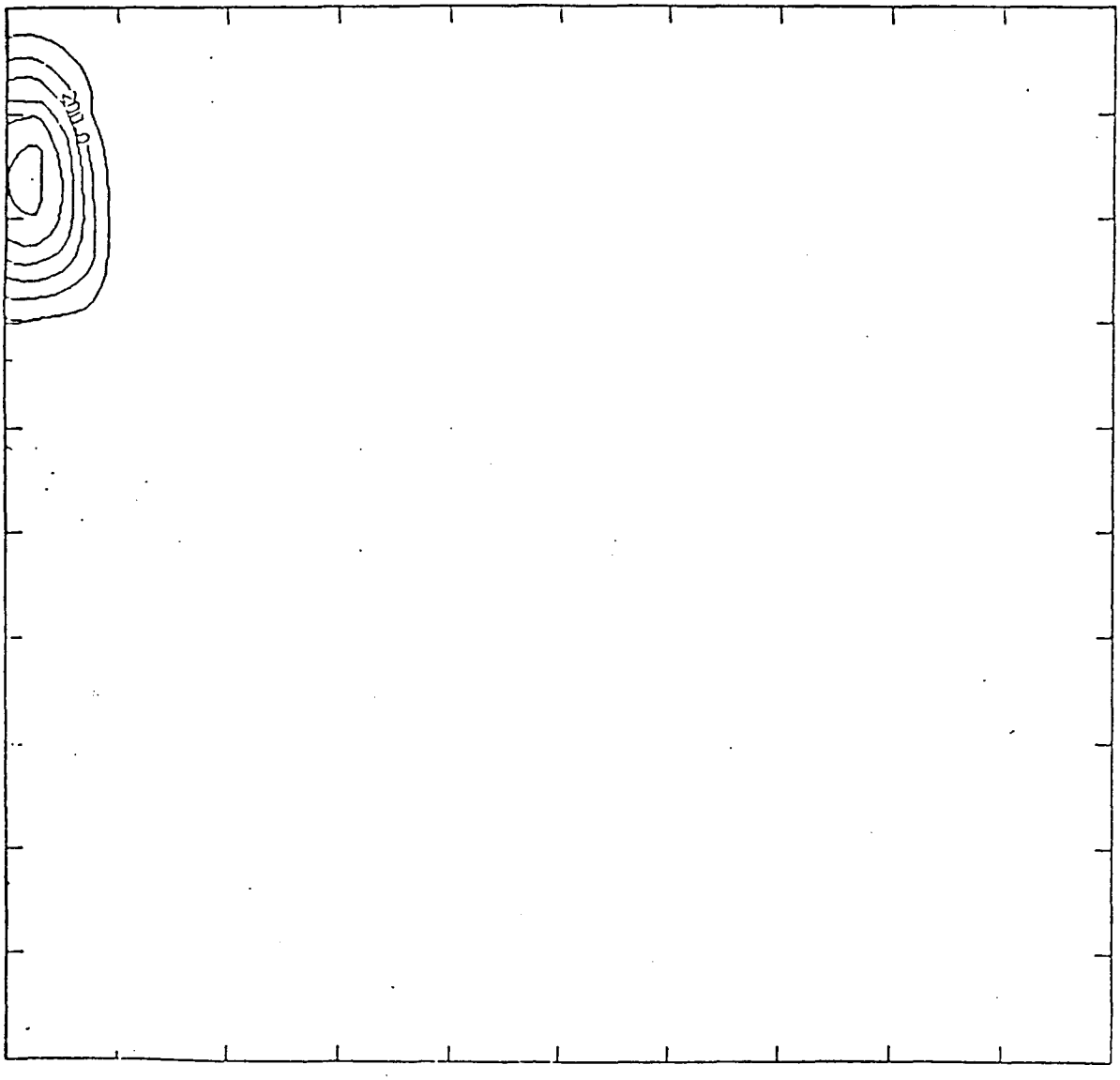

Figure A15. Kerogen density $\left(\frac{kg}{\mathrm{m}^3 \ of\ shale}\right)$ *at 27.7 hours into run.*

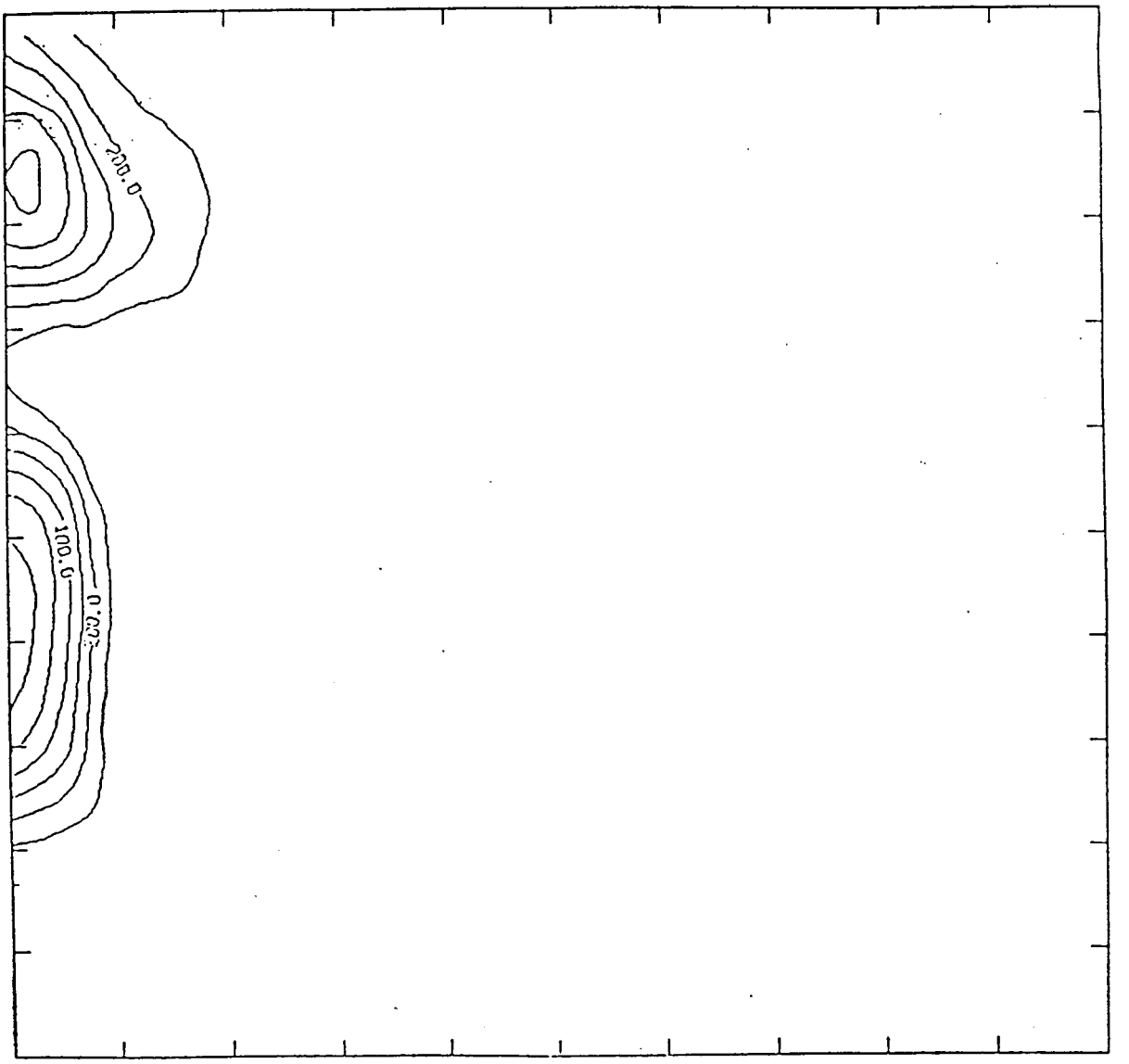

Figure A16. Same as Fig. A15 at 47.9 hours into run.

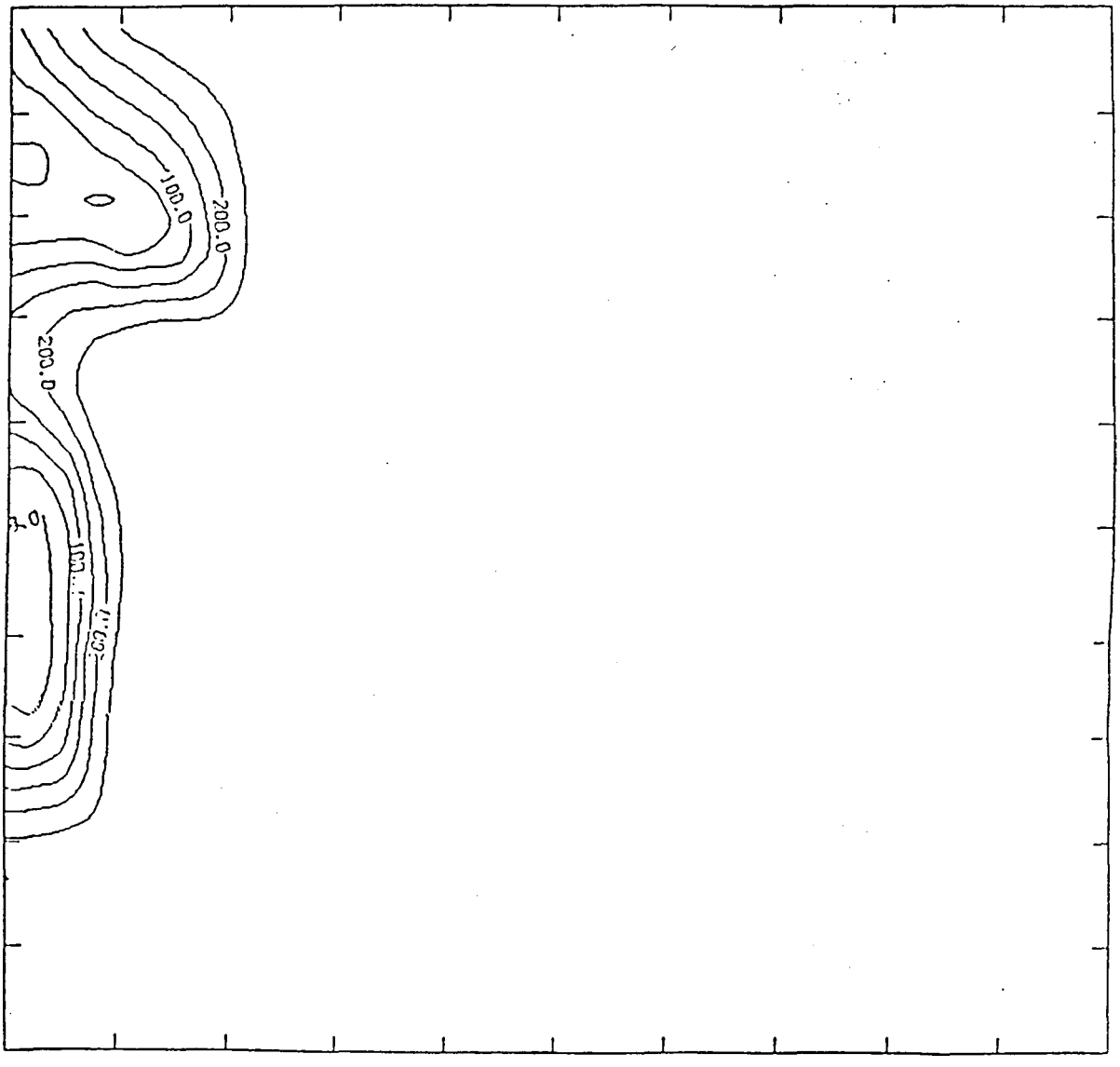

Figure A17. Same as Fig. A15 at 61.2 hours into run.

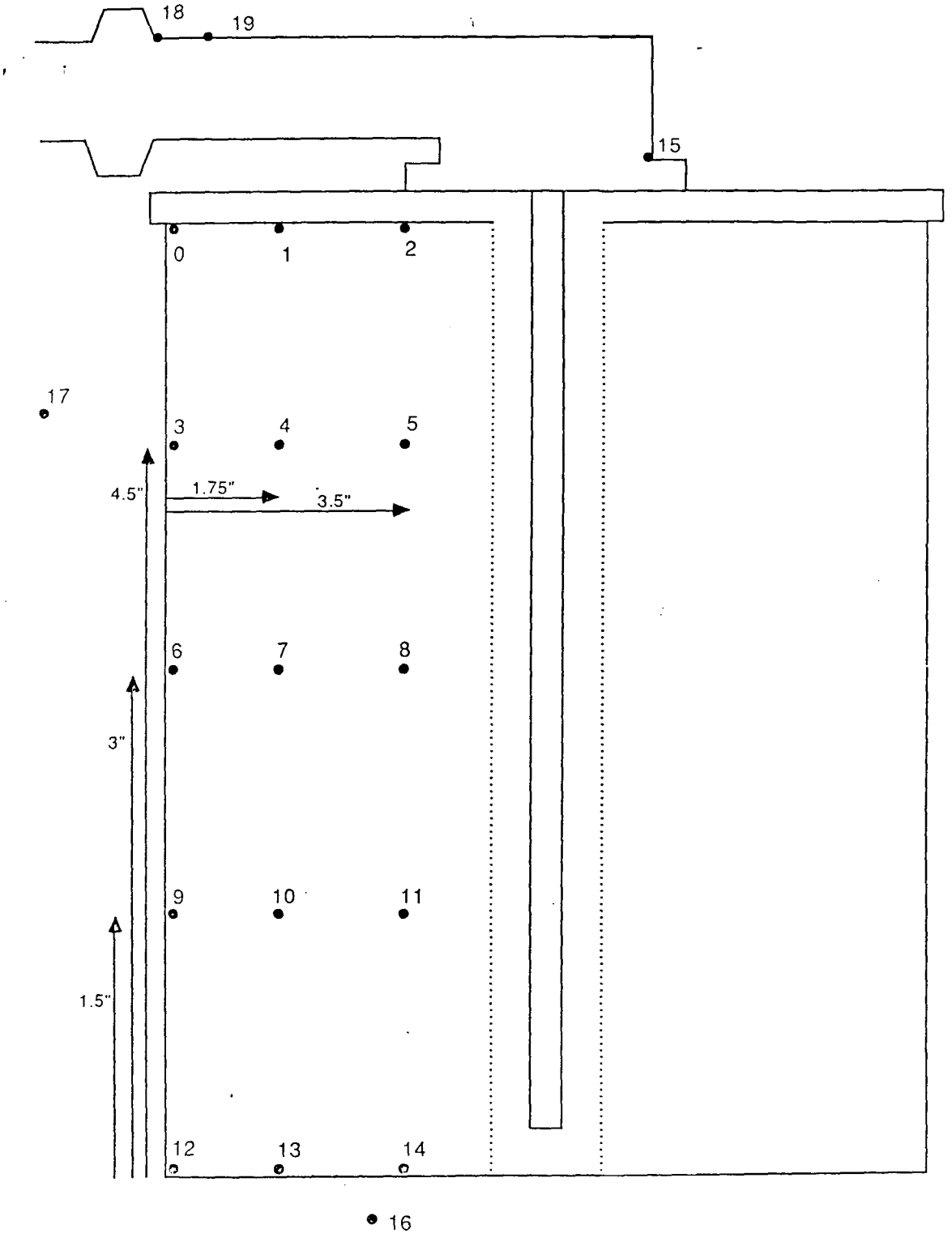

Figure A18. Thermocouple positions in shale block.

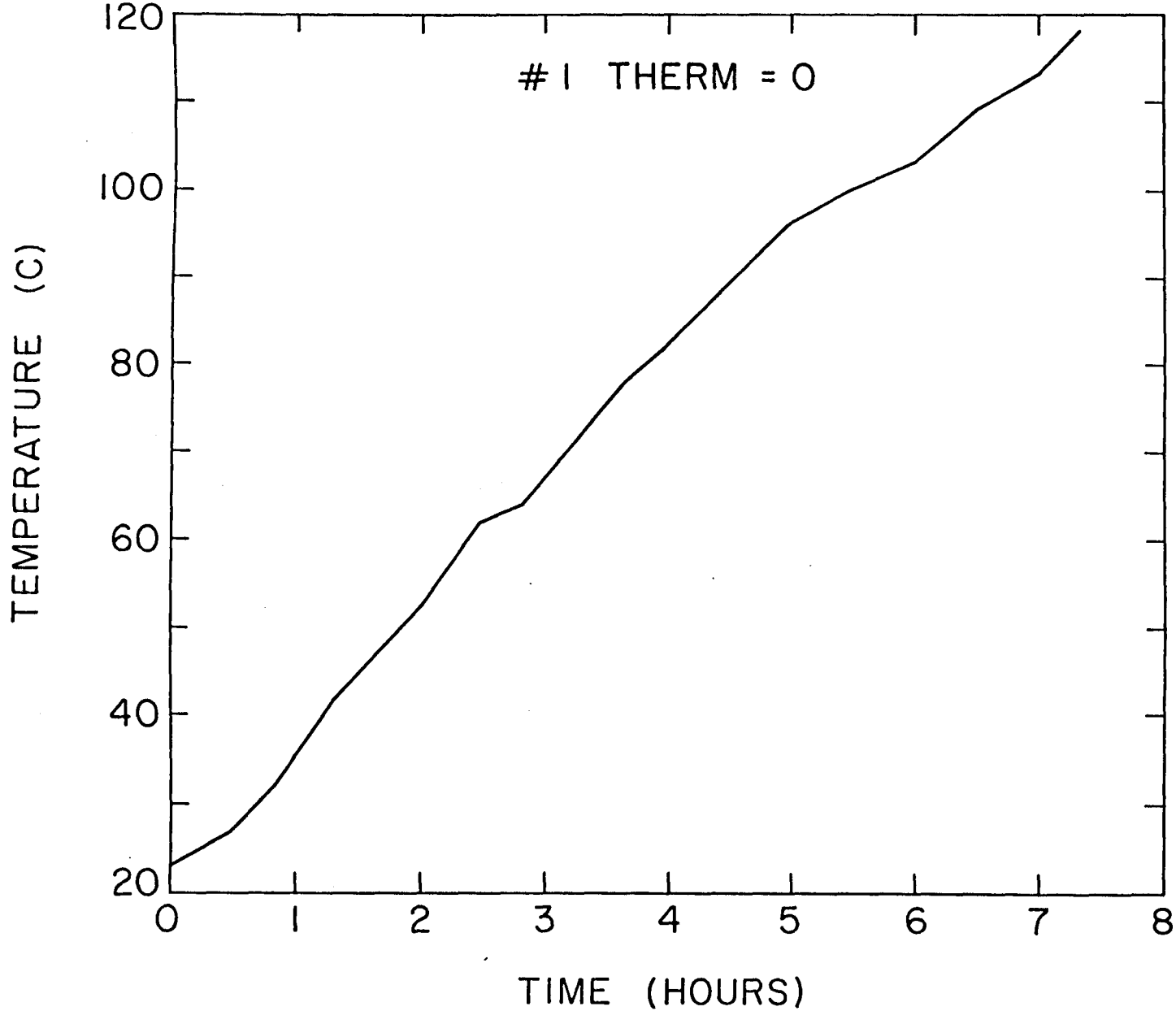

Figure A19. Temperature vs time.

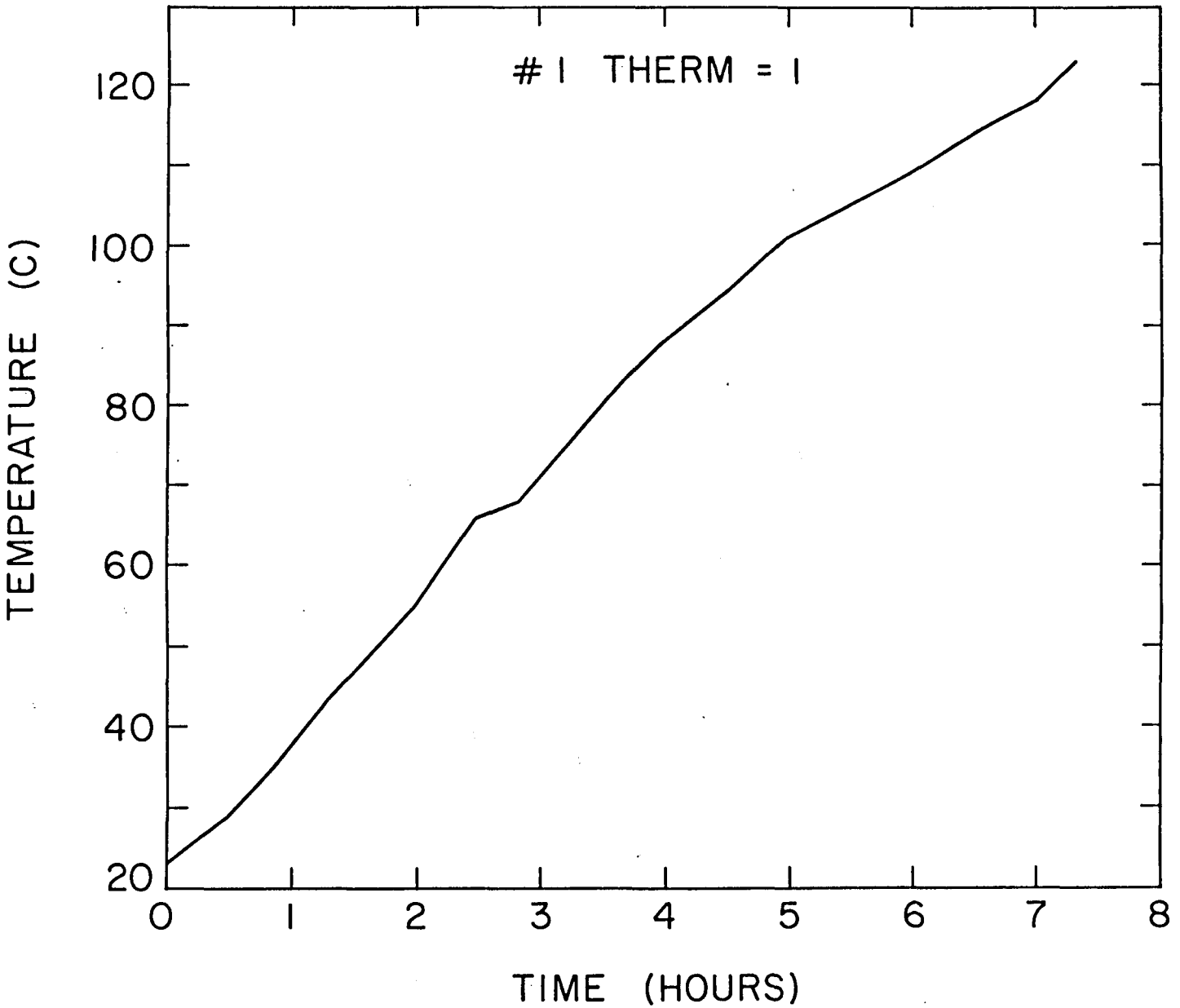

Figure A20. Temperature vs time.

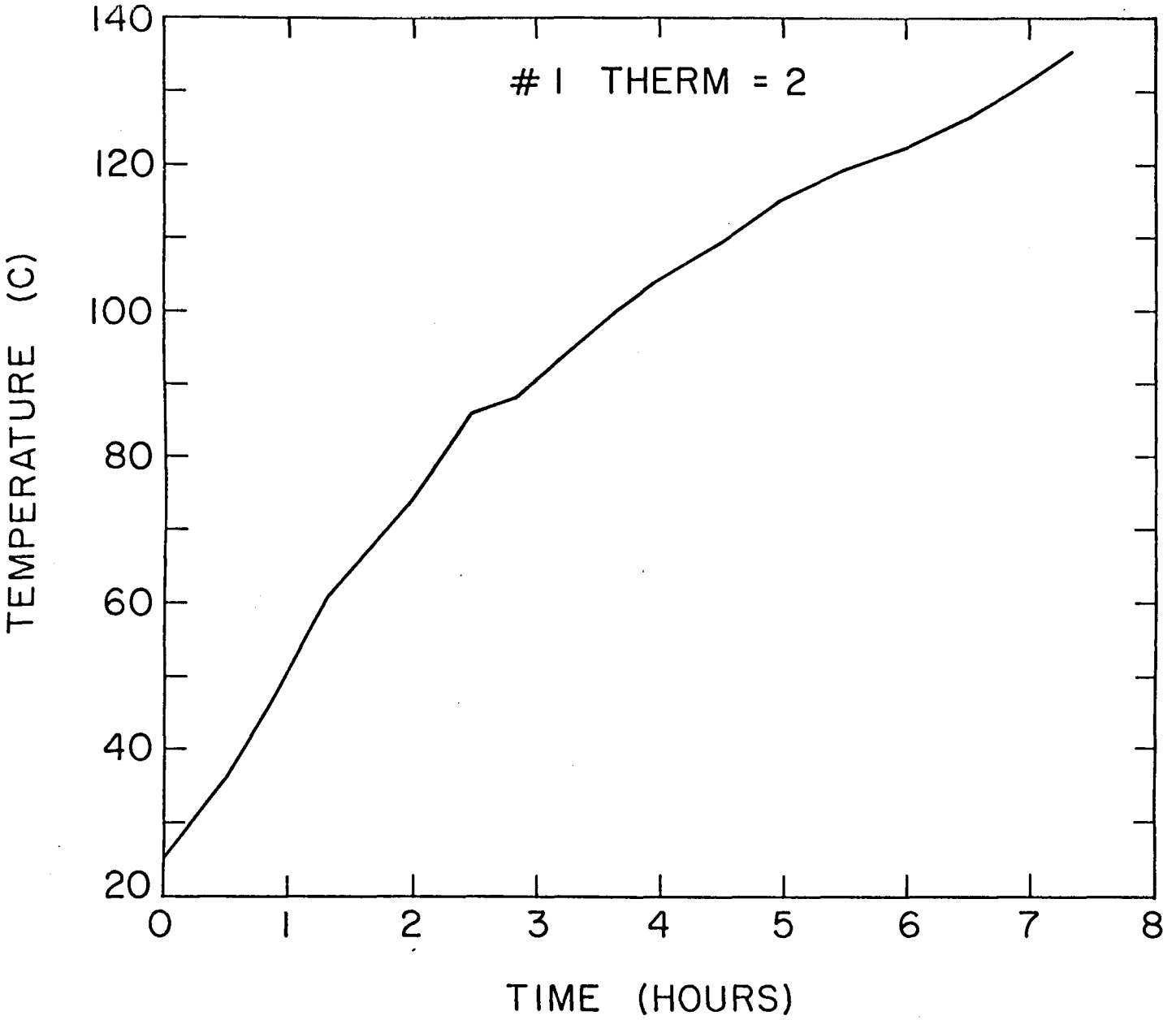

Figure A21. Temperature vs time.

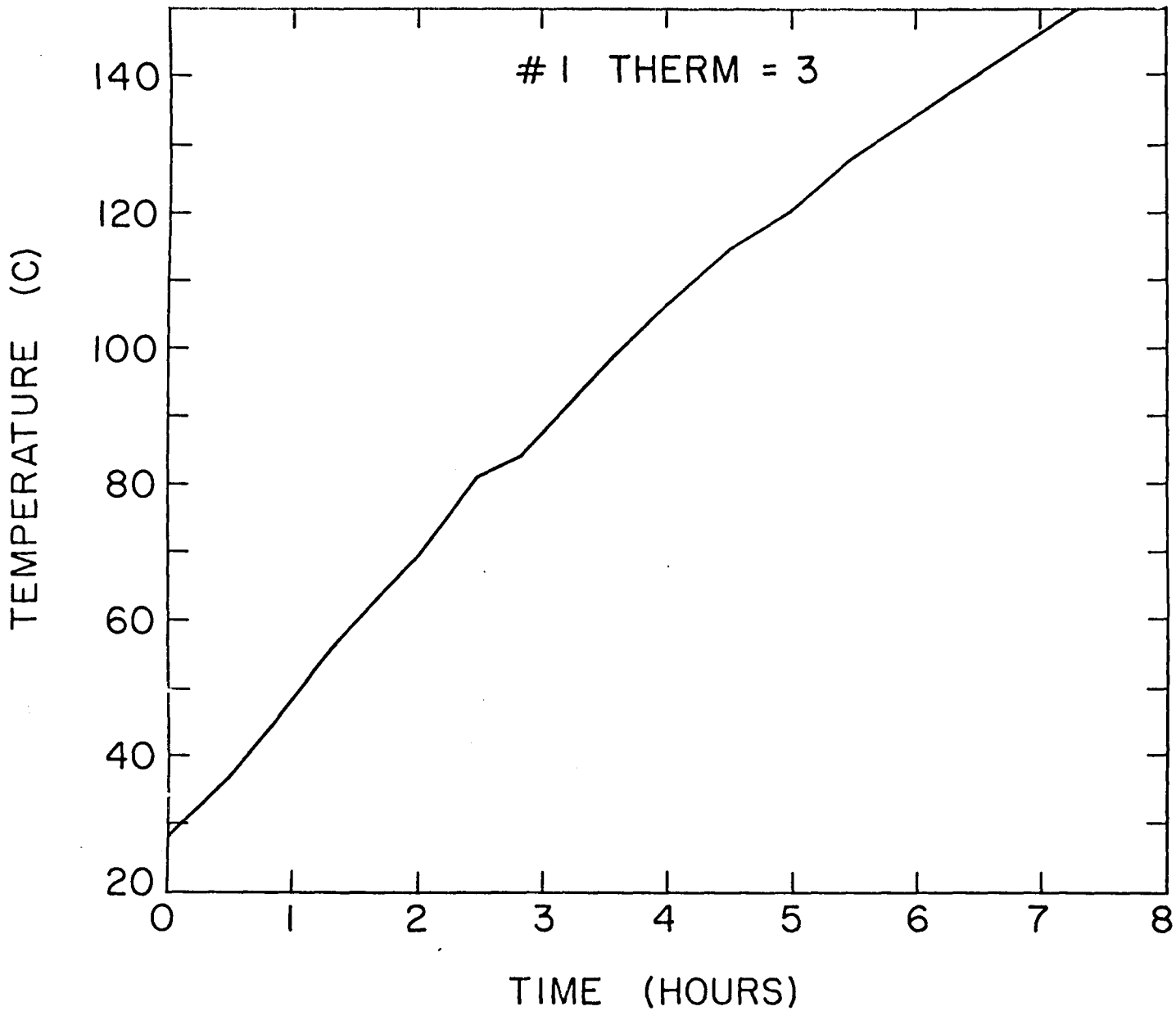

Figure A22. Temperature vs time.

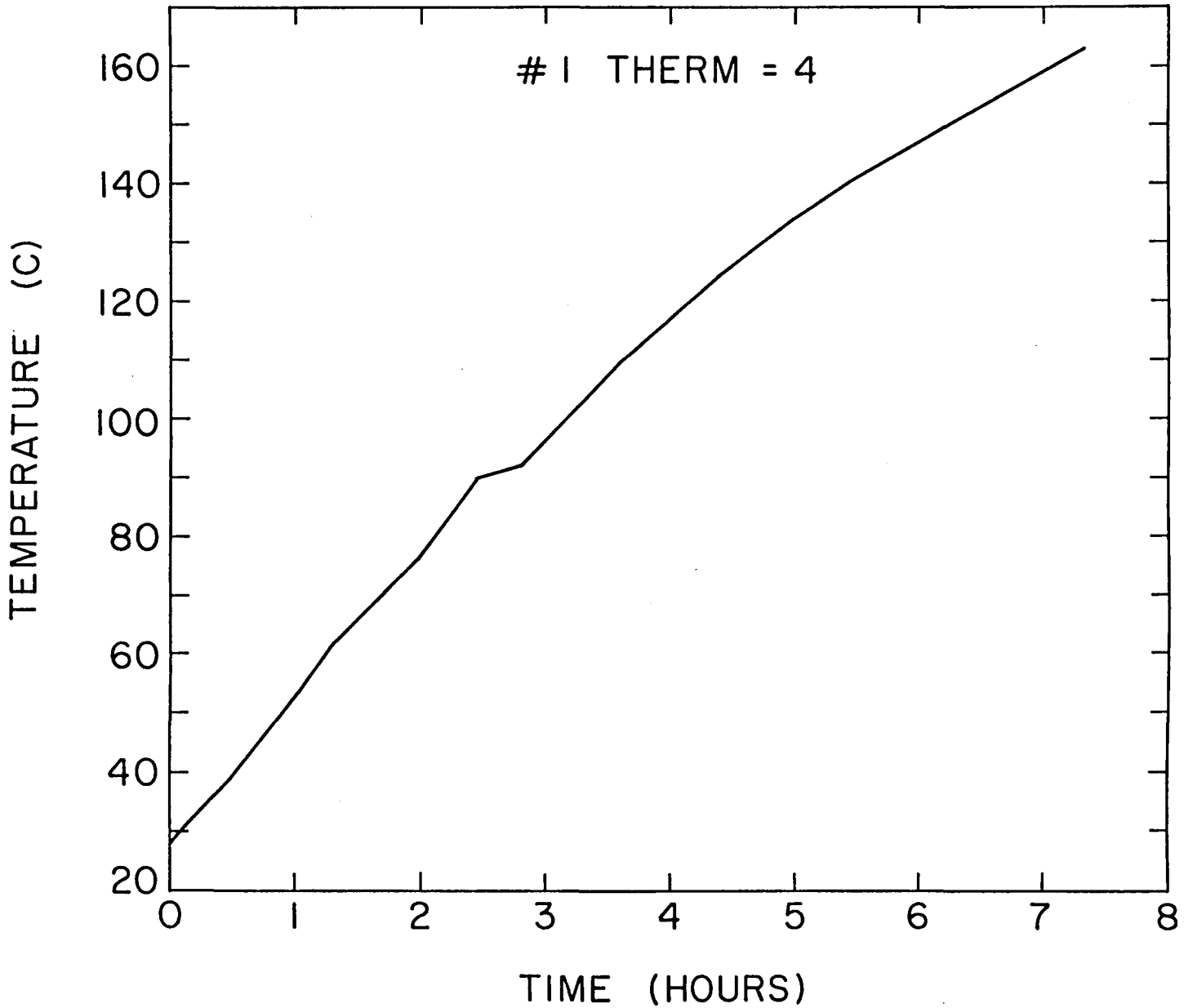

Figure A23. Temperature vs time.

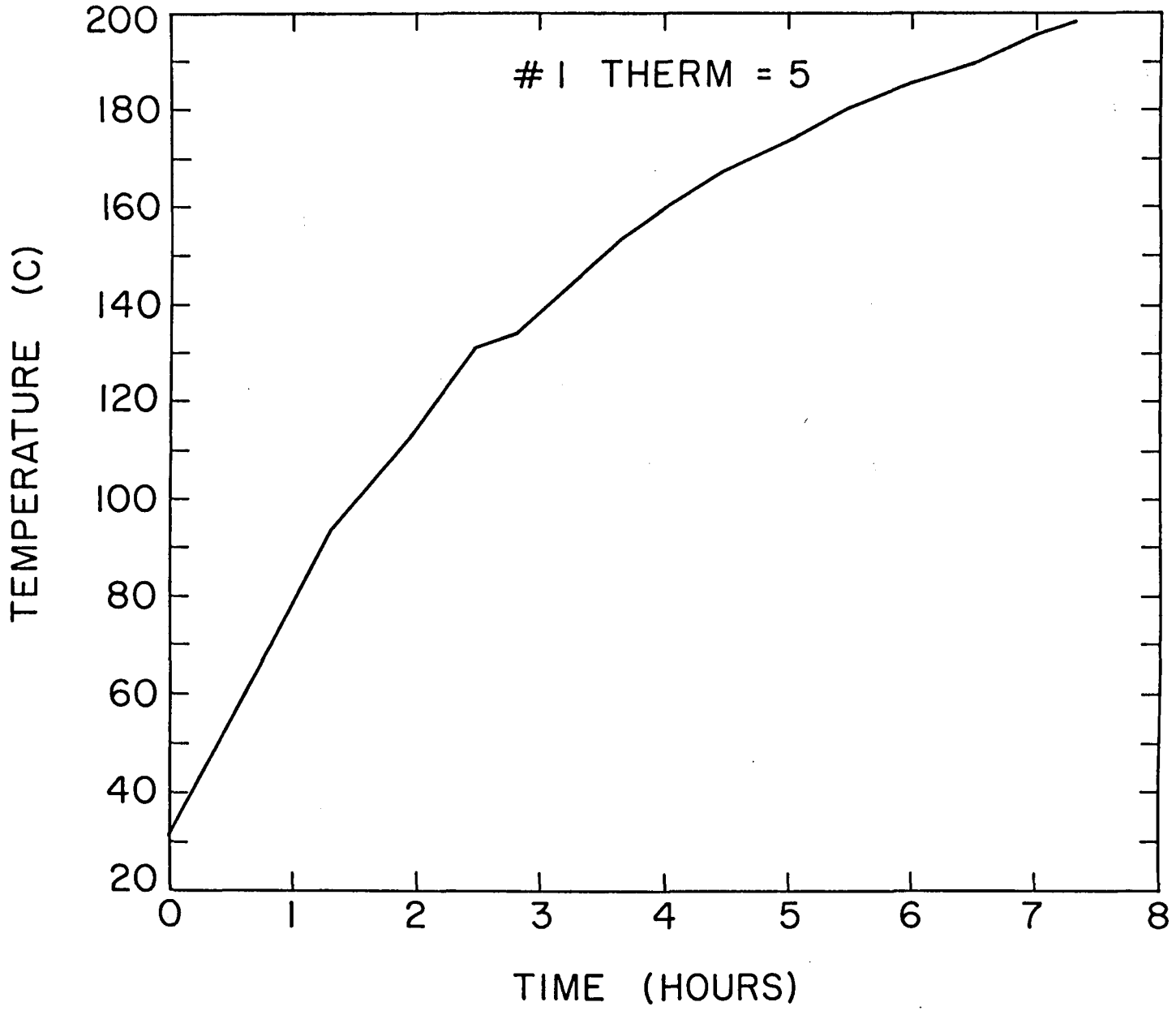

Figure A24. Temperature vs time.

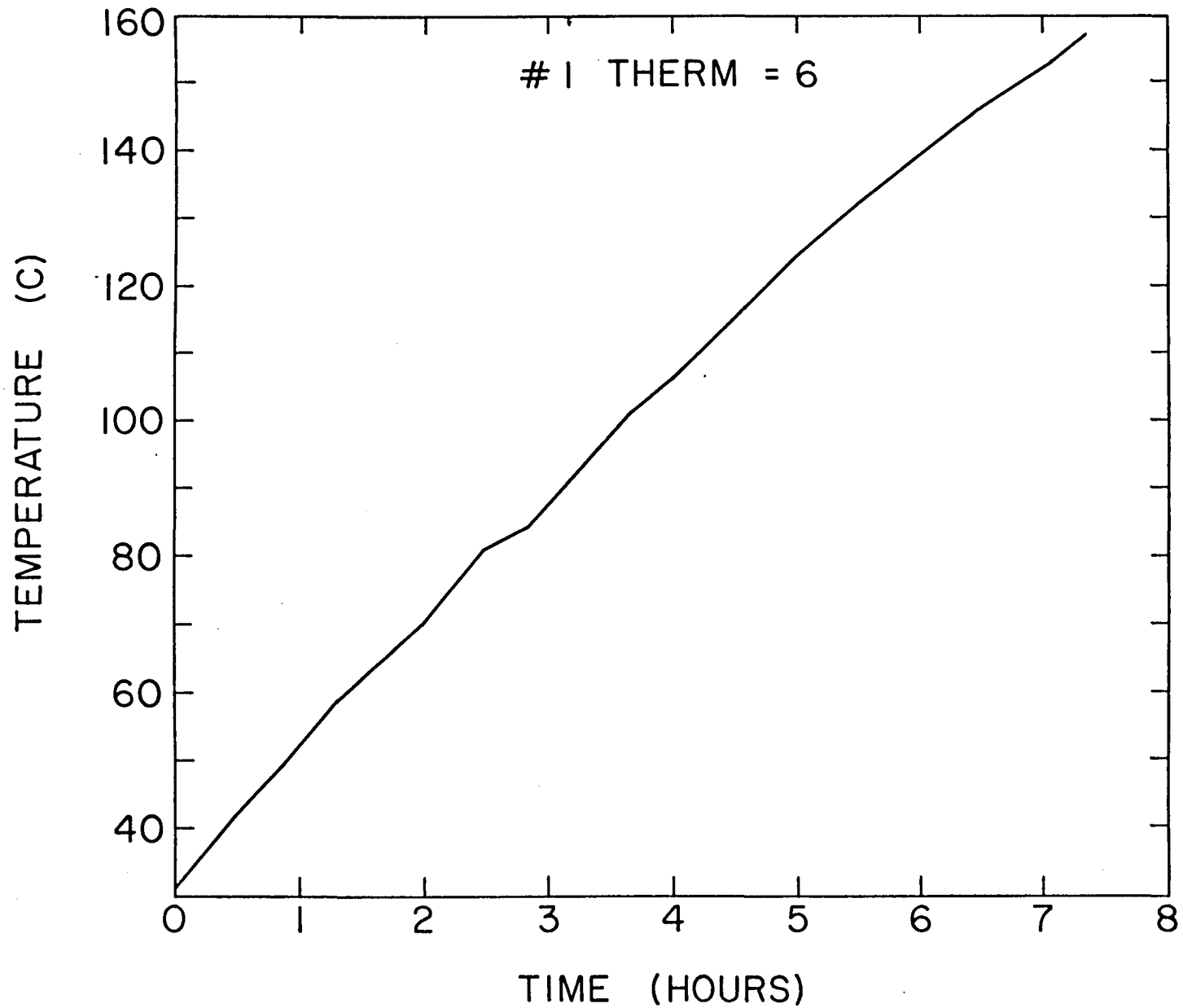

Figure A25. Temperature vs time.

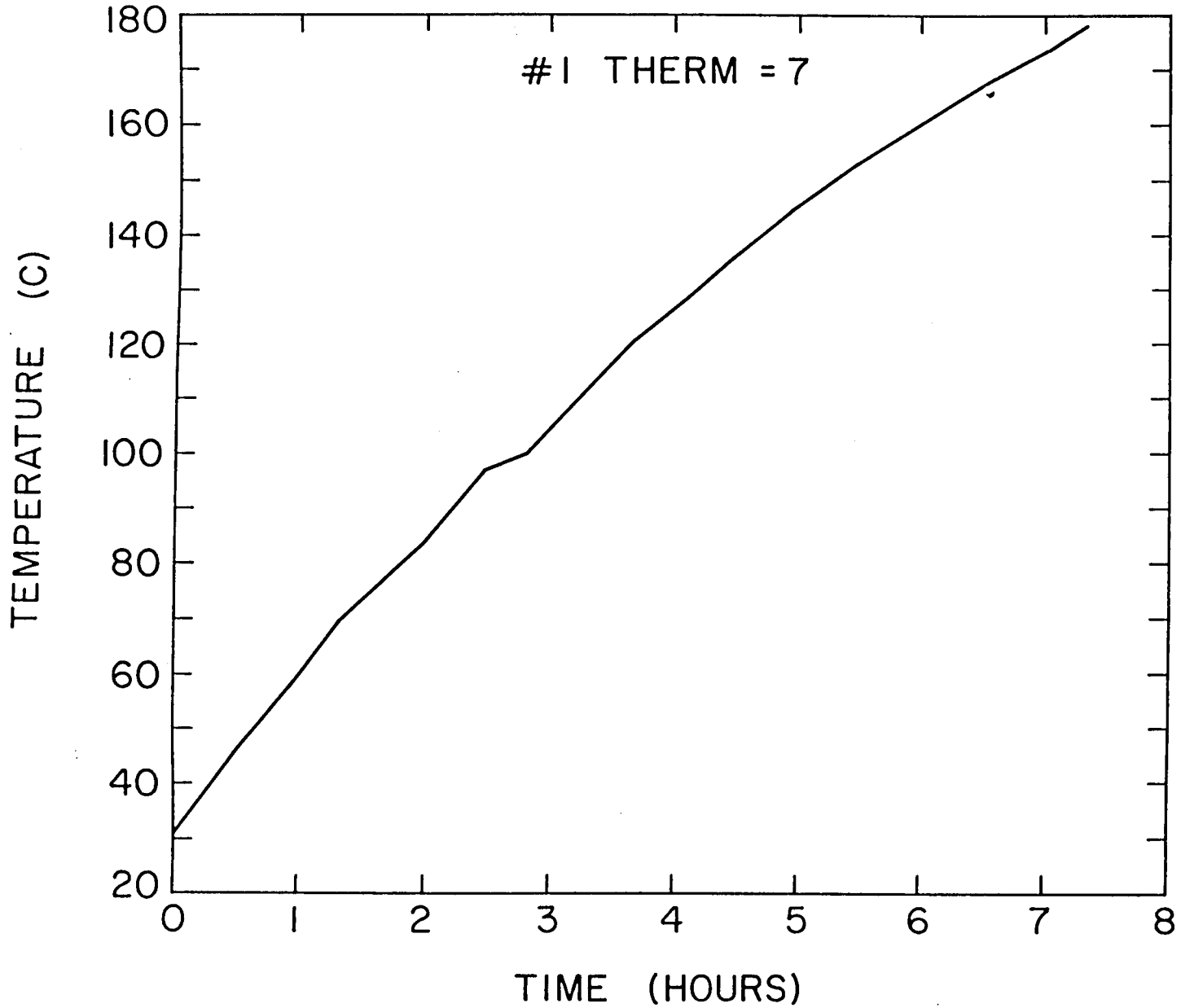

Figure A26. Temperature vs time.

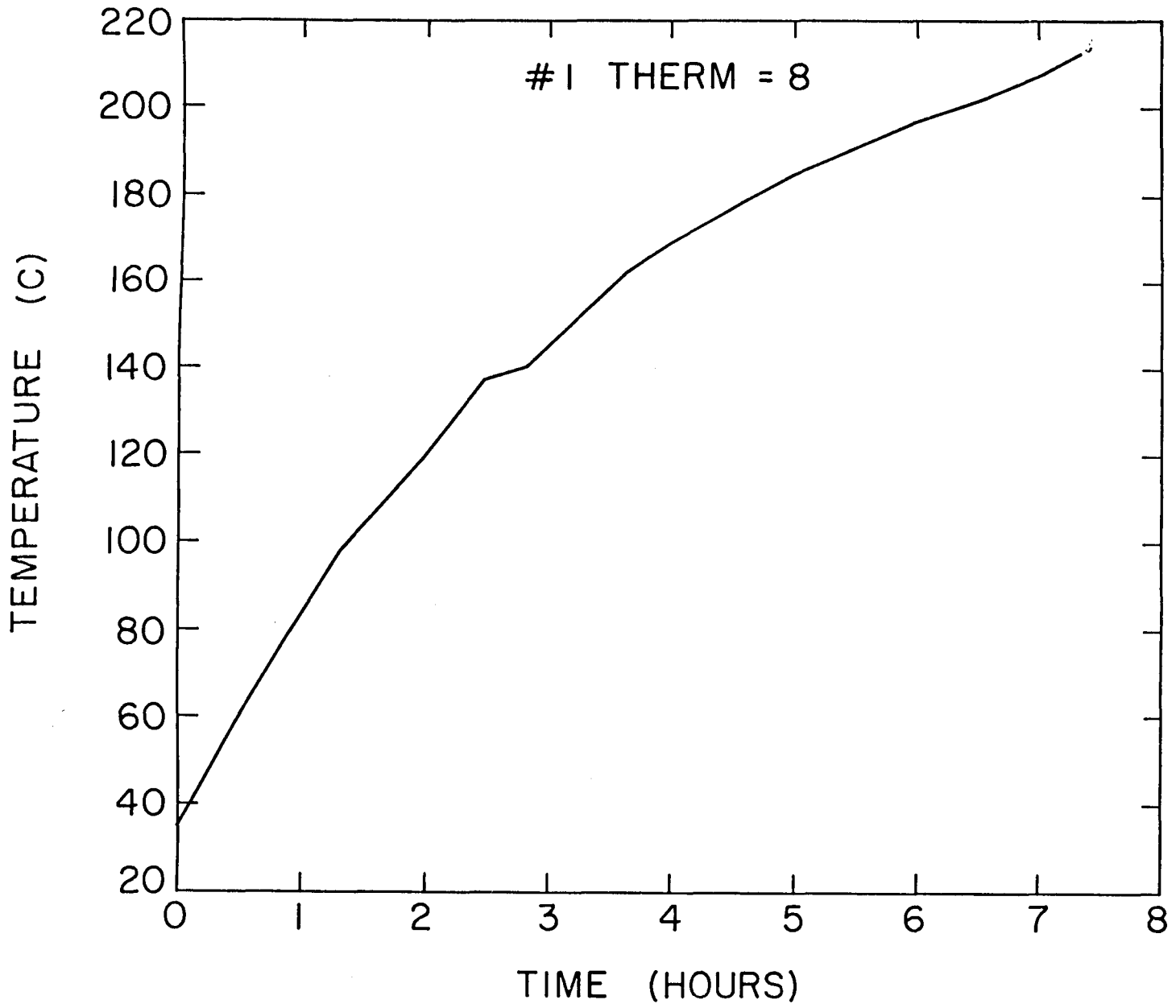

Figure A27. Temperature vs time.

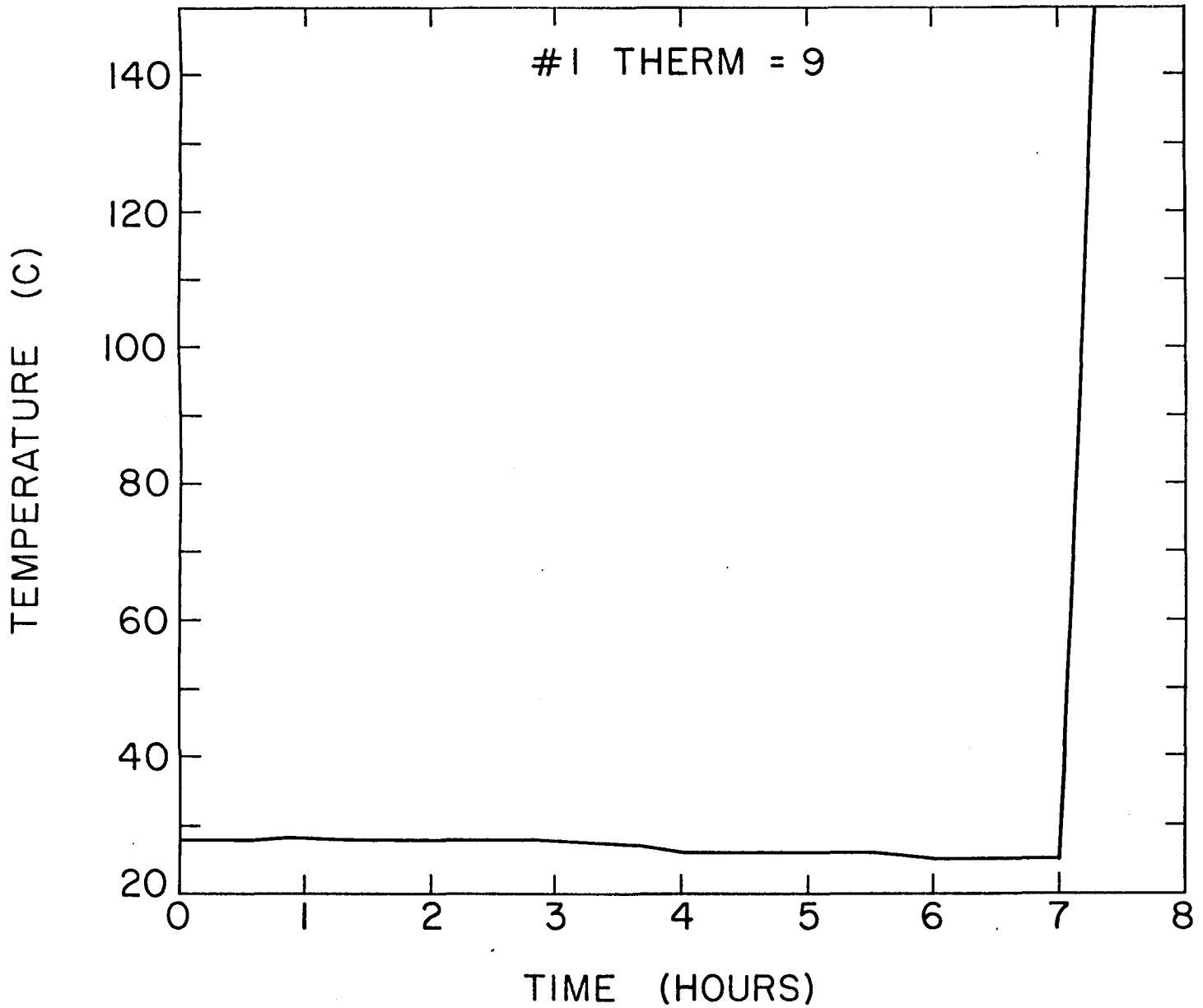

Figure A28. Temperature vs time.

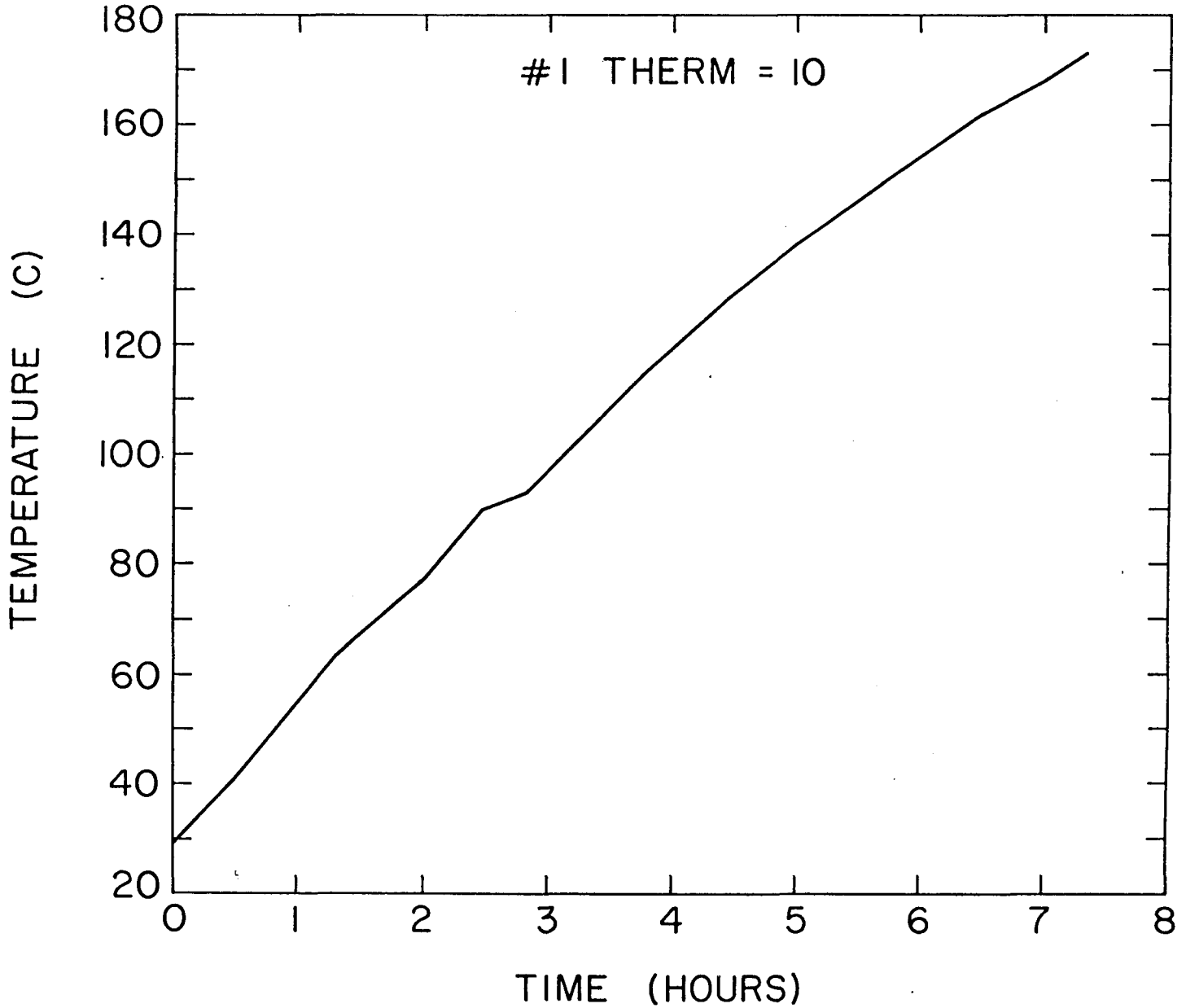

Figure A29. Temperature vs time.

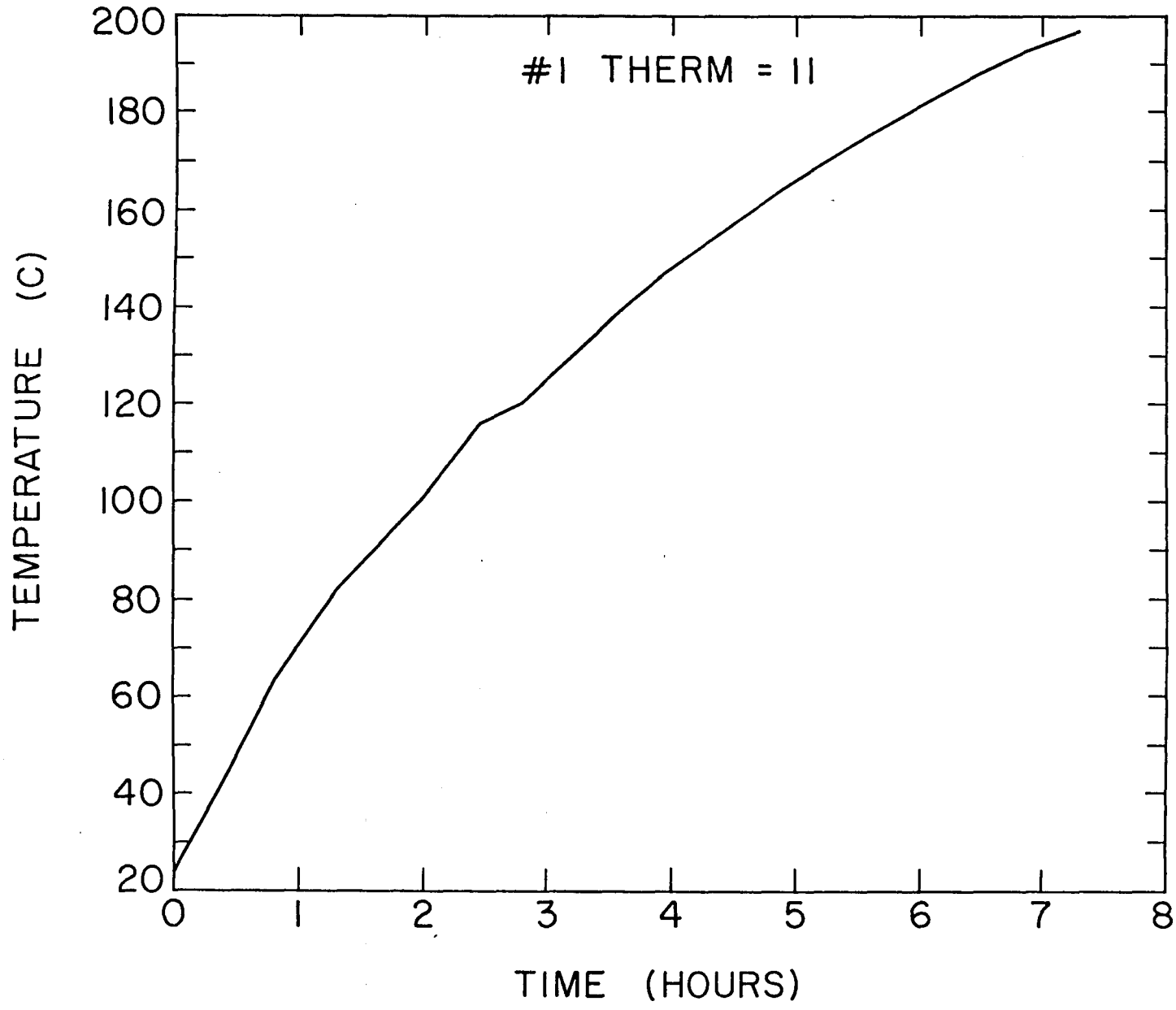

Figure A30. Temperature vs time.

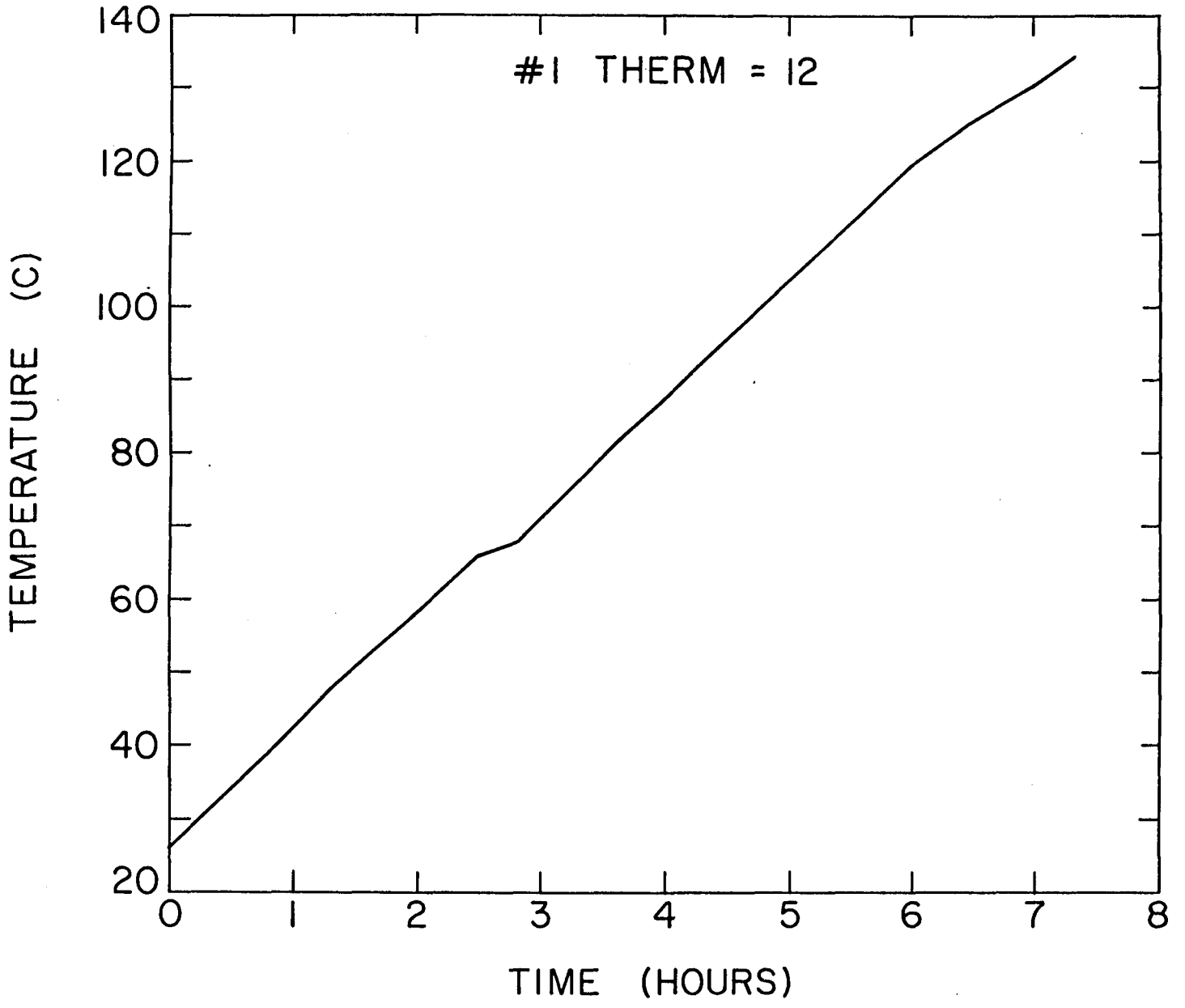

Figure A31. Temperature vs time.

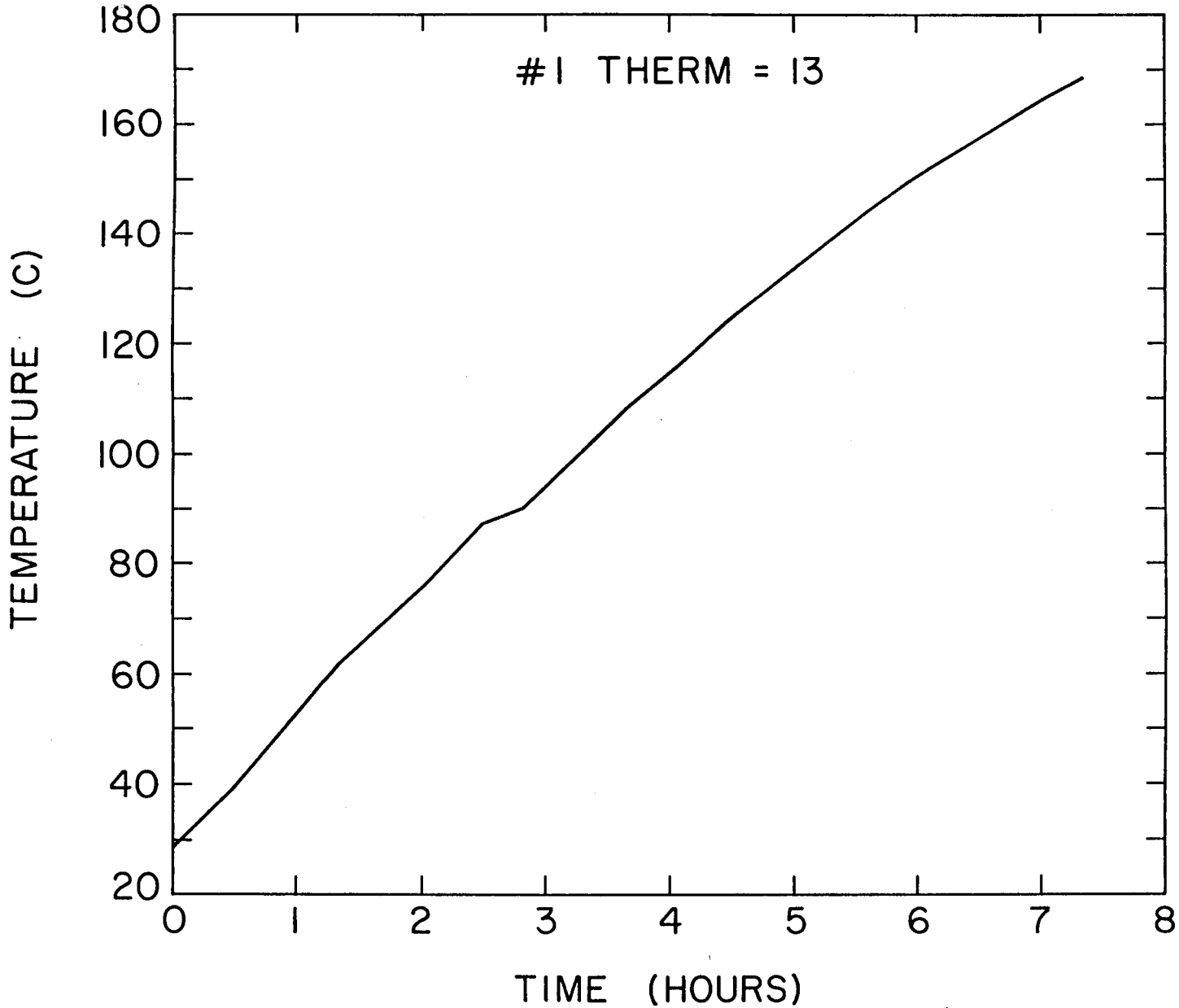

Figure A32. Temperature vs time.

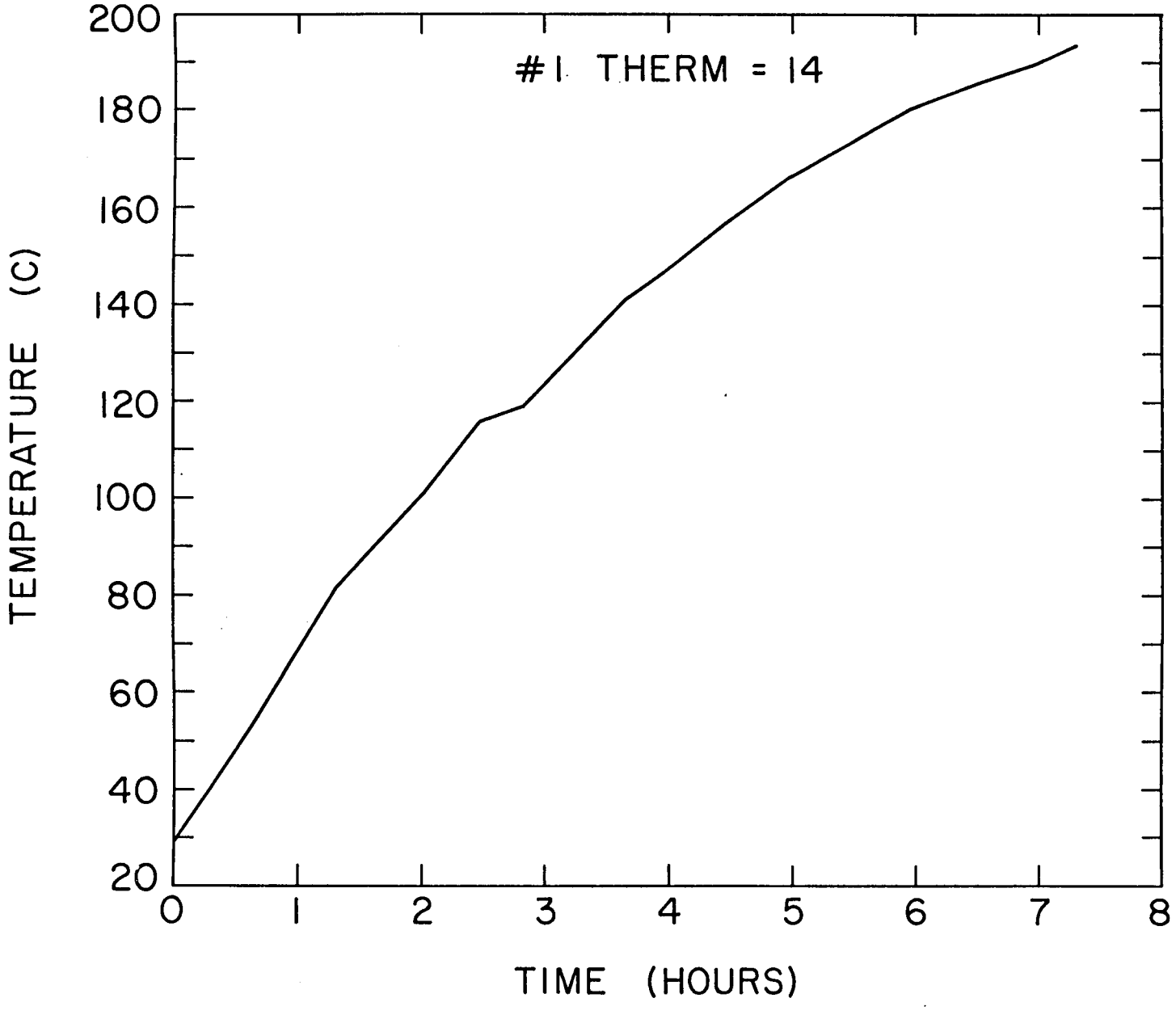

Figure A33. Temperature vs time.

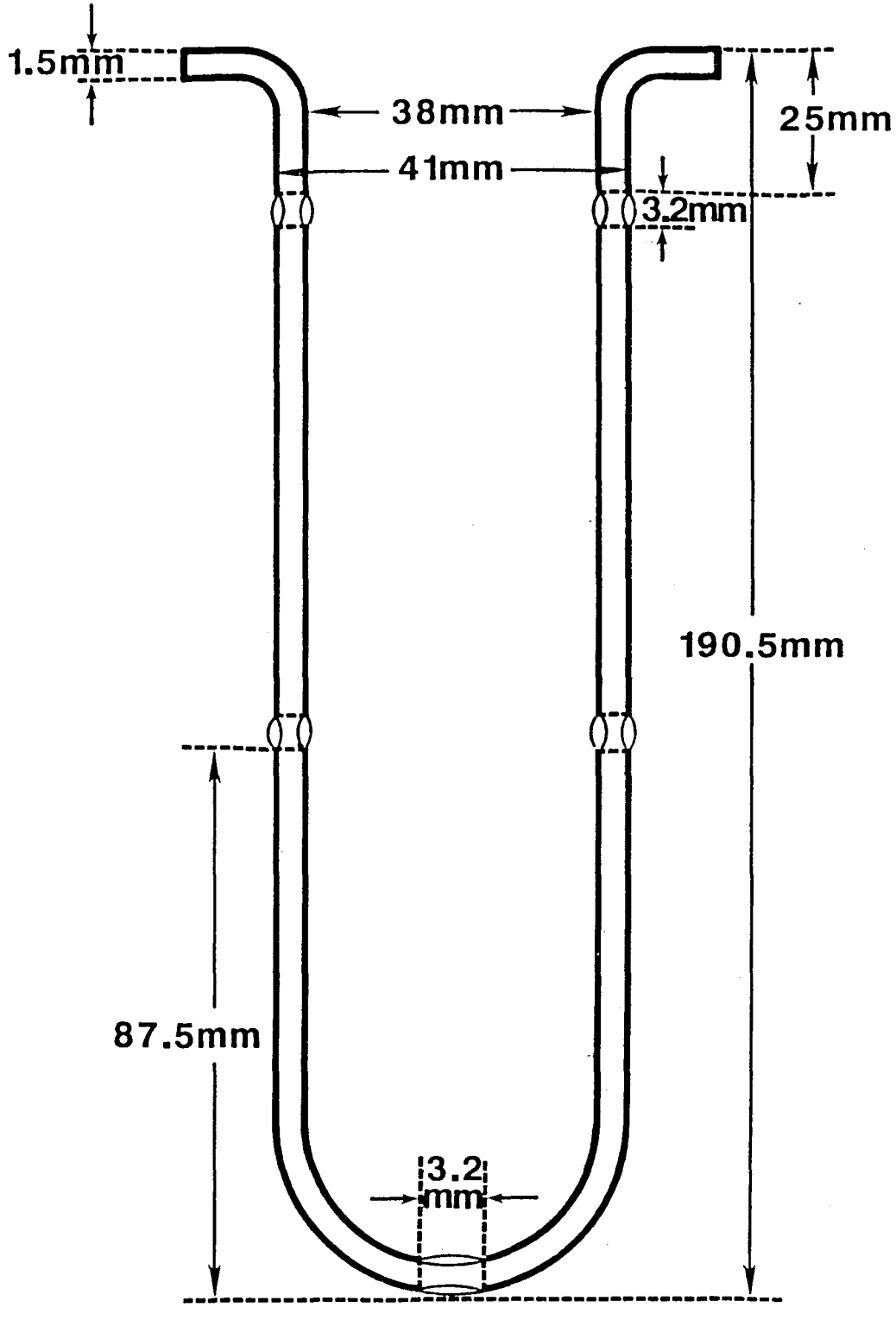

Figure A34. Insulated Antenna Sheath.

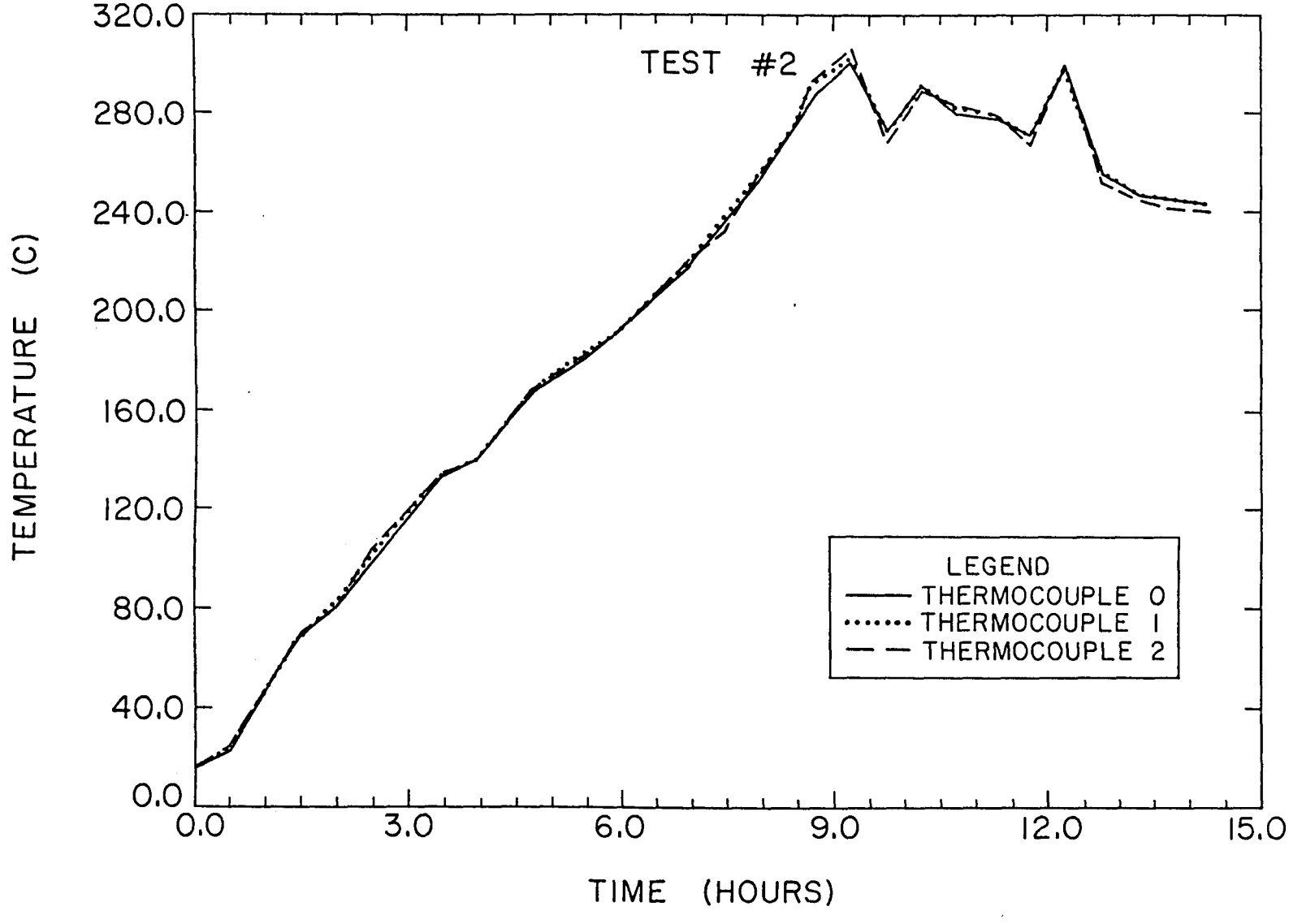

Figure A35. Temperature vs time profile for test #2 (monopole experiment).

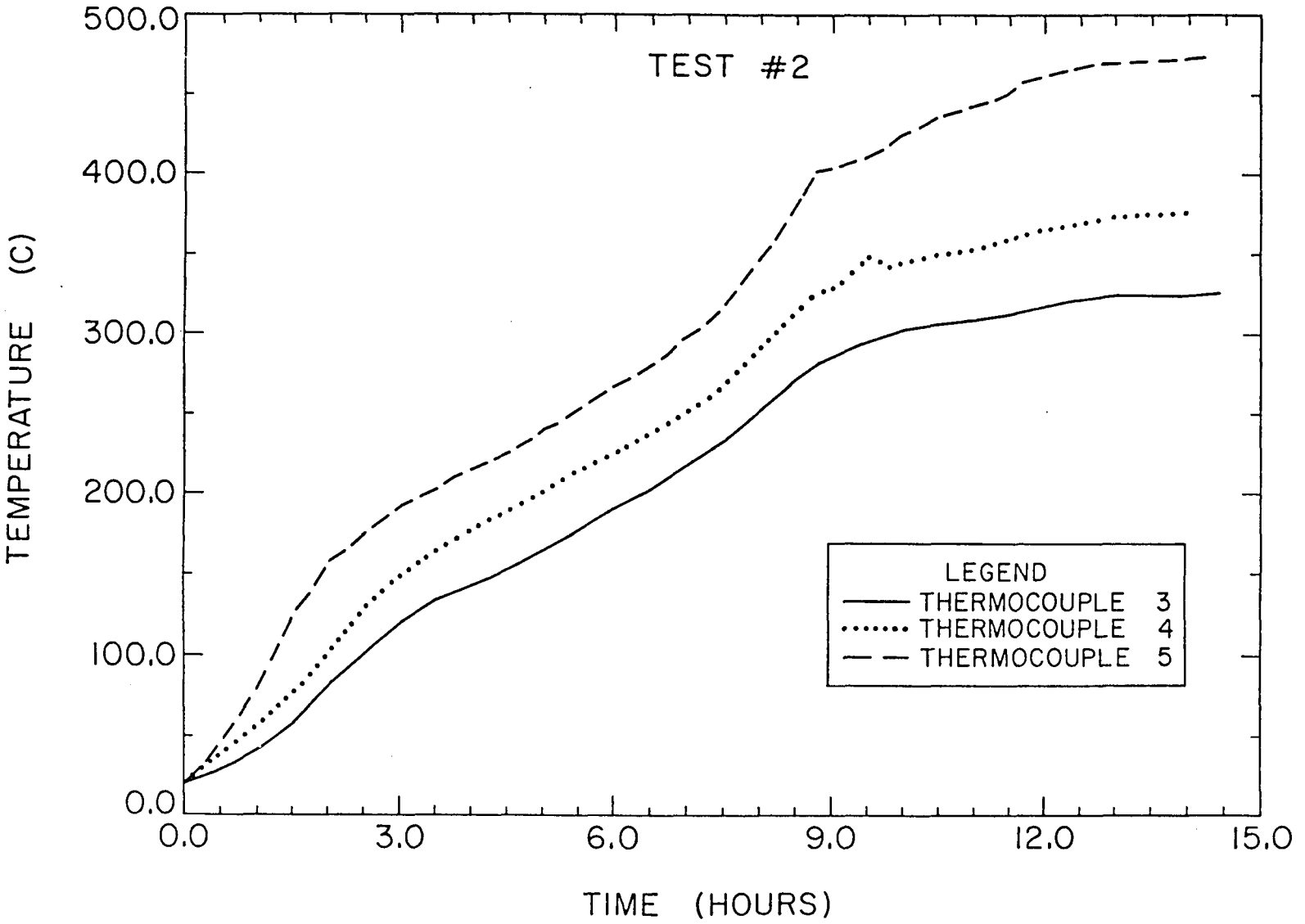

Figure A36. Temperature vs time profile for test #2 (monopole experiment).

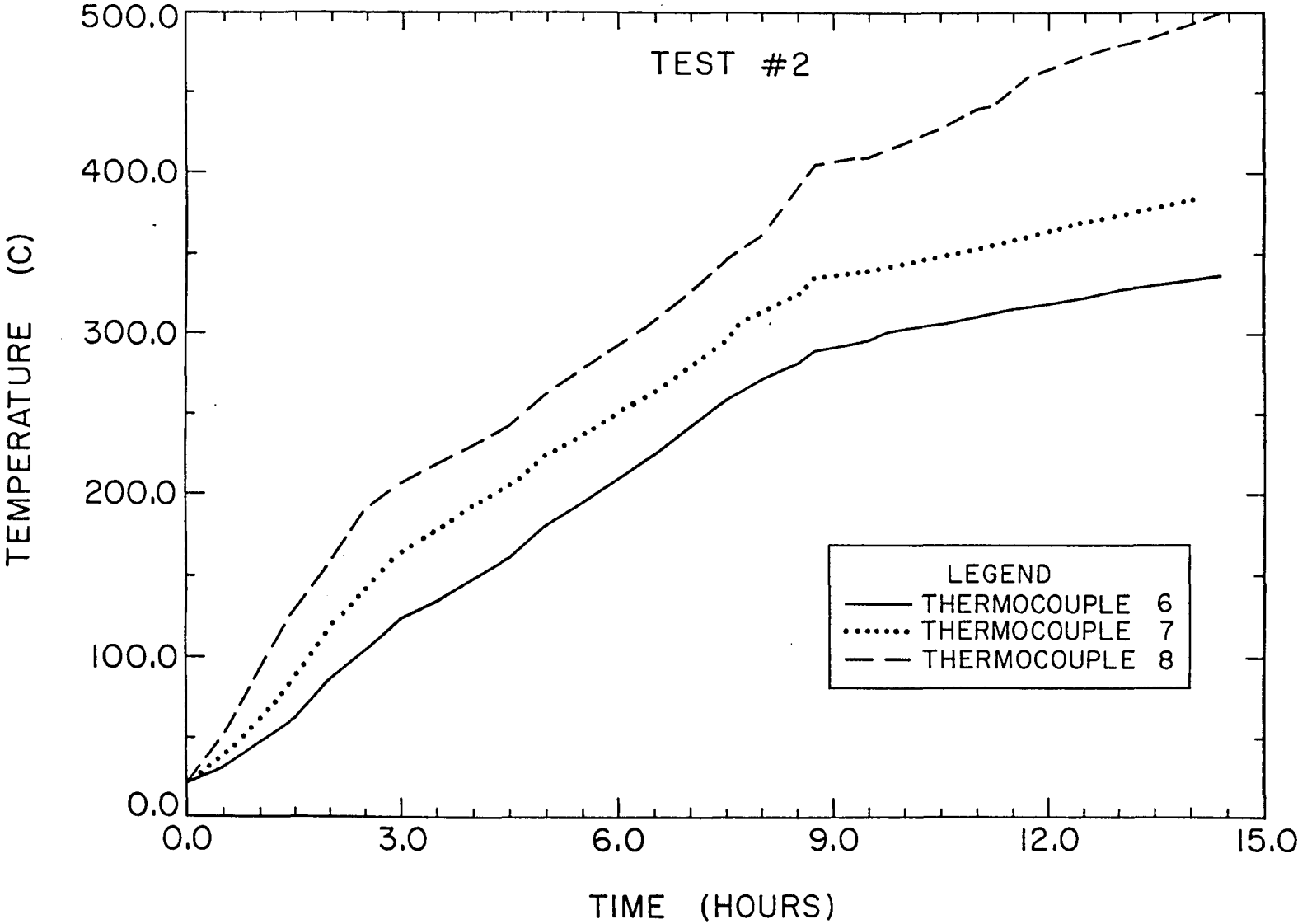

Figure A37. Temperature vs time profile for test #2 (monopole experiment).

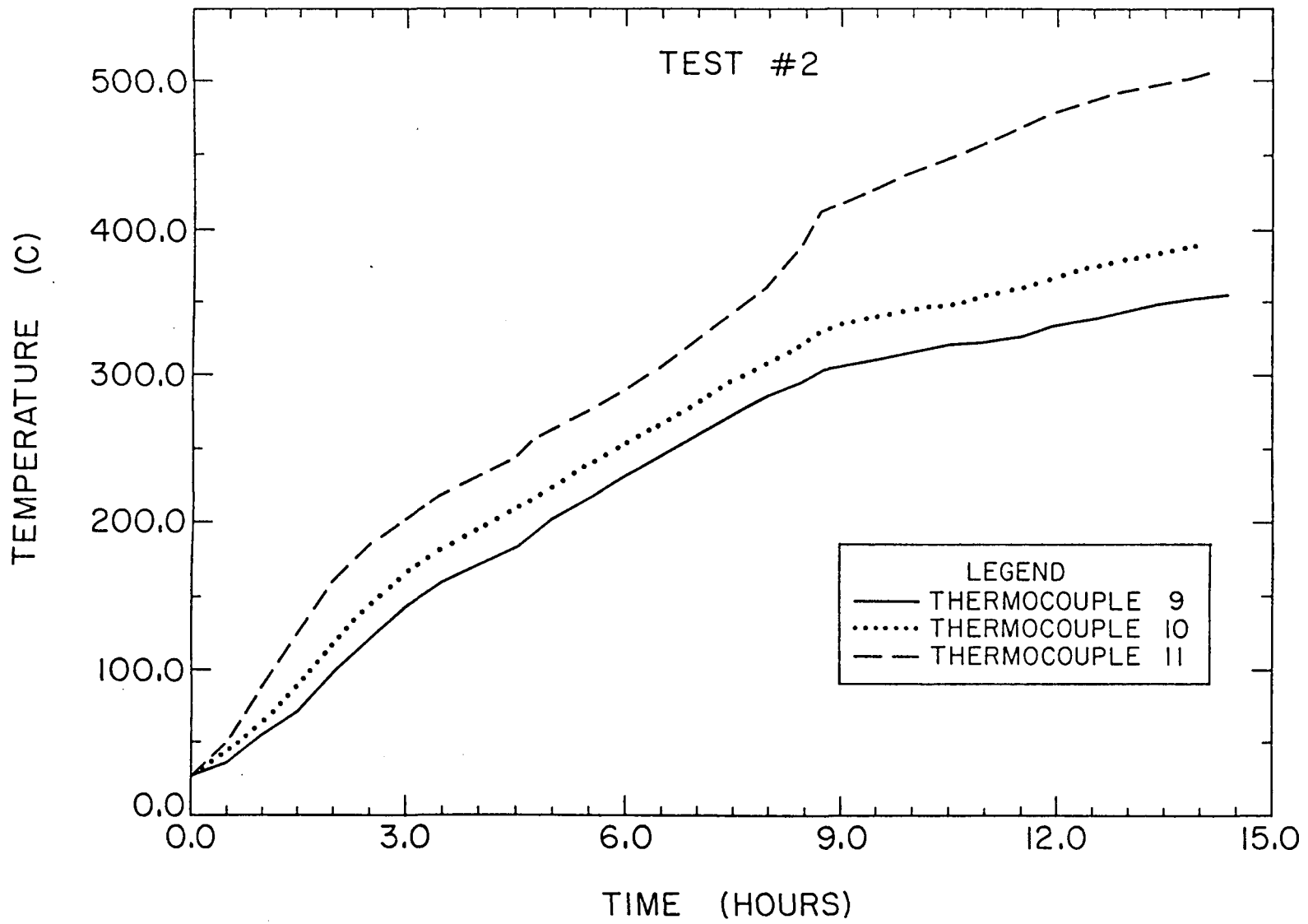

Figure A38. Temperature vs time profile for test #2 (monopole experiment).

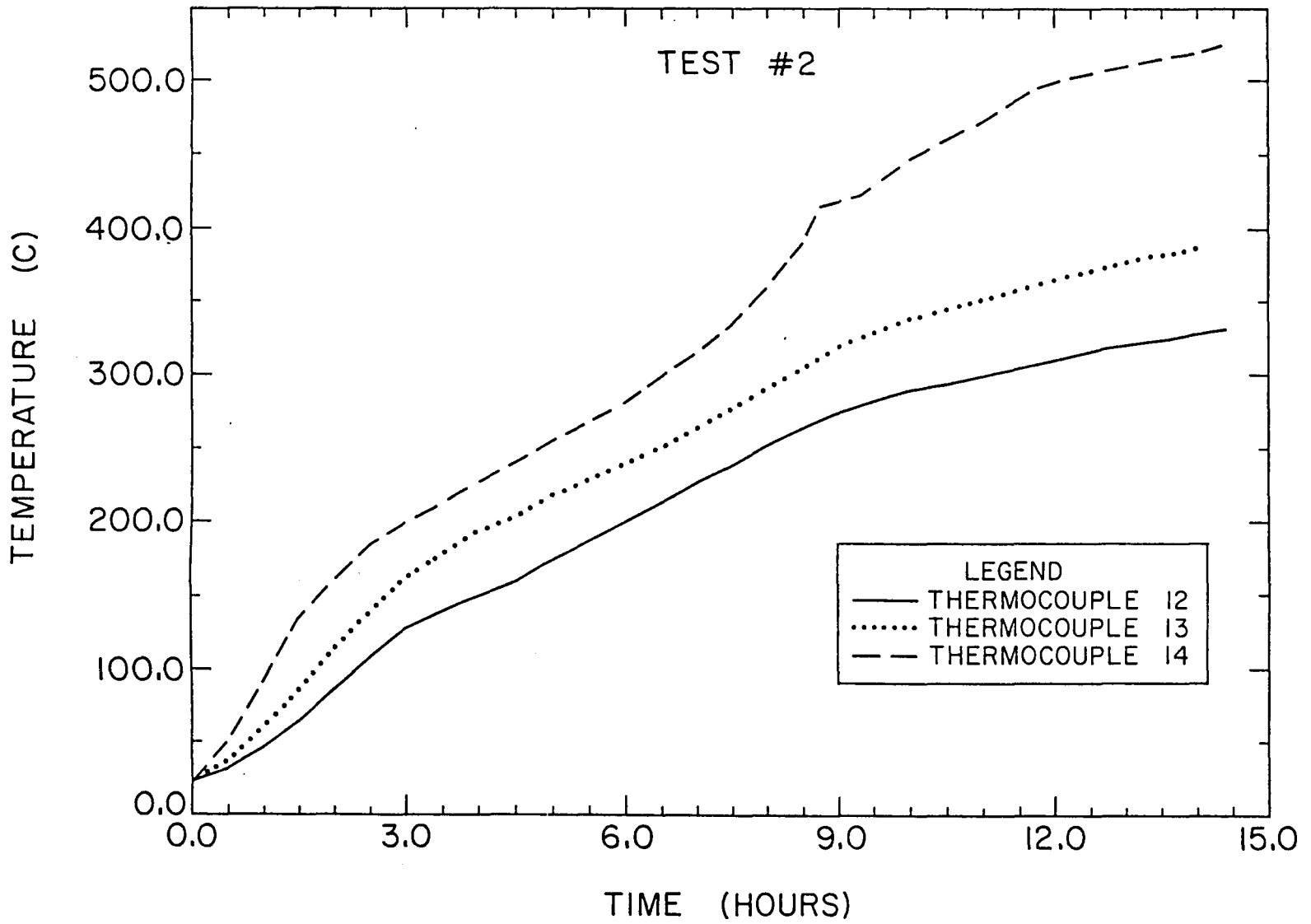

Figure A39. Temperature vs time profile for test #2 (monopole experiment).

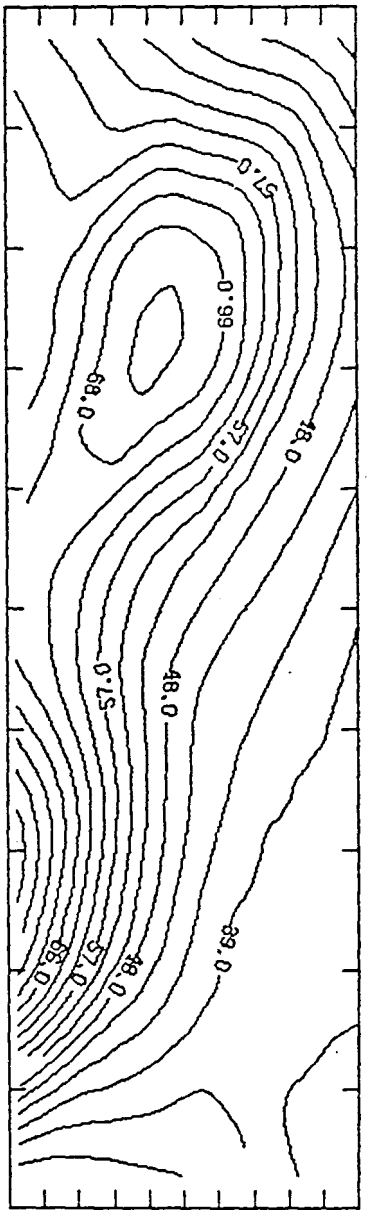

Figure A40. Temperature contours (°C).

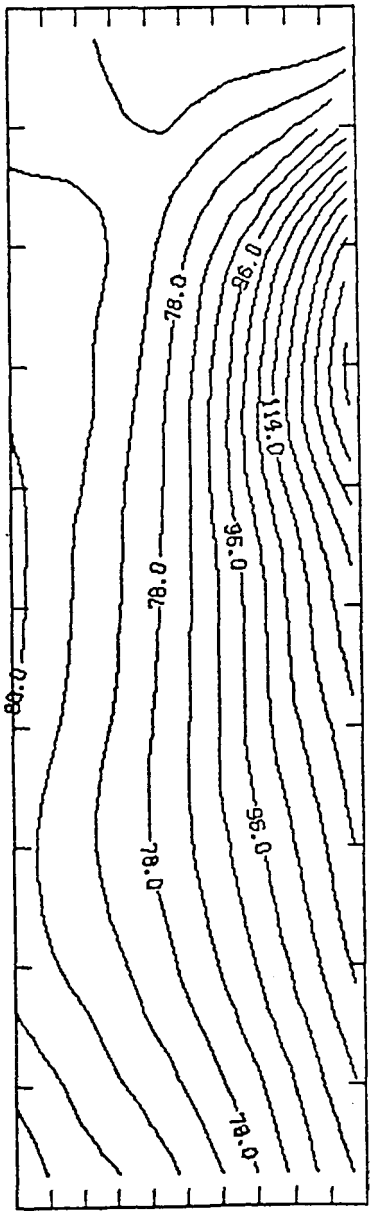

Figure A41. Temperature contours (°C).

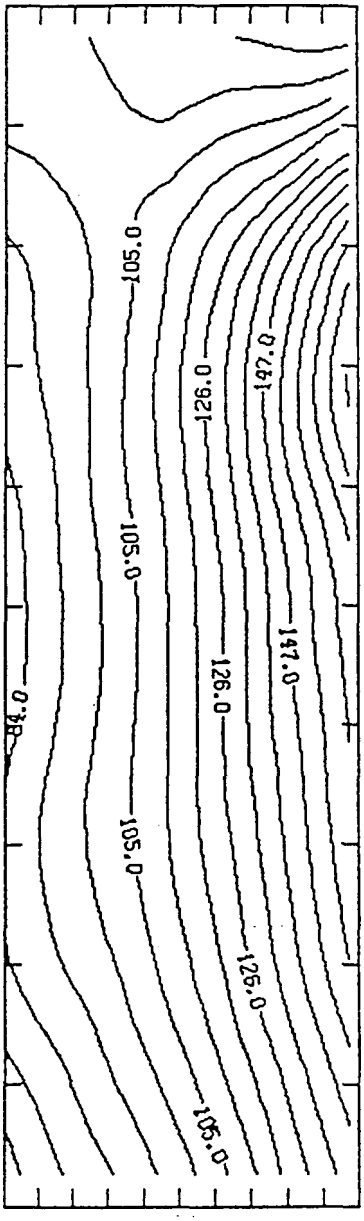

Figure A42. Temperature contours (°C).

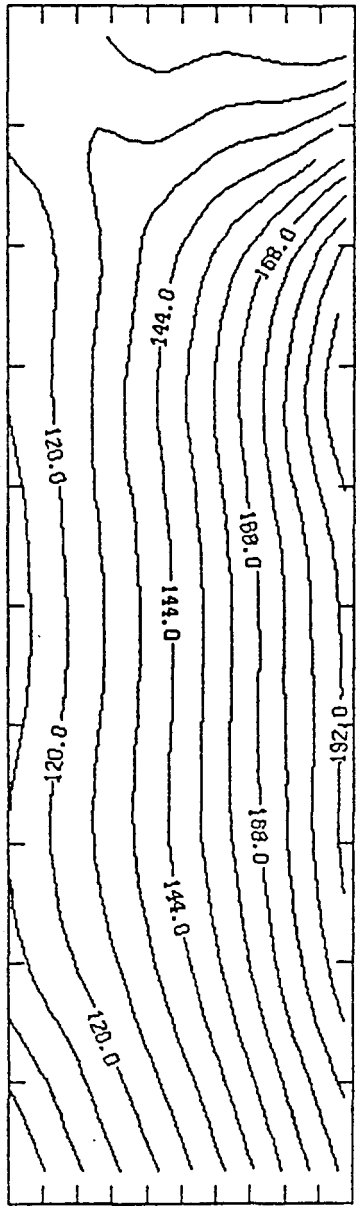

Figure A43. Temperature contours (°C).

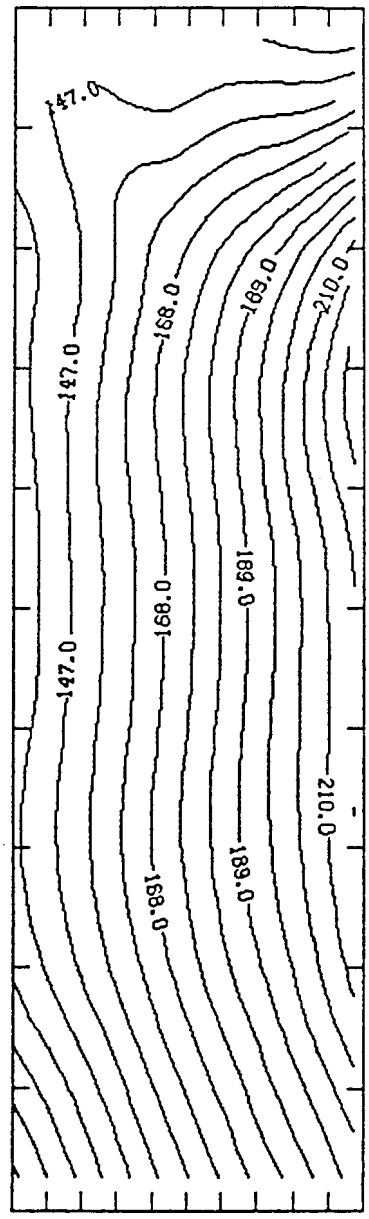

Figure A44. Temperature contours (°C).

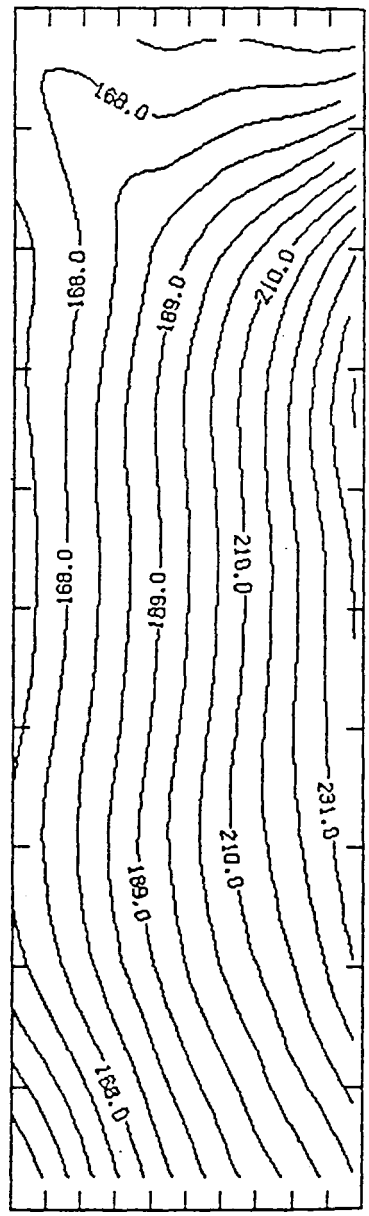

Figure A45. Temperature contours (°C).

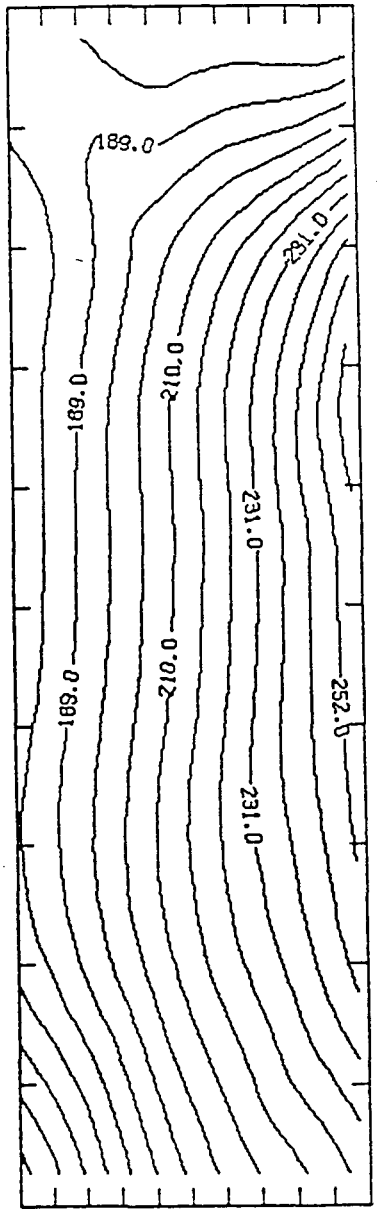

Figure A46. Temperature contours (°C).

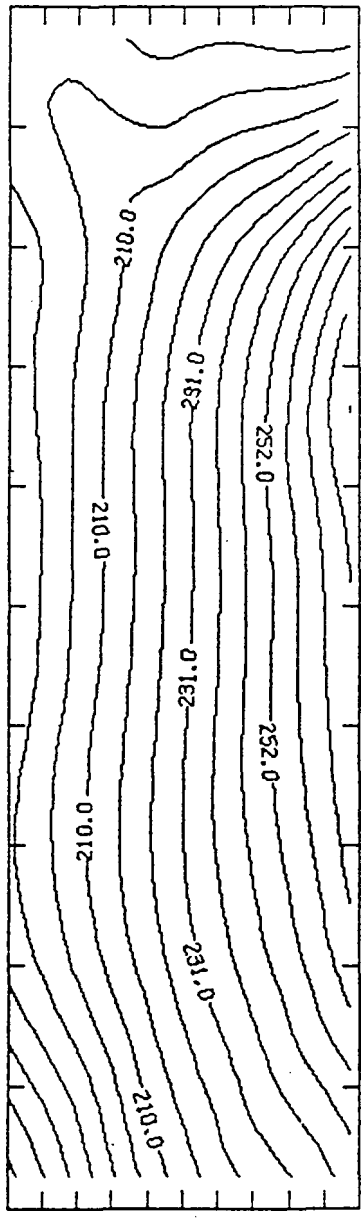

Figure A47. Temperature contours (°C).

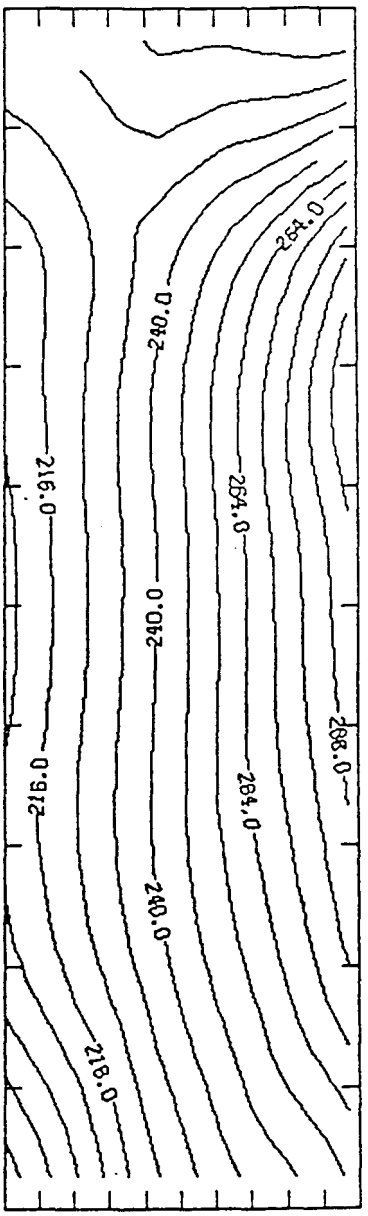

Figure A48. Temperature contours (°C).

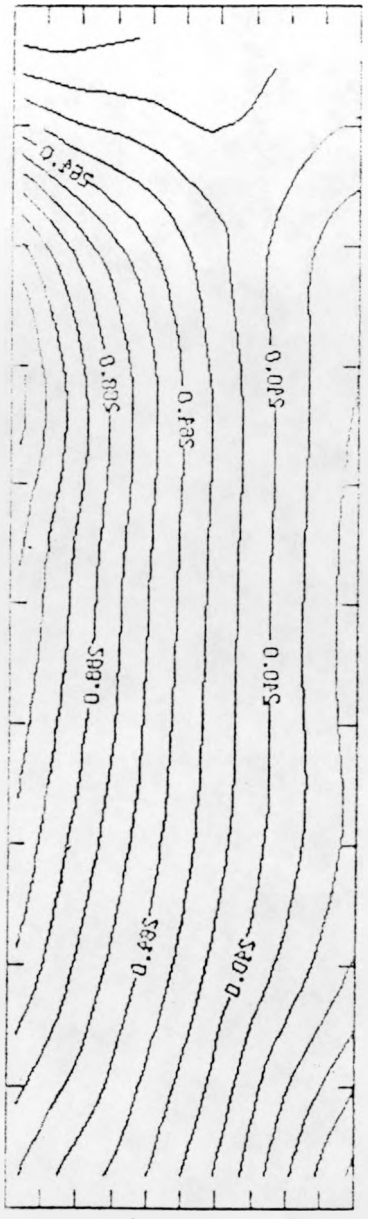

Figure A49. Temperature contours (°C).

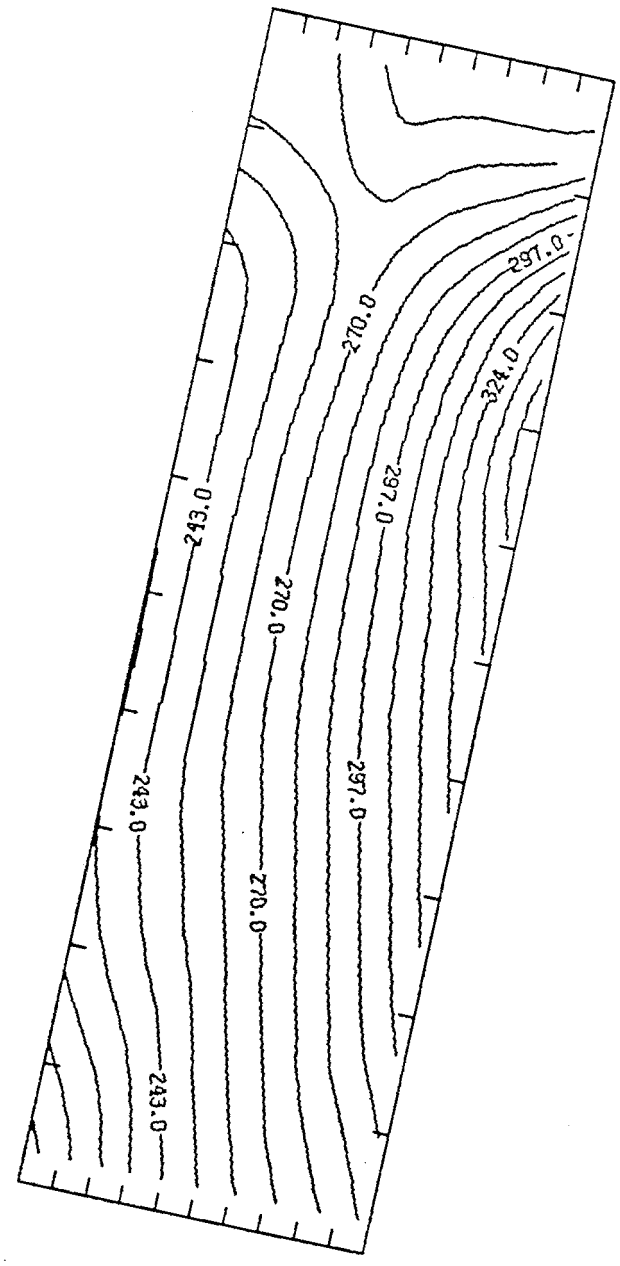

Figure A50. Temperature contours (°C).

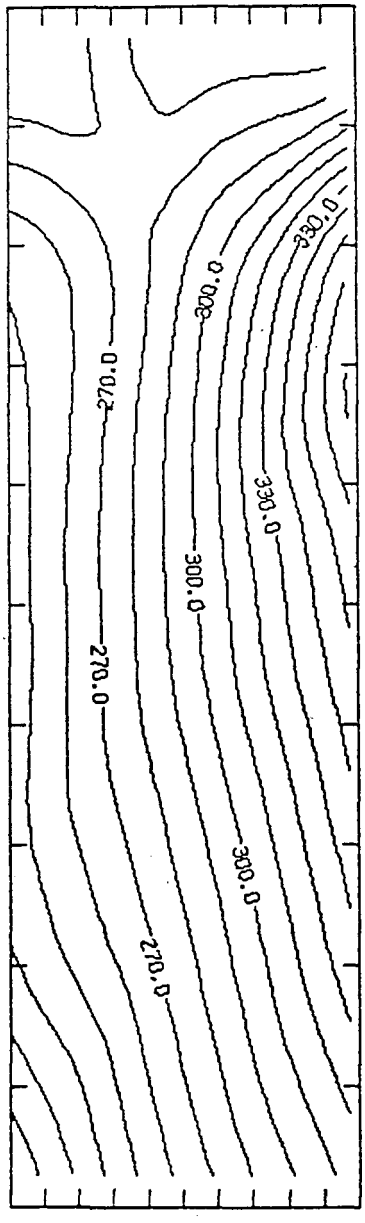

Figure A51. Temperature contours (°C).

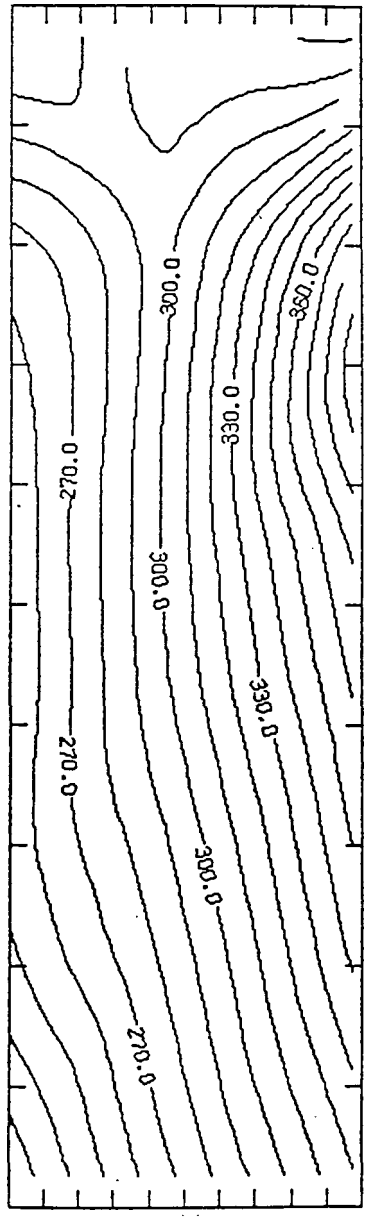

Figure A52. Temperature contours (°C).

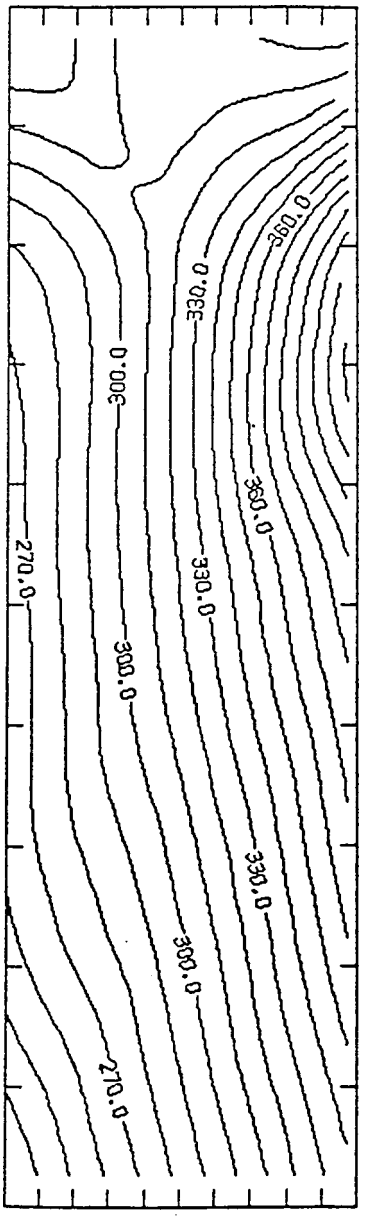

Figure A53. Temperature contours (°C).

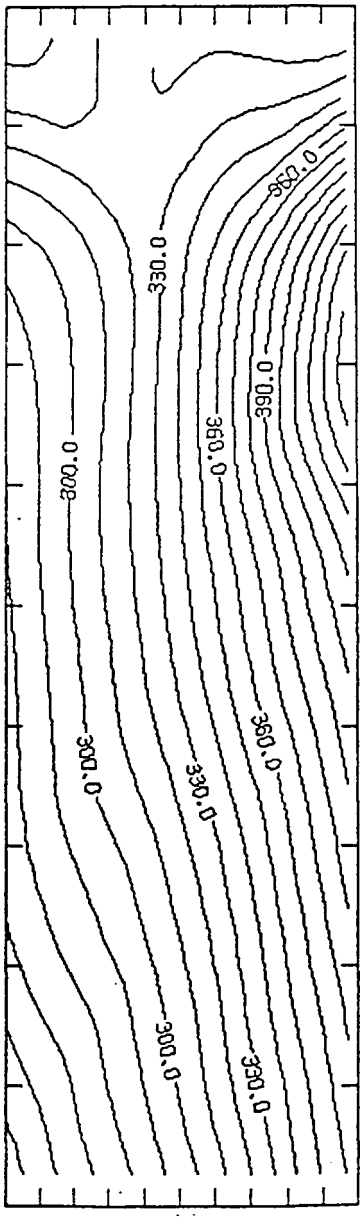

Figure A54. Temperature contours (°C).

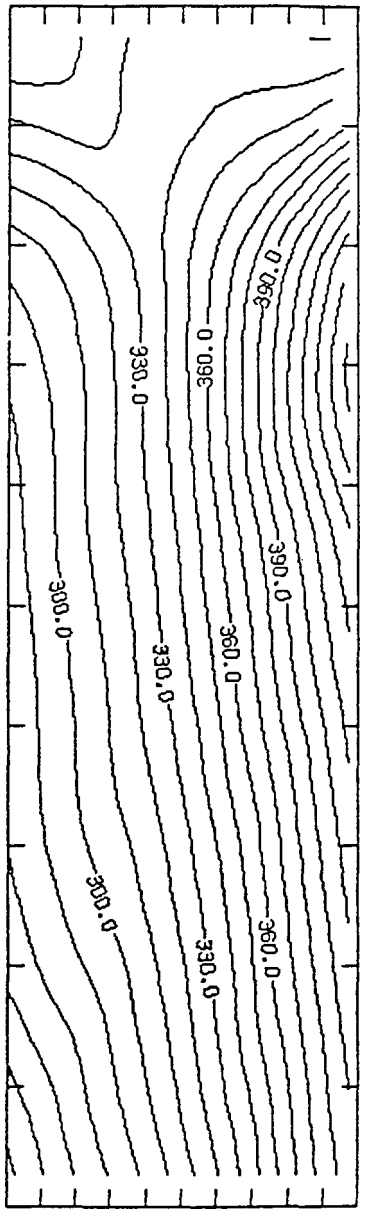

Figure A55. Temperature contours (°C).

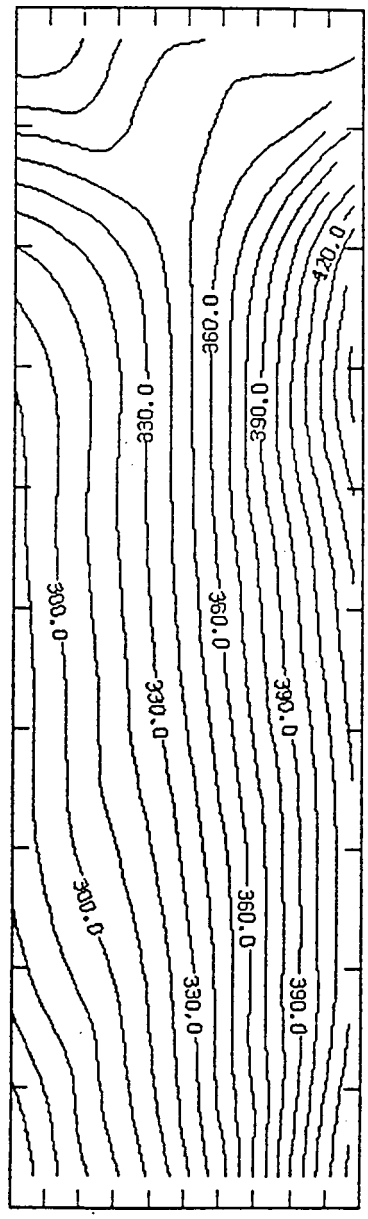

Figure A56. Temperature contours (°C).

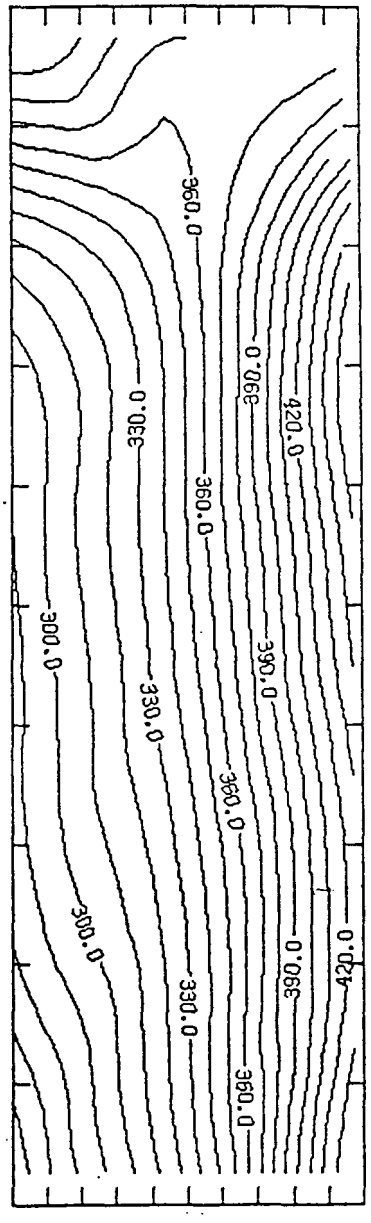

Figure A57. Temperature contours (°C).

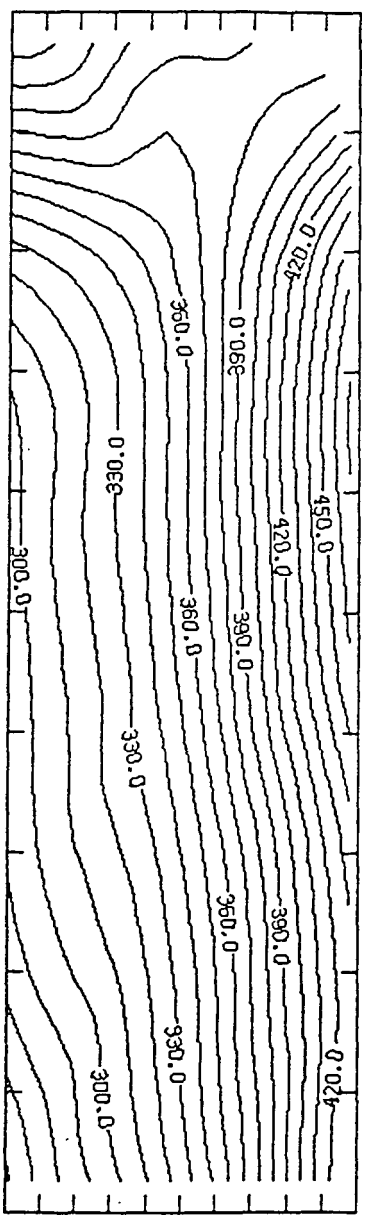

Figure A58. Temperature contours (°C).

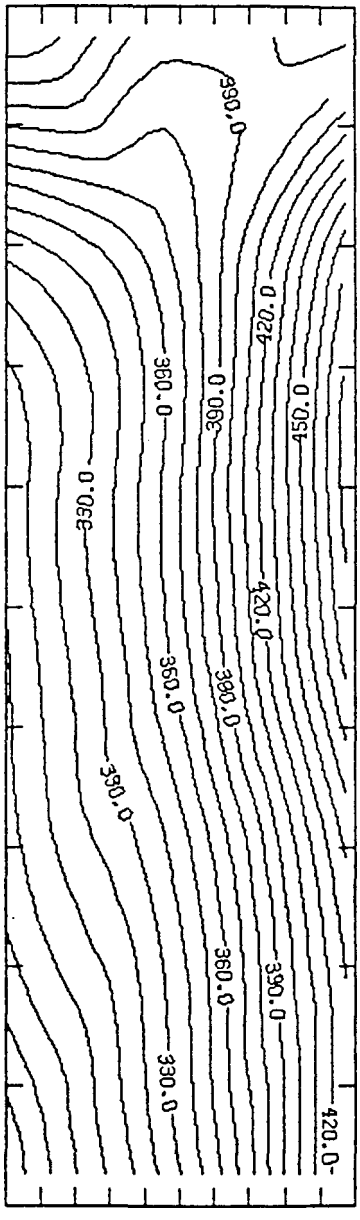

Figure A59. Temperature contours (°C).

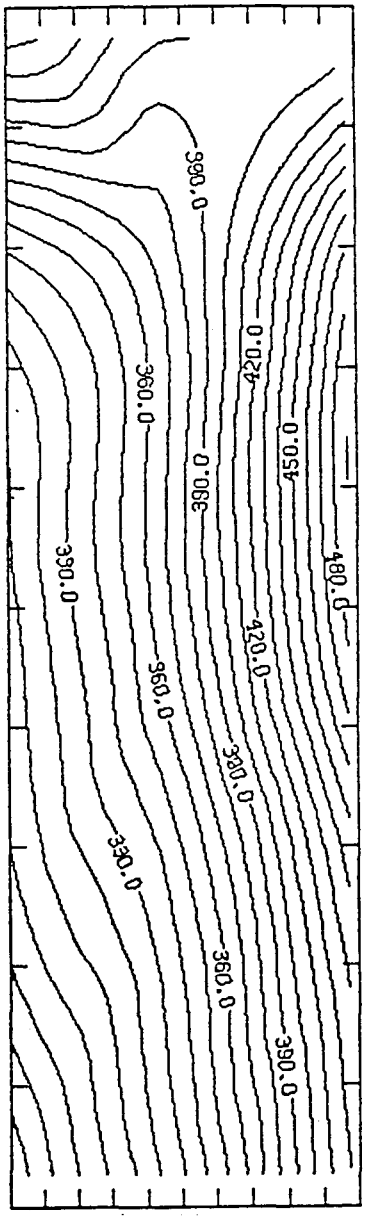

Figure A60. Temperature contours (°C).

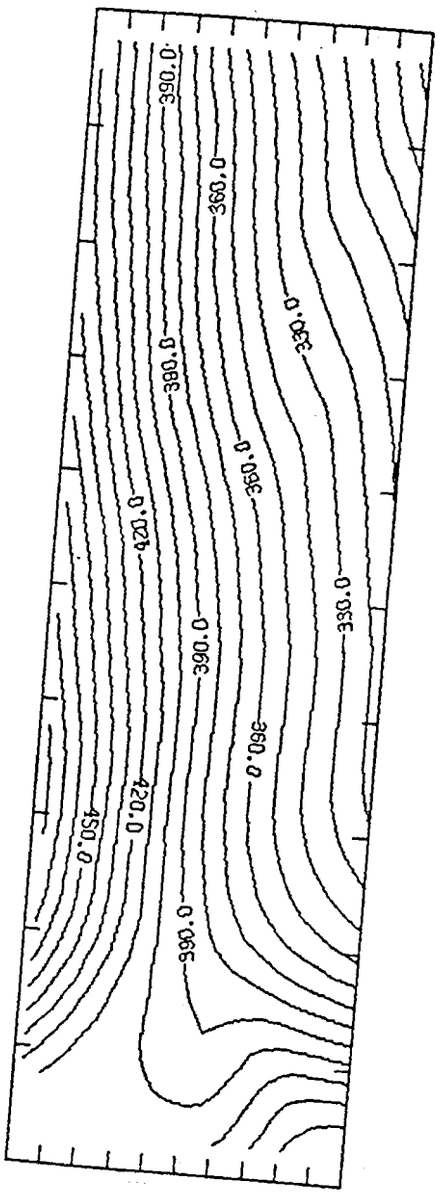

Figure A61. Temperature contours (°C).

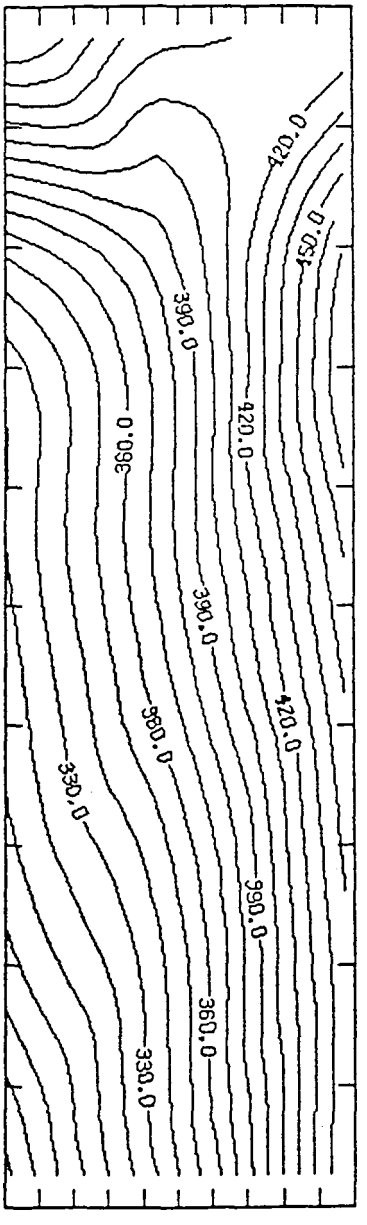

Figure A62. Temperature contours (°C).

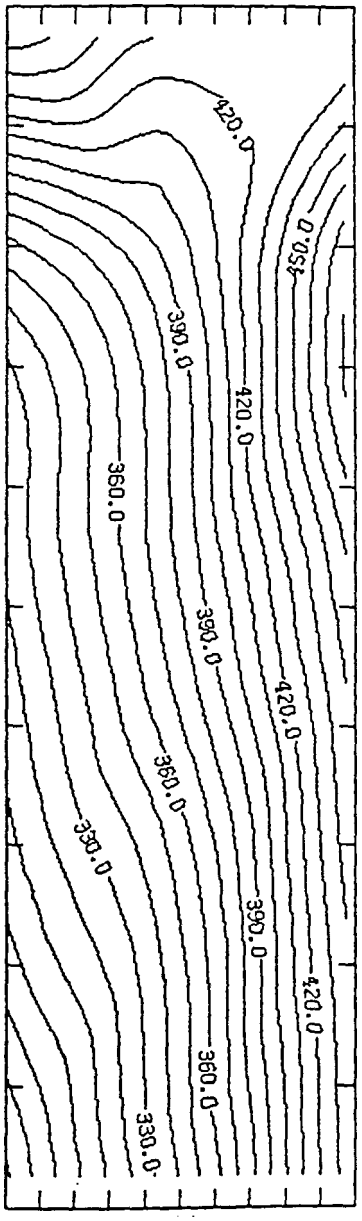

Figure A63. Temperature contours (°C).

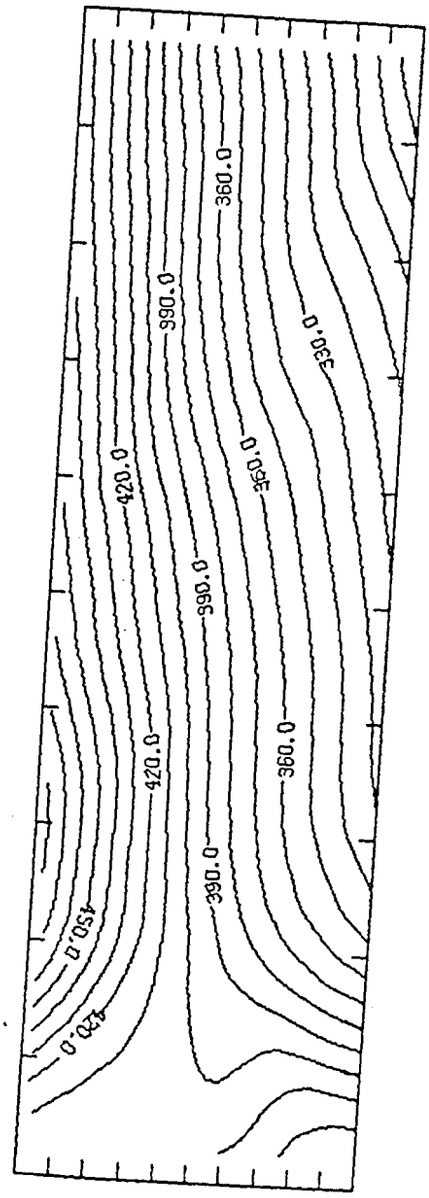

Figure A64. Temperature contours (°C).

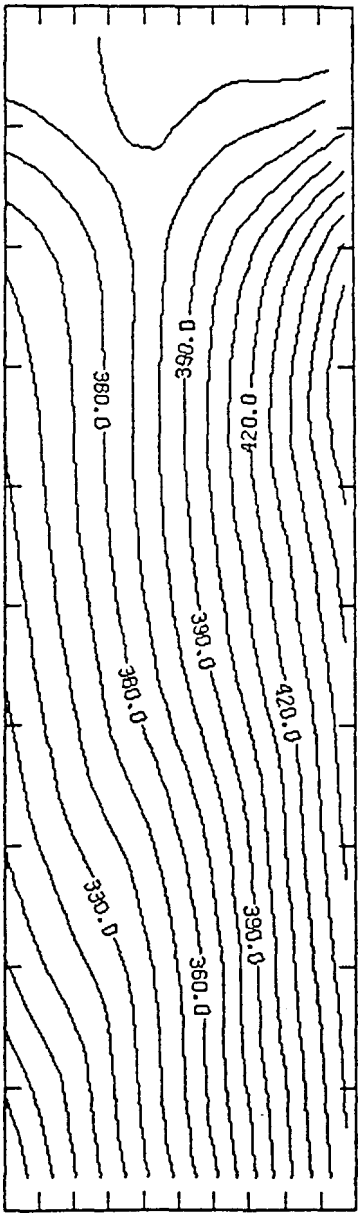

Figure A65. Temperature contours (°C).

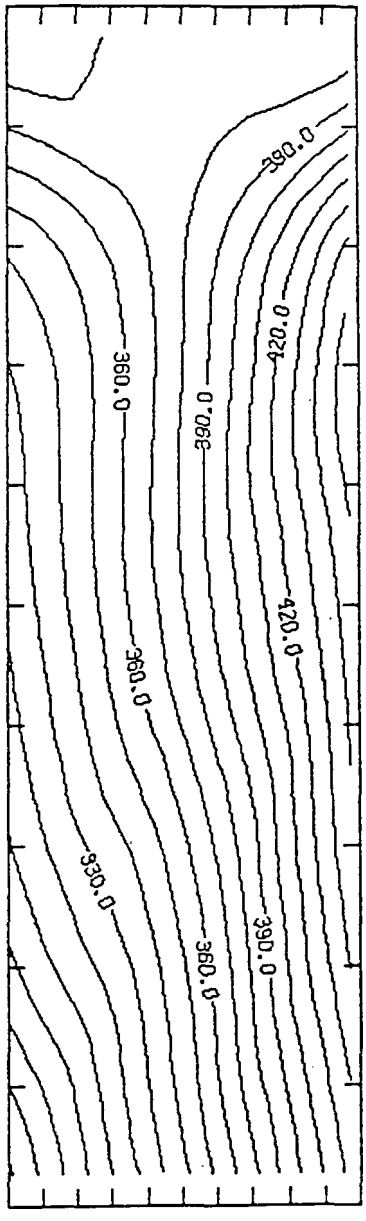

Figure A66. Temperature contours (°C).

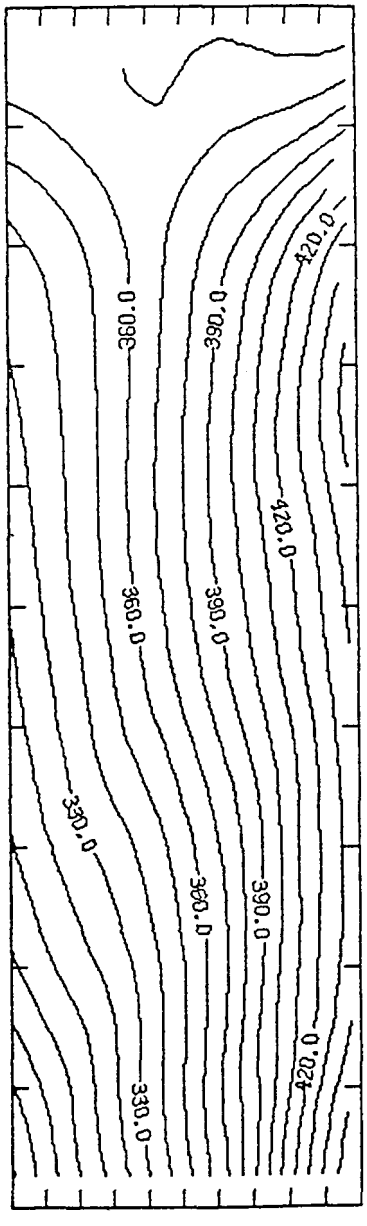

Figure A67. Temperature contours (°C).

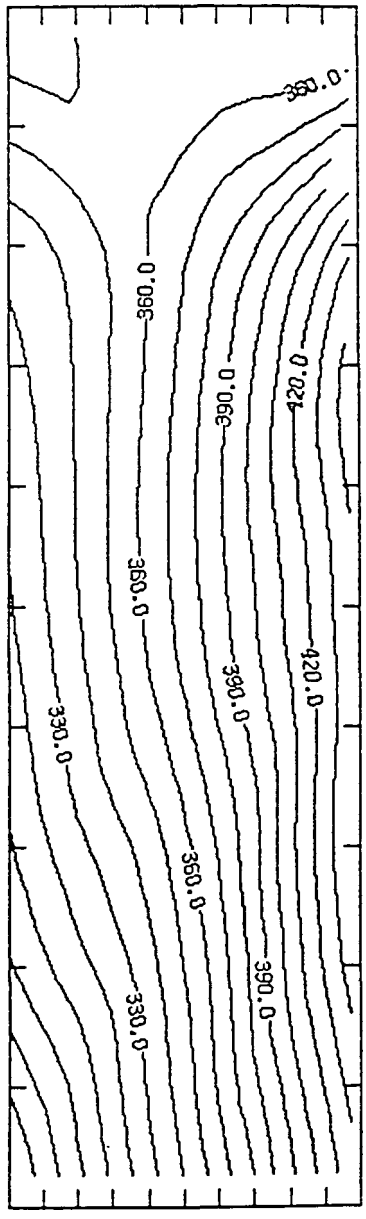

Figure A68. Temperature contours (°C).

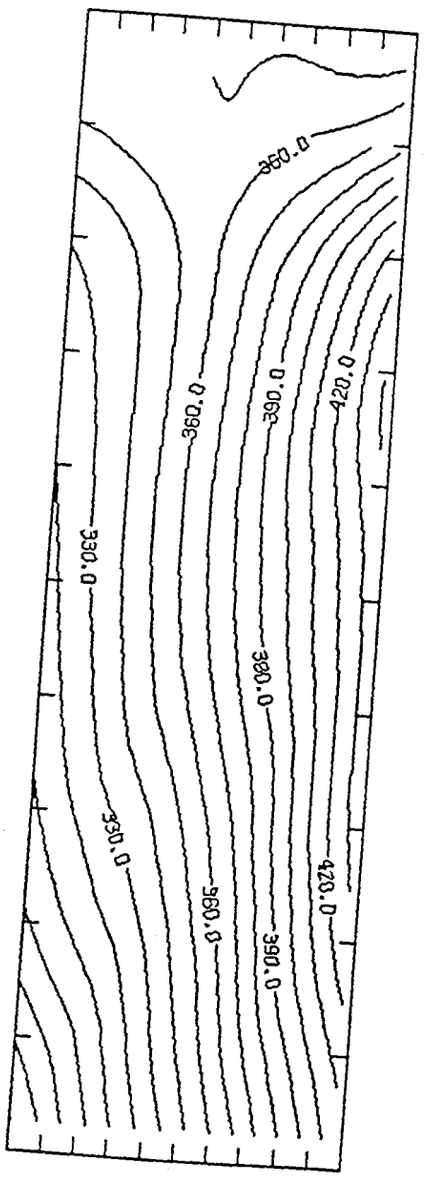

Figure A69. Temperature contours (°C).

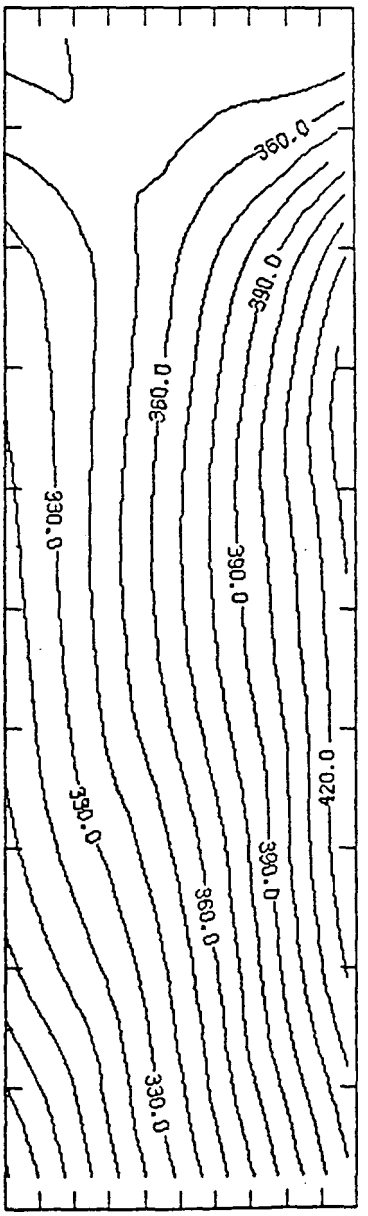

Figure A70. Temperature contours (°C).

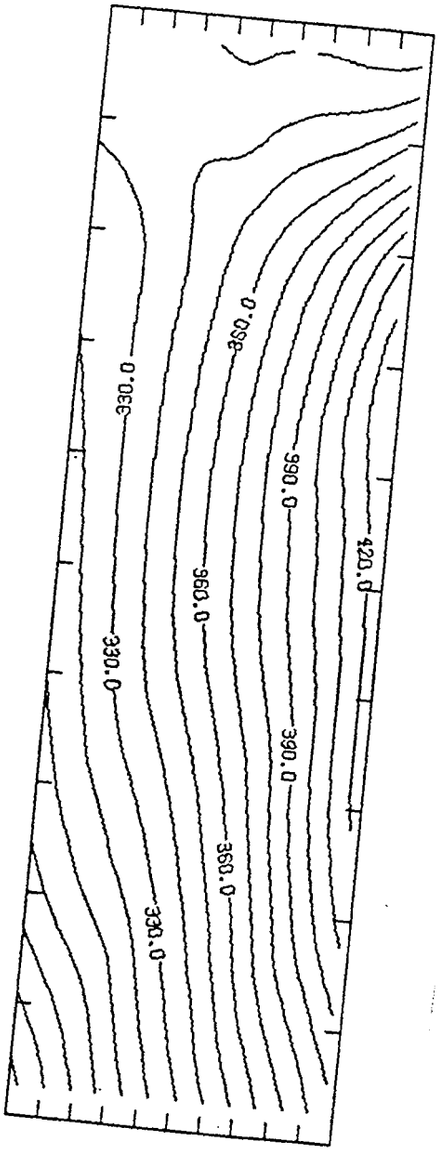

Figure A71. Temperature contours (°C).

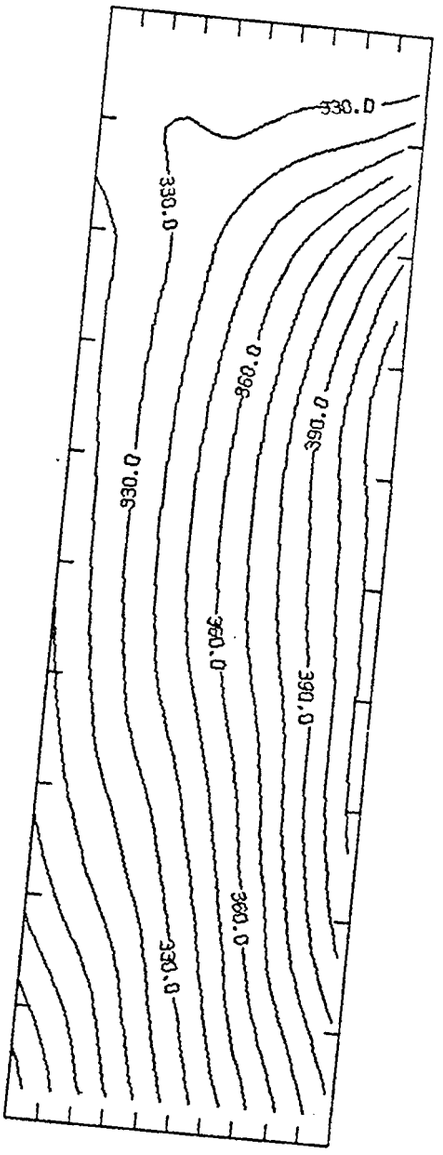

Figure A72. Temperature contours (°C).

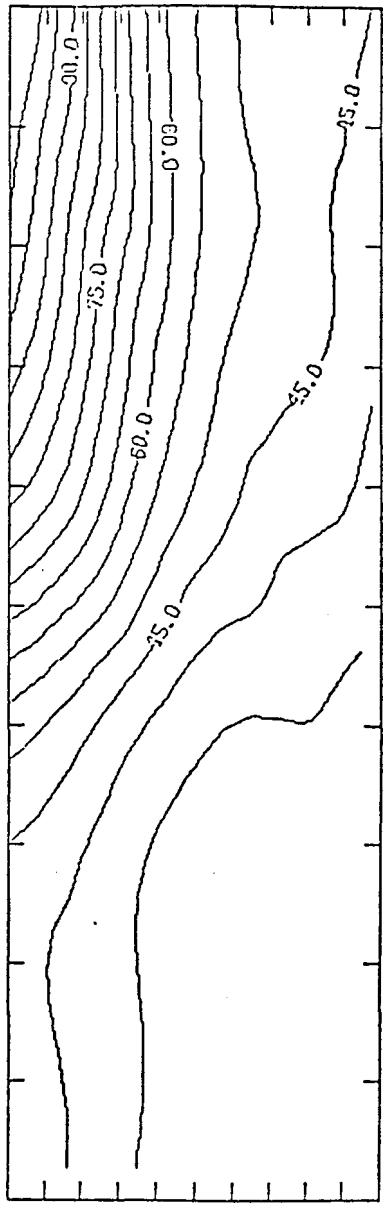

Figure A73. Experimental temperature contours (°C) at 3 hours in the rz plane.

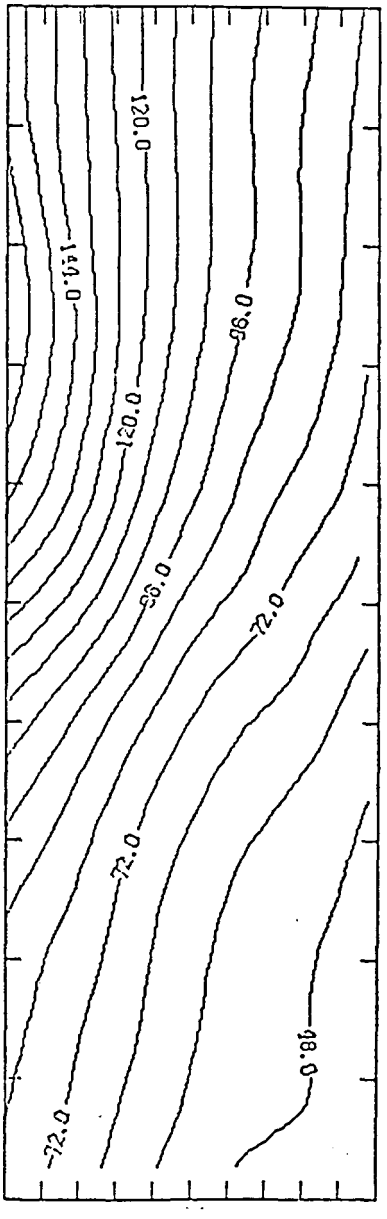

Figure A74. Experimental temperature contours (°C) at 5 hours in the rz plane.

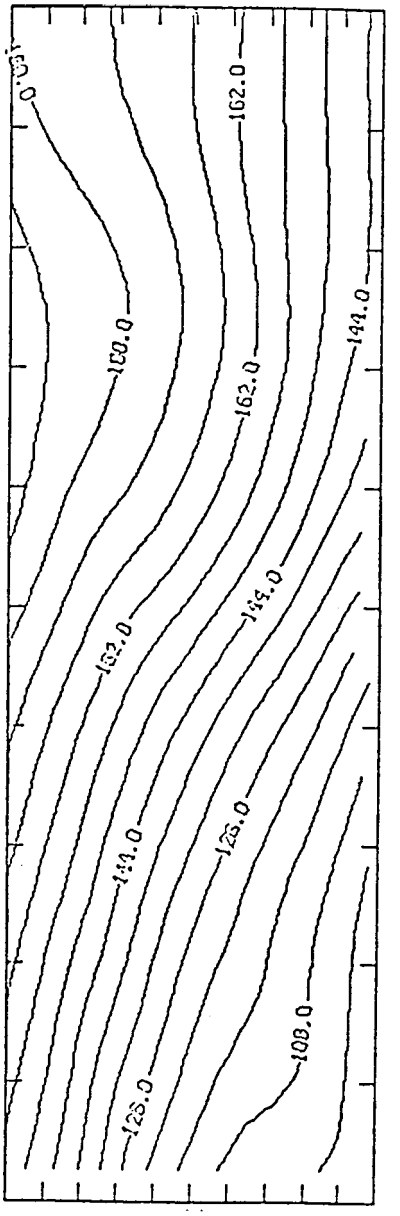

Figure A75. Experimental temperature contours (°C) at 10 hours in the rz plane.

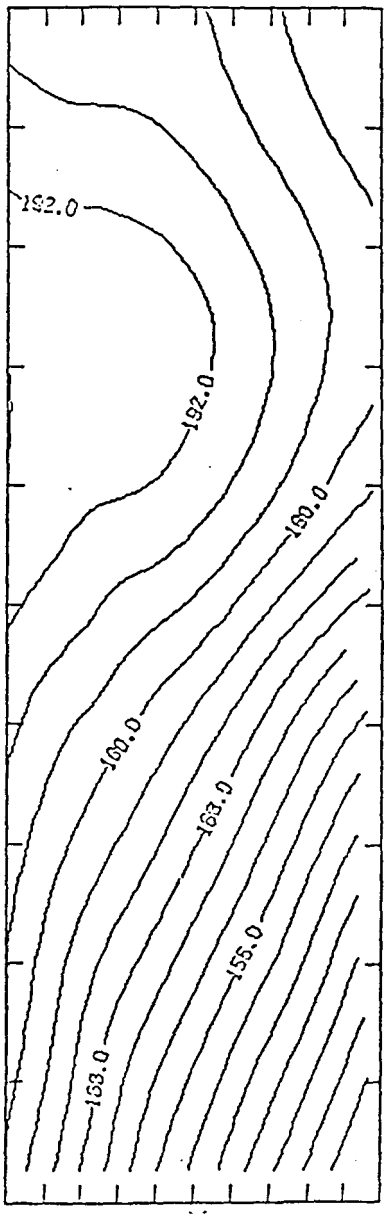

Figure A76. Experimental temperature contours (°C) at 15 hours in the rz plane.

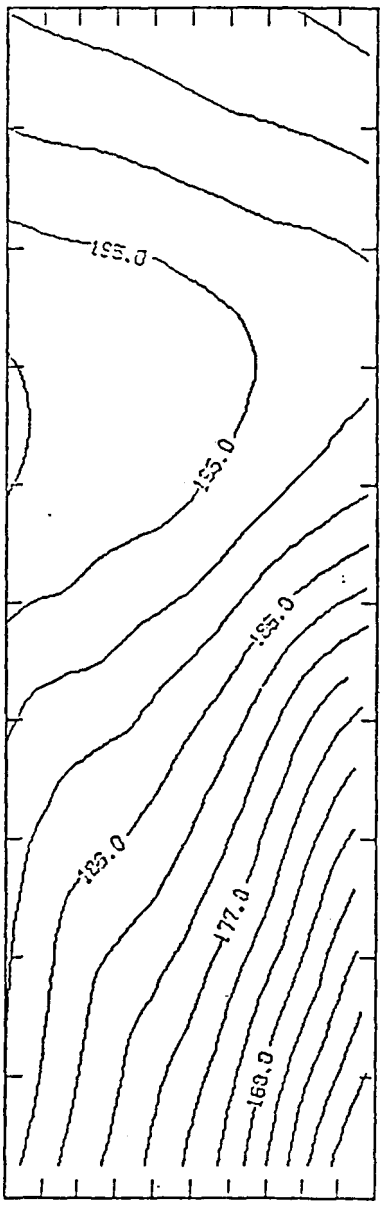

Figure A77. Experimental temperature contours (°C) at 20 hours in the rz plane.

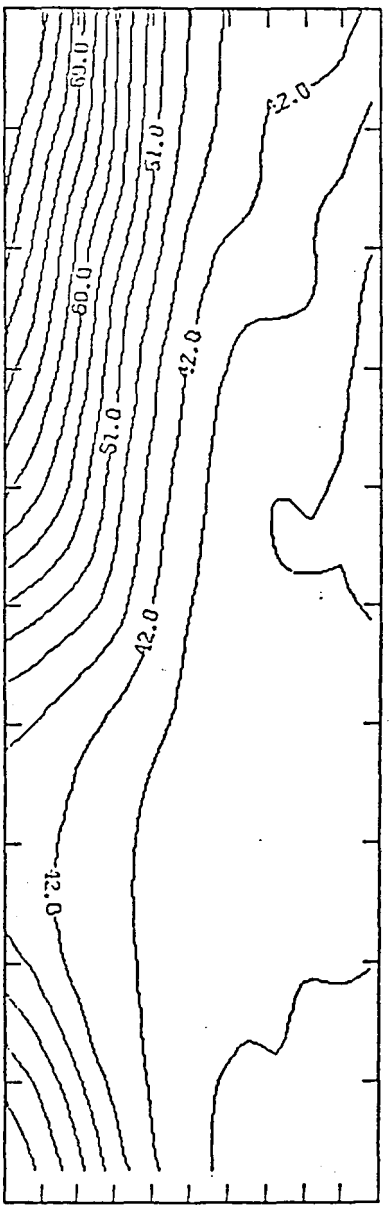

Figure A78. Model predictions for temperature contours (°C) at 3 hours in the rz plane.

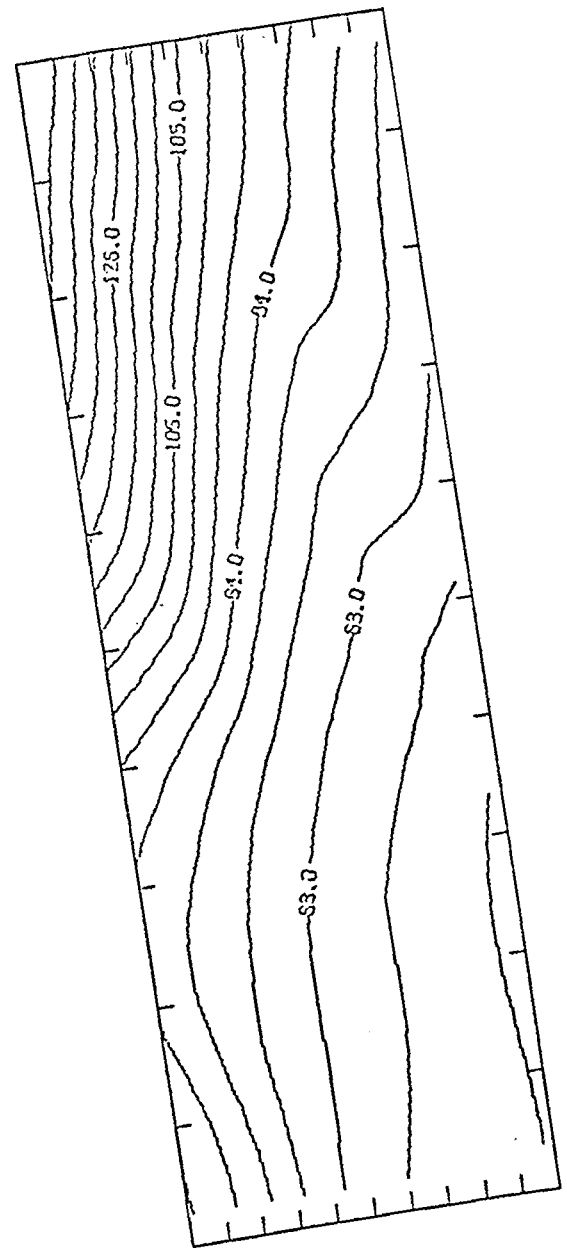

Figure A79. Model predictions for temperature contours (°C) at 5 hours in the rz plane.

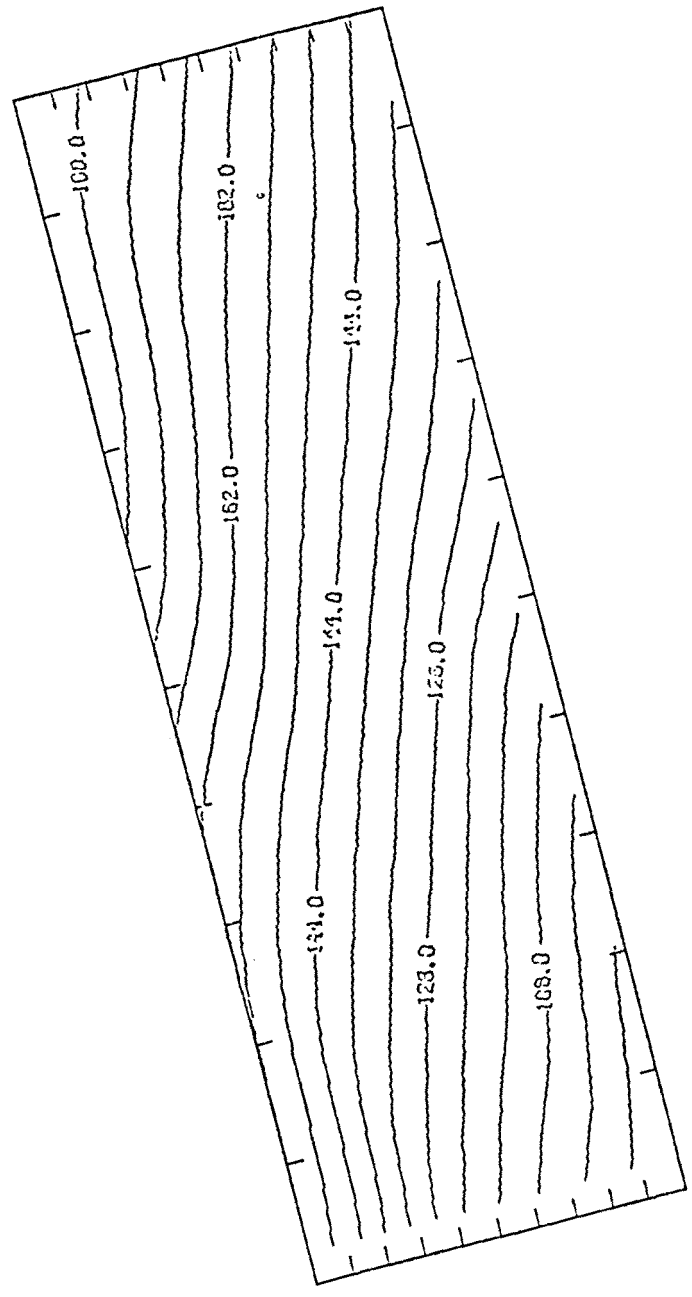

Figure A80. Model predictions for temperature contours (°C) at 10 hours in the rz plane.

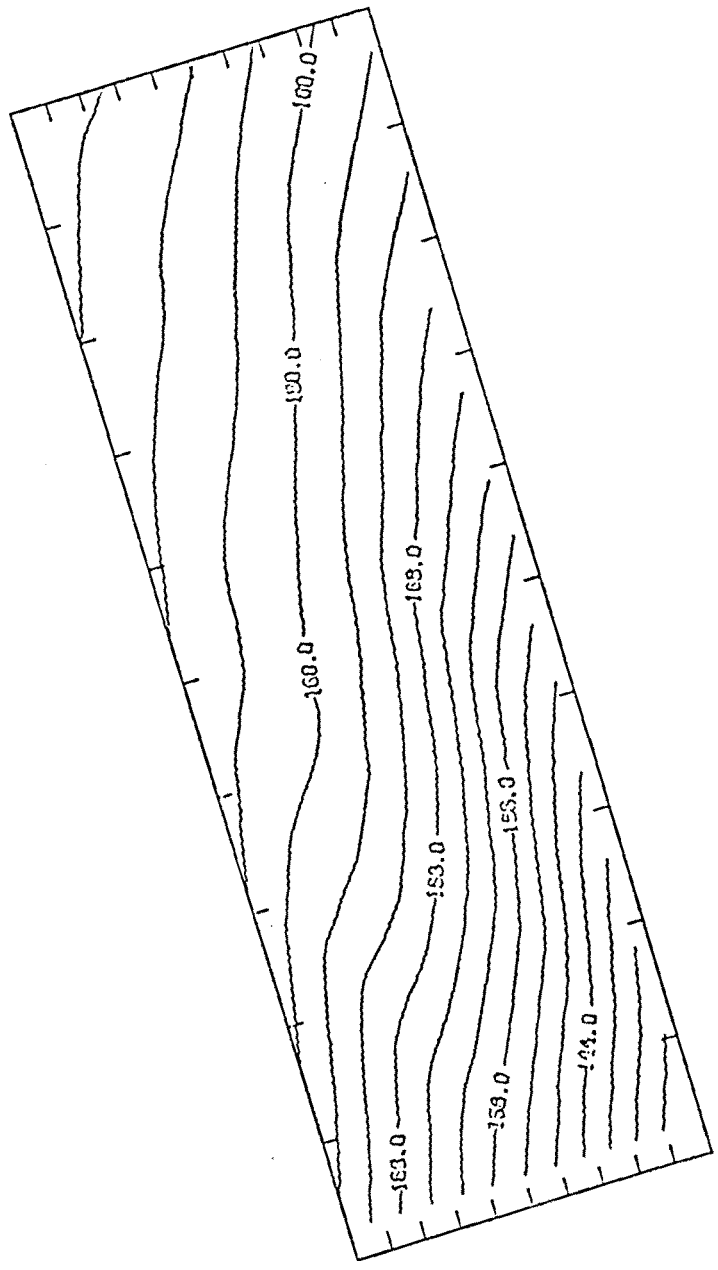

Figure A81. Model predictions for temperature contours (°C) at 15 hours in the rz plane.

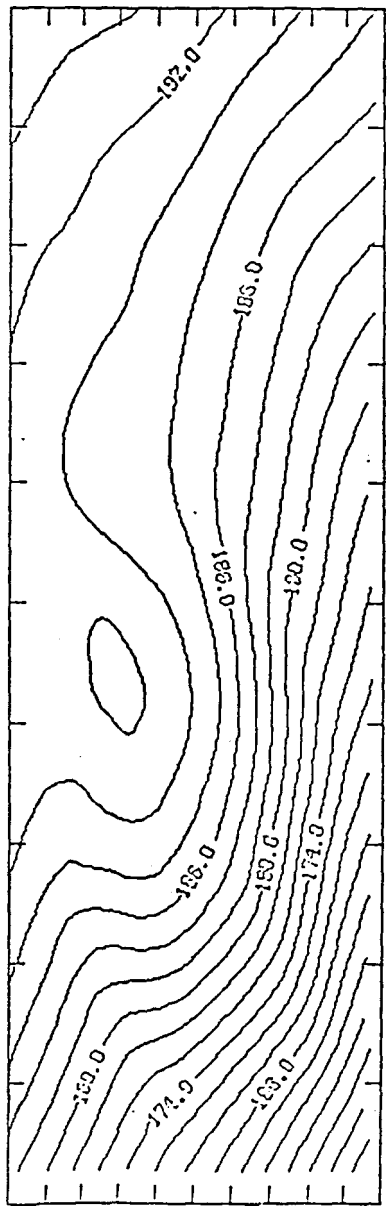

Figure A82. Model predictions for temperature contours (°C) at 20 hours in the rz plane.

APPENDIX B

HEATING OF A DIELECTRIC BY A MONOPOLE APPLICATOR

INTRODUCTION

In Chapter 2 we have attempted to model theoretically the feasibility of heating oil shales by insertion of arrays of monopole antennas into oil shale beds. The electromagnetic fields emitted from the monopole into the lossy media produce heat and thereby release oil. In order to obtain oil from shales it is necessary to heat the bed to temperatures to around 370°C. The advantage of using monopole applicators for large scale recovery operations is ease of insertion into the shale bed. The economics of the process has been studied by Bridges [1] and Mallon [8]. In the process of developing a useful array heating configuration we have studied in detail a single monopole. The purpose of this paper is to study a single monopole in a dielectric media.

Since the heating rate is proportional to the square of the electric fields, to describe the heating lossy dielectrics by a monopole applicator accurately it is necessary to obtain a good approximation to the electric fields surrounding a monopole. The field characterization problem is complicated by the fact that the near fields of a monopole antenna are difficult to calculate [11,31,54–60]. Harrison *et al.* [11] and Chang *et al.* [54] have presented approaches for calculating the near fields of a monopole antenna and King *et al.* [56,58,60] have given excellent fundamental theory of the monopole in dielectric media. These theories are quite accurate for distances from the monopole of greater than two antenna radii. In the present paper we calculate the electric fields of a single monopole and use these fields as a source terms in a heat-mass transfer model. We then analyze in detail the power patterns due to a single monopole.

ENERGY DISSIPATION IN A LOSSY MEDIUM

In a a low conducting, lossy media such as oil shale the heating due to high frequency electric fields is caused mainly by the rotation of polar molecules. In a rapidly fluctuating electromagnetic field polar molecules are rotated by the external torque applied to the dipole. This rotation is resisted by damping forces in the medium which in turn cause heating of the medium.

By considering conservation of energy for waves in a lossy media it is possible to obtain a formula for the dissipated heat energy as a function of the medium and field parameters. For a given volume of material Poynting's theorem states that

$$\int_S \vec{E}X\vec{H}^* \cdot \vec{n}dA = -\frac{1}{2}\int_V \sigma EE^* dV + \frac{j\omega}{2}\int_V [\mu HH^* - \epsilon EE^*]dV \qquad (B1)$$

where S is the surface surrounding the body, V is the volume, $\epsilon = \epsilon' - j\epsilon''$ is the dielectric constant, σ is the conductivity, ω is the radial frequency of the fields, E and H are the

Fourier transforms of the electric and magnetic fields, and μ is the permeability. If we assume that the magnetic loss is small then taking the real part of Equation (B1) yields the power dissipated into the body.

$$Re \int_S \vec{E} X \vec{H} \cdot \vec{n} dA = \frac{1}{2} \int_V \sigma |\vec{E}|^2 dV. \qquad (B2)$$

The conductivity σ consists of low frequency D.C. losses and high frequency polarization losses

$$\sigma = \sigma_{dc} + \omega \epsilon''. \qquad (B3)$$

At high frequencies the D.C. loss is small compared to polarization losses. So the power dissipated in a lossy medium due to high frequency electric fields is given by

$$P_{rmdiss} = \frac{1}{2} \omega \epsilon'' |E|^2. \qquad (B4)$$

In oil shales the dielectric polarization losses are due to bound water and polar molecules contained in kerogen. The dielectric loss in oil shales shows a strong temperature dependence which is due to the various chemical reactions occurring in the shale as it is heated and the release and migration of bound water in the form of steam.

In the far field where the waves are nearly plane, the power attenuates in an exponential manner. In the far field the power attenuation constant α is defined by

$$P = P_0 \ \exp\left(-\frac{z}{\alpha}\right). \qquad (B5)$$

It can be shown that α is a function of dielectric loss and frequency and for a plane wave is given by [58]

$$\alpha = \frac{1}{\omega} \left(\frac{2}{\mu \epsilon'}\right)^{\frac{1}{2}} \left[\left(1 + \left(\frac{\epsilon''}{\epsilon'}\right)^2\right)^{\frac{1}{2}} - 1\right]^{-\frac{1}{2}}. \qquad (B6)$$

For an applicator such as the monopole the near field region dissipates power more rapidly than the exponential function and Equation (B6) is not valid. Also, because of near field resistance the total power pumped from the monopole is not easily expressed as in the lossless media case as $\frac{1}{2}|I(o)|^2 R_{\text{rad}'}$ where R_{rad} is the radiation resistance of the monopole and $I(o)$ is the input current of the monopole. Therefore, in general, the power dissipated must be calculated from Equation (B4) by numerically integrating over a large enough volume.

The attenuation lengths are of critical interest when considering heating problems. It turns out that the fields of a monopole are attenuated both vertically down from the feed point of the monopole (due to damping of the excitation fields by the lossy media) and radially outward from the monopole.

THEORY OF THE MONOPOLE

In lossy media the near field effects are quite important. So in order to predict the heating due to a monopole, the fields of a monopole must be calculated both in near and far field

regions. The equations describing the fields of a monopole can be obtained from Maxwell's equations which in MKS units are given in the time domain by:

$$\vec{E} = -\vec{\nabla}\phi - \partial_t \vec{A} \tag{B7}$$

$$\vec{\nabla} X \vec{H} = \partial_t \vec{D} + \vec{J} \tag{B8}$$

$$\vec{\nabla} \cdot \vec{D} = \rho \tag{B9}$$

$$\vec{H} = \frac{1}{\mu} \vec{\nabla} X \vec{A}. \tag{B10}$$

From these equations we can form the following wave equation

$$\left[-\vec{\nabla}^2 \vec{A} + \vec{\nabla}(\vec{\nabla} \cdot \vec{A})\right] = \mu\epsilon\partial_t \left[\nabla\phi + \partial_t \vec{A}\right] + \mu\vec{J}. \tag{B11}$$

Using the Lorentz Gauge

$$\vec{\nabla} \cdot \vec{A} + \mu\epsilon\partial_t \phi = 0 \tag{B12}$$

we can obtain the wave equation for the vector potential

$$\vec{\nabla}^2 \vec{A} - \mu\epsilon \frac{\partial^2 \vec{A}}{\partial t^2} = -\mu\vec{J}. \tag{B13}$$

Fourier transformation of the time variable defined as

$$F(\omega) = \frac{1}{2\pi} \int_{-\infty}^{\infty} f(t)\ \exp(-j\omega t) dt \tag{B14}$$

which yields

$$\vec{\nabla}^2 \vec{A} + k^2 \vec{A} = -\mu\vec{J}, \tag{B15}$$

where

$$k^2 = \mu\epsilon\omega^2 = \left(\frac{2\pi}{\lambda}\right)^2. \tag{B16}$$

Now since

$$\nabla X \vec{H} = i\omega\epsilon\vec{E} + \vec{J} \tag{B17}$$

we obtain the electric field in terms of the vector potential by substitution of Equation (B10)

$$\frac{1}{\mu}[\nabla X \nabla X \vec{A}] = i\omega\epsilon\vec{E} + \vec{J}, \tag{B18}$$

or

$$\vec{E} = \frac{\nabla X \nabla X \vec{A} - \vec{J}}{i\mu\epsilon\omega}. \tag{B19}$$

For a dipole of length 2L oriented along the z axis (see Fig. B1) the current has only a z component. The vector potential can be obtained from Equation (B15)

$$A_z = \frac{\mu}{4\pi} \int_{-L}^{L} dz' I_z(z') K(r, r') \tag{B20}$$

where the kernal K is given by

$$K(r, r') = \frac{1}{2\pi} \int_{-\pi}^{+\pi} \frac{\exp(-jkr(\theta))}{r(\theta)} d\theta \tag{B21}$$

with

$$r = \left((z-z')^2 + \rho^2 + a^2 - 2a\rho\cos\theta\right)^{\frac{1}{2}}. \qquad (B22)$$

Here z is the observation point, a is the antenna radius, and θ is the angle between ρ and ρ'.

However, for the field calculations the reduced or average kernal was used to reduce computation time:

$$K = \frac{\exp(-ikR)}{R} \qquad (B23)$$

$$R = \left((z-z')^2 + \rho^2\right)^{\frac{1}{2}}. \qquad (B24)$$

This approximation is valid for thin antennas and introduces error in the field calculations only for points extremely close to the antenna. In the present heating experiments these very near fields are not important since an air gap of 2 cm was maintained around the monopole to prevent dielectric breakdown. In this approximation we have

$$A_z = \frac{\mu}{4\pi}\int_{-L}^{L} dz' I(z')\frac{\exp(-ikR)}{R}. \qquad (B25)$$

The electric field can then be obtained from Equations (B19) and (B25)

$$E_\rho = -\frac{i}{4\pi\omega\epsilon}\int_{-L}^{L} dz' I(z')\left[\frac{\partial^2}{\partial\rho\partial z}\right]K(R), \qquad (B26)$$

$$E_z = -\frac{i}{4\pi\omega\epsilon}\int_{-L}^{L} dz' I(z')\left[\frac{\partial^2}{\partial z^2} + k^2\right]K(R). \qquad (B27)$$

The derivatives of K can be calculated analytically to yield:

$$\frac{\partial^2 K}{\partial\rho\partial z} = \frac{(z-z')(\rho-\rho')}{4\pi}\frac{\exp(-ikR)}{R}\left[ik\left(\frac{ik}{R^2}+\frac{1}{R^3}\right)+\left(\frac{2ik}{R^3}+\frac{3}{R^4}\right)\right] \qquad (B28)$$

$$\frac{\partial^2 K}{\partial z^2} = \frac{1}{4\pi}\frac{\exp(-ikR)}{R}\left[-i\frac{k}{R} - \frac{(1+k^2)(z-z')^2}{R^2} + i\frac{3k(z-z')^2}{R^3} + \frac{3(z-z')^2}{R^4}\right] \qquad (B29)$$

FIELDS FOR SINUSOIDAL CURRENT DISTRIBUTION

It is often useful to obtain closed form solutions of Equations (B26) and (B27) (see for example Stutzman [31]). Exact expressions for the fields are possible when the current distribution is assumed sinusoidal. This corresponds to the case of an infinitely thin antenna. The current is given as

$$I(z) = I(0)\sin(k(L-\mid z\mid))/\sin(kL) - \; L < z < L \qquad (B30)$$

where L is the half length of the dipole and $I(o)$ is the input current. For this distribution Equations (B26 and B27) can be integrated exactly to obtain the fields

$$E_\rho = j(\mu/\epsilon)^{\frac{1}{2}} I(0)\frac{\frac{z-L}{\rho}\frac{\exp(-jkR_1)}{R_1} + \frac{z+L}{\rho}\frac{\exp(-jkR_2)}{R_2} - 2\cos(kL)\frac{z}{\rho}\frac{\exp(-jkr)}{r}}{\sin kL} \qquad (B31)$$

$$E_z = -j\left(\frac{\mu}{\epsilon}\right)^{\frac{1}{2}} I(0)\frac{\frac{\exp(-jkR_1)}{R_1} + \frac{\exp(-jkR_2)}{R_2} - 2cos(kL)\frac{\exp(-jkr)}{r}}{\sin\ kL} \tag{B32}$$

$$H^{\phi} = \frac{I(o)}{j4\omega\rho}\ \frac{\exp(-jkR_1 + \exp(-jkR_2) - 2\cos\ kL\exp(-jkR)}{\sin kL} \tag{B33}$$

where

$$R = (\rho^2 + z^2)^{\frac{1}{2}} \tag{B34}$$

$$R_1 = \left(\rho^2 + (z-L)^2\right)^{\frac{1}{2}} \tag{B35}$$

$$R_2 = \left(\rho^2 + (z+L)^2\right)^{\frac{1}{2}} \tag{B36}$$

Plots of these fields are given in Figs. B7–B9.

CURRENT DISTRIBUTION

The current distribution on the antenna is needed for the field calculations and can be found by solving the appropriate boundary value problem. The approach of the present paper was to solve Pocklington's equation subject to a coax excitation at the feed point. In the solution the following assumptions are made in this paper:

1. The excitation at the feed point is of the form of a TEM mode from a coaxial line. The input radial electric field is of the form

$$E = \frac{V}{2\ell n\left(\frac{b}{a}\right)\rho} \tag{B37}$$

   where a is the monopole radius, b is the outer coax radius, and ρ is the radial coordinate.

2. The averaged kernal (Equation (B23)) was utilized.

3. The antenna is assumed to have no conductive losses.

4. The antenna is assumed electrically thin ($L/a > 60$).

Pocklington's integral equation [31] for an antenna of length 2L is given by

$$E_z = \frac{1}{i\omega\epsilon}\int_{-L}^{L}\left[\frac{\partial^2 K(z,z')}{\partial z^2} + k^2 K(z,z')\right] I(z')dz'd\theta, \tag{B38}$$

where I is the source current on the antenna. Pocklington's equation was solved numerically using the method of moments.

It was assumed that the current was given by

$$I(z) = \sum_n c_n p_n(z) \tag{B39}$$

where the functions p_n are pulse functions.

$$\begin{aligned} p_n(z) &= 1 \text{ for } z_n < z < z_{n+1} \\ &= 0 \text{ otherwise} \end{aligned} \tag{B40}$$

where the grid points $z_1, z_2, ...z_{N+1}$ are given by

$$z_n = (n-1)L/N \tag{41}$$

The matching points which are in the center of each grid are given by $z_1, z_2, ...z_N$. In the numerical solution process the symmetries of the problem were utilized by using a Toeplitz matrix inversion routine [31].

The current distribution given by solving Equation (B38) is shown in Fig. B2 compared with the sinusoidal current distribution.

Using Equations (B26) and (B27) and the current distribution it is possible to integrate numerically to obtain the electric fields in the lossy material. Contour plots of the dissipated power are given in Figs. B18 and B19.

HEAT TRANSFER MODEL

In order to predict the heating due to a monopole inserted in oil shale a detailed heat-mass transfer model has been developed with the antenna as the heating source. Details of this model have been published elsewhere [9,61]. Basically, the program solves simultaneously equations for chemical reactions, mass conservation of species, energy balance, momentum, and electromagnetic sources. This model has been used to study the heating process using the monopole applicator as the heat source.

NUMERICAL RESULTS AND DISCUSSION

Although a sinusoidal current distribution is known to be exact only for very thin antennas it is useful to study how good an approximation it is in the near field of a finite diameter antenna. In Fig. B2 the current distribution is plotted as a function of axial distance on the antenna for the cases of sinusoidal and Pocklington's solution. Figs. B3 and B4 show the convergence of the solution to Pocklington's equation. The currents are normalized so as to have the same input impedances. As can be seen, the sinusoidal current distribution has much more pronounced peaks caused by the normalization. These sharper peaks tend to produce hot spots in the temperature profiles that are not found with Pocklington's current distribution. A contour plot of the dissipated power (Equation (B4)) is given in Fig. B5 in the $\rho - z$ plane. It can be seen that the fields are very intense in the near field region. These intense near fields cause non-uniformities of heating near the antenna. It can also be seen that the fields are more intense near the ground plane. This has been verified experimentally in unreported house lab experiments. The intense field concentration near the ground plane and the antenna can cause problems with dielectric breakdown of the media. Figs. B6 and B7 are iso-plots of the dissipated power using Pocklington's equation for the current which show the three dimensional character of the fields. Again the fields are more intense near the ground plane than they are near the bottom of the antenna. In Figs. B8 and B9 iso-plots for the power dissipated are given for various values of the iso-power. Comparison with Figs. B6 and B7 indicates that the sinusoidal current distribution gives a different power profile than that calculated from Pocklington's current. In particular the power is higher near the ground plane for the Pocklington current. In Figs. B10 and B15 the radial variation of the

magnitude of the square of the electric field is plotted for various axial distances along the monopole and for various loss factors for radial distances between 0.2L–2L. In these plots for comparison purposes the values for Pocklington's and sinusoidal currents are normalized to one at $r = 0.2$L. It can be seen that the fields due to Pocklington's currents decay more slowly than the sinusoidal case. In Figs. B16 and B17 the axial variation of $|E|^2$ is plotted for fixed radial coordinates for sinusoidal and Pocklington's current distributions. In the case of Pocklington's current the maximum occurs at the ground plane and decreases near the antenna bottom whereas the sinusoidal current gives various maxima. Experimentally it has been found that the fields calculated form Pocklington's distribution are much more representative.

For heating purposes it should be noted that the monopole dissipates most of its energy in the near field around the antenna and near the ground plane. In Figs. B18 and B19 the heat transfer model results which used the monopole fields calculated from Pocklington's current distribution as the heat source are shown. In Fig. B20 the temperature distribution is given for the sinusoidal current distribution for the same parameters as in Figs. B17 and B18. As can be seen the sinusoidal distribution gives a different temperature profile. Pocklington's current predicts higher temperature near the ground plane and few hot spots near the antenna.

If heating is attempted by a single monopole then two competing phenomena are found. On the one hand, to heat with a monopole high frequencies must be utilized to produce a large attenuation (also causing near field heating problems), on the other hand, high frequencies produce a large amount of vertical attenuation along the axis of the monopole (see Fig. (B7)), thus only the very top regions near the ground plane achieve high temperatures. Therefore, if one wishes a relatively uniform heating rate one must resort to arrays of monopoles to confine the fields.

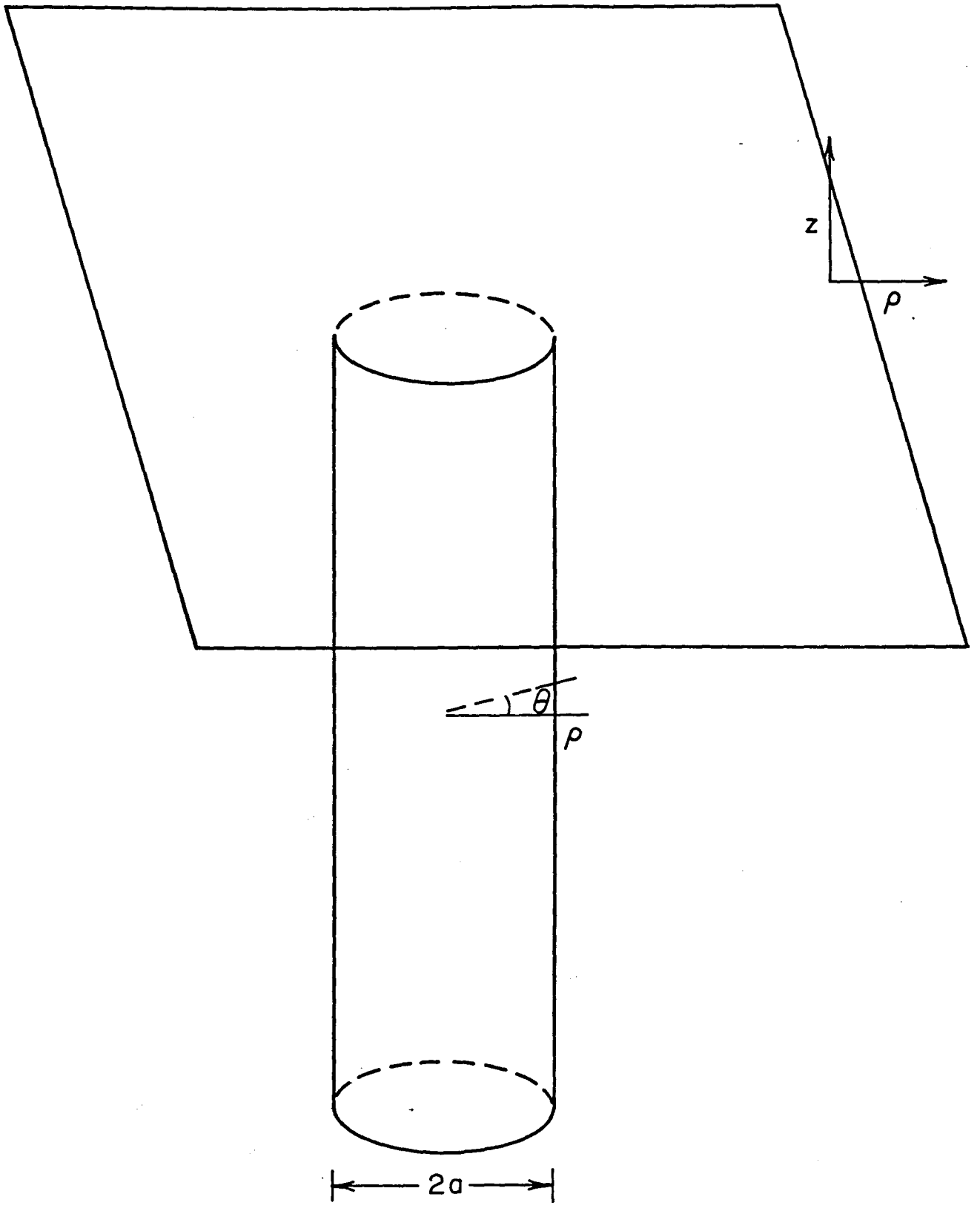

Figure B1. A monopole below a ground plane.

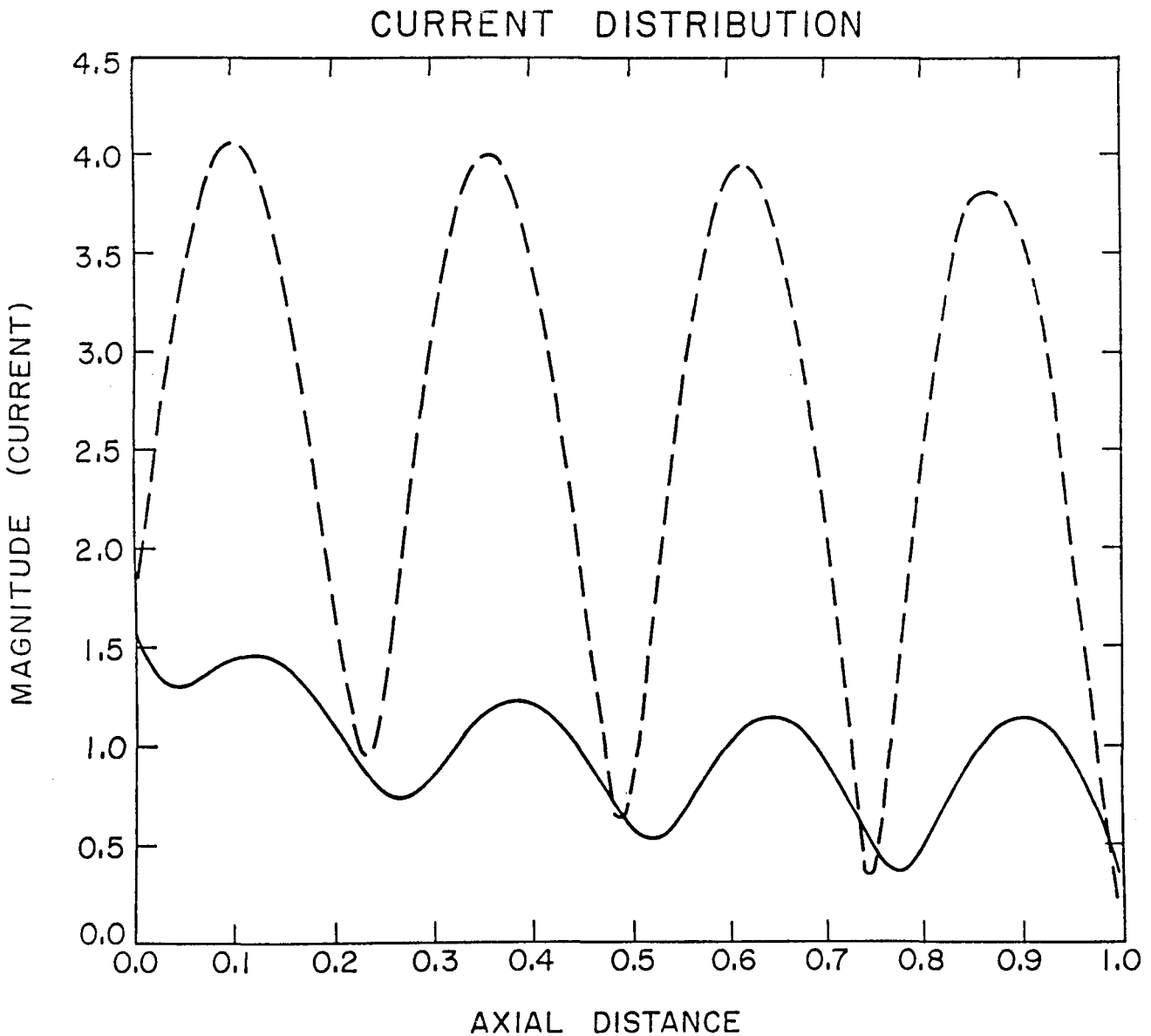

Figure B2. Current distribution for sinusoidal current (—) and for integration of Pocklington's Equation with $\epsilon = (6.0,0.3)$, $f = 470$ *MHz, and* $(2\ L/a = 250)$.

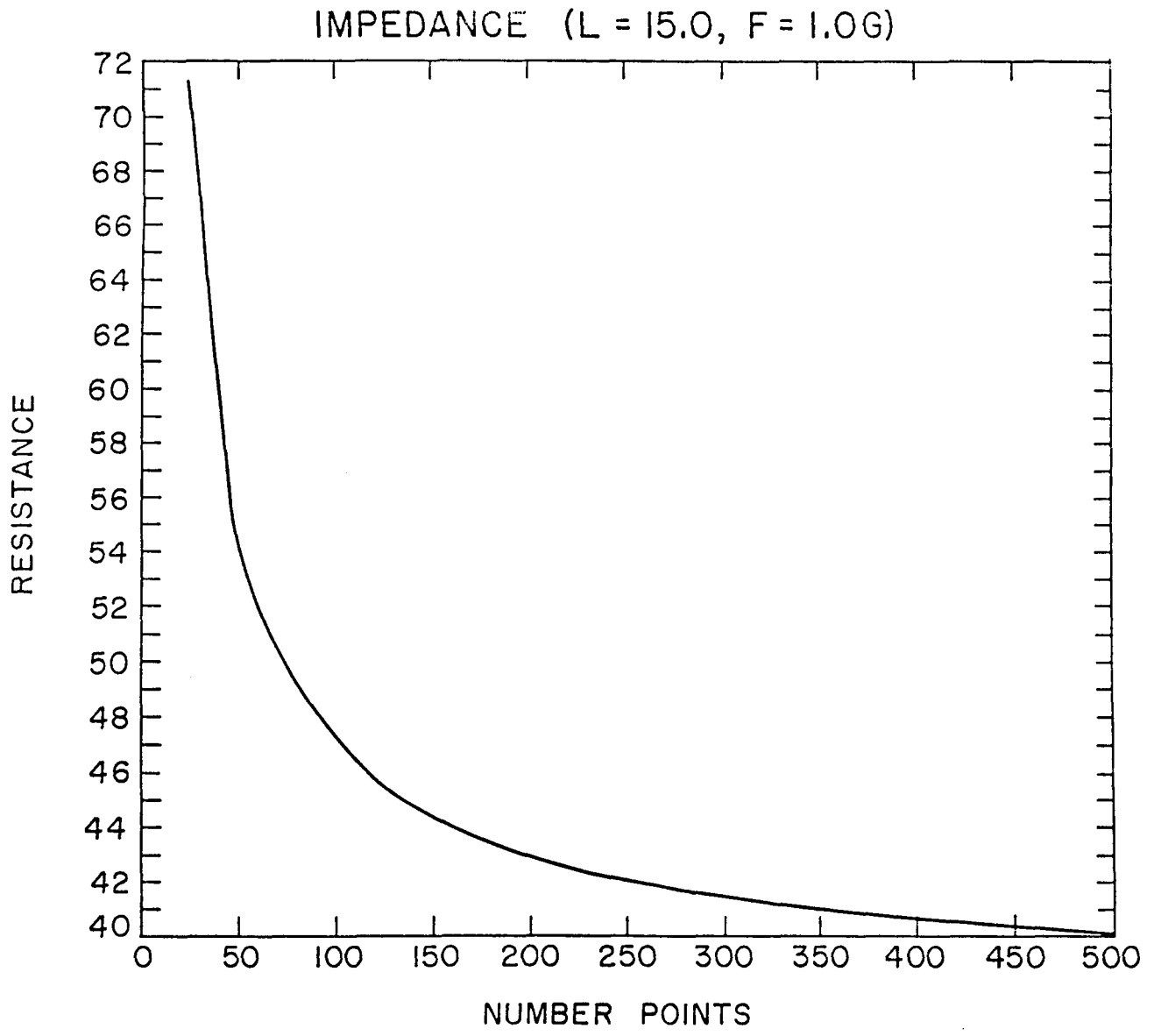

Figure B3. Convergence of the real part of the current distribution as a function of number of pulse function.

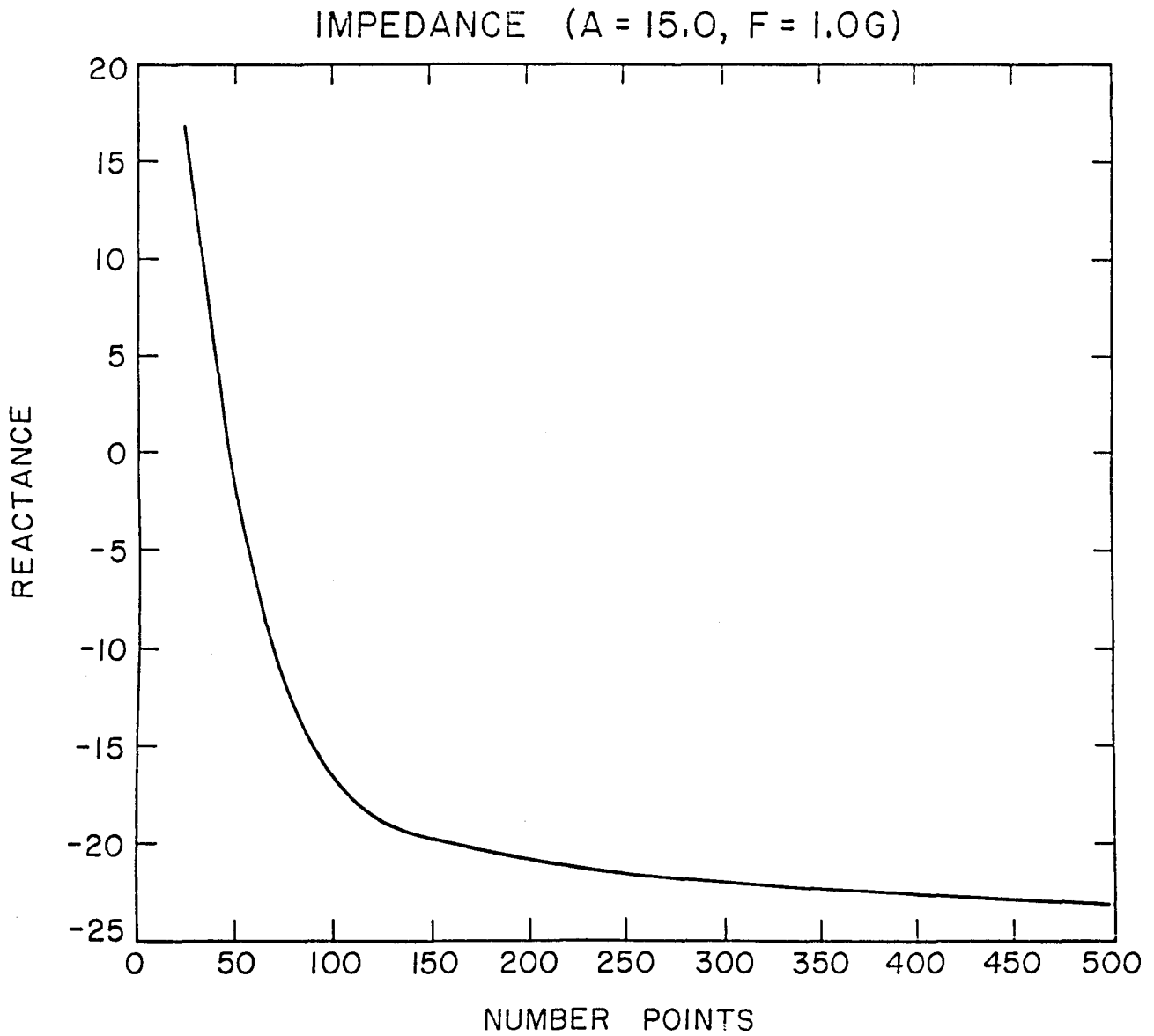

Figure B4. Convergence of the imaginary part of the current distribution as a function of the number of pulse functions.

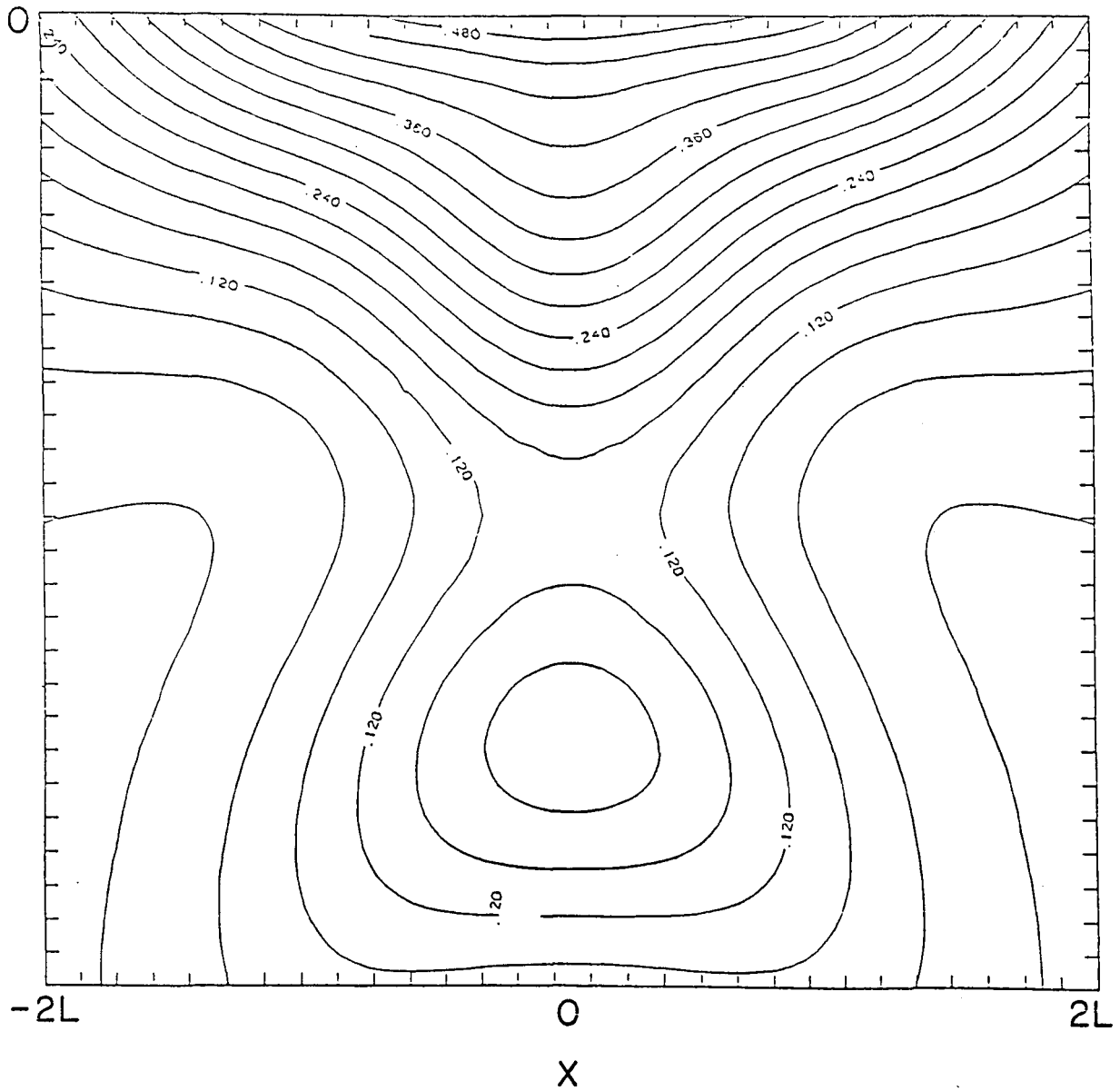

Figure B5. Contour plot of the power dissipated (Equation (B4)) in the ρ–z plane for distance $L/15$ from the monopole $2L/a$ = 250).

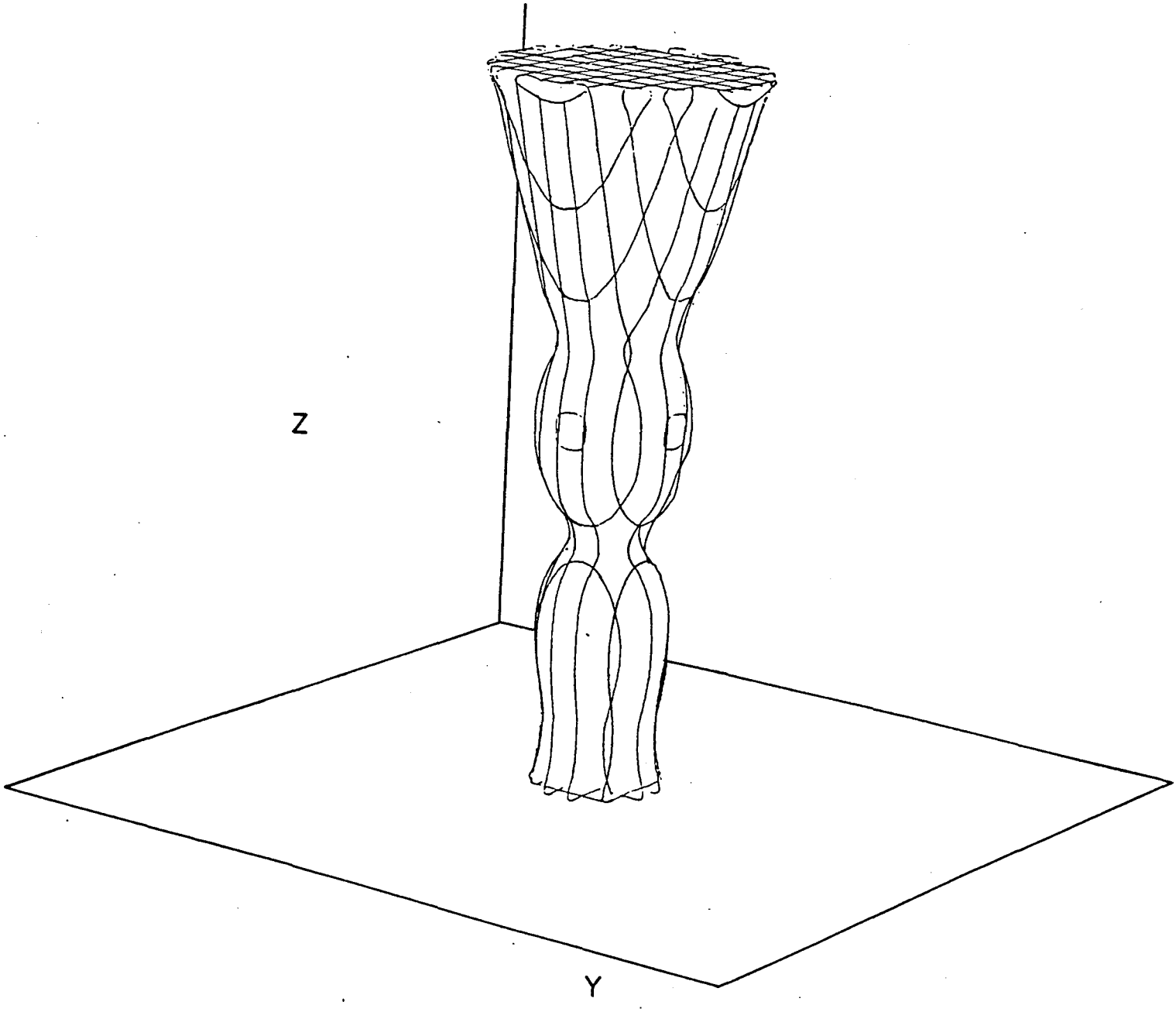

Figure B6. Three dimensional iso-surface plot of the dissipated power using Pocklington's equation for the current.

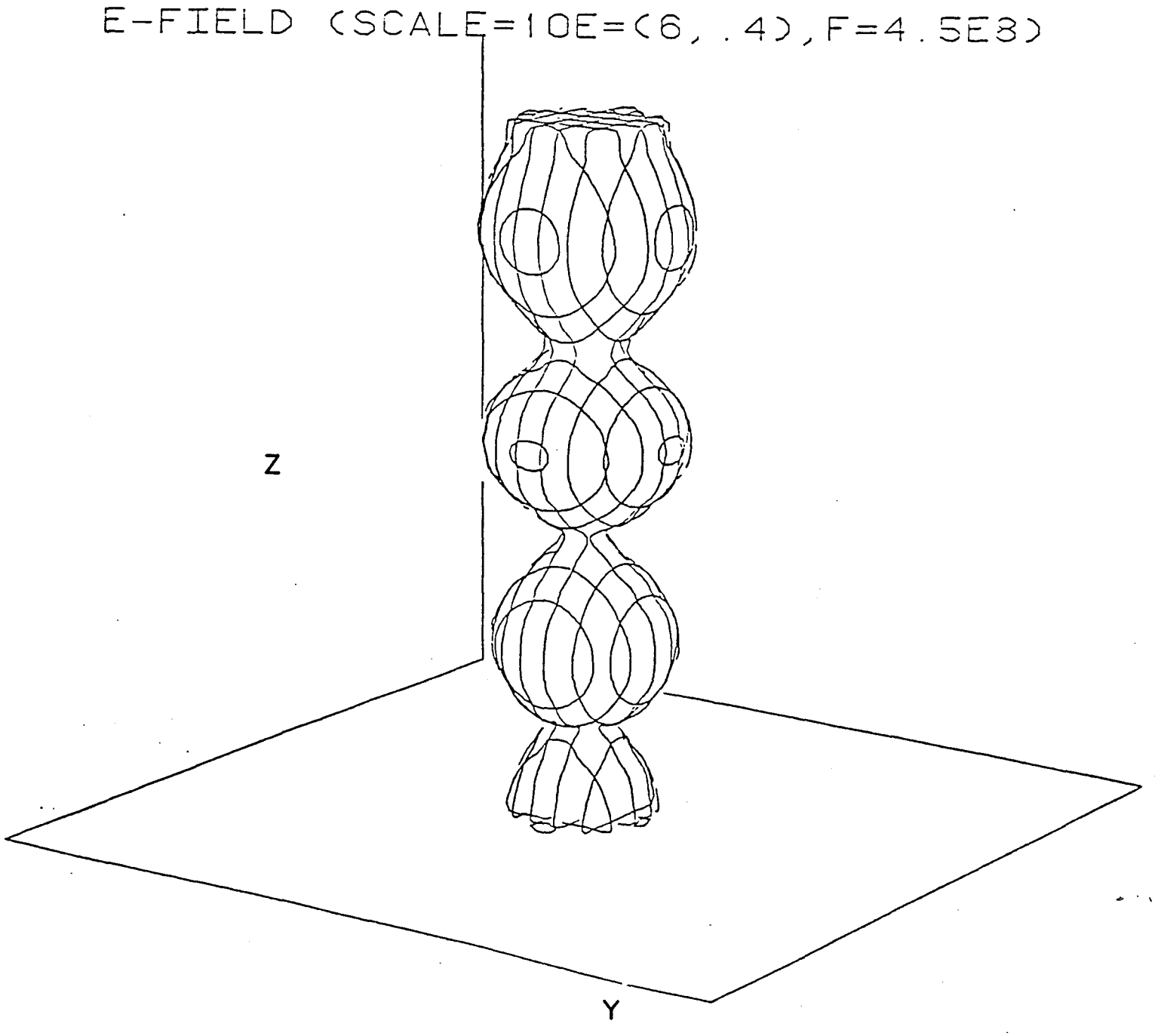

Figure B7. Three dimensional iso-surface plot of the dissipated power using Pocklington's current distribution for a iso-power surface of twice that of Fig. B5.

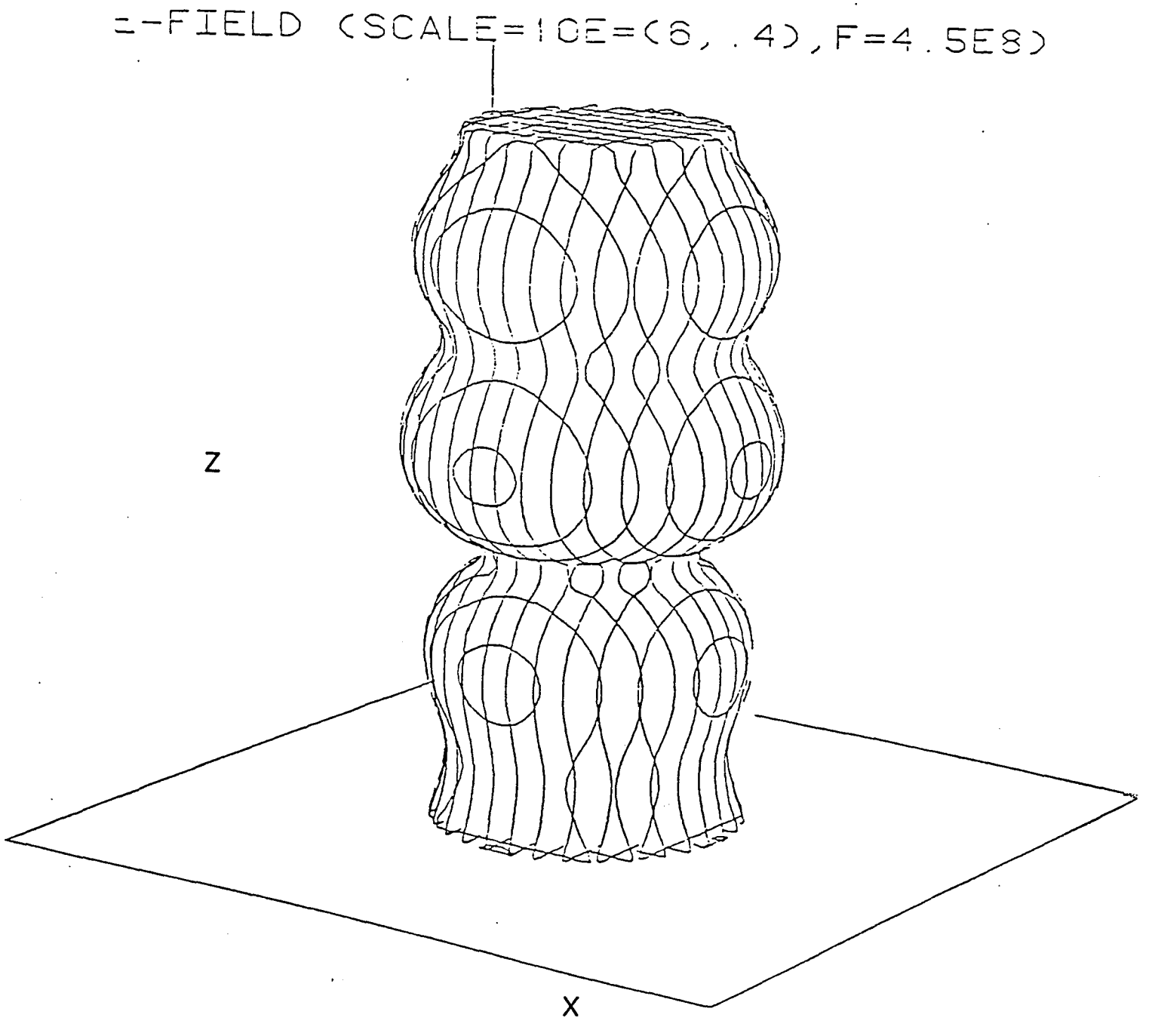

Figure B8. Iso-surface of the power dissipated using the sinusoidal current distribution for the electric field $E = 200V/M$.

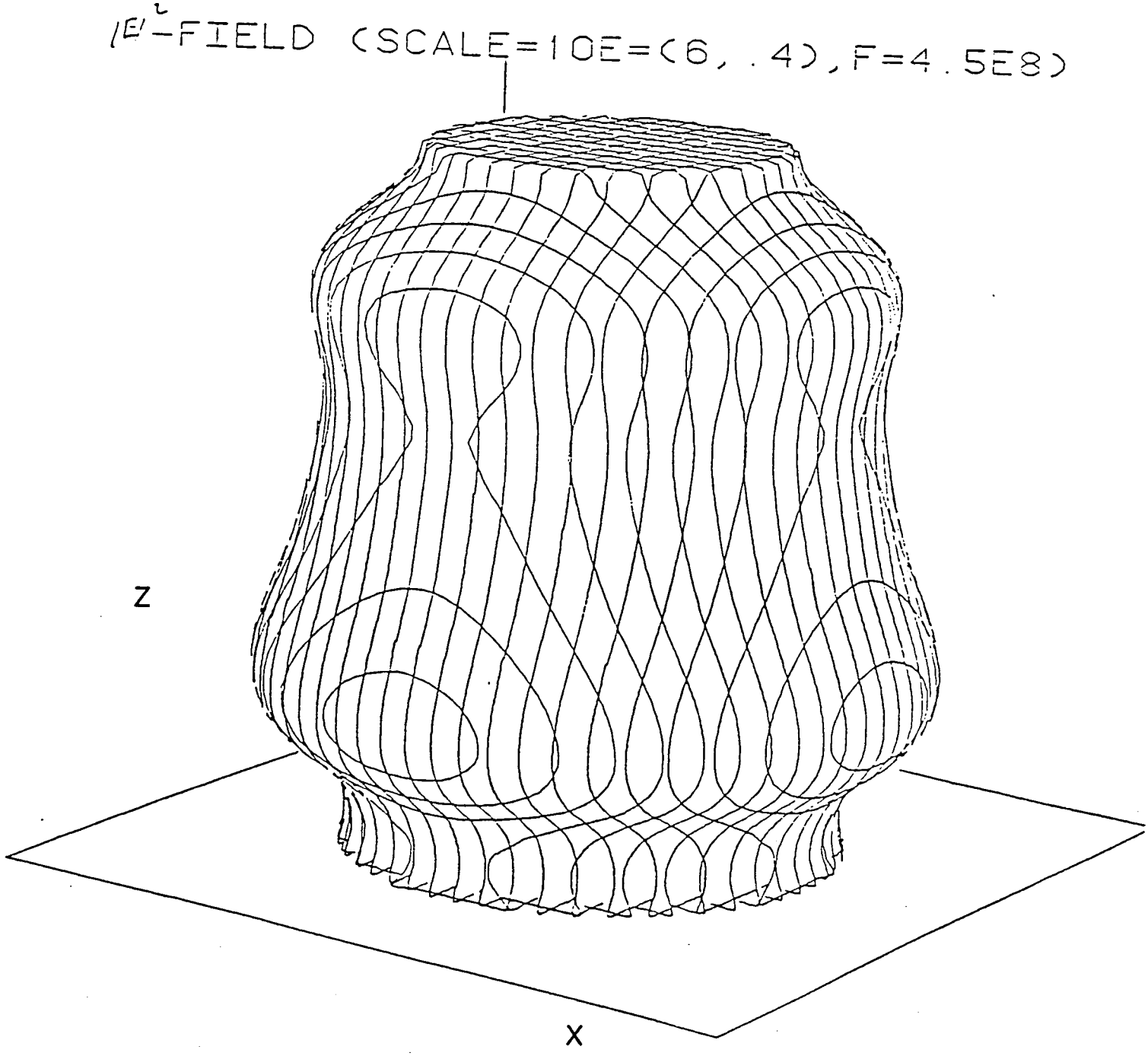

Figure B9. Iso-surface of the power dissipated using the sinusoidal current distribution for the electric field $E = 100V/M$.

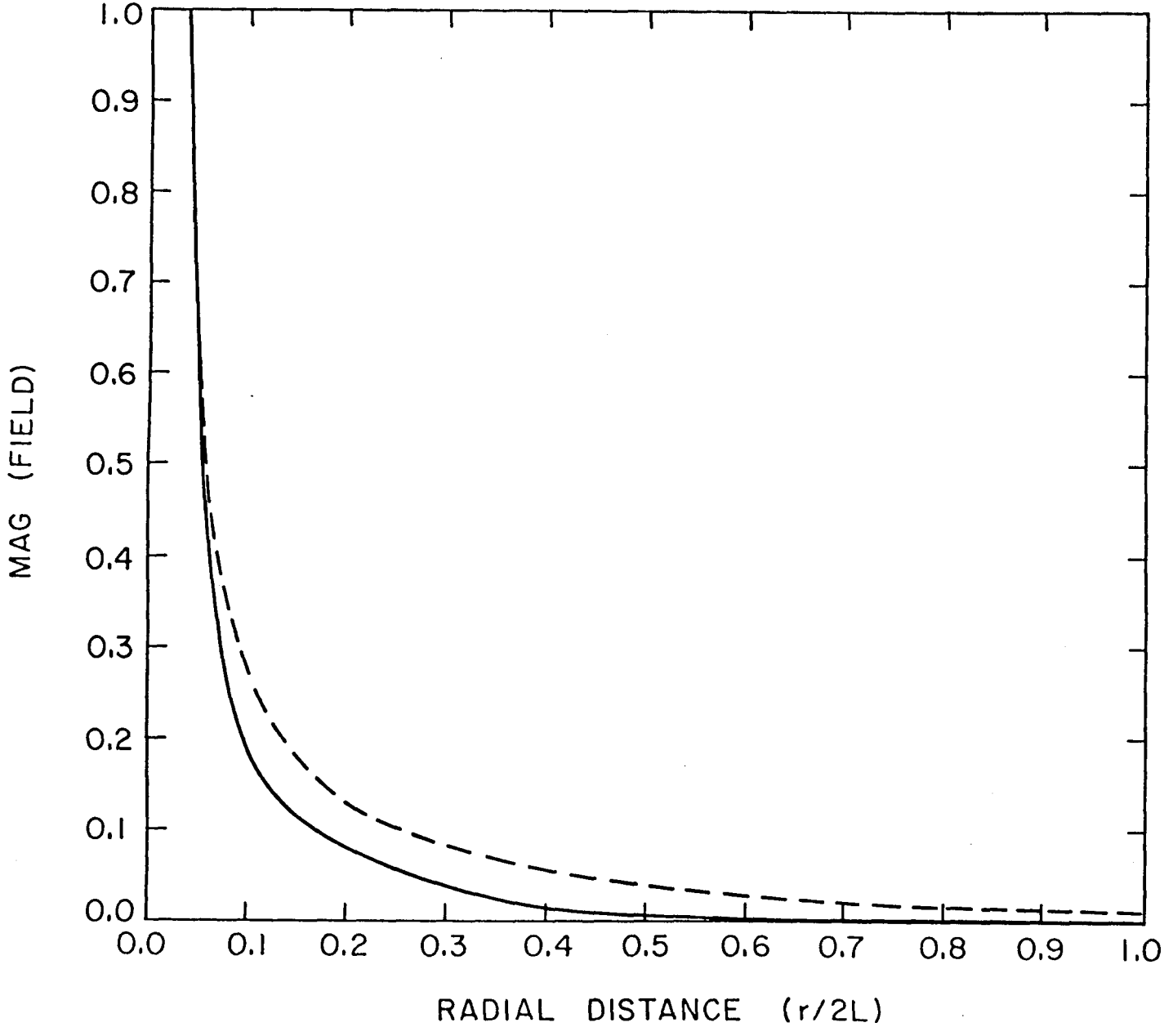

Figure B10. The radial distribution of the magnitude of the square of the electric field for $\epsilon = (6.0,0.1)$ *with Pocklington's equation* (–·–·–) *and sinusoidal current distribution* (—) *and an axial distance of* $L/4$, $2L/a = 250$.

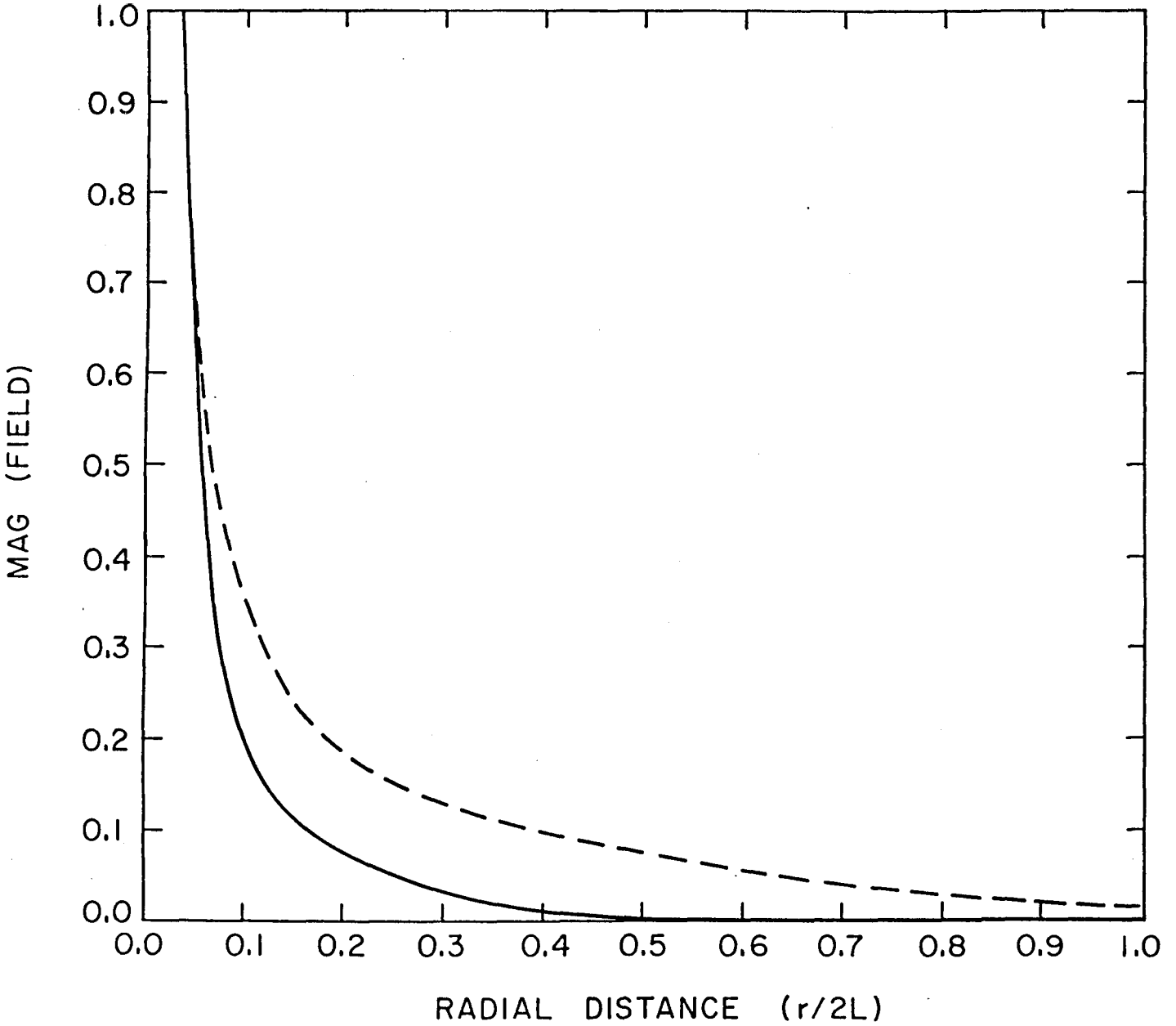

Figure B11. The radial distribution of the magnitude of the square of the electric field for $\epsilon = (6.0,0.1)$ *with Pocklington's equation* (—·—·—) *and sinusoidal current distribution* (—) *and an axial distance of* $L/4$, $2L/a = 250$.

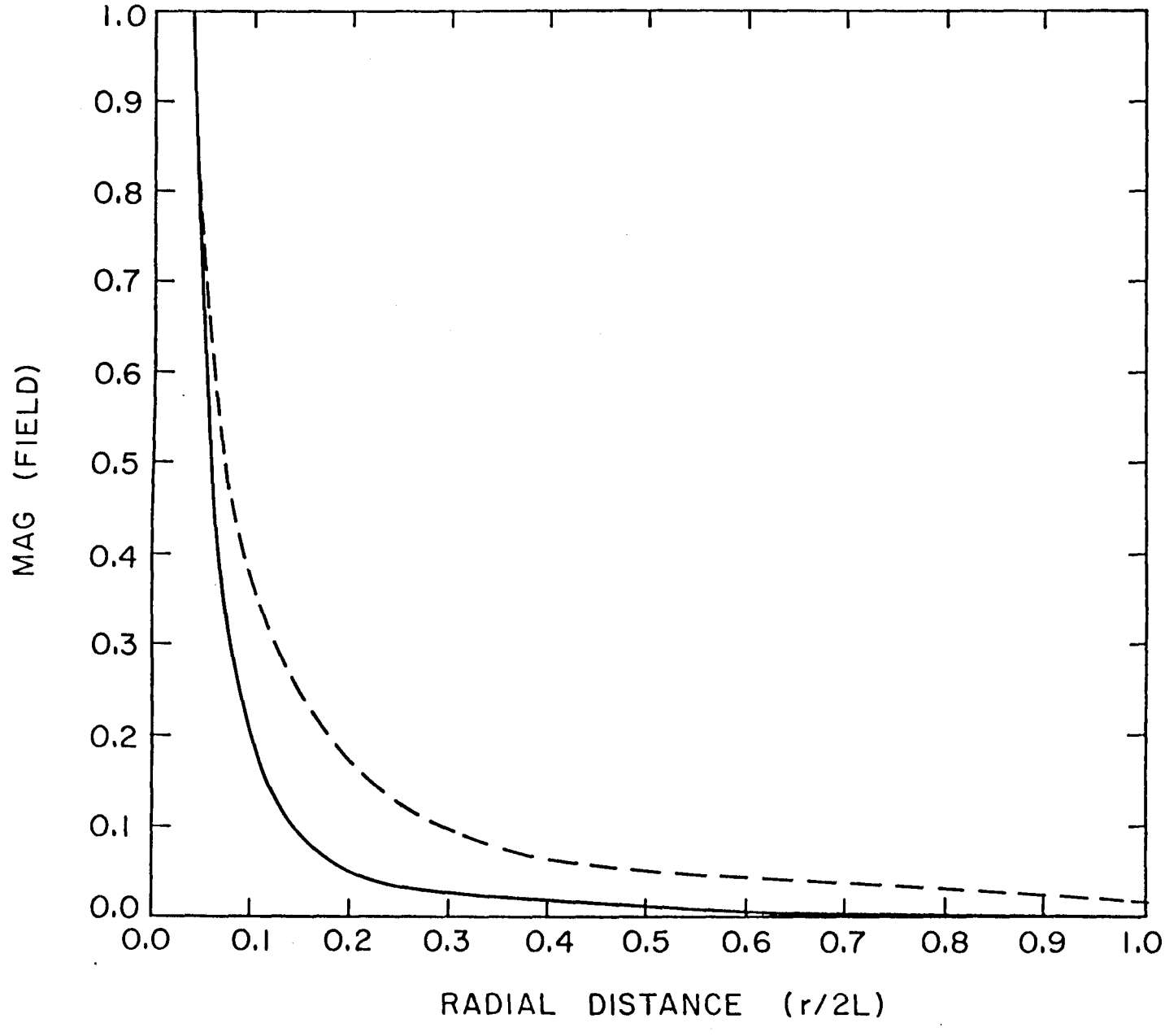

Figure B12. The radial distribution of the magnitude of the square of the electric field for $\epsilon = (6.0,0.1)$ *with Pocklington's equation* (—·—·—) *and sinusoidal current distribution* (—) *and an axial distance of* $3/4$, $2L/a = 250$.

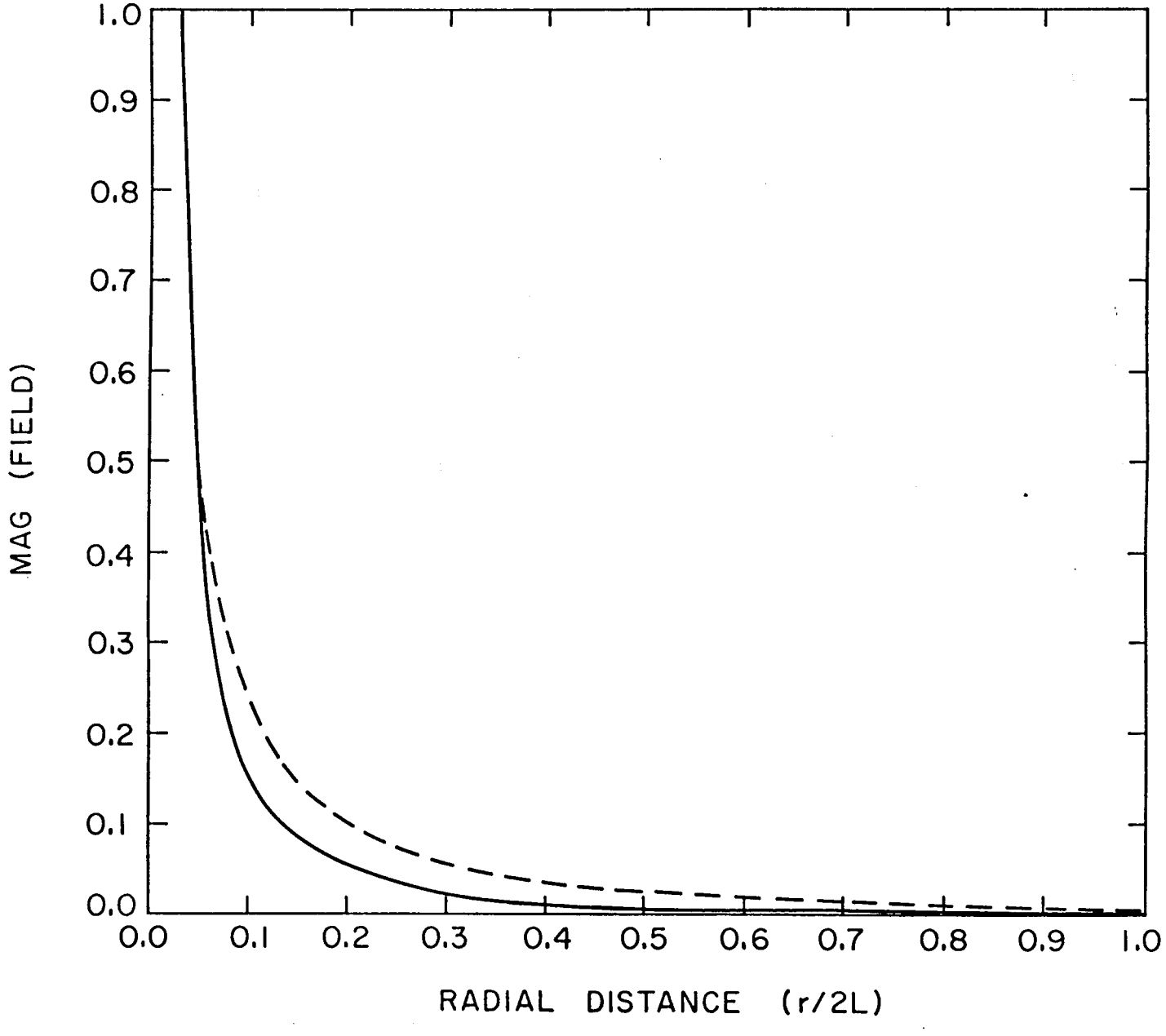

Figure B13. The radial distribution of the magnitude of the square of the electric field for $\epsilon = (6.0,0.4)$ *with Pocklington's equation* (—·—·—) *and sinusoidal current distribution* (—) *and an axial distance of* $L/4$, $2L/a = 250$.

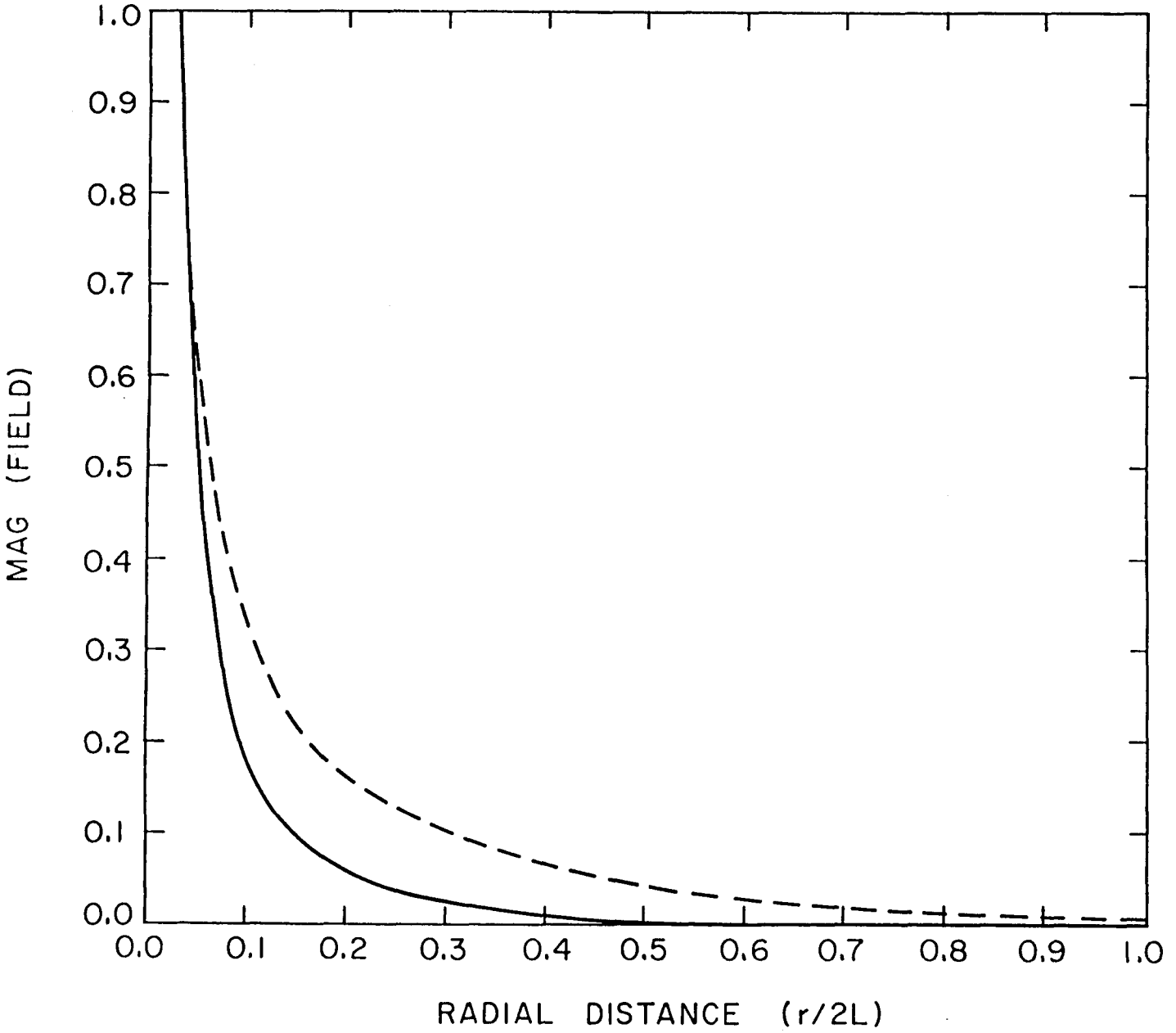

Figure B14. The radial distribution of the magnitude of the square of the electric field for $\epsilon = (6.0,0.2)$ *with Pocklington's equation* (–·–·–) *and sinusoidal current distribution* (—) *and an axial distance of* $L/2$, $2L/a = 250$.

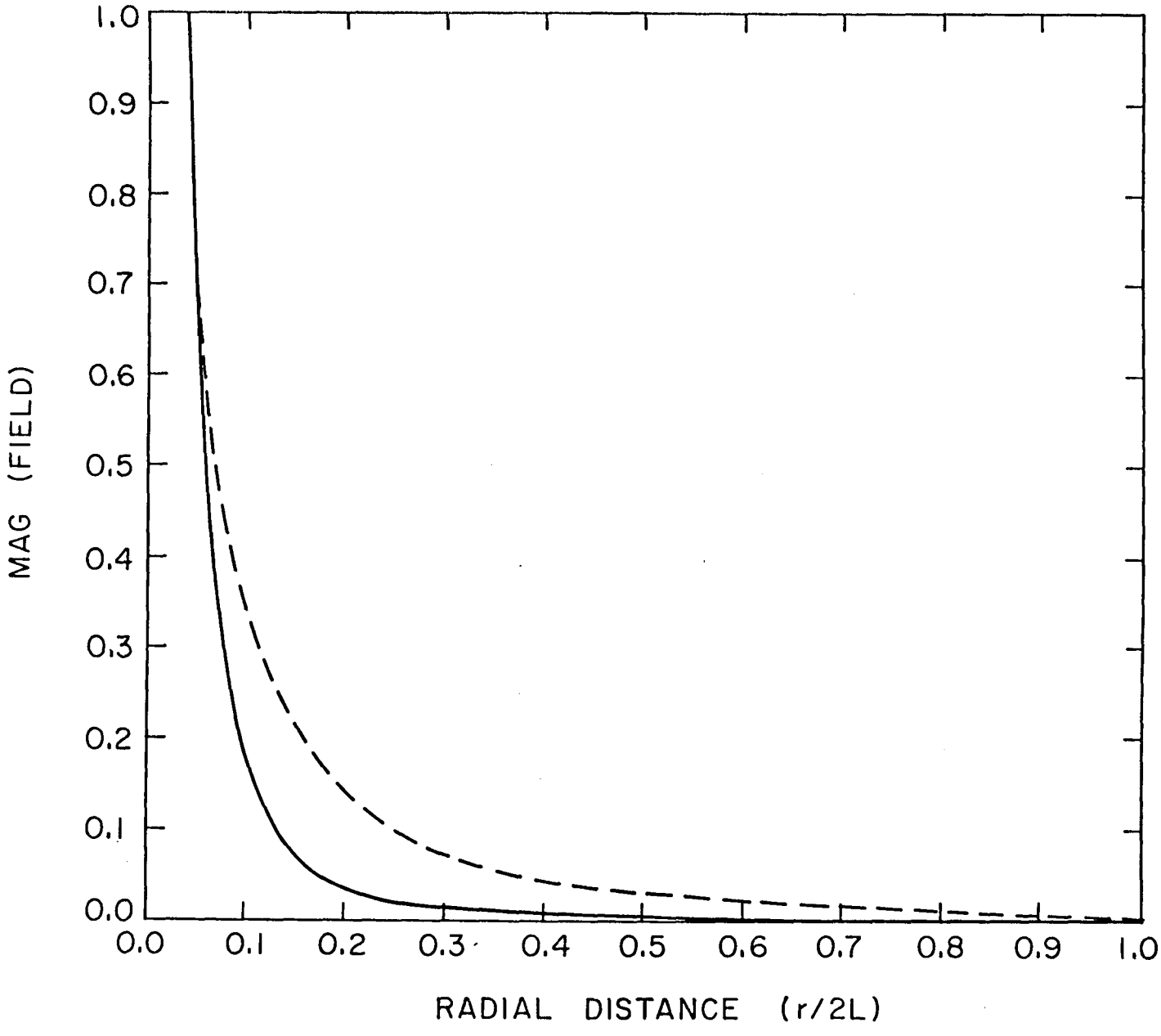

Figure B15. The radial distribution of the magnitude of the square of the electric field for $\epsilon = (6.0,0.4)$ *with Pocklington's equation* (—·—·—) *and sinusoidal current distribution* (—) *and an axial distance of* $3L/4$, $2L/a = 250$.

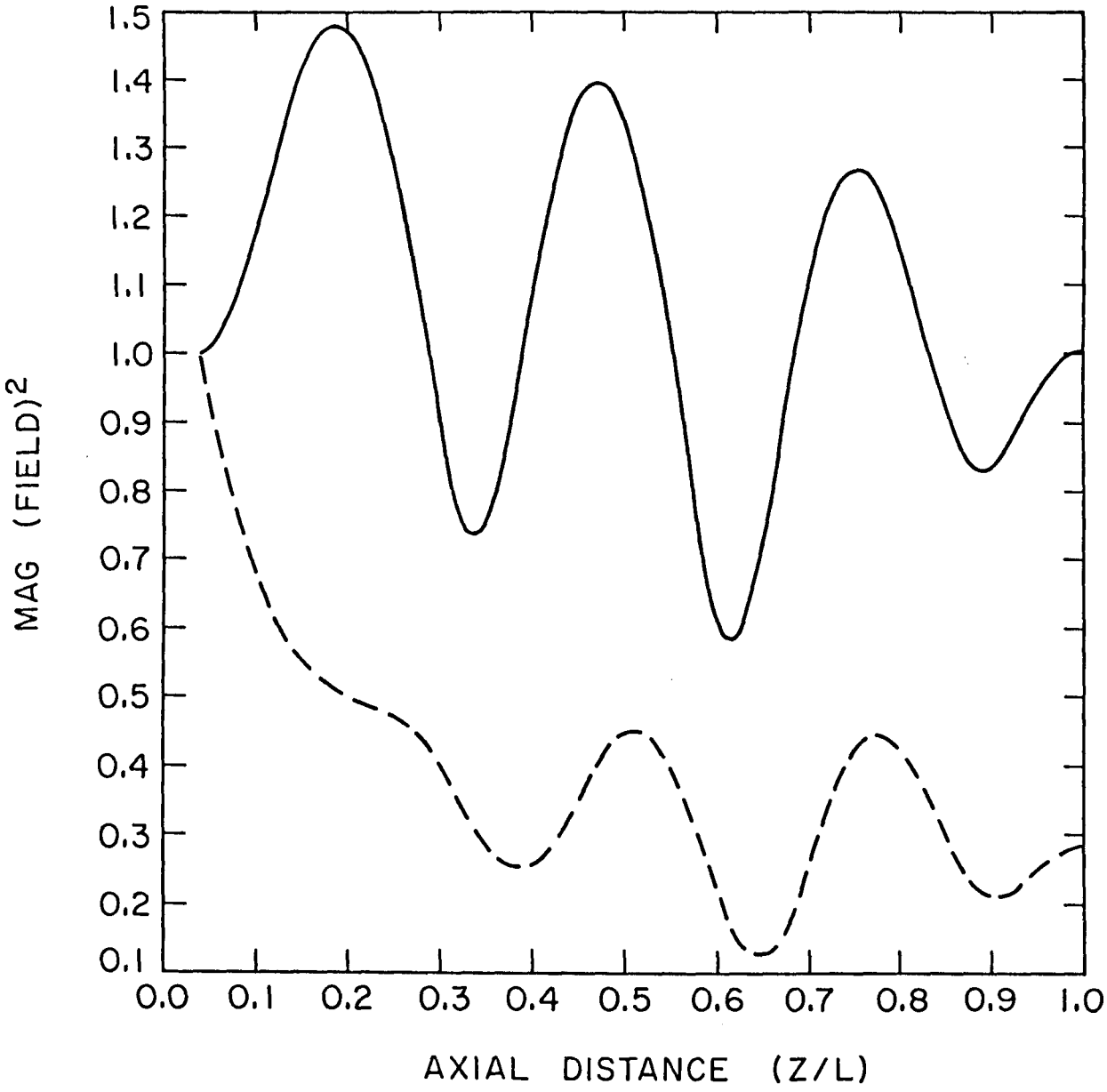

Figure B16. The axial variation of $|E|^2$ at a radial distance of 0.1L for $\epsilon = (6.0,0.4)$, $2L/a = 250$.

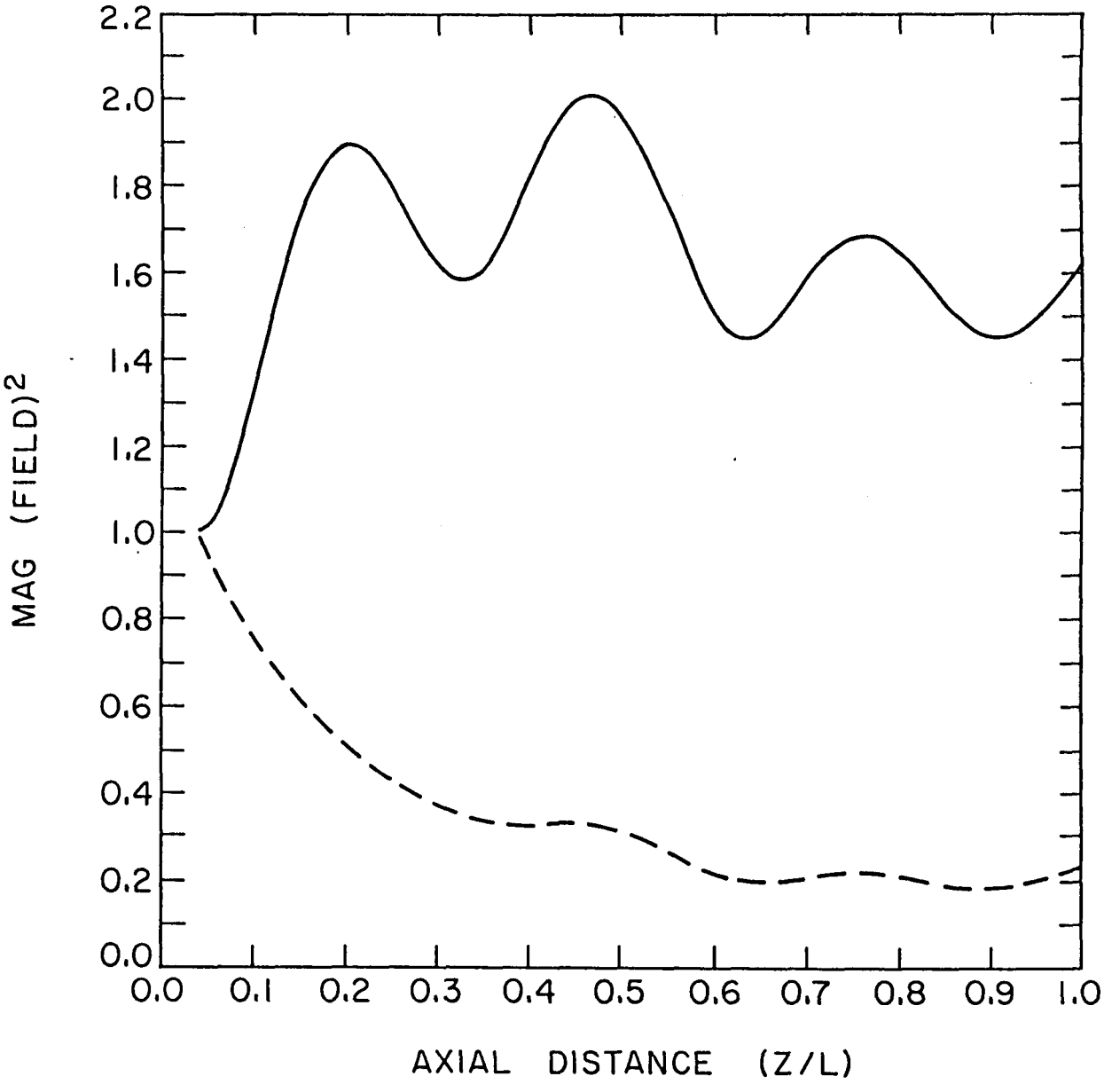

Figure B17. The axial variation of $|E|^2$ *at a radial distance of* $0.2L$ *for* $\epsilon = (6.0,0.4)$, $2L/a = 250$.

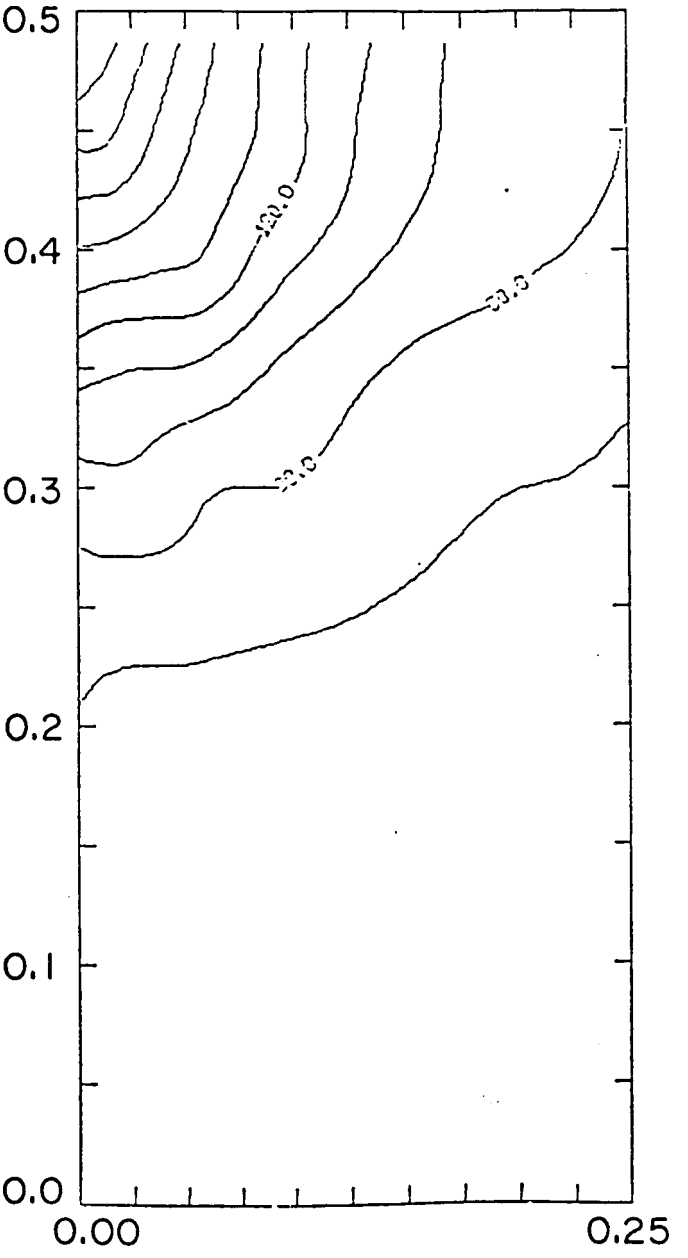

Figure B18. Temperature profiles using Pocklington's equation for the current predicted by the model for a frequency of 2450 MHz; $\epsilon = (3.0, 0.1)$, and a power of 1500 watts at a time of 2.8 hours. The radial dimensions are 0.0–0.25 m and axial dimensions are 0.0–0.5 m. The model run used 6 radial grid points and 7 axial points.

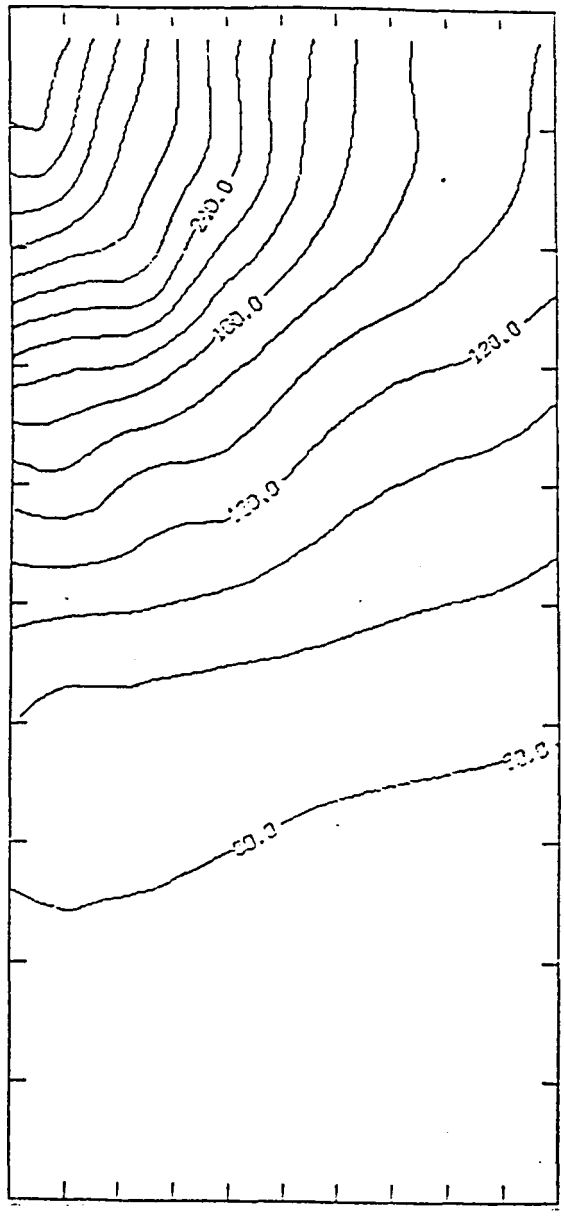

Figure B19. Temperature profiles using Pocklington's equation for current predicted by the model for a frequency of 2450 MHz; $\epsilon = (3.0, 0.1)$, and a power of 1500 watts at a time of 9.5 hours. The radial dimensions are 0.0–0.25 m and axial dimensions are 0.0–0.5 m. The model run used 6 radial grid points and 7 axial points.

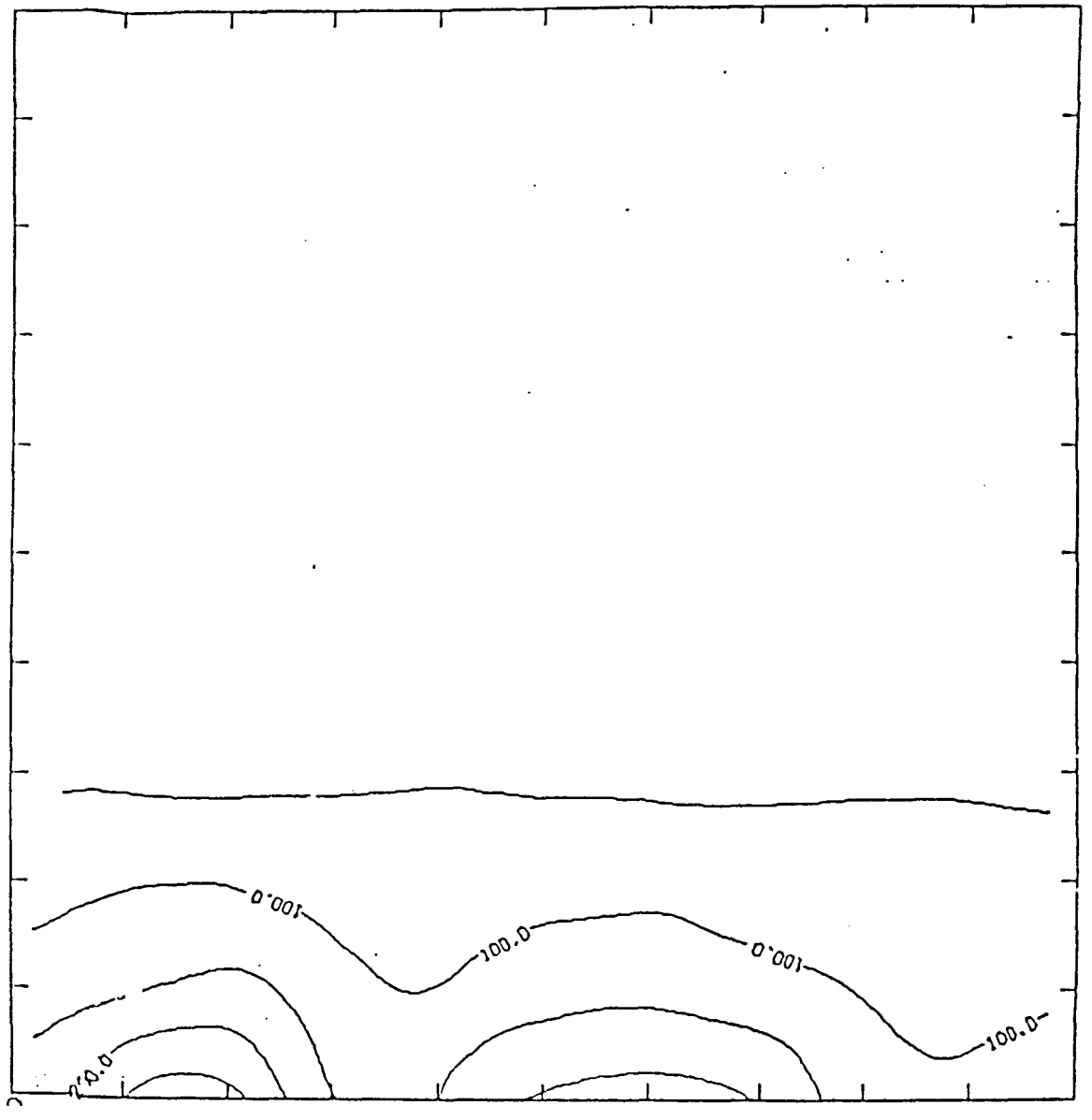

Figure B20. Temperature distributions using sinusoidal current distribution for same parameters as Fig. B19.

APPENDIX C

IMPEDANCE MODELING OF A COAX EXCITED MONOPOLE EMBEDDED IN OIL SHALE

It is of interest to determine the current distribution on an antenna embedded in an infinite bed of oil shale. The current distribution is needed for the calculations of the electromagnetic fields and the input impedance of the monopole. The impedance of the antenna can be calculated by knowledge of the input current at the driving point (a point where Hallen's equation fails). In this paper the general theory of the coaxially excited monopole is presented and numerical results are presented.

The following assumptions are made in this paper:

1. The excitation at the feed point is of the form of a TEM mode from a coaxial line. The input radial electric field is of the form

$$E = \frac{V}{2\ln\left(\frac{b}{a}\right)\rho} \tag{C1}$$

where a is the monopole radius and b is the coax radius.

2. The surface current is expressed as

$$G(z,z') = \frac{1}{2}\pi \int_{-\pi}^{\pi} \exp(-jkR(\theta))/R(\theta)d\theta \tag{C2}$$

where

$$R = \left((z-z')^2 + (2a\sin(\theta/2))^2\right)^{\frac{1}{2}}.$$

Here $k = 2\pi/\lambda$, is the observation point, and θ is the angle between ρ and ρ'.

3. The antenna is assumed to have no conductive losses. Pocklington's integral equation [31] for an antenna of length 2L is given by

$$E_z = \frac{1}{i\omega\epsilon} \int_{-L}^{L} \left[\frac{\partial^2 G(z,z')}{\partial z^2} + \beta^2 G(z,z')\right] J dz' d\theta \tag{C3}$$

where J is the source term on the antenna. Pocklington's equation was solved numerically using the method of moments. It was assumed that the current was given by $I(z) = \sum_n c_n p_n(z)$ where the function p_n are given as pulse functions.

$$p_n(z) = 1 \text{ for } z_m < z < z_{m+1} = 0 \text{ otherwise} \tag{C4}$$

where the grid points z_1, z_2, ..., z_{n+1} are given by

$$z_n = (n-1)L/N. \tag{C5}$$

The matching points which are in the center of each grid are given by z_1, z_2, ..., z_N.

In the numerical method the kernal K was approximated to avoid multiple integrals. It is possible to separate the integral in Equation (C1) as a sum of an elliptic integral and an additional term

$$K = \frac{\exp(-jkR_+) - 1}{R_+} + \frac{2E(p)}{\pi R_+} \qquad (C6)$$

where

$$R_+ = (z^2 + (\rho + a)^2)^{\frac{1}{2}}$$

$$p = 2a/R_+$$

$$E(p) = \frac{2}{\pi R_+} \int_0^{\frac{\pi}{2}} \frac{d\beta}{(1 - p^2 \sin^2 \beta)^{\frac{1}{2}}}.$$

NUMERICAL RESULTS AND DISCUSSION

In modeling the electromagnetic heating of oil shales it is important to determine the dielectric constants of the shales. Measurements of the input impedance of the monopole may in principle be used to determine the dielectric constant. In Figs. C1–C6 the input impedance of a monopole embedded in a block of shale ($V(0)/I(0)$) is plotted as a function of the real part of the dielectric constant for various values of the imaginary part of the dielectric constant. In Fig. C7 the current distribution is plotted along the antenna for an antenna length 0.152 and radius of .0027 m. In this case the coax has a radius of .0054 m.

The plots in Equation (C4) used 500 functions for each calculation of an input impedance and 60 input impedance points were calculated for each curve. Figs. C9 and C10 are plots of the convergence rates of Pocklington's equation and are a function of the number of pulse function. As can be seen the convergence is almost complete at about 200 points.

In Table C1 the experimentally determined impedance values are given for antenna of various lengths embedded in a shale block. When results given in Table C1 are compared to Figs. C1–C6 it can be seen that the dielectric constant of the shale is close to (3.0,0.1).

TABLE C1

EXPERIMENT INPUT IMPEDANCES

Data: Frequency: 1 GHz

Monopole Length	R	X
0.449	37.4	−20.8
0.385	37.1	−19.5
0.320	40.2	−22.3

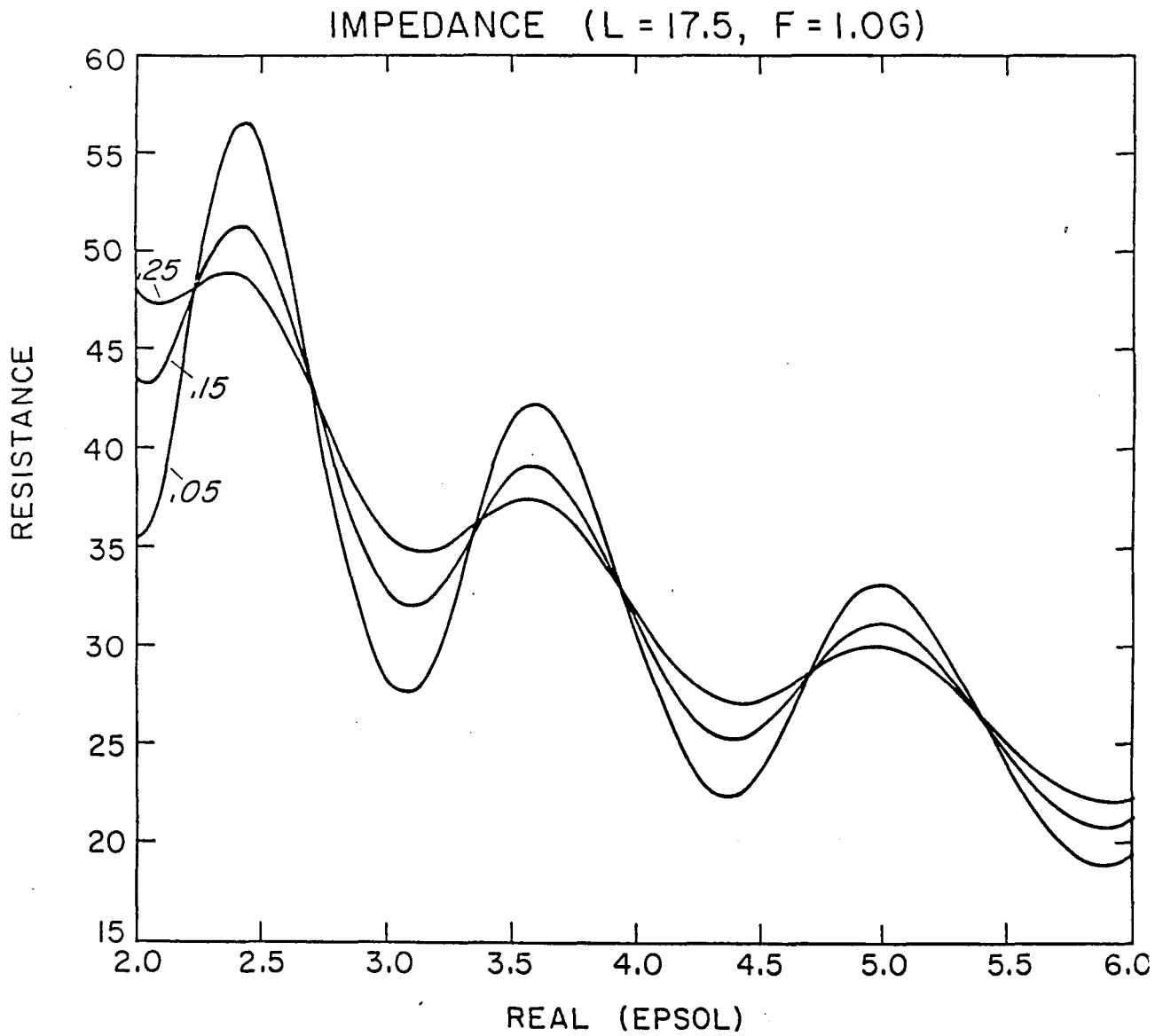

Figure C1. The real part of the impedance for various values of the imaginary dielectric constant. The antenna length is 0.435 meters, the frequency was 1.00 GHz. In this curve the radius of the antenna is A = .0082, B = 0208 m. The curves are for ϵ'' = −0.05, −0.15 and −0.25.

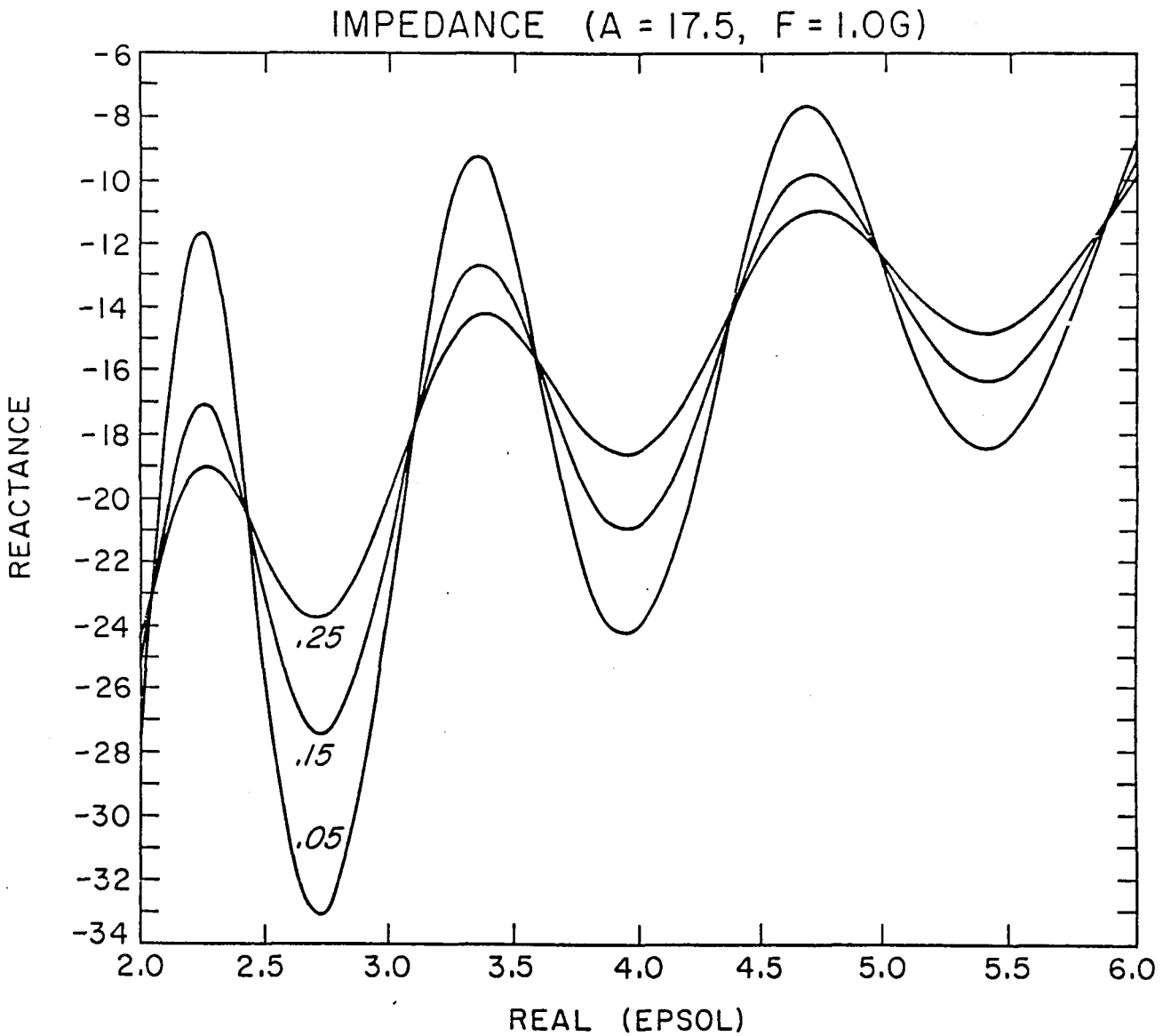

Figure C2. Similar to Fig. C1, but for the reactance part of the impedance.

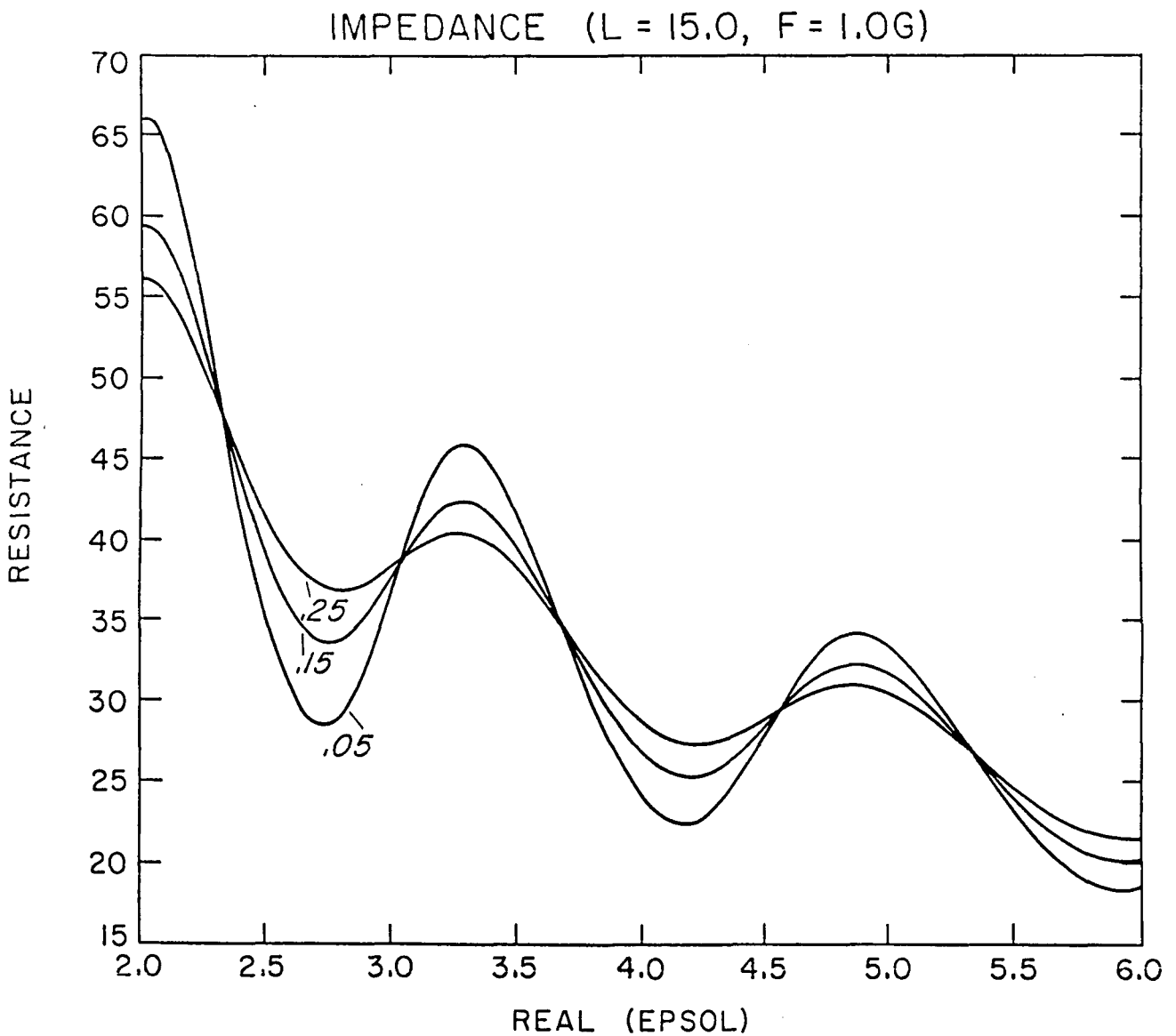

Figure C3. Similar to Fig. C1, but for an antenna length of 0.384 m.

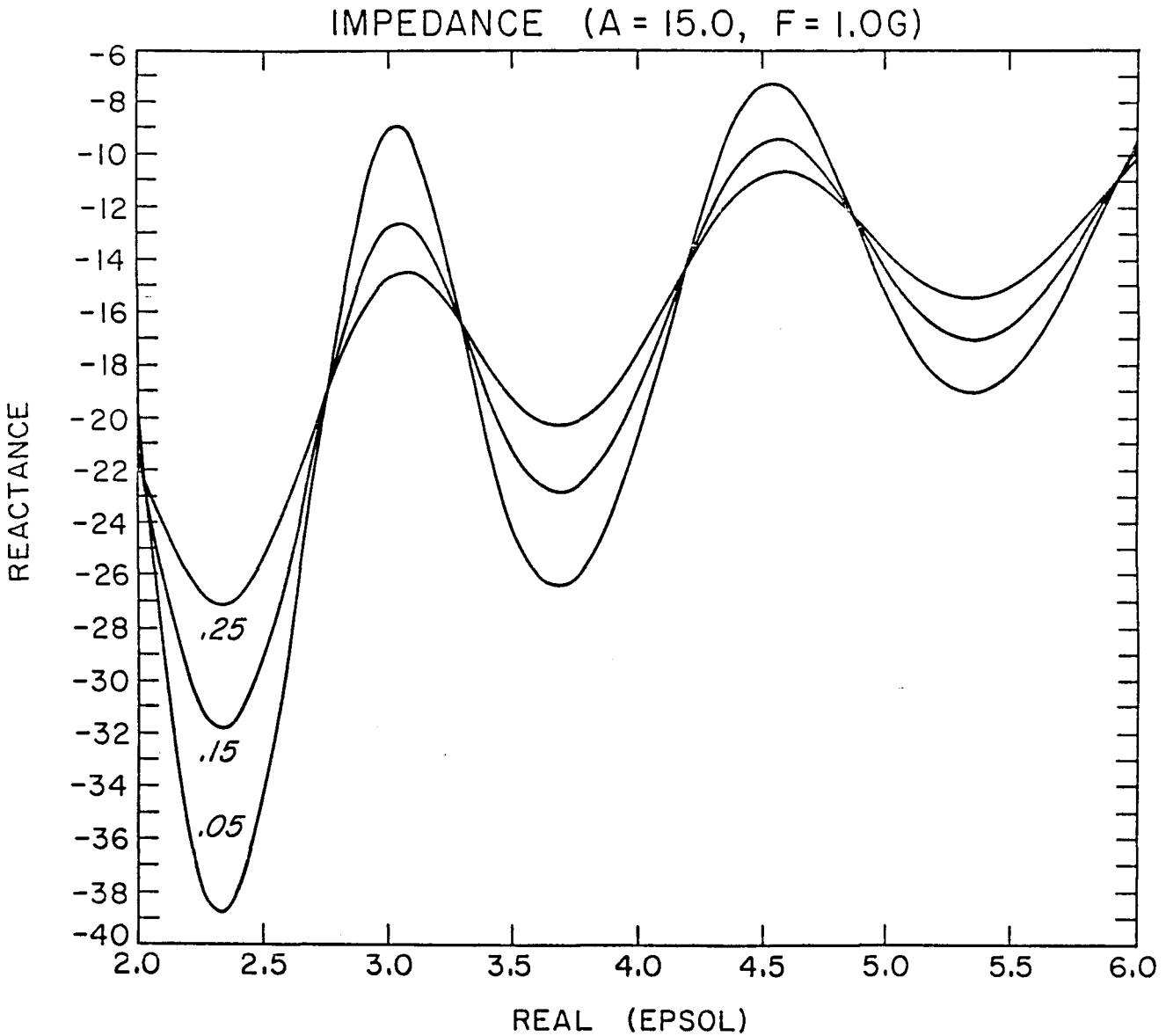

Figure C4. Similar to Fig. C2, but for antenna length 0.384 m.

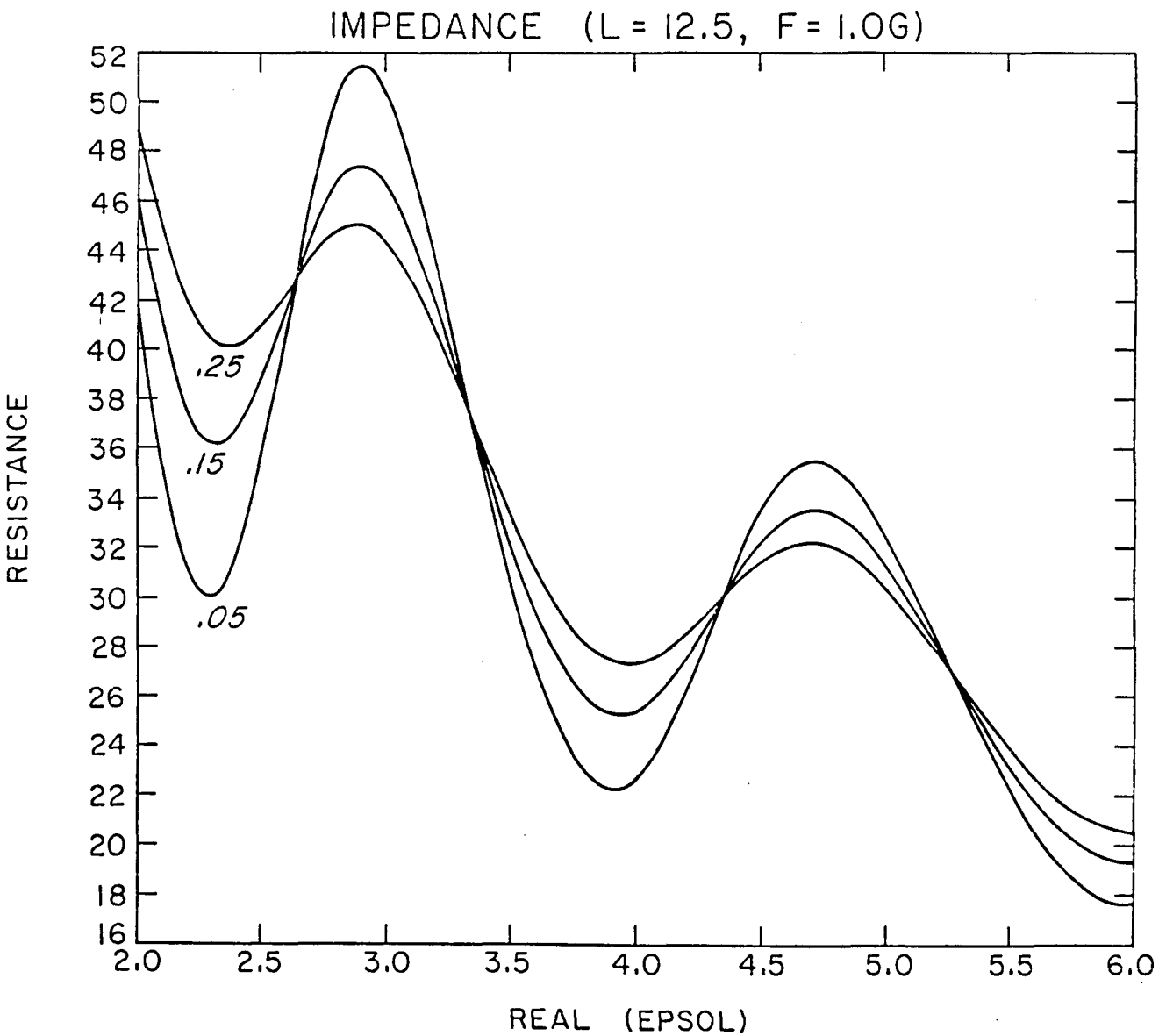

Figure C5. Similar to Fig. C1, but for antenna length 0.320 m.

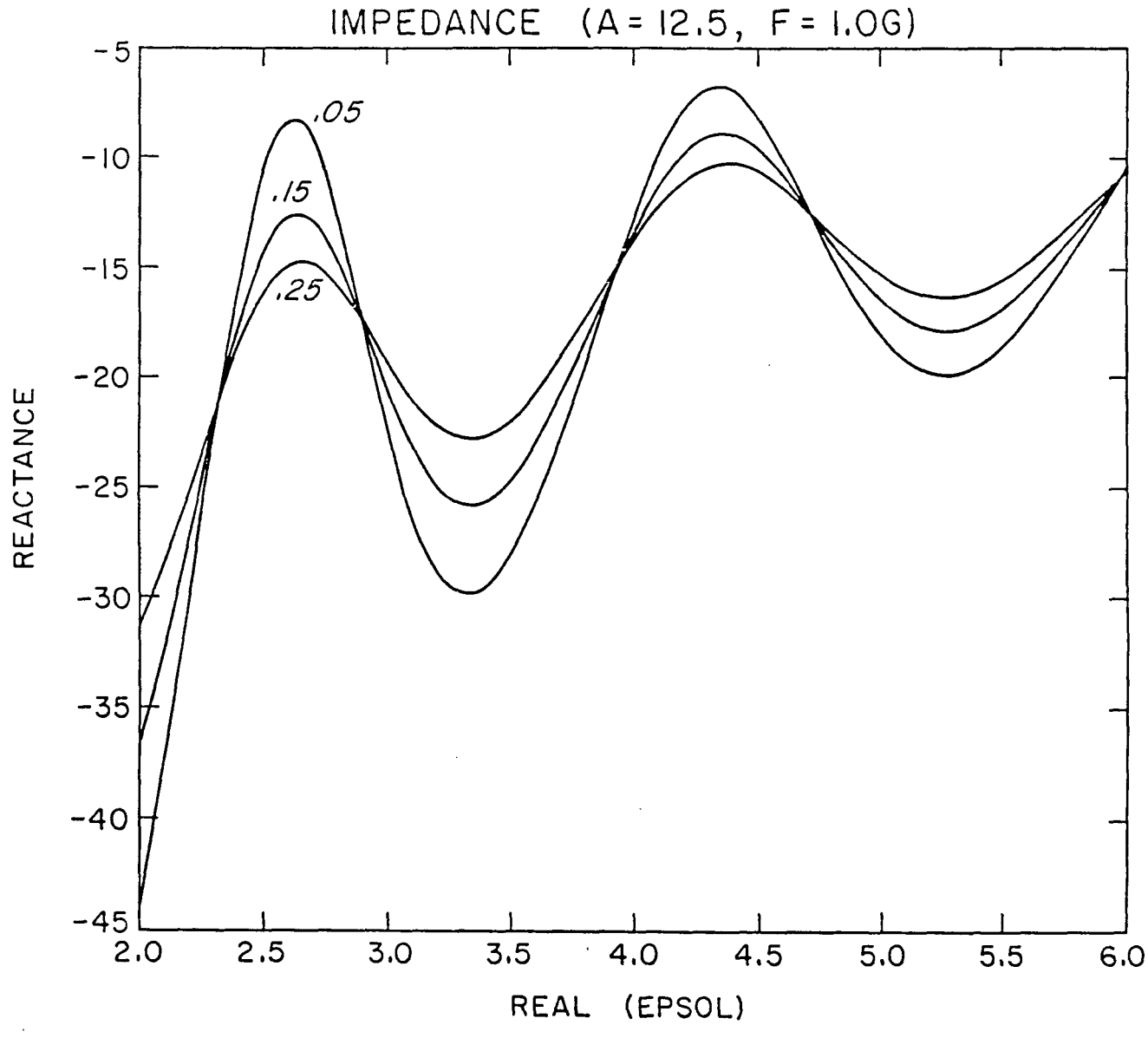

Figure C6. Similar to Fig. C2, but for antenna length 0.320 m.

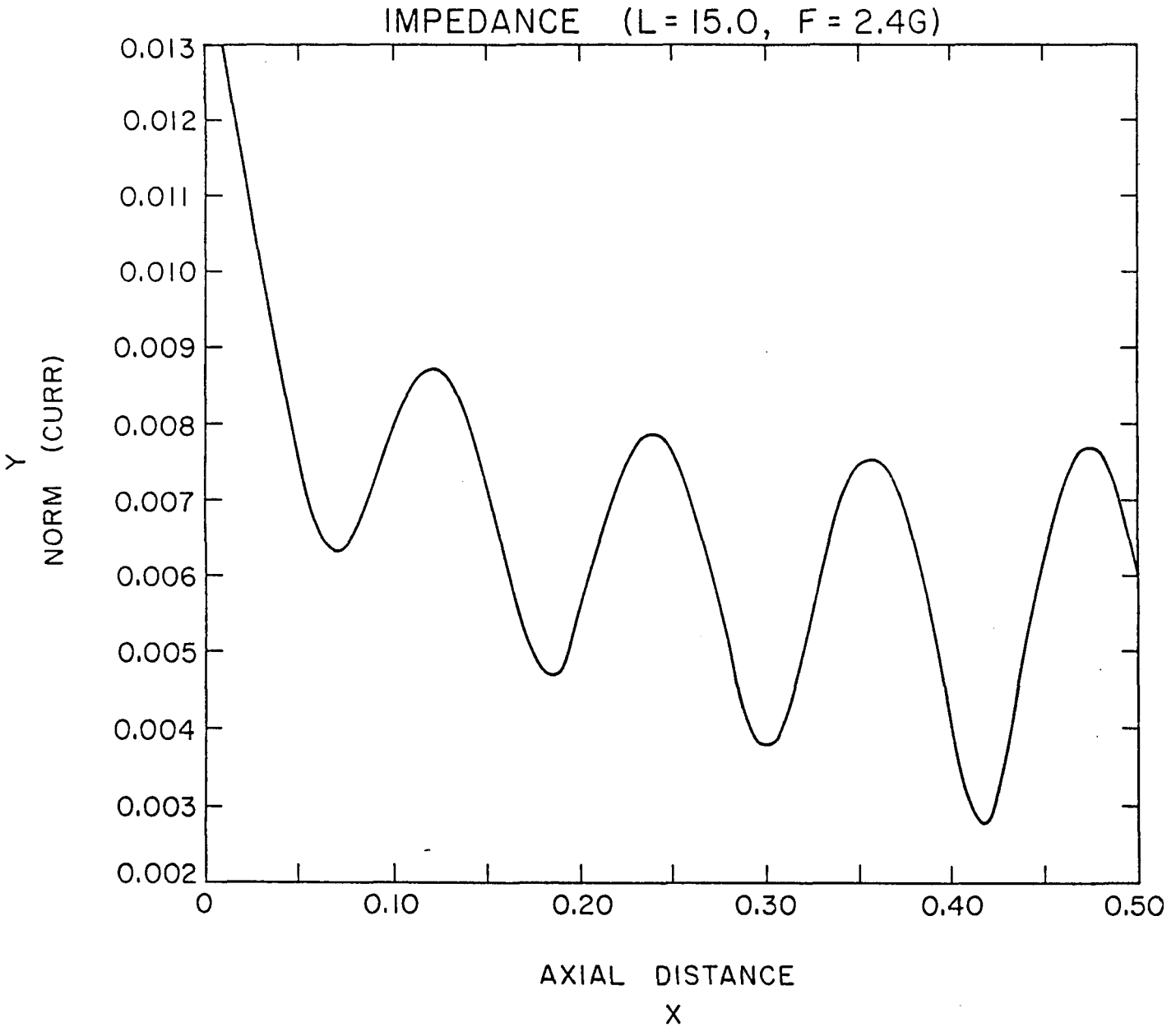

Figure C7. Current distribution (ampheres) on a monopole antenna of length 0.152 m, frequency of 2.45 GHz, $\epsilon = (3.0,-0.1)$.

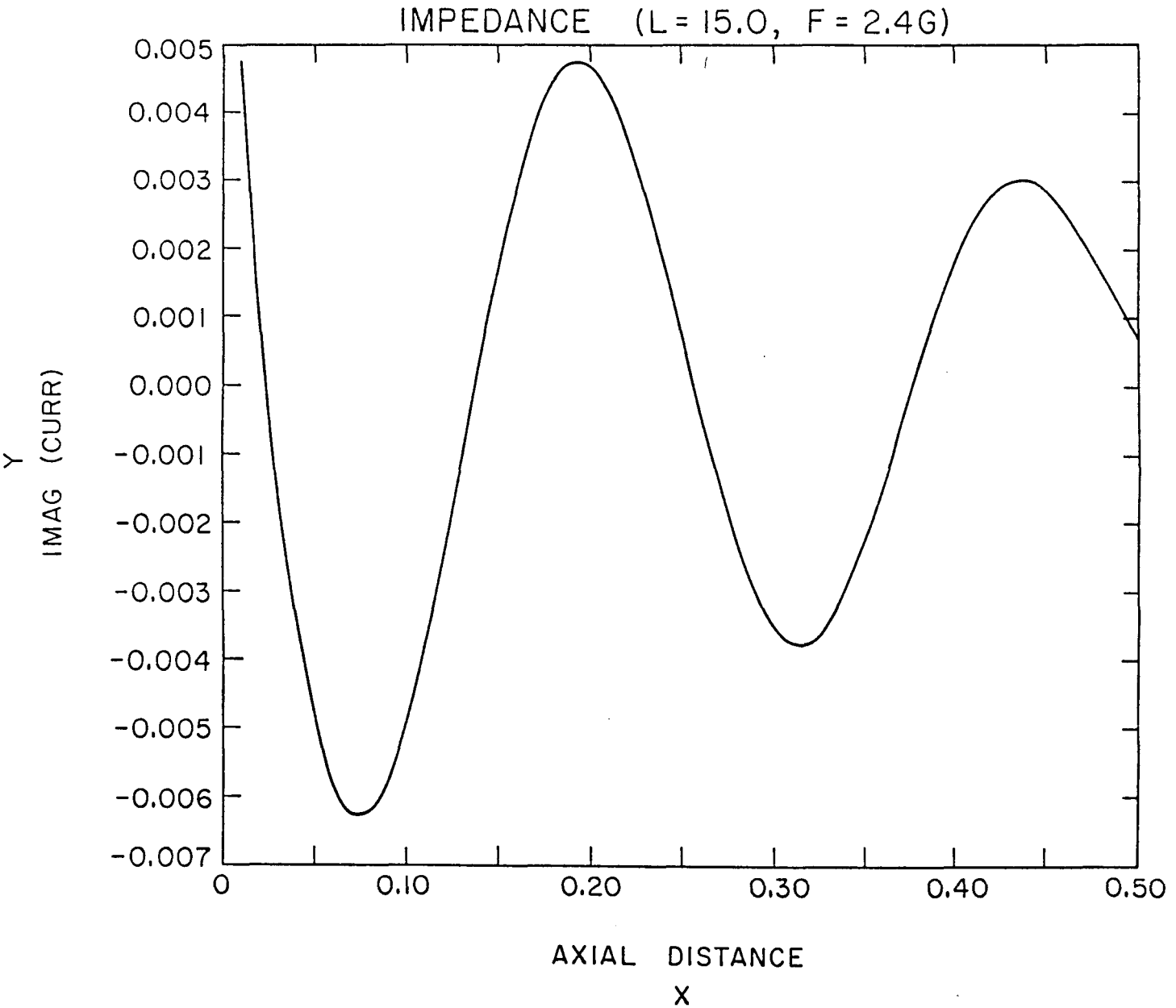

Figure C8. Imaginary (ampheres) part of the current distribution given in Fig. C7.

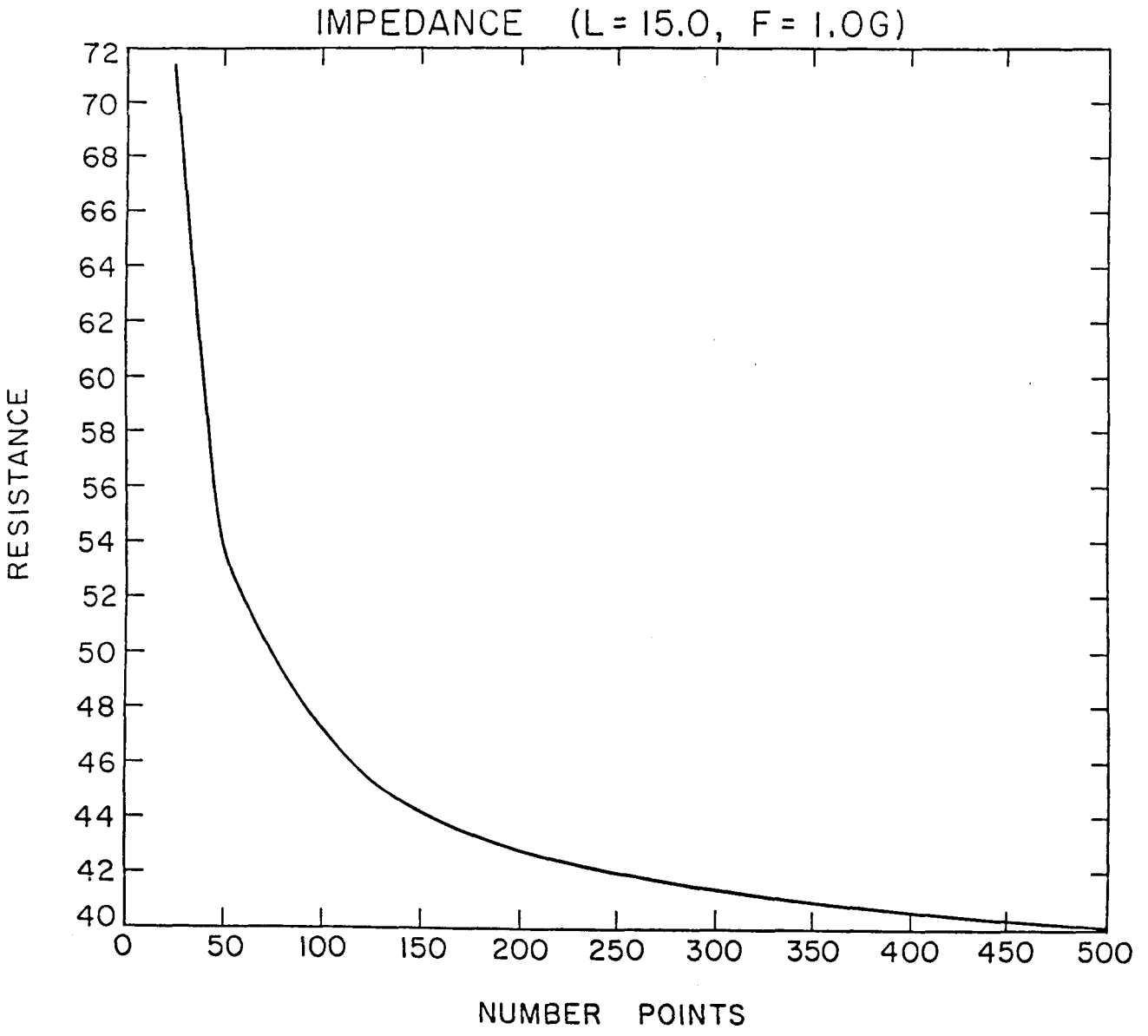

Figure C9. The convergence rate of the real part of the impedance as a function of the number of impulse functions.

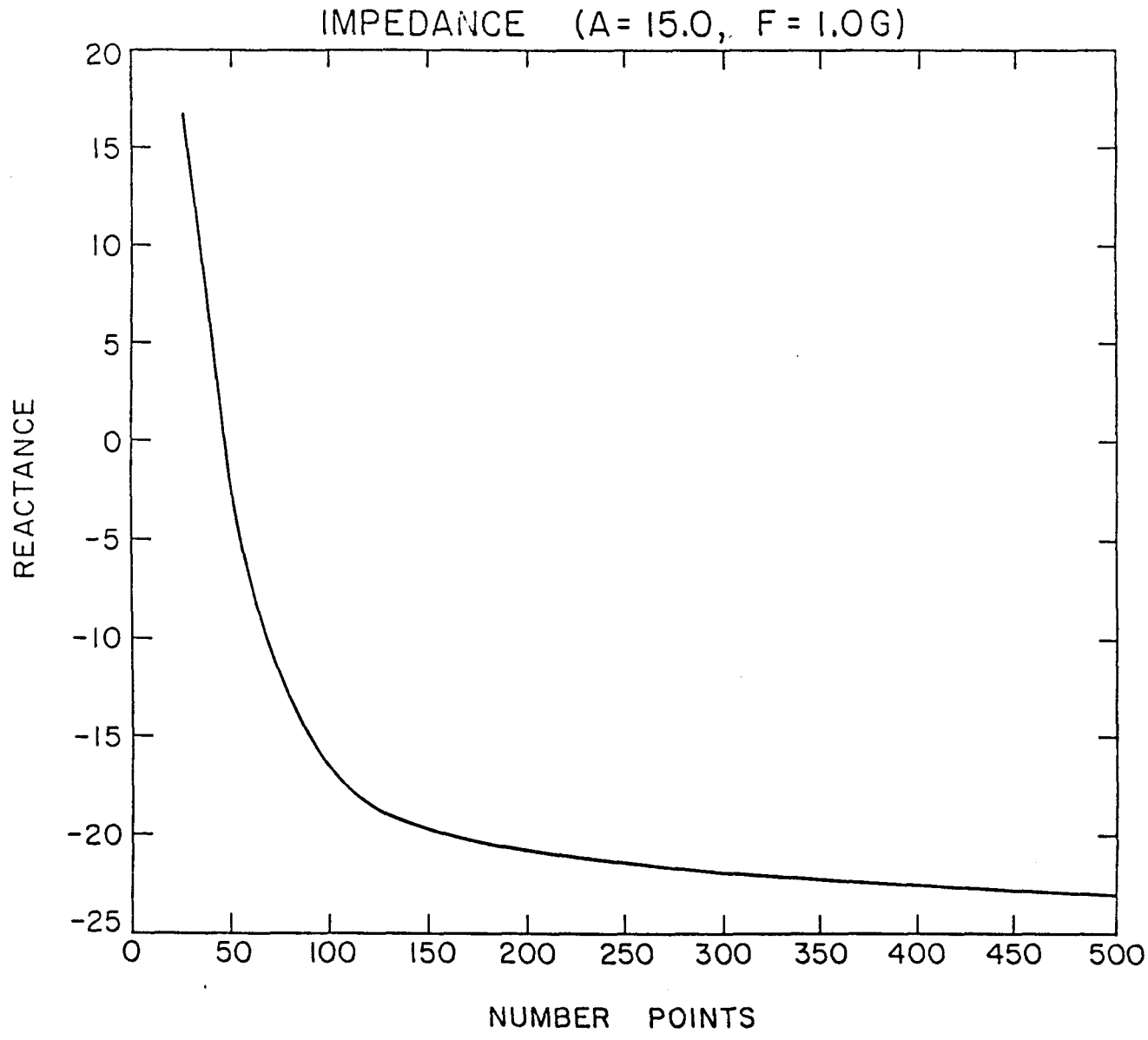

Figure C10. Same as Fig. C9, but for reactance.

APPENDIX D

MODEL SIMULATION RESULTS

The mathematical model outlined in Chapter 2 was used to simulate the various heating tests summarized in Appendix A. As an example, the simulation of test #7 is presented in detail here. In this test a block of dimensions (0.514 m × 0.505 m × 0.464 m) was heated with a monopole. The following simulation was performed before the test run to predict test results. In this simulation the following parameter were used:

Frequency	450 MHz
Input Power	2015 watts
Antenna Length	0.5
Shale Grade	27 gal/ton
ϵ	(6.0,−0.2)

The field distributions ($|E|^2$) are given in Fig. A8 and the simulation results are given in Figs. A9–A17.

The actual test was run with the following parameters:

Shale Grade	23 gal/ton
Input	500 watts for 30 min, 1000 watts for 30 min, and 1500 watts thereafter
Top Insulation	3.5″ John Mansville Fire Brick
Bottom Insulation	7.5″ John Mansville Fire Brick (#20)
Side Insulation	8″ shale blocks
Reflected Power	2 watts

The temperatures measured in the experiment in the r-z plane are shown in Figs. A73–A77.

Another model run of this test was performed tomatch the experimental parameters. In this run the following parameters were used:

Power	1500 watts
Field Distribution	$P(r,z) = P_0 \exp(-r/\alpha)[az + b]$ (where a and b are experimentally determined parameters).
Number of Model Grid Points	radial: 6, axial: 7

The heat losses from the block were estimated by knowledge of the experimental surface temperatures. These heat losses were then fed into the model. In the Figs. D1–D4 the model temperatures are plotted in the r-z plane. Comparison of the model predictions to the experimental results is very favorable. It is of interest to note that the pre-run test results were in the ballpark of the actual test.

In order to sort out the extent to which thermal conduction plays a role in the process, in Figs. D1–D4 the model was run with and without thermal conductivity. We see from the results that in a block size of dimensions 0.5 meters, after 8 hours thermal conductivity plays a very big role whereas for shorter times thermal conductivity effects are relatively minor.

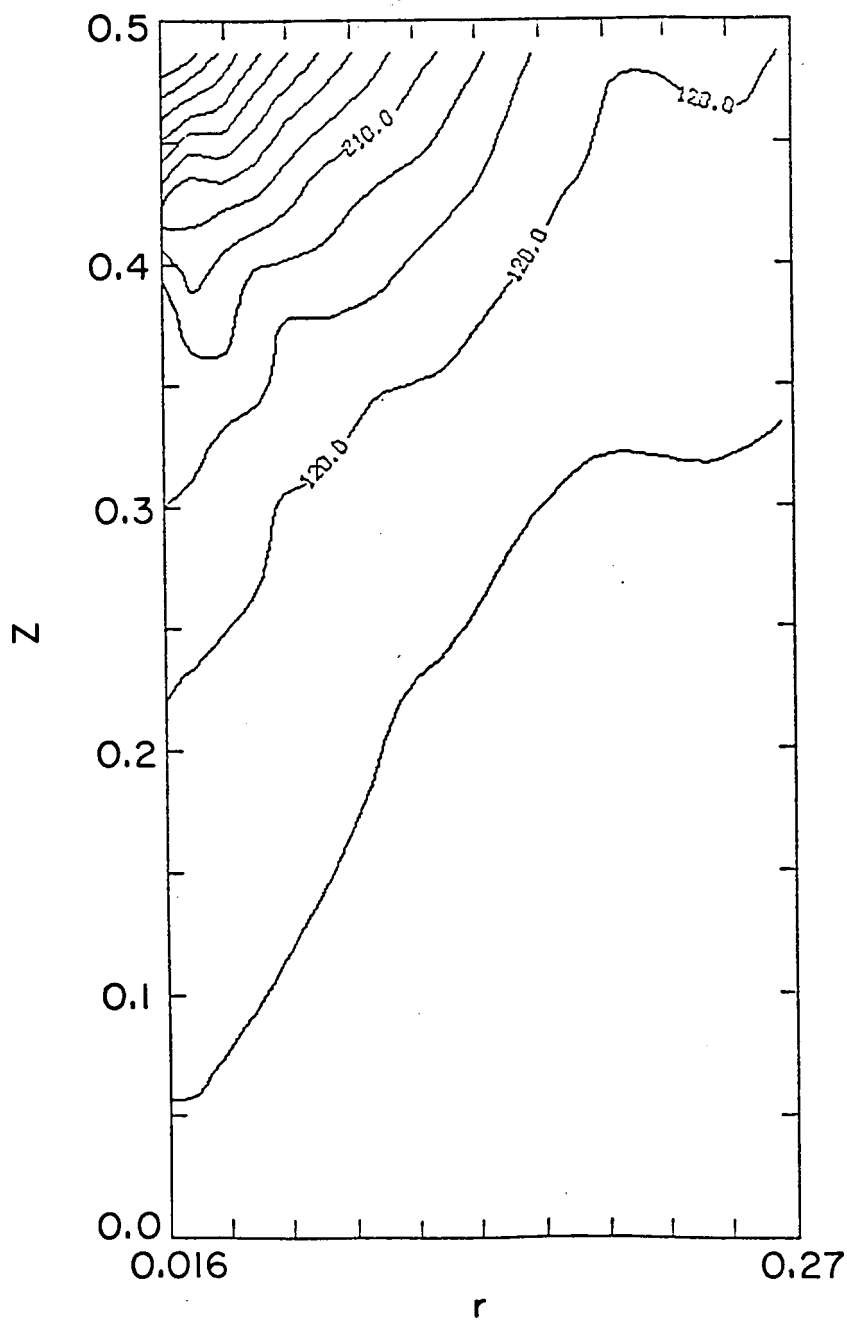

Figure D1. Temperature distributions in the r-z plane with and without thermal conductivity.

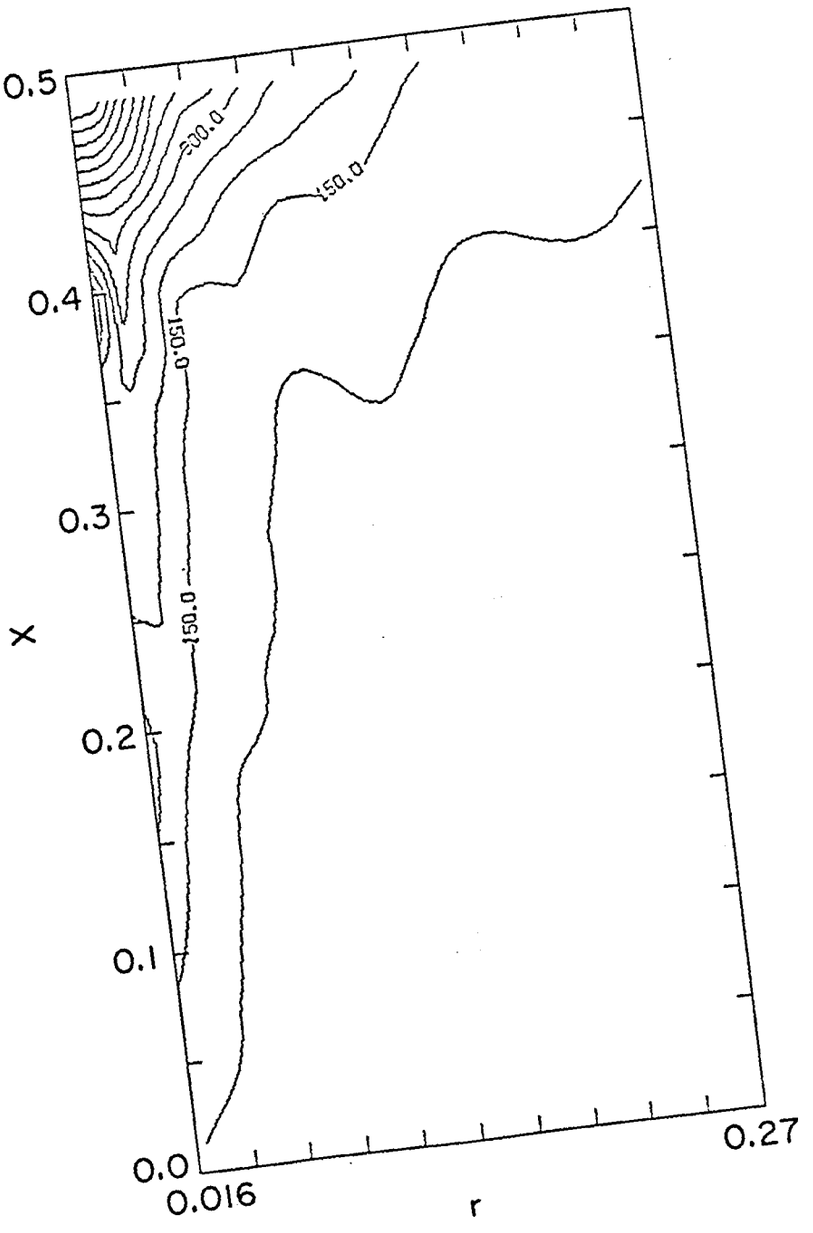

Figure D2. Temperature distributions in the r-z plane with and without thermal conductivity.

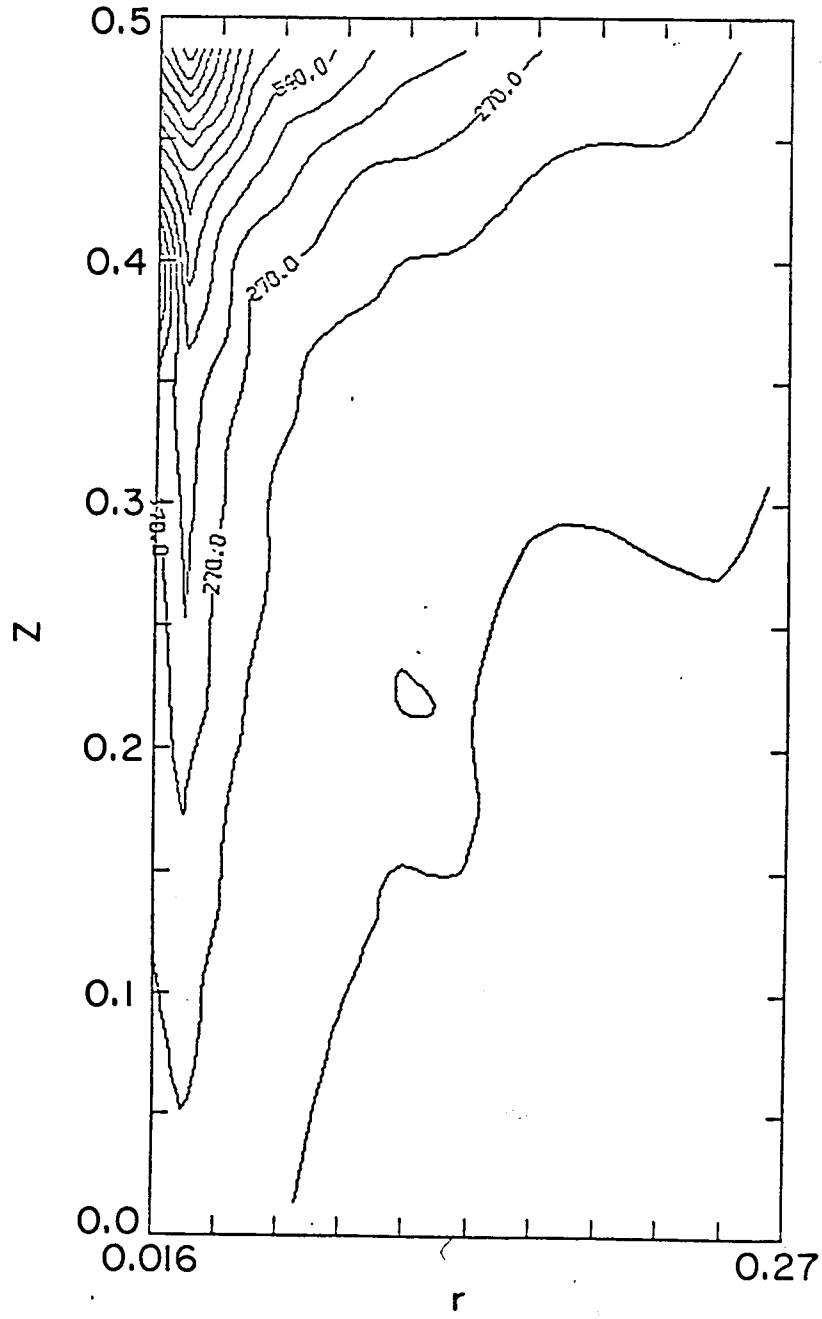

Figure D3. Temperature distributions in the r-z plane with and without thermal conductivity.

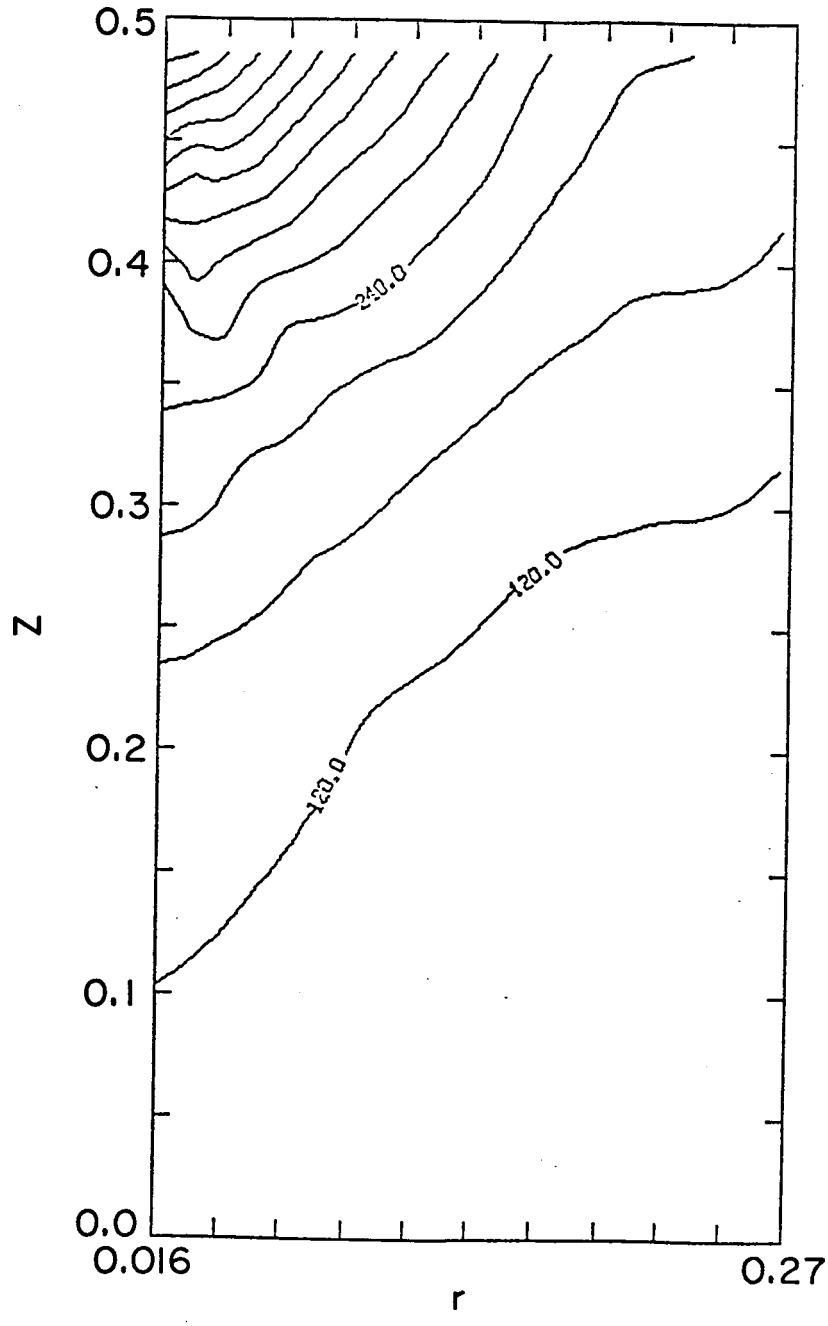

Figure D4. Temperature distributions in the r-z plane with and without thermal conductivity.

APPENDIX E:

IN SITU ELECTROMAGNETIC HEATING CODE

PROGRAM NAME: USHALE

DESCRIPTION: Simulates electromagnetic heating of oil shales.

DEVELOPED BY: J. Baker-Jarvis, University of Wyoming Physics Department

BACKGROUND

The present model simulates the retorting of oil shale around a single monopole applicator. The model solves equations for heat, mass, chemical reactions, and electromagnetic source terms simultaneously to produce temperatures, pressures, densities, oil yields, etc. The model uses Lawrence Livermore results for chemical reactions [22,23]. Cylindrical and cartesian coordinates may be used in two dimensions. The solution proceeds by discretizing the partial differential equations in the space variables and then solving the resulting system of coupled nonlinear partial differential equations by the IMSL differential equation routine DGEAR.

Details of the model are described in the publication by Baker-Jarvis [61]. Basically, the model assumes that initially the shale block consists of inert inorganics, dolomite, kerogen, bound water, and a small amount of void space. As the block is heated, the kerogen and dolomite react to form gases and oils, and permeability is achieved. The oil is assumed to be in either gaseous form or liquid form depending on the vapor pressure. Coking reactions are assumed to take place according to the kinetics developed by Lawrence Livermore [22,23]. As the kerogen and dolomite decompose, the porosity, and therefore the permeability increase and the oil begins to flow through the resource. The autogeneously produced gases produce the necessary pressures to push the products out to the monopole bore hole.

The boundary conditions employed are:

1. At the bore hole the pressure and temperature is assumed to be given.
2. Convection boundary conditions are given at all other sides of the retort for the temperature.

DIMENSIONAL UNITS USED IN PROGRAM

This program utilizes SI (metric units) throughout.

temperatures:	kelvin
pressure:	pascals
volume:	cubic meters
distance:	meters
mass:	kilograms
densities:	kilograms/cubic meters

A flow chart of equations and output parameters is given in Fig. E1. When setting up the code to be run, a number of parameters need to be set. These are:

setker	A subroutine used to set up kerogen density in the grid, in ukin(i,j)
gridr,gridz	number of grid points in r and z directions
xwel	radius of the well bore in meters
rmax	extent of the grid in the r direction in meters
zmax	extent of the grid in the z direction
coordty	type of coordinates to used (cylindrical = 3, rectangular = 2)
xend	time that you wish the first return of DGEAR (first print out)
field(i,j)	array of power density (watts/cu meter of shale) must be specified. Here one can either use subroutine MOMENT for a monopole or subroutine ELECP for a very thin monopole.
qrp1,qrm1,qzp1,qzm1	heat loss parameters must be set in subroutines FCN and FCNJ
epsol	complex dielectric constant of the shale
t01	initial temperature of the reservoir
initial saturation of gas	must be set in y(...)
initial pressure (pa)	must be set y(...)

HEATING SOURCE FUNCTIONS

The model was developed to use monopole applicators as the heating source, although any heat source could be used. The idea for determining the heating profile is to fill the array FIELD(i,j) (i = 1 to Gridr, j=i to Gridz) with the power dissipated at each grid point (watts/cubic meter). In the main routine there exists a function ELECP that gives the monopole power for a very thin monopole. To run this, one needs to specify frequency and epsol (dielectric constant). As an alternative one may use subroutine MOMENT to calculate the fields and fill array FIELD for a monopole that is not electrically thin. This routine integrates Maxwell's equations over the current distribution to find the dissipated power. A flow chart of the input of heat source is given in Fig. E2 and E3.

As the program runs it prints out various parameters such as values of the independent variables as a function of time, the time steps, integration order, oil yield, etc. Sample output of the program is given later in this appendix. The program to determine electromagnetic field distribution around two coupled, phased monopole antennas is given on pages 311–320 of this appendix.

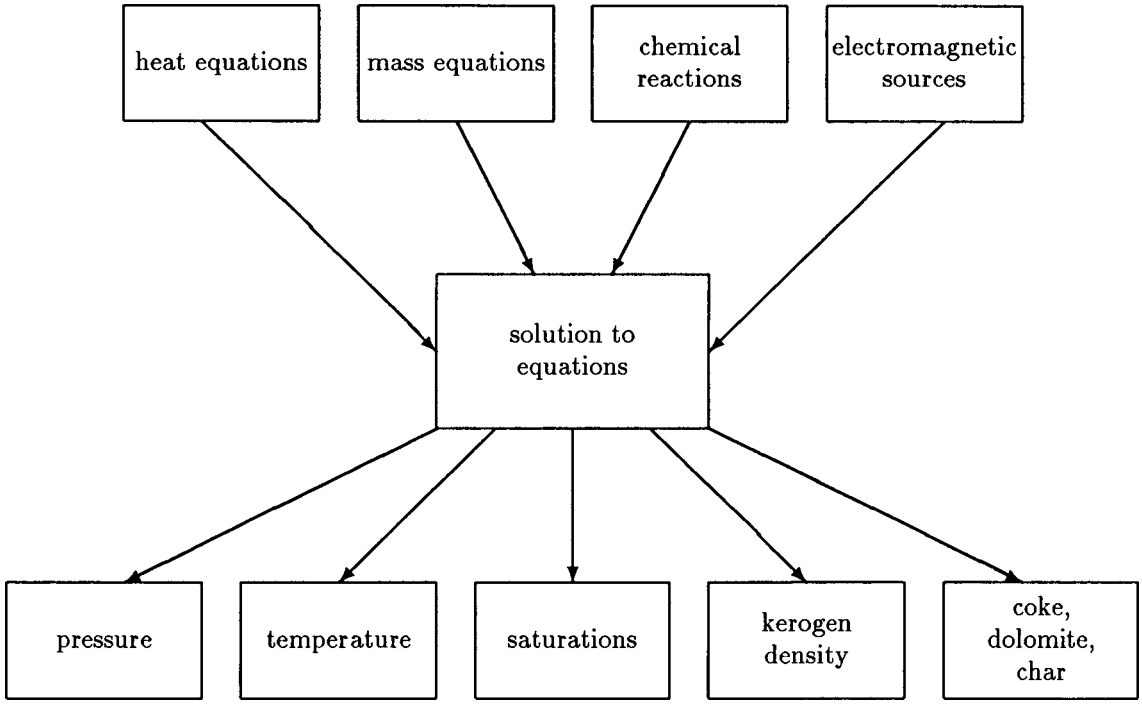

Figure E1. Flow chart of equations and output parameters.

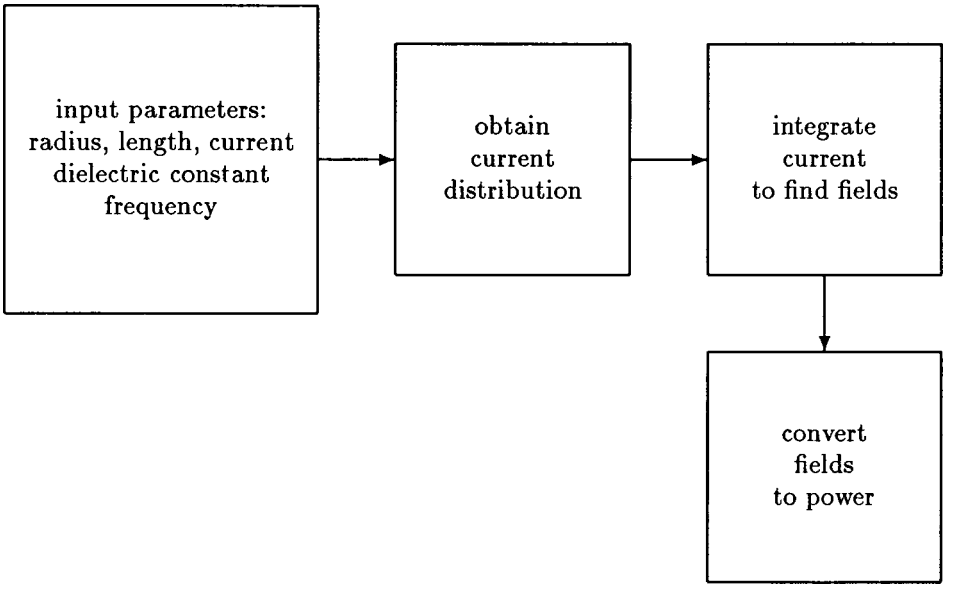

Figure E2. Program MOMENT.

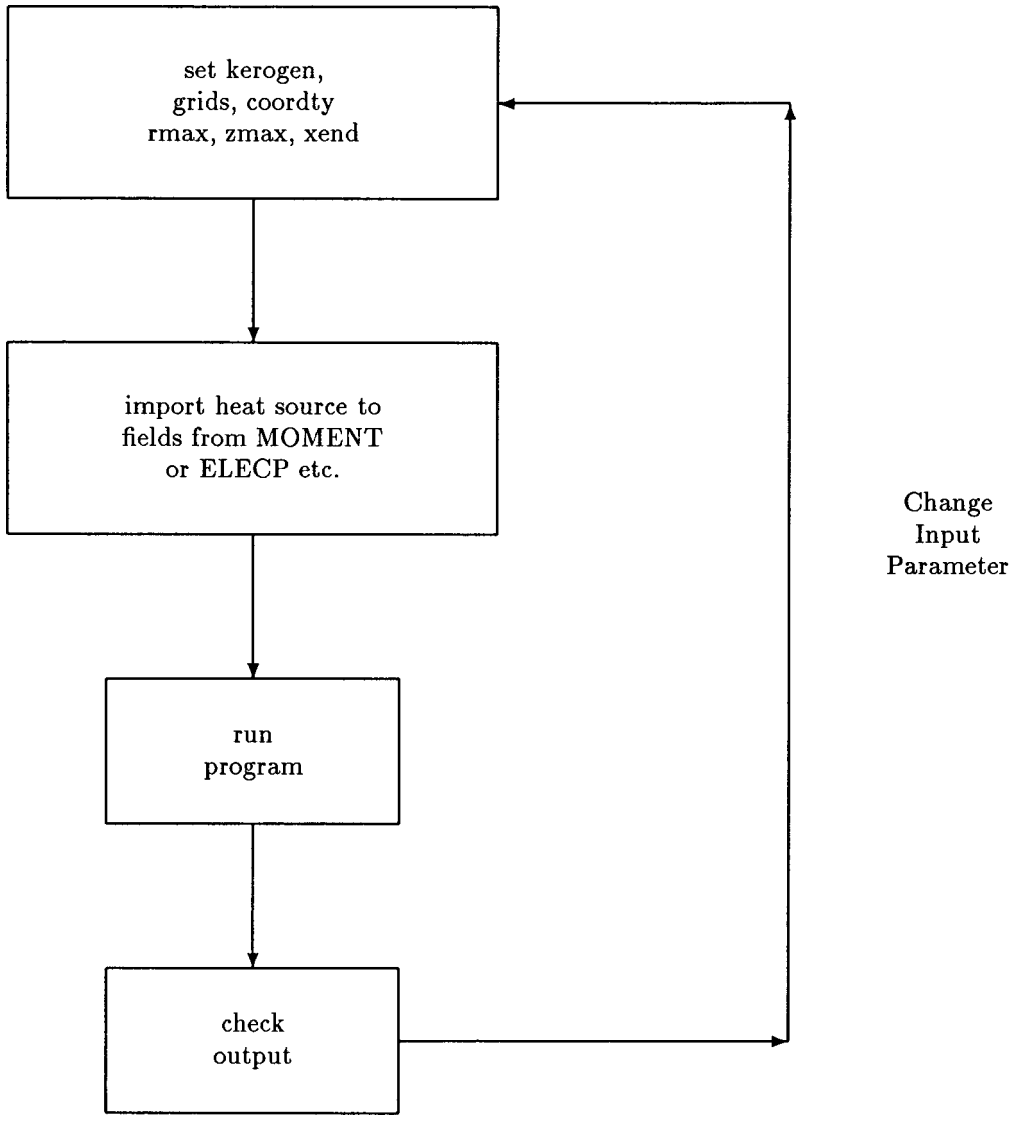

Figure E3. Program MOMENT.

krr	absolute permeability
soure	heat source
sourg	source of gases
kk,kmgco3,kcaco3	rate constants of kerogen, magnesium, calcium
delth	heats of reaction
upw,fx,tc	upstream weighting routines
vapor	vapor pressure of water
weigpar,per	weighting routine
xoilg	equilibrium constant for oil vapor
xkdt, xkdp	derivatives of xoilg w.r.t. t and p
densoil	density of oil
kcokel	rate constant of coking
elecp	power density for thin monopole
simp	complex integration routine
fields	subroutine for elecp
epower	power from fields dissipated
ay,by	routines for two dimensional intergation routine dblin
rresis	radiation resistance of antenna
coord	sets up grid for coordinates
setker	sets up kerogen concentration

Normal use of the program is depicted below:

cain	array of initial calcium carbonate composition (kg ca/cu m) shale
uca	array of $CaCo_3$ composition at time t
sg	array of gas saturations at grid points
pg	array of pressures at grid points
ol	array of light oil fraction at grid points
delt,deltz	arrays of dimensions of control volumes
rpts	array of r grid poitns as measured from well bore
vol	array of control volumes
tvol	total volume of retort
shdens	density of the shale
uktol	total kerogen
xi0	current on antenna (amps)
tcoke	total coke
coke	array of coke density
galton	shale grade

SUBROUTINES

The following is a summary of the subroutines:

velr,velz	velocities of oil and gas
cps,dcs	specific heat and derivative of specific with respect to temperature
ks	thermal conductivity of shale
kg	thermal conductivity of gas
vl,vg	viscosities of oil and gas
phi	porosity
perml,permg	permeability of liquid and gas

The routine also must evaluate the derivative of the differential equations with respect to the independent variables (temperature, pressure, kerogen density, gas saturation, light oil fraction). This is carried out in routine FCN.

VARIABLE DEFINITIONS

IMSL routine DEGEAR parameters:

H	last time step
tol	error tolerance
xend	time at first return
Idummy(6)	last order used in integration
Idummy(7)	cumulative number of time steps
T	time
Idummy(8)	number of Jacobians evaluated
y(i)	array containing independent variables at grid points
yprime(i)	array containing derivative of independent variable as a function of time

Main routine:

ukin	array of initial kerogen composition (kg ker/cu m shale)
uk	array of kerogen composition at time t
mgin	array of initial magnesium carbonate composition (kg mg/cu m shale)
umg	array of $mgco_3$ composition at time t

ROUTINE DGEAR [30]

In order to integrate the coupled system of ordinary differential equations produced after the spatial derivatives are discretized we use the IMSL package DGEAR. This routine operates on 1–12 integration orders and picks the best time step dynamically. The routine can either integrate "stiff" or "non-stiff" systems of equations. The present system is a "stiff system" of equations and for this case the DGEAR routine requires the evaluation of a Jacobian matrix. The Jacobian is evaluated in routine FCNJ.

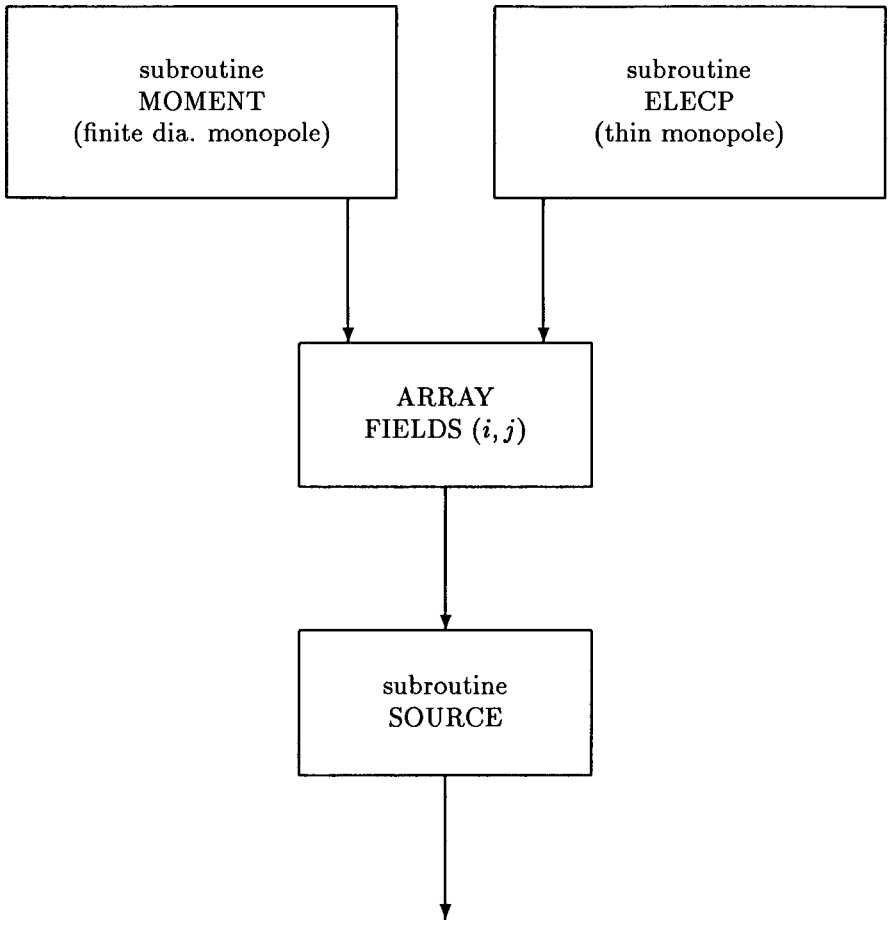

Figure E4. Flow Chart of Heat Source.

```
TOTAL VOLUME OF RETORT REGION(COORD=1,3,4) =.04236437693366
THE RADIAL GRID POINTS ARE
--------------------------
.01
.01974350485835
.03898059840916
.07096136340726
.1519487052336
.3
THE AXIAL GRID POINTS ARE
-------------------------
0.
.025
.05
.075
.1
.125
.15
THE DELTR ARE=
--------------
.00459512304566
.01422076523036
.0280767747415
.0553433938515
.1094449480823
.0782289950486
THE DELTZ ARE
-------------
.0125
.025
.025
.025
.025
.025
.0125
THE OUTER BOUNDARY OF CONTROL VOLUMES(RIP1)
-------------------------------------------
.01432363924376
.02827988409983
.05583440291186
.1102366805153
.2176458437323
.3
THE INNER BOUNDARY OF CONTROL VOLUMES ARE(RIM1)
-----------------------------------------------
.01
.01432363924376
.02827988409983
.05583440291186
.1102366805153
.2176458437323
NUMBER UPPER CODIAGONALS=39
NUMBER LOWER CODIAGONALS=39
FREQUENCY(HZ) =2.4E+9
MITER = -1
THE RADIATION RESISTANCE OF MONOPOLE(LOSSLESS) = 55.737796175
THE TOTAL RETORT VOLUME IS(CUBIC METERS) = .04236437693366
SHALE DENSITY IN KG./CUBIC METER = 2350.
SHALE GRADE IN GALLONS PER TON IS = 22.75777777778
PLANE WAVE POWER ATTENUATION (M)=.3444714582036
HEIGHT OF RETORT REGION(METERS)=.15
THE MAXIMUM RADIAL EXTENT OF RETORT = .3
DO YOU WISH TO CALCULATE THE TOTAL INPUT POWER?
IF YES ENTER 1, IF NO ENTER 2
```

```
*** WARNING WITH FIX ERROR  (IER =  66) FROM IMSL ROUTINE DBLIN
THE TOTAL INPUT POWER =2463.996874417
-----------------------------------------
POWER(W)/(CU M)AT GRID POINTS(J=1 ON BOTTOM OF BLOCK)
-----------------------------------------
 .100E+08  .100E+08  .100E+08  .100E+08  .100E+08  .100E+08  .100E+08
 .100E+08  .100E+08  .100E+08  .100E+08  .100E+08  .100E+08  .100E+08
 .100E+08  .100E+08  .100E+08  .100E+08  .100E+08  .100E+08  .100E+08
 .100E+08  .100E+08  .100E+08  .100E+08  .100E+08  .100E+08  .100E+08
 .100E+08  .100E+08  .100E+08  .100E+08  .100E+08  .100E+08  .100E+08
 .100E+08  .100E+08  .100E+08  .100E+08  .100E+08  .100E+08  .100E+08
DO YOU WHICH TO FIND POWER DISSIPATED IN SHALE BLOCK?
IF YES ENTER 1, IF NO ENTER 2
THE TOTAL POWER DISSIPATED IN SHALE BLOCK IS(W)423643.7693366
XIO=9.
*** WARNING WITH FIX ERROR  (IER =  67) FROM IMSL ROUTINE DGEAR
INPUT ENERGY (JOULES)=42364376.93366
TOTAL PRODUCED OIL (GALLONS) IS = .001072707628566
OIL EXTRACTED(SATURATION METHOD)=.00158755411627
UK=99.53830406279
POTENTIAL  OIL IN RESOURCE=2.808997796684
THE TOTAL OIL=.06074025900098
POROSITY=.01035008963791
VELOCITY(M/S) OF LIQUID OIL AT WELL BORE=.000031673115457 87
VELOCITY OF GAS(M/S) AT WELL BORE=.02783256936235
WATER DENSITY UWDMI(1,GRIDZ/2)=0.
THE LAST USED ORDER=  4
THE CUMULATIVE # STEPS= 37
THE CUMULATIVE # FCN EVALUATIONS= 89
MITER=-1
THE CUMULATIVE # JACOBIAN EVALUATIONS= 14
LAST STEP SIZE (SECONDS)=4.053927331023
TIME (CURENT TIME IN SECONDS) = 100.
ELAPSED TIME(SECONDS)=100.
ERROR TOLORANCE=.005
-----------------------------------------------
        THE TIME IN DAYS = .001157407407407
-----------------------------------------------
THE KEROGEN DENSITY(KG/CU. METER)
-----------------------------------------
 250.      250.      250.      250.      250.      250.      250.
 250.      250.      250.      250.      250.      250.      250.
 250.      250.      250.      250.      250.      250.      250.
 250.      250.      250.      250.      250.      250.      250.
 250.      250.      250.      250.      250.      250.      250.
 250.      250.      250.      250.      250.      250.      250.
THE LIGHT OIL GAS MOLE FRACTION
-----------------------------------------
 .324      .323      .323      .323      .323      .323      .324
 .325      .324      .324      .324      .324      .324      .325
 .325      .324      .324      .324      .324      .324      .324
 .325      .323      .323      .323      .323      .323      .324
 .324      .323      .323      .323      .323      .323      .324
 .326      .324      .324      .324      .324      .324      .325
-----------------------------------------
THE TEMPERATURES (KELVIN) AT THE GRID POINTS
-----------------------------------------
 673.      674.      674.      674.      674.      674.      673.
 677.      677.      677.      677.      677.      677.      677.
 677.      677.      677.      677.      677.      677.      677.
 677.      677.      677.      677.      677.      677.      677.
 677.      677.      677.      677.      677.      677.      677.
 676.      676.      676.      676.      676.      676.      676.
-----------------------------------------
```

THE GAS SATURATIONS AT THE GRID POINTS

.991	.991	.991	.991	.991	.991	.991
.991	.991	.991	.991	.991	.991	.991
.989	.989	.989	.989	.989	.989	.989
.987	.988	.988	.988	.988	.988	.987
.987	.987	.987	.987	.987	.987	.987
.986	.986	.986	.986	.986	.986	.986

THE PRESSURES AT THE GRID POINTS (N/SQ. M.)

.744E+06	.744E+06	.744E+06	.744E+06	.744E+06	.744E+06	.744E+06
.106E+07	.106E+07	.106E+07	.106E+07	.106E+07	.106E+07	.106E+07
.131E+07	.131E+07	.131E+07	.131E+07	.131E+07	.131E+07	.131E+07
.153E+07	.153E+07	.153E+07	.153E+07	.153E+07	.153E+07	.153E+07
.169E+07	.169E+07	.169E+07	.169E+07	.169E+07	.169E+07	.169E+07
.177E+07	.177E+07	.177E+07	.177E+07	.177E+07	.177E+07	.177E+07

THE CHAR CONCENTRATION (KG./CUBIC METER OF SHALE)

1.12	1.15	1.16	1.16	1.16	1.16	1.13
1.38	1.43	1.43	1.43	1.43	1.43	1.39
1.40	1.45	1.45	1.45	1.45	1.45	1.41
1.40	1.45	1.45	1.45	1.45	1.45	1.41
1.40	1.45	1.45	1.45	1.45	1.45	1.41
1.31	1.37	1.37	1.37	1.37	1.37	1.33

THE COKE CONCENTRATION (KG.)

.201E-40	.433E-40	.433E-40	.433E-40	.433E-40	.434E-40	.204E-40
.186E-39	.403E-39	.404E-39	.404E-39	.404E-39	.403E-39	.189E-39
.944E-39	.205E-38	.205E-38	.205E-38	.205E-38	.205E-38	.963E-39
.420E-38	.913E-38	.914E-38	.914E-38	.914E-38	.913E-38	.428E-38
.173E-37	.376E-37	.376E-37	.376E-37	.376E-37	.376E-37	.176E-37
.168E-37	.373E-37	.374E-37	.374E-37	.374E-37	.374E-37	.172E-37

THE DOLUMITE DENSITY(KG/CU. METER)

493.	493.	493.	493.	493.	493.	493.
493.	493.	493.	493.	493.	493.	493.
493.	493.	493.	493.	493.	493.	493.
493.	493.	493.	493.	493.	493.	493.
493.	493.	493.	493.	493.	493.	493.
493.	493.	493.	493.	493.	493.	493.

THE CALCIUM CARBONTAE(KG/CU. METER)

282.	282.	282.	282.	282.	282.	282.
282.	282.	282.	282.	282.	282.	282.
282.	282.	282.	282.	282.	282.	282.
282.	282.	282.	282.	282.	282.	282.
282.	282.	282.	282.	282.	282.	282.
282.	282.	282.	282.	282.	282.	282.

XIO=9.
INPUT ENERGY (JOULES)=2007730.291532
TOTAL PRODUCED OIL (GALLONS) IS = .001145636791878
OIL EXTRACTED(SATURATION METHOD)=.004444837721536
UK=199.05007608 7
POTENTIAL OIL IN RESOURCE=2.808997796684
THE TOTAL OIL=.06751160057
POROSITY=.01086723052249
VELOCITY(M/S) OF LIQUID OIL AT WELL BORE=.000004284082705519
VELOCITY OF GAS(M/S) AT WELL BORE=.05159137797401
WATER DENSITY UWOM1(1,GRIDZ/2)=0.
THE LAST USED ORDER= 4
THE CUMULATIVE # STEPS= 38

```
 copy,ushale
C  THIS PROGRAM MODELS THE TIME EVOLUTION OF OIL SHALE

C  AS IT IS HEATED.  THE MODEL IS TWO DIMENSIONAL IN
C  CYLINDERICAL COORDINATES (R, Z).  THE SHALE IS ORIGINALLY
C  ASSUMED TO CONSIST OF KEROGEN, CARBONATES, WATER, AND
C  INORGANICS.  AS THE SHALE HEATS THE VARIOUS COMPONENTS
C  DECOMPOSE TO FORM GASES, OIL, AND CHAR.
C*************************************************************
C
C
      PROGRAM OILSHAL(INPUT,OUTPUT,TAPE7,TAPE12,TAPE13,TAPE11,TAPE16,
     1 TAPE15,TAPE17)
      REAL Y(400),WK(44320),T,TOL,XEND,G,H,DUMMY,KRR
      REAL PERML,VL,ULI,PRODGAS,AZ,BZ,FIELD,DENSOIL
      REAL PM1,SM1(15,15),POTENT,TUK,ENERGY,KIM1,KO
      REAL FREQ,ATTEN,YYY(42),VGO,PC,PC1,PHI,OLM1(15,15)
      REAL VAPORP,UKTOL,UWTOL,TVOL,KCOKEL,KCHAR,OMEGA
      REAL RPTS,DELRAV,RIP1,RIM1,DENSS,TM1,HEIGHT,CPS
      REAL KKERO,KHYO,CHYO,KWO,CWO,CKO,CCARB,KCAC,KMGC,CGO
      REAL  KCOKEG,KK,TM2,KCARB,GALTON ,COKE(15,15)
      REAL DENSO,R,GMOLE,OMOLE,UWIN,UKIN,XFRAC,VOL,DENSW
      REAL DUWO,XTEMP,UMG,UCA,CARBDEN,XIO,QL,UGIM1(15),ULIM1(15)
      REAL MGIN,CAIN,UKM1(15,15),UMGM1(15,15),UCAM1(15,15)
      REAL DENSIN,UK(15,15),HI,PM2(15,15),ULIM2(15),UGIM2(15)
      REAL ULIM3(15),UGIM3(15)
      REAL DELTR,DELTZ,CLO,KLO,GALT,PERCW,HEXT,SDUMMY,SHDENS
      REAL CCC(3),AA(3,3),BB(3),WKA(1000),DDD(3,3),XTIME(5)
      INTEGER N,METH,INDEX,IWK(400),IER,IDUMMY,GRGZ
      INTEGER GRIDR,GRIDZ,MITER,NUC,NLC,NLCC,NUCC,FLAG,COORDTY
      COMPLEX EPSOL
      COMMON/ONE/UKIN(15,15),WKK,CCACO3,CMGCO3,CARBDEN(15,15)
      COMMON /ONEE/XIO,XMU,DIA,XLO
      COMMON/SIXX/EPSOL,OMEGA,XQL
      COMMON/TWO/DELTR(60),DELTZ(60),GRIDR,GRIDZ,G,SHDENS
      COMMON/THREE/XFRAC,UWIN,KKERO,KHYO,CHYO,KWO,CWO,CKO,KMGC,KCAC
      COMMON/FOUR/DENSO,R,GMOLE,OMOLE,CC,DENSW,XPERMZ
      COMMON/SIX/GRGZ,DUWO(15,15)
      COMMON/SEVEN/CHAR(15,15)
      COMMON/EIGHT/CLO,KLO,CGO,TOI
      COMMON/TEN/DENSS(15,15),MGIN(15,15),CAIN(15,15),DENSIN(15,15)
      COMMON/ELEVEN/DELRAV(60),RIP1(60),RIM1(60),VOL(50,50)
      COMMON/TWELVE/CCARB,KCARB
      COMMON/FOURT/UMG(15,15),UCA(15,15)
      COMMON/SEVENT/TT(15,15),PM1(15,15)
      COMMON/EIGTT/XWEL,HEXT,FREQ
      COMMON/TWENTTH/UWOM1(15,15)
      COMMON/TWENTF/HEIGHT,COORDTY,ZPTS(60),RPTS(60)
      COMMON/FIEL/FIELD(35,35),XP,XDBLIN
      COMMON/THITF/UKM1,UCAM1,UMGM1,XM1,XKM1(15,15)
      COMMON/GAL/GALTON
      COMMON/GEAR/DUMMY(48),SDUMMY(4),IDUMMY(38)
      COMMON/DBAND/NLC,NUC
      COMMON/TWENTT/NLCC,NUCC,NCP
      EXTERNAL FCN,FCNJ,AY,BY,EPOWER,RRESIS,AAY,BBY
C
C  NUMBER OF GRIDZ POINTS IN Z COORDINATE(GRIDZ) AND R COORDINATE
C  (GRIDR).  ALSO THE SIZE OF THE GRID BLOCKS (DELTZ,DELTR)
C  (IF COORDTY.EQ.2 OR 4)
C  THE RELATIVE ERROR IS GIVEN BY TOL IN THE DATA STATEMENT
C  (TOL IS GENERALLY .01 - .001).  THE INITIAL CONCENTRATION
C  OF BOUND WATER IN THE SHALE IS GIVEN BY UWIN.  THE FREQUENCY
C  OF THE APPLIED FIELDS IS GIVEN BY FREQ.
C  THE MAXIMUM RADIAL EXTENT OF THE RETORT IS GIVEN BY RMAX. XWEL
```

```
C  GIVES THE RADIUS OF THE WELL.
C  THE DIELECTRIC CONSTANT IS GIVEN BY EPSOL(COMPLEX), XQL IS THE NUMBER
C  OF QUARTER WAVELENGTHS IN THE ANTENNA, XIO IS THE CURRENT
C  THE INITIAL CONCENTRATION OF KEROGEN IN THE SHALE IS INPUT
C  BY SPECIFYING UKIN(I,J)
C
C*************************************************************
C   THE FOLLOWING PARAMTERS SHOULD BE SET BY THE USER
C
       ISKIP=2
       DATA GRIDR/6/,GRIDZ/7/,FREQ/2.4E9/,XPERMZ/1./
C  THE NUMBER OF TIMESTEPS PER PLOT IS INPUT IN IPLOTIT
      DATA IPLOTIT/20/
       DATA XIO/9./,XQL/14.5/
C   XEND IS THE TIME THAT DGEAR WILL FIRST RETURN SPECIFY
C   XEND IN SECONDS FROM START OF HEATING
       XEND=100.
        XDBLIN=1.
        TCOKE=0.0
       IORDER=2
       EPSOL=(3.,-.10)*8.85E-12
C
       DATA TOL/.0050/,UWIN/00./,XWEL/.01/,RMAX/.30/,NCP/5/,ZMAX/.15/
C
       DIA=XWEL
C
C   SET UP THE KEROGEN CONCENTRATIONS
C
       CALL SETKER(UKIN,GRIDR,GRIDZ)
C
C
C INITIAL VALUES ARE INPUT (PRESSURE,SATURATION,TEMPERATURE AND
C
       DO 10 I=1,GRIDR
       DO 1011 J=1,GRIDZ
C
C   INITIAL LIGHT OIL(GAS) MOLE FRACTION
C
          Y(NCP*J-4+NCP*(I-1)*GRIDZ)=.5*XKOILG(1,1,293.,1.E5,.3)
C
C     INITIAL KEROGEN
C
          Y(NCP*J-3+NCP*(I-1)*GRIDZ)=UKIN(I,J)
C
C  INITIAL TEMPERATURE
C
                TOI=295.
          Y(NCP*J-2+NCP*(I-1)*GRIDZ)=TOI
C
C  INITIAL SATURATION
C
          Y(NCP*J-1+NCP*(I-1)*GRIDZ)=.98
C
C  INITIAL PRESSURE
C
          Y(NCP*J+NCP*(I-1)*GRIDZ)=1.E5
C
          PM1(I,J)=Y(NCP*J+NCP*(I-1)*GRIDZ)/1.1
          UWOM1(I,J)=UWIN
          SM1(I,J)=Y(NCP*J-1+NCP*(I-1)*GRIDZ)
          PM2(I,J)=Y(NCP*J+NCP*(I-1)*GRIDZ)
          TT(I,J)=Y(NCP*J-2+NCP*(I-1)*GRIDZ)/1.1
          OLM1(I,J)=Y(NCP*J-4+NCP*(I-1)*GRIDZ)
C
 1011  CONTINUE
 10      CONTINUE
```

```
C
C
C  ENTER TYPE OF COORDINATES (1,3,OR 4 CYLINDRICAL, 2
C  (RECTANGULAR))
C  COORDTY .EQ. 1 OR 3 USES AN NON-UNIFORM GRID IN R COORDINATE
C
       COORDTY=3
C
       IF(COORDTY.EQ.1)PRINT*,'YOU ARE IN CYLINDRICAL COORDINATES'
       IF(COORDTY.EQ.2)PRINT*,'YOU ARE IN RECTANGULAR COODINATES'
C
C
C    IF COORDTY EQUALS 2 OR 4 THEN SPECIFY DELTR(I)
C
        DO 3 I=1,GRIDR
         DELTR(I)=(RMAX-XWEL)/FLOAT(GRIDR)
  3     CONTINUE
C
        DELTR(1)=DELTR(2)/2.
        DELTR(GRIDR)=DELTR(GRIDR-1)/2.
C
C    SET UP THE GRID SPACINGS (DELTR,DELTZ)
C
       DO 6 I=1,4*GRIDZ
        DELTZ(I)=ZMAX/(FLOAT(GRIDZ-1))
  6    CONTINUE
C
       DELTZ(1)=DELTZ(2)/2.
       DELTZ(GRIDZ)=DELTZ(GRIDZ-1)/2.
C
**********************************************************************
C
C   SET UP THE COORDINATE SYSTEM
C
       CALL COORD(RPTS,VOL,RIP1,RIM1,DELRAV,DELTR,ZPTS
     1  ,TOLVOL,HEIGHT,DELTZ,GRIDR,GRIDZ,COORDTY,XWEL,RMAX,UKIN,UWIN
     1 ,UKTOL,UWTOL)
C
       IF(COORDTY.EQ.1.OR.COORDTY.EQ.3.OR.COORDTY.EQ.4)THEN
        XPHI=2.*ACOS(-1.)
        SCALR=RPTS(1)
       ELSE
        XPHI=1.
        SCALR=1.
       ENDIF
C
C
C  THESE PARAMETERS IN THE FOLLOWING DATA STATEMENTS GENERALLY
C  DO NOT HAVE TO BE MODIFIED FOR EACH RUN.
C
       XMU=4.*ACOS(-1.)*1.E-7
       OMEGA=2.*ACOS(-1.)*FREQ
       XL0 = 2.*ACOS(-1.)/SQRT(OMEGA**2*REAL(EPSOL)*XMU)
       DATA ICOUNT/0/,PRODGAS/0.0/,PRODOL/0.0/
C
       DATA XKM1/225*0.0/,CHAR/225*0.0/,DUW0/225*0.0/,COKE/225*0.0/
       DATA TT/225*0./,CARBDEN/225*0./
       DATA R/8314./,GMOLE/25./,DENSO/1000./,CL0/1500./,DENSW/1000./
       DATA KL0/.20/,XFRAC/0.0/,G/9.8/,ENERGY/0.0/,XENERL0/0.0/
       DATA OMOLE/200./
       DATA CG0/1000./
       DATA ULIM1/15*0.0/,UGIM1/15*0.0/,ULIM2/15*0./,UGIM2/15*0./
       DATA CCACO3/1000./,CMGCO3/1000./
       DATA KKER0/.15/,KHY0/2./,KW0/.04/,CW0/4190./
       DATA CCARB/800./,KCARB/2./
       DATA CHY0/1000./.CK0/1200./.KMGC/1.1/.KCAC/1.1/
```

```
C
C    INPUT FOR IMSL ROUTINE DGEAR
C
      DATA T/.002/,H/10.0/,METH/2/,MITER/-1/,INDEX/1/
      DATA HEXT/6./,FLAG/1/
C
C   CALL ELECP TO CALCULATE POWER ARRAY (FIELD(GRIDR,GRIDZ)
C
      CALL ELECP(FREQ,XQL,XIO,GRIDR,GRIDZ,FIELD)
C
C  THE NUMBER OF UPPER (NUC,NUCC) AND LOWER (NLC, NLCC) CODIAGONALS
C  ARE FIXED
C
      NUC=(GRIDZ+1)*NCP-1
      NLC=NUC
      NUCC=NUC
      NLCC=NLC
C
C
C      PRINT VARIOUS INPUT PARAMTERS
C
      PRINT*,'NUMBER UPPER CODIAGONALS=',NUC
      PRINT*,'NUMBER LOWER CODIAGONALS=',NLC
      PRINT*,'FREQUENCY(HZ) =',FREQ
      PRINT*,'MITER = ',MITER
C
      PRINT*,'THE RADIATION RESISTANCE OF MONOPOLE(LOSSLESS) = ',
     1       DCADRE(RRESIS,0.000,.999,.001,.001,ERROR,IER)
     1    +  DCADRE(RRESIS,-.999,0.00,.001,.001,ERROR,IER)
C
C
C    GRGZ IS THE PRODUCT OF NUMBER OF GRID POINTS
C
      GRGZ=GRIDR*GRIDZ
C
      WRITE(15,3088) GRIDR
      WRITE(15,3088)GRIDZ
 3088 FORMAT(I4)
      WRITE(14,3041) IPLOTIT
 3041   FORMAT(I2)
C
C
C
C
C
C
C
C
C
C
      TVOL=0.0
      IF(COORDTY.EQ.1.OR.COORDTY.EQ.3.OR.COORDTY.EQ.4)THEN
C
C
        TVOL=ACOS(-1.)*(RIP1(GRIDR)**2-RPTS(1)**2)*HEIGHT
C
C
C
        PRINT*,'THE TOTAL RETORT VOLUME IS(CUBIC METERS) = ',TVOL
C
        SHDENS=(UKTOL+UWTOL+(1.-(UKTOL/1000.+UWTOL/1000.)/TVOL)*2800.
     1   *TVOL)/TVOL
C
      ELSE IF(COORDTY.EQ.2)THEN
C
        TVOL=((RMAX-RPTS(1))*HEIGHT)
C
```

```
        SHDENS=(UKTOL+UWTOL+(1.-(UKTOL/1000.+UWTOL/1000.)/TVOL)*2800.
     1   *TVOL)/TVOL
C
      ENDIF
C
      PRINT*,'SHALE DENSITY IN KG./CUBIC METER = ',SHDENS
C
C
      GALTON=-(SHDENS/1000.-2.616)/(.9/77.)
C
C   SET UP DENSITIES OF INORGANICS
C
      PRINT*,'SHALE GRADE IN GALLONS PER TON IS = ',GALTON
C
      DO 412 I=1,GRIDR
       DO 411 J=1,GRIDZ
        MGIN(I,J)=.21*SHDENS
        CAIN(I,J)=.12*SHDENS
        DENSS(I,J)=SHDENS-UKIN(I,J)-UWIN-MGIN(I,J)-CAIN(I,J)
        DENSIN(I,J)=DENSS(I,J)
 411    CONTINUE
 412   CONTINUE
C
      N=GRGZ*NCP
C
C
C
C
      XM1=1.E-20
     XM2=1.E-21
      XM3=1.E-50
      TM2=0.0
C
      TMASS=0.0
      DO 21 I=1,GRIDR
      DO 22 J=1,GRIDZ
       UK(I,J)=UKIN(I,J)
       UKM1(I,J)=UK(I,J)
       UCA(I,J)=CAIN(I,J)
       UCAM1(I,J)=UCA(I,J)
       UMG(I,J)=MGIN(I,J)
       UMGM1(I,J)=UMG(I,J)
       TMASS=TMASS + (DENSS(I,J)+UKIN(I,J)+UMG(I,J)+ UCA(I,J))
     1 *VOL(I,J)*XPHI
 22    CONTINUE
 21    CONTINUE
C
C
C    PRINT ATTENUATION LENGHTS AND HEIGHT OF RETORT AND RMAX
C
      PRINT*,'PLANE WAVE POWER ATTENUATION (M)=',ATTEN(OMEGA,XMU,EPSOL)
      PRINT*,'HEIGHT OF RETORT REGION(METERS)=',HEIGHT
      PRINT*,'THE MAXIMUM RADIAL EXTENT OF RETORT = ',RMAX
C
C
      PRINT*,'DO YOU WISH TO CALCULATE THE TOTAL INPUT POWER?'
      PRINT*,'IF YES ENTER 1, IF NO ENTER 2'
      READ*,ITYPE
      IF(ITYPE.EQ.1)THEN
      XP=0.0
      DO 7311 IX=1,GRIDR*2
       DO 7222 JX=1,3*GRIDZ
         XP=FIELD(IX,JX)*2.*ACOS(-1.)*VOL(IX,JX)+XP
 7222  CONTINUE
 7311  CONTINUE
      XPP=DBLIN(EPOWER,XWEL,20.*RMAX,AAY,BBY,1.E-3,ERROR,IER)
```

```
C
      PRINT*,'THE TOTAL INPUT POWER =',XPP
      ENDIF
      XENDM1=0.0
C
      FLAG=1
C
C   THE TOTAL POTENTIAL KEROGEN IN THE SHALE IS CALCULATED
C
      POTENT=0.0
      IF(COORDTY.EQ.1.OR.COORDTY.EQ.3.OR.COORDTY.EQ.4)THEN
C
       DO 804  J=1,GRIDZ
        POTENT=POTENT+(RMAX**2-RPTS(1)**2)*ACOS(-1.)
     1   *DELTZ(J)*2.204/8.31*UKIN(1,J)
 804    CONTINUE
C
      ELSE IF(COORDTY.EQ.2)THEN
C
       DO 814  J=1,GRIDZ
        POTENT=POTENT+(RMAX-RPTS(1))
     1   *DELTZ(J)*2.204/8.31*UKIN(1,J)
 814    CONTINUE
C
      ENDIF
C
C
C
C
      IC=1
      DO 2066 II=1,GRIDR
       DO 9887 JJ=1,GRIDZ
       YYY(IC)=FIELD(II,JJ)
       IC=IC+1
 9887   CONTINUE
 2066  CONTINUE
C
      PRINT*,'----------------------------------------'
      PRINT*,'POWER(W)/(CU M)AT GRID POINTS(J=1 ON BOTTOM OF BLOCK)'
      PRINT*,'----------------------------------------'
      PRINT 99,YYY
C
C
      PRINT*,'DO YOU WHICH TO FIND POWER DISSIPATED IN SHALE BLOCK?'
      PRINT*,'IF YES ENTER 1, IF NO ENTER 2'
C
      READ*,ITYPE
C
      IF(ITYPE.EQ.1)THEN
      XP=0.0
      DO 7211 IX=1,GRIDR
       DO 6222 JX=1,GRIDZ
         XP=FIELD(IX,JX)*2.*ACOS(-1.)*VOL(IX,JX)+XP
 6222  CONTINUE
 7211  CONTINUE
C
      PRINT*,'THE TOTAL POWER DISSIPATED IN SHALE BLOCK IS(W)',
     1  XP
      ENDIF
C
        XSUBST=0.0
      DO 40 III=1,5
C
C
      WRITE(13,708) T
 708   FORMAT(E12.5)
```

```
C
        PRINT*,'XIO=',XIO
       IF(ICOUNT.EQ.21)THEN
        ICOUNT=1
        PRINT*,'IF YOU WISH TO TERMINATE ENTER,1 IF NOT ENTER,2'
C
        READ*,ITYPE
C
        IF(ITYPE.EQ.1)THEN
        PRINT*,'DO YOU REALLY WISH TO END? IF SO ENTER,1 IF NOT ENTER,2'
        READ*,ITYPE
        IF(ITYPE.EQ.1)GO TO 41
        ENDIF
C
       ENDIF
C
C  CALL SUBROUTINE DGEAR TO INTEGRATE EQUATIONS,N IS NUMBER OF
C  EQUATIONS, FCN IS THE SUBBROUTINE WHICH CALCULATES THE
C  PARTIAL DERIVATIVES FOR NEWTONS ITERATION, T IS THE STARTING
C  TIME, H IS THE STEP SIZED USED, XEND IS THE TIME AT WHICH
C  SOLUTION IS DESIRED, TOL IS THE ERROR TOLORANCE. FOR A
C  DESCRIPTION OF DGEAR SEE IMSL INFORMATION.
C
       IF(III.EQ.2)XEND=1.E10
C
       CALL DGEAR(N,FCN,FCNJ,T,H,Y,XEND,TOL,METH,MITER,INDEX,
     1 IWK,WK,IER)
C
       INDEX=3
C
C   THE TOTAL INPUT ENERGY IS CALCULAFTERED AFTER EACH CALL OF DGEAR
C
       XP=0.0
       DO 4112 I=1,GRIDR
        DO 8112 J=1,GRIDZ
         XP=XP+FIELD(I,J)*VOL(I,J)*XPHI*(T-XM1)
 8112    CONTINUE
 4112  CONTINUE
C
       PRINT*,'INPUT ENERGY (JOULES)=',XP
C
C
C
C  THE TOTAL ENERGY DISSIPATED OUTSIDE OF BLOCK IS CALCULATED
C
C
C
       TCHAR=0.0
C
       DO 104 I=1,GRIDR
       DO 105 J=1,GRIDZ
C
         TT(I,J)=Y(NCP*J-2 +NCP*(I-1)*GRIDZ)
C
         PM2(I,J)=PM1(I,J)
C
        UKM1(I,J)=Y(NCP*J-3+NCP*(I-1)*GRIDZ)
       UK(I,J)=Y(NCP*J-3+NCP*(I-1)*GRIDZ)
         XUK=KK(TT(I,J))*UKM1(I,J)*.6585
         PM1(I,J)=Y(NCP*J+NCP*(I-1)*GRIDZ)
C
         SM1(I,J)=Y(NCP*J-1+NCP*(I-1)*GRIDZ)
C
         XKM1(I,J)=XKOILG(I,J,TT(I,J),PM1(I,J),SM1(I,J))
C
         IF(OLM1(I,J).GT..98.OR.OLM1(I,J).LT.
```

```
     1 0.)THEN
           PRINT*,'YOIL NOT IN RANGE',OLM1(I,J)
          ENDIF
C
C
C
C
C       CALCULATE TOTAL CHAR PRODUCED UP TO THIS TIME
          XKOGO=XKOILG(I,J,TT(I,J),PM1(I,J),SM1(I,J))
          WMOLE=(1.-OLM1(I,J))*GMOLE+OLM1(I,J)*OMOLE
C
          COKE(I,J)=VOL(I,J)*XPHI*(T-XM1)*(
     1    PHI(TT(I,J),UK(I,J),UMG(I,J),UCA(I,J),I,J)
     1      *(.75*KCOKEL(TT(I,J))*(1.-SM1(I,J))*DENSOIL(PM1(I,J))
     1      + .31*KCOKEG(TT(I,J))*SM1(I,J)*OLM1(I,J)*OMOLE
     1      *PM1(I,J)/R/TT(I,J))) + COKE(I,J)
C
          TCOKE=VOL(I,J)*XPHI*(T-XM1)*(
     1    PHI(TT(I,J),UK(I,J),UMG(I,J),UCA(I,J),I,J)
     1      *(KCOKEL(TT(I,J))*(1.-SM1(I,J))*DENSOIL(PM1(I,J))
     1      + KCOKEG(TT(I,J))*SM1(I,J)*OLM1(I,J)*OMOLE
     1      *PM1(I,J)/R/TT(I,J))) + TCOKE
C
          CHAR(I,J)=(T-XM1)*(
     1    PHI(TT(I,J),UK(I,J),UMG(I,J),UCA(I,J),I,J)
     1      *(.75*KCOKEL(TT(I,J))*(1.-SM1(I,J))*DENSOIL(PM1(I,J))
     1      + .31*KCOKEG(TT(I,J))*SM1(I,J)*OLM1(I,J)*OMOLE
     1      *PM1(I,J)/R/TT(I,J))) + .1710*KK(TT(I,J))*UK(I,J)
     2 *(T-XM1) + CHAR(I,J)
C
          TCHAR=TCHAR+CHAR(I,J)*VOL(I,J)*XPHI
          TUK=TUK+(UMG(I,J)+UCA(I,J)+UK(I,J)+DENSS(I,J))*VOL(I,J)
     1 *XPHI
C
C
          UMGM1(I,J)=UMG(I,J)
          UCAM1(I,J)=UCA(I,J)
C
C
C
 105    CONTINUE
 104    CONTINUE
C
C
C
C
C
         DO 746 J=1,GRIDZ
C
          XKOGO=XKOILG(1,J,TT(1,J),PM1(1,J),SM1(1,J))
          WMOLE=(1.-OLM1(1,J))*GMOLE+OLM1(1,J)*OMOLE
          PC1=PC(1,J,1.-SM1(1,J))
        KO=KRR(TT(1,J),UK(1,J),UMG(1,J),UCA(1,J),1,J)
        KIM1=WEIGPAR(KRR(TT(1,J),UK(1,J),UMG(1,J),UCA(1,J),1,J),KO,1,2)
          ULI=KIM1*PERML(1.-
     1    SM1(1,J))/VL(TT(1,J))*MAX(((PM1(1,J)-PC1)-1.E5),0.)
     1 /((RPTS(2)-RPTS(1)))
C
          UGI=KIM1*PERMG(1.-
     1    SM1(1,J))/VG(TT(1,J))*MAX((PM1(1,J)-1.E5),0.)
     1 /((RPTS(2)-RPTS(1)))
C
          PHO=PHI(TT(1,J),UK(1,J),UMG(1,J),UCA(1,J),1,J)
          PRODGAS= PRODGAS+ XPHI*SCALR*DELTZ(J)*GMOLE*
     1    PM1(2,J)/R/TT(2,J)*(UGI*(T-XM1))*(1.-OLM1(2,J))
          PRODOL= PRODOL+ XPHI*SCALR*DELTZ(J)*(DENSOIL(PM1(1,J))
```

```
     1 *(ULI)*(T-XM1)+
     1   UGI*(T-XM1)*OMOLE*OLM1(2,J)*PM1(2,J)/R/TT(2,J))*
     1   2.204/8.310
C
       UGIM2(J)=UGIM1(J)
       ULIM2(J)=ULIM1(J)
         UGIM1(J)=UGI
         ULIM1(J)=ULI
 746    CONTINUE
C
C
       PRINT*,'TOTAL PRODUCED OIL (GALLONS) IS = ',PRODOL
C
C  THE % OF THE TOTAL OIL PRODUCED
C
C
       XOIL=0.0
       XGAS=0.0
       DO 5677 I=1,GRIDR
        DO 5678 J=1,GRIDZ
C
         XKOGO=XKOILG(I,J,TT(I,J),PM1(I,J),SM1(I,J))
         WMOLE=(1.-OLM1(I,J))*GMOLE+OLM1(I,J)*OMOLE
C
         PHO=PHI(TT(I,J),UK(I,J),UMG(I,J),UCA(I,J),I,J)
C
         XOIL=XOIL+ PHI(TT(I,J),UK(I,J),UMG(I,J),UCA(I,J),I
     1   ,J)*VOL(I,J)*XPHI*2.204/8.31
     1   *((1.-SM1(I,J))*DENSOIL(PM1(I,J))+SM1(I,J)*OMOLE*OLM1(I,J)
     1 *PM1(I,J)/R/TT(I,J))
C
        XGAS=XGAS+VOL(I,J)*XPHI*PHO*SM1(I,J)*GMOLE*(1.-OLM1(I,J))
     1       *PM1(I,J)/R/TT(I,J)
 5678   CONTINUE
 5677  CONTINUE
        IF(III.EQ.1)XOILN1=XOIL+XGAS
C
       XOIL2=0.0
C
       DO 987 I=1,GRIDR
        DO  988 J=1,GRIDZ
          XOIL2 = XOIL2 + MAX(0.0,UK(I,J))*VOL(I,J)*XPHI*2.204/8.31
     1  *.6585
 988    CONTINUE
 987   CONTINUE
C
       XOIL2 = XOIL +XOIL2 +TCOKE*2.204/8.31
C
       XXXOIL = POTENT*.6585-XOIL2 -XSUBST
         IF(III.EQ.1)THEN
             XSUBST=XXXOIL
         ENDIF
C
       PRINT*,'OIL EXTRACTED(SATURATION METHOD)=',MAX(XXXOIL,0.)
C
        WRITE(11,607) MAX(0.0,XXXOIL)
C
 607    FORMAT(E12.5)
C
C
        PRINT*,'UK=',TUK
        PRINT*,'POTENTIAL  OIL IN RESOURCE=',POTENT
       DO 8111 I=1,GRIDR
        DO 9111 J=1,GRIDZ
          XTO=XTO+KK(TT(I,J))*UK(I,J)*(T-XM1)*VOL(I,J)*.6585*XPHI
     1 *2.204/8.31
```

```
 9111   CONTINUE
 8111   CONTINUE
        PRINT*,'THE TOTAL OIL=',XTO
C
       PRINT*,'POROSITY=',PHI(TT(1,GRIDZ/2),UK(1,GRIDZ/2),
     1 UMG(1,GRIDZ/2),UCA(1,GRIDZ/2),1,GRIDZ/2)
C
C      PRINT THE OIL VELOCITY AT THE WELL BORE
C
       PRINT*,'VELOCITY(M/S) OF LIQUID OIL AT WELL BORE=',(PM1(2,GRIDZ/2
     1 )-1.E5)*PERML(1.-
     2 SM1(1,GRIDZ/2))/VL(TT(1,GRIDZ/2))*KRR(TT(1,GRIDZ/2)
     2 ,UK(1,GRIDZ/2),UMG(1,GRIDZ/2),UCA(1,GRIDZ/2),1,GRIDZ/2)
     3 /2./(RPTS(2)-RPTS(1))
C
       PRINT*,'VELOCITY OF GAS(M/S) AT WELL BORE=',(PM1(1,GRIDZ/2)-1.E5)
     1 *PERMG(1.-
     2 SM1(1,GRIDZ/2))/VG(TT(1,GRIDZ/2))/DELTR(1)*KRR(TT(1,GRIDZ/2)
     2 ,UK(1,GRIDZ/2),UMG(1,GRIDZ/2),UCA(1,GRIDZ/2),1,GRIDZ/2)
C
C
C  PRINT OUTPUT AT VARIOUS TIMES
C
       PRINT*,'WATER DENSITY UWOM1(1,GRIDZ/2)=',MAX(0.,UWOM1(1,GRIDZ/2))
       PRINT*,'THE LAST USED ORDER=  ',IDUMMY(6)
       PRINT*,'THE CUMULATIVE # STEPS= ',IDUMMY(7)
       PRINT*,'THE CUMULATIVE # FCN EVALUATIONS= ',IDUMMY(8)
       PRINT*,'MITER=',MITER
       PRINT*,'THE CUMULATIVE # JACOBIAN EVALUATIONS= ',IDUMMY(9)
       PRINT*,'LAST STEP SIZE (SECONDS)=',H
       PRINT*,'TIME (CURENT TIME IN SECONDS) = ',T
       PRINT*,'ELAPSED TIME(SECONDS)=',T
       PRINT*,'ERROR TOLORANCE=',TOL
C
       IC=1
       DO 1234 II=1,GRIDR
        DO 2897 JJ=1,GRIDZ
         YYY(IC)=  Y(NCP*JJ-3+NCP*(II-1)*GRIDZ)
         IC=IC+1
 2897   CONTINUE
 1234  CONTINUE
C
       PRINT*,'-----------------------------------------------'
       PRINT*,'        THE TIME IN DAYS = ',T/3600./24.
       PRINT*,'-----------------------------------------------'
       PRINT*,'THE KEROGEN DENSITY(KG/CU. METER)'
       PRINT*,'--------------------------------------'
       PRINT 99,YYY
C
       IC=1
       DO 566 II=1,GRIDR
        DO 5558 JJ=1,GRIDZ
         YYY(IC)=  Y(NCP*JJ-4+NCP*(II-1)*GRIDZ)
         IC=IC+1
 5558   CONTINUE
  566  CONTINUE
C
       PRINT*,'THE LIGHT OIL GAS MOLE FRACTION'
       PRINT*,'--------------------------------------'
       PRINT 99,YYY
C
 5676  CONTINUE
       IC=1
       DO 466 II=1,GRIDR
        DO 4558 JJ=1,GRIDZ
         YYY(IC)=  Y(NCP*JJ-2+NCP*(II-1)*GRIDZ)
```

```
        IC=IC+1
 4558   CONTINUE
  466  CONTINUE
C
      PRINT*,'----------------------------------------'
      PRINT*,'THE TEMPERATURES (KELVIN) AT THE GRID POINTS'
      PRINT*,'----------------------------------------'
      PRINT 99,YYY
 99   FORMAT(7G10.3)
C
 5666   IF(ISKIP.EQ.1)GO TO 7111
      IC=1
      DO 4033 II=1,GRIDR
       DO 4222 JJ=1,GRIDZ
       YYY(IC)= Y(NCP*JJ-1+NCP*(II-1)*GRIDZ)
       IC=IC+1
 4222   CONTINUE
 4033  CONTINUE
C
      PRINT*,'-------------------------------------'
      PRINT*,'THE GAS SATURATIONS AT THE GRID POINTS'
      PRINT*,'-------------------------------------'
      PRINT 99,YYY
C
      IC=1
      DO 5066 II=1,GRIDR
       DO 4229 JJ=1,GRIDZ
       YYY(IC)=Y(NCP*JJ+NCP*(II-1)*GRIDZ)
       IC=IC+1
 4229   CONTINUE
 5066  CONTINUE
C
      PRINT*,'----------------------------------------'
      PRINT*,'THE PRESSURES AT THE GRID POINTS (N/SQ. M.)'
      PRINT*,'----------------------------------------'
      PRINT 99,YYY
C
      IC=1
      DO 6788 II=1,GRIDR
       DO 6557 JJ=1,GRIDZ
       YYY(IC)=CHAR(II,JJ)
       IC=IC+1
 6557   CONTINUE
 6788  CONTINUE
C
      PRINT*,'----------------------------------------'
      PRINT*,'THE CHAR CONCENTRATION (KG./CUBIC METER OF SHALE)'
      PRINT*,'----------------------------------------'
      PRINT 99,YYY
C
      IC=1
      DO 3788 II=1,GRIDR
       DO 3557 JJ=1,GRIDZ
       YYY(IC)=COKE(II,JJ)
       IC=IC+1
 3557   CONTINUE
 3788  CONTINUE
C
      PRINT*,'----------------------------------------'
      PRINT*,'THE COKE CONCENTRATION (KG.)'
      PRINT*,'----------------------------------------'
      PRINT 99,YYY
C
      IC=1
      DO 7643 II=1,GRIDR
       DO 8415 JJ=1,GRIDZ
```

```
         YYY(IC)=  UMG(II,JJ)
         IC=IC+1
 8415   CONTINUE
 7643   CONTINUE
C
       PRINT*,'THE DOLOMITE DENSITY(KG/CU. METER)'
       PRINT*,'-------------------------------------'
       PRINT 99,YYY
C
       IC=1
       DO 7322 II=1,GRIDR
        DO 7321 JJ=1,GRIDZ
         YYY(IC)=  UCA(II,JJ)
         IC=IC+1
 7321   CONTINUE
 7322   CONTINUE
C
       PRINT*,'THE CALCIUM CARBONTAE(KG/CU. METER)'
       PRINT*,'-------------------------------------'
       PRINT 99,YYY
C
 7111    CONTINUE
C
       DO 6038 II=1,GRIDR
        DO 8229 JJ=1,GRIDZ
          WRITE(7,500) Y(NCP*JJ-4+NCP*(II-1)*GRIDZ)
 8229   CONTINUE
 6038  CONTINUE
C
       DO 93 II=1,GRIDR
        DO 933 JJ=1,GRIDZ
         WRITE(7,500) Y(NCP*JJ-3+NCP*(II-1)*GRIDZ)
 933    CONTINUE
  93   CONTINUE
C
       DO 43 II=1,GRIDR
        DO 433 JJ=1,GRIDZ
         WRITE(7,99) Y(NCP*JJ-2+NCP*(II-1)*GRIDZ)
 500     FORMAT(E15.5)
 433    CONTINUE
  43   CONTINUE
C
       DO 3033 II=1,GRIDR
        DO 3222 JJ=1,GRIDZ
         WRITE(7,500) Y(NCP*JJ-1+NCP*(II-1)*GRIDZ)
 3222   CONTINUE
 3033  CONTINUE
C
       DO 3038 II=1,GRIDR
        DO 3229 JJ=1,GRIDZ
          WRITE(7,500) Y(NCP*JJ+NCP*(II-1)*GRIDZ)
 3229   CONTINUE
 3038  CONTINUE
C
C
       DO 4677 I=1,GRIDR
         DO 4678 J=1,GRIDZ
          WRITE(7,500) CHAR(I,J)
C
 4678    CONTINUE
 4677  CONTINUE
C
       XM3=XM2
       XM2=XM1
        XM1=T
C
```

```
      ICOUNT=ICOUNT+1
 40   CONTINUE
C
 41    WRITE(12,608) III
 608   FORMAT(I4)
      STOP
      END
C
*****************************************************************************
*****************************************************************************
*****************************************************************************
      SUBROUTINE FCN(N,TI,Y,YPRIME)
      REAL VOL,GMOLE,OMOLE,R,DENSO,DENSS,TI,QRM1,QRP1,QZP1,QZM1,DENSW
      REAL KIP1,KIM1,KJP1,KJM1,KO,PM1,DDENSO,DENSOIL,KCOKEL,KCOKEG
      REAL UKIP1,UKIM1,UKJP1,UKJM1,WEIGPAR,WEIGPER,UKM1(15,15)
      REAL WKA(50),AMAT(4,4),BMAT(4)
      REAL VSLIP1,VSLIM1,VSLJP1,VSLJM1
      REAL  XA,XB,XC,XD,XF,XG,XH,XK,VLO,VGO,SOUROG
      REAL FEL,FEG,FWL,FWG,FNL,FNG,FSL,FSG
      REAL MGRRO,MLRRO,YO(15,15),UMGM1(15,15),UCAM1(15,15)
      REAL RIM1,RIP1,UW
      REAL KSIM1,KSIP1,KSJP1,KSJM1,OL(15,15)
      REAL YT,XT,KCAC,KMGC,DUWO,SHDENS
      REAL KMGCO3,KCACO3
      REAL PERML,PERMG,UWO
      REAL MGO,MGZO,MLZO,FX,TC,TCLJM1,COKE
      REAL TCGIM1,TCGIP1,TCLIM1,TCLIP1,TCGJP1,TCLJP1,TCGJM1
      REAL T(15,15),PG(15,15),SG(15,15),UK(15,15),PL(15,15)
      REAL PLIM1,PLIP1,PLJP1,PLJM1,SGIM1,SGIP1,SGJP1,SGJM1
      REAL UKO,DELTZ,DELTR,DELRAV,KKERO,KHYO,KWO,CWO,CHYO
      REAL MGRM1,MGRP1,MGZP1,MGZM1,MLRM1,MLRP1,MLZP1,MLZM1
      REAL MLO,UKIN,CGO,CSO,KMG,KCA
      REAL PGO,PGIM1,PGIP1
      REAL PGJP1,PGJM1,TO,TIM1,TIP1,TJP1,TJM1,KKTO
      REAL VELR,VELZ,KS,PHI,SOURE,KRR,PC
      REAL VGRM1,VGRP1,VGZP1,VGZM1,VLRM1,VLRP1,VLZP1,VLZM1
      REAL UCA,UMG,CCACO3,CMGCO3,CARBDEN,FREQ
      REAL UPW,KCARB,CCARB,DPGT
      REAL SOURG,KK,DELTH
      REAL Y(N),YPRIME(N),RPTS,G,DENSIN,KLO,CLO,HEXT,CC,MGIN,CAIN
      INTEGER MAIM1,MIIP1,MAJM1,MIJP1,GRIDR,GRIDZ,N,GRGZ
      INTEGER COORDTY
      COMMON/ONE/UKIN(15,15),WKK,CCACO3,CMGCO3,CARBDEN(15,15)
      COMMON/TWO/DELTR(60),DELTZ(60),GRIDR,GRIDZ,G,SHDENS
      COMMON/THREE/XFRAC,UWIN,KKERO,KHYO,CHYO,KWO,CWO,CKO,KMGC,KCAC
      COMMON/FOUR/DENSO,R,GMOLE,OMOLE,CC,DENSW,XPERMZ
      COMMON/SIX/GRGZ,DUWO(15,15)
      COMMON/SEVEN/CHAR(15,15)
      COMMON/EIGHT/CLO,KLO,CGO,TOI
      COMMON/TEN/DENSS(15,15),MGIN(15,15),CAIN(15,15),DENSIN(15,15)
      COMMON/ELEVEN/DELRAV(60),RIP1(60),RIM1(60),VOL(50,50)
      COMMON/SEVENT/TT(15,15),PM1(15,15)
      COMMON/TWELVE/CCARB,KCARB
      COMMON/FOURT/UMG(15,15),UCA(15,15)
      COMMON/EIGTT/XWEL,HEXT,FREQ
      COMMON/TWENTTH/UWOM1(15,15)
      COMMON/TWENTT/NLCC,NUCC,NCP
      COMMON/TWENTF/HEIGHT,COORDTY,ZPTS(60),RPTS(60)
      COMMON/THITF/UKM1,UCAM1,UMGM1,XM1,XKM1(15,15)
C
C     UKO IS KEROGEN AT T,UKIN IS ORIGINAL  ,KK IS ARREN COEFF
C     GRIDR ,GRIDZ ARE GRID PTS
C
      DO 10 I=1,GRIDR
      DO 20 J=1,GRIDZ
C
```

```
      MAIM1=MAX(I-1,1)
      MIIP1=MIN(I+1,GRIDR)
      MAJM1=MAX(J-1,1)
      MIJP1=MIN(J+1,GRIDZ)
C
      NL=NCP*J-4+NCP*(I-1)*GRIDZ
      NY=NCP*J-3+NCP*(I-1)*GRIDZ
      NT=NCP*J-2+NCP*(I-1)*GRIDZ
      NS=NCP*J-1+NCP*(I-1)*GRIDZ
      NP=NCP*J+NCP*(I-1)*GRIDZ
C
      OL(I,J)=Y(NL)
      UK(I,J)=Y(NY)
      T(I,J)=Y(NT)
      SG(I,J)=Y(NS)
      PG(I,J)=Y(NP)
C
      IF(I.NE.GRIDR)THEN
        OL(I+1,J)=Y(NCP*J-4+NCP*I*GRIDZ)
        UK(I+1,J)=Y(NCP*J-3+NCP*I*GRIDZ)
        T(I+1,J)=Y(NCP*J-2+NCP*I*GRIDZ)
        SG(I+1,J)=Y(NCP*J-1+NCP*I*GRIDZ)
        PG(I+1,J)=Y(NCP*J+NCP*I*GRIDZ)
      ENDIF
C
C
      IF(J.NE.GRIDZ)THEN
        OL(I,J+1)=Y(NCP*(J+1)-4+NCP*(I-1)*GRIDZ)
        UK(I,J+1)=Y(NCP*(J+1)-3+NCP*(I-1)*GRIDZ)
        T(I,J+1)=Y(NCP*(J+1)-2+NCP*(I-1)*GRIDZ)
        SG(I,J+1)=Y(NCP*(J+1)-1+NCP*(I-1)*GRIDZ)
        PG(I,J+1)=Y(NCP*(J+1)+NCP*(I-1)*GRIDZ)
      ENDIF
C
C
      IF(J.NE.1)THEN
        OL(I,J-1)=Y(NCP*(J-1)-4+NCP*(I-1)*GRIDZ)
        UK(I,J-1)=Y(NCP*(J-1)-3+NCP*(I-1)*GRIDZ)
        T(I,J-1)=Y(NCP*(J-1)-2+NCP*(I-1)*GRIDZ)
        SG(I,J-1)=Y(NCP*(J-1)-1+NCP*(I-1)*GRIDZ)
        PG(I,J-1)=Y(NCP*(J-1)+NCP*(I-1)*GRIDZ)
      ENDIF
C
      IF(I.NE.1)THEN
        OL(I-1,J)=Y(NCP*J-4+NCP*(I-2)*GRIDZ)
        UK(I-1,J)=Y(NCP*J-3+NCP*(I-2)*GRIDZ)
        T(I-1,J)=Y(NCP*J-2+NCP*(I-2)*GRIDZ)
        SG(I-1,J)=Y(NCP*J-1+NCP*(I-2)*GRIDZ)
        PG(I-1,J)=Y(NCP*J+NCP*(I-2)*GRIDZ)
      ENDIF
C
C INITIALIZE VALUES OF TEMP,PRESSURE,SATURATION ETC AT GRID PTS
C
C
      OLO=OL(I,J)
      OLRP1=OL(MIIP1,J)
      OLRM1=OL(MAIM1,J)
      OLZM1=OL(I,MAJM1)
      OLZP1=OL(I,MIJP1)
      UKO=UK(I,J)
      TO=T(I,J)
      TIP1=(T(MIIP1,J)+T(I,J))/2.
      TIM1=(T(MAIM1,J)+T(I,J))/2.
      TJM1=(T(I,MAJM1)+T(I,J))/2.
      TJP1=(T(I,MIJP1)+T(I,J))/2.
      SGO=MIN(1.,SG(I,J))
```

```
      SGIM1=MIN(1.,(SG(MAIM1,J)+SG0)/2.)
      SGIP1=MIN(1.,(SG(MIIP1,J)+SG0)/2.)
      SGJP1=MIN(1.,(SG(I,MIJP1)+SG0)/2.)
      SGJM1=MIN(1.,(SG(I,MAJM1)+SG0)/2.)
      PG0=PG(I,J)
      PGIP1=(PG(MIIP1,J)+PG0)/2.
      PGIM1=(PG(MAIM1,J)+PG0)/2.
      PGJM1=(PG(I,MAJM1)+PG0)/2.
      PGJP1=(PG(I,MIJP1)+PG0)/2.
      DENSOI=DENSOIL(PG0)
      DENSIM1=DENSOIL(PGIM1)
      DENSIP1=DENSOIL(PGIP1)
      DENSJM1=DENSOIL(PGJM1)
      DENSJP1=DENSOIL(PGJP1)
      PL0=PG0-PC(I,J,1.-SG0)
      PLIM1=PGIM1-PC(I,J,1.-SGIM1)
      PLJP1=PGJP1-PC(I,J,1.-SGJP1)
      PLIP1=PGIP1-PC(I,J,1.-SGIP1)
      PLJM1=PGJM1-PC(I,J,1.-SGJM1)
      PL(MAIM1,J)=PG(MAIM1,J)-PC(I,J,1.-SG(MAIM1,J))
      PL(MIIP1,J)=PG(MIIP1,J)-PC(I,J,1.-
     1  SG(MIIP1,J))
      PL(I,MAJM1)=PG(I,MAJM1)-PC(I,J,1.-SG(I,MAJM1))
      PL(I,MIJP1)=PG(I,MIJP1)-PC(I,J,1.-
     1  SG(I,MIJP1))
      KKT0=KK(T0)
      UKIM1=(UK(MAIM1,J)+UK0)/2.
      UKIP1=(UK(MIIP1,J)+UK0)/2.
      UKJP1=(UK(I,MIJP1)+UK0)/2.
      UKJM1=(UK(I,MAJM1)+UK0)/2.
      KSIM1=WEIGPAR(KS(UK0,I,J),KS(UK0,I,J),I,2)
      KSIP1=WEIGPAR(KS(UK0,I,J),KS(UK0,I,J),I,1)
      KSJP1=WEIGPER(KS(UK0,I,J),KS(UK0,I,J),J,1)
      KSJM1=WEIGPER(KS(UK0,I,J),KS(UK0,I,J),J,2)
      CS0=CPS(T(I,J))
      KMG=KMGCO3(T0)
      KCA=KCACO3(T0)
      UMG0=UMGM1(I,J)/(1.+(TI-XM1)*KMG)
      UMG(I,J)=UMG0
      UCA0=UCAM1(I,J)/(1.+(TI-XM1)*KCA)
      UCA(I,J)=UCA0
      K0=KRR(T0,UK(I,J),UMG0,UCA0,I,J)
      KIP1=WEIGPAR(K0,KRR(T(MIIP1,J),UKIP1,UMG0,UCA0,MIIP1,J),I,1)
      KIM1=WEIGPAR(KRR(T(MAIM1,J),UKIM1,UMG0,UCA0,MAIM1,J),K0,I,2)
      KJP1=WEIGPER(K0,KRR(T(I,MIJP1),UKJP1,UMG0,UCA0,I,MIJP1),J,1)
      KJM1=WEIGPER(KRR(T(I,MAJM1),UKJM1,UMG0,UCA0,I,MAJM1),K0,J,2)
      MG0=PERMG(1.-SG0)
      MGZ0=MG0*XPERMZ
      ML0=PERML(1.-SG0)
      MLZ0=ML0*XPERMZ
      MLRM1=PERML(1.-SG(MAIM1,J))
      MLRP1=PERML(1.-SG(MIIP1,J))
      MLZP1=PERML(1.-SG(I,MIJP1))
     1 *XPERMZ
      MLZM1=PERML(1.-SG(I,MAJM1))
     1 *XPERMZ
      MGRM1=PERMG(1.-SG(MAIM1,J))
      MGRP1=PERMG(1.-SG(MIIP1,J))
      MGZP1=PERMG(1.-SG(I,MIJP1))
     1 *XPERMZ
      MGZM1=PERMG(1.-SG(I,MAJM1))
     1 *XPERMZ
      VSLIP1=WEIGPAR(VL(T0),VL(T(MIIP1,J)),I,1)
      VSLIM1=WEIGPAR(VL(T(MAIM1,J)),VL(T0),I,2)
      VSLJP1=WEIGPER(VL(T0),VL(T(I,MIJP1)),J,1)
      VSLJM1=WEIGPER(VL(T(I,MAJM1)),VL(T0),J,2)
```

```
      PHO=PHI(TO,UKO,UMGO,UCAO,I,J)
      DPHUKO=DPHUK(I,J)
      XDIFZ=1.
      XKDTO=XKDT(TI,I,J,TO,PGO,SGO)
      XKOGO= XKOILG(I,J,TO,PGO,SGO)*(1.-SGO+1.E-10)/(1.-SGO+1.E-4)
      XKDSG=-(1./(1.-SGO+1.E-4)-(1.-SGO+1.E-10)/(1.-SGO+1.E
     1 -4)**2)*XKOILG(I,J,TO,PGO,SGO)
      XKRP1=XKOILG(I,J,T(MIIP1,J),PG(MIIP1,J),SGO)
      XKRM1=XKOILG(I,J,T(MAIM1,J),PG(MAIM1,J),SGO)
      XKZP1=XKOILG(I,J,T(I,MIJP1),PG(I,MIJP1),SGO)
      XKZM1=XKOILG(I,J,T(I,MAJM1),PG(I,MAJM1),SGO)
      XKOGPO=XKDP(TO,PGO)
C
      WMOLE=(1.-OLO)*GMOLE+OLO*OMOLE
      WMRP1=(1.-OLRP1)*GMOLE+OLRP1*OMOLE
      WMRM1=(1.-OLRM1)*GMOLE+OLRM1*OMOLE
      WMZP1=(1.-OLZP1)*GMOLE+OLZP1*OMOLE
      WMZM1=(1.-OLZM1)*GMOLE+OLZM1*OMOLE
C
      DENSG=OMOLE*PGO/R/TO*OLO
C
C   COEFFICIENTS LEFT SIDE OF LIGHT OIL EQN
C
C
      XA=VOL(I,J)*OMOLE/R/TO*PHO*SGO*PGO*(-1./TO)*OLO
     1 -VOL(I,J)*DENSOI*(1.-SGO)*PHO*OLO/XKOGO**2*XKDTO
C
      XB=VOL(I,J)*(OMOLE/R/TO*PHO*PGO*OLO-PHO*DENSOI*OLO/XKOGO
     1 -(1.-SGO)*PHO*DENSOI*OLO/XKOGO**2*XKDSG)
C
      XC=VOL(I,J)*PHO*(DDENSO(PGO)*(1.-SGO)*OLO/XKOGO -
     1 (1.-SGO)*DENSOI*OLO/XKOGO**2*XKOGPO
     1 +OMOLE*OLO*SGO/R/TO)
C
      XCOL=VOL(I,J)*(OMOLE/R/TO*PHO*SGO*PGO
     1 +PHO*DENSOI*(1.-SGO)/XKOGO)
C
C
C  COEFFIENTS LEFT HAND SIDE OF HEAVY OIL EQN
C
C
C
      XU= VOL(I,J)*PHO*DENSOI*OLO/XKOGO**2*XKDTO*(1.-SGO)
C
      XF=VOL(I,J)*(-PHO*DENSOI*(1.-OLO/XKOGO)
     1 +(1.-SGO)*PHO*DENSOI*OLO/XKOGO**2*XKDSG)
C
      XV=VOL(I,J)*PHO*(1.-SGO)*(DDENSO(PGO)*(1.-OLO/XKOGO)
     1 +DENSOI*OLO/XKOGO**2*XKOGPO)
C
      XW=-VOL(I,J)*PHO*DENSOI*(1.-SGO)/XKOGO
C
C    LEFT HAND SIDE OF INERT GAS EQN
      XL=VOL(I,J)*PHO*SGO*PGO*GMOLE/R/TO*(-1./TO*(1.-OLO))
C
      XM=VOL(I,J)*PHO*PGO*GMOLE/R/TO*(1.-OLO)
C
      XN= VOL(I,J)*PHO*SGO/R/TO*GMOLE*((1.-OLO))
C
      XO=-VOL(I,J)*PHO*SGO*PGO*GMOLE/R/TO
C
C
COEFFIENTS LEFT HAND SIDE OF HEAT EQN
C
      XH=VOL(I,J)*(PHO*(1.-SGO)*DENSOI*CLO+
     1 DENSS(I,J)*CSO+UCA(I,J)*CCACO3+UMG(I,J)*CMGCO3
```

```
     2  +CKO*UKO
     1 +CGO*SGO*PGO/R*PHO*TOI/TO/TO*WMOLE
     3 +CCARB*CHAR(I,J)+DENSS(I,J)*(TO-TOI)*DCS(TO))
C
       XI=VOL(I,J)*PHO*SGO*WMOLE/R/TO*CGO*(TO-TOI)
C
       XJ=XI/SGO*PGO-VOL(I,J)*DENSOI*PHO*CLO*(TO-TOI)
C
       XOL=VOL(I,J)*CGO*PHO*SGO*PGO/R*(OMOLE-GMOLE)*(TO-TOI)/TO
C
C
C
C
C    VELOCITES AT GRIDS ARE CALCULATED
C
          VGRM1=VELR(UPW(MGRM1,MGO,PG(MAIM1,J),PGO)*KIM1/VG(TIM1),
     1 PG(MAIM1,J),PGO
     2 ,PGJP1,PGJM1,PGIM1*WMOLE/R/TIM1,I,J,1)
C
          VGRP1=VELR(UPW(MGO,MGRP1,PGO,PG(MIIP1,J))*KIP1/VG(TIP1)
     1    ,PGO,PG(MIIP1,J),
     2 PGJP1,PGJM1,PGIP1*WMOLE/R/TIP1,I,J,2)
C
          VGZP1=VELZ(UPW(MGZO,
     1 MGZP1,PGO,PG(I,MIJP1))*KJP1/VG(TJP1)
     2    ,PGIM1,PGIP1,PG(I,MIJP1),PGO,PGJP1*WMOLE/R/TJP1,
     3 I,J,1)
C
          VGZM1=VELZ(UPW(MGZM1,MGZO,PG(I,MAJM1),PGO)*KJM1/VG(TJM1),
     1    PGIM1,PGIP1,PGO,PG(I,MAJM1),
     2 PGJM1*WMOLE/R/TJM1,I,J,2)
C
          VLRM1=VELR(UPW(MLRM1,MLO,PL(MAIM1,J),PLO)*KIM1/VSLIM1
     1   ,PL(MAIM1,J),PLO,
     2 PLJP1,PLJM1,DENSOI,I,J,1)
C
          VLRP1=VELR(UPW(MLO,MLRP1,PLO,PL(MIIP1,J))*KIP1/VSLIP1
     1    ,PLO,PL(MIN(I+1,
     2 GRIDR),J),PLJP1,PLJM1,DENSOI,I,J,2)
C
          VLZP1=VELZ(UPW(MLZO,
     1 MLZP1,PLO,PL(I,MIJP1))*KJP1/VSLJP1   ,
     2    PLIM1,PLIP1,PL(I,MIJP1),PLO,DENSOI,I,J,1)
C
          VLZM1=VELZ(UPW(MLZM1,MLZO,
     1  PL(I,MAJM1),PLO)*KJM1/VSLJM1,PLIM1,PLIP1,PLO,PL(I,MAJM1)
     2 ,DENSOI,I,J,2)
C
C     BOUNDARY CONDITIONS ON VELOCITIES
C
       IF (I .EQ. GRIDR) THEN
          VGRP1=0.0
          VLRP1=0.0
       ENDIF
C
       IF (J .EQ. 1) THEN
          VGZM1=0.0
          VLZM1=0.0
       ENDIF
C
       IF (J .EQ. GRIDZ) THEN
          VGZP1=0.0
          VLZP1=0.0
       ENDIF
C
C
```

```
        IF (I .EQ. 1) THEN
         VGRM1= PERMG(1.-SG(1,J) )*KIM1/VG(TIM1)
     1  *(-(PG(1,J)-1.E5))/((RPTS(2)-RPTS(1)))
         VLRM1= PERML(1.-SG(1,J) )*KIM1/VL(TIM1)
     1  *(-(PL(1,J)-1.E5))/((RPTS(2)-RPTS(1)))
        ENDIF
C
CALCULATES CONVECTION COEFFICIENTS (FEG,FWG,FSG,FNG,FNL,FSL,FEL,FWL)
C
         FEG=RIM1(I)*DELTZ(J)*VGRM1*UPW(PG(MAIM1,J)/T(MAIM1,J),PGO
     1  /TO,PG(MAIM1,J),PGO)/R
         FWG=RIP1(I)*DELTZ(J)*VGRP1*UPW(PGO/TO,PG(MIIP1,J)/
     1  T(MIIP1,J),PGO,PG(MIIP1,J))/R
         FNG=DELRAV(I)*VGZP1*UPW(PG(I,MIJP1)/T(I,MIJP1)
     1  ,PGO/TO,PG(I,MIJP1),PGO)/R
         FSG=DELRAV(I)*VGZM1*UPW(PGO/TO,PG(I,MAJM1)
     1  /T(I,MAJM1),PGO,PG(I,MAJM1))/R
         FEL=RIM1(I)*VLRM1*DELTZ(J)*DENSIM1
         FWL=RIP1(I)*VLRP1*DELTZ(J)*DENSIP1
         FNL=VLZP1*DENSJP1*DELRAV(I)
         FSL=VLZM1*DENSJM1*DELRAV(I)
C
C
        TCGIM1=WMOLE*CGO*(TIM1-TOI)
        TCLIM1=CLO*(TIM1-TOI)
        TCGIP1=WMOLE*CGO*(TIP1-TOI)
        TCLIP1=CLO*(TIP1-TOI)
        TCGJP1=WMOLE*CGO*(TJP1-TOI)
        TCLJP1=CLO*(TJP1-TOI)
        TCGJM1=WMOLE*CGO*(TJM1-TOI)
        TCLJM1=CLO*(TJM1-TOI)
C
COEFFIENTS RIGHT HAND SIDE OF LIGHT OIL EQN.
C
        XUK=.6585*UKO*KKTO
C
        XD= VOL(I,J)*(1.*XUK
     2-PHO*((1.-SGO)*DENSOI*KCOKEL(TO)*OLO/XKOGO
     3 +DENSG*KCOKEG(TO)*SGO))
     1 +FEG*OMOLE*UPW(OLRM1,OLO,PG(MAIM1,J),PGO)
     1 -FWG*UPW(OLO,OLRP1,PGO,PG(MIIP1,J))*OMOLE
     1 +FSG*OMOLE*UPW(OLZM1,OLO,PG(I,MAJM1),PGO)
     1 -FNG*OMOLE*UPW(OLO,OLZP1,PGO,PG(I,MIJP1))
C
     1 +FEL*(OLRM1/XKRM1+OLO/XKOGO)/2.
     1 -FWL*(OLRP1/XKRP1+OLO/XKOGO)/2.
     1 +FSL*(OLZM1/XKZM1+OLO/XKOGO)/2.
     1 -FNL*(OLZP1/XKZP1+OLO/XKOGO)/2.
     1+VOL(I,J)*OMOLE/R/TO*KKTO*DPHUKO*UKO*SGO*PGO*OLO
     1 +VOL(I,J)*DENSOI*(1.-SGO)*OLO/XKOGO*DPHUKO*UKO*KKTO
C
COEFFIENTS RIGHT HAND SIDE OF HEAVY OIL EQN.
C
        XG= VOL(I,J)*(0.*XUK
     2-PHO*((1.-SGO)*DENSOI*KCOKEL(TO)*(1.-OLO/XKOGO)))
     1 +FEL*(1.-(OLO/XKOGO+OLRM1/XKRM1)/2.)
     1 -FWL*(1.-(OLO/XKOGO+OLRP1/XKRP1)/2.)
     1 +FSL*(1.-(OLO/XKOGO+OLZM1/XKZM1)/2.)
     1 -FNL*(1.-(OLO/XKOGO+OLZP1/XKZP1)/2.)
     1 +VOL(I,J)*DENSOI*(1.-SGO)*DPHUKO*KKTO*UKO*(1.-OLO/XKOGO)
C
C   RIGHT HAND SIDE OF INERT GAS EQN.
C
      XP=VOL(I,J)*SOURG(XUK,UCAO,UMGO,KCA,KMG,DUWO,DENSOI,TO,
     1 SGO,PHO,DENSG,XKOGO,OLO)
     1 + FEG*GMOLE*UPW(1.-OLO.1.-OLRM1.PGO.PG(MAIM1.J))
```

```
     1 - FWG*GMOLE*UPW(1.-OLO,1.-OLRP1,PGO,PG(MIIP1,J))
     1 + FSG*GMOLE*UPW(1.-OLO,1.-OLZM1,PGO,PG(I,MAJM1))
     1 - FNG*GMOLE*UPW(1.-OLO,1.-OLZP1,PGO,PG(I,MIJP1))
     1 +VOL(I,J)*PHO*(.25*(1.-SGO)*DENSOI*KCOKEL(TO)+.69*DENSG*SGO
     1 *KCOKEG(TO))
     1 +VOL(I,J)*DPHUKO*SGO*PGO*GMOLE/R/TO*KKTO*UKO*(1.-OLO)
C
C
COEFFIENTS RIGHT HAND SIDE OF HEAT EQN
C
C    QRP1,QZP1 ARE NEGATIVE
       QRM1=100./(2.*ACOS(-1.)*XWEL*.5)*(TO-TOI)/700.
       QRP1=-MAX(0.,10.*(TO-TOI))
       QZM1=MAX(0.,1.3*(TO-TOI))
       QZP1=MIN(0.,-10.*(TO-TOI)*.1)
C
       XE=1.E-50
       XK=VOL(I,J)*(SOURE(I,J,TO,FREQ,XWEL,TI)+DELTH(UKO,KKTO,
     1 DUWO(I,J),I,J))+(FEL*TCLIM1+FEG*TCGIM1)-(FNL*TCLJP1+FNG*
     2 TCGJP1)-(FWL*TCLIP1+FWG*TCGIP1)+(FSL*TCLJM1+FSG*TCGJM1)
     3+DELTZ(J)*FX(QRP1,KSIP1
     4 *(T(MIIP1,J)-TO)/(RPTS(MIIP1)-RPTS(I)+XE),I,J,2)*RIP1(I)
     5 -DELTZ(J)*FX(QRM1,KSIM1
     6 *(TO-T(MAIM1,J))/(RPTS(I)-RPTS(MAIM1)+XE),I,J,1)*RIM1(I)
     7 +DELRAV(I)*FX(QZP1,XDIFZ*KSJP1
     8 *(T(I,MIJP1)-TO)/(ZPTS(MIJP1)-ZPTS(J)+XE),I,J,3)
       XK=XK-DELRAV(I)*FX(QZM1,XDIFZ*KSJM1/(ZPTS(J)-ZPTS(MAJM1)+XE)
     A *(TO-T(I,MAJM1)),I,J,4)+VOL(I,J)*(CKO*(TO-TOI)*UKO*KKTO
     1 +KCA*UCAO*(TO-TOI)*CCACO3+KMG*UMGO*(TO-TOI)*CMGCO3-CCARB*
     1 (TO-TOI)*.171*UKO*KKTO
     1 -CCARB*PHO*(.31*SGO*DENSG*(TO-TOI)*KCOKEG(TO)+
     1 .75*(1.-SGO)*DENSOI*KCOKEL(TO)*(TO-TOI))+CGO*SGO*PGO*WMOLE
     1 /R*DPHUKO*KKTO*UKO*(TO-TOI)/TO)
C
C
C   CALCULATE PRIME COORD
C
C
C   THE DERIVATIVES OF THE TEMP (DTT), SATURATIONS OF GASES (DSGT),
C   OIL GAS (NY), AND PRESSURE (DPGT) WITH RESPECT TO THE INDEPENDENT
C    VARIABLES T, SG, YO, AND P.
C
       AMAT(1,1)=XA
       AMAT(1,2)=XB
       AMAT(1,3)=XC
       AMAT(1,4)=XCOL
        BMAT(1)=XD
       AMAT(2,1)=XU
       AMAT(2,2)=XF
       AMAT(2,3)=XV
       AMAT(2,4)=XW
       BMAT(2)=XG
       AMAT(3,1)=XL
       AMAT(3,2)=XM
       AMAT(3,3)=XN
       AMAT(3,4)=XO
       BMAT(3)=XP
       AMAT(4,1)=XH
       AMAT(4,2)=XJ
       AMAT(4,3)=XI
       AMAT(4,4)=XOL
       BMAT(4)=XK
        CALL LEQT2F(AMAT,1,4,4,BMAT,6,WKA,IER)
C
C
       YPRIME(NS)=BMAT(2)
```

```
C
      YPRIME(NT)=BMAT(1)
C
      YPRIME(NL)=BMAT(4)
C
      YPRIME(NP) =BMAT(3)
C
      YPRIME(NY)=-KKTO*UKO

 20    CONTINUE
 10    CONTINUE
       RETURN
       END
C*******************************************************************************
C*******************************************************************************
C*******************************************************************************
C*******************************************************************************
C    RADIAL VELOCITIES VIA DARCY'S LAW
C
      REAL FUNCTION VELR(MR1,PR1,PR2,PZ1,PZ2
     1 ,DENS,I,J,K)
      REAL MR1,MZ1,PR1,PR2,PZ1,PZ2,RPTS,SHDENS
      REAL B,KV,DENS,DELTR,DELTZ,G
      INTEGER GRIDR,GRIDZ,K
      COMMON/TWO/DELTR(60),DELTZ(60),GRIDR,GRIDZ,G,SHDENS
      COMMON/TWENTF/HEIGHT,COORDTY,ZPTS(60),RPTS(60)
C
      IF(I.EQ.GRIDR.AND.K.EQ.2)THEN
        VELR=0.0
        RETURN
      ENDIF
C
      IF(I.EQ.GRIDR.AND.K.EQ.1)THEN
        VELR=-(PR2-PR1)*MR1/(RPTS(GRIDR)-RPTS(GRIDR-1))
        RETURN
      ENDIF
C
      IF(K.EQ.2)THEN
        VELR=-(PR2-PR1)*MR1/(RPTS(I+1)-RPTS(I))
        RETURN
      ENDIF
C
      IF(K.EQ.1.AND.I.NE.1)THEN
        VELR=-(PR2-PR1)*MR1/(RPTS(I)-RPTS(I-1))
        RETURN
     ENDIF
      END
C
C*******************************************************************
C  AXIAL VELOCITIES CALCULATED USING DARCY'S LAW
C
      REAL FUNCTION VELZ(MZ1,PR1,PR2,PZ1,PZ2
     1 ,DENS,I,J,K)
      REAL MR1,MZ1,PR1,PR2,PZ1,PZ2
      REAL DELTR,DELTZ,G
      REAL B,KV,DENS,YDELTA,RPTS,SHDENS
      INTEGER GRIDR,GRIDZ,K
      COMMON/TWO/DELTR(60),DELTZ(60),GRIDR,GRIDZ,G,SHDENS
      COMMON/TWENTF/HEIGHT,COORDTY,ZPTS(60),RPTS(60)
C
      IF(J.EQ.1.AND.K.EQ.2)THEN
        VELZ=0.0
        RETURN
      ENDIF
C
      IF(J.EQ.GRIDZ.AND.K.EQ.1)THEN
```

```
        VELZ=0.0
        RETURN
      ENDIF
C
C
       IF(K.EQ.1)THEN
      VELZ=-(PZ1-PZ2)*MZ1/(ZPTS(J+1)-ZPTS(J))
     ELSE IF(K.EQ.2)THEN
      VELZ=-(PZ1-PZ2)*MZ1/(ZPTS(J)-ZPTS(J-1))
      ENDIF
C
      RETURN
      END
C
C**********************************************************************
C  SPECIFIC HEAT OF THE SOLID MATRIX AS A FUNCTION OF TEMPERATURE
C
      REAL FUNCTION CPS(T)
      REAL T
      COMMON/GAL/GALTON
C
      CPS=(800.+4./3.*T)*(.4/50.*GALTON+.5)
      RETURN
      END
C
**********************************************************************
C
      REAL FUNCTION DCS(T)
      REAL T
      COMMON/GAL/GALTON
C
      DCS=4./3.*(.4/50.*GALTON+.5)
      RETURN
      END
**********************************************************************
C   THERMAL CONDUCTIVITY OF SOLID  MATRIX AS A FUNCTION OF KEROGEN
C  REMAINING IN THE SHALE
C
      REAL FUNCTION KS(UK0,I,J)
      REAL UK0
      COMMON/ONE/UKIN(15,15),WKK,CCACO3,CMGCO3,CARBDEN(15,15)
C
      KS=UK0/UKIN(I,J) + .5*(1.-UK0/UKIN(I,J))
      RETURN
      END
C
C**************************************************************************
C    THERMAL CONDUCTIVITY OF GASES AS A FUNCTION OF TEMPERATURE
C
      REAL FUNCTION KG(T0)
      REAL T0
C
      KG=.56
      RETURN
      END
C
C**************************************************************************
C  VISCOSITY OF OIL AS A FUNCTION OF THE TEMPERATIURE
C
      REAL FUNCTION VL(T)
      REAL T
C       PG 38 CHRISTENSEN THESIS
C
C
      VL=6.3E-7*EXP(5182./T)
      RETURN
```

```
      END
C
C*************************************************************************
C  VISCOSITY OF GASES AS A FUNCTION OF TEMPERATURE
C
C
       REAL FUNCTION VG(T)
       REAL T,T1
CC  FROM WAYNE STATE REPORT PG. 57
       T1=T-273.
      VG=5.E-5
      RETURN
      END
C
*************************************************************************
C   POROSITY AS A FUNCTION OF ORGANIC MATERIAL REMAINING
C
      REAL FUNCTION PHI(T,UK,UMG,UCA,I,J)
      REAL UK,UKIN,CCACO3,CMGCO3,CARBDEN,T,UWO,WKK
      REAL MGIN,CAIN,UMG,UCA,DENSIN,KCAC,KMGC
      REAL XFRAC,KKERO,KHYO,CHYO,KWO,CKO,DENSS
      COMMON/ONE/UKIN(15,15),WKK,CCACO3,CMGCO3,CARBDEN(15,15)
      COMMON/THREE/XFRAC,UWIN,KKERO,KHYO,CHYO,KWO,CWO,CKO,KMGC,KCAC
      COMMON/TEN/DENSS(15,15),MGIN(15,15),CAIN(15,15),DENSIN(15,15)
C
      XX=.010
      PHI=MIN(ABS(UKIN(I,J)/1000.+(MGIN(I,J)+CAIN(I,J)+DENSIN(I,J))
     1 /2800.-UK/1000.-(UMG+UCA+DENSS(I,J))/2800.)
     2+XX,1.)
      IF(PHI.LE.0.0)PHI=.01
      RETURN
      END
C
C*************************************************************************
C  RELATIVE PERMEABILITY OF OIL AS A FUNCTION OF OIL SATURATION
C
      REAL FUNCTION PERML(SO)
      REAL SO,K(15),S(15)
      INTEGER IX,JY
C
      DATA S(1)/0.0/,S(2)/.33/,S(3)/.36/,S(4)/.42/,S(5)/.48/
     1 ,S(6)/.54/,S(7)/.60/,S(8)/.66/,S(9)/.72/,S(10)/.78/
     2 ,S(11)/.84/,S(12)/.9/,S(13)/1.0/
C
      DATA K(1)/.000/,K(2)/.001/,K(3)/.006/,K(4)/.008/,K(5)/.011/
     1 ,K(6)/.02/,K(7)/.03/,K(8)/.10/,K(9)/.15/,K(10)/.30/
     2 ,K(11)/.500/,K(12)/.80/,K(13)/1.0/
C
C
      PERML=SO
      RETURN
      DO 10 I=1,12
       IF (SO .GE. S(I).AND.SO .LT. S(I+1)) THEN
        GO TO 5
       ENDIF
  10   CONTINUE
       IF (SO .EQ. 1.) THEN
         PERML=1.0
         RETURN
       ENDIF
       IF (SO .GT. 1.) THEN
        PERML=1.0
        RETURN
       ELSE IF (SO .LT. 0.0) THEN
        PERML=0.0
        RETURN
```

```
      ENDIF
C
   5  IF (S(I) .EQ. SO) THEN
        PERML=K(I)
        RETURN
      ENDIF
      IF (S(I+1) .EQ. SO) THEN
       PERML=K(I+1)
       RETURN
      ELSE
       XM=(K(I+1)-K(I))/(S(I+1)-S(I))
       XB=K(I)-XM*S(I)
       PERML=XM*SO+XB
      ENDIF
      RETURN
      END
CC
C*************************************************************************
C   RELATIVE PERMEABILITY OF GASES AS A FUNCTION OF OIL SATURATION
C
      REAL FUNCTION PERMG(SO)
      REAL SO,S(15),K(13)
      INTEGER IX,JY
C
      DATA S(1)/0.0/,S(2)/.33/,S(3)/.36/,S(4)/.42/,S(5)/.48/
     1 ,S(6)/.54/,S(7)/.6/,S(8)/.66/,S(9)/.72/,S(10)/.78/
     2 ,S(11)/.84/,S(12)/.9/,S(13)/1.0/
C
      DATA K(1)/1.0/,K(2)/.89/,K(3)/.84/,K(4)/.725/,K(5)/.595/
     1 ,K(6)/.45/,K(7)/.315/,K(8)/.21/,K(9)/.13/,K(10)/.073/
     2 ,K(11)/.035/,K(12)/.015/,K(13)/0.0/
C
        PERMG=(1.-SO)
      RETURN
      DO 10 I=1,12
       IF (SO .GE. S(I).AND.SO .LT. S(I+1)) THEN
        GO TO 5
       ENDIF
  10  CONTINUE
      IF (SO .EQ. 1.) THEN
        PERMG=0.0
        RETURN
      ENDIF
      IF (SO .GT. 1.) THEN
       PERMG=0.0
       RETURN
      ELSE IF (SO .LT. 0.0) THEN
       PERMG=1.0
       RETURN
      ENDIF
C
   5  IF (S(I) .EQ. SO) THEN
        PERMG=K(I)
        RETURN
      ENDIF
      IF (S(I+1) .EQ. SO) THEN
        PERMG=K(I+1)
       RETURN
      ELSE
       XM=(K(I+1)-K(I))/(S(I+1)-S(I))
       XB=K(I)-XM*S(I)
       PERMG=XM*SO+XB
      ENDIF
      RETURN
      END
*************************************************************************
```

```
C   ABSOLUTE PERMEABILITY AS A FUNCTION OF POROSITY ( USING
C   KOZENY'S FORMULA)
C
      REAL FUNCTION KRR(T,UK,UMG,UCA,I,J)
      REAL DELTR,DELTZ,GRIDR,GRIDZ,G,UMG,UCA,T,PH,PHI
      REAL UK,UKIN,WKK,CCACO3,CMGCO3,CARBDEN,DENSS,DENSIN
      REAL CAIN,MGIN
      COMMON/ONE/UKIN(15,15),WKK,CCACO3,CMGCO3,CARBDEN(15,15)
      COMMON/TWO/DELTR(60),DELTZ(60),GRIDR,GRIDZ,G,SHDENS
      COMMON/TEN/DENSS(15,15),MGIN(15,15),CAIN(15,15),DENSIN(15,15)
C     1 CM DIAMETER
      PH=PHI(T,UK,UMG,UCA,I,J)
      KRR=MIN(ABS(.5E-12/.026*PH*PH*PH/((1.-PH)**2)),.5E-12)+1.E-14
      RETURN
      END
C*************************************************************************
C
C   ELECTROMAGNETIC SOURCE TERM AS A FUNCTION OF R,Z, AND TEMPERATURE
C
      REAL FUNCTION SOURE(I,J,T,FREQ,XWEL,TI)
      REAL MAX,DELTR,DELTZ,G,GR,GZ,LOSSTAN,DIELCST,ELECNRM,R
      REAL RPTS,PERCDIS,T,ATTEN,FREQ,ZPTS,FIELD
      INTEGER GRIDR,GRIDZ,I,J,COORDTY
      COMMON/TWO/DELTR(60),DELTZ(60),GRIDR,GRIDZ,G,SHDENS
       COMMON/FIEL/FIELD(35,35),XP,XDBLIN
      COMMON/ELEVEN/DELRAV(60),RIP1(60),RIM1(60),VOL(50,50)
      COMMON/TWENTF/HEIGHT,COORDTY,ZPTS(60),RPTS(60)
C
      SOURE=FIELD(I,J)
C
C
      RETURN
      END
C
C*************************************************************************
C   SOURCE OF GASES
C
      REAL FUNCTION SOURG(XUK,UCAO,UMGO,KCA,KMG,DUWO,DENSOI,TO
     1 ,SGO,PHO,DENSG,XKOGO,OLO)
      REAL UKO,KK,UWIN,TL,TH,TO,KKERO,KHYO,CHYO,KCOKEL,KCOKEG
      REAL UCAO,UMGO,KMG,KCA
      REAL CWO,CKO,KMGC,KCAC,DUWO,KWO
      COMMON/THREE/XFRAC,UWIN,KKERO,KHYO,CHYO,KWO,CWO,CKO,KMGC,KCAC
      COMMON/SEVEN/CHAR(15,15)
C
       SOURG=XUK/.6585*(.1705)+PHO*(.250*(1.-SGO)*DENSOI*KCOKEL(TO)
     1 + .69*DENSG*KCOKEG(TO)*SGO)+KMG*UMGO+KCA*UCAO
       RETURN
       END
C
C*************************************************************************
C    SOURCE OF OILS
C
      REAL FUNCTION SOURO(XUK,SGO,DENSOI,PHO,TO,VOL,DENSG,XKOGO,OLO)
      REAL UKO,KK,XFRAC,TO,UWIN,DUWO,COKE
      REAL KKERO,KHYO,CHYO,KWO,CWO,CKO,KMGC,KCAC,KCOKEL
      REAL KCOKEG
      COMMON/SEVEN/CHAR(15,15)
      COMMON/THREE/XFRAC,UWIN,KKERO,KHYO,CHYO,KWO,CWO,CKO,KMGC,KCAC
C
      SOURO=XUK
      RETURN
      END
C
C*************************************************************************
C    KEROGEN RATE CONSTANT
```

```
C
        REAL FUNCTION KK(T)
        REAL T,KKTM1(15,15),TTT(15,15)
        INTEGER IX,JY
        COMMON/SIXT/KKTM1,TTT
        IF(-26390./T.LE.-100.)THEN
        KK=1.E-9
        RETURN
        ENDIF
        IF(-26390./T.GE.100.)THEN
         KK=1.E50*2.38E13
         RETURN
        ENDIF
        KK=2.81E13*EXP(-26390./T)
        RETURN
        END
C
C*******************************************************************************
C
C*****************************************************************
C   MAGNESIUM CARBONATE RATE CONSTANT
C
       REAL FUNCTION KMGCO3(T)
       REAL T
       IF(-29090./T.GT.200.)THEN
        KMGCO3=1.E-9
        RETURN
       ELSE
        KMGCO3=1.7E10*EXP(-29090./T)
        RETURN
       ENDIF
       END
C
*****************************************************************
C   CALCIUM CARBONATE RATE CONSTANT
C
       REAL FUNCTION KCACO3(T)
       REAL T
       IF(-36050./T.GT.200.)THEN
        KCACO3=1.E-9
        RETURN
       ELSE
        KCACO3=9.6E10*EXP(-36050./T)
        RETURN
       ENDIF
       END
C
*****************************************************************
C   SOURCE FOR HEAT EQUATION FOR CHEMICAL REACTIONS
C
       REAL FUNCTION DELTH(UKO,KKTO,DUWO,I,J)
       REAL UKO,KK,TO,UWIN,XFRAC,DUWO,UWO,KKTO
       REAL UK(15,15),UMG,UCA,YO,DYO
       REAL UCAO,UMGO,KCA,KMG,COKE
       REAL KKERO,KHYO,CHYO,KWO,CWO,CKO,KMGC,KCAC
       COMMON/THREE/XFRAC,UWIN,KKERO,KHYO,CHYO,KWO,CWO,CKO,KMGC,KCAC
       COMMON/SEVEN/CHAR(15,15)
       COMMON/FOURT/UMG(15,15),UCA(15,15)
       DELTH=-3.3E5*UKO*KKTO
       RETURN
       END
C
C*******************************************************************************
C   DERIVATIVE OF POROSITY WITH RESPECT TO KEROGEN DENSITY
       REAL FUNCTION DPHUK(I,J)
       REAL UKIN,WKK,CCACO3,CMGCO3,CARBDEN,N,DENSS,UK(15,15)
```

```
      REAL MGIN,CAIN,DENSIN
      COMMON/ONE/UKIN(15,15),WKK,CCACO3,CMGCO3,CARBDEN(15,15)
      COMMON/FOURT/UMG(15,15),UCA(15,15)
      COMMON/TEN/DENSS(15,15),MGIN(15,15),CAIN(15,15),DENSIN(15,15)
C
      DPHUK=-1./1000.
C
      RETURN
      END
C
C*************************************************************************
C   UPSTREAM WEIGHTING OF THE CONVECTION COEFFICIENTS
      REAL FUNCTION UPW(K1,K2,P1,P2)
      REAL K1,K2,P1,P2
C
      IF (P1 .GE. P2) THEN
         UPW=K1
      ELSE
        UPW=K2
        ENDIF
      RETURN
      END
C*************************************************************************
C   UPSTREAM WEIGHTING ROUTINE
C
      REAL FUNCTION FX(X,Y,I,J,K)
      REAL X,Y,DELTR,DELTZ,G,B,RPTS,SHDENS
      INTEGER I,J,GRIDR,GRIDZ,K
      COMMON/TWO/DELTR(60),DELTZ(60),GRIDR,GRIDZ,G,SHDENS
C
      IF (K .EQ. 1.AND.I .EQ. 1) THEN
        FX=X
        GO TO 5
      ELSE IF (K .EQ. 2.AND.I .EQ. GRIDR) THEN
        FX=X
        GO TO 5
      ELSE IF (K .EQ. 4.AND.J .EQ. 1) THEN
       FX=X
       GO TO 5
      ELSE IF (K .EQ. 3.AND.J .EQ. GRIDZ) THEN
       FX=X
      ELSE
       FX=Y
      ENDIF
 5    RETURN
      END
C
C*************************************************************************
C   UPSTREAM WEIGHTING OF ENTHALPY
C
       REAL FUNCTION TC(FEG,X,Y)
       REAL FEG,X,Y
       IF (FEG .LT. 0.0) THEN
        TC=X
       ELSE
        TC=Y
       ENDIF
       RETURN
       END
C
C*************************************************************************
C   CAPILLARY PRESSURE AS A FUNCTION OF OIL SATURATION
C
      REAL FUNCTION PC(IX,JY,SO)
      REAL SO
      INTEGER IX,JY
```

```
      PC=MAX(.001,3.E4*(1.-SO)**3)
       PC=0.0
      RETURN
      END
C
C
C
**********************************************************************
C
**********************************************************************
C   ATTENUATION LENGTHS
C
      REAL FUNCTION ATTEN(OMEGA,XMU,EPSOL)
      REAL OMEGA
       COMPLEX EPSOL
C
      ATTEN=1./2./OMEGA*SQRT(2./XMU/REAL(EPSOL)/(SQRT(1.+
     1 (AIMAG(EPSOL)/REAL(EPSOL))**2) -1.))
      RETURN
      END
**********************************************************************
C      VAPOR PRESSURE OF WATER
      REAL FUNCTION VAPORP(T)
      REAL T
C
      VAPORP=1.1833E10*EXP(-3818.15/(T-45.92))
      RETURN
      END
**********************************************************************
C
C  PARALLEL WEIGHTING TERM
       REAL FUNCTION WEIGPAR(X,Y,I,K)
       REAL X,Y,DELTR,DELTZ,G,B,RPTS,SHDENS
       INTEGER I,J,K,GRIDR,GRIDZ
       COMMON/TWO/DELTR(60),DELTZ(60),GRIDR,GRIDZ,G,SHDENS
C
       IF(K.EQ.1)WEIGPAR=(DELTR(I)*X+DELTR(MIN(I+1,GRIDR))*Y)/(DELTR(I)
     1 +DELTR(MIN(I+1,GRIDR)))
C
       IF(K.EQ.2) WEIGPAR=(DELTR(MAX(I-1,1))*X+DELTR(I)*Y)/
     1 (DELTR(MAX(I-1,1))+DELTR(I))
C
       RETURN
       END
**********************************************************************
C    PERPENDICULAR WEIGHTING TERM
C
       REAL FUNCTION WEIGPER(X,Y,I,K)
       REAL X,Y,DELTR,DELTZ,G,SHDENS
       INTEGER I,K,GRIDR,GRIDZ
       COMMON/TWO/DELTR(60),DELTZ(60),GRIDR,GRIDZ,G,SHDENS
C
       IF(K.EQ.1)WEIGPER=1./(DELTZ(I)*Y+DELTZ(MIN(I+1,GRIDZ))*X)*(
     1 DELTZ(I)+DELTZ(MIN(I+1,GRIDZ)))*X*Y
C
       IF(K.EQ.2) WEIGPER=1./(DELTZ(MAX(I-1,1))*Y+DELTZ(I)*X)*
     1 (DELTZ(MAX(I-1,1))+DELTZ(I))*X*Y
C
       RETURN
       END
C**********************************************************************
C  CALCULATES JACOBIAN FOR IMSL ROUTINE DGEAR
       SUBROUTINE FCNJ(N,TI,Y,PD)
       REAL PD(30000),YO(15,15),SOUROG,WEIGPAR,WEIGPER
       REAL KMGCO3,KCACO3,PM1,OL(15,15),KCOKEL,KCOKEG
       REAL VOL,GMOLE,OMOLE,R,DENSOI,DENSS,TI,QRM1,QRP1,QZP1,QZM1
```

```
      REAL VSLIP1,VSLIM1,VSLJP1,VSLJM1,UMG0,UCA0
      REAL KIP1,KIM1,KJP1,KJM1,K0,BMAT(4),AMAT(4,4),WKA(50)
      REAL UKIP1,UKIM1,UKJP1,UKJM1
      REAL  XA,XB,XC,XD,XF,XG,XH,XK,VL0,VG0,CPS
      REAL FEL,FEG,FWL,FWG,FNL,FNG,FSL,FSG,DELTT,DELTS,DELTY
      REAL MGRR0,MLRR0,DSGT,DTT,DYT
      REAL RIM1,RIP1,UW,DUW,KS,UCAM1(15,15),UMGM1(15,15)
      REAL KSIM1,KSIP1,KSJP1,KSJM1
      REAL YT,XT,KCA,KMG,KCAC,KMGC,DUW0,SHDENS
      REAL PL0,PERML,PERMG,UW0
      REAL MG0,MGZ0,FX,TC,TCLJM1
      REAL TCGIM1,TCGIP1,TCLIM1,TCLIP1,TCGJP1,TCLJP1,TCGJM1
      REAL T(15,15),PG(15,15),SG(15,15),UK(15,15),PL(15,15)
      REAL PLIM1,PLIP1,PLJP1,PLJM1,SGIM1,SGIP1,SGJP1,SGJM1
      REAL UK0,DELTZ,DELTR,DELRAV,KKER0,KHY0,KW0,CW0,CHY0
      REAL MGRM1,MGRP1,MGZP1,MGZM1,MLRM1,MLRP1,MLZP1,MLZM1
      REAL MLZ0,UKIN,CG0,CS0,ML0
      REAL PGIM1,PGIP1,PG0
      REAL PGJP1,PGJM1,T0,TIM1,TIP1,TJP1,TJM1,KKT0
      REAL VELR,VELZ,PHI,SOURE,KRR,PC
      REAL VGRM1,VGRP1,VGZP1,VGZM1,VLRM1,VLRP1,VLZP1,VLZM1
      REAL UCA,UMG,CCACO3,CMGCO3,CARBDEN,FREQ,COKE
      REAL UPW,KCARB,CCARB,DPGT,KS0,UKM1(15,15)
      REAL SOURG,KK,DELTH
      REAL Y(N),YPRIME(400),RPTS,G,DENSIN,KL0,CL0,HEXT,CC,MGIN,CAIN
      INTEGER MAIM1,MIIP1,MAJM1,MIJP1,GRIDR,GRIDZ,N,GRGZ,COORDTY
      INTEGER NLCC,NUCC,NCP
      COMMON/ONE/UKIN(15,15),WKK,CCACO3,CMGCO3,CARBDEN(15,15)
      COMMON/TWO/DELTR(60),DELTZ(60),GRIDR,GRIDZ,G,SHDENS
      COMMON/THREE/XFRAC,UWIN,KKER0,KHY0,CHY0,KW0,CW0,CK0,KMGC,KCAC
      COMMON/FOUR/DENS0,R,GMOLE,OMOLE,CC,DENSW,XPERMZ
      COMMON/SIX/GRGZ,DUW0(15,15)
      COMMON/SEVEN/CHAR(15,15)
      COMMON/EIGHT/CL0,KL0,CG0,T0I
      COMMON/TEN/DENSS(15,15),MGIN(15,15),CAIN(15,15),DENSIN(15,15)
      COMMON/ELEVEN/DELRAV(60),RIP1(60),RIM1(60),VOL(50,50)
      COMMON/SEVENT/TT(15,15),PM1(15,15)
      COMMON/TWELVE/CCARB,KCARB
      COMMON/FOURT/UMG(15,15),UCA(15,15)
      COMMON/EIGTT/XWEL,HEXT,FREQ
      COMMON/TWENTTH/UW0M1(15,15)
      COMMON/THITF/UKM1,UCAM1,UMGM1,XM1,XKM1(15,15)
      COMMON/TWENTT/NLCC,NUCC,NCP
      COMMON/TWENTF/HEIGHT,COORDTY,ZPTS(60),RPTS(60)
C
C     UK0 IS KEROGEN AT T,UKIN IS ORIGINAL  ,KK IS ARREN COEFF
C     GRIDR ,GRIDZ ARE GRID PTS
C
      DELTT=.01
      DELTS=.00010
      DELTY=.01
      DELTP=10.00
      DELTL=.0001
C
      CALL FCN(N,TI,Y,YPRIME)
C
      DO 1022 I=1,GRIDR
       DO 1023 J=1,GRIDZ
         DO 10 ITER2=1,GRIDR
          DO 20 ITER3=1,GRIDZ
           DO 2046 ITER4=1,NCP
C
      IITER=NCP*ITER3-(NCP-ITER4)+NCP*(ITER2-1)*GRIDZ
      II=NCP*J+NCP*(I-1)*GRIDZ
C
      IF(IITER.GT.II+NUCC)GO TO 2000
```

```
      IF(IITER.LT.II-NLCC  )GO TO 2000
      IF(IITER.LT.NUCC+II-3*NCP.AND.IITER.GT.II+3*NCP)GO TO 2000
      IF(IITER.GT.II-NUCC+3*NCP.AND.IITER.LT.II-3*NCP)GO TO 2000
C
      MAIM1=MAX(I-1,1)
      MIIP1=MIN(I+1,GRIDR)
      MAJM1=MAX(J-1,1)
      MIJP1=MIN(J+1,GRIDZ)
C
      INT=NCP*ITER3-2+NCP*(ITER2-1)*GRIDZ
      INS=NCP*ITER3-1+NCP*(ITER2-1)*GRIDZ
      INP=NCP*ITER3+NCP*(ITER2-1)*GRIDZ
      INY=NCP*ITER3-3+NCP*(ITER2-1)*GRIDZ
      INL=NCP*ITER3-4+NCP*(ITER2-1)*GRIDZ
C
      NL=NCP*J-4+NCP*(I-1)*GRIDZ
      NY=NCP*J-3+NCP*(I-1)*GRIDZ
      NT=NCP*J-2+NCP*(I-1)*GRIDZ
      NS=NCP*J-1+NCP*(I-1)*GRIDZ
      NP=NCP*J+NCP*(I-1)*GRIDZ
C
      OL(I,J)=Y(NL)
      UK(I,J)=Y(NY)
      T(I,J)=Y(NT)
      SG(I,J)=Y(NS)
      PG(I,J)=Y(NP)
C
      IF(I.NE.GRIDR)THEN
        OL(I+1,J)=Y(NCP*J-4+NCP*I*GRIDZ)
        UK(I+1,J)=Y(NCP*J-3+NCP*I*GRIDZ)
        T(I+1,J)=Y(NCP*J-2+NCP*I*GRIDZ)
        SG(I+1,J)=Y(NCP*J-1+NCP*I*GRIDZ)
        PG(I+1,J)=Y(NCP*J+NCP*I*GRIDZ)
      ENDIF
C
C
      IF(J.NE.GRIDZ)THEN
        OL(I,J+1)=Y(NCP*(J+1)-4+NCP*(I-1)*GRIDZ)
        UK(I,J+1)=Y(NCP*(J+1)-3+NCP*(I-1)*GRIDZ)
        T(I,J+1)=Y(NCP*(J+1)-2+NCP*(I-1)*GRIDZ)
        SG(I,J+1)=Y(NCP*(J+1)-1+NCP*(I-1)*GRIDZ)
        PG(I,J+1)=Y(NCP*(J+1)+NCP*(I-1)*GRIDZ)
      ENDIF
C
C
      IF(J.NE.1)THEN
        OL(I,J-1)=Y(NCP*(J-1)-4+NCP*(I-1)*GRIDZ)
        UK(I,J-1)=Y(NCP*(J-1)-3+NCP*(I-1)*GRIDZ)
        T(I,J-1)=Y(NCP*(J-1)-2+NCP*(I-1)*GRIDZ)
        SG(I,J-1)=Y(NCP*(J-1)-1+NCP*(I-1)*GRIDZ)
        PG(I,J-1)=Y(NCP*(J-1)+NCP*(I-1)*GRIDZ)
      ENDIF
C
      IF(I.NE.1)THEN
        OL(I-1,J)=Y(NCP*J-4+NCP*(I-2)*GRIDZ)
        UK(I-1,J)=Y(NCP*J-3+NCP*(I-2)*GRIDZ)
        T(I-1,J)=Y(NCP*J-2+NCP*(I-2)*GRIDZ)
        SG(I-1,J)=Y(NCP*J-1+NCP*(I-2)*GRIDZ)
        PG(I-1,J)=Y(NCP*J+NCP*(I-2)*GRIDZ)
       ENDIF
C
      IF(ITER4.EQ.2)THEN
       T(ITER2,ITER3)=Y(INT)+DELTT
      ENDIF
C
      IF(ITER4.EQ.3)THEN
```

```
        SG(ITER2,ITER3)=Y(INS)+DELTS
       ENDIF
C
       IF(ITER4.EQ.4)THEN
       PG(ITER2,ITER3)=Y(INP)+DELTP
       ENDIF
C
       IF(ITER4.EQ.1)THEN
        UK(ITER2,ITER3)=Y(INY)+DELTY
       ENDIF
C
       IF(ITER4.EQ.5)THEN
        OL(ITER2,ITER3)=Y(INL)+DELTL
       ENDIF
C
       OL0=OL(I,J)
       OLRP1=OL(MIIP1,J)
       OLRM1=OL(MAIM1,J)
       OLZM1=OL(I,MAJM1)
       OLZP1=OL(I,MIJP1)
       UK0=UK(I,J)
       T0=T(I,J)
       TIP1=(T(MIIP1,J)+T(I,J))/2.
       TIM1=(T(MAIM1,J)+T(I,J))/2.
       TJM1=(T(I,MAJM1)+T(I,J))/2.
       TJP1=(T(I,MIJP1)+T(I,J))/2.
       SG0=MIN(1.,SG(I,J))
       SGIM1=MIN(1.,(SG(MAIM1,J)+SG0)/2.)
       SGIP1=MIN(1.,(SG(MIIP1,J)+SG0)/2.)
       SGJP1=MIN(1.,(SG(I,MIJP1)+SG0)/2.)
       SGJM1=MIN(1.,(SG(I,MAJM1)+SG0)/2.)
       PG0=PG(I,J)
       PGIP1=(PG(MIIP1,J)+PG0)/2.
       PGIM1=(PG(MAIM1,J)+PG0)/2.
       PGJM1=(PG(I,MAJM1)+PG0)/2.
       PGJP1=(PG(I,MIJP1)+PG0)/2.
       DENSOI=DENSOIL(PG0)
       DENSIM1=DENSOIL(PGIM1)
       DENSIP1=DENSOIL(PGIP1)
       DENSJM1=DENSOIL(PGJM1)
       DENSJP1=DENSOIL(PGJP1)
       PL0=PG0-PC(I,J,1.-SG0)
       PLIM1=PGIM1-PC(I,J,1.-SGIM1)
       PLJP1=PGJP1-PC(I,J,1.-SGJP1)
       PLIP1=PGIP1-PC(I,J,1.-SGIP1)
       PLJM1=PGJM1-PC(I,J,1.-SGJM1)
       PL(MAIM1,J)=PG(MAIM1,J)-PC(I,J,1.-SG(MAIM1,J))
       PL(MIIP1,J)=PG(MIIP1,J)-PC(I,J,1.-
     1  SG(MIIP1,J))
       PL(I,MAJM1)=PG(I,MAJM1)-PC(I,J,1.-SG(I,MAJM1))
       PL(I,MIJP1)=PG(I,MIJP1)-PC(I,J,1.-
     1  SG(I,MIJP1))
       KKT0=KK(T0)
       UKIM1=(UK(MAIM1,J)+UK0)/2.
       UKIP1=(UK(MIIP1,J)+UK0)/2.
       UKJP1=(UK(I,MIJP1)+UK0)/2.
       UKJM1=(UK(I,MAJM1)+UK0)/2.
       KSIM1=WEIGPAR(KS(UK0,I,J),KS(UK0,I,J),I,2)
       KSIP1=WEIGPAR(KS(UK0,I,J),KS(UK0,I,J),I,1)
       KSJP1=WEIGPER(KS(UK0,I,J),KS(UK0,I,J),J,1)
       KSJM1=WEIGPER(KS(UK0,I,J),KS(UK0,I,J),J,2)
       CS0=CPS(T(I,J))
       KMG=KMGCO3(T0)
       KCA=KCACO3(T0)
       UMG0=UMGM1(I,J)/(1.+(TI-XM1)*KMG)
       UMG(I,J)=UMG0
```

```
      UCA0=UCAM1(I,J)/(1.+(TI-XM1)*KCA)
      UCA(I,J)=UCA0
      K0=KRR(T0,UK(I,J),UMG0,UCA0,I,J)
      KIP1=WEIGPAR(K0,KRR(T(MIIP1,J),UKIP1,UMG0,UCA0,MIIP1,J),I,1)
      KIM1=WEIGPAR(KRR(T(MAIM1,J),UKIM1,UMG0,UCA0,MAIM1,J),K0,I,2)
      KJP1=WEIGPER(K0,KRR(T(I,MIJP1),UKJP1,UMG0,UCA0,I,MIJP1),J,1)
      KJM1=WEIGPER(KRR(T(I,MAJM1),UKJM1,UMG0,UCA0,I,MAJM1),K0,J,2)
      MG0=PERMG(1.-SG0)
      MGZ0=MG0*XPERMZ
      ML0=PERML(1.-SG0)
      MLZ0=ML0*XPERMZ
      MLRM1=PERML(1.-SG(MAIM1,J))
      MLRP1=PERML(1.-SG(MIIP1,J))
      MLZP1=PERML(1.-SG(I,MIJP1))
     1 *XPERMZ
      MLZM1=PERML(1.-SG(I,MAJM1))
     1 *XPERMZ
      MGRM1=PERMG(1.-SG(MAIM1,J))
      MGRP1=PERMG(1.-SG(MIIP1,J))
      MGZP1=PERMG(1.-SG(I,MIJP1))
     1 *XPERMZ
      MGZM1=PERMG(1.-SG(I,MAJM1))
     1 *XPERMZ
      VSLIP1=WEIGPAR(VL(T0),VL(T(MIIP1,J)),I,1)
      VSLIM1=WEIGPAR(VL(T(MAIM1,J)),VL(T0),I,2)
      VSLJP1=WEIGPER(VL(T0),VL(T(I,MIJP1)),J,1)
      VSLJM1=WEIGPER(VL(T(I,MAJM1)),VL(T0),J,2)
      PH0=PHI(T0,UK0,UMG0,UCA0,I,J)
      DPHUK0=DPHUK(I,J)
      XDIFZ=1.
      KKT0=KK(T0)
      KMG=KMGCO3(T0)
      KCA=KCACO3(T0)
      KKT0=KK(T0)
      XDIFZ=1.
      UW0=UWOM1(I,J)
      XKDT0=XKDT(TI,I,J,T0,PG0,SG0)
      XKOG0= XKOILG(I,J,T0,PG0,SG0)*(1.-SG0+1.E-10)/(1.-SG0+1.E-4)
      XKDSG=-(1./(1.-SG0+1.E-4)-(1.-SG0+1.E-10)/(1.-SG0+1.E
     1 -4)**2)*XKOILG(I,J,T0,PG0,SG0)
      XKRP1=XKOILG(I,J,T(MIIP1,J),PG(MIIP1,J),SG0)
      XKRM1=XKOILG(I,J,T(MAIM1,J),PG(MAIM1,J),SG0)
      XKZP1=XKOILG(I,J,T(I,MIJP1),PG(I,MIJP1),SG0)
      XKZM1=XKOILG(I,J,T(I,MAJM1),PG(I,MAJM1),SG0)
      XKOGP0=XKDP(T0,PG0)
C
      WMOLE=(1.-OL0)*GMOLE+OL0*OMOLE
      WMRP1=(1.-OLRP1)*GMOLE+OLRP1*OMOLE
      WMRM1=(1.-OLRM1)*GMOLE+OLRM1*OMOLE
      WMZP1=(1.-OLZP1)*GMOLE+OLZP1*OMOLE
      WMZM1=(1.-OLZM1)*GMOLE+OLZM1*OMOLE
C
      DENSG=OMOLE*PG0/R/T0*OL0
C
C   COEFFICIENTS LEFT SIDE OF LIGHT OIL EQN.
C
C
      XA=VOL(I,J)*OMOLE/R/T0*PH0*SG0*PG0*(-1./T0)*OL0
     1 -VOL(I,J)*DENSOI*(1.-SG0)*PH0*OL0/XKOG0**2*XKDT0
C
      XB=VOL(I,J)*(OMOLE/R/T0*PH0*PG0*OL0-PH0*DENSOI*OL0/XKOG0
     1 -(1.-SG0)*PH0*DENSOI*OL0/XKOG0**2*XKDSG)
C
      XC=VOL(I,J)*PH0*(DDENSO(PG0)*(1.-SG0)*OL0/XKOG0 -
     1 (1.-SG0)*DENSOI*OL0/XKOG0**2*XKOGP0
     1 +OMOLE*OL0*SG0/R/T0)
```

```
C
      XCOL=VOL(I,J)*(OMOLE/R/TO*PHO*SGO*PGO
     1 +PHO*DENSOI*(1.-SGO)/XKOGO)
C
C  COEFFIENTS LEFT HAND SIDE OF HEAVY OIL EQN
C
C
        XF=VOL(I,J)*(-PHO*DENSOI*(1.-OLO/XKOGO)
     1 +(1.-SGO)*PHO*DENSOI*OLO/XKOGO**2*XKDSG)
C
        XU= VOL(I,J)*PHO*DENSOI*OLO/XKOGO**2*XKDTO*(1.-SGO)
C
        XV=VOL(I,J)*PHO*(1.-SGO)*(DDENSO(PGO)*(1.-OLO/XKOGO)
     1 +DENSOI*OLO/XKOGO**2*XKOGPO)
        XW=-VOL(I,J)*PHO*DENSOI*(1.-SGO)/XKOGO
C
C    LEFT HAND SIDE OF INERT GAS EQN.
C
        XL=VOL(I,J)*PHO*SGO*PGO*GMOLE/R/TO*(-1./TO*(1.-OLO))
        XM=VOL(I,J)*PHO*PGO*GMOLE/R/TO*(1.-OLO)
C
        XN= VOL(I,J)*PHO*SGO/R/TO*GMOLE*((1.-OLO))
C
        XO=-VOL(I,J)*PHO*SGO*PGO*GMOLE/R/TO
C
C
COEFFIENTS LEFT HAND SIDE OF HEAT EQN
C
C
        XH=VOL(I,J)*(PHO*(1.-SGO)*DENSOI*CLO+
     1 DENSS(I,J)*CSO+UCA(I,J)*CCACO3+UMG(I,J)*CMGCO3
     2  +CKO*UKO
     1 +CGO*SGO*PGO/R*PHO*TOI/TO/TO*WMOLE
     3 +CCARB*CHAR(I,J)+DENSS(I,J)*(TO-TOI)*DCS(TO))
C
        XI=VOL(I,J)*PHO*SGO*WMOLE/R/TO*CGO*(TO-TOI)
C
        XJ=XI/SGO*PGO-VOL(I,J)*DENSOI*PHO*CLO*(TO-TOI)
C
        XOL=VOL(I,J)*CGO*PHO*SGO*PGO/R*(OMOLE-GMOLE)*(TO-TOI)/TO
C
C
C
C
C    VELOCITES AT GRIDS ARE CALCULATED
C
         VGRM1=VELR(UPW(MGRM1,MGO,PG(MAIM1,J),PGO)*KIM1/VG(TIM1),
     1 PG(MAIM1,J),PGO
     2 ,PGJP1,PGJM1,PGIM1*WMOLE/R/TIM1,I,J,1)
C
         VGRP1=VELR(UPW(MGO,MGRP1,PGO,PG(MIIP1,J))*KIP1/VG(TIP1)
     1    ,PGO,PG(MIIP1,J),
     2 PGJP1,PGJM1,PGIP1*WMOLE/R/TIP1,I,J,2)
C
         VGZP1=VELZ(UPW(MGZO,
     1 MGZP1,PGO,PG(I,MIJP1))*KJP1/VG(TJP1)
     2    ,PGIM1,PGIP1,PG(I,MIJP1),PGO,PGJP1*WMOLE/R/TJP1,
     3 I,J,1)
C
         VGZM1=VELZ(UPW(MGZM1,MGZO,PG(I,MAJM1),PGO)*KJM1/VG(TJM1),
     1    PGIM1,PGIP1,PGO,PG(I,MAJM1),
     2 PGJM1*WMOLE/R/TJM1,I,J,2)
C
         VLRM1=VELR(UPW(MLRM1,MLO,PL(MAIM1,J),PLO)*KIM1/VSLIM1
     1  ,PL(MAIM1,J),PLO,
     2 PLJP1,PLJM1,DENSOI,I.J.1)
```

```
C
        VLRP1=VELR(UPW(MLO,MLRP1,PLO,PL(MIIP1,J))*KIP1/VSLIP1
     1   ,PLO,PL(MIN(I+1,
     2 GRIDR),J),PLJP1,PLJM1,DENSOI,I,J,2)
C
        VLZP1=VELZ(UPW(MLZO,
     1 MLZP1,PLO,PL(I,MIJP1))*KJP1/VSLJP1   ,
     2   PLIM1,PLIP1,PL(I,MIJP1),PLO,DENSOI,I,J,1)
C
        VLZM1=VELZ(UPW(MLZM1,MLZO,
     1  PL(I,MAJM1),PLO)*KJM1/VSLJM1,PLIM1,PLIP1,PLO,PL(I,MAJM1)
     2 ,DENSOI,I,J,2)
C
C     BOUNDARY CONDITIONS ON VELOCITIES
C
       IF (I .EQ. GRIDR) THEN
          VGRP1=0.0
          VLRP1=0.0
       ENDIF
C
       IF (J .EQ. 1) THEN
          VGZM1=0.0
          VLZM1=0.0
       ENDIF
C
       IF (J .EQ. GRIDZ) THEN
          VGZP1=0.0
          VLZP1=0.0
       ENDIF
C
C
       IF (I .EQ. 1) THEN
        VGRM1= PERMG(1.-SG(1,J) )*KIM1/VG(TIM1)
     1  *(-(PG(1,J)-1.E5))/((RPTS(2)-RPTS(1)))
        VLRM1= PERML(1.-SG(1,J) )*KIM1/VL(TIM1)
     1  *(-(PL(1,J)-1.E5))/((RPTS(2)-RPTS(1)))
       ENDIF
C
CALCULATES CONVECTION COEFFICIENTS (FEG,FWG,FSG,FNG,FNL,FSL,FEL,FWL)
C
        FEG=RIM1(I)*DELTZ(J)*VGRM1*UPW(PG(MAIM1,J)/T(MAIM1,J),PGO
     1  /TO,PG(MAIM1,J),PGO)/R
        FWG=RIP1(I)*DELTZ(J)*VGRP1*UPW(PGO/TO,PG(MIIP1,J)/
     1  T(MIIP1,J),PGO,PG(MIIP1,J))/R
        FNG=DELRAV(I)*VGZP1*UPW(PG(I,MIJP1)/T(I,MIJP1)
     1  ,PGO/TO,PG(I,MIJP1),PGO)/R
        FSG=DELRAV(I)*VGZM1*UPW(PGO/TO,PG(I,MAJM1)
     1  /T(I,MAJM1),PGO,PG(I,MAJM1))/R
        FEL=RIM1(I)*VLRM1*DELTZ(J)*DENSIM1
        FWL=RIP1(I)*VLRP1*DELTZ(J)*DENSIP1
        FNL=VLZP1*DENSJP1*DELRAV(I)
        FSL=VLZM1*DENSJM1*DELRAV(I)
C
C
       TCGIM1=WMOLE*CGO*(TIM1-TOI)
       TCLIM1=CLO*(TIM1-TOI)
       TCGIP1=WMOLE*CGO*(TIP1-TOI)
       TCLIP1=CLO*(TIP1-TOI)
       TCGJP1=WMOLE*CGO*(TJP1-TOI)
       TCLJP1=CLO*(TJP1-TOI)
       TCGJM1=WMOLE*CGO*(TJM1-TOI)
       TCLJM1=CLO*(TJM1-TOI)
C
COEFFIENTS RIGHT HAND SIDE OF LIGHT OIL EQN.
C
       XUK=.6585*UKO*KKTO
```

```
C
        XD= VOL(I,J)*(1.*XUK
     2-PHO*((1.-SGO)*DENSOI*KCOKEL(TO)*OLO/XKOGO
     3 +DENSG*KCOKEG(TO)*SGO))
     1 +FEG*OMOLE*UPW(OLRM1,OLO,PG(MAIM1,J),PGO)
     1 -FWG*UPW(OLO,OLRP1,PGO,PG(MIIP1,J))*OMOLE
     1 +FSG*OMOLE*UPW(OLZM1,OLO,PG(I,MAJM1),PGO)
     1 -FNG*OMOLE*UPW(OLO,OLZP1,PGO,PG(I,MIJP1))
C
     1 +FEL*(OLRM1/XKRM1+OLO/XKOGO)/2.
     1 -FWL*(OLRP1/XKRP1+OLO/XKOGO)/2.
     1 +FSL*(OLZM1/XKZM1+OLO/XKOGO)/2.
     1 -FNL*(OLZP1/XKZP1+OLO/XKOGO)/2.
     1+VOL(I,J)*OMOLE/R/TO*KKTO*DPHUKO*UKO*SGO*PGO*OLO
     1 +VOL(I,J)*DENSOI*(1.-SGO)*OLO/XKOGO*DPHUKO*UKO*KKTO
C
COEFFIENTS RIGHT HAND SIDE OF HEAVY OIL EQN.
C
        XG= VOL(I,J)*(0.*XUK
     2-PHO*((1.-SGO)*DENSOI*KCOKEL(TO)*(1.-OLO/XKOGO)))
     1 +FEL*(1.-(OLO/XKOGO+OLRM1/XKRM1)/2.)
     1 -FWL*(1.-(OLO/XKOGO+OLRP1/XKRP1)/2.)
     1 +FSL*(1.-(OLO/XKOGO+OLZM1/XKZM1)/2.)
     1 -FNL*(1.-(OLO/XKOGO+OLZP1/XKZP1)/2.)
     1 +VOL(I,J)*DENSOI*(1.-SGO)*DPHUKO*KKTO*UKO*(1.-OLO/XKOGO)
C
C   RIGHT HAND SIDE OF INERT GAS EQN
C
      XP=VOL(I,J)*SOURG(XUK,UCAO,UMGO,KCA,KMG,DUWO,DENSOI,TO,
     1 SGO,PHO,DENSG,XKOGO,OLO)
     1 + FEG*GMOLE*UPW(1.-OLO,1.-OLRM1,PGO,PG(MAIM1,J))
     1 - FWG*GMOLE*UPW(1.-OLO,1.-OLRP1,PGO,PG(MIIP1,J))
     1 + FSG*GMOLE*UPW(1.-OLO,1.-OLZM1,PGO,PG(I,MAJM1))
     1 - FNG*GMOLE*UPW(1.-OLO,1.-OLZP1,PGO,PG(I,MIJP1))
     1 +VOL(I,J)*PHO*(.25*(1.-SGO)*DENSOI*KCOKEL(TO)+.69*DENSG*SGO
     1 *KCOKEG(TO))
     1 +VOL(I,J)*DPHUKO*SGO*PGO*GMOLE/R/TO*KKTO*UKO*(1.-OLO)
C
C
COEFFIENTS RIGHT HAND SIDE OF HEAT EQN
C
C    QRP1,QZP1 ARE NEGATIVE
       QRM1=100./(2.*ACOS(-1.)*XWEL*.5)*(TO-TOI)/700.
       QRP1=-MAX(0.,10.*(TO-TOI))
       QZM1=MAX(0.,1.3*(TO-TOI))
       QZP1=MIN(0.,-10.*(TO-TOI)*.1)
C
       XE=1.E-50
       XK=VOL(I,J)*(SOURE(I,J,TO,FREQ,XWEL,TI)+DELTH(UKO,KKTO,
     1 DUWO(I,J),I,J))+(FEL*TCLIM1+FEG*TCGIM1)-(FNL*TCLJP1+FNG*
     2 TCGJP1)-(FWL*TCLIP1+FWG*TCGIP1)+(FSL*TCLJM1+FSG*TCGJM1)
     3+DELTZ(J)*FX(QRP1,KSIP1
     4 *(T(MIIP1,J)-TO)/(RPTS(MIIP1)-RPTS(I)+XE),I,J,2)*RIP1(I)
     5 -DELTZ(J)*FX(QRM1,KSIM1
     6 *(TO-T(MAIM1,J))/(RPTS(I)-RPTS(MAIM1)+XE),I,J,1)*RIM1(I)
     7 +DELRAV(I)*FX(QZP1,XDIFZ*KSJP1
     8 *(T(I,MIJP1)-TO)/(ZPTS(MIJP1)-ZPTS(J)+XE),I,J,3)
       XK=XK-DELRAV(I)*FX(QZM1,XDIFZ*KSJM1/(ZPTS(J)-ZPTS(MAJM1)+XE)
     A *(TO-T(I,MAJM1)),I,J,4)+VOL(I,J)*(CKO*(TO-TOI)*UKO*KKTO
     1 +KCA*UCAO*(TO-TOI)*CCACO3+KMG*UMGO*(TO-TOI)*CMGCO3-CCARB*
     1 (TO-TOI)*.171*UKO*KKTO
     1 -CCARB*PHO*(.31*SGO*DENSG*(TO-TOI)*KCOKEG(TO)+
     1 .75*(1.-SGO)*DENSOI*KCOKEL(TO)*(TO-TOI))+CGO*SGO*PGO*WMOLE
     1 /R*DPHUKO*KKTO*UKO*(TO-TOI)/TO)
C   CALCULATE PRIME COORD
C
```

```
      XUP=XU*XO -XW*XL
      XFP=XF*XO-XW*XM
      XVP=XV*XO-XW*XN
      XGP=XG*XO-XP*XW
C
C
C   THE JACOBIAN MATRIX (PD) IS CONTRUCTED IN THE FOLLOWING STEPS
C   THE DERIVATIVES OF THE TEMP (DTT), SATURATIONS OF GASES (DSGT),
C   OIL GAS (NY), AND PRESSURE (DPGT) WITH RESPECT TO THE INDEPENDENT
C    VARIABLES T, SG, YO, AND P.
C
C
        A1=XB*XU-XA*XF
        A2=XU*XC-XV*XA
        A3=XCOL*XU-XA*XW
         A4=XU*XD-XA*XG
         B1=XL*XB-XA*XM
         B2=XL*XC-XN*XA
         B3=XCOL*XL-XA*XO
         B4=XD*XL-XA*XP
         C1=XB*XH-XA*XJ
        C2=XH*XC-XI*XA
        C3=XCOL*XH-XA*XOL
        C4=XH*XD-XK*XA
        D1=B1*A2-A1*B2
        D2=B1*A3-A1*B3
          D3=A4*B1-A1*B4
        E1=A2*C1-A1*C2
          E2=C1*A3-A1*C3
          E3=A4*C1-C4*A1
          DLT=(D3*E1-E3*D1)/(D2*E1-D1*E2)
          DPGT=(E3-E2*DLT)/E1
          DSGT=(C4-C3*DLT-C2*DPGT)/C1
          DTT=(XD-XCOL*DLT-XC*DPGT-XB*DSGT)
     1 /XA
          DYT=-KKTO*UKO
C
C
         IF(ITER4.EQ.2)THEN
C
          IF(N*(INT-NT+NLCC)+NT.GT.0)THEN
           PD(N*(INT-NT+NLCC)+NT)=(DTT-YPRIME(NT))/DELTT
          ENDIF
C
          IF(N*(INT-NS+NLCC)+NS.GT.0)THEN
           PD(N*(INT-NS+NLCC)+NS)= (DSGT-YPRIME(NS))/DELTT
          ENDIF
C
          IF(N*(INT-NP+NLCC)+NP.GT.0)THEN
           PD(N*(INT-NP+NLCC)+NP)=(DPGT-YPRIME(NP))/DELTT
          ENDIF
C
          IF(N*(INT-NY+NLCC)+NY.GT.0)THEN
           PD(N*(INT-NY+NLCC)+NY)=(DYT-YPRIME(NY))/DELTT
          ENDIF
C
          IF(N*(INT-NL+NLCC)+NL.GT.0)THEN
           PD(N*(INT-NL+NLCC)+NL)=(DLT-YPRIME(NL))/DELTT
          ENDIF
C
         ELSE IF(ITER4.EQ.3)THEN
C
          IF(N*(INS-NT+NLCC)+NT.GT.0)THEN
           PD(N*(INS-NT+NLCC)+NT)=(DTT-YPRIME(NT))/DELTS
          ENDIF
C
```

```
          IF(N*(INS-NS+NLCC)+NS.GT.0)THEN
           PD(N*(INS-NS+NLCC)+NS )=(DSGT-YPRIME(NS))/DELTS
          ENDIF
C
          IF(N*(INS-NP+NLCC)+NP.GT.0)THEN
           PD(N*(INS-NP+NLCC)+NP)=(DPGT-YPRIME(NP))/DELTS
          ENDIF
C
          IF(N*(INS-NY+NLCC)+NY.GT.0)THEN
           PD(N*(INS-NY+NLCC)+NY)=(DYT-YPRIME(NY))/DELTS
          ENDIF
C
          IF(N*(INS-NL+NLCC)+NL.GT.0)THEN
           PD(N*(INS-NL+NLCC)+NL)=(DLT-YPRIME(NL))/DELTS
          ENDIF
C
         ELSE IF(ITER4.EQ.4)THEN
C
          IF(N*(INP-NT+NLCC)+NT.GT.0)THEN
           PD(N*(INP-NT+NLCC)+NT)=(DTT-YPRIME(NT))/DELTP
          ENDIF
C
          IF(N*(INP-NS+NLCC)+NS.GT.0)THEN
           PD(N*(INP-NS+NLCC)+NS)=(DSGT-YPRIME(NS))/DELTP
          ENDIF
C
          IF(N*(INP-NP+NLCC)+NP.GT.0)THEN
           PD(N*(INP-NP+NLCC)+NP)=(DPGT-YPRIME(NP))/DELTP
          ENDIF
C
          IF(N*(INP-NY+NLCC)+NY.GT.0)THEN
           PD(N*(INP-NY+NLCC)+NY)=(DYT-YPRIME(NY))/DELTP
          ENDIF
C
          IF(N*(INP-NL+NLCC)+NL.GT.0)THEN
           PD(N*(INP-NL+NLCC)+NL)=(DLT-YPRIME(NL))/DELTP
          ENDIF
         ELSE IF(ITER4.EQ.5)THEN
C
          IF(N*(INL-NT+NLCC)+NT.GT.0)THEN
           PD(N*(INL-NT+NLCC)+NT)=(DTT-YPRIME(NT))/DELTL
          ENDIF
C
          IF(N*(INL-NS+NLCC)+NS.GT.0)THEN
           PD(N*(INL-NS+NLCC)+NS)=(DSGT-YPRIME(NS))/DELTL
          ENDIF
C
          IF(N*(INL-NP+NLCC)+NP.GT.0)THEN
           PD(N*(INL-NP+NLCC)+NP)=(DPGT-YPRIME(NP))/DELTL
          ENDIF
C
          IF(N*(INL-NY+NLCC)+NY.GT.0)THEN
           PD(N*(INL-NY+NLCC)+NY)=(DYT-YPRIME(NY))/DELTL
          ENDIF
C
          IF(N*(INL-NL+NLCC)+NL.GT.0)THEN
           PD(N*(INL-NL+NLCC)+NL)=(DLT-YPRIME(NL))/DELTL
          ENDIF
C
         ELSE IF(ITER4.EQ.1)THEN
C
          IF(N*(INY-NT+NLCC)+NT.GT.0)THEN
           PD(N*(INY-NT+NLCC)+NT)=(DTT-YPRIME(NT))/DELTY
          ENDIF
C
          IF(N*(INY-NS+NLCC)+NS.GT.0)THEN
```

```
          PD(N*(INY-NS+NLCC)+NS)=(DSGT-YPRIME(NS))/DELTY
         ENDIF
C
         IF(N*(INY-NP+NLCC)+NP.GT.0)THEN
          PD(N*(INY-NP+NLCC)+NP)=(DPGT-YPRIME(NP))/DELTY
         ENDIF
C
         IF(N*(INY-NY+NLCC)+NY.GT.0)THEN
          PD(N*(INY-NY+NLCC)+NY)=(DYT-YPRIME(NY))/DELTY
         ENDIF
C
         IF(N*(INY-NL+NLCC)+NL.GT.0)THEN
          PD(N*(INY-NL+NLCC)+NL)=(DLT-YPRIME(NL))/DELTY
         ENDIF
C
        ENDIF
C
C
 2000       CONTINUE
 2046      CONTINUE
 20       CONTINUE
 10      CONTINUE
 1023  CONTINUE
 1022 CONTINUE
        RETURN
        END
C
*************************************************************
C
*************************************************************
C    EQUILIBRIUM CONSTANT FOR OIL
       REAL FUNCTION XKOILG(I,J,T,P,S)
       REAL T,P
C
C
       XKOILG=EXP(12.12-6538./(T*1.8-167.))/P*1.E5/14.7
C
       RETURN
       END
C
*************************************************************
C
C DERIVATIVE OF OIL K CONSTANT WITH RESPECT TO TEMPERATURE
       REAL FUNCTION XKDT(TI,I,J,T,P,S)
       REAL T,P,UKM1(15,15),UCAM1(15,15),UMGM1(15,15)
       COMMON/SEVENT/TT(15,15),PM1(15,15)
       COMMON/THITF/UKM1,UCAM1,UMGM1,XM1,XKM1(15,15)
C
       XKDT=EXP(12.12-6538./(T*1.8-167.))/P*1.E5/14.7
     1 *6538.*1.8/(T*1.8-167.)**2
      RETURN
      END
C
*************************************************************
C  DERIVATIVE WITH RESPECT TO PRESSURE OF K CONSTANT
C
       REAL FUNCTION XKDP(T,P)
       REAL T,P
C
         XKDP=-EXP(12.12-6538./(T*1.8-167.))/(P**2)*1.E5/14.7
        RETURN
        END
C
*************************************************************
C
C DENSITY OF OIL
```

```
      REAL FUNCTION DENSOIL(P)
      REAL DENSO,R,GMOLE,OMOLE,CC,DENSW,XPERMZ
      COMMON/FOUR/DENSO,R,GMOLE,OMOLE,CC,DENSW,XPERMZ
C
      DENSOIL=DENSO*EXP(MAX(1.E-5,1.E-5*14.5*(P/1.E5-1.)))
C
      RETURN
      END
C
*****************************************************************
C DERIVATIVE OF DENSITY OF OIL WITH RESPECT TO PRESSURE
      REAL FUNCTION DDENSO(P)
      REAL DENSO,R,GMOLE,OMOLE,CC,DENSW,XPERMZ
      COMMON/FOUR/DENSO,R,GMOLE,OMOLE,CC,DENSW,XPERMZ
C
      DDENSO=DENSO*EXP(MAX(1.E-10,1.E-5*14.5*(P/1.E5-1.)))*1.E-10*14.5
      RETURN
      END
C
C*************************************************************
C RATE CONSTANT FOR COKE OF LIQUID OIL
C
      REAL FUNCTION KCOKEL(T)
C
      KCOKEL=3.1E7*EXP(-67681./T)
C
      RETURN
      END
C
*************************************************************
C
C  RATE CONSTANT FOR COKE OF OIL IN GAS PHASE
      REAL FUNCTION KCOKEG(T)
C
      KCOKEG=4.8E8*EXP(-69340./T)
C
      RETURN
      END
C
C*************************************************************************
C   CALCULATES POWER MATRIX
C
      SUBROUTINE ELECP(FREQ,XQL,XIO,GRIDR,GRIDZ,FIELD)
      REAL A,OMEGA,R,Z,FIELD(35,35),XP,XDBLIN,L
      REAL B,IO,MU,FREQ,DIA,DD,LO
      INTEGER GRIDR,GRIDZ
      COMPLEX EPSOL,SIMP,ELEC,CTEMP,FIELDS,CEPSOL,K
       COMMON/TWENTF/HEIGHT,COORDTY,ZPTS(60),RPTS(60)
      COMMON /ONEE/IO,MU,DIA,LO
      COMMON/SIXX/EPSOL,OMEGA, QL
C
      IO=XIO
C
C
      DATA C/3.E8/
      DATA DIA/.01/
C
      XSCALE =1.0
C
          XB=QL/4.*LO
C
C
C
      K=CSQRT(OMEGA**2*EPSOL*MU)
C
C
```

```
C
        DO 89 I=1,GRIDR*2
         DO 90 J=1,2*GRIDZ
C
C
           CTEMP=FIELDS(RPTS(I),0.0,ZPTS(GRIDZ)-ZPTS(J),EPSOL,OMEGA,QL)
C
C
C
          FIELD(I,J)=-1./2.*OMEGA*AIMAG(EPSOL)*CTEMP
         FIELD(I,J)=1.E7
 90      CONTINUE
 89     CONTINUE
C
C
      RETURN
      END
C*************************************************************
C
C
C   CALCULATES INTEGRAND FOR ELECTRIC FIELD INTEGRAL
       COMPLEX FUNCTION ELEC(XP,X,YP,Y,ZP,Z,QL,OMEGA,EPSOL)
       REAL X,Y,Z,QL,OMEGA,MU ,IO,DIA,DD,LO,ZP
       COMPLEX EPSOL ,K,ER,EZ,IMA
       COMMON /ONEE/IO,MU,DIA,LO
C
       IMA=(0.,1.)
C
       XT= SQRT((X-XP)**2+(Y-YP)**2+(Z-ZP)**2)
C
      K=CSQRT(OMEGA**2*EPSOL*MU)
C
       ELEC = -1./4/ACOS(-1.)*IMA*OMEGA*MU*CEXP(-IMA*K
     1  *XT)/XT*CSIN(K*(QL/8.*LO-ABS(ZP)))*IO
C
       RETURN
       END
CCCCCCCCCCCCCCCCCCCCCCCCCCCCCCCCCCCCCCCCCCCCCCCCCCCCCCCCCC
C  INTEGRATES A COMPLEX FUNCTION OVER REAL LIMITS
      COMPLEX FUNCTION SIMP(XP,YP,A,B,M,X,Y,Z,QL,OMEGA,EPSOL)
      REAL A,B,ZR(50),QL,OMEGA,L,IO,MU,DIA,DD,LO
      INTEGER ITER
      COMPLEX EPSOL,K,I2,F,ELEC
      COMMON/FIVE/ZR
C
C
      H=(B-A)/(FLOAT(M)-1.)
      I2=0.0
      DO 5 I=1,M
C
         ZR(I)=A+FLOAT(I-1)*H
C
         IF((I-1).EQ.0)THEN
           I2=I2+ELEC(XP,X,YP,Y,ZR(1),Z,QL,OMEGA,EPSOL)
            GO TO 5
         ELSEIF((I-1).EQ.M-1)THEN
           I2=I2+ELEC(XP,X,YP,Y,ZR(M),Z,QL,OMEGA,EPSOL)
           GO TO 5
         ELSEIF(2*(I/2).EQ.I)THEN
           I2=I2+ELEC(XP,X,YP,Y,ZR(I),Z,QL,OMEGA,EPSOL)*4.
C
         GO TO 5
C
         ENDIF
          I2=I2+2.*ELEC(XP,X,YP,Y,ZR(I),Z,QL,OMEGA,EPSOL)
   5     CONTINUE
```

```
        SIMP=1./3.*H*I2
      RETURN
      END
C
C*************************************************************
C  CALCULATES ELECTRIC FIELDS
C
      COMPLEX FUNCTION FIELDS(X,Y,Z,EPSOL,OMEGA,QL)
      REAL IO,MU,DIA,DD,QL,X,Y,Z,OMEGA,LO
      COMPLEX K,EZ,EY,EPSOL,EX,IMA
C
      COMMON /ONEE/IO,MU,DIA,LO
       COMMON/EIGTT/XWEL,HEXT,FREQ
C
C
C
C
      DATA C/3.E8/
      DATA DIA/.01/
C
      XSCALE =1.0
C
C
      XB=QL/4.*LO
C
C
C
            IMA=(0.,1.)
      K=CSQRT(OMEGA**2*EPSOL*MU)
C
       XT=SQRT(X**2+(Z-XB/2.)**2)
       XT2=SQRT(X**2+(Z+XB/2.)**2)
        R=SQRT(X**2+Z**2)
             EX=IMA*CSQRT(MU/EPSOL)*IO/4./ACOS(-1.)/X
     1    *((Z-XB/2.)*CEXP(-IMA*K*XT)/XT+(Z+XB/2.)*CEXP(-IMA*K*XT2)/XT2
     2    -2.*Z*CCOS(K*XB/2.)*CEXP(-IMA*K*R)/R)
C
       EZ=-IMA*CSQRT(MU/EPSOL)*IO/4./ACOS(-1.)*(CEXP(-IMA*K*XT)/XT
     1  +CEXP(-IMA*K*XT2)/XT2-2.*CCOS(K*XB/2.)*CEXP(-IMA*K*R)/R)
C
C
C
       FIELDS=CABS(EX)**2+CABS(EZ)**2
      RETURN
      END
C
*************************************************************
C
C  CALCULATES POWER DUE TO ELECTRIC FIELDS
       REAL FUNCTION EPOWER(X,Z)
       REAL OMEGA,QL
       INTEGER COORDTY
       COMPLEX FIELDS,EPSOL
       COMMON/TWENTF/HEIGHT,COORDTY,ZPTS(60),RPTS(60)
       COMMON/SIXX/EPSOL,OMEGA,QL
C
       IF(COORDTY.EQ.2.OR.COORDTY.EQ.4)THEN
        XTEMP=1.
       ELSE
        XTEMP=2.*ACOS(-1.)*X
       ENDIF
C
      EPOWER=-.5*AIMAG(EPSOL)*OMEGA*FIELDS(X,.0001,Z,EPSOL,OMEGA
     1 ,QL)*XTEMP
C
       RETURN
```

```
      END
C
*****************************************************************
C   Y LIMITS FOR IMSL ROUTINE DBLIN
C
      REAL FUNCTION  AY(X)
       REAL HEIGHT
       INTEGER GRIDR,GRIDZ,COORDTY
       COMMON/TWO/DELTR(60),DELTZ(60),GRIDR,GRIDZ,G,SHDENS
       COMMON/TWENTF/HEIGHT,COORDTY,ZPTS(60),RPTS(60)
      AY=-ZPTS(GRIDZ)
      RETURN
      END
C
*****************************************************************
C  Y LIMITS FOR IMSL ROUTINE DBLIN
C
      REAL FUNCTION  BY(X)
      BY = .00
      RETURN
      END
C
      REAL FUNCTION  AAY(X)
       REAL HEIGHT
       INTEGER GRIDR,GRIDZ,COORDTY
       COMMON/TWO/DELTR(60),DELTZ(60),GRIDR,GRIDZ,G,SHDENS
       COMMON/TWENTF/HEIGHT,COORDTY,ZPTS(60),RPTS(60)
      AAY=-20.*ZPTS(GRIDZ)
      RETURN
      END
C
      REAL FUNCTION  BBY(X)
       REAL HEIGHT,COORDTY
       COMMON/TWENTF/HEIGHT,COORDTY,ZPTS(60),RPTS(60)
      BBY = 0.0
      RETURN
      END
C
*****************************************************************
C   CALCULATES RADIATION RESITANCE OF THE ANTENNA
       REAL FUNCTION RRESIS(Z)
      COMPLEX EPSOL
      COMMON /ONEE/XIO,XMU,DIA,XLO
      COMMON/SIXX/EPSOL,OMEGA,XQL
C
      XB=XQL/4.*XLO
      XK=2.*ACOS(-1.)/XLO
      RRESIS=60.*(COS(XK*XB/2.*Z)-COS(XK*XB/2.))**2 /(1.-Z*Z)/2.
     1 /SQRT(REAL(EPSOL)/8.85E-12)
       RETURN
       END
C
*****************************************************
C  CALCULATES COORDINATES, AND GRID BLOCK BOUNDARIES
       SUBROUTINE COORD(RPTS,VOL,RIP1,RIM1,DELRAV,DELTR,ZPTS
     1  ,TOLVOL,HEIGHT,DELTZ,GRIDR,GRIDZ,COORDTY,XWEL,RMAX,UKIN,UWIN
     1 ,UKTOL,UWTOL)
       REAL VOL(50,50),DELTR(60),DELTZ(60),RPTS(60),RIP1(60)
       REAL RIM1(60),DELRAV(60),ZPTS(60),UKIN(15,15)
      REAL RIP11(60),RIM11(60)
       INTEGER GRIDR,GRIDZ,COORDTY
C
       HEIGHT=0.0
C
       DO 59 I=1,GRIDZ
        HEIGHT=HEIGHT+DELTZ(I)
```

```
 59    CONTINUE
C
      IF  (COORDTY .EQ. 1) THEN
C
C
C        SET UP RADIAL CORDINATES
C
       RPTS(1)=XWEL
C
           DO 1144 I=1,2*GRIDR
                RPTS(I+1)=RPTS(I)*(RMAX/XWEL)**(1./(GRIDR-1))
 1144      CONTINUE
C
C
           DO 2222 J=1,GRIDZ
               VOL(1,J)=((RPTS(2)**2-RPTS(1)**2)/ALOG((RPTS(2)/RPTS(1))
     1         **2)-RPTS(1)    **2)*DELTZ(J)*.5
 2222      CONTINUE
C
C
           DO 4444 I=2,GRIDR*2
           DO 5 J=1,GRIDZ
C
               VOL(I,J)=.5*DELTZ(J)*((RPTS(I+1)**2-RPTS(I)**2)/
     1         ALOG((RPTS(I+1)/RPTS(I))**2) - (RPTS(I)**2-RPTS(I-1)**2)
     2      /   ALOG((RPTS(I)/RPTS(I-1))** 2))
C
  5        CONTINUE
 4444      CONTINUE
C
C          RIP1 IS THE RADIAL COORDINATE OF THE EAST SIDE OF THE
C          CONTROL VOLUME,RIM1 IS ON THE WELL SIDE OF CONTROL VOLUME
C
           RIP1(1)=(RPTS(2)-RPTS(1))/ALOG(RPTS(2)/RPTS(1))
           RIM1(1)=RPTS(1)
           RIP1(GRIDR)=RPTS(GRIDR)
           RIM1(GRIDR)=(RPTS(GRIDR)-RPTS(GRIDR-1))/ALOG(
     1     RPTS(GRIDR)/RPTS(GRIDR-1))
C
           DO 6666 I=2,GRIDR*2
               RIP1(I)=(RPTS(I+1)-RPTS(I))/ALOG(RPTS(I+1)/RPTS(I))
               RIM1(I)=(RPTS(I)-RPTS(I-1))/ALOG(RPTS(I)/RPTS(I-1))
 6666      CONTINUE
C
C
           DO 159 J=1,GRIDZ
              VOL(GRIDR,J)=DELTZ(J)*(RIP1(GRIDR)-RIM1(GRIDR-1))*
     1        (RIP1(GRIDR)+RIM1(GRIDR-1))/2.
 159       CONTINUE
C
           DO 143 I=1,GRIDR*2
             DO 348 J=1,GRIDZ
               DELRAV(I)=VOL(I,J)/DELTZ(J)
               DELTR(I)=(RIP1(I)-RIM1(I))
 348         CONTINUE
 143       CONTINUE
C
      ELSE IF  ( COORDTY .EQ. 2 ) THEN
C
C
           XTEMP=XWEL
           DO 7 I=2,GRIDR*2
               RPTS(I-1)=XTEMP
               XTEMP=XTEMP+ABS(DELTR(I))
   7       CONTINUE
C
```

```
            RPTS(GRIDR)=RMAX
C
C
            DO 62 I=1,GRIDR
             DELRAV(I)=DELTR(I)
  62        CONTINUE
C
            DO 13 II=1,GRIDR
            IF(II.EQ.1)THEN
              RIM1(1)=1.
              RIP1(1)=1.
            ELSE IF(II.EQ.GRIDR)THEN
              RIM1(GRIDR)=1.
              RIP1(GRIDR)=1.
            ELSE
              RIP1(II)=1.
              RIM1(II)=1.
            ENDIF
  13        CONTINUE
C
C            CONSTRUCT VOLUME ELEMENT
C
            DO 8 I=1,GRIDR*2
             DO 469 J=1,GRIDZ
              VOL(I,J)=DELTR(I)*DELTZ(J)
  469        CONTINUE
  8         CONTINUE
            TOLVOL=0.0
C
            DO 7666 I=1,GRIDR
              DO 7667 J=1,GRIDZ
                TOLVOL=TOLVOL+VOL(I,J)
 7667         CONTINUE
 7666       CONTINUE
C
      ELSE IF ( COORDTY .EQ. 3 .OR. COORDTY .EQ. 4)THEN
C
            IF(COORDTY.EQ.4)THEN
C
C
             HEIGHT=0.0



C
             DO 599 I=1,GRIDZ
               HEIGHT=HEIGHT+DELTZ(I)
 599         CONTINUE
C
C  SET UP R CORDINATES
C
             XTEMP=XWEL
             DO 789 I=2,GRIDR*2
               RPTS(I-1)=XTEMP
               XTEMP=XTEMP+ABS(DELTR(I))
 789         CONTINUE
C
             RPTS(GRIDR) = RMAX
C
         ENDIF
C
C
        IF(COORDTY.EQ.3)THEN
C
           RPTS(1)=XWEL
             DO 1111 I=1,GRIDR*2
```

```
                RPTS(I+1)=RPTS(I)*(RMAX/XWEL)**(1./(GRIDR-1))
 1111         CONTINUE
        ENDIF
C
             DO 234 II=1,GRIDR*2
C
             IF(II.EQ.1)THEN
              RIM11(1)=RPTS(1)
              RIP11(1)=SQRT((RPTS(2)**2-RPTS(1)**2)/2./ALOG(
     1 RPTS(2)/RPTS(1)))
             ELSE IF(II.EQ.GRIDR)THEN
          RIM11(GRIDR)=SQRT((RPTS(GRIDR)**2-RPTS(GRIDR-1)**2)/2./ALOG(
     1 RPTS(GRIDR)/RPTS(GRIDR-1)))
              RIP11(GRIDR)=RPTS(GRIDR)
             ELSE
          RIM11(II)=SQRT((RPTS(II)**2-RPTS(II-1)**2)/2./ALOG(
     1 RPTS(II)/RPTS(II-1)))
          RIP11(II)=SQRT((RPTS(II+1)**2-RPTS(II)**2)/2./ALOG(
     1 RPTS(II+1)/RPTS(II)))
             ENDIF
C
 234       CONTINUE
        DO 411 I=1,GRIDR*2
C
        IF(I.EQ.1)THEN
        RIP1(I)=(RPTS(I+1)-RPTS(I))/ALOG(RPTS(I+1)/RPTS(I))
        RIM1(I)=RPTS(1)
       ELSE IF(I.EQ.GRIDR)THEN
       RIP1(GRIDR)=RPTS(GRIDR)
       RIM1(I)=(RPTS(I)-RPTS(I-1))/ALOG(RPTS(I)/RPTS(I-1))
        ELSE
        RIP1(I)=(RPTS(I+1)-RPTS(I))/ALOG(RPTS(I+1)/RPTS(I))
       RIM1(I)=(RPTS(I)-RPTS(I-1))/ALOG(RPTS(I)/RPTS(I-1))
        ENDIF
C
 411         CONTINUE
C
             DO 977 J=1,GRIDR*2
               DELTR(J)=(RIP11(J)-RIM11(J))
               DELRAV(J)=RPTS(J)*DELTR(J)
 977         CONTINUE
C
C  CONSTRUCT VOLUME ELEMENT
C
             DO 768 I=1,GRIDR*2
             DO 9 J=1,4*GRIDZ
               VOL(I,J)= (RIP11(I)**2-RIM11(I)**2)*DELTZ(J)/2.
  9          CONTINUE
  768        CONTINUE
C
       ENDIF
C
C
           ZPTS(1)=0.0
           DO 755 I=1,3*GRIDZ
            ZPTS(I+1)=ZPTS(I) + DELTZ(I+1)
 755       CONTINUE
           ZPTS(GRIDZ)=HEIGHT
C
           TTOLVOL=0.0
           DO 5666 I=1,GRIDR
           DO 5667 J=1,GRIDZ
            TTOLVOL=TTOLVOL+VOL(I,J)*2.*ACOS(-1.)
 5667      CONTINUE
 5666      CONTINUE
C
```

```
      IF(COORDTY.EQ.1.OR.COORDTY.EQ.3.OR.COORDTY.EQ.4)THEN
C
       PRINT*,'TOTAL VOLUME OF RETORT REGION(COORD=1,3,4) =',TTOLVOL
C
      ENDIF
C
C
      UWTOL=0.0
      UKTOL=0.0
      DO 922 I=1,GRIDR
       DO 923 J=1,GRIDZ
C
        IF(COORDTY.EQ.1.OR.COORDTY.EQ.3.OR.COORDTY.EQ.4)THEN
          UKTOL=UKTOL+UKIN(I,J)*VOL(I,J)*2.*ACOS(-1.)
          UWTOL=UWTOL+UWIN*VOL(I,J)*2.*ACOS(-1.)
        ELSE IF(COORDTY.EQ.2)THEN
          UKTOL=UKTOL+UKIN(I,J)*VOL(I,J)
          UWTOL=UWTOL+UWIN*VOL(I,J)
        ENDIF
C
 923    CONTINUE
 922    CONTINUE
C
C
C    PRINT OUT THE RADIAL GRID POINTS
C
      PRINT*,'THE RADIAL GRID POINTS ARE'
      PRINT*,'-------------------------'
C
      DO 1331 I=1,GRIDR
       PRINT*,RPTS(I)
      WRITE(17,3067) RPTS(I)
 1331 CONTINUE
C
      PRINT*,'THE AXIAL GRID POINTS ARE'
      PRINT*,'-------------------------'
C
      DO 1132 I=1,GRIDZ
       PRINT*,ZPTS(I)
 1132 CONTINUE
C
      PRINT*,'THE DELTR ARE='
      PRINT*,'--------------'
C
      DO 3389 I=1,GRIDR
       PRINT*,DELTR(I)
 3389 CONTINUE
C
      PRINT*,'THE DELTZ ARE'
      PRINT*,'-------------'
C
      DO 3354 I=1,GRIDZ
       PRINT*,DELTZ(I)
     WRITE(16,3067)DELTZ(I)
 3067 FORMAT(E12.5)
 3354 CONTINUE
C
      PRINT*,'THE OUTER BOUNDARY OF CONTROL VOLUMES(RIP1)'
      PRINT*,'-------------------------------------------'
C
      DO 3655 I=1,GRIDR
       PRINT*,RIP1(I)
 3655 CONTINUE
C
      PRINT*,'THE INNER BOUNDARY OF CONTROL VOLUMES ARE(RIM1)'
      PRINT*,'-------------------------------------------'
```

```
C
      DO 7623 I=1,GRIDR
       PRINT*,RIM1(I)
 7623  CONTINUE
      RETURN
      END
C
C*******************************************************
C
C  SET UP KEROGEN CONCENTRATION IN SHALE (KG./CUBIC METER) AT
      SUBROUTINE SETKER(UKIN,GRIDR,GRIDZ)
      REAL UKIN(15,15)
      INTEGER GRIDR,GRIDZ,COORDTY
C
C  AT EACH GRID POINT OF THE OIL SHALE BED
C
      DO 4 I=1,GRIDR
C
      DO 577 J=1,GRIDZ
C
         IF (J .EQ. 1) THEN
              UKIN(I,J)=250.
           ELSE IF (J .EQ. 2) THEN
              UKIN(I,J)=250.
           ELSE IF (J .EQ. 3) THEN
              UKIN(I,J)=250.
           ELSE IF (J .EQ. 4) THEN
              UKIN(I,J)=250.
           ELSE IF (J .EQ. 5) THEN
              UKIN(I,J)=250.
           ELSE IF (J .EQ. 6) THEN
              UKIN(I,J)=250.
           ELSE IF (J .EQ. 7) THEN
              UKIN(I,J)=250.
           ELSE IF (J .EQ. 8) THEN
              UKIN(I,J)=250.
           ELSE IF (J .EQ. 9) THEN
              UKIN(I,J)=250.
         ENDIF
C
  577  CONTINUE
C
 4     CONTINUE
C
C
C
      RETURN
     END
2
2
2
2
2
2
2
2
2
2
2
2
2
2
2
2
2
1
1
```

PROGRAM NAME: MOMENT

DESCRIPTION: Simulates electromagnetic field around a single monopole antenna

DEVELOPED BY: J. Baker-Jarvis, University of Wyoming Physics Department

SUBROUTINE MOMENT

This subroutine calculates the current distribution on a monopole antenna fed from a coaxial line. The routine also calculates the field distribution due to the current distribution by integrating the appropriate expression numerically. A flow chart of the system is given in Fig. E5.

Important parameters:

Epsol	dielectric constant
Omega	angular frequency
IO	current in amps
Freq	frequency in hertz
gridr,gridz	number of grid points
k	wave number
xlam	wavelength
xlength	length of monopole in meters
field	2 dimensional array of power at grid points
moment	subroutine that calculates current on antenna
elecp	subroutine that calculates power
simp	complex integration routine
elecc	subroutine that has field kernals for integration
powerin	subroutine that calculates grid points

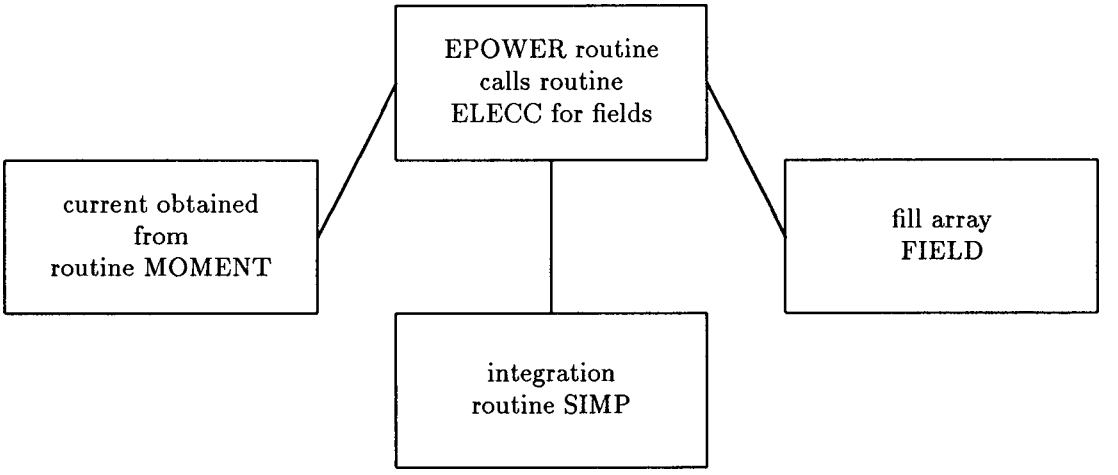

Figure E5. Flow chart of subroutine MOMENT.

```
copy,field1
      PROGRAM CURENT(INPUT,OUTPUT,TAPE7,TAPE8,TAPE111,TAPE17,TAPE27)
C   THIS PROGRAM CALCULATES THE ELECTRIC FIELDS DUE TO A MONOPOLE
C   ANTENNA EMBEDDED IN A DIELECTRIC MEDIA.  THE CURRENT DISTRIBUTION
C   IS SOLVED FOR USING POCKLINGTON'S EQUATION.  THE CURRENT DISTRIBUTION
C   IS THEN INTEGRATED TO FIND BOTH NEAR AND FAR FIELDS.
C
C
      REAL MU,LO,DELTZ,DELTZM(300),VOL(150,150),ZZPTS(150),RRPTS(150)
      REAL Z(300),RPTS(10),ZPTS(10),FIELD(10,10),YYY(100)
      COMPLEX EPSOL,A,AA(39,39),BB(39),K,CT,FUNC,W,INTE,KK(300)
      COMPLEX CURR,IC(300),B,B2,IMA
      INTEGER GRIDR,GRIDZ
      EXTERNAL AY,BY,ELECP,EPOWER,POYNT
      COMMON/FOUR/K
      COMMON /ONEE/IO,MU,DIA,LO
      COMMON/CNSTNS/ADIA,A2,B,B2,IMA,BDIA
      COMMON/FIVEE/XLENGTH,XVOLT
      COMMON/THREE/ZN(300),N,IC
      COMMON/SIX/XB
      COMMON/TWO/OMEGA,EPSOL,FREQ
      COMMON/SEVEN/DELTZ
C
      EPSOL=(1.0,-.000)*8.85E-12
      DATA IO/1./,FREQ/2.45E9/
      DATA BB/39*(0.0,0.0)/,ZN/300*0.0/
      V=1.
C   ENTER NUMBER OF MATCH POINTS
C
      N=101
      OMEGA=2.*ACOS(-1.)*FREQ
      MU=4.*ACOS(-1.)*1.E-7
      K=CSQRT(OMEGA**2*EPSOL*MU)
3067 FORMAT(E12.5)
      GRIDR=6
      GRIDZ=7
      IFLAG=1

C
      CALL POWERIN(.01,GRIDR,GRIDZ,1.,1.,VOL,RPTS,ZPTS)
C
      XI=3.
      XVOLT=1.00000
      XLAM=2.*ACOS(-1.)/REAL(K)
      XLENGTH=XLAM*.1875*2.
      XB=XLENGTH
      XMIN=1.E29
C
C   THE RADIUS OF MONOPOLE IS 'A'
C
     ADIA=.00317*XLAM
C
C   THE RADIUS OF COAXIAL LINE IS 'BDIA'
C
     BDIA=1.868*ADIA
     XMAX=0.0
C
C
      LO = 2.*ACOS(-1.)/SQRT(OMEGA**2*REAL(EPSOL)*MU)
      PRINT*,'LO=',LO
C   CALL PROGRAM TO CALCULATE CURRENT DISTRIBUTION
      CALL MOMENT(N)
      DO 671 I=1,N
      READ(99,502) ZN(I)
```

```
 502   FORMAT(E12.5)
 671   CONTINUE
 501   FORMAT(I5)
C
       PRINT*,'THE MONOPOLE LENGTH=  ',XLENGTH/2.
       PRINT*,'THE INNER RADIUS= ',ADIA,'OUTER RAD= ',BDIA
       PRINT*,'KA=',K*ADIA
       PRINT*,'K=',K
       XB=XLENGTH
       PRINT*,'KL=',K*XB/2.
C
       XK=REAL(K)
C
       DO 77 I=1,N
        READ(77,504) IC(I)
  504   FORMAT(2E12.5)
       IC(I)=IC(I)
 77    CONTINUE
C
C
C
      ICC=1
        DO 333 I=1,GRIDR
          DO 222 J=1,GRIDZ
           FIELD(I,J)=EPOWER(RPTS(I),ZPTS(GRIDZ+1-J)+.002)/2./ACOS(-1.)
         PRINT*,'FIEL=',FIELD(I,J)
       YYY(ICC)=FIELD(I,J)
       WRITE(111,502) YYY(ICC)
        ICC=ICC+1
 222      CONTINUE
 333    CONTINUE
       PO=0.0

       NX=100
       NY=70
       RRMAX=3.*2.45E9/FREQ
      ZZMAX=1.*2.45E9/FREQ
 776     CONTINUE

        PRINT 99,YYY
 99    FORMAT(7G10.3)
C
C
       ZZ=-XB/2.
C
       DO 451 KKK=1,30
C
         Y=-XB
C
       DO 450 J=1,30
C
         X=-XB
C
          DO 45 I=1,30
C
           CTEMP=ELECP(X,Y,ZZ)
C
           XMAX=MAX(XMAX,(CTEMP))
           XMIN=MIN(XMIN,(CTEMP))
C
 500       FORMAT(E17.8)
C
           WRITE(18,500) CTEMP
C
           X=X+XB/29.*2.
C
```

```
  45     CONTINUE
C
        Y=Y+XB/29.**2.
C
 450   CONTINUE
C
        ZZ=ZZ+XB/29./2.
C
 451    CONTINUE
       WRITE(17,500) XMAX
       WRITE(17,500) XMIN
C
       STOP
       END
C
C
************************************************************
C
       COMPLEX FUNCTION CURR(NN,S,K,Z)
       REAL Z,S(NN)
       COMPLEX K(NN) ,XM,XB
       INTEGER IX,JY
C
C
       DO 10 I=1,NN-1
C
        IF (Z .LE. S(I).AND.Z .GT. S(I+1)) THEN
         GO TO 5
        ENDIF

  10   CONTINUE
C
       IF(Z.LT.S(NN))THEN
         CURR=K(NN)
         RETURN
        ENDIF
C
       IF(Z.GT.S(1))THEN
         CURR=K(1)
         RETURN
        ENDIF
       PRINT*,'Z IN CURR IS BAD','Z  =',Z,'S(I)=',S(I-1),'I=',I-1
C
   5   IF (S(I) .EQ. Z) THEN
         CURR=K(I)
         RETURN
       ENDIF
C
       IF (S(I+1) .EQ. Z) THEN
        CURR=K(I+1)
        RETURN
       ELSE
       XMR=(REAL(K(I+1))-REAL(K(I)))/(S(I+1)-S(I))
       XBR=REAL(K(I))-XMR*S(I)
       CURRR=XMR*Z+XBR
       XMI=(AIMAG(K(I+1))-AIMAG(K(I)))/(S(I+1)-S(I))
       XBI=AIMAG(K(I))-XMI*S(I)
       CURRI=XMI*Z+XBI
       CURR=CMPLX(CURRR,CURRI)
       ENDIF
C
       RETURN
       END
C
************************************************************
C
```

```
      REAL FUNCTION ELECP(XXX,YYY,ZZZ)
      REAL A,OMEGA,R,Z,FIELD(15,15),XP,XDBLIN,L
      REAL B,IO,MU,FREQ,DIA,DD,LO
      INTEGER GRIDR,GRIDZ
      COMPLEX EPSOL,SIIM,ELECC,FIELDS,K,KK(300)
      EXTERNAL ELECC
      COMMON/TWENTF/HEIGHT,COORDTY,ZPTS(42),RPTS(42)
      COMMON/THREE/ZN(300),IA,KK
      COMMON /ONEE/IO,MU,DIA,LO
      COMMON/SIX/XB
      COMMON/TWO/OMEGA,EPSOL,FREQ
C
C
       CTEMP=0.0
       DO 99 IX=1,3
         IF(IX.EQ.2)GO TO 99
C
         CTEMP= CABS(SIIM(1.E-8,1.E-5,-XB/2.,-1.E-5,10,XXX,
     1   YYY ,ZZZ,OMEGA,EPSOL,ELECC,IX))**2+CTEMP
 99    CONTINUE
C
C
       ELECP=-.5*OMEGA*AIMAG(EPSOL)*CTEMP
       RETURN
C
C
       END
C*************************************************************
C
C*************************************************************
C
C
       COMPLEX FUNCTION ELECC(XP,X,YP,Y,ZPP,Z,OMEGA,EPSOL,IX)
       REAL X,Y,Z,OMEGA,MU ,IO,DIA,DD,LO,ZP
       COMPLEX EPSOL ,K,ER,EZ,IMA,XEXP,CURR,KK(300)
       COMMON /ONEE/IO,MU,DIA,LO
       COMMON/THREE/ZN(300),IA,KK
C
       IMA=(0.,1.)
C
       ZP=ZPP
       ELECC =0.0
C
       DO 99 KKK=1,2
       XT= SQRT((X-XP)**2+(Y-YP)**2+(Z-ZP)**2)
C
       K=CSQRT(OMEGA**2*EPSOL*MU)
       XEXP=CEXP(-IMA*K
     1  *XT)/XT
C
       IF(IX.EQ.3)THEN
       ELECC =-1./4/ACOS(-1.)*IMA*CSQRT(MU/EPSOL)/K*XEXP*(
     1  -IMA*K/XT-(1.+K**2*(Z-ZP)**2)/XT**2
     2   + IMA*3.*K*(Z-ZP)**2/XT**3
     3  + 3.*(Z-ZP)**2/XT**4 + K**2)
     1  *CURR(IA,ZN,KK,ZP) + ELECC
C
       ELSE IF(IX.EQ.1)THEN
C
       ELECC = -1./4./ACOS(-1.)*IMA/EPSOL/OMEGA*XEXP*
     1 (Z-ZP)*( IMA*K*(X-XP)*(IMA*K/XT**2
     2  + 3./XT**3) + ( 3./XT**4)*(X-XP))
     1  *CURR(IA,ZN,KK,ZP) + ELECC
C
       ELSE IF(IX.EQ.2)THEN
C
```

```
        ELECC = -1./4./ACOS(-1.)*IMA/EPSOL/OMEGA*XEXP*
      1 (Z-ZP)*( IMA*K*(Y-YP)*(IMA*K/XT**2
      2  + 3./XT**3) + ( 3./XT**4)*(Y-YP))
      1  *CURR(IA,ZN,KK,ZP) + ELECC
C
        ELSE IF(IX.EQ.4)THEN
C
        ELECC= 1/4./ACOS(-1.)*(X-XP)*XEXP*(1.+IMA*K*XT)/XT**2
      1 *CURR(IA,ZN,KK,ZP) +ELECC
         ENDIF
C
        ZP=-ZP
 99     CONTINUE
C
        RETURN
        END
CCCCCCCCCCCCCCCCCCCCCCCCCCCCCCCCCCCCCCCCCCCCCCCC
C
      COMPLEX FUNCTION SIIM(XP,YP,A,B,M,X,Y,Z,OMEGA,EPSOL,FUNCT,IX)
      REAL A,B,ZR(100),OMEGA,L,IO,MU,DIA,DD,LO
      INTEGER ITER
      COMPLEX EPSOL,K,I2,F,FUNCT
      EXTERNAL FUNCT
      COMMON/FIVE/ZR
C
C
      H=(B-A)/(FLOAT(M)-1.)
      I2=0.0
      DO 5 I=1,M
C
         ZR(I)=A+FLOAT(I-1)*H
C
         IF((I-1).EQ.0)THEN
           I2=I2+FUNCT(XP,X,YP,Y,ZR(1),Z,OMEGA,EPSOL,IX)
            GO TO 5
         ELSEIF((I-1).EQ.M-1)THEN
           I2=I2+FUNCT(XP,X,YP,Y,ZR(M),Z,OMEGA,EPSOL,IX)
           GO TO 5
         ELSEIF(2*(I/2).EQ.I)THEN
           I2=I2+FUNCT(XP,X,YP,Y,ZR(I),Z,OMEGA,EPSOL,IX)*4.
C
         GO TO 5
C
         ENDIF
          I2=I2+2.*FUNCT(XP,X,YP,Y,ZR(I),Z,OMEGA,EPSOL,IX)
   5     CONTINUE
C
         SIIM=1./3.*H*I2
      RETURN
      END
C
C**********************************************************
C
        REAL FUNCTION AY(X)
        AY=-2.04
        RETURN
        END
C
        REAL FUNCTION BY(X)
        BY=-1.E-3
        RETURN
        END
C
**********************************************************
C
      SUBROUTINE MOMENT(NNN)
```

```
      REAL L,LL,LLP,MU,LO ,ZN(1001)
      COMPLEX I(1001),V(1001),J,ZZ(1001),AM(1001),AM1(1001),B,K
      COMPLEX EZ
      COMPLEX EPSOL,B2
      COMPLEX INGRLK,EINC,KERNAL
      COMMON/CNSTNS/A,A2,B,B2,J,XB
      COMMON /ONEE/IO,MU,DIA,LO
      COMMON/TWO/OMEGA,EPSOL,FREQ
      COMMON/FIVEE/XLENGTH,XVOLT
C
       OMEGA=2.*ACOS(-1.)*FREQ
       B=CSQRT(OMEGA**2*EPSOL*MU)
       LO= 2.*ACOS(-1.)/SQRT(OMEGA**2*REAL(EPSOL)*MU)
       PRINT*,'LO=',LO
       PRINT*,'MONOPOLE ANTENNA LENGTH=',XLENGTH/2.
C
C
      N=NNN*2-1
 501  FORMAT(I5)
C
      L=XLENGTH
      DELZ=L/N
      PI=ACOS(-1.)
      TEMP=0.0
      J=(0.,1.)
      B2=B**2
      A2=A**2
      LL=-.5*L
      LLP=LL
      DELZO2=DELZ*.5
      Z=LL+DELZO2
C
C  FILL IN VOLTAGE MATRIX
C
      PRINT*,'LN(L/A)2=',2.*ALOG(L/A)
      DO 100 II=1,N
        UL=LL+DELZ
        ZM=LL+DELZO2
        ZN(II)=ZM
        NINT=INT(80.0001-II*(60./FLOAT(N)))
        ZZ(II)=-1./EPSOL/OMEGA/4./ACOS(-1.)*J*INGRLK(NINT,LL,UL,Z)
        CALL MAG(EZ,A,XB,ZM,A,OMEGA,EPSOL)
        V(II)=-EINC(ZM)
        LL=UL
 100  CONTINUE
       DO 888 II=1,N/2+1
        WRITE(99,502) ZN(N/2+2-II)
 888   CONTINUE
 502   FORMAT(E12.5)
C
C
       PRINT*,'N=  ',N
       PRINT*,'L=  ',L
       PRINT*,'A=  ',A
       PRINT*,'THE FIRST ROW OF IMPEDANCE MATRIX IS:'
C
      CALL TPLZ(ZZ,AM,AM1,N,V,I,1,XNORM,IER)
C
       PRINT*,'THE CURRENT MATRIX IS:'
       DO 300 KK=1,N/2+1
       PRINT*,'ZN=',ZN(KK),'  CURR=',(I(KK))
       WRITE(8,509) CABS(I(KK))
 509   FORMAT(E12.5)
 887    CONTINUE
 300   CONTINUE
       PRINT*,'THE INPUT IMPEDANCE(MONOPOLE)=',1./I(N/2)/2.
```

```
      PRINT*,'THE  POWER(MONOPOLE)=',CABS(XVOLT**2*I(N/2.))/4.
      PRINT*,'THE CURRENT=',I(N/2)
      PRINT*,'EPSOL=',EPSOL/8.85E-12
 88   CONTINUE
C
      DO 999 KK=1,N/2+1
         WRITE(77,500) I(N/2+2-KK)*XVOLT
 500     FORMAT(2E12.5)
 999  CONTINUE
      REWIND(UNIT=77)
      REWIND(UNIT=99)
C
      RETURN
      END
C
      COMPLEX FUNCTION INGRLK(NINT,LL,UL,Z)
      REAL LL
      COMPLEX KERNAL,S,HALF
C
      H=(UL-LL)/FLOAT(NINT)
      HOVER2=.5*H
      S=(0.,0.)
      HALF=KERNAL(Z,LL+HOVER2)
      NINTM1=NINT-1
C
      DO 100 I=1,NINTM1
        ZP=LL+I*H
        S=S+KERNAL(Z,ZP)
        HALF=HALF+KERNAL(Z,ZP+HOVER2)
 100  CONTINUE
C
      INGRLK=H/6.*(KERNAL(Z,LL)+KERNAL(Z,UL)+4.*HALF+2.*S)
C
      RETURN
      END
C
      COMPLEX FUNCTION KERNAL(Z,ZP)
      COMPLEX J,B,B2
      COMMON/CNSTNS/A,A2,B,B2,J,XB
C
      R=SQRT((Z-ZP)**2+A2)
      R2=R**2
      R5=R2**2*R
      KERNAL=CEXP(-J*B*R)*((1.+J*B*R)*(2.*R2-3.*A2)+B2*A2*R2)/R5
      RETURN
      END
C
      COMPLEX FUNCTION EINC(Z)
      COMPLEX J,B,B2
      COMMON/CNSTNS/A,A2,B,B2,J,XB
      R1=SQRT(Z**2+A2)
      R2=SQRT(Z**2+XB**2)
      EINC=.5/ALOG(XB/A)*((CEXP(-J*B*R1)/R1)-(CEXP(-J*B*R2)/R2))
      RETURN
      END
C
      SUBROUTINE TPLZ(TAU,A,A1,NZ,VIN,VOUT,MM,XNORM,IER)
      COMPLEX TAU1,ALMDA,ALPHA,COEF,FAC,C1,C2,V,V1,V2
      COMPLEX TAU(NZ),A(1001),A1(1001),VIN(1001),VOUT(1001),ONE,ZERO
C
      DATA ONNE/1D0/,ZRRO/0D0/
      ONE=1.
      ZERO=0.0
C
      N=NZ-1
      IER=0
```

```
      TAU1=TAU(1)
C
      DO 2000 II=1,N
        TAU(II)=TAU(II+1)/TAU1
 2000 CONTINUE
C
      ALMDA=ONE-TAU(1)**2
      A(1)=-TAU(1)
      I=2
 1    KK=I-1
      ALPHA=ZERO
C
      DO 2 M=1,KK
       LL=I-M
       ALPHA=ALPHA+A(M)*TAU(LL)
2     CONTINUE
C
      ALPHA=-(ALPHA+TAU(I))
      IF(CABS(ALPHA).EQ.0.D0)GO TO 15
      COEF=ALPHA/ALMDA
C
      ALMDA=ALMDA-COEF*ALPHA
C
      DO 3 J=1,KK
       L=I-J
       A1(J)=A(J)+COEF*A(L)
 3    CONTINUE
C
      DO 7 J=1,KK
       A(J)= A1(J)
 7    CONTINUE
C
      A(I)=COEF
C
      IF(I.GE.N)GO TO 5
C
      I=I+1
      GO TO 1
 5    NH=(NZ+1)/2
      FAC=ALMDA*TAU1
      XNORM=ZRRO
      NP=NZ+1
C
      DO 51 I=1,NH
       XNM=ZRRO
       IF(I.NE.1)GO TO 52
      A1(1)=ONE/FAC
      XNM=CABS(A1(1))
C
      DO 53 J=2,NZ
       A1(J)=A(J-1)/FAC
       XNM=CABS(A1(J))+XNM
 53   CONTINUE
C
      GO TO 54
 52   XNM=ZRRO
      JH=I-1
      C1=A(JH)
      NNP1=NP-I
      C2=A(NNP1)
C
      DO 55 JJ=1,N
         J=NP-JJ
     INPJ=NP-J
       JL=J-1
       A1(J)=A1(JL)+(C1*A(JL)-C2*A(INPJ))/FAC
```

```
        XNM=CABS(A1(J))+XNM
 55     CONTINUE
C
        A1(1)=A(I-1)/FAC
        XNM=XNM+CABS(A1(1))
 54     IF(XNM.GT.XNORM)XNORM=XNM
C
        DO 56 II=1,MM
         ID=(II-1)*NZ
         V=ZERO
         V1=ZERO
C
           DO 57 J=1,NZ
            NIDJ=ID+J
            V2=VIN(NIDJ)
            V=V+V2*A1(J)
            KNPJ=NP-J
            V1=V1+V2*A1(KNPJ)
 57         CONTINUE
C
         NIDI=ID+I
         VOUT(NIDI)=V
         KIDNPI=ID+NP-I
         VOUT(KIDNPI)=V1
 56     CONTINUE
C
 51     CONTINUE
        RETURN
 15     PRINT*,'ERROR HAS OCCURRED(SINGULAR MATRIX)'
        IER =I
        RETURN
        END
C
C*****************************************************************
C
      SUBROUTINE MAG(EZB,AB,BB,ZB,RB,OMEGA,EPSOL)
      COMPLEX EZB,FINT,XMB(5),T1,T2,T3,TPI,EPSOL,HPHB,K,J
C
       ZPB=0.0
      PI=ACOS(-1.)
      J=(0.,1.)
      TPI=CSQRT(EPSOL*4.*PI*1.E-7*OMEGA**2)
      DAB=(BB-AB)/3.
      D=RB/50.
      BAL=ALOG(BB/AB)
C
      IF(RB.NE.0.)GO TO 10
C
      TO=SQRT((ZB-ZPB)**2+AB**2)
      TT=SQRT((ZB-ZPB)**2+BB**2)
      EZB=(CEXP(-J*TPI*TO)/TO-CEXP(-J*TPI*TT)/TT)/BAL/2.
      GO TO 200
C
  10   H=PI/5.
      RO=SQRT((ZB-ZPB)**2+RB**2)
C
      IF(RO.LT..05.AND.RB.NE.0.) GO TO 25
C
      BMA=BB**2-AB**2
      BPA=BB**2+AB**2
      RO2=RO**2
      RO3=RO**3
      T1=BMA/8./BAL/RO2*CEXP(-J*TPI*RO)
      T2=1./TPI/RO+(1.-BPA/2./RO2)*J
      T3=-1./TPI/RO2+BPA/RO3*J
      EZB=T1*(2.*T2+(RB**2)/RO*(T2*(-2./RO-TPI*J)+T3))*TPI
```

```
      GO TO 200
C
 25   DO 150 JJ=1,5
       R=RB
       Z=ZB
       RP=AB+DAB/2.
       IF(JJ.EQ.2)Z=ZB+D
       IF(JJ.EQ.3)Z=ZB-D
       IF(JJ.EQ.4)R=RB-D
       IF(JJ.EQ.5)R=RB+D
       XMB(JJ)=0.0
C
       DO 100 I=1,3
       R1=SQRT((Z-ZPB)**2+(R+RP)**2)
       PP=4.*R*RP/R1**2
       CALL ELPING(ELT,PP)
      TEMP=2./R1*ELT
      CON1=(Z-ZPB)**2+R**2+RP**2
      CON2=2.*R*RP
      CALL FUNCT(FR1,FL1,CON1,CON2,0.)
      CALL FUNCT(FR2,FL2,CON1,CON2,PI)
      FINT=CMPLX(FR1+FR2,FL1+FL2)
      U=H
      P=2.
  50    CALL FUNCT(FR3,FL3,CON1,CON2,U)
      FINT=FINT+P*CMPLX(FR3,FL3)
      U=U+H
      IF(U+H/4..LT.PI)GO TO 50
      U=H/2.
      P=2.*P
      IF(P.LT.5.)GO TO 50
      FINT=FINT*H/6.+TEMP
      RP=RP+DAB
      XMB(JJ)=XMB(JJ)+FINT*DAB
 100  CONTINUE
      XMB(JJ)=XMB(JJ)/(TPI*BAL)
C
 150  CONTINUE
      EZB=XMB(1)/RB+(XMB(5)-XMB(4))/D/2.
 200  CONTINUE
      RETURN
      END
C
C*************************************************************
C
      SUBROUTINE FUNCT(FCR,FCI,CONS1,CONS2,V)
      RR=SQRT(CONS1-CONS2*COS(V))
      RPI=6.283185*RR
      FCR=(COS(V)*COS(RPI)-1.)/RR
      FCI=-(COS(V)*SIN(RPI))/RR
      RETURN
      END
C
C ******************************************************
C
      SUBROUTINE ELPING(ELPO,ELPC)
      ELPI=1.-ELPC
      A0=1.3862944
      A1=.096663443
      A2=.035900924
      A3=.037425637
      A4=.014511962
      B0=.5
      B1=.12498594
      B2=.068802486
      B3=.033283553
```

```
      B4=.0044178701
      ELPO=(((((((A4*ELPI)+A3)*ELPI)+A2)*ELPI+A1)*ELPI)+A0+ALOG(1./ELPI)
     1*(((((((B4*ELPI)+B3)*ELPI)+B2)*ELPI)+B1)*ELPI)+B0)
      RETURN
      END
*************************************************************
C
      REAL FUNCTION EPOWER(XXX,ZZZ)
      REAL A,OMEGA,R,Z,FIELD(15,15),XP,XDBLIN,L
      REAL B,IO,MU,FREQ,DIA,DD,LO
      INTEGER GRIDR,GRIDZ
      COMPLEX EPSOL,SIIM,ELECC,FIELDS,K,KK(300)
      EXTERNAL ELECC
      COMMON/TWENTF/HEIGHT,COORDTY,ZPTS(42),RPTS(42)
      COMMON/THREE/ZN(300),IA,KK
      COMMON /ONEE/IO,MU,DIA,LO
      COMMON/SIX/XB
      COMMON/TWO/OMEGA,EPSOL,FREQ
C
C
       CTEMP=0.0
       DO 99 IX=1,3
C
         CTEMP= CABS(SIIM(1.E-8,0.,-XB/2.,0.,20,XXX,
     1   0.0 ,ZZZ,OMEGA,EPSOL,ELECC,IX))**2+CTEMP
 99    CONTINUE
C
C
       EPOWER=-.5*OMEGA*AIMAG(EPSOL)*CTEMP*2.*ACOS(-1.)
       RETURN
C
C
       END
C
*****************************************************
C
      REAL FUNCTION POYNT(ZZZ)
      REAL A,OMEGA,R,Z,FIELD(15,15),XP,XDBLIN,L
      REAL IO,MU,FREQ,DIA,DD,LO
      INTEGER GRIDR,GRIDZ
      COMPLEX EPSOL,SIIM,ELECC,FIELDS,K,KK(300),ER,EZ,HP,B,B2,IMA
      EXTERNAL ELECC
      COMMON/TWENTF/HEIGHT,COORDTY,ZPTS(42),RPTS(42)
       COMMON/CNSTNS/ADIA,A2,B,B2,IMA,BDIA
      COMMON/THREE/ZN(300),IA,KK
      COMMON /ONEE/IO,MU,DIA,LO
      COMMON/SIX/XB
      COMMON/TWO/OMEGA,EPSOL,FREQ
C
C
         ER= SIIM(1.E-8,1.E-5,-XB/2.,-1.E-5,100,.27,
     1   1.E-6 ,ZZZ,OMEGA,EPSOL,ELECC,1)
C
         EZ= SIIM(1.E-8,1.E-5,-XB/2.,-1.E-5,100,.27,
     1   1.E-6 ,ZZZ,OMEGA,EPSOL,ELECC,3)
C
         HP= SIIM(1.E-8,1.E-5,-XB/2.,-1.E-5,100,.27,
     1   1.E-6 ,ZZZ,OMEGA,EPSOL,ELECC,4)
C
       POYNT=-.5*REAL((EZ)*CONJG(HP))*.27*2.*ACOS(-1.)
C
C
       RETURN
C
C
       END
```

```
C
C*****************************************************
C
      SUBROUTINE POWERIN(XWEL,GRIDR,GRIDZ,RMAX,ZMAX,VOL,RPTS,ZPTS)
      REAL RPTS(1000),DELTR(1000),DELTZ(1000),RIM1(1000),RIP1(1000)
      REAL DELRAV(1000),ZPTS(1000)
      REAL VOL(150,150),RIM11(1000),RIP11(1000)
      INTEGER GRIDR,GRIDZ
C
          RPTS(1)=XWEL
            DO 1111 I=1,GRIDR
                RPTS(I+1)=RPTS(I)*(RMAX/XWEL)**(1./(GRIDR-1))
 1111       CONTINUE
C
      DO 999 I=1,GRIDZ
        DELTZ(I)=ZMAX/FLOAT(GRIDZ-1)
 999  CONTINUE
      DELTZ(1)=DELTZ(2)/2.
      DELTZ(GRIDZ)=DELTZ(GRIDZ-1)/2.
C
      DO 5551 I=1,GRIDZ
       ZPTS(I)=-(I-1)*DELTZ(2)
 5551  CONTINUE
C
            DO 234 II=1,GRIDR
C
            IF(II.EQ.1)THEN
             RIM11(1)=RPTS(1)
             RIP11(1)=SQRT((RPTS(2)**2-RPTS(1)**2)/2./ALOG(
     1 RPTS(2)/RPTS(1)))
            ELSE IF(II.EQ.GRIDR)THEN
           RIM11(GRIDR)=SQRT((RPTS(GRIDR)**2-RPTS(GRIDR-1)**2)/2./ALOG(
     1 RPTS(GRIDR)/RPTS(GRIDR-1)))
             RIP11(GRIDR)=RPTS(GRIDR)
            ELSE
           RIM11(II)=SQRT((RPTS(II)**2-RPTS(II-1)**2)/2./ALOG(
     1 RPTS(II)/RPTS(II-1)))
           RIP11(II)=SQRT((RPTS(II+1)**2-RPTS(II)**2)/2./ALOG(
     1 RPTS(II+1)/RPTS(II)))
            ENDIF
C
 234      CONTINUE
      DO 411 I=1,GRIDR
C
      IF(I.EQ.1)THEN
      RIP1(I)=(RPTS(I+1)-RPTS(I))/ALOG(RPTS(I+1)/RPTS(I))
      RIM1(I)=RPTS(1)
     ELSE IF(I.EQ.GRIDR)THEN
     RIP1(GRIDR)=RPTS(GRIDR)
     RIM1(I)=(RPTS(I)-RPTS(I-1))/ALOG(RPTS(I)/RPTS(I-1))
      ELSE
      RIP1(I)=(RPTS(I+1)-RPTS(I))/ALOG(RPTS(I+1)/RPTS(I))
     RIM1(I)=(RPTS(I)-RPTS(I-1))/ALOG(RPTS(I)/RPTS(I-1))
      ENDIF
C
 411          CONTINUE
C
            DO 977 J=1,GRIDR
              DELTR(J)=(RIP11(J)-RIM11(J))
              DELRAV(J)=RPTS(J)*DELTR(J)
 977          CONTINUE
C
C  CONSTRUCT VOLUME ELEMENT
C
            DO 768 I=1,GRIDR
            DO 9 J=1.GRIDZ
```

```
                VOL(I,J)= (RIP11(I)**2-RIM11(I)**2)*DELTZ(J)/2.
  9           CONTINUE
  768         CONTINUE
C
       RETURN
       END
x2
1
2
 EOI ENCOUNTERED.
/
```

PROGRAM NAME: PHASE5

DESCRIPTION: Simulates the electromagnetic field distribution around two coupled, phased monopole antennas

DEVELOPED BY: V.J. Nargaraj, University of Wyoming, Physics Department

PHASED ARRAY CODE

The phased array program is for two coupled monopoles in a lossy medium, fed from a coaxial line, that may be phased together in such a fashion to produce a given power pattern. The algorithm is based on the mathematical analysis given in King's book. The problem is complicated by the fact that the field distribution from one antenna induces a current on the other antenna, thus the current distributions form a coupled system of equations. The program consists of first calculating the current distribution on the antennas and then integrating the distribution times the appropriate coupled Green function to determine the electric field pattern.

Important variables and functions:

epsol	dielectric constant
freq	frequency
xlam	wavelength
L	antenna length in meters
a	antenna radius
Tplz	subroutine to solve a matrix problem
I	array containing current values
N	number of grid points
siim	integration routine
kernel1,kernel2	Green functions
einc1,einc2	excitation functions
power	function to calculate power

```
 copy,phase5
      PROGRAM MIME (INPUT,OUTPUT)
C*************************************************************************
C     MOMENT METHOD  (POINT MATCHING) PROGRAM FOR A CENTER FED DIPOLE
C     OF LENGTH L AND RADIUS A WITH MAGNETIC FRILL GENERATOR
C*************************************************************************

      REAL L,LL,LLP,MU,ZU,ZN(201),Y1ARAY(201),X1ARAY(201),POWER
      REAL Y2ARAY(201),PARRAY(20,20),P1ARRAY(20,20),P2ARRAY(20,20)
      COMPLEX R(201),I(201),V(201),J,ZZ(201),AM(201),AM1(201),B,B2,EPSOL
      COMPLEX INGRLK,EINC,KERNEL,IU,M,BB,CURR,KRZ,KZZ,G11,G12,EINC1,V2,
     &EINC2,KERNEL1,KERNEL2,I1(201),I2(201),IONEZ(201),ITWOZ(201)
      COMMON/CNSTNS/A,A2,B,B2,J,PI
      COMMON/ONE/ADIA,BDIA,D
      COMMON/TWO/ZN,N,IJ,IONEZ,ITWOZ
      COMMON/THREE/V1,V2
      COMMON/FOUR/OMEGA,EPSOL
      COMMON/SIX/L
      EXTERNAL KERNEL1,KERNEL2,KRZ,KZZ

      DO 106 JJ=1,2
      EPSOL=(1.,0.)*8.854E-12
      PI=ACOS(-1.)
      FREQ=.450E09
      MU=PI*4.0E-07
      OMEGA=2.*PI*FREQ
      N=100

      B=OMEGA*CSQRT(EPSOL*MU)
      XLAM=2*PI/REAL(B)
      L=1.334
      A=0.005
       PRINT*,'A =',A
      DELZ=(L/N)
      J=(0.,1.)
      B=OMEGA*CSQRT(EPSOL*MU)
      B2=B*B
      A2=A*A
      ADIA=A
      BDIA=.0208
      THETA=180
      LL=-.5*L
      LLP=LL
      DELZ02=DELZ*.5
      Z=LL+DELZ02
      D=.33334
       PRINT*,'D/2.=',D/2.
      V1=1.
      V2=CEXP(J*THETA)

C*************************************************************************
C     TO FILL THE VOLTAGE MATRIX AND THE FIRST ROW OF THE IMPEDANCE
C     MATRIX
C*************************************************************************

      DO 100 II=1,N
      UL=LL+DELZ
      ZM=LL+DELZ02
      ZN(II)=ZM
      NINT=INT(80.0001-II*(60./N))

      IF(JJ.EQ.1)THEN
            ZZ(II)=-(J/(4.*PI*EPSOL*OMEGA))*INGRLK(NINT,LL,UL,Z,KERNEL1)
             V(II)=-EINC1(ZM)
```

```
      ELSEIF(JJ.EQ.2)THEN

           ZZ(II)=-(J/(4.*PI*OMEGA*EPSOL))*INGRLK(NINT,LL,UL,Z,KERNEL2)
             V(II)=-EINC2(ZM)

      ENDIF
  100 LL=UL

C*************************************************************************
C   CALL THE TOEPLITZ MATRIX SOLVING SUBROUTINE
C*************************************************************************

      CALL TPLZ(ZZ,AM,AM1,N,V,I,1,XNORM,IER)

C*************************************************************************

      DO 118 JP=1,N
       IF (JJ.EQ.1) THEN
         I1(JP)=I(JP)
          ELSE IF(JJ.EQ.2)THEN
        I2(JP)=I(JP)
       ENDIF
 118   CONTINUE

 106   CONTINUE
C*************************************************************************
C  TO PRINT THE INDIVIDUAL CURRENTS IN THE TWO ANTENNAS DRIVEN BY VOLTAGES
C   V(1) AND V(2).
C*************************************************************************
      DO 900 KK=1,N
      IONEZ(KK)=I1(KK)+I2(KK)
      ITWOZ(KK)=I1(KK)-I2(KK)
 900  CONTINUE

C*************************************************************************

C  30 FORMAT(1H //1H ,29X,'CURRENT VECTOR I(N)'//1H ,19X,'N'
C    &,12X,'REAL',14X,'IMAGINARY'/)
C
C  40 FORMAT(1H ,18X,I3,2(1PE20.7))
C
C     DO 444 TT=1,2
C
C     WRITE(*,30)
C
C     IF (TT.EQ.1)THEN
C           DO 300 KK=1,N,5
C300         WRITE(*,40) KK,CABS(IONEZ(KK))
C       ELSEIF(TT.EQ.2)THEN
C           DO 303 KK=1,N,5
C303         WRITE(*,40) KK,CABS(ITWOZ(KK))
C     ENDIF
C
C444   CONTINUE
C
C*************************************************************************

        PTS = XLAM*5.

        Y=PTS
        X=-PTS

        DO 970 KA=1,11
        Y=PTS
```

```
      DO 980 KB=1,11

      PARRAY(KA,KB)=POWER(XLAM/2.,X,Y)


      Y=Y-XLAM
 980  CONTINUE
      PRINT*

      X=X+XLAM
 970  CONTINUE

C*************************************************************************
C TO PLOT IONEZ AND ITWOZ
C*************************************************************************

 525  FORMAT(3E20.6)

      DO 555 IA=1,N

      Y1ARAY(IA)=CABS(IONEZ(IA))
      Y2ARAY(IA)=CABS(ITWOZ(IA))


      WRITE(7,525) Y1ARAY(IA),Y2ARAY(IA),ZN(IA)

 555  CONTINUE
C*************************************************************************
C DEFINE STORAGE FOR COMBINED POWER OF ANTENNA1 AND ANTENNA2
C*************************************************************************

 505  FORMAT (1E12.4)

      DO 420 LA=1,11
      DO 430 LB=1,11

      WRITE(8,505) PARRAY(LA,LB)

 430  CONTINUE
 420  CONTINUE

      STOP
      END

C*************************************************************************
C THIS SUBPROGRAM USES SIMPSONS RULE TO NUMERICALLY INTEGRATE
C    POCKLINGTONS EQUATION
C*************************************************************************

      COMPLEX FUNCTION INGRLK(NINT,LL,UL,Z,KERNEL)
      REAL LL
      COMPLEX KERNEL,S,HALF
      EXTERNAL KERNEL
      H=(UL-LL)/NINT
      HOVER2=.5*H
      S=(0.,0.)
      HALF=KERNEL(Z,LL+HOVER2)
      NINTM1=NINT-1
      DO 100 I=1,NINTM1
      ZP=LL+I*H
      S=S+KERNEL(Z,ZP)
  100 HALF=HALF+KERNEL(Z,ZP+HOVER2)
      INGRLK=(H/6.)*(KERNEL(Z,LL)+ KERNEL(Z,UL)+4.*HALF+2.*S)
      RETURN
      END
```

```
C*************************************************************************
C  TPLZ SUBROUTIONE - PURPOSE
C                            TO SOLVE A SYSTEM INVOLVING A TOEPLITZ
C   MATRIX. TPLZ REQUIRES ONLY 5N STORGE LOCATIONS FOR AN NBY N MATRIX
C
C   REMARKS@D
C            A TOEPLITZ MATRIX HAS THE FIRST ROW EQUAL TO THE FIRST COLUMN.
C            ALL ELEMENTS ALONG THE MAIN DIAGONAL ARE EQUAL.
C            ANY DIAGONAL OFF THE MAIN DIAGONAL WILL THE SAME PROPERTY.
C   DESCRIPTION OF PARAMETERS@D
C     NZ       - ORDER OF THE MATRIX
C     TAU      - FIRST ROW OR COLUMN OF THE TOEPLITZ MATRIX (VECTOR LENGTH NZ).
C     A,A1     - ARE VECTORS OF LENGTH NZ NEEDED FOR SCRATCH AREA.
C     VIN      - FOR THE MATRIX EQUATION (Z)(I)=(V), VIN IS V.
C              - (Z,I,&V MAY BE THOUGHT AS GENERALISED IMPEDANCES,
C              - CURRENTS,AND VOLTAGES RESPECTIVELY).
C              - V IS A NZ BY NM MATRIX
C     MM       - NUMBER OF COLUMN VECTORS ON RIGHT SIDE OF MATRIX EQUATION
C              - (Z)(I)=(V)
C     VOUT     - SOLUTION OF THE MATRIX EQUATION. SOLUTION I WILL BE AN
C              - NZ BY MM MATRIX
C     XORM     - UPON RETURN THIS IS INFINITE MATRIX NORM OF INVERSE.
C     IER      - ERROR CODE WHICH IS 0 IF NO TROUBLE.
C*************************************************************************

      SUBROUTINE TPLZ(TAU,A,A1,NZ,VIN,VOUT,MM,XNORM,IER)
      COMPLEX TAU1,ALMDA,ALPHA,COEF,FAC,C1,C2,V,V1,V2
      COMPLEX TAU(NZ),A(100),A1(100),VIN(100),VOUT(100),ONE,ZERO
      DATA ONE/(1.0,0.0)/,ZERO/(0.0,0.0)/
      DATA ONNE/1.0/,ZRRO/0.0/
      N=NZ-1
      IER=0
C*************************************************************************
C  TO NORMALIZE THE INPUT MATRIX.
C
C*************************************************************************
      TAU1=TAU(1)
      DO 2000 II=1,N
 2000 TAU(II)=TAU(II+1)/TAU1

C*************************************************************************
C  THE FOLLOWING CALCULATES THE ITERATIVE VARIABLES TO OBTAIN
C  A(N) AND ALMDA.
C NOTE @D
C       VECTOR A(I) HAS I ELEMENTS AND IS STORED AS A(I,J),J=1,N
C*************************************************************************

      ALMDA=ONE-TAU(1)*TAU(1)
      A(1)=-TAU(1)
      I=2
    1 KK=I-1
      ALPHA=ZERO
      DO 2 M=1,KK
      LL=I-M
   2  ALPHA=ALPHA+A(M)*TAU(LL)
      ALPHA=-(ALPHA+TAU(I))
      IF(CABS(ALPHA).EQ.0.D0)GO TO 15
      COEF=ALPHA/ALMDA
      ALMDA=ALMDA-COEF*ALPHA
      DO 3 J=1,KK
      L=I-J
    3 A1(J)=A(J)+COEF*A(L)
      DO 7 J=1,KK
    7 A(J)=A1(J)
      A(I)=COEF
```

```
      IF(I.GE.N)GO TO 5
    4 I=I+1
      GO TO 1

C*************************************************************************
C  THE FOLLOWING COMPUTES THE VALUES OF EACH ELEMENT OF THE INVERSE
C*************************************************************************

    5 NH=(NZ+1)/2
      FAC=ALMDA*TAU1
      XNORM=ZRRO
      NP=NZ+1
      DO 51 I=1,NH
      XNM=ZRRO
      IF(I.NE.1)GO TO 52
      A1(1)=ONE/FAC
      XNM=CABS(A1(1))
      DO 53 J=2,NZ
      A1(J)=A(J-1)/FAC
   53 XNM=CABS(A1(J))+XNM
      GO TO 54
   52 XNM=ZRRO
      JH=I-1
      C1=A(JH)
      NNPI=NP-I
      C2=A(NNPI)
      DO 55 JJ=1,N
      J=NP-JJ
      INPJ=NP-J
      JL=J-1
      A1(J)=A1(JL)+(C1*A(JL)-C2*A(INPJ))/FAC
   55 XNM=CABS(A1(J))+XNM
      A1(1)=A(I-1)/FAC
      XNM=XNM+CABS(A1(1))
   54 IF(XNM.GT.XNORM)XNORM=XNM

C*************************************************************************
C   MATRIX MULTIPLY
C*************************************************************************

      DO 56 II=1,MM
      ID=(II-1)*NZ
      V=ZERO
      V1=ZERO
      DO 57 J=1,NZ
      NIDJ=ID+J
      V2=VIN(NIDJ)
      V=V+V2*A1(J)
      KNPJ=NP-J
   57 V1=V1+V2*A1(KNPJ)
      NIDI=ID+I
      VOUT(NIDI)=V
      KIDNPI=ID+NP-I
   56 VOUT(KIDNPI)=V1
   51 CONTINUE
      RETURN
   15 WRITE(*,700)


  700 FORMAT('ERROR HAS OCCURED. MATRIX IS NOT NONSINGULAR')
      IER=I
      RETURN
      END
C*************************************************************************
C     SUBROUTINE CURRENT - PURPOSE
C           TO FIND THE CURRENT FOR ANY Z
```

```
C     ZU = IMPEDANCE FOR WHICH I IS TO BE DETERMINED
C     IU = CURRENT CORRESPONDING TO ZU
C*************************************************************************

      COMPLEX FUNCTION CURR(ZU)
      COMMON/TWO/ZN,N,IJ,IONEZ,ITWOZ
      REAL ZN(201),ZU
      COMPLEX IONEZ(201),ITWOZ(201)
      COMPLEX IU,M,BB


      IF (IJ.EQ.1)THEN
         IF (ZU.GE.ZN(100)) THEN
                   CURR=IONEZ(100)
                   RETURN

         ELSE
           DO 100 K=1,99
              IF(ZU.LE.ZN(K))THEN
                     CURR=IONEZ(K)
                     RETURN
              ELSE IF(ZU.GT.ZN(K).AND.(ZU.LT.ZN(K+1)))THEN
                     M=(IONEZ(K+1)-IONEZ(K))/(ZN(K+1)-ZN(K))
                     BB=IONEZ(K)-(M*ZN(K))
                     CURR=M*ZU+BB
                     RETURN
              ENDIF
 100        CONTINUE
         ENDIF

      ELSE IF (IJ.EQ.2)THEN

         IF (ZU.GE.ZN(100))THEN
                   CURR=ITWOZ(100)
                   RETURN

         ELSE
           DO 123 K=1,99

              IF (ZU.LE.ZN(K))THEN
                     CURR=ITWOZ(K)
                     RETURN

              ELSE IF(ZU.GT.ZN(K).AND.(ZU.LT.ZN(K+1)))THEN
                     M=(ITWOZ(K+1)-ITWOZ(K))/(ZN(K+1)-ZN(K))
                     BB=ITWOZ(K)-(M*ZN(K))
                     CURR=M*ZU+BB
                     RETURN
              ENDIF
 123        CONTINUE

         ENDIF

      ENDIF

      PRINT*,'ERROR HAS OCURRED IN FUNCTION CURR '
      END

C*************************************************************************
C   SUBPROGRAMS TO EVALUATE THE DIFFERENTIALS
C*************************************************************************

      COMPLEX FUNCTION KRZ(X,XP,Y,YP,ZP,Z)
      COMPLEX J,B,B2,CURR,EPSOL,IONEZ(201),ITWOZ(201)
      REAL ZN(201)
      COMMON/CNSTNS/A,A2,B,B2,J,PI
```

```
      COMMON/TWO/ZN,N,IJ,IONEZ,ITWOZ
      COMMON/FOUR/OMEGA,EPSOL

      RMRP=SQRT((X-XP)**2+(Y-YP)**2)
      RR=SQRT((Z-ZP)**2+(X-XP)**2+(Y-YP)**2)
      RR2=RR*RR
      RR3=RR*RR2
      RR4=RR*RR3

      KRZ=((Z-ZP)*(RMRP)/(4.*PI))*(CEXP(-J*B*RR)/RR)
     & *((J*B*((J*B/RR2)+(1./RR3)))+((2.*J*B/RR3)+(3./RR4)))
     & *(CURR(ZP)*J/(OMEGA*EPSOL))
      RETURN
      END

C*************************************************************************
C SUBPROGRAM TO EVALUATE THE DIFFERENTIAL   DK/DZ2
C*************************************************************************

      COMPLEX FUNCTION KZZ(X,XP,Y,YP,ZP,Z)
      COMPLEX J,B,B2,CURR,EPSOL,IONEZ(201),ITWOZ(201)
      COMMON/CNSTNS/A,A2,B,B2,J,PI
      REAL ZN(201)
      COMMON/TWO/ZN,N,IJ,IONEZ,ITWOZ
      COMMON/FOUR/OMEGA,EPSOL

      RIR=(Z-ZP)**2
      RR=SQRT(RIR+(X-XP)**2+(Y-YP)**2)
      RR2=RR*RR
      RR3=RR*RR2
      RR4=RR*RR3

      KZZ=(1./(4.*PI))*(CEXP(-J*B*RR)/RR)*((-J*B/RR)-((1+B2*RIR)/RR2)
     & +((J*3.*B*RIR)/RR3)+((3.*RIR)/RR4)+B2)
     & *(CURR(ZP)*J/(OMEGA*EPSOL))
      RETURN
      END
C*************************************************************************
C      TO COMPUTE THE FIELDS GOVERNED BY EQUATIONS (3) AND (4)
C*************************************************************************

      COMPLEX FUNCTION EINC1(Z)
      COMPLEX J,B,B2,G11,G12,V2
      COMMON/ONE/ADIA,BDIA,D
      COMMON/CNSTNS/A,A2,B,B2,J,PI
      COMMON/THREE/V1,V2

       R1=SQRT(ADIA**2+Z**2)
       R2=SQRT(BDIA**2+Z**2)
C
      EINC1=(((V1-V2)/2.)/ALOG(BDIA/ADIA))*(CEXP(-J*B*R1)/R1
     1 -CEXP(-J*B*R2)/R2)
      RETURN
      END
C*************************************************************************
C    TO COMPUTE  RHS OF EQUATION (4)
C*************************************************************************

      COMPLEX FUNCTION EINC2(Z)
      COMPLEX G11,G12,J,B,B2,V2
      COMMON/ONE/ADIA,BDIA,D
      COMMON/CNSTNS/A,A2,B,B2,J,PI
      COMMON/THREE/V1,V2

       R1=SQRT(ADIA**2+Z**2)
       R2=SQRT(BDIA**2+Z**2)
```

```
C
      EINC2=(((V1+V2)/2.)/ALOG(BDIA/ADIA))*(CEXP(-J*B*R1)/R1
     1 +CEXP(-J*B*R2)/R2)

      RETURN
      END
C*************************************************************************
C    SUBPROGRAMS TO COMPUTE KERNEL1 AND KERNEL2
C*************************************************************************

      COMPLEX FUNCTION KERNEL1(Z,ZP)
      COMPLEX J,B,B2
      COMMON/CNSTNS/A,A2,B,B2,J,PI
      COMMON/ONE/ADIA,BDIA,D
C
C
      RD=SQRT((Z-ZP)**2+D**2)
      RD2=RD**2
      RD5=RD2**2*RD
C
      R=SQRT((Z-ZP)**2+A2)
      R2=R**2
      R5=R2**2*R
      KERNEL1=CEXP(-J*B*R)*((1.+J*B*R)*(2.*R2-3.*A2)+B2*A2*R2)/R5
     1 -  CEXP(-J*B*RD)*((1.+J*B*RD)*(2.*RD2-3.*A2)+B2*A2*RD2)/RD5
       RETURN
       END

C*************************************************************************
C     PROGRAM TO COMPUTE KERNEL2
C*************************************************************************

      COMPLEX FUNCTION KERNEL2(Z,ZP)
      COMMON/ONE/ADIA,BDIA,D
      COMPLEX J,B,B2
      COMMON/CNSTNS/A,A2,B,B2,J,PI
C
C
      RD=SQRT((Z-ZP)**2+D**2)
      RD2=RD**2
      RD5=RD2**2*RD
C
      R=SQRT((Z-ZP)**2+A2)
      R2=R**2
      R5=R2**2*R
      KERNEL2=CEXP(-J*B*R)*((1.+J*B*R)*(2.*R2-3.*A2)+B2*A2*R2)/R5
     1 +  CEXP(-J*B*RD)*((1.+J*B*RD)*(2.*RD2-3.*A2)+B2*A2*RD2)/RD5
       RETURN
       END
C*************************************************************************
C  THE FOLLOWING PROGRAM INTEGRATES THE CURRENT TO OBTAIN THE FIELD
C   DISTRIBUTION.
C
      COMPLEX FUNCTION SIIM(XP,YP,A,B,M,X,Y,Z,FUNCT)
      REAL A,B,ZR(100),ZN(201),OMEGA,L,IO,MU,DIA,DD,LO
      INTEGER ITER
      COMPLEX EPSOL,K,I2,F,FUNCT,KRZ,KZZ,IONEZ(201),ITWOZ(201)
      EXTERNAL FUNCT
      COMMON/TWO/ZN,N,IJ,IONEZ,ITWOZ
      COMMON/FIVE/ZR
C
C
      H=(B-A)/(FLOAT(M)-1.)
      I2=0.0
      DO 5 I=1,M
C
```

```
         ZR(I)=A+FLOAT(I-1)*H
C
         IF((I-1).EQ.0)THEN
           I2=I2+FUNCT(X,XP,Y,YP,ZR(1),Z)
            GO TO 5
         ELSEIF((I-1).EQ.M-1)THEN
           I2=I2+FUNCT(X,XP,Y,YP,ZR(M),Z)
           GO TO 5
         ELSEIF(2*(I/2).EQ.I)THEN
           I2=I2+FUNCT(X,XP,Y,YP,ZR(I),Z)
C
         GO TO 5
C
         ENDIF
          I2=I2+2.*FUNCT(X,XP,Y,YP,ZR(I),Z)
   5     CONTINUE
C
         SIIM=1./3.*H*I2
       RETURN
        END

C*******************************************************************************

       REAL FUNCTION POWER (Z,X,Y)
       EXTERNAL KZZ,KRZ
       COMMON/CNSTNS/A,A2,B,B2,J,PI
       COMMON/ONE/ADIA,BDIA,D
       COMMON/TWO/ZN,N,IJ,IONEZ,ITWOZ
       COMMON/SIX/L
       REAL L,ZN(201)
       COMPLEX KRZ,KZZ,B,B2,J,SIIM,C1,C2,C3,C4,IONEZ(201),ITWOZ(201)

       DO 222 IJ=1,2

       IF (IJ.EQ.1)THEN
           C1=SIIM(D/2.,0.0,-L/2.,L/2.,20,X,Y,Z,KZZ)
           C3=SIIM(D/2.,0.0,-L/2.,L/2.,20,X,Y,Z,KRZ)

       ELSEIF (IJ.EQ.2)THEN
           C2=SIIM(-D/2.,0.0,-L/2.,L/2.,20,X,Y,Z,KRZ)
           C4=SIIM(-D/2.,0.0,-L/2.,L/2.,20,X,Y,Z,KZZ)

       ENDIF
 222   CONTINUE


       POWER=(CABS(C1+C4))**2+(CABS(C3+C2))**2

       RETURN
       END
 EOI ENCOUNTERED.
/
```

REFERENCES

1. J.E. Bridges, A. Taflove, and R.H. Snow (1978), Net energy recoveries from in situ dielectric heating of oil shales *Proceedings of 11th Annual Oil Shale Symposium*, Colorado School of Mines, Golden, Colorado.

2. J.E. Bridges, J. Enk, R.H. Snow, and G. Sresty (1982), Physical and electrical properties of oil shales, *Proceedings of Fifteenth Oil Shale Symposium*, Colorado School of Mines, Golden, Colorado, 311–330.

3. J. duBow and K. Rajewhwar (1979), Thermophysical properties of oil shales, *Final Technical Report #EF–77–5—3–1584*, DOE.

4. E.T. Wall, R. Damrauer, W. Lutz, R. Bies, and M. Cranney (1978), Retorting oil shales by microwave power, *Thermal Hydrocarbon Chemistry*, 330.

5. E.T. Wall (1983), Interaction of microwave energy with fuel precursors, *J. Micro. Power*, **18(1)**, 131–134.

6. J.E. Bridges, G. Sresty, A. Taflove, and R. Snow (1979), Radio frequency heating to recover oil from Utah tar sands, *Proceedings First International Conference on Future of Heavy Crude and Tar Sand*, McGraw-Hill, New York.

7. F.E. Vermeulen and F.S. Chute (1983), Electromagnetic techniques in the in situ recovery of heavy oils, *J. Microwave Power*, **18**, 15–29.

8. R.G. Mallon (1982), Economics of shale oil production by radio frequency heating, Lawrence Livermore Lab., *Report UCRL–52942.*

9. J. Baker-Jarvis and R. Inguva (1988), Mathematical model for in situ oil shale retorting by electromagnetic radiation, *Fuel*, **67**, 916.

10. Raytheon Patents 4,196,329 and 4,320,801 by Rowland; 4,301,865 by Kasevich; 4,193,451 by Dauphine.

11. C.W. Harrison, C.D. Taylor, E.A. Aronson, and M.L. Houston (1970), An accurate representation of the complete electromagnetic field in the vicinity of a base-driven monopole, *IEEE Trans.*, **12(4)**, 164–173.

12. A.C. Metaxas and R.J. Meredith (1983), *Industrial Microwave Heating*, Peter Peregrinus Ltd., London.

13. P.I. Somlo (1967), The discontinuity capacitance and effective position of a shielded open circuit in a coax line, *Proceedings Inst. Radio Elec., Australia*, **28(7)**.

14. R.L. Braun (1981), Mathematical modeling of modified in-situ aboveground oil shale retorting, *Report #UCRL–53119*, Lawrence Livermore Laboratory.

15. T.J. Travis, P.S. Hommert, and C.E. Tyner (1982), A two dimensional numerical model of underground oil shale retorting, *Los Alamos Laboratory Report.*

16. K.H. Coats (1980), An equation of state compositional model, *SPEJ*, **Oct.**, 363–376.

17. G.C. Sresty, Kinetics of low temperature pyrolysis of oil shale by the IITRI RF process, *Proceedings of the 13th Oil Shale Symposium*, Colorado School of Mines, Golden, Colorado.

18. E. Sarapuu (1965), Underground electrocarbonization of oil shale, *Quart. Colo. Sch.*, **60(4)**.

19. B.K. Erodskaya, *Use of Electric Current for the Purpose of Preparing Oil Shale Layers for Underground Strip Mine Gasification*, NSF, Washington, D.C.

20. S.T. Fisher (1980), Processing of solid fuel deposits by electrical induction heating, *IEEE Transactions of Industrial Electronics and Control Instrumentation*, **IECI–27(1)**.

21. E.R. Abernathy (1974), Production increase of heavy crude oils by electromagnetic heating, *Paper No. 37007*, Ann. Tech. Meeting of Pet. Soc. of CIM, Calgary, Alberta, Canada.

22. J.H. Campbell, G.J. Koskinas, and N.D. Stout (1980), Oil shale retorting: Effects of particle size and heating rate on oil evolution and intraparticle oil degradation, *In Situ*, **2**.

23. A.K. Burnham and R.L. Braun (1985), General kinetics of oil shale pyrolysis, *In Situ*, **9(1)**, 1–23.

24. J. Bear (1972), *Dynamics of Fluids in Porous Media*, Elsevier Press, New York.

25. G.R. Jenkins and J.W. Kirkpatrick (1979), Twenty years operation of an in-situ combustion project, *J. of Canadian Pet.*, **Mar.-Jun.**, 60–66.

26. R. Christenson (1980), *Viscosity Characteristics of Bitumen*, Masters Thesis, University of Wyoming.

27. K. Abou-Kassem and K.Aziz (1985), Handling of phase change in thermal simulators, *J. Pet. Tech.*, **Sep.**, 1661– 1663.

28. J. Baker-Jarvis and R. Inguva (1985), Heat conduction in heterogeneous materials, *J. Heat Transfer*, **107**, 39–43.

29. J. Baker-Jarvis and R. Inguva (1984), Heat conduction in layered media, *Fuel*, **63**, 1726–1730.

30. de Gear (1971), *Numerical Initial Value Problems in Ordinary Differential Equations*, Prentice-Hall, Englewood Cliffs, New Jersey.

31. W.L. Stutzman and G.A. Thiele (1981), *Antenna Theory and Design*, John Wiley and Sons, New York.

32. G.K. Youngren (1980), Development and application of an in situ combustion reservoir simulator, *SPE*, **Feb.**, 39– 51.

33. R.L. Jesch and R.H. McLaughlin (1984), Dielectric measurements of oil shales as functions of temperature and frequency, *IEEE Trans. Geosci. Remote Sensing*, **GE– 22(2)**, 99–105.

34. R.L. Jesch and R.H. McLaughlin (1983), Dielectric measurements of oil shales as functions of temperature and frequency, *NBSIR 83–1683*, **Jan.**

35. M. Freeman (1979), *Techniques for Dielectric Spectroscopy of Materials*, Masters Thesis, Colorado State University.

36. A.R. von Hippel ed. (1954), *Dielectric Materials and Applications*, John Wiley and Sons, Inc., New York, 47–139.

37. R.N. Jones, H.E. Bussey, W.E. Little, and R.F. Metzer (1978), Electrical characteristics of corn, wheat and soya in the 1–200 MHz range, *NBSIR 78–897.*

38. R.L. Jesch (1978), Dielectric measurements of five different soil textural types as functions of frequency and moisture content, *NBSIR 78–896.*

39. H.E. Bussey (1978), Dielectric measurements of lunar soil, *Lunar Planet. Sci. Conf. IX, Abstract Papers*, 140–142.

40. S. Ramo, J.R. Whinnery, and T. van Druzer (1984), *Fields and Waves in Communication Electronics*, John Wiley and Sons, New York, Chaper 5.

41. J.R. Whinnery and H.W. Jamieson (1944), Equivalent circuits for discontinuities in transmission lines, *Proceedings I.R.E.*, **32**, 98–114.

42. J.R. Whinnery, H.W. Jamieson, and T.E. Robbins (1944), Coaxial line discontinuities, *Proceedings I.R.E.*, **32**, 695–709.

43. H.E. Bussey (1980), Dielectric measurements in a shielded open circuit coaxial line, *IEEE Trans. Inst. Meas.*, **IM–29(2)** 120–124.

44. R.C. West, ed. (1987), *Handbook of Chemistry and Physics*, 68th Edition, CRC Press, Inc., Boca Raton, Florida.

45. R. Inguva (1984), Physics of oil shales, *Final Technical Report #DE–AS20–81LC–10783.*

46. S.C. Jones (1971), A rapid accurate unsteady-state Klinkenberg permeability permeameter, *SPE #3535*, 46th Annual Fall Meeting, New Orleans, October 3–6.

47. J.W. Amyx, D.M. Bass, and R.L. Whiting (1960), *Petroleum Reservoir Engineering*, McGraw Hill, New York.

48. B.C. Craft and M.F. Hawkins (1959), *Applied Petroleum Reservoir Engineering*, Prentice Hall, New Jersey.

49. G.C. Wallick and J.S. Aronofsky (1954), Effect of gas slip on unsteady flow of gas through porous media, *Transactions of AIME*, **201**, 322–324.

50. R.L. Wise, R.C. Miller (1971), and H.W. Sohns, Heat contents of some Green River oil shales, *Report of Investigation, 7482*, U.S. Bureau of Mines, Washington, DC.

51. S.K. Kumschal (1975), Energy requirements in oil shale retorting, *Quart. Colo. Sch. Mines*, **70(3)**, 237– 272.

52. N.M. Melton and T.S. Cross (1967), Fracturing oilshale with electricity, *Quart. Colo. Sch. Mines*, **62(3)**, 45–60.

53. J.R. Butt, J.E. Lewis, and F.R. Steward (1983), *J. Microwave Power*, **18(1)**.

54. D.C. Chang, R. Halbegwachs, and C.H. Harrison, Jr. (1975), The electromagnetic field very near to a monopole, *IEEE Transactions of Electromagnetic Compatibility*, **EMC–17(2)**, 97–105.

55. D.C. Chang (1968), On the electrically thick monopole, *IEEE Trans. Ant. Prop.*, **AP–16(1)**, 58–64.

56. R.W. King and C.H. Harrison (1969), *Antennas and Waves: A Modern Approach*, The M.I.T. Press, Cambridge, Massachusetts.

57. L.A. Ames, J.T. deBettencourt, J.W. Frazier, and A.S. Orange (1963), Radio communications via rock strata, *IEEE Trans. on Communications*, **21**.

58. R.W.P. King and K. Iizuka (1963), The complete electromagnetic field of a half-wave dipole in a dissipative medium, *IEEE Trans. on Ant. Prop.*, **May**, 275–285.

59. M.K. Moore (1963), Effects of a surrounding conducting medium on antenna analysis, *IEEE Trans. Ant. Prop.*, **May**.

60. R.W.P. King, M. Owens and T.T. Wu (1981), *Antennas in Matter*, M.I.T. Press, Cambridge, Massachusetts.

61. J. Baker-Jarvis (1984), *Volumetric Heating of Oil Shales and Heat Transfer in Heterogeneous Media*, Ph.D. Thesis, University of Wyoming.